WOODHEAD PUBLISHING SERIES IN ENERGY

# Coal Combustion Products (CCP's)

## Characteristics, Utilization and Beneficiation

**Edited by Tom Robl, Anne Oberlink and Rod Jones**

WP
WOODHEAD
PUBLISHING

# Coal Combustion Products (CCP's)

## Related titles

*The Coal Handbook: Towards Cleaner Production, Volume 2: Coal Utilisation*
(ISBN 978-1-78242-116-0)

*Materials for Energy Efficiency and Thermal Comfort in Buildings*
(ISBN 978-1-84569-526-2)

*Structures, Processing, Properties and Industrial Applications*
(ISBN 978-1-84569-449-4)

Woodhead Series in Energy

# Coal Combustion Products (CCP's)

## Characteristics, Utilization and Beneficiation

*Edited by*

***Tom Robl***

***Anne Oberlink***

***Rod Jones***

ELSEVIER

WP
WOODHEAD
PUBLISHING
An imprint of Elsevier

Woodhead Publishing is an imprint of Elsevier
The Officers' Mess Business Centre, Royston Road, Duxford, CB22 4QH, United Kingdom
50 Hampshire Street, 5th Floor, Cambridge, MA 02139, United States
The Boulevard, Langford Lane, Kidlington, OX5 1GB, United Kingdom

Copyright © 2017 Elsevier Ltd. All rights reserved.
Copyright © 2017 Electric Power Research Institute Inc. Published by Elsevier Ltd.
All rights reserved.

No part of this publication may be reproduced or transmitted in any form or by any means, electronic or mechanical, including photocopying, recording, or any information storage and retrieval system, without permission in writing from the publisher. Details on how to seek permission, further information about the Publisher's permissions policies and our arrangements with organizations such as the Copyright Clearance Center and the Copyright Licensing Agency, can be found at our website: www.elsevier.com/permissions.

This book and the individual contributions contained in it are protected under copyright by the Publisher (other than as may be noted herein).

**Notices**

Knowledge and best practice in this field are constantly changing. As new research and experience broaden our understanding, changes in research methods, professional practices, or medical treatment may become necessary.

Practitioners and researchers must always rely on their own experience and knowledge in evaluating and using any information, methods, compounds, or experiments described herein. In using such information or methods they should be mindful of their own safety and the safety of others, including parties for whom they have a professional responsibility.

To the fullest extent of the law, neither the Publisher nor the authors, contributors, or editors, assume any liability for any injury and/or damage to persons or property as a matter of products liability, negligence or otherwise, or from any use or operation of any methods, products, instructions, or ideas contained in the material herein.

**Library of Congress Cataloging-in-Publication Data**
A catalog record for this book is available from the Library of Congress

**British Library Cataloguing-in-Publication Data**
A catalogue record for this book is available from the British Library

ISBN: 978-0-08-100945-1 (print)
ISBN: 978-0-08-101047-1 (online)

For information on all Woodhead publications visit our website at https://www.elsevier.com/books-and-journals

ELSEVIER
Book Aid International
Working together to grow libraries in developing countries
www.elsevier.com • www.bookaid.org

*Publisher:* Joe Hayton
*Acquisition Editor:* Maria Convey
*Editorial Project Manager:* Charlotte Kent
*Production Project Manager:* Omer Mukthar
*Cover Designer:* Victoria Pearson

Typeset by SPi Global, India

# Contents

# List of contributors

**T. Adams** American Coal Ash Association, Lexington, KY, United States

**P. Amaya** American Electric Power, Columbus, OH, United States

**D.P. Bentz** NIST, Gaithersburg, MD, United States

**J.D. Bittner** Orca Technical Interests LLC, Tacoma, WA, United States

**A. Bittner** Gradient, Cambridge, MA, United States

**G.M. Blythe** AECOM, Blythe, CA, United States

**L.J.N. Bradley** Haley & Aldrich, Inc., Burlington, MA, United States

**T. Butalia** The Ohio State University, Columbus, OH, United States

**N.E. Carriker** Tennessee Valley Authority, Knoxville, TN, United States

**J. Castleman** The SEFA Group, Inc., Lexington, SC, United States

**L.J. Csetenyi** University of Dundee, Dundee, United Kingdom

**S. Dai** China University of Mining and Technology, Beijing, China

**J.L. Daniels** UNC Charlotte, Charlotte, NC, United States

**D. French** University of New South Wales, Sydney, NSW, Australia

**U.M. Graham** University of Kentucky Center for Applied Energy Research, Lexington, KY, United States

**J. Groppo** University of Kentucky, Lexington, KY, United States

**D. Harris** Asian Coal Ash Association, Beijing, China

**K.R. Henke** University of Kentucky Center for Applied Energy Research, Lexington, KY, United States

**B. Hensel** Electric Power Research Institute, Palo Alto, CA, United States

**J.C. Hower** University of Kentucky Center for Applied Energy Research, Lexington, KY, United States

**F.J. Hrach** ST Equipment & Technology LLC, Needham, MA, United States

**R. Jewell** University of Kentucky, Lexington, KY, United States

**R. Jones** University of Dundee, Dundee, Scotland

**J. Jow** National Institute of Clean-and-Low-Carbon Energy (NICE), Beijing, China

**R.A. Kruger** South African Coal Ash Association, Pretoria, South Africa

**K.J. Ladwig** Electric Power Research Institute, Palo Alto, CA, United States

**L. Lemay** National Ready Mixed Concrete Association, Silver Spring, MD, United States

**A. Lewis** Gradient, Cambridge, MA, United States

**S. Liu** China University of Mining and Technology, Beijing, China

**M.J. McCarthy** University of Dundee, Dundee, United Kingdom

**R. Minkara** Headwaters Incorporated, Kennesaw, GA, United States

**H.W. Nugteren** Delft University of Technology, Delft, The Netherlands

**K. Radloff** Gradient, Cambridge, MA, United States

**T. Robl** University of Kentucky, Lexington, KY, United States

**R.V.R. San Nicolas** The University of Melbourne, Melbourne, VIC, Australia

**L.L. Sutter** Michigan Technological University, Houghton, MI, United States

**M. Thomas** University of New Brunswick, Fredericton, NB, Canada

**J.S.J. van Deventer** The University of Melbourne, Melbourne, VIC, Australia

**B. Walkley** The University of Sheffield, Sheffield, United Kingdom

**C.R. Ward** University of New South Wales, Sydney, NSW, Australia

**W. Wolfe** The Ohio State University, Columbus, OH, United States

# Editors biography

**Thomas Robl** is a Senior Advisor for the Materials Technologies Group at the University of Kentucky Center for Applied Energy Research (UK CAER). He is a member of the University of Kentucky Graduate Faculty and is Co-Chairman of the World of Coal Ash Conference (WOCA). He received his PhD from the University of Kentucky in 1977 in Geology.

**Anne Oberlink** is a Senior Research Scientist for the Materials Technologies group at the University of Kentucky Center for Applied Energy Research (UK CAER). She is a co-editor of the *Coal Combustion and Gasification Products Journal*, a journal collaboratively published by UK CAER and the American Coal Ash Association (ACAA). She received her second Masters of Science in Chemistry from the University of Kentucky in 2010.

**Rod Jones** is Professor of Civil Engineering and the Director of the Concrete Technology Unit at the University of Dundee in Scotland. He's a Chartered Civil Engineer and is a leading researcher in the field of cement and concrete technology. His research work lies in the areas of engineering design, sustainable construction, durability performance, utilization of industrial by-products, and enhancing service-life performance.

# Preface

A seismic change is underway in the production and use of coal combustion products. In many countries, coal power plants are being retired, which is affecting the market dynamics of coal combustion products. As plants close the point sources of coal ash become more distant. The haulage costs increase and the pricing structure changes, making recovery, processing, and beneficiation technologies more viable.

This is transforming coal combustion by-products into a consistent, reliable, and valued commodity. A large surplus of high-quality ash remains in countries such as China, India, and Poland, while shortages develop in North America, Western Europe, Japan, and Australia. In these regions, coal fly ash is changing from a grossly oversupplied and underpriced commodity to one where pricing is more reflective of a true value proposition. The international shipping of coal products is already underway; thus coal products are undergoing a rapid change from a by-product to a product, the value of which is expected to reach 100 billion dollars in the next 10 years.

Over the past three quarters of a century, our understanding of coal ash as a concrete additive has changed. Originally used to control heat, the value of coal ash in both displacing cement, improving concrete durability, and extending structural life is now well documented, as is the value of scrubber materials (e.g., synthetic gypsum) in other construction applications, such as plasterboard and related products.

The era of fly ash as a multibillion-dollar, internationally traded commodity has arrived and will shape the future of the industry. The power has shifted from the utility to the ash resource trader.

However, there are many other geopolitical forces in place.

Greenhouse gas emissions and other related environmental concerns are an important driving force. Both industrialized and developing countries are rapidly embracing new infrastructure development, which is consuming immense quantities of natural resources. Globally, Portland cement is the most important building material, but it is also the third-largest source of global anthropologic carbon emissions. Indeed, the greatest materials engineering challenge of our time may be to reduce the carbon footprint of Portland cement concrete and other construction materials. The use of fly ash is the most important solution in meeting this challenge.

Fracking has changed the energy supply paradigm, providing what amounts to a limitless supply of unconventional oil and gas. Abundant fuel supplies and lower costs combined with environmental pressures have resulted in the closing of coal combustion power plants at an unprecedented pace in North America and parts of Europe.

These coal plant closings are bringing to the forefront issues about the management of ash stored in ponds and landfills at plant sites that have been closed or converted to other fuel. The long-term potential for groundwater contamination and the stability of the containment structures must be addressed now rather than in some distant future, when new policies and regulations are under development.

This book attempts to provide a timely portrait of this industry in transition, from the basics of the origin of materials and their chemistry to their current and future utilizations. Also covered are technologies for the beneficiation of coal ash. Environmental and human health risks are also discussed, including the impacts of ash pond failures.

We have enlisted international authors with acknowledged expertise in both industry and academia. We have also attempted to provide something of a global perspective, at least to the extent that the topic and our own backgrounds permit.

**The Editors**

# Acknowledgments

We would like to thank the editorial staff at Elsevier for all their support and encouragement for this project.

**Tom, Anne and Rod**

# Part One

# Nature of coal combustion products

# An introduction to the nature of coal

# 1

*J. Groppo*
University of Kentucky, Lexington, KY, United States

## 1.1 Coal formation and rank

Coal is a heterogeneous material essentially comprised of fossilized carbon that originates from organic material accumulated in low-lying areas or sediment basins. The parent organic material was typically vegetative in origin, consisting of trees, plants, leaves, roots, branches, pollen, and spores. As these materials accumulated in a saturated environment, partially decayed vegetation would settle to the bottom of the swamp or bog and transform into peat, provided suitable acidity and anaerobic conditions existed to prevent full decay. This process, termed humification, refers to the decomposition of plant matter as it is transformed into organic residue (Fuchsman, 1980). Over time, massive amounts of vegetative matter cyclically accumulated. As long as the water table continued to rise and prevent the swamp from drying out, more peat formed.

Several different systems are used to classify peat, using characteristics such as geology, botanical content, or physiochemical properties (Fuchsman, 1980; Boron, Evans, & Peterson, 1987). Table 1.1 shows an increase in carbon content and a decrease in oxygen content as the level of humification increases. As decomposition proceeds, readily degraded components, such as cellulose and hemicellulose, are the first to be attacked by microorganisms, while more resistant lignin remains (Boron et al., 1987). In addition the amount of bitumen and humic acids also increase, with humic acids comprising up to 60% of the organic material present (Table 1.2). The organic matter composition of peat is important because it comprises the parent material that will eventually be transformed with time and pressure into coal.

Infiltration of sediments via flooding events or erosion resulted in the burial of the peat. The burial depth increased with a continued deposition of sediment layers, eventually progressing to depths where temperature and pressure both increase. As a result the peat would be compacted and transformed into lignite (brown coal), the initial step in the coalification process. Moisture is reduced via dehydration, while carboxylic acids and volatile matter (primarily methane), along with $CO_2$, are also reduced as pressure compacts organic material into a denser solid (Taylor et al., 1998). With time, heat, and pressure, lignite matures into subbituminous coal, then into bituminous coal, and eventually into anthracite. The various stages that occur over time result in changes to the chemistry of the organic matter during the coalification process. Coal rank is the term used to define the extent to which the organic matter has progressed

**Coal Combustion Products (CCP's).** **http://dx.doi.org/10.1016/B978-0-08-100945-1.00001-0**

**Table 1.1** **Elemental composition of peat as a function of humification (Fuchsman, 1980)**

| Element (dry basis) | H1 to H3 | H4 to H7 | H8 to H10 |
|---|---|---|---|
| Carbon (%) | 43–53 | 56–58 | 59–63 |
| Hydrogen (%) | 5.0–6.1 | 5.5–6.1 | 5.1–6.1 |
| Oxygen (%) | 40–46 | 34–39 | 31–34 |
| Nitrogen (%) | 0.5–1.0 | 0.8–1.1 | 0.9–1.9 |
| Sulfur (%) | 0.1–0.2 | 0.1–0.3 | 0.2–0.5 |

**Table 1.2** **Organic matter components in peat as a function of humification (Boron et al., 1987)**

| Organic material | H1 to H2 | H5 to H6 | H9 to H10 |
|---|---|---|---|
| Cellulose (%) | 15–20 | 5–15 | – |
| Hemicellulose (%) | 15–30 | 10–30 | 0–1 |
| Lignin (%) | 5–40 | 5–30 | 5–20 |
| Humic Acids (%) | 0–5 | 20–30 | 50–60 |
| Bitumens (%) | 1–10 | 5–15 | 5–20 |
| Nitrogen Compounds (%) | 3–14 | 5–20 | 5–25 |

through the coalification process, and each rank is defined by several physiochemical properties. One generally accepted classification scheme, shown in Table 1.3, utilizes fixed carbon, volatile matter, calorific value, and agglomerating characteristics to determine the specific coal rank (ASTM, 2015). In this scheme, fixed carbon and volatile matter are expressed on a dry mineral matter free basis (dmmf), while calorific value is expressed on a moist mineral-matter-free basis (mmf). There are two classifications for lignite and three classifications for subbituminous, all based on calorific value. The bituminous coal rank is determined by both calorific value and composition (i.e., fixed carbon and volatile matter). The high-volatile-matter subbituminous coals all contain <69% fixed carbon and >31% volatile matter. The calorific value increases with rank, as volatile matter is converted into fixed carbon as the coalification process proceeds. Through continued coalification, increasing amounts of volatile matter are converted into fixed carbon, as rank increases to low volatile bituminous. Once the amount of fixed carbon increases to 86% and the volatile matter decreases to 14%, the rank is classified as Anthracite. One very important observation is that as coalification proceeds through the various ranks, volatile matter is converted into fixed carbon, resulting in an increasing energy density.

Specific coal rank classifications vary between countries, but in general, formation begins with peat and sequentially progresses to lignite, subbituminous coal, bituminous coal, and anthracite. As this progression proceeds, several important compositional transformations occur. As previously mentioned, carbon content increases

**Table 1.3** Classification of coal by bank (ASTM D388-12, 2015)

| | | Fixed carbon | Volatile matter | Gross calorific value | | |
|---|---|---|---|---|---|---|
| | | % | % | Btu/lb | MJ/kg | |
| **Coal rank** | | **dmmf** | **dmmf** | **Moisture mmf** | **Moisture mmf** | **Agglomerating characteristics** |
| Anthracite | Meta-anthracite | ≥98% | <2% | | | Non-agglomerating |
| | Anthracite | 92–98% | 2–8% | | | |
| | Semianthracite | 86–92% | 8–14% | | | |
| Bituminous | Low-volatile bituminous | 78–86% | 14–22% | | | Commonly agglomerating |
| | Medium-volatile bituminous | 69–78% | 22–31% | | | |
| | High-volatile A Bituminous | <69% | >31% | ≥14,000 | ≥32.557 | |
| | High-volatile B Bituminous | <69% | >31% | 13,000–14,000 | 30.232–32.557 | |
| | High-volatile C Bituminous | <69% | >31% | 11,500–13,000 | 26.743–30.232 | |
| | High-volatile C Bituminous | | >31% | 10,500–11,500 | 24.418–26.743 | Agglomerating |
| Subbituminous | Subbituminous A | | | 10,500–11,500 | 24.418–26.743 | |
| | Subbituminous B | | | 9500–10,500 | 22.09–24.418 | |
| | Subbituminous C | | | 8300–9500 | 19.30–22.09 | |
| Lignite | Lignite A | | | 6300–8300 | 14.65–19.30 | Nonagglomerating |
| | Lignite B | | | <6300 | <14.65 | |

with coal rank as volatile matter is converted into carbon, thus volatile matter decreases with rank. Another important change is that moisture content decreases with rank. This moisture is not free or surface water, but rather it is moisture within the chemical structure of the coal itself. Peat can contain as much as 75% chemically bound water, which decreases to 35% in lignite, further decreasing to 25% in subbituminous coal and to less than 10% moisture in bituminous coal (Teichmüller & Teichmüller, 1982). Moisture content is particularly important when considering thermal properties of coal, since higher moisture content results in a lower heating value.

This type of classification scheme is relevant to fly ash for one very important reason: it is the single most determining factor as to which type of fly ash will be produced by combustion. In almost all cases, lower-rank coals lignite and subbituminous will produce Class C ash, while higher-rank coals bituminous and anthracite will produce Class F ash. A detailed discussion on the differences between these types of fly ash will be provided later in this chapter.

## 1.2 Coal composition and mineralogy

### 1.2.1 Organic material

Coal is a not actually a mineral; rather, it is a heterogeneous material comprised of varying quantities of different organic components termed macerals. Macerals comprise coal in much the same way that minerals comprise rocks. The distinction is that minerals retain their physical and chemical properties regardless of their size, while macerals do not. When describing the composition of coal in geologic terms, the components are grouped by maceral type, an evaluation that is done microscopically. In general, coal can petrographically be described as an assemblage of macerals and mineral matter. One classification system (Table 1.4) shows the parent material that

**Table 1.4** Coal maceral classification and parent material

| Maceral type | Maceral | Parent material |
|---|---|---|
| Macerals comprised of woody or cortical tissues | Vitrinite | Woody tissue |
| | Fusinite | Fossilized charcoal |
| | Semifusinite | Transition between woody tissue and fossilized charcoal |
| Macerals of plant matter other than woody tissue | Spornite | Spores |
| | Culinite | Cuticles |
| | Resinite | Plant resins and waxes |
| | Alginite | Algal bodies |
| | Sclerotinite | Fungi |
| Not traced to a specific vegetable tissue | Micronite | Humic mud |

(Modified from Van Krevlin, 1961)

formed each maceral. While all of these macerals are important in determining the combustion properties of the coal, four are typically associated with the unburned carbon found in fly ash, fusinite, semifusinite, and less notably, sclerotinite and micronite.

### 1.2.2 Mineral phases

In addition to carbon, volatile matter, and moisture, inorganic material is also found in coal. One source of the inorganic material is weathering and erosion of associated minerals from the surrounding area that are deposited along with organic matter during flooding events or streamflow throughout the coal formation process. Other sources include the inorganic components of the parent vegetation itself, along with ash deposition during volcanic events. A variety of minerals can commonly be found in coal, as shown in Table 1.5. These minerals can be found in varying concentrations, depending on the depositional environment. The quantity and composition of these

**Table 1.5 Classification of common minerals found in coal (Nelson, 1953; Spackman & Moses, 1961)**

| **Shale group (Group M)** | **Accessory minerals** |
|---|---|
| Muscovite $(KAl_2(AlSiO_3O_{10})(OH)_2)$ | Sphalerite (ZnS) |
| Hydromuscovite | Feldspar $(K,Na)_2O \cdot Al_2O_3 \cdot 6SiO_2$ |
| Illite $(K(MgAl,Si)(Al,Si_3)O_{10}(OH)_8)$ | Garnet $(3CaO \cdot Al_2O_3 \cdot 3SiO_2)$ |
| Bravaisite | Hornblende $(CaO \cdot 3FeO \cdot 4SiO_2)$ |
| Montmorillonite $(MgAl)_3(Si_4O_{10})_3(OH)_{10} \cdot 12H_2O$ | Gypsum $(CaSO_4 \cdot 2H_2O)$ |
| Kaolin Group (Group K) | Apatite $(9CaO \cdot 3P_2O_5 \cdot CaF_2)$ |
| Kaolinite $(Al_2SI_sO_5)OH)_4)$ | Zircon $(ZrSiO_4)$ |
| Levisite | Epidote $(4CaO \cdot 3Al_2O_3 \cdot 6SiO_2 \cdot H_2O)$ |
| Metahalloysite | Biotite $(K_2O \cdot MgO \cdot Al_2O_3 \cdot 3SiO_2 \cdot H_2O)$ |
| Sulfide Group (Group S) | Augite $(CaO \cdot MgO \cdot 2SiO_2)$ |
| Pyrite $(FeS_2)$ | Prochlorite $(2FeO \cdot 2MgO \cdot Al_2O_3 \cdot 2SiO_2 \cdot 2H_2O$ |
| Marcasite $(FeS_2)$ | Chlorite $(Mg,Fe,Al)_8(Si,Al)_4O_{10}(OH)_8$ |
| Carbonate Group (Group C) | Diaspore $(Al_2O_3 \cdot H_2O)$ |
| Ankerite $CaCO_3 \cdot (Mg, Fe, Mn)CO_3$ | Lepidocrocite $(Fe_2O_3 \cdot H_2O)$ |
| Calcite $(CaCO_3)$ | Barite $(BaSO_4)$ |
| Siderite $(FeCO_3)$ | Kyanite $(Al_2O_3 \cdot SiO_2)$ |
| Chloride Group (Group O) | Staurolite $(2FeO \cdot 5Al_2O_3 \cdot 4SiO_2 \cdot H_2O)$ |
| Sylvite (KCl) | Topaz $(AlF)_2SiO_4$ |
| Halite (NaCl) | Tourmaline $(H_9Al_3(BOH)_2Si_4O_{19}$ |
| Oxide Group (Group O) | Pyrophyllite $(Al_2Si_4O_{10}(OH)_2)$ |
| Quartz $(SiO_2)$ | Penninite $(5MgO \cdot Al_2O_3 \cdot 3SiO_2 \cdot 2H_2O)$ |
| Hematite $(Fe_3O_4)$ | |
| Magnatite $(Fe_2O_3)$ | |

minerals are a critical consideration for fly ash chemistry, as these inorganic phases are not combustible and will determine the chemistry of the ash that remains after the parent coal is combusted. Coals with higher concentrations of sulfide minerals pyrite and marcasite will obviously produce ash with elevated concentrations of iron. The most common minerals found in most coals are from the shale and kaolin groups, which contain appreciable elemental concentrations of Al and Si, therefore it is not surprising that most fly ashes are predominantly aluminosilicates.

Water chemistry and conditions during peat formation also play important roles in determining which minerals and elements will be present. For example, western US subbituminous coals were formed under fresh water conditions, while eastern US bituminous coals were formed under brackish water conditions. Since fresh water conditions were likely more alkaline in nature, soluble cations, such as calcium and sodium, precipitated as calcium and sodium carbonate species during peat formation and remained throughout the coalification process. As such, western US bituminous coals contain appreciable amounts of Na and Ca. Brackish or saline water quality prevalent during peat formation in eastern US bituminous coals contained appreciable amounts of sulfur from marine life decomposition, resulting in lower pH limiting Ca and/or Na precipitation. As a result, when the incursion water receded, soluble Ca and Na remained in solution and were not deposited as precipitates. As such, eastern US bituminous coals have a much lower Ca and Na content, though they contain appreciable amounts of sulfur.

Similarly, trace elements are also found in coal in varying concentrations (Table 5.2). Coal preparation or cleaning with physical beneficiation methods can remove some of the inorganic mineral and trace elements associated with coal; however, the extent of removal is dependent on the liberation of the inorganic species. If minerals and trace elements are associated with the organic matrix, physical cleaning will do little to remove them prior to combustion. As a result, the inorganic elements contained in the coal will be effectively concentrated during combustion, as the carbon and volatile matter are removed by combustion. The implication is that these elements will be concentrated in the combustion by-products in either gaseous or solid form.

### 1.2.3 Trace elements

As with mineral phases, a variety of other elements can also be found in coal at trace concentration well below 1%. These trace elements originate from the same sources as mineral phases: erosion and/or weathering and transport of surrounding rocks, those contained in the parent vegetation, volcanic events and precipitation or sorption from the aqueous phase during intrusion. A comparison of the trace elements found in international coals is shown in Table 1.6 (IEA, 2012). The range for each element present varies considerably, and it is noteworthy that these values are the average total amounts of specific elements present.

More detailed trace element data for US coals are summarized in Table 1.7. While mean concentrations vary considerably, one general observation is that subbituminous western US coals generally have lower trace element concentrations, with the exception of Ba and Sr. From an environmental perspective, the amount of various trace

## Table 1.6 Average values for trace elements in international coals[a] (IEA, 2012)

| Element | Average (mg/kg) | Average range (mg/kg) |
|---|---|---|
| As | 2.69 | 0.36–9.8 |
| B | 47 | 11–123 |
| Be | 1.0 | 0.1–2.0 |
| Cd | 0.093 | 0.01–0.19 |
| Co | 4.5 | 1.2–7.8 |
| Hg | 0.091 | 0.03–0.19 |
| Pb | 7.0 | 1.1–22 |
| Se | 2.15 | 0.15–5.0 |
| Cr | 17.6 | 2.9–34 |
| Cu | 10.8 | 1.8–20 |
| Mn | 40 | 8–93 |
| Ni | 11.1 | 1.5–21 |
| Zn | 12.7 | 5.1–18 |
| F | 120 | 15–305 |
| Cl | 440 | 25–1420 |

[a] Coals from Australia, Austria, Brazil, Canada, China, Denmark, Germany, India, Italy, South Korea, the Netherlands, New Zealand, Poland, Russia, South Africa, Sweden Thailand, the United Kingdom, and the United States.
(Taken from Nalbandian, H. (2012). Trace element emissions from coal, CCC/203, IEA Clean Coal Centre, ISBN 978-92-9029-523-5, 89 pp, September. http://bookshop.iea-coal.org.uk/reports/ccc-203/83084.)

## Table 1.7 Mean concentration (ppm) of trace elements in US coals (Gluskoter, Ruch, Miller, et al., 1977)

| Element | Eastern US | Illinois Basin | Western US |
|---|---|---|---|
| Ag | 0.02 | 0.03 | 0.03 |
| As | 25 | 14 | 2.3 |
| B | 42 | 110 | 56 |
| Ba | 200 | 100 | 500 |
| Be | 1.3 | 1.7 | 0.46 |
| Br | 12 | 13 | 4.7 |
| Cd | 0.24 | 2.2 | 0.18 |
| Ce | 25 | 14 | 11 |
| Co | 9.8 | 7.3 | 1.8 |
| Cr | 20 | 18 | 9 |
| Cs | 2 | 1.4 | 0.42 |
| Cu | 18 | 14 | 10 |
| Dy | 2.3 | 1.1 | 0.63 |
| Eu | 0.52 | 0.26 | 0.2 |
| F | 89 | 67 | 62 |
| Ga | 5.7 | 3.2 | 2.5 |
| Ge | 1.6 | 6.9 | 0.91 |
| Hf | 1.2 | 0.54 | 0.78 |
| Hg | 0.2 | 0.2 | 0.09 |

*Continued*

**Table 1.7 Continued**

| Element | Eastern US | Illinois Basin | Western US |
|---|---|---|---|
| I | 1.7 | 1.7 | 0.52 |
| In | 0.23 | 0.16 | 0.1 |
| La | 15 | 6.8 | 5.2 |
| Lu | 0.22 | 0.09 | 0.07 |
| Mn | 18 | 53 | 49 |
| Mo | 4.6 | 8.1 | 2.1 |
| Ni | 15 | 21 | 5 |
| P | 150 | 64 | 130 |
| Pb | 5.9 | 32 | 3.4 |
| Rb | 22 | 19 | 4.6 |
| Sb | 1.6 | 1.3 | 0.58 |
| Sc | 5.1 | 2.7 | 1.8 |
| Se | 4 | 2.2 | 1.4 |
| Sm | 2.6 | 1.2 | 0.61 |
| Sn | 2 | 3.8 | 1.9 |
| Sr | 130 | 35 | 260 |
| Ta | 0.33 | 0.15 | 0.15 |
| Tb | 0.34 | 0.22 | 0.21 |
| Th | 4.5 | 2.1 | 2.3 |
| Tl |  | 0.66 |  |
| U | 1.5 | 1.5 | 1.2 |
| V | 38 | 32 | 14 |
| W | 0.69 | 0.82 | 0.75 |
| Yb | 0.83 | 0.56 | 0.38 |
| Zn | 25 | 250 | 7 |
| Zr | 45 | 47 | 33 |
| No. of Samples | 23 | 114 | 28 |

elements present is not of general concern; rather, it is the amount of leachable elements and the conditions under which they can leach that are of more specific concern.

Leaching potential of substrates can be determined by numerous well-established procedures. In the US, the toxicity characteristics leaching procedure (TCLP) was developed by the US Environmental Protection Agency (EPA) to simulate leaching through a landfill in order to determine whether a solid waste is hazardous (EPA, 1992). The procedure essentially consists of leaching solid material for 18 h at 5% solids after the pH has been adjusted using acetic acid or sodium hydroxide to simulate an extended period of time in a landfill. The filtrate is then analyzed to determine the concentration of elements that have been leached. Data presented thus far has been limited to trace elements associated with coals prior to combustion. Trace elements are effectively concentrated in combustion as the organic phases are converted to CO2, while the inorganic mineral matter is thermally altered but remains as ash.

Coal combustion proceeds in stages as coal is introduced to the boiler. The initial stage is moisture evaporation, followed by combustion of volatile matter. The final stage is combustion of remaining fixed carbon, leaving noncombustible inorganic phases to cool and solidify as ash particulates. Nonvolatile elements that were present in the parent coal either as mineral matter or trace elements are concentrated in the residual ash particulates as carbon, the primary component of coal, is combusted. Thus a coal containing 10% ash will produce ash with approximately an order of magnitude higher nonvolatile elemental concentration.

An excellent review of leaching characteristics of fly ash was presented by Izquierdo and Querol (2012). This review of over 90 publications showed that the mode of occurrence of elements in coal determines their solubility in fly ash and that most elements are tightly bound to fly ash and are not easily released. Most elements display pH dependent solubility and are poorly leached in the pH range of 7–10. The mobility of most elements is highly sensitive to pH, and the amount of calcium present exerts dominant influence on the pH of the system. Alkalinity decreases the release of Cd, Co, Cu, Hg, Ni, Pb, Sn, and Zn, but simultaneously enhances the release of oxyanionis of As, B, Cr, Mom Sb, Se, V, and W. Several elements, including As, B, Cr, Sb, Se, and V can be bound by the formation of secondary phases, such as ettringite ($Ca_6Al_2(SO_4)_3(OH)_{12}\cdot 26H_2O$).

## 1.3 Coal beneficiation

### *1.3.1 Coal beneficiation processes*

Coal beneficiation, or coal preparation as it is also termed, refers to the processes through which inorganic impurities are separated from raw mined coal, thereby providing improved combustion characteristics to the fuel produced. The separation processes used are primarily based on exploiting the physical differences between the organic (i.e., coal) and inorganic (i.e., ash) components. Given the low unit value of coal, it is imperative for these separation processes to be both efficient and cost effective. The most commonly used processes are jig washing, density separation, sizing, and froth flotation. Typical configurations divide the run of mine coal into size fractions and utilize different separation processes for each size fraction (Luttrell, Barbee, & Stanley, 2003).

Density separation exploits the differences in density between the organic and inorganic components found in mined coal. As previously described, coal typically is comprised of an assemblage of macerals and inorganic material. Macerals containing primarily organic matter generally have a density of $<1.4$ g/cm$^3$, and as the amount of ash associated with the macerals increases, the density of the particles also increases, because the primary composition of ash associated with coal is essentially the weathered products of quartz (density 2.65 g/cm$^3$). Thus particles in the density range of 1.6–1.8 g/cm$^3$ have a higher ash content. Pyrite ($FeS_2$), another commonly associated mineral, has a much higher density of 5.0 g/cm$^3$. Given the difference in density between the desired material (coal) and undesired material (ash and pyrite), density separation can be an efficient approach for producing low-ash coal, provided the high-ash content particles are liberated from the low-ash particles.

Density separation processes employed in coal preparation are typically performed in a medium suspension of fine ground (−45 μm) magnetite ($Fe_3O_4$) dispersed in water. Magnetite is added to the suspension to maintain the desired medium density. For example, if the medium density is maintained at a density of 1.45 g/cm$^3$, all particles with lower density will float to the top of a separation vessel while the higher density particles sink. The float- and- sink products are separately removed and washed on an appropriately sized screen. Magnetite particles are recovered from washwater with magnetic separators and recycled back into the process. Dense medium separation of coarse particles (>50 mm) is typically accomplished in vessels, while intermediate-size particles (50–1 mm) are treated in cyclones. The operating principles of dense medium cyclones are essentially the same as those of conventional cyclone sizing processes; however, with dense medium cyclones, the fluid density can be increased to the desired separation density by the addition of magnetite. Jig washing employs similar separation principles, but rather than adjusting the medium density, particles are separated in a water medium that is pulsated pneumatically or hydraulically. The pulsation of the jigging motion stratifies particles based on density. Lighter particles migrate to the top of the particle bed, and denser particles migrate to the bottom, thus producing a separation based on particle density. The choice between using jigging or dense medium separation is generally made depending on the amount of near-gravity material, or the amount of material within ±0.1 specific gravity units of the desired separation specific gravity. With 0–7% of the feed near gravity, almost any separation process will work effectively, though jigs are commonly employed under these conditions. With 7%–10% near-gravity material, jigs operate with decreased efficiency, and so dense medium separation processes are appropriate. With >10% near gravity material, dense medium separation processes have application, but the process needs to be more closely controlled. With >25% near-gravity material, dense medium separation is very difficult, but can still find application in limited situations (Wills, 2006).

Size separation processes are the simplest to implement. These processes exploit distinct difference in sizes between coal and ash particles. If, for example, the coal to be processed is coarse while the ash is fine, then efficient separation can be achieved by a simple screening at the appropriate size. The same is true for the converse (i.e., coarse ash and fine coal). As this approach is so simple, it is used wherever possible; however, it is dependent upon the size distribution of the coal and ash particles. When particles are too small to screen efficiently, the size difference between coal and ash particles is exploited using classifying cyclones.

For fine particles (<150 μm), dense medium separation and sizing do not produce efficient separations. These particles are separated by flotation, which exploits differences in particle hydrophobicity. Most bituminous and higher-rank coals have some natural hydrophobic properties, while ash particles are hydrophilic. Coal hydrophobicity can be increased by selective adsorption of small quantities (100–200 g/tonne) of nonpolar collectors, such as diesel or fuel oil. The coal/ash suspension (10–15% solids w/w) is agitated in a tank or cell, and air bubbles are introduced at the bottom of the cell. Surface-active agents, such as short-chain alcohols, are typically added to increase bubble surface area by reducing surface tension at the air/liquid interface, thus producing copious amounts of small air bubbles. Hydrophobic coal particles adsorb onto the rising air bubble and are transported to the top of the cell, where they coalesce and form a stable froth layer. The froth layer overflows the cell or is removed by mechanical scrapers while ash particles remain in suspension and are withdrawn from the cell. Flotation cells used in coal preparation are either mechanically agitated or column flotation cells with no agitator.

### 1.3.2 Coal beneficiation practice

The extent to which the coal is cleaned is dependent upon the market for which the cleaned coal is intended. Utility markets generally require coal that contains <10% ash, depending on the heating value and other fuel considerations specified in fuel contracts. If the mined coal meets contract specifications, then cleaning is not necessary. However, if the mined coal contains excessive amounts of ash and/or sulfur, then coal cleaning is practiced using the various techniques described previously, and the separation density is adjusted to maximize plant yield within the ash and sulfur limits of the fuel desired.

Coal preparation practices vary globally as coal properties and market conditions vary. In the US and Australia, dense medium separation accounted for over half of the preparation done in 2001, as shown in Table 1.8 (Cleaner Coal Technology Program, 2001). In South Africa, dense medium separation accounted for 85% of the coal preparation, due to the very high levels of near-gravity material present in coal mined in this region. In China and Germany, jig washing is the dominant separation process used, again, due to the nature of the coal mined.

US coal preparation practice is well documented. In 2014, there were 252 coal preparation plants operating in the US with an average feed rate of 842 tonnes/h with a range of 227–7444 tonnes/h (Coal Age, 2015). Of these plants, 235 were cleaning bituminous coal, while only 17 were cleaning anthracite. There were no plants

**Table 1.8** Coal preparation processes used by country (Cleaner Coal Technology Program, 2001)

| Process | US | Australia | South Africa | China | India | Germany | Russia | UK |
|---|---|---|---|---|---|---|---|---|
| Jig Washing (%) | 13 | 22 | 0 | 60 | 47 | 79 | 48 | 30 |
| Dense Media Separation (%) | 52 | 60 | 85 | 23 | 35 | 15 | 24 | 30 |
| Froth Flotation (%) | 18 | 10 | 5 | 14 | 2 | 6 | 10 | 15 |
| Other (%) | 17 | 8 | 10 | 3 | 16 | 0 | 18 | 25 |

cleaning subbituminous coal or lignite, because these lower rank coals are not amenable to processing. Low-rank coals that are actively mined globally are found close to the surface and can be selectively mined by removing overburden and high-ash areas; thus coal preparation is not necessary to improve quality by rejecting ash. The ash that is present in these seams is finely disseminated and would require extensive grinding to achieve any degree of ash liberation. The low-energy density of subbituminous coals precludes the economic viability of coal preparation practice, as well as more costly underground mining methods. The low-energy density is attributed primarily to the high moisture content of these coals, which is typically 20–30%. The moisture is not due to the presence of free water, but rather to chemically bound water in hydrated organic species, which can only be removed by thermal treatment. The high energy cost of thermal drying, along with the risk of spontaneous combustion, precludes upgrading by moisture reduction, thus low-rank coals are selectively mined from thick seams without further processing to improve energy density.

Bituminous coals are cleaned to improve coal quality whenever practicable. The need for coal cleaning continually increases as thinner and more marginal-quality coal seams are mined. Thinner seams often require the removal of strata above and/or below the coal seam to facilitate equipment access, as well as access to stable roof and floor strata. Any strata removed during the mining process will be separated from the coal in coal preparation processes.

## 1.4 Coal pulverizing

In general, coal is transported and stored as fuel for use at as coarse a size as possible in order to minimize losses during handling and transport, moisture absorption, and spontaneous combustion, among other considerations. In pulverized coal combustion (PCC), the feed coal is typically pulverized to a fine size by mechanical mills, generally 80% finer than 75 μm, and conveyed into the boiler pneumatically. The grindability of coal varies significantly depending on composition and is commonly assessed by the Hardgrove Grindability Index, or HGI, which is much the same as the relative ease or difficulty of grinding ores as assessed by the Bond Work Index (Bond, 1961). The HGI is determined by using standard techniques and equipment as described in ASTM D409 (ASTM, 2009), where coal specimens are ground in a device under standard conditions. The ground coal is then screened to quantify the amount that is reduced to finer than 75 μm; thus the more fines produced, the higher the HGI.

The HGI of coal has been shown to be influenced by petrographic composition, where HGI values increase with carbon content up to 90%, then drops rapidly with at carbon content exceeding approximately 92% (Fitton, Hughes, & Hurtley, 1957). It is generally accepted that the occurrence of vitrinite in coal increases the HGI value, while other macerals, such as micronite (Hower, Greasem, & Klapheake, 1987), decrease grinadability, as do elevated concentrations of ash in the coal (Wang, Guo, Yingling, & Parekh, 1996). Coals with <40 HGI are generally classified as very hard, coals with 40–60 HGI are classified as hard, 60–80 HGI as medium hard, 80–100 HGI as soft, and 100–120 HGI as very soft. Coal HGI > 120 is classified as extremely soft and includes only some types of brown coal (Tichanek, 2008).

Regardless of any specific correlation between grindability and maceral type, it is clear that some macerals are more difficult to grind than others. This results in a coal pulverizer generating a size range of particles with a general trend of lower HGI (i.e., harder) macerals that are coarser than higher HGI (i.e., softer) macerals. As previously described, some macerals, such as fusinite, semifusinite, sclerotinite, and alginite, are typically associated with the unburned carbon found in fly ash. Their presence can be attributed to both their hardness as well as their relatively poor combustion characteristics in comparison to other macerals. Maceral hardness results in coarser particles, with a lower surface area being introduced into the boiler after pulverization. Meanwhile, poorer combustion properties result in higher proportions of these macerals, which comprise the unburned carbon remaining in fly ash after combustion. Their occurrence in fly ash is exacerbated by what are now commonly used staged combustion low $NO_x$ burners, which essentially lower the flame temperature in order to limit $NO_x$ formation.

## 1.5 Future trends for clean coal technologies

### 1.5.1 Clean coal technologies ash

Clean coal technologies (CCT) were developed as an effort to continue utilizing coal to generate electricity while addressing the environmental liabilities of this fuel. Early efforts focused on sulfur reduction to mitigate concerns over acid rain formation and resulted in the development and widespread implementation of postcombustion $SO_2$ scrubbing technologies, such as wet and dry scrubbing. The adoption of efficient scrubbing technologies in recent years has enabled the usage of higher sulfur coals that were not suitable for fuel use. Since much of the elevated sulfur content of these high sulfur coals is associated with pyrite ($FeS_2$), the resulting fly ash will contain higher concentrations of iron. The principle adverse quality impact this will have on fly ash will be with respect to color, as high iron fly ash is generally darker than that derived from low-sulfur coals. The other important difference is more relevant to bottom ash, as high-sulfur coals produce bottom ashes with higher bulk density. Low-sulfur coals produce bottom ash with a loose bulk density less than 880 kg/$m^3$, significantly lower than crushed limestone and gravel (1360–1600 kg/$m^3$), making them suitable for use as lightweight aggregate in concrete masonry units (Groppo & Robl, 2002). Increased use of higher-sulfur coal will result in the decreased availability of bottom ash that is marketable as lightweight aggregate.

Adoption of low NOx burners, another CCT, to mitigate $NO_x$ formation has also had an adverse impact on fly ash quality by increasing the amount of unburned carbon (Hower et al., 1996). While optimization of burner operation can minimize the impact, fly ash beneficiation has become more commonly employed as a means to selectively remove or passivate carbon. Electrostatic (Bittner, Gasiorowski, Tondu, & Vasiliauskas, 1997) and thermal (Keppeler, 2001) processes have been in commercial use over the past few decades to address this issue and will see continued uses in the future.

Perhaps the most significant CCT to impact ash quality in the future is fluidized bed combustion (FBC), technology where solid fuel is fluidized by air in a combustion chamber, producing turbulent mixing of fuel and gases. A significant difference from pulverized coal combustion is the velocity of the air used, generally high enough to fluidize the fuel bed. FBC technologies achieve very low SOx emission levels by adding a sorbent such as limestone into the fluidization vessel so that sulfur capture occurs during combustion, thus eliminating the need for a downstream flue-gas treatment. As FBC boilers operate at lower temperatures (760–930°C) than those of PC boilers, $NO_x$ formation is also minimized. An additional benefit of FBC technology is fuel flexibility, which allows for a variety of less expensive lower-quality fuels (typically coal, biomass, or a mixture of both) to be efficiently combusted.

The earliest commercial versions of FBC technology were operated at atmospheric pressure; hence the term atmospheric fluidized bed combustion (AFBC). A later variation known as pressurized fluidized bed combustion (PFBC) operates at elevated pressure and produces a high-pressure gas stream, which can be used to drive a gas turbine, while steam generated from water tubes in the chamber is used to drive a steam turbine, providing higher thermal efficiency with this combined cycle. Circulating fluidized bed combustion (CFBC) circulates large volumes of air and entrains sorbent material from the combustion chamber, where it is separated with large cyclones. Air is returned to fluidize the bed, while sorbent is also recycled to maximize sulfur capture. Spent sorbent is periodically removed, and fresh sorbent is added as necessary to maintain emission requirements.

Of the nearly 12 M tonnes of FBC ash produced in the United States in 2015, almost 90% was utilized in mining applications, while a minor amount (65 K tonnes) was also used for waste stabilization (ACAA, 2016). In Europe (EU15), FBC ash production in 2010 was only 912 K tonnes, with 77% utilized in a variety of applications, including cement kiln feed, subgrade stabilization, and infill (ECOBA, 2011). What is noteworthy of the utilization data is that unlike fly ash, FBC ash is not used as a pozzolan in cement and concrete (ASTM, 2008). Chemistry and variability precludes the use of FBC ash for use in these types of applications. Given the fuel flexibility and low $NO_x$ and $SO_x$ emissions produced by these technologies, it is reasonable to speculate that the amount of FBC by-products produced globally will increase significantly as this technology becomes more widely adapted, particularly for the combustion and cocombustion of biomass.

### 1.5.2 Biomass ash

Biomass has become a fuel source of increasing interest worldwide, particularly when considering sustainable fuel resources. Biomass (e.g., energy crops, agricultural residue, trees, etc.) can be used as primary fuel, or cofired with another fuel source, such as coal. The by-product from these combustion processes (i.e., ash) does not conform to combustion ash specifications in the United States, so it cannot be used as a pozzolan in concrete. Provisions have been made in Europe to allow biomass-derived ash to be used in cementitious applications, limited to when a maximum of 10% of the ash is derived from secondary fuel resources (European Standard EN-450, 2005).

The composition of ash derived from numerous biomass sources has been compiled by the Energy Research Center of the Netherlands (ECN, 2011). While there is a significant variation of composition between sources, biomass-derived ash is generally higher in alkali content and lower in ash content than ash derived from coal. The ash resulting from the cocombustion of biomass and coal is comprised of proportional properties of the ash derived from both fuel components. Since biomass has a low ash content and usually represents a minor proportion of the fuel mix, it typically has a minor impact on utilization properties. Cocombustion ash has been shown to be equivalent to the ash produced from full coal firing with respect to environmental, technical, and occupational health properties. Even when it is derived from high proportions of biomass fuel, it conforms to the technical requirements of European standards (EN450) for utilization in concrete (te Winkel, Meij, & Saraber, 2007). Ashes derived from utility cocombustion of coal with forest residues (i.e., tree limbs) and mill residue (i.e., sawdust) were evaluated for use in mortar and concrete by Shearer, Yeboah, Kustis, and Burns (2011). While cofiring impacted morphology, no correlation was found between increased cofiring percentages and increased LOI or alkali content of the ash.

### *1.5.3 Gasification slag*

Although currently limited in the production of electricity, gasification is a CCT that shows great promise for the future, particularly if coal is to remain a significant part of the electrical production fuel mix. Rather than using coal as a fuel to produce steam, gasification converts a host of fuels into syngas (i.e, a mixture of CO and $H_2$) via controlled oxidation. Additional $H_2$ can be produced by reacting the CO with steam in a separate reactor. Hydrogen can then be combusted in a gas turbine, from which heat is recovered from the exhaust gases to produce steam, which is directed to a steam turbine. Electricity is produced from generators driven by both the gas turbine and the steam turbine, thus the term “integrated gasification combined cycle,” or IGCC. Because electricity is generated from two thermodynamic cycles, the combined cycle operates at a higher conversion efficiency (>40%) than the separate cycles. In gasification, sulfur is converted to $H_2S$, which is readily converted into salable sulfuric acid. $NO_x$ is not formed in the reducing environment of the gasifier; rather, ammonia is created and easily stripped from the gas stream. There are currently 15 IGCC projects operating globally, in addition to another 22 proposed plants in the United States and another 72 in other countries (NETL, 2016).

Ash produced from gasification processes is very dissimilar to that produced through pulverized coal combustion. Most gasification processes cyclically tap molten slag from the gasifier, where it flows into a quench tank. This rapid quenching produces a vitreous, fine-grained slag that is similar in chemistry to coal ash.

However, most gasification slag is essentially a coarse (i.e., >150 μm) mixture of vitreous aluminosilicates (often called frit) and porous carbon. The frit is often suitable for use as aggregate, provided that the porous carbon can be removed. While the frit can be pozzolanic, comminution to fine sizes is required; thus utilization is currently limited primarily to applications such as kiln feed or roofing granules.

A significant environmental benefit of fossil fuel gasification is that unlike pulverized coal combustion; it provides a concentrated by-product stream of $CO_2$, an important consideration for potential utilization and sequestration. Despite the increased cost and complexity of generation with IGCC, increased efficiency, cleaner emissions, and concentrated $CO_2$ are important advantages that will likely play a significant role in the future of generation technologies, particularly with coal as a fuel.

## References

American Coal Ash Association (ACAA). (2016). *2015 Coal combustion product (CCP) production & use survey report*. [online] Available at: https://www.acaa-usa.org/Portals/9/Files/PDFs/2015-Survey_Results_Table.pdf [Accessed 7 November 2016].

American Society for Testing and Materials (ASTM). (2015). *ASTM D388–15, Standard classification of coals by rank, Annual Book of ASTM Standards, Volume 05.06*. West Conshohocken, PA: ASTM International.

American Society for Testing and Materials (ASTM). (2009). *ASTM D409, Standard test method for grindability of coal by the Hardgrove-Machine method, Volume 05.06*. West Conshohocken, PA: ASTM International.

American Society for Testing and Materials (ASTM). (2008). *ASTM C618, Standard specifications for coal fly ash and raw or calcined natural pozzolan for use as a mineral admixture in concrete, Annual Book of ASTM Standards, Volume 04.02*. West Conshohocken, PA: ASTM International. pp. 330–332.

Bittner, J., Gasiorowski, S., Tondu, E., & Vasiliauskas, A. (1997). STI fly ash separation system 10% in, 1% out; 160,000 tons of STI ash in the new England ready mix concrete market. In *Proceedings of the 1997 International Ash Utilization Symposium* (pp. 630–636).

Bond, F. C. (1961). Crushing and grinding calculations, Part I. *British Chemical Engineering*, *6*(6), 378–385.

Boron, D. J., Evans, E. W., & Peterson, J. M. (1987). *International Journal of Coal Geology*, *8*, 1–31.

Cleaner Coal Technology Program. (2001). *Coal preparation, technology status report 015, Department of Trade and Industry, London, January*. [online] found at http://webarchive.nationalarchives.gov.uk/+/http:/www.berr.gov.uk/files/file19296.pdf [Accessed 4 November 2016].

Coal Age. (2015). *2014 Preparation Plant Census*. pp. 26–30.

U.S. Environmental Protection Agency (EPA). (1992). Method 1311: Toxicity characteristic leaching procedure. *Test methods for evaluating solid waste, physical/chemical methods. Document no. SW-846. Washington, DC*,(July).

European Standard EN-450. (2005). *Fly ash for concrete-part 1: Definition, specifications and conformity criteria*. Belgium: Brussels.

Energy Research Center of the Netherlands (ECN). (2011). *Phyllis, database for biomass and waste*. [online] Available at https://www.ecn.nl/phyllis2/ [Accessed 7 November 2016].

European Coal Combustion Products Association (ECOBA). (2011). *Production and utilisation of CCP's in 2010 in Europe (EU 15)*. [online] Available at: http://www.ecoba.org/evjm, media/ccps/ECO-STAT_2010.pdf [Accessed 7 November 2016].

Fitton, A., Hughes, T. H., & Hurtley, T. F. (1957). The grindability of British coals: A laboratory examination. *Journal of the Institute of Fuel*, *30*, 54–65.

Fuchsman, C. H. (1980). *Peat: Industrial chemistry and technology*. New York, London, Toronto, Sydney, San Francisco: Academic Press.

Gluskoter, H. J., Ruch, R. R., Miller, W. G., et al. (1977). *Trace elements in coal: Occurrence and distribution*. Urbana, IL: Illinois State Geological Survey Circular 499.

Groppo, J., & Robl, T. (2002). Commercial-scale recovery of lightweight block sand from stored coal combustion ash. In R. Dhir, T. Dyer, & J. Halliday (Eds.), *Sustainable concrete construction, Proceedings of the international conference, University of Dundee, Scotland, UK* (pp. 485–493). London: Thomas Telford.

Hower, J. C., Robl, T. L., Rathbone, R. F., Groppo, J. G., Graham, U. M., & Taulbee, D. N. (1996). Case studies of the impact of conversion to low-$NO_X$ combustion on fly ash petrology and mineralogy. In: *Proceedings of 7th Australian Coal Science Conference, Gippsland, Australia, Dec. 2–4*, pp. 347–354.

Hower, J. C., Greasem, A. M., & Klapheake, J. G. (1987). Influence of microlithotype composition on Hardgrove Grindability for selected eastern Kentucky coals. *Internationals Journal of Coal Geology*, *7*, 227–244.

Izquierdo, M., & Querol, X. (2012). Leaching behaviour of elements from coal combustion fly ash: An overview. *International Journal of Coal Geology*, *94*, 54–66.

International Energy Agency (IEA). (2012). *Profiles: Trace element emissions from coal* (p. 2012). Clean Coal Centre. No 12/13, November.

Keppeler, J. (2001). Carbon burnout, an update on commercial applications. In *Proceedings of 2001 International Ash Utilization Symposium, Oct. 20–24, Lexington, KY*.

Luttrell, G. H., Barbee, C. J., & Stanley, F. L. (2003). *Optimum cutpoints for heavy medium separations, Advances in Gravity Concentration*. Littleton, CO: Society of Mining, Metallurgy, and Exploration. 189 p.

National Energy Technology Laboratory (NETL). (2016). *Proposed gasification plant database*. [online] Available at https://www.netl.doe.gov/research/coal/energy-systems/gasification/gasification-plant-databases [Accessed 7 November 2016].

Nelson, J. B. (1953). Assessment of the mineral species associated with coal. *Monthly Bulletin, British Coal Utilization Research Association*, *17*(2), 41–45.

Shearer, C. R., Yeboah, N., Kustis, K. E., & Burns, S. E. (2011). The early age behavior of biomass fired and co-fired fly ash in concrete. In *Proceedings 2011 World of Coal Ash (WOCA) Conference, Denver, CO, May 9–12*.

Spackman, W., & Moses, R. G. (1961). The nature and occurrence of ash-forming minerals in anthracite. In *Bulletin 75, Mineral Industries Experiment Station* (pp. 1–15): Pennsylvania State University.

Taylor, G. H., Teichmuller, M., Davis, A., Diessel, C. F. K., Littke, R., & Robert, P. (1998). *Organic petrology*. Berlin: Gebrüder Borntraeger. 704 p.

Teichmüller, M., & Teichmüller, R. (1982). The geological basis of coal formation. In E. Stachet al. (Ed.), *Coal petrology* (3rd ed., pp. 5–86). Berlin, Stuttgart: Borntraeger.

te Winkel, H., Meij, R., & Saraber, A. (2007). Environmental and health aspects of ashes produced at co-combustion of biomass. In *Proceedings 2007 World of Coal Ash (WOCA), Northern Kentucky, USA, May 7-10*.

Tichanek, F. (2008). Contribution to determination of coal grindability using Hardgrove method. *GeoScience Engineering*, *LVI*(1), 27–32.

Wills, B. A. (2006). In T. Mapier-Munn (Ed.), *Will's Mineral Processing Technology* (7th ed.). Amsterdam: Elsevier. 444 pp.

Van Krevlin, D. W. (1961). Coal: Typology, chemistry, physics and constitution. L. L. Anderson (Ed.), *Coal science and technology: Vol. 3*. Amsterdam: Elsevier. 514 p.

Wang, X. H., Guo, Q., Yingling, J. C., & Parekh, B. K. (1996). Improving pyrite liberation and grinding efficiency in fine coal comminution by swelling pretreatment. *Coal Preparation*, *17*, 185–198.

# Generation and nature of coal fly ash and bottom ash

## 2

*J.C. Hower*, K.R. Henke*, S. Dai†, C.R. Ward‡, D. French‡,*
*S. Liu†, U.M. Graham**
*University of Kentucky Center for Applied Energy Research, Lexington, KY, United States,
†China University of Mining and Technology, Beijing, China, ‡University of New South Wales, Sydney, NSW, Australia

## 2.1 Common types of coal utilization

The basic types of coal combustion and gasification systems have been described in detail by Kitto and Stultz (2005, Chapters 14–18), with further discussions by Berkowitz (1979) and Henderson (2003). The details of the various plant designs are discussed in those references. While we may make references to certain engineering aspects, our emphasis is on the transition of the organic and inorganic portions of coal to fly ash and bottom ash (BA).

The behavior of mineral matter during coal utilization is complex and depends upon a number of factors, such as the particular utilization technology employed, the temperature, gas composition, residence time, mineral particle size, and mineral association. For example, the operating temperature may range from 800°C in fluidized bed combustors to 1600°C in slagging gasifiers. In many utilization technologies, particle residence time is short and heating rates are rapid (Elliott, 1981; Juniper, 2000), resulting in nonequilibrium conditions. The mineral reactions are strongly dependent on the particular technology employed, and the following discussion is based on the individual technologies that may be responsible for the production of ash materials.

### *2.1.1 Pulverized coal and stoker combustion systems*

The most common method of coal combustion, especially for large-scale power production, is pulverized-fuel (pf) combustion, also referred to as entrained-phase or suspension-fired combustion. In this process the coal is ground to a fine powder and injected with a stream of air into the furnace chamber, where it ignites to form a fireball at temperatures that usually range between 1300 and 1700°C. Most of the ash from this process travels as suspended particles with the combustion gases, then collected by electrostatic precipitators (ESPs) or fabric filters as fly ash. Some ash, however, along with fragments detached from deposits that may form on the walls of the furnace, falls to the bottom of the combustion chamber and is removed as BA. Residence times for the particles, especially those that form the fly ash fraction, are relatively short, which may affect the extent to which interactions between the different phases occur.

**Coal Combustion Products (CCP's).** http://dx.doi.org/10.1016/B978-0-08-100945-1.00002-2

### 2.1.2 Stoker boilers

Coal may also be burned in stoker boilers, in which a relatively coarse-crushed (typically $<50$ mm) feedstock is burned in a stream of air that passes through a permeable bed of granular coal particles. Several different types of stoker systems are used, including underfeed, chain grate, and sprinkler systems. The ash remaining after combustion either falls to the bottom of the furnace or is forced over the edge of the combustion chamber as new coal is fed in to replace the burned material. Such furnaces are mainly used for relatively small industrial or institutional settings. The coal and its mineral matter in such systems are inherently exposed to heating for some time, which may cause some components to melt or fuse and result in clinker formation.

### 2.1.3 Fluidized bed combustion systems

Fluidized bed combustion (FBC), a system in which the fuel (e.g., coal) is fed into a solid bed, which has been fluidized by an upward movement of air, includes technologies such as atmospheric fluidized bed combustion, circulating fluidized bed combustion (CFBC), pressurized fluidized bed combustion, pressurized circulating fluidized bed combustion, and bubbling fluidized bed combustion. Such systems offer several advantages, including a simple construction and flexibility in use of fuel types, as well as high combustion efficiency at a significantly lower temperature (750–950°C) in comparison to other coal utilization technologies. Also, unlike other coal utilization technologies, ash recycling causes residence times in the combustor to be on the order of hours or even days. A major advantage is the ability to remove $SO_2$ using added limestone or dolomite in the bed material.

### 2.1.4 Coal gasification processes

Although there are a number of coal gasification technologies, Collot (2006) provides details of three different types with potential significance to modern industry: moving-bed or fixed-bed, fluidized-bed, and entrained-flow gasifiers. Only two are considered here: the fixed-bed Lurgi process and entrained-flow slagging gasification, as these represent two extremes of operating conditions. For example, temperatures in the Lurgi process are in the range 1100–1350°C and in slagging gasifiers as high as 1600°C (Matjie, Li, Ward, & French, 2008; Riley, French, Ward, Stephenson, & Gurba, 2014; Wagner, Coertzen, Matjie, & van Dyk, 2008). The ash products of fixed-bed gasifiers are mainly coarse-grained aggregates of coal ash and heated or fused rock particles with a range of crystalline and amorphous or glassy components (Hlatshwayo, Matjie, Li, & Ward, 2009; Matjie et al., 2008). In slagging gasifiers, however, most of the ash forms a molten material that is removed in liquid form. Although it is generally considered that the only ash product of a slagging gasifier is glass, Riley et al. (2014) indicate that the actual glass contents of entrained-flow gasifier ashes may range from as low as 74 to a maximum of 100 wt%.

## 2.2 Methods for CCP analysis

Applications specific to CCPs (Coal combustion products) are described below. These and other techniques are also described in a review paper by Vassilev and Vassileva (2005).

### 2.2.1 *Physical characterization techniques*

#### *2.2.1.1 Particle size distribution*

The determination of the particle size of fly ash has been a fundamental part of considerations of utilization size. Davis, Carlson, Kelly, and Davis (1937) used a 45-μm size (325 mesh) in the definition of pozzolanic activity. The simplest technique for determining particle size distribution is sieve analysis. Ashes may be sieved on nylon mesh sieves so as to avoid possible contamination from metal meshes; gentle brushing helps reduce the aggregation of the particles. This may provide data on size distribution down to about 20–30 μm. Sieving can be carried out with water (wet sieving) or in air (dry sieving); wet sieving, however, may remove some of the mobile major and trace elements from the ash, which may affect the interpretation of element partitioning with particle size for use in environmental studies.

Laboratory-scale, air-based cyclone separators can also be used to provide data on sizes down to 10–20 μm. This technique actually provides separation based on a combination of size and density (i.e., classification), and not on particle size alone. If density is constant, however, the separation is inherently based on particle size. Another instrument using classification principles is the air-based Bahco Aerodynamic Classifier, which is applicable to ash particles between 100 and 4 μm in size.

The most commonly used instrument for determining the particle size distribution of fly ash is the laser particle size analyzer, which is based on the diffraction of laser light by ash particles suspended in a variety of fluids, including air, water, ethanol, and propanol. The diffraction intensity pattern is dependent on the particle size. A mathematical deconvolution of the diffraction pattern is then used to determine the particle size distribution, assuming a spherical particle shape. The refractive index of the ash, which may vary with composition, should also be taken into account (Jewell & Rathbone, 2009).

Cascade impactors are inertial aerosol particle collection devices, widely used to investigate fine particulates in combustion streams (e.g., Buhre, Hinkley, Gupta, Nelson, & Wall, 2006). However, they typically cover the 20 μm to submicrometer range, thus they are less readily applicable to the main bulk of fly ash streams.

#### *2.2.1.2 Particle density and surface area*

The relative density of ash particles can be determined by measuring the displacement volume obtained using a Le Chatelier flask. The true density of the particles can be determined using helium pycnometry.

Surface area can be determined by measuring the absorption of either nitrogen or carbon dioxide by the fly ash sample. Nitrogen surface area determinations report the surface area due to mesopores and macropores, whereas the use of carbon dioxide enables the determination of surface area due to microporosity.

### 2.2.2 Chemical analysis techniques

The chemical analysis techniques used for coal ash are essentially the same as those used for the analysis of other geological materials, and as such are well established in the technical literature. X-ray fluorescence and inductively coupled plasma atomic emission spectrometry (ICP-AES) are commonly used for the major oxides. Trace elements are generally determined using ICP-AES and inductively coupled plasma mass spectrometry. However, some trace elements, specifically mercury and selenium, require special atomic absorption spectrometric techniques.

#### 2.2.2.1 X-ray diffraction

X-ray diffraction (XRD) is useful in the mineralogical characterization of fly ash, partly because the individual inorganic particles are usually too small to be reliably identified by optical microscopy or other techniques. However, glass, which is usually the most abundant component of coal ash, is amorphous or noncrystalline and therefore does not have regular arrays of atoms that produce definitive peaks in X-ray diffraction studies. Broad patterns or "humps" are typically seen in X-ray diffractograms of fly ashes and other CCPs (Fig. 2.1), derived from the amorphous or glassy material.

As with the mineral matter in coal, a quantitative assessment of the percentages of the different components in CCPs may be determined from X-ray diffractograms using the profile-refinement techniques originally developed by Rietveld (1969). The proportion of amorphous material in a CCP sample may be determined either by fitting an "observed" pattern to the glass diffraction "hump" or by spiking the sample with a known weight of another (crystalline) phase, following procedures outlined by Ward and French (2006) and Font et al. (2010).

X-ray diffraction may be combined with other methods to provide a better basis for characterization, including, for example, information on the association of elements with particular phases in the ash material. Rivera et al. (2015) used conventional and synchrotron-based XRD in conjunction with X-ray absorption spectroscopy and electron probe microanalysis, as well as electron microscopy (SEM).

#### 2.2.2.2 Unburnt carbon and loss on ignition

This is an important characteristic of fly ash used in concrete, as it is considered that unburnt carbon has a major influence on entrained air, both in terms of total air entrained and bubble size characteristics.

Loss on ignition (LOI) is considered to be a simplified measure of the unburnt carbon content of the fly ash sample and conveniently determined by measuring the weight loss of a sample on heating to a high temperature, usually 950°C. The total carbon content of an ash sample may also be determined more precisely, however, by elemental analysis techniques.

Not all weight loss associated with the heating of coal ashes in an LOI determination is necessarily due to carbon. As shown in Table 2.1 and Fig. 2.2, a reasonable correlation may exist between LOI and total carbon at low LOI levels, but significant discrepancies may be observed, probably due to breakdown of mineral phases in ashes with higher LOI values (Figs. 2.3–2.5).

**Table 2.1** **Loss on ignition and total carbon content (wt%) for some Australian fly ashes (French et al., 2007)**

| Power station | Moisture | LOI | Total carbon | Sulfur as $SO_3$ |
|---|---|---|---|---|
| NSW #1 | 0.15 | 0.76 | 0.52 | 0.09 |
| NSW #3 | 0.19 | 2.78 | 2.54 | 0.05 |
| NSW #5 | 0.11 | 1.36 | 1.33 | 0.05 |
| NSW #6 | 0.56 | 5.72 | 4.59 | 0.09 |
| QLD #11 | 0.33 | 3.87 | 3.51 | 0.12 |
| QLD #12 | 0.21 | 4.71 | 4.69 | 0.10 |
| WA #13 | 0.58 | 2.68 | 2.31 | 0.30 |
| WA #14 | 0.62 | 3.39 | 2.57 | 0.05 |
| WA #15 | 0.68 | 4.31 | 3.09 | 0.55 |

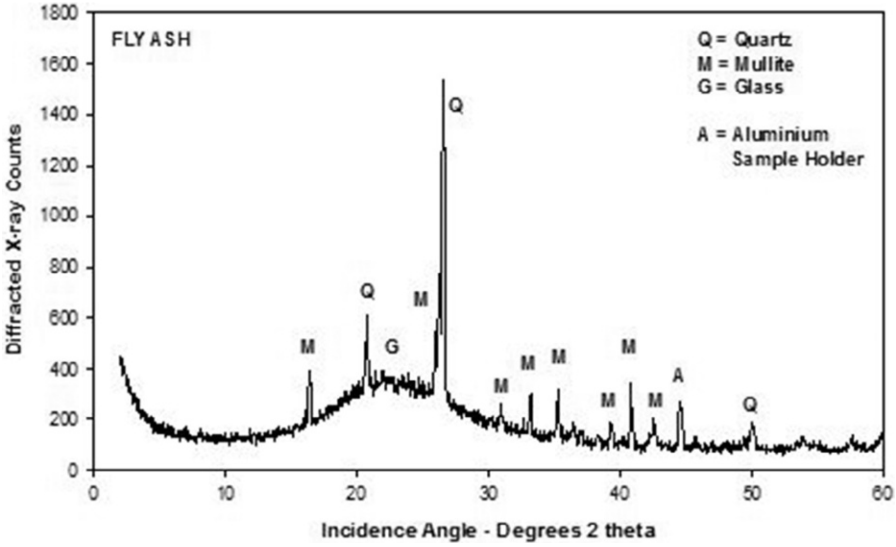

**Fig. 2.1** X-ray diffractogram of a fly ash sample, showing the peaks due to the different crystalline phases (*Q*, quartz; *M*, mullite) and the broad hump around 22 degrees 2-theta, representing the amorphous or glassy (G) component.

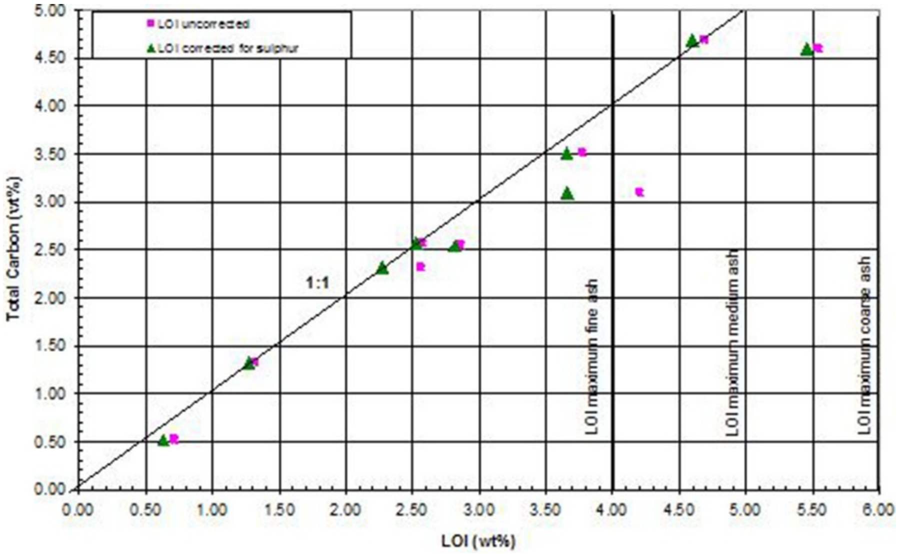

**Fig. 2.2** Plot of LOI at 750°C against total carbon for ashes in Table 2.2, showing greater differences and poorer correlations at high LOI values.
Courtesy of French, D., Smitham, J., Nelson, P. (2007). *A preliminary assessment of the variability of Australian fly ashes*. Research Report 65, Co-operative Research Centre for Coal in Sustainable Development, Brisbane, Australia, 52 p. http://pandora.nla.gov.au/pan/64389/20080828-1328/www.ccsd.biz/publications/757.html.

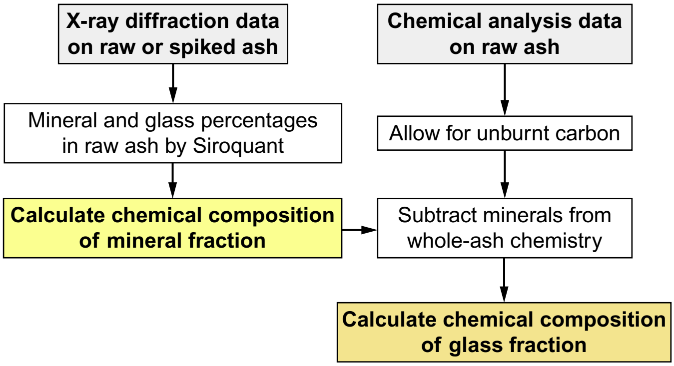

**Fig. 2.3** Estimation of the chemical composition of amorphous material (glassy component) in coal ash using quantitative XRD and chemical analysis data.
Courtesy of Ward, C.R., &French, D. (2006). Determination of glass content and estimation of glass composition in fly ash using quantitative X-ray diffractometry. *Fuel*, *85*, 2268–2277.

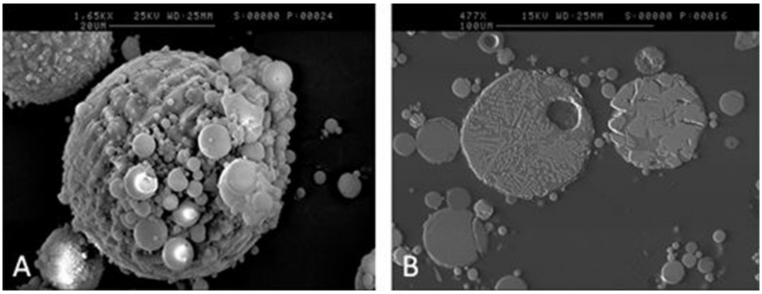

**Fig. 2.4** Scanning electron microscope (SEM) images of fly ash particles: (A) secondary electron image of mounted particles showing topographic characteristics; and (B) back-scattered electron image of particles in polished section showing bright and often dendritic iron oxide particles and darker aluminosilicate materials.
Courtesy of French, D., Riley, K., & Ward, C. R. (2014). Characterisation, classification and properties of coal combustion products. In C. R. Ward, C. Heidrich, O. Yeatman (Eds.), *Coal combustion products handbook* (2nd ed.) (pp. 35–99). Wollongong: Ash Development Association of Australia.

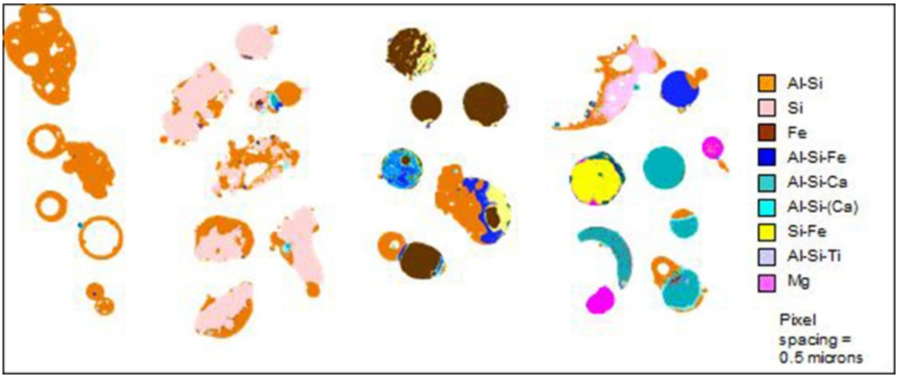

**Fig. 2.5** Fly ash particles analyzed by QemSCAN showing the distribution of inorganic phases (minerals and glassy components), defined by different elemental compositions within the individual particles.
Courtesy of French, D., Ward, C.R., & Butcher, A. (2008). *QemSCAN for characterisation of coal and coal utilisation by-products*. Research report 93 (103 p). Brisbane: Co-operative Research Centre for Coal in Sustainable Development. http://pandora.nla.gov.au/pan/64389/20080828-1328/www.ccsd.biz/publications/970.html.

The total carbon content of an ash may also only be an indicator of the proportion of unburnt organic carbon; it would also include any inorganic carbon that may be present as carbonates (Brown & Dykstra, 1995), although the proportion of such inorganic carbon in fly ash is usually low. As the LOI value is often used as a proxy for unburned carbon, the discrepancy between total carbon and LOI may be significant when assessing the suitability of a particular fly ash for use as a cementitious material. A high LOI value could lead, for example, to an ash being classed as unsuitable, even though the total or unburned carbon content might suggest otherwise.

#### 2.2.2.3 Other determinations

As with coal, the moisture content of an ash sample is determined by measuring the weight loss at 105°C.

The sulfuric anhydride content is determined gravimetrically, following precipitation as barium sulfate after the addition of a barium chloride solution to a concentrated hydrochloric acid digest of the sample.

Available alkali is determined by mixing a fly ash sample with calcium hydroxide and dissolving the resultant material in dilute hydrochloric acid. The sodium and potassium contents of the solution are determined instrumentally using flame photometry, atomic absorption spectroscopy, or inductively coupled plasma atomic emission spectroscopy.

Chloride ion content is determined by digesting the sample with nitric acid and determining the chloride content of the resultant solution by potentiometric titration with silver nitrate.

### 2.2.3 Optical petrology

The basic method for reflected-light, oil-immersion optical petrology of fly ash and BA differs from the procedures outlined for coal only in generally not needing blue-light excitation and in relying more comprehensively on polarized light. Dispersing a Sudan Black dye in the epoxy helps the optical contrast by dampening the subsurface reflections from bright fly ash particles. The basic nomenclature was outlined by Hower (2012), and the nature of the components is discussed later in this chapter.

## 2.3 Classification for standards

### 2.3.1 Basic fly ash classification for use as a cementitious component

Fly ashes may be classified under various schemes, depending in part on the purpose for which the ash might be marketed or used. In the most common standards, the ASTM C618 (ASTM, 2015) and EN450ash is classified into Type F (low lime) or C (high lime) using the criteria summarized in Table 2.2. Class F fly ash is pozzolanic and requires the addition of Portland cement or hydrated lime in order to produce cementitious compounds. Class C fly ash, is both pozzolanic and is hydraulic is form cementitious hydrates in the presence of water. While it is generally considered that Class F fly ash is derived from geologically older bituminous- and anthracite-rank coals and Class C fly ash is the product of younger, lower-rank coals, neither geologic age nor coal rank should be considered to be an absolute predictor of fly ash chemistry.

Table 2.2 **Chemical criteria for ASTM classification of fly ashes (ASTM, 2015)**

| Chemical requirements | Fly ash Class F | Fly ash Class C |
|---|---|---|
| Silicon dioxide, aluminum oxide, iron oxide ($SiO_2+Al_2O_3+Fe_2O_3$), min % | 70 | 50 |
| Sulfur trioxide ($SO_3$), max % | 5.0 | 5.0 |
| Moisture content, max % | 3.0 | 3.0 |
| Loss on ignition, max % | 6.0[a] | 6.0 |

[a] The use of Class F ash with up to 12% loss on ignition may be approved by the user if either acceptable performance records or laboratory tests results are made available.

The Canadian standard classification of fly ash, CSA A3001 (Thomas, Shehata, & Shashiprakash, 1999), is similar to ASTM C618 but uses three classes, namely F, CI, and CH, which are differentiated by their calcium oxide content. Class F has a low lime content (<8% CaO by mass), Class CI has medium lime (between 8% and 20% CaO by mass) and Class CH has high lime (more than 20% CaO by mass).

## *2.3.2 Carbon forms in fly ash*

As a simple statement of fact for a complex problem, carbon in fly ash is a consequence of the incomplete combustion of coal. Why carbon remains is a function of a number of factors including, but not limited to, the rank and maceral composition of the coal, poor grinding of the feed coal, the use of a coal not suited for the boiler, and combustion conditions, among other factors.

Pulverization plays a role in the control of the amount of carbon burnout, reflecting the efficiency of carbon combustion in the boiler, with increased carbon burnout being important both for increased boiler efficiency and for the potential use and value of the fly ash (Yu et al., 2005). A high proportion of >100 mesh (>150 μm) coal in a pulverized coal feed decreases the carbon burnout and negatively impacts the efficiency of $NO_x$ reduction (Maier, Spliethoff, Kicherer, Fingerle, & Hein, 1994). As an example of the effectiveness of pulverizers in reducing fly ash carbon, Hower, Robertson, et al. (1996) found in a plant burning Central Appalachian high volatile bituminous coal that maintenance of the pulverizers coincident with conversion to low-$NO_x$ combustion resulted in a decreased particle size and, consequently, reduced fly ash carbon. This was contrary to experience with other power plants (Barranco, Colechin, Cloke, Gibb, & Lester, 2006; Hower et al., 1997; Hower, Thomas, & Palmer, 1999), where the lower combustion temperatures in the low-$NO_x$ setting resulted in a reduced carbon burnout.

Rank plays a role in combustion, with low-rank, high-volatile coals being more ignitable. Conversely, the combustion of low-volatile coals, particularly anthracites, requires attention to engineering parameters in order to achieve and sustain combustion (Hough & Sanyal, 1987). Combustion temperatures are also rank dependent, as they rise with an increase in rank (Bengtsson, 1986; Crelling, Hippo, Woerner, & West, 1992).

The term "unburned coal" is often used but, in most cases, it is not an accurate reflection of the nature of the carbon in the fly ash. Bituminous coals in the caking coal range undergo rapid melting and devolatilization in the boiler. While vaguely recognizable forms of the original macerals are seen in some fly ashes (Fig. 2.6), fly ash carbons are not coal and, given the devolatilization, are not chemically representative of the original coal particle.

Carbons from lignites and subbituminous coals below the rank of caking coals will form a char. Instead of melting, there will be devolatilizing as the vitrinite structure is lost (Fig. 2.7; see Kostova, Hower, Mastalerz, & Vassilev, 2011). The combustion of anthracite, above the rank of caking coals, leads to some devolatilization and

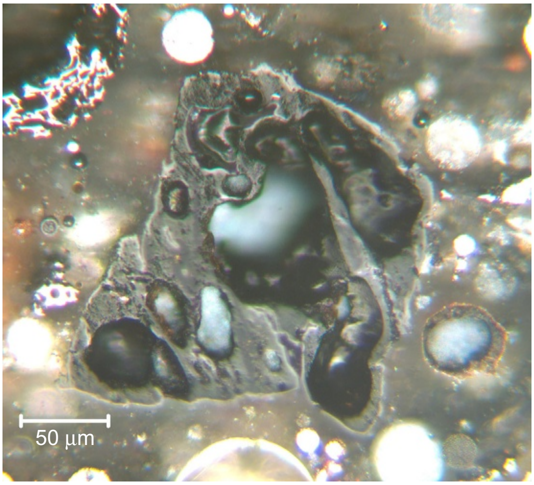

**Fig. 2.6** Unburned coal showing devolatilization vacuoles in melted vitrinite and a thin oxidation rim surrounding the particle. Class F fly ash. Image 93903 01.

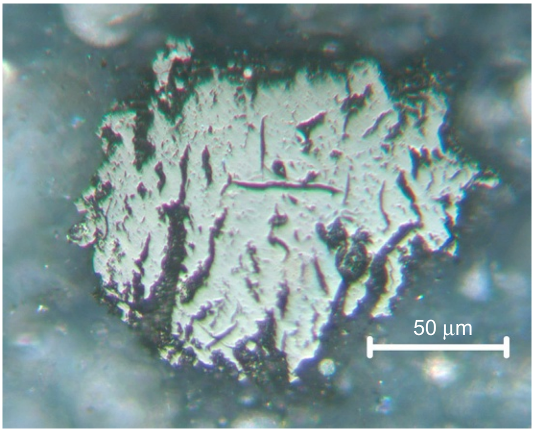

**Fig. 2.7** Char from the combustion of subbituminous coal. Class C fly ash. Image 93922 04.

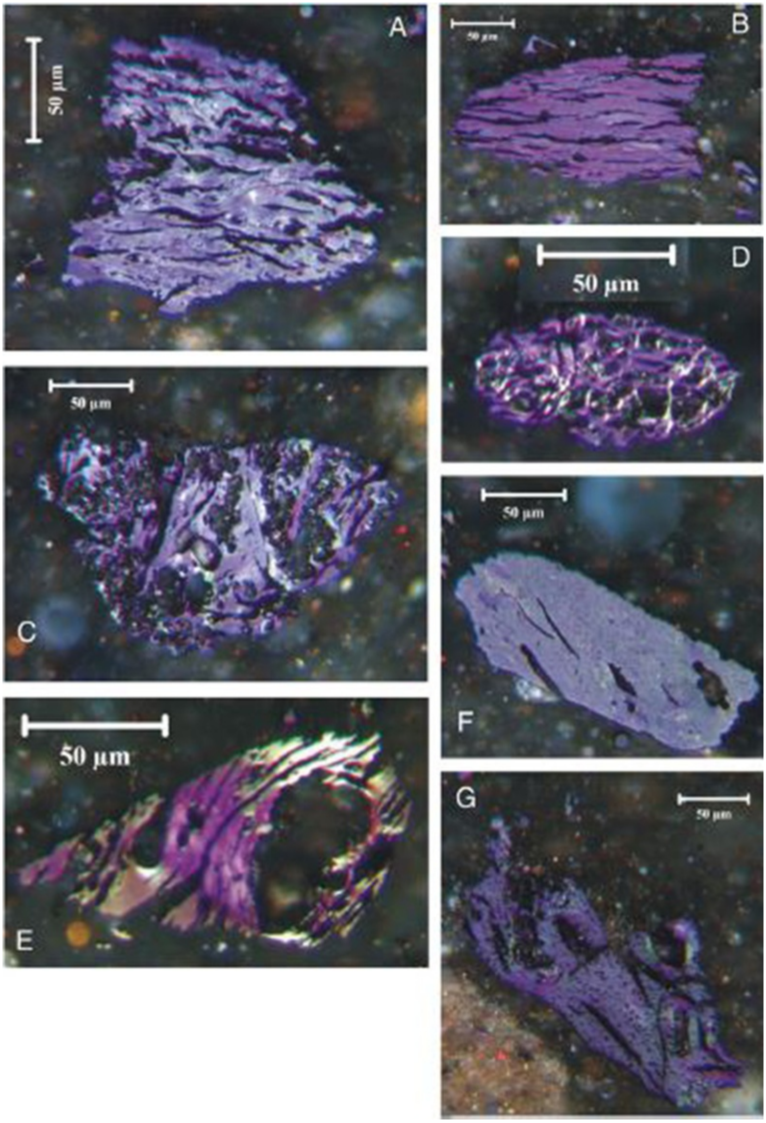

**Fig. 2.8** Selected petrology images; all reflected light, oil immersion. (A) Unburned coal showing thermally induced fractures and minor devolatilization of anisotropic vitrinite. Photo Yunnan 1 06; (B) unburned coal showing thermally induced fractures and minor devolatilization of anisotropic vitrinite. Photo Yunnan 1 08; (C) anisotropic coke. Photo Yunnan 1 09; (D) anisotropic coke. Photo Yunnan 2 01; (E) anisotropic coke. Photo Yunnan 2 03; (F) unburned coal showing devolatilization of anisotropic vitrinite. Photo Yunnan 2 02; and (G) unburned coal showing devolatilization of anisotropic vitrinite. Photo Yunnan 4 06.

thermally induced fracturing (Fig. 2.8; Silva et al., 2012). Within the bituminous-rank range and largely overlapping with caking coals, some of the vitrinite macerals are melted, devolatilized, and, ultimately, passed through the boiler to the ash-collection system (Fig. 2.9A, B, and E). The vitrinite-derived carbons can be classified as isotropic and anisotropic coke. While "coke" does have a distinct meaning in the metallurgical coke industry, it can be applied here due to the structural ties to the thermoplastic properties of the vitrinite. There appears to be a rank dependence, with isotropic coke being more common in fly ash carbons originating from high volatile C bituminous coals (Hower et al., 1995). Inertinite macerals (Fig. 2.9) generally pass through the boiler relatively intact, although indications of devolatilization and combustion can be found (Fig. 2.9C, F, and G).

Graphitic and fullerene and nanotube carbons have been found to be associated with coals from Eastern Kentucky and the Illinois Basin (Hower, Graham, Dozier, Tseng, & Khatri, 2008; Silva, DaBoit, Serra, Mardon, & Hower, 2010; Wilcox

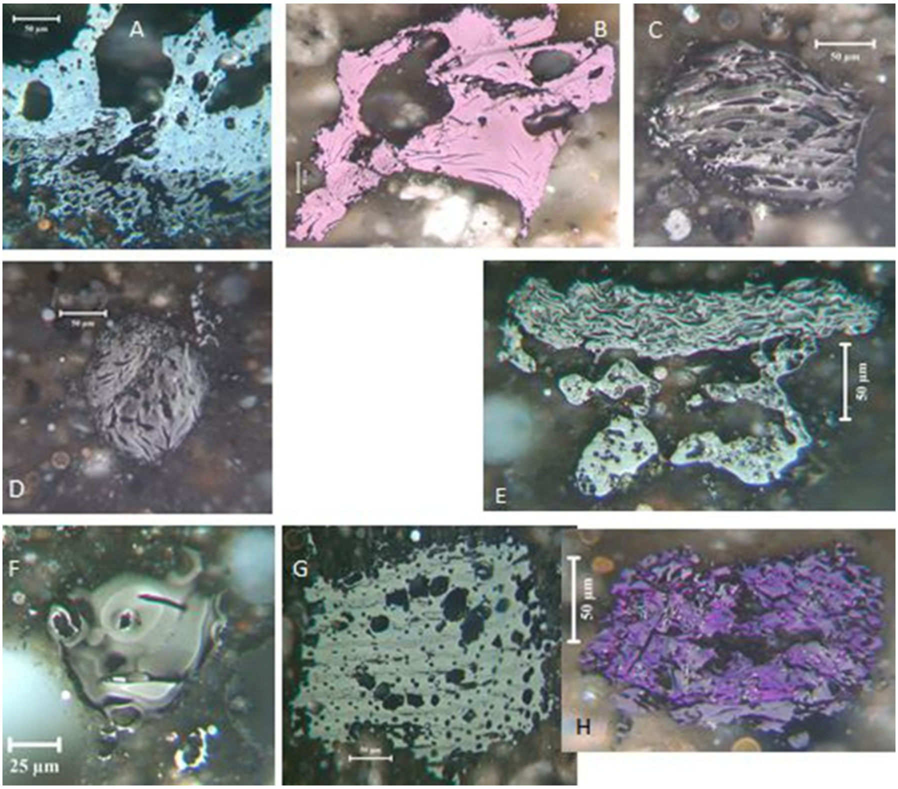

**Fig. 2.9** Carbon: (A) inertinite (bottom) and anisotropic coke (top). Class F fly ash. Image 93705 04; (B) char. Class F bottom ash. Image 93694 08; (C) char and inertinite. Class F fly ash. Image 93900 02; (D) char. Class F fly ash. Image 93901 02; (E) inertinite (top) and anisotropic coke (bottom). Class F fly ash. Image 93914 04; (F) inertinite. Class F fly ash. Image 93907 01; (G) inertinite. Class F fly ash. Image 93907 11; and (H) Inertinite. Class F fly ash. Image 93701 14.

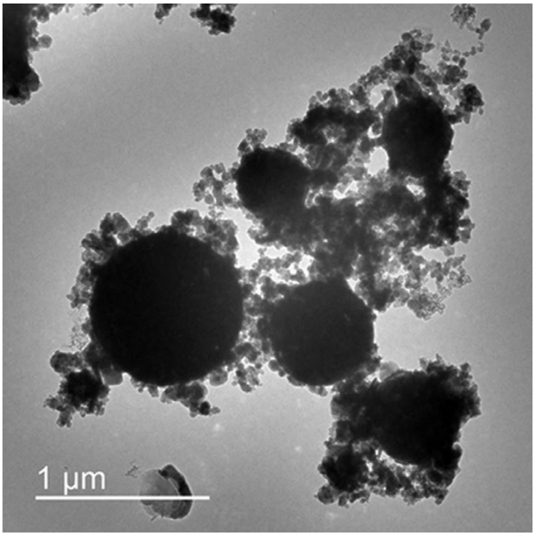

**Fig. 2.10** Transmission electron image of fine carbon surrounding spherical Al-Si-rich glassy fly ash particles. Class F fly ash. Image TEM 93644 (Wilcox et al., 2015).

et al., 2015). The fine carbons (Figs. 2.10 and 2.11), generally too fine to be resolved in optical microscopy, are loosely attached to the surface of the Al-Si glass and Fe-spinel particles in the fly ash assemblage. Nanoscale particles encased within the nanocarbons could be the site of Hg, As, Se, and other trace elements.

## 2.3.3 Inorganic forms in fly ash and BA

### 2.3.3.1 Basic chemistry-related ash properties

In most fly ashes and BAs, inorganic forms comprise the majority of the material. It is important to clearly delineate mineral reactions in the melting and cooling history of the fly ash and BA. Similar to carbons, certain inorganic phases may represent partial melting and/or recrystallization of the minerals, others may represent minerals that passed through the boiler without significant reaction, and still others may represent neoformed glass or mineral components (Creelman, Ward, Schumacher, & Juniper, 2013).

Some of the fundamental behaviors of oxides in coal combustion have been simplified to the proportions of the base and acid oxides (Vaninetti & Busch, 1982):

$$\mathrm{Base/acid} = (\mathrm{Fe_2O_3} + \mathrm{CaO} + \mathrm{MgO} + \mathrm{K_2O} + \mathrm{Na_2O})/(\mathrm{SiO_2} + \mathrm{Al_2O_3} + \mathrm{TiO_2})$$

For example, slagging, which is the buildup of molten ash on furnace walls, is a function of

$$\text{Slagging factor} = (\text{base/acid}) \cdot \left(S_{\mathrm{dry}}\right) [\text{for eastern US bituminous coals}]$$

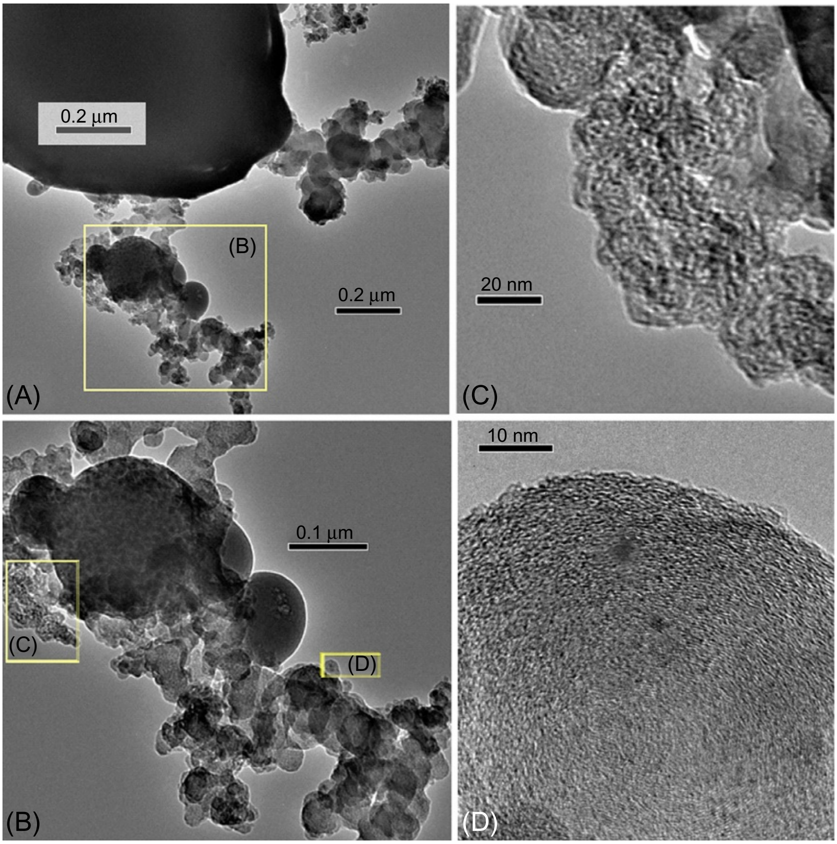

**Fig. 2.11** HRTEM images of C-rich nanoclusters. Large, dark, round bodies in (A) and (B) and at extreme upper right of (C) are Si-Al glass fly ash particles. Few-nm dark spots in (D) are metal grains (Hower et al., 2008).

The slagging tendency increases with a rise in the slagging factor (SF), with $\mathrm{SF} < 0.6$ indicating a low slagging tendency and $\mathrm{SF} > 2.6$ indicating a severe slagging tendency.

Fouling, which is the buildup of ash deposits in the convection pass at a rate faster than a soot blower can remove, is defined as

$$\text{Fouling factor}(R_f) = (\text{base}/\text{acid})/\mathrm{Na_2O}[\text{for eastern US bituminous coals}]$$

$R_f < 0.2$ indicates a low fouling tendency, and $R_f > 1.0$ indicates a severe fouling tendency.

### 2.3.3.2 Rock fragments and quartz

The behavior of the common coal minerals in combustion and gasification is summarized in Table 2.3 (after Mraw et al., 1983). Querol, Fernandez Turiel, and Lopez Soler (1994) discussed the mineral transformations in a Spanish subbituminous coal (see Table 2.3 for the balanced equations).

**Table 2.3** **Generalized scheme of behavior of coal minerals during combustion and gasification**

| Mineral matter | Combustion | Gasification |
|---|---|---|
| Ca, Na, etc., in carboxylates | Mostly to sulfates; can also react with $SiO_2$, etc. to form silicates | Oxides (?), sulfides (?) |
| Pyrite | Oxidation to hematite ($Fe_2O_3$) or magnetite ($Fe_3O_4$); reaction with silicates | Reduction to pyrrhotite |
| Carbonates | Dissociation to oxides; reaction with silicates | Dissociation to oxides; reaction with silicates |
| Clays | Dehydration and sintering; possible mullite; reactions of products with $Fe_2O_3$ from pyrite, CaO from carbonates, $SiO_2$, etc. | Same as combustion, but $FeS_2 \rightarrow FeS$, not oxide; does not react with oxides |
| Quartz | Relict; reaction with aluminosilicates from clays, with CaO and $Fe_2O_3$ to form crystalline and molten silicate phases | Similar to combustion, but with less melting |

(After Mraw, S. C., De Neufville, J. P., Freund, H., Baset, A., Gorbaty, M. L., & Wright, F. J. The science of mineral matter in coal. In *Coal science*, **Vol. 2**, 1983, Academic Press; Cambridge, MA, 1–63.)

Partially vitrified rock fragments (Fig. 2.12) represent incomplete combustion, most likely fragments of carbonaceous shale. In some cases, coked carbons are seen within the less melted portion of the particle, indicating that the heating was sufficient to devolatilize the carbonaceous shale but not capable of thoroughly vitrifying the entire grain. Sulfides, probably as pyrrhotite, have been observed in partially melted fly ash and BA particles.

Quartz (Fig. 2.13) is the most common and recognizable mineral to pass through from the coal to the ashes.

### *2.3.3.3 Fe-bearing minerals*

Iron-bearing minerals may react to form discrete iron oxide particles, but Fe in other forms (e.g., nonmineral inorganic material) may interact with aluminosilicate residues and represent a potential source of slagging. Pyrite decomposition in the combustion flame is rapid: 400 ms for 53- to 63-μm pyrite and 575 ms for 75- to 90-μm pyrite (Srinivasachar, Helble, & Boni, 1990). As noted in Table 2.4, the initial transformation of pyrite (py) is to pyrrhotite (po). Srinivasachar, Helble, and Boni (1990) found a sharp interface between inner py cores and the po rim of Fe-sulfides in ashes. At 1500 K and an $S/(S\text{-}Fe) < 0.1$ or 1400 K and $S/(S\text{-}Fe) < 0.17$, magnetite should crystallize from the melt. The conversion of magnetite to hematite is slow and kinetically limited, requiring more time in the hot zone of the furnace. Magnetite is the stable oxide in fresh fly ash (Patil, Eaton, & Tittlebaum, 1984). In contrast to the free pyrite

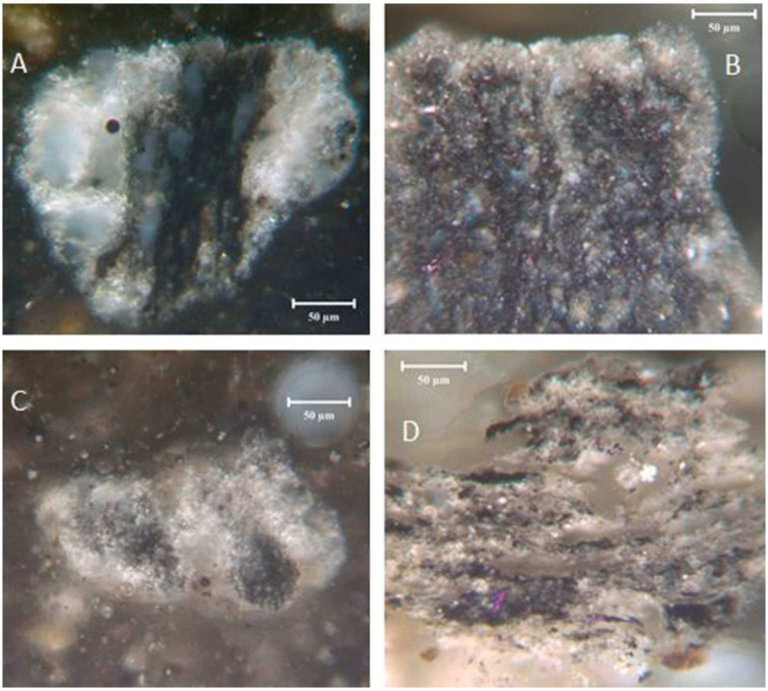

**Fig. 2.12** Rock fragments: (A) partially melted rock through center of particle flanked by glass. Class F fly ash. Image 93670 03; (B) glass on rim around less vitrified core. Class F bottom ash. Image 93686 06; (C) small fragments of partially melted rock surrounded by glass. Class F fly ash. Image 93884 02; and (D) Small fragments of partially melted rock surrounded by glass. Class F bottom ash. Image 93690 04.

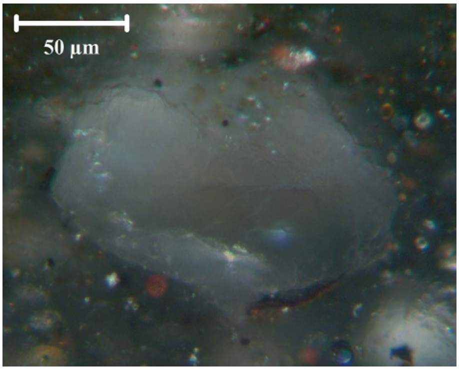

**Fig. 2.13** Quartz grain. Class F fly ash. Image 93809 01.

Table 2.4 **Quantitative X-ray diffraction data for selected Australian fly ashes (French et al., 2014)**

| | New South Wales | | | | | Queensland | | | Western Australia | | | | |
|---|---|---|---|---|---|---|---|---|---|---|---|---|---|
| | Station no. | | | | | | | | | | | | |
| **Mineral** | **1** | **2** | **3** | **12** | **13** | **5** | **7** | **14** | **8** | **9** | **10** | **15** | **South Australia** |
| Quartz | 4.9 | 11.2 | 9.7 | 5.2 | 5.3 | 7.2 | 10.0 | 2.3 | 18.1 | 25.1 | 26.3 | 17.8 | 31.9 |
| Mullite | 8.5 | 16.0 | 10.2 | 8.9 | 18.5 | 7.2 | 21.3 | 8.9 | 18.5 | 15.2 | 20.3 | 8.8 | 15.6 |
| Cristobalite | 0.0 | | 0.1 | 0.1 | 0.0 | | 0.0 | 0.0 | 0.0 | 0.1 | 0.1 | | |
| Spinel | | 0.2 | | | | | 0.5 | | | | | | |
| Magnetite | 0.0 | 0.2 | 0.7 | 0.0 | 0.3 | 1.1 | 0.0 | 1.9 | 0.6 | 1.5 | 0.6 | 7.7 | |
| Maghemite | 0.1 | | 0.8 | 0.4 | 1.1 | 1.0 | 0.4 | 1.3 | 1.1 | 1.8 | 0.4 | | |
| Hematite | 0.0 | 0.4 | 0.4 | 0.0 | 0.0 | 0.7 | 0.0 | 0.5 | 0.7 | 1.3 | 2.2 | 4.1 | 0.6 |
| Calcite | | | | | | 0.3 | | | | | | | |
| Amorphous | 86.4 | 72.0 | 78.1 | 85.4 | 74.8 | 82.2 | 68.2 | 85.0 | 61.0 | 55.1 | 50.2 | 61.6 | 49.2 |

grains, pyrite within clay bands tends to coalesce with the clay and silica minerals to form Fe-K-Al-Si glass (Abbott & Austin, 1985; Huffman, Huggins, Shah, & Shah, 1990; Srinivasachar, Helble, & Boni, 1990; Srinivasachar, Helble, Boni, et al., 1990).

In our petrographic nomenclature, we use the term "spinel" as a broad category of minerals, including magnetite. Many of the minerals in the spinel family have defect structures and include a number of elements such as Al, Mg, Ni, Cr, among others. The iron in the secondary minerals comes from the decomposition of Fe-sulfides and other Fe-bearing minerals in the coal. The spinel minerals can form delicate dendrites in a glass matrix (Fig. 2.14A), coarser dendritic assemblages in glass (Fig. 2.14B and C),

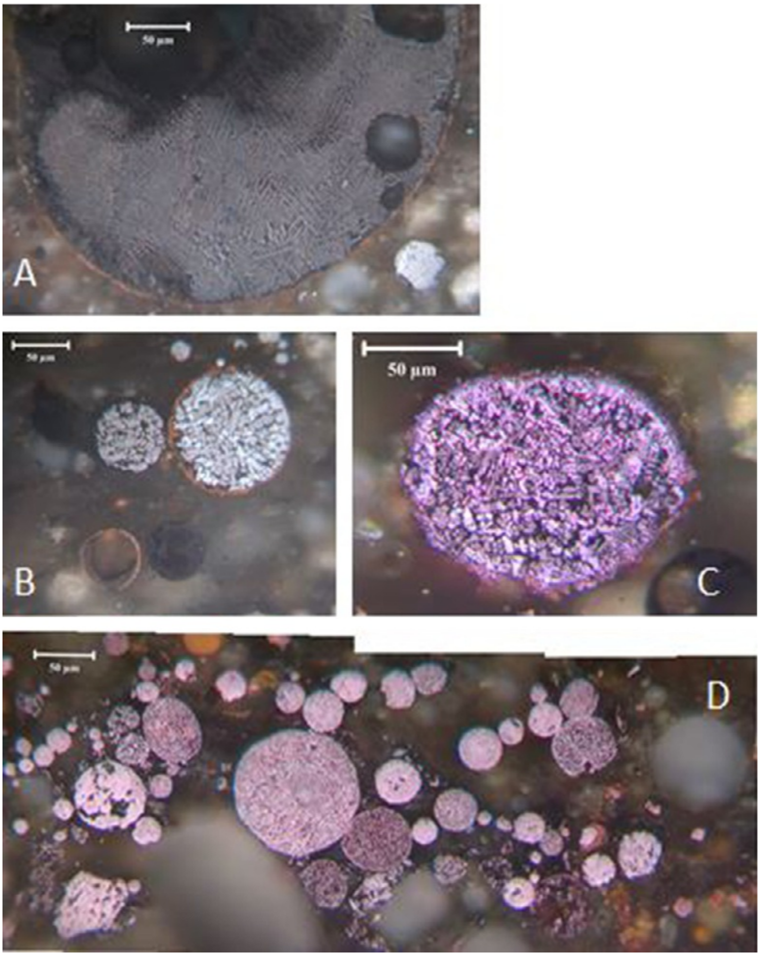

**Fig. 2.14** Spinel: (A) fine spinel in glass matrix. Class F fly ash. Image 93891 07; (B) four spinel-glass aggregates of 40-μm or more diameter, including hollow sphere (lower left quadrant). Note the red oxidation rim on the largest particle (upper right quadrant). Class F fly ash. Image 93898 01; (C) spinel in glass. Class F fly ash. Image 93696 13; and (D) multiple spinel and spinel-glass grains in a glass matrix in Class F bottom ash. Image 93662 01.

or solid or nearly solid grains (e.g., some of the grains in Fig. 2.14D). Oxidation rims can be seen around the edges of many of the rounded particles (Fig. 2.14A, B, and possibly C).

### 2.3.3.4 High-temperature silicates

Mullite, anorthite, and other Al-Si minerals (Fig. 2.15) may be formed by solid-state reactions (French et al., 2001) or may crystallize from the melt. The mineral phase depends upon the temperature attained and the rapidity of cooling, with the BA tending to cool more slowly, as well as the chemical composition of the material and the potential for interaction between the phases involved. For example, within the $CaO-Al_2O_3-SiO_2$ field, the crystallization of mullite versus anorthite depends upon the balance between $Al_2O_3$ and CaO (Fig. 2.16) (Alekseev & Vereshchagin, 1997; Ehlers, 1972; Osborn & Muan, 1960). The $CaO-SiO_2-Al_2O_3$ system has several eutectics in the 1200–1300°C range. In a study of fly ash and BA from Indian coals, Tazaki, Fyfe, Sahu, and Powell

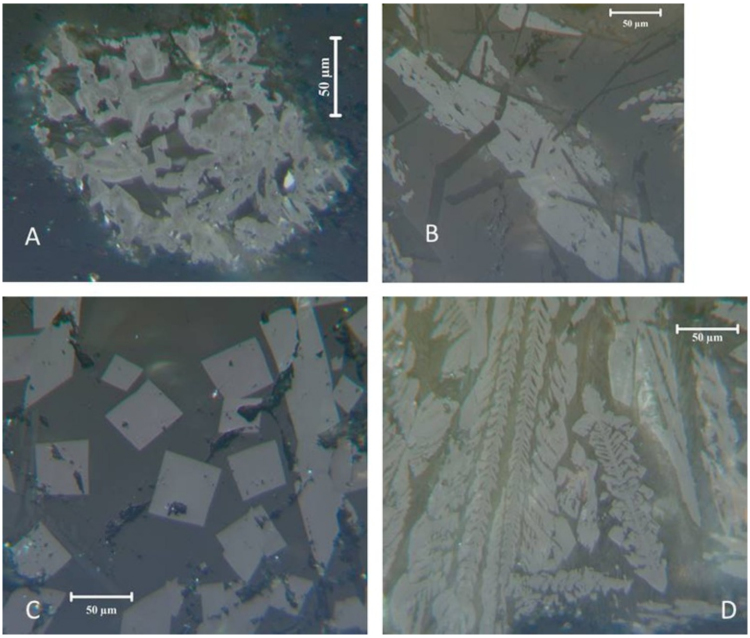

**Fig. 2.15** Mullite and other neoformed minerals: (A) neoformed crystals in glass. Class C bottom ash. Image 93972 06; (B) neoformed crystals in glass. Class C bottom ash. Image 93972 07; (C) neoformed crystals in glass. Class C bottom ash. Image 93972 09; and (D) neoformed crystals in glass. Class C bottom ash. Image 93972 11.

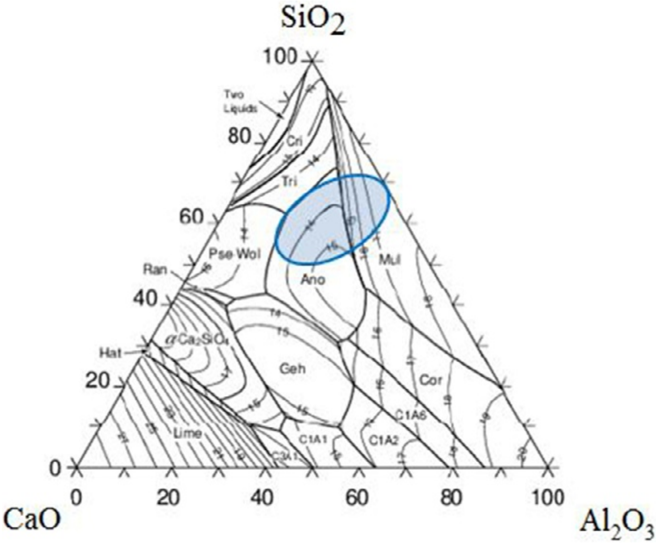

**Fig. 2.16** Range of normalized $SiO_2$-$Al_2O_3$-CaO compositions (*blue oval*) for Central Appalachian, Illinois Basin, and Powder River Basin coal-derived bottom ashes from the University of Kentucky Center for Applied Energy Research (CAER) collection. Crystallization of solid phases from melts in this range would be to mullite on the right side of the mullite-anorthite liquidus and to anorthite or the left side of the liquidus. The chemical compositions are based on the whole-ash analysis. *Ano*, anorthite; C1A1, $CaO{\cdot}Al_2O_3$; C1A2, $CaO{\cdot}2Al_2O_3$; C1A6, $CaO{\cdot}6Al_2O_3$; C3A1, $3CaO{\cdot}Al_2O_3$; *Cor*, corundum; *Cri*, cristobalite; *Geh*, gehlenite; *Hat*, hatrurite; *Mul*, mullite; *Pse-Wol*, pseudowollastonite; *Ran*, rankinite; *Tri*, tridymite.

(1989) found agglomerates of sillimanite and mullite polymorphs, spheroidal nonopaque forms with an opaque nucleus, wüstite, ilmenite, and glass.

### 2.3.3.5 Glass and included minerals

Glass is usually the most abundant constituent in fly ash and BA (Fig. 2.17). Quantitative X-ray diffraction studies (e.g., Font et al., 2010; Valentim, Guerdes, Flores, Ward, & Hower, 2009; Ward & French, 2006), as well as petrographic examinations (e.g., Hower, Robl, et al., 1996; Mardon & Hower, 2004), indicate that amorphous aluminosilicate glass is the dominant phase in nearly all fly ashes from pf combustion systems. Quartz and mullite are usually the dominant crystalline phases in Class F fly ashes, while the Fe oxides (i.e., hematite, maghemite, and magnetite) are usually minor components. Lime, gehlenite, and anorthite are the crystalline phases in Class C fly ashes. Spinel, cristobalite, and calcite are rare or trace phases also found in some ashes.

Fly ashes from Western Australian power stations were found to be distinctive in containing relatively abundant Fe oxide phases, higher quartz, and lower glass contents (Table 2.4) (French, Riley, & Ward, 2014). Two of the Queensland ashes in

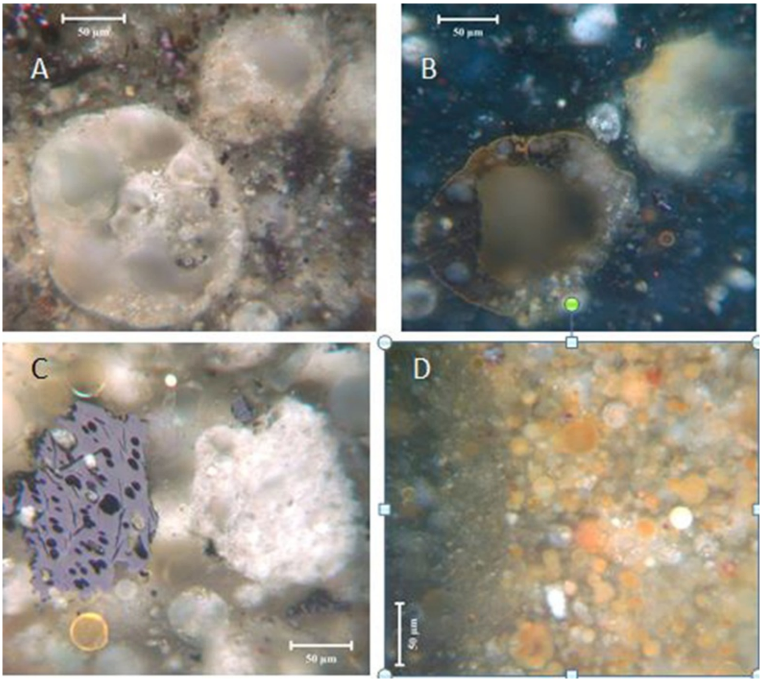

**Fig. 2.17** Glass: (A) glass pleiospheres. Class F bottom ash portion of comingled bottom ash/pulverizer rejects waste stream. Image 93685 06; (B) glass cenospheres. Class F fly ash from dry FGD material. Image 93866 04; (C) inertinite (left) and glass. Class F fly ash. Image 93701 13; and (D) agglomerated glass spheres with other ash forms (very bright spinel on right center). Class C fly ash. Image 93811 03.

Table 2.4 (5 and 14) also have relatively high Fe oxide contents, similar to those of the Western Australian samples; the remaining Queensland ash (7) is similar to New South Wales fly ashes. The ash from South Australia contains a higher proportion of crystalline quartz and a lower proportion of amorphous material than those of the other stations listed. As discussed later in this chapter, these variations mainly reflect differences in the rank of the feed coals. The ashes from Western Australia, South Australia, and two of the Queensland power stations were derived from lower-rank coals, and the remaining ashes were derived from high volatile bituminous materials.

Based on XRD analysis, Moreno et al. (2005) noted a considerable variability in the mineralogy of European fly ashes. While amorphous aluminosilicate glass was still the dominant phase, it varied in abundance from 48 to 86 wt%. Quartz and mullite contents ranged from 1.7 to 12.5 wt% and from <0.3 to 40.4 wt%, respectively. Calcite was found in two of the ashes, and lime and anhydrite were found in several of the ashes, with contents varying from <0.3 to 5.8 wt% and from <0.3 to 15.0 wt%, respectively. While hematite was found to be relatively uncommon, magnetite was present in all of the ashes, reaching a maximum of 3.8 wt%. Feldspar was sometimes present as a minor phase, and ettringite was found in one ash sample. Unfortunately, Moreno et al. (2005) did not discuss the possible causes of the observed variation. Ural (2005) found very low glass contents and abundant Ca-bearing phases in Turkish fly ashes, but the results are not directly comparable to bituminous coal ashes as the feed coal was a high-Ca lignite. Font et al. (2010) also show a range of mineralogical characteristics for European fly ashes, including ashes from coals cofired with biomass, depending on the temperature of combustion, the type of fuel (coal rank and nature of any cofired biomass), and the combustion technology employed. Amorphous material (glass) was found to be less abundant in ashes from FBC (57%–82%) than from pulverized-coal plants (80%–97%), mainly due to the lower temperatures involved. Similarly, while mullite (up to 16%) and quartz (up to 5%) were the principal crystalline phases in pulverized coal ashes, quartz (9%–26%), illite (up to 8%), K-feldspar (up to 2%) and anorthite (up to 2.6%), along with minor calcite and anhydrite, were the main components of ashes derived from FBC processes.

### 2.3.3.6 Nonfuel components

Extraneous, nonfuel objects can show up in fly ash and BA. Fig. 2.18 shows a piece of metal with exsolution structures, not expected for something forming from the coal minerals in the boiler. Such material can come from abraded parts of the steam tubes in the boiler, from the pulverizer, or from other places along the path of the coal or the flue gas with its entrained fly ash.

### 2.3.3.7 Mineralogical variation within ash-collection systems

As well as variations in bulk properties between power stations, significant variations in mineralogy may exist among the fly ashes collected from different zones of individual ESP systems, depending in part on particle size and density characteristics. Table 2.5, for example, shows the variations in mineralogy for fly ashes across the ESP zones of two Queensland power stations, and the BA and fly ash from different ESP zones for a South Australian power station (French et al., 2014; Narukawa,

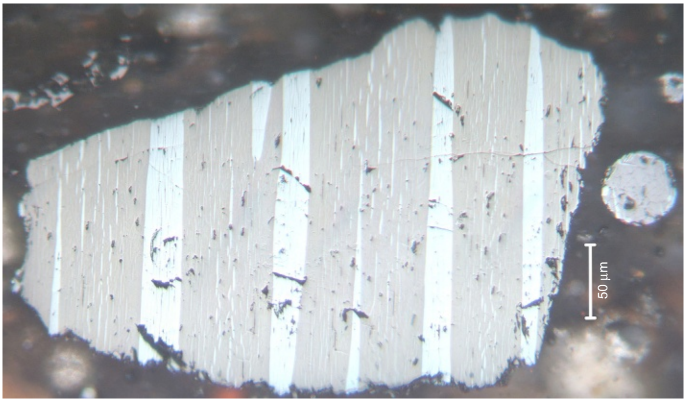

**Fig. 2.18** Metal. Exsolution of metal phases. Class F fly ash. Image 93898 03.

Table 2.5 **Quantitative X-ray diffraction mineralogy across the electrostatic precipitator zones of two Queensland power stations (A and B) and one South Australian power station (Station X) (French et al., 2014)**

| **Mineral** | **Station A** | | | | | |
|---|---|---|---|---|---|---|
| **ESP zone** | **Z1A** | **Z1B** | **Z2** | **Z3** | **Z4** | **Z5** |
| Quartz | 4.7 | 5.4 | 2.1 | 1.1 | 0.9 | 0.8 |
| Mullite | 17.4 | 17.9 | 11.2 | 9.5 | 9.1 | 9.3 |
| Hematite | 1.0 | 0.9 | 0.9 | 0.9 | 0.8 | 0.8 |
| Maghemite | 1.6 | 1.4 | 1.3 | 1.7 | 1.3 | 1.8 |
| Magnetite | 3.1 | 3.6 | 3.1 | 2.3 | 3.0 | 2.0 |
| Amorphous | 72.2 | 70.7 | 81.3 | 84.5 | 85.0 | 85.3 |

| **Mineral** | **Station B** | | | | | |
|---|---|---|---|---|---|---|
| **ESP zone** | **Z1** | **Z2** | **Z3** | **Z4** | **Z5** | **Z6** |
| Quartz | 9.6 | 11.9 | 12.0 | 11.5 | 12.0 | 11.6 |
| Mullite | 12.0 | 9.0 | 9.8 | 9.7 | 9.1 | 10.1 |
| Hematite | nd | nd | nd | nd | nd | nd |
| Maghemite | nd | nd | nd | nd | nd | nd |
| Magnetite | nd | nd | nd | nd | nd | nd |
| Amorphous | 78.5 | 79.1 | 78.3 | 78.9 | 78.9 | 78.3 |

| **Mineral** | **Station X** | | | |
|---|---|---|---|---|
| **ESP zone** | **BA** | **Z1** | **Z2** | **Z3** |
| Quartz | 34.1 | 36.2 | 17.1 | 10.7 |
| Mullite | 14.6 | 18.2 | 6.0 | 6.3 |
| Rutile | 1.0 | 1.4 | 0.9 | 0.8 |
| Hematite | 2.3 | 0.5 | 0.7 | 0.9 |
| Anhydrite | 0 | 1.1 | 2.2 | 2.8 |
| Gehlenite | 0 | 0 | 0 | 4.5 |
| Albite | 8.3 | 0 | 0 | 0 |
| Spinel | 1.4 | 0 | 0 | 0 |
| Halite | 1.9 | 0 | 0 | 0 |
| Amorphous | 36.4 | 42.6 | 73.1 | 74.0 |

nd, not detected.

Riley, & French, 2003). Quartz and mullite, in association with amorphous aluminosilicate glass, are the dominant crystalline phases present in the ashes from all three stations. Iron-rich phases, such as hematite, maghemite, and magnetite, are also present in the ashes from one of the Queensland stations (Station A) and to a lesser extent from the South Australian station (Station X).

Both quartz and mullite contents decrease across the ESP rows in the ashes from Stations A and X, with quartz decreasing at a faster rate than mullite. This is probably a function of decreasing particle size. Iron oxide (hematite, maghemite, magnetite) contents tend to remain relatively constant across the precipitator zones for these stations, and amorphous (glass) contents increase with decreasing particle size. The proportion of anhydrite ($CaSO_4$) in the fly ashes of Station X also increases across the precipitator zones. These results suggest that quartz and mullite may be more abundant in the relatively coarse particles of the ash stream, whereas the iron oxides are uniformly distributed across the particle size range. Albite (Na-feldspar) is also present in the BA of Station X, possibly reflecting the high-temperature mineral transformations (cf. French et al., 2001) in that part of the furnace system.

By contrast, mullite initially decreases and then remains relatively constant in the Station B samples, whereas the quartz contents initially increase. The glass content remains constant across the zones for these ashes. The limited mineralogical variation in the ash from Station B suggests that the phases are uniformly distributed across the particle size range, an observation which, in the case of quartz, is supported by SEM examination.

X-ray diffraction studies by Valentim et al. (2009) also showed amorphous material (glass) to be the dominant constituent in fly ash from a Portuguese power plant (64.7%–78.2%), together with mullite (11%–20%), quartz (4%–9%), and iron oxide minerals (3%–5%). Small proportions of calcite, anhydrite, and gypsum were also found in some of the fly ash samples. As with the Australian examples, the proportions of quartz, mullite, and Fe oxides were higher in ash from precipitator zones that collected the coarser ash particles, and glass (and anhydrite/gypsum) was most abundant in the ash of the zones collecting finer-sized material. Ribiero, Valentim, Ward, and Flores (2011) indicate similar mineralogy for fly ashes derived from combustion of Portuguese anthracites, with 14%–19% mullite, 15%–18% quartz, and 60%–70% amorphous material.

### 2.3.3.8 Relation of fly ash mineralogy to coal characteristics

Ward and French (2006) have investigated the relationships between the mineralogy of Australian feed coals (as determined by quantitative XRD of the mineral matter) and that of the resultant fly ash. As shown in Fig. 2.19, the quartz contents of the fly ash and the low-temperature ash of the feed coal show a strong positive correlation, with two exceptions. The quartz content of the fly ash is generally a little lower than that of the corresponding coal mineral matter, which is probably due to the reaction of fine-grained quartz during combustion. The two aberrant points may also possibly be explained by that reaction mechanism if the quartz in the coal is present mainly as fine-grained material.

Fig. 2.19 also shows a similar but less pronounced positive correlation between the iron-bearing minerals in the fly ash and siderite and pyrite contents (the two dominant iron-bearing minerals) in the corresponding coal mineral matter. One reason for the greater variability may be the presence of other Fe-bearing minerals, such as Fe-rich chlorite, illite, or ankerite. The two aberrant points in the plot are of samples from relatively low-rank (subbituminous) coals, in which the Fe may be present in other minerals as described above, as amorphous phases, or in an organic association.

Ward and French (2006) also showed that the glass composition of a fly ash sample could be estimated if the quantitative mineralogy (by XRD) and bulk chemistry of

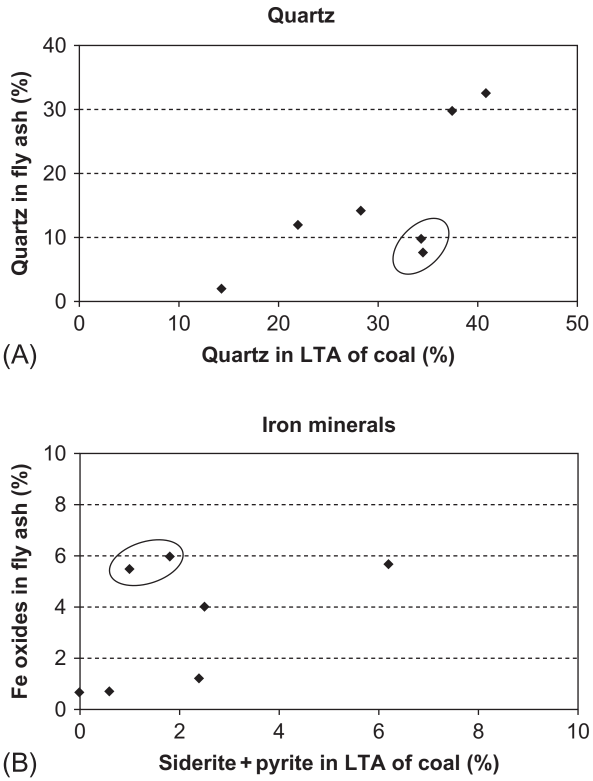

**Fig. 2.19** Relations between (A) quartz contents and (B) iron-bearing minerals in Australian fly ashes and the low-temperature ash of the corresponding feed coal as determined by quantitative X-ray diffraction (Ward & French, 2006); data points circled are discussed in the text.

the ash are known. Based on this approach, Table 2.6 shows that the inferred glass composition of Australian fly ashes can be divided into two groups. The ashes of Group A are derived from subbituminous coals and characterized by glass with a relatively low (inferred) percentage of silica (45%–60%) and a high (generally $>10.0\%$) proportion of $Fe_2O_3$; ashes of Group B are derived from bituminous coals, have glass with high (inferred) silica (60%–70%) and low Fe contents ($<5.3\%$ $Fe_2O_3$).

Hower, Robl, et al. (1996) noted a positive correlation between the intensity of the X-ray diffraction peaks of magnetite and hematite in the ash and the sulfur content of the feed coal, although no quantitative mineralogical data were provided for the ash. Mastalerz, Hower, Drobniak, Mardon, and Lis (2004) found spinel to be higher in ash derived from high sulfur coal, which was considered to reflect the higher pyrite content of the feed coal in question. A similar trend was observed by Hower, Trimble, Eble, Palmer, and Kolker (1999): based on optical microscopy, spinel contents were higher in fly ash produced from combustion of a high-sulfur coal than in ash from a low-sulfur coal. Mullite contents were also higher and glass contents lower in the ash produced from the high-sulfur coal.

Table 2.6 **Chemical composition of Australian fly ash samples, together with inferred composition of mineral and glass fractions (Ward & French, 2006)**

**Whole ash chemistry**

| Property | Station no. | | | | | | | | |
|---|---|---|---|---|---|---|---|---|---|
| | **15** | **19** | **18** | **16** | **20** | **17** | **21** | **22** | **23** |
| $SiO_2$ | 56.8 | 57.0 | 58.3 | 44.5 | 62.9 | 67.0 | 61.5 | 57.5 | 65.9 |
| $Al_2O_3$ | 26.3 | 25.0 | 22.2 | 30.7 | 29.3 | 24.8 | 22.4 | 28.2 | 27.6 |
| $Fe_2O_3$ | 9.5 | 9.9 | 13.6 | 14.4 | 1.8 | 3.1 | 7.6 | 5.6 | 1.1 |
| CaO | 1.4 | 1.5 | 1.3 | 4.2 | 1.3 | 1.0 | 3.3 | 3.8 | 0.4 |
| BaO | 0.4 | 0.5 | 0.4 | 0.1 | 0.1 | 0.0 | 0.1 | 0.1 | 0.0 |
| MgO | 0.8 | 0.7 | 0.8 | 1.6 | 1.1 | 0.6 | 1.1 | 1.2 | 0.3 |
| $Na_2O$ | 0.2 | 0.2 | 0.2 | 0.4 | 0.8 | 0.6 | 0.9 | 0.2 | 0.2 |
| $K_2O$ | 0.7 | 0.5 | 0.4 | 0.9 | 0.5 | 1.6 | 1.9 | 1.1 | 2.9 |
| $TiO_2$ | 1.7 | 1.5 | 1.7 | 1.9 | 1.8 | 1.0 | 0.9 | 1.6 | 1.3 |
| $P_2O_5$ | 1.9 | 2.7 | 1.0 | 1.0 | 0.1 | 0.2 | 0.2 | 0.5 | 0.2 |
| $SO_3$ | 0.3 | 0.5 | 0.1 | 0.3 | 0.2 | 0.1 | 0.1 | 0.2 | 0.1 |
| Total | 100.0 | 100.0 | 100.0 | 100.0 | 100.0 | 100.0 | 100.0 | 100.0 | 100.0 |

**Inferred chemistry—minerals**

| Property | Station no. | | | | | | | | |
|---|---|---|---|---|---|---|---|---|---|
| | **Group A** | | | | **Group B** | | | | |
| | **15** | **19** | **18** | **16** | **20** | **17** | **21** | **22** | **23** |
| Minerals % | 52.7 | 55.0 | 53.9 | 20.0 | 39.0 | 20.9 | 33.7 | 34.0 | 26.3 |
| $SiO_2$ | 61.3 | 68.5 | 65.0 | 27.8 | 50.2 | 53.7 | 55.1 | 40.7 | 54.5 |
| $TiO_2$ | 0.0 | 0.0 | 0.0 | 0.0 | 0.0 | 0.0 | 0.0 | 0.0 | 0.0 |

| | | | | | | | | | |
|---|---|---|---|---|---|---|---|---|---|
| $Al_2O_3$ | 33.0 | 21.5 | 24.4 | 42.7 | 48.1 | 40.5 | 33.0 | 51.9 | 42.9 |
| $Fe_2O_3$ | 5.7 | 10.0 | 10.6 | 29.5 | 1.8 | 5.7 | 11.9 | 7.4 | 2.7 |
| MgO | 0.0 | 0.0 | 0.0 | 0.0 | 0.0 | 0.0 | 0.0 | 0.0 | 0.0 |
| CaO | 0.0 | 0.0 | 0.0 | 0.0 | 0.0 | 0.0 | 0.0 | 0.0 | 0.0 |
| $Na_2O$ | 0.0 | 0.0 | 0.0 | 0.0 | 0.0 | 0.0 | 0.0 | 0.0 | 0.0 |
| $K_2O$ | 0.0 | 0.0 | 0.0 | 0.0 | 0.0 | 0.0 | 0.0 | 0.0 | 0.0 |
| $P_2O_5$ | 0.0 | 0.0 | 0.0 | 0.0 | 0.0 | 0.0 | 0.0 | 0.0 | 0.0 |
| $SO_3$ | 0.0 | 0.0 | 0.0 | 0.0 | 0.0 | 0.0 | 0.0 | 0.0 | 0.0 |
| Total | 100.0 | 100.0 | 100.0 | 100.0 | 100.0 | 100.0 | 100.0 | 100.0 | 100.0 |

**Inferred chemistry—glass**

| | **Station no.** | | | | | | | | |
|---|---|---|---|---|---|---|---|---|---|
| | **Group A** | | | | **Group B** | | | | |
| **Property** | **15** | **19** | **18** | **16** | **20** | **17** | **21** | **22** | **23** |
| Glass % | 47.3 | 45.0 | 46.1 | 80.0 | 61.0 | 79.1 | 66.3 | 66.0 | 73.7 |
| $SiO_2$ | 52.3 | 43.8 | 50.8 | 48.8 | 71.1 | 70.5 | 64.9 | 66.2 | 66.0 |
| $TiO_2$ | 3.7 | 3.3 | 3.7 | 2.4 | 3.0 | 1.2 | 1.4 | 2.5 | 1.3 |
| $Al_2O_3$ | 19.2 | 29.5 | 19.8 | 27.8 | 17.4 | 20.6 | 17.0 | 16.0 | 27.6 |
| $Fe_2O_3$ | 13.9 | 9.8 | 17.5 | 10.6 | 1.8 | 2.4 | 5.4 | 4.7 | 1.1 |
| MgO | 1.6 | 1.6 | 1.9 | 2.0 | 1.8 | 0.8 | 1.7 | 1.7 | 0.3 |
| CaO | 2.9 | 3.4 | 2.8 | 5.3 | 2.1 | 1.2 | 5.0 | 5.8 | 0.4 |
| $Na_2O$ | 0.4 | 0.3 | 0.3 | 0.4 | 1.4 | 0.7 | 1.3 | 0.2 | 0.2 |
| $K_2O$ | 1.4 | 1.2 | 0.9 | 1.1 | 0.8 | 2.1 | 2.9 | 1.7 | 2.9 |
| $P_2O_5$ | 3.9 | 6.0 | 2.2 | 1.2 | 0.2 | 0.3 | 0.2 | 0.7 | 0.2 |
| $SO_3$ | 0.6 | 1.1 | 0.2 | 0.3 | 0.3 | 0.1 | 0.2 | 0.4 | 0.1 |
| Total | 100.0 | 100.0 | 100.0 | 100.0 | 100.0 | 100.0 | 100.0 | 100.0 | 100.0 |

In contrast to ash from higher-rank coals, the fly ash produced from the combustion of very low-rank coals may be dominated by sulfates and other nonsilicate minerals. For example, Mudd and Kodikara (2000) indicate that the main minerals in fly ashes from the Latrobe Valley, Victoria, Australia, are thenardite ($Na_2SO_4$), halite (NaCl), periclase (MgO), hematite ($Fe_2O_3$), magnetite ($Fe_3O_4$), lime (CaO), anhydrite ($CaSO_4$), quartz ($SiO_2$), and alumina ($Al_2O_3$). Gypsum ($CaSO_4 \cdot 2H_2O$) and calcite ($CaCO_3$) may also be found in ash that has been emplaced in ponds, which formed by interaction of the Ca-bearing components with water and the atmosphere. This unusual mineralogy reflects the abundance of nonmineral inorganic elements, such as Na, Ca, and Mg, in the mineral matter of the feed coal materials (Brockway & Borsaru, 1985; Kiss & King, 1977).

## 2.3.4 Fate of coal major oxides and minor and trace elements

### 2.3.4.1 Volatility of elements in combustion

The relative volatility of elements determines much of the chemistry of BA and fly ash, with BA having relatively large concentrations of refractory elements than fly ash (Fig. 2.20 after Clarke (1993) and Meij (1994), among others). These are not absolute rules; obviously Al, Si, and Fe are important constituents of fly ash. For the more

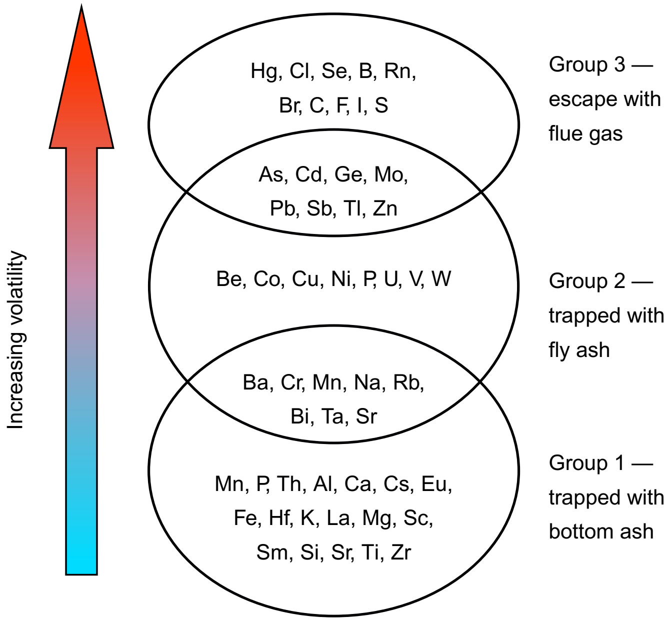

**Fig. 2.20** Distribution of elements among bottom ash, fly ash, and flue gas after Clarke (1993) and Meij (1994). This is a generalized concept and actual performance in pollution control systems may vary. For example, fly ash carbons may capture Hg.

volatile elements, however, high concentrations in the BA may be an indication of an anomaly in the production of the material.[1] Mardon and Hower (2004), in a detailed study of a single unit at a utility burning eastern Kentucky coal, demonstrated an increase in volatile elements (Zn and As being good examples) with a decrease in flue-gas temperature and fly ash particle size from the mechanical (cyclone) hoppers to the third-row ESP hoppers. In the latter investigation, as well as in Hower and Robertson (2004), selenium exhibited a behavior out of character with its known volatility, with the greatest Se concentration in the first-row ESP hoppers.

### 2.3.4.2 Mercury

Mercury, a potential neurotoxin when microbially converted to methylmercury (Trasande, Schechter, Haynes, & Landrigan, 2006), is an exception to the capture behavior of volatile trace elements. Arsenic and Zn, for example, show a relationship between increases in concentration and decreases in flue gas temperature and fly ash particle size. In contrast, Hg capture by fly ash improves with an increase in the amount of fly ash carbon, a decrease in the ambient flue-gas temperature, and an apparent increase in surface area from inertinite to isotropic carbon to anisotropic carbon (Hower et al., 2010). Mercury is known to be associated with <3-nm Fe-, As-, Se-, and Pb- (and other metals) bearing metal or mineral (possibly Fe spinel) inclusions in fullerene carbons, as well as directly with the fullerenes (Hower et al., 2008; Silva et al., 2010). In general, only $Hg^{2+}$ is captured by emission control systems, with elemental Hg passing through the system and into the atmosphere (Senior et al., 1997; Senior, Sarofim, Zeng, Helble, & Mamani-Paco, 2000). Chlorine enhances the oxidation of $Hg^0$ to $Hg^{2+}$, increasing the potential for Hg capture by fly ash carbons or by FGD gypsum (Senior et al., 1997). Enhanced flue-gas desulfurization, in place at many US power stations, and powdered activated carbon (PAC) for medium- and high-Cl coals or brominated PAC for low-Cl coals are used to control Hg emissions (Reisch, 2015). The carbons from low-rank coals are more efficient per unit of carbon than carbons from bituminous coals (Goodarzi & Hower, 2008; Kostova et al., 2011; Lu, Rostam-Abadi, Chang, Richardson, & Paradis, 2007) owing to the greater surface area of subbituminous-derived versus bituminous-derived chars (Külaots, Hurt, & Suuberg, 2004). In an investigation of anthracite-derived fly ashes from two Chinese power plants, Silva et al. (2012) found that Hg was higher (2300–2500 ppb vs. 300–860 ppb) in the fly ash with higher fly ash C (10.5%–13.9% dry vs. 3.9%–9.8% dry) and Cl (118 ppm average vs. 2–12 ppm).

### 2.3.4.3 Selenium and arsenic

#### Fly ash and BA

Due to its semivolatile behavior, selenium in coal combustion systems tends to occur as a vapor in flue gas, accumulate in fly ash, and be depleted in BA (Agnihotri, Chauk, Mahuli, & Fan, 1998; Al-Abed, Jegadeesan, Scheckel, & Tolaymat, 2008; Shah, Strezov, Strezov, & Nelson, 2007). Studies of Se in CCBs have been conducted by

---

[1] Anecdotally, an unusually high lead concentration in the bottom ash at a Kentucky power plant was ultimately traced to the use of lead shotgun pellets in the removal of slag from the wall of the boiler.

Shah et al. (2007), Shah, Strezov, Prince, and Nelson (2008), Huggins, Senior, Chu, Ladwig, and Huffman (2007), and Luo, Glammer, Huhmann, and Catalano (2011), among others.

Depending on combustion conditions and the chemistry of the coal, some arsenic may accumulate in BAs (Yudovich & Ketris, 2005). However, because of its semi-volatility, arsenic mostly concentrates in flue gases and then largely condenses onto high surface-area, fine-grained fly ash particles, especially during postcombustion cooling (Galbreath & Zygarlicke, 2004; Guo, Yang, & Liu, 2004; Helble, 2000; Hower, Trimble, et al., 1999; Llorens, Fernández-Turiel, & Querol, 2001; López-Antón, Díaz-Somoano, Spears, & Martínez-Tarazona, 2006; Mukherjee & Kikuchi, 1999; Shah et al., 2008). Some very fine-grained, arsenic-bearing fly ash particles will readily pass through flue gas treatment systems and enter the atmosphere, where they may be inhaled (Yudovich & Ketris, 2005).

### *2.3.4.4 Rare earth elements*

#### Classification and origin of REY in coal

Coal deposits are considered as potential alternative sources for REY, or REE if yttrium is not included (Seredin & Dai, 2012), which are crucial metals for alternative power and energy-efficient technologies. Identification of REY during coal combustion may not only increase the beneficiation of coal deposits themselves, but also will promote humanity's further movement on the "green road" (Seredin & Dai, 2012).

According to the Seredin and Dai (2012), regarding the classification of REY in coal or in coal ash, two classifications are recognized based on geological and industrial perspectives, respectively:

**(1)** Geochemical classification. REY are classified into light (LREY-La, Ce, Pr, Nd, and Sm), medium (MREY-Eu, Gd, Tb, Dy, and Y), and heavy (HREY-Ho, Er, Tm, Yb, and Lu) groups. Accordingly, in comparison with the upper continental crust (UCC; Taylor & McLennan, 1985), three enrichment types are identified: L-type (light-REY; $La_N/Lu_N > 1$), M-type (medium-REY; $La_N/Sm_N < 1$, $Gd_N/Lu_N > 1$), and H-type (heavy REY; $La_N/Lu_N < 1$). Coal or coal ash with REY distribution patterns similar to UCC (normal or N-type) are rarely observed (e.g., Dai et al., 2015).

**(2)** Industrial classification. This classification divides REY into critical (Nd, Eu, Tb, Dy, Y, and Er), uncritical (La, Pr, Sm, and Gd), and excessive (Ce, Ho, Tm, Yb, and Lu) groups.

#### Assessment criteria for coal ashes as REY raw materials

The criteria of Seredin and Dai (2012) for the assessment of REY in coal ash as raw materials suggested that data on REY grade and their individual composition are adequate for a preliminary estimation. The first assessment criterion is the concentration of REY in coal ash. REO content $\geq$1000 μg/g in ash is considered as the cut-off grade for beneficial recovery. The second criterion is the individual composition of the metals in coal ash. A $REY_{def,\ rel}$-$C_{outl}$ graph was proposed to evaluate high-REY coal ash in terms of potential industrial value (Fig. 2.21), where the $y$-axis is the percentage of critical elements in total REY ($REY_{def,\ rel}$) and the $x$-axis represents the outlook coefficient ($C_{outl}$). The $C_{outl}$ proposed for primary estimation of ore quality is the ratio of the relative amount of critical REY metals in the total REY to the relative amount of excessive REY, calculated as follows:

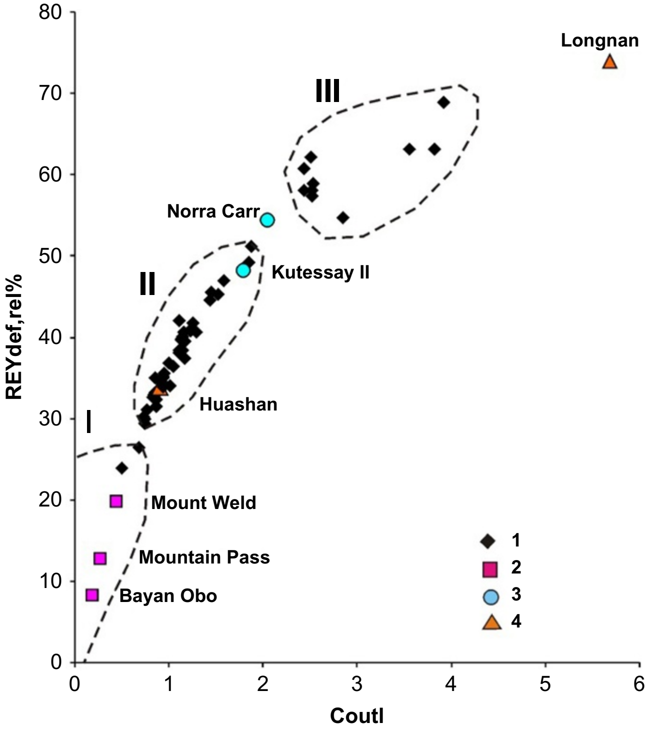

**Fig. 2.21** Classification of REE-rich coal ashes by outlook for individual REY composition in comparison with selected deposits of conventional types. 1, REE-rich coal ashes; 2, carbonatite deposits; 3, hydrothermal deposits; 4, weathered crust elution deposited (ion-adsorbed) deposits. Clusters of REE-rich coal ashes distinguished by outlook for REY composition (numerals in figure): I-unpromising, II-promising, and III-highly promising.

$$C_{\text{outl}} = \frac{(\text{Nd} + \text{Eu} + \text{Tb} + \text{Dy} + \text{Er} + \text{Y})/\sum \text{REY}}{(\text{Ce} + \text{Ho} + \text{Tm} + \text{Yb} + \text{Lu})/\sum \text{REY}}$$

Based on $\text{REY}_{\text{def, rel}}$-$C_{\text{outl}}$ relationship (Fig. 2.21), three categories can be classified: (1) The first category has $\text{REY}_{\text{def,rel}}$ and $C_{\text{outl}}$ values $\leq 26\%$, respectively. The coal ashes that fall into this category are considered unpromising in terms of REY recovery, in spite of the high total REO content (0.16%–0.17%) in the ashes. The coal ashes in this category generally have L-type enrichment type. (2) The coal ashes that fall into the second category with $30\% \leq \text{REE}_{\text{def,rel}} \leq 51$ and $0.7 \leq C_{\text{outl}}$ are regarded as promising REY raw materials for economic development and have various (L-, M-, and H-) REY enrichment types. (3) The coal ashes in the third category with $\text{REE}_{\text{def,rel}} > 60\%$ and $C_{\text{outl}} > 2.4$ require attention because they are considered as highly promising economic REY raw materials. REY-rich coal ashes in this category are generally characterized by an H-type REY enrichment type.

### Fate of REY in coal ash

In order to fully investigate the fate of REY and its behavior during coal combustion productions, the following changes between feed coal and coal combustion productions (e.g., fly ash and BA) should be taken into account: concentrations, distribution patterns (e.g., normalized to UCC), fractions between the L-, M-, and H-REY, and modes of occurrence.

Due to the low volatility of REY during coal combustion (Clarke, 1993), not only the concentration but also the distribution patterns of REY are expected to be overall similar between laboratory ash, fly ash, and BA. Additionally, studies by Dai et al. (2014) showed that the REY distribution patterns of the fly ash and BA are similar to those of the corresponding feed coals.

Hower et al. (2013) used Ce, the most abundant of the REY, as a proxy for other REY in their wavelength-dispersive spectrometry electron microprobe study of the associations of REY in fly ash. Cerium appears to be dispersed in the glass; therefore, an increased Ce concentration as the glass content of the fly ash increases in the finer sizes makes sense. Dai et al. (2014) showed that REY concentrations increases from 192 in plus-120-mesh fly ash through 230 μg/g (120×160 mesh), 293 μg/g (160×300 mesh), 373 μg/g (300×360 mesh), 412 μg/g (360×500 mesh), and to 550 μg/g in minus-500 mesh fly ashes. In addition, some REY (e.g., Y, La, Ce, Pr, and Nd) were observed in REY-bearing calcite and $CaCO_3(F)$ (probably parisite) in high-REY fly ash (Dai et al., 2014).

## 2.3.5 Ash formation in FBC

As a consequence of the lower operating temperatures, large grains of quartz may pass though FBC systems with minimal alteration (although micron-size grains with a high surface area may participate in some mineralogical reactions); even some clays, such as illite, may undergo only slight alteration (Riley et al., 2014). Although the operating temperature is significantly lower than for pulverized fuel systems, the mineralogy of fluidized bed fly ash is often complex due to the use of limestone or dolomite as an in situ desulfurizing agent (Table 2.7). Thus sulfates, typically calcium sulfates, are abundant, but complex alkali metal sulfates may also be present along with unreacted decomposition products of limestone, such as lime. Reaction of the silicate mineral matter in the coal with limestone may form a series of calcium silicates, such as anorthite, gehlenite, and diopside. Oxide phases (e.g., magnetite, hematite, and hercynite) may also be present. Depending on the sodium and silica contents of the coal ash, felspathoids such as nepheline may form.

As a consequence of the lower operating temperature, the proportion of amorphous material is lower than that in ash from pulverized fuel combustion. Unlike pulverized fuel fly ash, glass is a minor component of the amorphous material. Due to the frequent occurrence of abundant sulfates and unreacted lime and portlandite, ash derived from FBC may behave very differently to that from pulverized fuel combustion. For example, leachates of FBC ashes may be very alkaline.

Table 2.7 **Mineralogy of typical ashes from fluidized bed combustion systems (compiled from various sources)**

| | Atmospheric FBC | | Pressurized FBC | |
|---|---|---|---|---|
| Minerals | Silo ash | Bottom ash | Fly ash | Bottom ash |
| Quartz | 25.8 | 30.0 | 3.7 | 9.8 |
| Mullite | 0.9 | 2.3 | 6.1 | |
| Gehlenite | | | 8.5 | 6.3 |
| Melilite, sodic | | | 5.8 | 5.7 |
| Merwinite | | | 6.6 | 5.0 |
| Anorthite | 0.7 | 3.7 | 11.8 | 4.4 |
| Periclase (?) | | | 0.7 | |
| Hematite | 1.0 | 1.9 | | |
| Maghemite | 0.7 | 0.6 | 1.0 | |
| Magnetite | 0.3 | 0.2 | | |
| Lime | | | 3.0 | 16.7 |
| Portlandite | | 4.2 | 0.6 | 2.6 |
| Calcite | 1.6 | 0.9 | 3.1 | 43.6 |
| Anhydrite | 0.4 | 1.2 | 7.5 | 5.8 |
| Gypsum | 3.0 | | | |
| Amorphous | 65.5 | 54.8 | 41.6 | |
| Total | 99.9 | 99.8 | 100.0 | 99.9 |

| | CFBC Unit A | | CFBC Unit B | | CFBC Unit C |
|---|---|---|---|---|---|
| Minerals | Bed ash | Fly ash | Bed ash | Fly ash | Fly ash |
| Quartz | 1.8 | 1.5 | 15.8 | 5.9 | 6.6 |
| Cristobalite | | | | | 3.5 |
| Mullite | | | 10.8 | | 27.4 |
| Diopside | 0.9 | | | | |
| Anorthite | 3.1 | 8.5 | 2.3 | 2.9 | 9.1 |
| Nepheline | 9.1 | 6.8 | | | |
| Hauyne | 1.6 | | | | |
| Rutile | | | 0.6 | | |
| Hematite | 4.5 | 20.7 | 6.9 | 4.6 | |
| Maghemite | 6.9 | 9.8 | 5.5 | 0.1 | |
| Magnetite | | | 9.5 | 3.5 | |
| Ilmenite | | | 2.1 | | |
| Spinel | | | 4.1 | | |
| Lime | | | 1.8 | 1.4 | |
| Portlandite | | | | 4.2 | |
| Calcite | | 0.8 | | 14.0 | |
| Anhydrite | 47.0 | 50.9 | 4.4 | 14.8 | 0.7 |
| Hexahydrite | | 0.5 | | | |
| Butlerite | 0.3 | 0.6 | | | |
| Aphthitalite | | | | 0.5 | |
| Srebrodolskite | | | | 3.6 | |
| Amorphous | 24.6 | | 36.3 | 44.6 | 52.6 |
| Total | 99.8 | 100.1 | 100.1 | 100.1 | 99.9 |

### 2.3.6 Ash and slag formation during coal gasification

The mineral transformations in coal gasification are important to commercialization of gasifiers (Shannon et al., 2009). Since gasifiers operate in substoichiometric conditions, the transformation of the mineral matter during gasification is quite different from that in combustion (Zhang, Jackson, & Vuthaluru, 1999). In general, the sintering and softening temperatures of minerals in coal during gasification are lower than those in combustion. The solid residue in fluidized-bed gasifiers is a dry ash or a fused agglomerated ash according to the operating conditions, gasifier design, and ash fusibility temperature. Entrained-flow gasifiers mainly produce vitreous slag because of the very high temperatures, while fixed-bed gasifiers generate dry ash (Sasol-Lurgi) or slag (high-temperature gasifiers) depending upon the design. Atmosphere, mineral matter composition, the presence of carbonaceous components, and aerodynamics of ash particles can also make a difference in the mineral matter transformation besides design (Koyama, Morimoto, Ueda, & Matsuoka, 1996; Wagner et al., 2008). Above all, the dependability of the operation of gasifiers relies on the generation of ash/slag in accordance with its design.

Similar to combustion, the mineral matter transformations during gasification include the processes of char/ash fragmentation, ash coalescence, and volatilization and condensation of inorganics. Slag is always formed after the generation of ash. Because of the difference in temperature history and residence time, ash and slag are similar in chemical composition, but different in mineral composition and the morphology of the mineral matter (Li & Bai, 2013). The generation of ash/slag in different gasifiers has a notable diversity, and therefore a discussion is presented on specific reaction types in this chapter.

#### 2.3.6.1 Fixed-bed gasifier

The Lurgi gasifier is the main commercialized fixed-bed gasifier (Fig. 2.22), in which the coal moves slowly from top to bottom in the gasifier and has countercurrent contacts with the rising gas agent and reactant gas. Physical and chemical changes include drying, pyrolysis, gasification, and combustion.

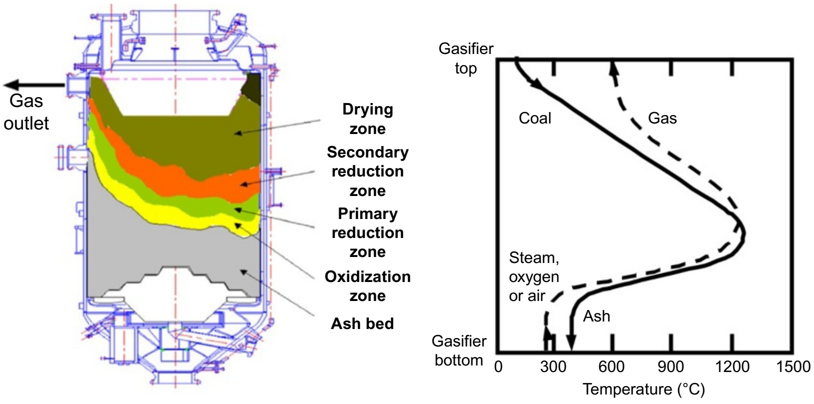

**Fig. 2.22** Typical zones in the Sasol-Lurgi gasification process (van Dyk et al., 2006).

The ash produced from the fixed-bed Lurgi process tends to be coarser than that produced by other coal utilization technologies, ranging in particle size from 4 to 75 mm, and is extremely heterogeneous (Matjie et al., 2008). Apart from coal, extraneous fragments of sedimentary rock, such as mudstone, siltstone, and sandstone, that occur in the feedstock may pass through the process with minimal alteration, except for some marginal reaction rims. The mineralogy of fused clinkers in South African Lurgi ashes is dominated by anorthite and mullite, which occur in association with quartz, cristobalite, and diopside (Table 2.8). Amorphous contents range from 20 to 73 wt%, although contents less than 50 wt% are more typical. The overall proportion of amorphous material is considerably lower than in the almost completely fused products of slagging gasification (see below). Unreacted quartz, K feldspar, and illite may occur in the rock fragments of the Lurgi ash, with mullite, anorthite, and amorphous material occurring in the reaction rims.

More detailed mineralogical studies (Matjie, French, Ward, Pistorius, & Li, 2011; Matjie, Ward, & Li, 2012a,2012b) indicate that the breakdown of organic particles in the coarse (<6 mm) feedstocks for South African Lurgi gasifiers produces a Ca-rich ash at the high temperatures in the reaction chamber, due to a combination of carbonate minerals as fracture fillings in the vitrinite macerals and nonmineral Ca in the organic matter. This material then melts or fuses in the bed of the gasifier, flows around the heat-altered yet solid stony particles in the feedstock, and on cooling binds them together to form clinkered aggregates within the ash (Figs. 2.23–2.25).

As indicated in Table 2.9, slags from entrained-flow coal gasification mainly consist of amorphous glass, derived from the melting of the mineral-matter residues to facilitate their removal from the reaction chamber. Where glass contents are lower, graphitic carbon is often the most abundant component, suggesting that the gasifier is operating under less than optimum conditions (Riley et al., 2014). Anorthite is typically the most abundant crystalline silicate phase, although its concentration rarely exceeds 8 wt%; mullite, quartz, and, possibly, cristobalite occur in trace amounts. Oxide phases are a minor component, the most common being the iron oxides magnetite, maghemite, and hematite; the spinels, hercynite and spinel *sensu stricto*, are rare in overall occurrence. The fine particulate stream is dominated by glass with only trace proportions of quartz.

The BGL (British Gas-Lurgi) gasification process is another typical fixed-bed gasifier with melting slag discharge. The steam and oxygen are sprayed into the gasifier, and their proportion is sufficient to maintain high temperatures so that ash/slag melts and gathers in the bottom of furnace. The molten ash/slag is chilled after feeding into a slag chamber below the gasifier, deposited on a hermetic ash bucket, and then finally discharged from the gasifier. The formation mechanisms of ash/slag in BGL gasifier should be similar to a fixed-bed gasifier, and the largest difference is that the ash has been transformed into slag. However, few papers focus on specific transformation law and mechanisms (Li & Bai, 2013).

### Fluidized-bed gasifier

By controlling the velocity of the gas agent, the coal in a fluidized-bed gasifier is kept in a fluidized state, the coal particles and gas agents are in sufficient contact with each other, and the chemical reactions and heat transfer are underway with the support

**Table 2.8** Mineralogy of Lurgi gasification ash (Matjie et al., 2008)

| Mineral | Bulk gasification ash | Clinker 1 | Clinker 2 | Clinker 3 | Clinker 4 | Clinker 5 | Clinker 6 |
|---|---|---|---|---|---|---|---|
| Quartz | 10.7 | 3.9 | 0.2 | 3.7 | 10.6 | 5.5 | 14.6 |
| Cristobalite | 1.8 | 0.0 | 1.7 | 5.5 | 10.2 | 4.2 | 0.0 |
| Anorthite | 13.1 | 27.0 | 51.6 | 19.5 | 10.4 | 38.8 | 2.3 |
| Mullite | 17.7 | 5.7 | 9.5 | 13.9 | 22.1 | 10.7 | 29.7 |
| Diopside | 0.7 | 12.1 | 0.0 | 1.9 | 0.9 | 0.0 | 0.0 |
| Amorphous | 56.0 | 51.3 | 37.0 | 55.7 | 45.8 | 40.8 | 53.4 |
| Total | 100.0 | 100.0 | 100.0 | 100.2 | 100.0 | 100.0 | 100.0 |

| | Clinker 7 | Clinker 8 | Heated stone 1 | Heated stone 2 | Heated stone 3 | Heated stone 4 |
|---|---|---|---|---|---|---|
| Quartz | 12.9 | 1.5 | 61.8 | 50.8 | 21.3 | 24.9 |
| Cristobalite | 0.0 | 1.0 | 0.0 | 0.0 | 0.0 | 0.0 |
| Anorthite | 8.4 | 62.3 | 3.2 | 2.3 | 0.0 | 0.0 |
| Mullite | 17.0 | 5.8 | 14.8 | 7.7 | 19.7 | 0.0 |
| Diopside | 0.0 | 12.1 | 0.0 | 0.0 | 0.0 | 0.0 |
| Illite | 0.0 | 0.0 | 0.0 | 0.0 | 7.9 | 0.0 |
| Anatase | 0.1 | 0.0 | 0.0 | 0.0 | 0.6 | 1.1 |
| Rutile | 0.0 | 0.0 | 0.0 | 0.0 | 0.0 | 0.8 |
| Dolomite | 0.0 | 0.0 | 0.0 | 0.0 | 0.0 | 0.3 |
| Pyrrhotite | 0.0 | 0.0 | 0.0 | 0.0 | 6.4 | 0.0 |
| Amorphous | 61.6 | 17.3 | 20.1 | 39.2 | 44.2 | 73.0 |
| Total | 100.0 | 100.0 | 99.9 | 100.0 | 100.1 | 100.1 |

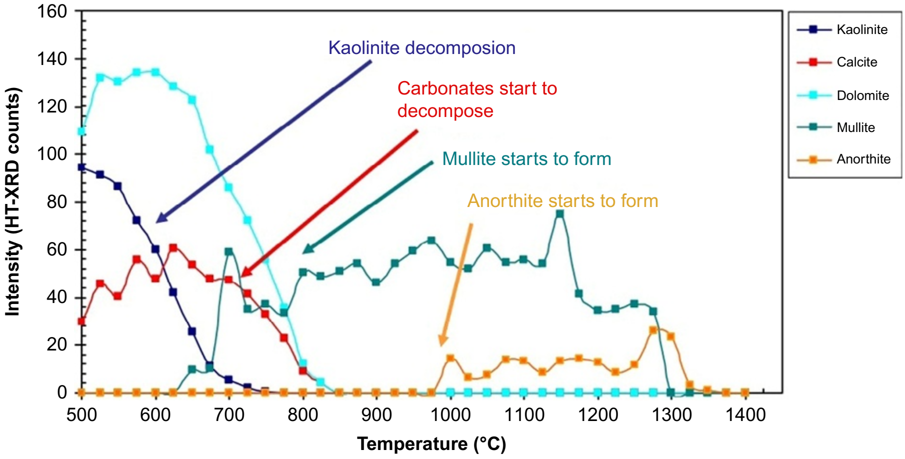

**Fig. 2.23** Integral intensities of identified phases as a function of temperature (van Dyk et al., 2006).

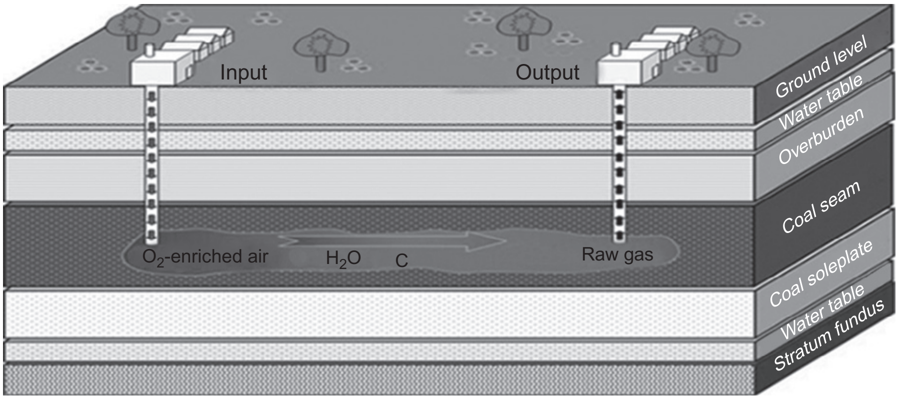

**Fig. 2.24** An overview of the UCG process (Liu et al., 2016).

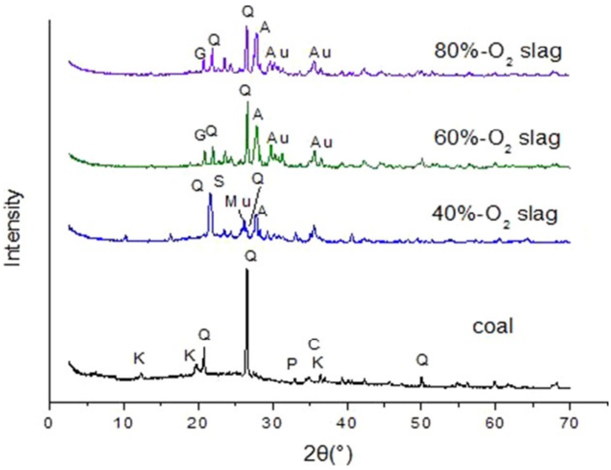

**Fig. 2.25** Mineral composition of coal and UCG slag by XRD analysis (*Q*, Quartz; *Py*, Pyroxene; *A*, Anorthite; *S*, Sekaninaite; *G*, Gehlenite; *P*, Pyrite; *C*, Chlorite; *K*, Kaolinite; *Mu*, Mullite) (Liu et al., 2016).

**Table 2.9** Mineralogy of slagging gasifier ash from different coal feedstocks

| Coal | Coal A | | | | Coal B | | | Coal C | | | Coal D | | | Coal E | Coal F |
|---|---|---|---|---|---|---|---|---|---|---|---|---|---|---|---|
| | Slag | Slag | Slag | Fine ash | Slag | Slag | Fine ash | Slag | Slag | Fine ash | Slag | Slag | Fine ash | Slag | Slag |
| Quartz | 0.1 | 1.1 | 0.5 | 0.3 | 0.8 | 2.5 | 0.4 | 0.1 | 0.1 | | | 0.2 | 0.2 | | |
| Cristobalite | | | 0.6 | | | | | | | | | | | | |
| Mullite | | | | | 0.9 | | | 0.2 | | | | | | | |
| Anorthite | 5.4 | 0.6 | | | | | | | 2.4 | | | 8.5 | | | 2.2 |
| Hematite | | | | | | | | | | | | | | | 0.6 |
| Maghemite | 2.8 | | | | | | | | | | | | | | 0.5 |
| Magnetite | 2.5 | 0.2 | | | 0.3 | | | | | | | | | | 1.0 |
| Hercynite | 0.5 | | | | | | | | | | | | | | |
| Spinel | | | | | | | | | | | | | | | 0.6 |
| Goethite | 3.2 | 0.2 | | | | | | | | | | | | | |
| Calcite | | | | | 0.2 | | | 0.2 | | | | | | | |
| Melanterite | | | | | | 0.5 | | | | | | | | | |
| Gypsum | | | | | | 0.7 | | | 0.6 | | | 0.3 | 0.9 | | |
| Greigite | | | | | | | 0.5 | | | 0.5 | | | | | |
| Carbon | | | | | 11.7 | | | 24.9 | | | | | | | |
| Amorphous | 85.5 | 97.9 | 98.9 | 99.7 | 86.1 | 96.4 | 99.1 | 74.6 | 96.9 | 99.5 | 100. | 91.0 | 98.9 | 100. | 95.0 |
| Total | 100.0 | 100.0 | 100.0 | 100.0 | 100.0 | 100.1 | 100.0 | 100.0 | 100.0 | 100.0 | 100.0 | 100.0 | 100.0 | 100.0 | 99.9 |

(Partly after Riley, K., French, D., Ward, C. R., Stephenson, L. G., & Gurba, L. W. (2014). Characterisation, impact and use of products from other technologies. In C. R. Ward, C. Heidrich, & O. Yeatman (Eds.), Coal combustion products handbook (2nd ed.) (pp. 409–439).Wollongong: Ash Development Association of Australia.)

agitation and back mixing. Partial- gasification ash and fine coal particles are carried by the gas, while most of the ash is discharged from the bottom of the furnace. The fine coal particles carried by gas will move back again to the bed layer in a cyclical process. The reaction temperature in fluidized bed gasifier is relatively low; however, the pyrolysis temperature is higher and is same as that for reduction.

#### Entrained-flow bed gasifier

In an entrained-flow gasifier, a gas agent entrained with pulverized coal or coal slurry is fed into a furnace through special nozzles. Oxygen mixtures will ignite in a flash, burn rapidly, and generate plenty of heat as a result of temperature radiation. In that case, the temperature of the flame center can reach 2000°C, which melts the mineral matter. With char gasification, the droplets generated by mineral matter are deposited on furnace walls by the entrainment of partly airflow, thus forming liquid ash/slag sheets. Then, the liquid sheets and partly undeposited ash/slag particles, which are considered gasification slag, are discharged from the bottom of furnace. Some ash/slag particles are discharged from the top of furnace with the airflow (Li & Bai, 2013).

## 2.4 Other solid fuels

### 2.4.1 Tire-derived fuel

A few utility power plants, generally units equipped with cyclone-fired boilers, and industrial boilers have used small amounts of chopped tires as a supplement to their coal supply (Hower & Robertson, 2004; Hower et al., 2007; Hower, Robertson, & Roberts, 2001). The use of tires in power plants has been driven by regulations; for example, the incentive for the Tennessee Valley Authority to burn tires in their Allen Fossil Plant was a 1991 Tennessee law banning tires in landfills (Maize, 1993). Zinc is a significant inorganic constituent in the tires, both from the steel belts and bead wire, with 34% Zn and 98% Zn-Cu alloy, respectively, and from ZnO used as a curing agent in the rubber (Amari, Themelis, & Wernick, 1999). In a Kentucky utility cyclone boiler, the concentration of Zn in the fly ash increased from 570 ppm in a run without added tires to 6763, 10,860, and 17,940 ppm for fly ashes from first, second, and third-ESP rows at a time when 2%–3% tires were part of the fuel mix (Hower et al., 2007).

### 2.4.2 Petroleum coke

Petroleum coke has been used as a substitute for portions of the coal feed; although the use varies with the price of the coke. Petroleum coke has high concentrations of Ni and V, with up to 9463 ppm Ni and 1425 ppm V in the fourth-row ESP fly ash, and 26,440 ppm Ni and 3340 V in the 100 × 200-mesh portion of the latter ash, at a western Kentucky power plant (Hower, Thomas, Mardon, & Trimble, 2005). In addition, the fly ash has large amounts of petroleum coke, up to 55% in the first-row ESP fly ash, pointing towards inherent inefficiencies in attempting to burn a coke in a boiler designed for high-volatile C bituminous coal.

# References

Abbott, M. F., & Austin, L. G. (1985). Studies on slag deposit formation in pulverized-coal combustors. 6. Sticking behaviour of slag drops from three Pennsylvania steam coals. *Fuel*, *64*, 832–838.

Agnihotri, R., Chauk, S., Mahuli, S., & Fan, L. -S. (1998). Selenium removal using Ca-based sorbents: Reaction kinetics. *Environmental Science and Technology*, *32*, 1841–1846.

Al-Abed, S. R., Jegadeesan, G., Scheckel, K. G., & Tolaymat, T. (2008). Speciation, characterization, and mobility of As, Se, and Hg in flue gas desulphurization residues. *Environmental Science and Technology*, *42*, 1693–1698.

Alekseev, Y. I., & Vereshchagin, V. I. (1997). Formation of crystalline phases in electroceramics of the system CaO-MgO-$Al_2O_3$-$SiO_2$ (a review). *Glass and Ceramics*, *54*, 340–343.

Amari, T., Themelis, N. J., & Wernick, I. K. (1999). Resource recovery from used rubber tires. *Resources Policy*, *25*, 179–188.

American Society for Testing and Materials (ASTM), 2015. Standard specification for coal fly ash and raw or calcined natural pozzolan for use in concrete (ASTM C618-15). ASTM International, West Conshohocken, PA, 5 pp.

Barranco, R., Colechin, M., Cloke, M., Gibb, W., & Lester, E. (2006). The effects of pf grind quality on coal burnout in a 1 MW combustion test facility. *Fuel*, *85*, 1111–1116.

Bengtsson, M. (1986). *Combustion behavior for a range of coals of various origins and petrographic composition* (PhD dissertation). Stockholm, Sweden: The Royal Institute of Technology, variously paginated.

Berkowitz, N. (1979). *An introduction to coal technology*. New York, NY: Academic Press. 345 p.

Brockway, D. J., & Borsaru, R. M. (1985). Ion profiles in Victorian brown coals. In *Proceedings of international conference on coal science, Sydney, Australia, October* (pp. 593–596): Pergamon Press, Oxford.

Brown, R. C., & Dykstra, J. (1995). Systematic errors in the use of loss-on-ignition to measure unburnt carbon in fly ash. *Fuel*, *74*, 570–574.

Buhre, B. J. P., Hinkley, J. T., Gupta, R. P., Nelson, P. F., & Wall, T. F. (2006). Fine ash formation during combustion of pulverised coal-coal property impacts. *Fuel*, *85*, 185–193.

Clarke, L. B. (1993). The fate of trace elements during coal combustion and gasification: An overview. *Fuel*, *72*, 731–736.

Collot, A. -G. (2006). Matching gasification technologies to coal properties. *International Journal of Coal Geology*, *65*, 191–212.

Creelman, R. A., Ward, C. R., Schumacher, G., & Juniper, L. (2013). Relation between coal mineral matter and deposit mineralogy in pf furnaces. *Energy and Fuels*, *27*, 5714–5724.

Crelling, J. C., Hippo, E. J., Woerner, B. A., & West, D. P. (1992). Combustion characteristics of selected whole coals and macerals. *Fuel*, *71*, 151–158.

Dai, S., Hower, J. C., Ward, C. R., Guo, W., Song, H., O'Keefe, J. M. K., et al. (2015). Elements and phosphorus minerals in the middle Jurassic inertinite-rich coals of the Muli Coalfield on the Tibetan Plateau. *International Journal of Coal Geology*, *144–145*, 23–47.

Dai, S., Zhao, L., Hower, J. C., Johnston, M. N., Song, W., Wang, P., et al. (2014). Petrology, mineralogy, and chemistry of size-fractioned fly ash from the Jungar power plant, Inner Mongolia, China, with emphasis on the distribution of rare earth elements. *Energy and Fuels*, *28*, 1502–1514.

Davis, R. E., Carlson, R. W., Kelly, J. W., & Davis, H. E. (1937). Properties of cements and concretes containing fly ash. *Journal of the American Concrete Institute*, *33*, 577–611.

Ehlers, E. G. (1972). *The interpretation of geological phase diagrams*. San Francisco, CA: W.H. Freeman & Co. 280 p.

Elliott, M. A. (Ed.), (1981). *Chemistry of coal utilization: Second supplementary volume*. New York, NY: Wiley. 2374 p.

Font, O., Moreno, N., Querol, X., Izquierdo, M., Alvarez, E., Diez, S., et al. (2010). X-ray powder diffraction-based method for the determination of the glass content and mineralogy of coal (co)-combustion fly ashes. *Fuel*, *89*, 2971–2976.

French, D., Dale, L., Matulis, C., Saxby, J., Chatfield, P., & Hurst, H. J. (2001). Characterization of mineral transformations in pulverized fuel combustion by dynamic high-temperature X-ray diffraction analysis. In *Proceedings of 18th Pittsburgh international coal conference, Newcastle, Australia, December*. 7 p. (CD-ROM).

French, D., Smitham, J., & Nelson, P. (2007). A preliminary assessment of the variability of Australian fly ashes. Research Report 65, Co-operative Research Centre for Coal in Sustainable Development, Brisbane, Australia, 52 p. http://pandora.nla.gov.au/pan/64389/20080828-1328/www.ccsd.biz/publications/757.html.

French, D., Riley, K., & Ward, C. R. (2014). Characterisation, classification and properties of coal combustion products. In C. R. Ward, C. Heidrich, & O. Yeatman (Eds.), *Coal combustion products handbook* (2nd ed., pp. 35–99). Wollongong: Ash Development Association of Australia.

Galbreath, K. C., & Zygarlicke, C. J. (2004). Formation and chemical speciation of arsenic-, chromium-, and nickel-bearing coal combustion PM2.5. *Fuel Processing Technology*, *85*, 701–726.

Goodarzi, F., & Hower, J. C. (2008). Classification of carbon in Canadian fly ashes and their implications in the capture of mercury. *Fuel*, *87*, 1949–1957.

Guo, R., Yang, J., & Liu, Z. (2004). Thermal and chemical stabilities of arsenic in three Chinese coals. *Fuel Processing Technology*, *85*, 903–912.

Helble, J. J. (2000). Model for the air emissions of trace metallic elements from coal combustors equipped with electrostatic precipitators. *Fuel Processing Technology*, *63*, 125–147.

Henderson, C. (2003). *Clean coal technologies*. London: IEA Clean Coal Centre. CC/74, 42 p.

Hlatshwayo, T. B., Matjie, R. H., Li, Z., & Ward, C. R. (2009). Mineralogical characterization of Sasol feed coals and corresponding gasification ash constituents. *Energy and Fuels*, *23*, 2867–2873.

Hough, D. C., & Sanyal, A. (1987). The role of petrography in the classification and combustion of coal. *Energy World*, *146*, 7–10.

Hower, J. C. (2012). Petrographic examination of coal-combustion fly ash. *International Journal of Coal Geology*, *92*, 90–97.

Hower, J. C., Graham, U. M., Dozier, A., Tseng, M. T., & Khatri, R. A. (2008). Association of sites of heavy metals with nanoscale carbon in a Kentucky electrostatic precipitator fly ash. *Environmental Science and Technology*, *42*, 8471–8477.

Hower, J. C., Groppo, J. G., Joshi, P., Dai, S., Moecher, D. P., & Johnston, M. N. (2013). Location of cerium in coal-combustion fly ashes: Implications for recovery of lanthanides. *Coal Combustion and Gasification Products*, *5*, 73–78.

Hower, J. C., Rathbone, R. F., Graham, U. M., Groppo, J. G., Brooks, S. M., Robl, T. L., et al. (1995). Approaches to the petrographic characterization of fly ash. In *International coal testing conference, 11th, Lexington, KY, May 10-12* (pp. 49–54).

Hower, J. C., Rathbone, R. F., Robl, T. L., Thomas, G. A., Haeberlin, B. O., & Trimble, A. S. (1997). Case study of the conversion of tangential- and wall-fired units to low-$NO_x$ combustion: Impact on fly ash quality. *Waste Management*, *17*, 219–229.

Hower, J. C., & Robertson, J. D. (2004). Chemistry and petrology of fly ash derived from the co-combustion of western United States coal and tire-derived fuel. *Fuel Processing Technology*, *85*, 359–377.

Hower, J. C., Robertson, J. D., Elswick, E. R., Roberts, J. M., Brandsteder, K., Trimble, A. S., et al. (2007). Further investigation of the impact of the co-combustion of tire-derived fuel and petroleum coke on the petrology and chemistry of coal combustion products. *Energy Sources, Part A: Recovery, Utilization, and Environmental Effects*, *29*, 431–461.

Hower, J. C., Robertson, J. D., & Roberts, J. M. (2001). Combustion by-products from the co-combustion of coal, tire-derived fuel, and petroleum coke at a Western Kentucky cyclone-fired unit. *Fuel Processing Technology*, *74*, 125–142.

Hower, J. C., Robertson, J. D., Thomas, G. A., Wong, A. S., Schram, W. H., Graham, U. M., et al. (1996). Characterisation of fly ash from Kentucky power plants. *Fuel*, *75*, 403–411.

Hower, J. C., Robl, T. L., Rathbone, R. F., Groppo, J. G., Graham, U. M., & Taulbee, D. N. (1996). Case studies of the impact of conversion to low-$NO_x$ combustion on fly ash petrology and mineralogy. In *Australian coal science conference, 7th, 2-4 Dec. 1996, Gippsland, Victoria, Australia* (pp. 347–354).

Hower, J. C., Senior, C. L., Suuberg, E. M., Hurt, R. H., Wilcox, J. L., & Olson, E. S. (2010). Mercury capture by native fly ash carbons in coal-fired power plants. *Progress in Energy and Combustion Science*, *36*, 510–529.

Hower, J. C., Thomas, G. A., Mardon, S. M., & Trimble, A. S. (2005). Impact of co-combustion of petroleum coke and coal on fly ash quality: Case study of a Western Kentucky power plant. *Applied Geochemistry*, *20*, 1309–1319.

Hower, J. C., Thomas, G. A., & Palmer, J. (1999). Impact of the conversion to low-$NO_x$ combustion on ash characteristics in a utility boiler burning western US coal. *Fuel Processing Technology*, *61*, 175–195.

Hower, J. C., Trimble, A. S., Eble, C. F., Palmer, C. A., & Kolker, A. (1999). Characterization of fly ash from low-sulphur and high-sulphur coal sources: Partitioning of carbon and trace elements with particle size. *Energy Sources*, *21*, 511–525.

Huffman, G. P., Huggins, F. E., Shah, N., & Shah, A. (1990). Behavior of basic elements during coal combustion. *Progress in Energy and Combustion Science*, *16*, 243–251.

Huggins, F. E., Senior, C. L., Chu, P., Ladwig, K., & Huffman, G. P. (2007). Selenium and arsenic speciation in fly ash from full-scale coal-burning utility plants. *Environmental Science and Technology*, *41*, 3284–3289.

Jewell, R. B., & Rathbone, R. F. (2009). Optical properties of coal combustion byproducts for particle-size analysis by laser diffraction. *Coal Combustion and Gasification Products*, *1*, 1–7.

Juniper, L. A. (2000). Thermal coal technology: A manual for Australian coal. In *QTHERM program*. Brisbane: Department of Mines and Energy, Queensland Government. 180 p.

Kiss, L. T., & King, T. N. (1977). The expression of results of coal analysis: The case for brown coals. *Fuel*, *56*, 340–341.

Kitto, J. B., & Stultz, S. C. (2005). *Steam: Its generation and use* (41st ed.). Barberton, OH: Babcock & Wilcox. variously paginated in 50 chapters.

Kostova, I. J., Hower, J. C., Mastalerz, M., & Vassilev, S. V. (2011). Mercury capture by selected Bulgarian fly ashes: Influence of coal rank and fly ash carbon pore structure on carbon efficiency. *Applied Geochemistry*, *26*, 18–27.

Koyama, S., Morimoto, T., Ueda, A., & Matsuoka, H. (1996). A microscopic study of ash deposits in a two-stage entrained-bed coal gasifier. *Fuel*, *75*, 459–465.

Külaots, I., Hurt, R. H., & Suuberg, E. M. (2004). Size distribution of unburned carbon in fly ash and its implications. *Fuel*, *83*, 223–230.

Li, W., & Bai, J. (2013). *Chemistry of ash from coal*. Beijing: Science Press. 330 p.

Liu, S. Q., Qi, C., Zhang, S. J., & Deng, Y. P. (2016). *Minerals in the Ash and Slag from Oxygen-enriched Underground Coal Gasification,* Minerals 6. http://dx.doi.org/10.3390/min6020027.

Llorens, J. F., Fernández-Turiel, J. L., & Querol, X. (2001). The fate of trace elements in a large coal-fired power plant. *Environmental Geology*, *40*, 409–416.

López-Antón, M. A., Díaz-Somoano, M., Spears, D. A., & Martínez-Tarazona, M. R. (2006). Arsenic and selenium capture by fly ashes at low temperature. *Environmental Science and Technology*, *40*, 3947–3951.

Lu, Y., Rostam-Abadi, M., Chang, R., Richardson, C., & Paradis, J. (2007). Characteristics of fly ashes from full-scale coal-fired power plants and their relationship to mercury adsorption. *Energy and Fuels*, *21*, 2112–2120.

Luo, Y., Glammer, D. E., Huhmann, B. L., & Catalano, J. G. (2011). Speciation of selenium, arsenic, and zinc in Class C fly ash. *Energy & Fuels*, *25*, 2980–2987.

Maier, H., Spliethoff, H., Kicherer, A., Fingerle, A., & Hein, K. R. G. (1994). Effect of coal blending and particle size on $NO_x$ emission and burnout. *Fuel*, *73*, 1447–1452.

Maize, K. (1993). Tires to energy: Where the rubber meets the grid. *Public Power*, *51*(1), 18–22.

Mardon, S. M., & Hower, J. C. (2004). Impact of coal properties on coal combustion by-product quality: Examples from a Kentucky power plant. *International Journal of Coal Geology*, *59*, 153–169.

Mastalerz, M., Hower, J. C., Drobniak, A., Mardon, S., & Lis, G. (2004). From in situ coal to fly ash: A study of coalmines and power plants from Indiana. *International Journal of Coal Geology*, *59*, 171–192.

Matjie, R. H., French, D., Ward, C. R., Pistorius, P. C., & Li, Z. (2011). Behaviour of coal mineral matter in sintering and slagging of ash during the gasification process. *Fuel Processing Technology*, *92*, 1426–1433.

Matjie, R. H., Li, Z., Ward, C. R., & French, D. (2008). Chemical composition of glass and crystalline phases in coarse gasification ash. *Fuel*, *87*, 857–869.

Matjie, R. H., Ward, C. R., & Li, Z. (2012a). Mineralogical transformations in coal feedstocks during carbon conversion, based on packed bed combustor tests, Part 1: Bulk coal ash studies. *Coal Combustion and Gasification Products*, *4*, 45–54.

Matjie, R. H., Ward, C. R., & Li, Z. (2012b). Mineralogical transformations in coal feedstocks during carbon conversion, based on packed bed combustor tests, Part 2: Behaviour of individual particles. *Coal Combustion and Gasification Products*, *4*, 55–67.

Meij, R. (1994). Trace element behavior in coal-fired power plants. *Fuel Processing Technology*, *39*, 199–217.

Moreno, N., Querol, X., Andres, J. M., Stanton, K., Towler, M., Nugteren, H., et al. (2005). Physico-chemical characteristics of European pulverized coal combustion fly ashes. *Fuel*, *84*, 1351–1363.

Mraw, S. C., De Neufville, J. P., Freund, H., Baset, A., Gorbaty, M. L., & Wright, F. J. (1983). The science of mineral matter in coal. *Coal science: Vol. 2*(pp. 1–63): Cambridge, MA: Academic Press.

Mudd, G. M., & Kodikara, J. (2000). Field studies of the leachability of aged brown coal ash. *Journal of Hazardous Materials*, *76*(2–3), 159–192.

Mukherjee, A. B., & Kikuchi, R. (1999). Coal ash from thermal power plants in Finland. In K. S. Sajwan, A. K. Alva, & R. F. Keefer (Eds.), *Biogeochemistry of trace elements in coal and coal combustion byproducts* (pp. 59–76). New York, NY: Kluwer Academic/Plenum Publishers.

Narukawa, T., Riley, K. W., & French, D. (2003). The distribution of trace elements through the ESPs of two Australian power stations. In *Proceedings 12th international conference on coal science, 2-6 November 2003, Cairns, Queensland, Australia* [CD publication].

Osborn, E. F., & Muan, A. (1960). *Phase equilibrium diagrams of oxide systems. The system* $CaO\text{-}Al_2O_3\text{-}SiO_2$*. Plate 1*. Columbus, OH: The American Ceramic Society and the Edward Orton Jr. Ceramic Foundation.

Patil, M. D., Eaton, H. C., & Tittlebaum, M. E. (1984). $^{57}$Fe Mössbauer spectroscopic studies of fly ash from coal-fired power plants and bottom ash from lignite-natural gas combustion. *Fuel*, *63*, 788–792.

Querol, X., Fernandez Turiel, J. L., & Lopez Soler, A. (1994). The behaviour of mineral matter during combustion of Spanish subbituminous and brown coals. *Mineralogical Magazine*, *58*, 119–133.

Reisch, M. S. (2015). Bromine comes to the rescue for Mercury power plant emissions. *Chemical and Engineering News*, *93*(11), 17–19.

Ribiero, J., Valentim, B., Ward, C. R., & Flores, D. (2011). Comprehensive characterization of anthracite fly ash from a thermo-electric power plant and its potential environmental impact. *International Journal of Coal Geology*, *86*, 204–212.

Rietveld, H. M. (1969). A profile refinement method for nuclear and magnetic structures. *Journal of Applied Crystallography*, *2*, 65–71.

Riley, K., French, D., Ward, C. R., Stephenson, L. G., & Gurba, L. W. (2014). Characterisation, impact and use of products from other technologies. In C. R. Ward, C. Heidrich, & O. Yeatman (Eds.), *Coal combustion products handbook* (2nd ed., pp. 409–439). Wollongong: Ash Development Association of Australia.

Rivera, N., Kaur, N., Hesterberg, D., Ward, C. R., Austin, R. E., & Duckworth, O. W. (2015). Chemical composition, speciation and elemental associations in coal fly ash samples related to the Kingston ash spill. *Energy and Fuels*, *29*(2), 954–967.

Senior, C. L., Bool, L. E., III, Huffman, G. P., Huggins, F. E., Shah, N., Sarofim, A., et al. (1997). *Fundamental study of mercury partitioning in coal fired power plant flue gas*. Proceedings of the Air & Waste Management Association's annual meeting & exhibition, Toronto, ON, Canada, June 8–13.

Senior, C. L., Sarofim, A. F., Zeng, T., Helble, J. J., & Mamani-Paco, R. (2000). Gas-phase transformations of mercury in coal-fired power plants. *Fuel Processing Technology*, *63*, 197–213.

Seredin, V. V., & Dai, S. (2012). Coal deposits as potential alternative sources for lanthanides and yttrium. *International Journal of Coal Geology*, *94*, 67–93.

Shah, P., Strezov, V., Prince, K., & Nelson, P. F. (2008). Speciation of As, Cr, Se and Hg under coal fired power station conditions. *Fuel*, *87*, 1859–1869.

Shah, P., Strezov, V., Strezov, C., & Nelson, P. F. (2007). Speciation of arsenic and selenium in coal combustion products. *Energy and Fuels*, *21*, 506–512.

Shannon, G. N., Matsuura, H., Rozelle, P., Fruehan, R. J., Pisupati, S., & Sridhar, S. (2009). Effect of size and density on the thermodynamic predictions of coal particle phase formation during coal gasification. *Fuel Processing Technology*, *90*, 1114–1121.

Silva, L. F. O., DaBoit, K., Serra, C., Mardon, S. M., & Hower, J. C. (2010). Fullerenes and metallofullerenes in coal-fired stoker fly ash. *Coal Combustion and Gasification Products*, *2*, 66–79.

Silva, L. F. O., Jasper, A., Andrade, M. L., Sampaio, C. H., Dai, S., Li, X., et al. (2012). Applied investigation on the interaction of hazardous elements binding on ultrafine and nanoparticles in Chinese anthracite-derived fly ash. *The Science of the Total Environment*, *419*, 250–264.

Srinivasachar, S., Helble, J. J., & Boni, A. A. (1990). Mineral behavior during coal combustion 1. Pyrite transformations. *Progress in Energy and Combustion Science*, *16*, 281–292.

Srinivasachar, S., Helble, J. J., Boni, A. A., Shah, N., Huffman, G. P., & Huggins, F. E. (1990). Mineral behavior during coal combustion 2. Illite transformations. *Progress in Energy and Combustion Science*, *16*, 293–302.

Taylor, S. R., & McLennan, S. M. (1985). *The continental crust: Its composition and evolution*. London: Blackwell. 312 p.

Tazaki, K., Fyfe, W. S., Sahu, K. C., & Powell, M. (1989). Observations on the nature of fly ash particles. *Fuel*, *68*, 727–734.

Thomas, M., Shehata, M., & Shashiprakash, S. (1999). The use of fly ash in concrete: Classification by composition. *Cement, Concrete and Aggregates*, 0149-6123. *21*(2), 105–110. http://dx.doi.org/10.1520/CCA10423J.

Trasande, L., Schechter, C. B., Haynes, K. A., & Landrigan, P. J. (2006). Mental retardation and prenatal methylmercury toxicity. *American Journal of Industrial Medicine*, *49*, 153–158.

Ural, S. (2005). Comparison of fly ash properties from Afsin-Elbistan coal basin, Turkey. *Journal of Hazardous Materials*, *B119*, 85–92.

Valentim, B., Guerdes, A., Flores, D., Ward, C. R., & Hower, J. C. (2009). Variations in fly ash composition with sampling location: Case study from a Portuguese power plant. *Coal Combustion and Gasification Products*, *1*, 14–24.

van Dyk, J. C., Melzer, S., & Sobiecki, A. (2006). Mineral matter transformation during Sasol-Lurgi fixed bed dry bottom gasification-utilization of HT-XRD and FactSage modelling. *Minerals Engineering*, *19*, 1126–1135.

Vaninetti, G. E., & Busch, C. F. (1982). Mineral analysis of ash data: A utility perspective. *Journal of Coal Quality*, *1*, 22–31.

Vassilev, S. V., & Vassileva, C. G. (2005). Methods for characterization of composition of fly ashes from coal-fired power stations: A critical overview. *Energy and Fuels*, *19*, 1084–1098.

Wagner, N. J., Coertzen, M., Matjie, R. H., & van Dyk, J. C. (2008). Coal gasification. In I. Suárez-Ruiz & J. C. Crelling (Eds.), *Applied coal petrology* (pp. 119–144): Burlington, MA: Academic Press.

Ward, C. R., & French, D. (2006). Determination of glass content and estimation of glass composition in fly ash using quantitative X-ray diffractometry. *Fuel*, *85*, 2268–2277.

Wilcox, J., Wang, B., Rupp, E., Taggart, R., Hsu-Kim, H., Oliveira, M. L. S., et al. (2015). Observations and assessment of fly ashes from high-sulfur bituminous coals and blends of high-sulfur bituminous and subbituminous coals: Environmental processes recorded at the macro and nanometer scale. *Energy & Fuels*, *29*, 7168–7177. http://dx.doi.org/10.1021/acs.energyfuels.5b02033.

Yu, D., Xu, M., Sui, J., Liu, X., Yu, Y., & Cao, Q. (2005). Effect of coal particle size on the proximate composition and combustion properties. *Thermochimica Acta*, *439*, 103–109.

Yudovich, Ya. E., & Ketris, M. P. (2005). Arsenic in coal: A review. *International Journal of Coal Geology*, *61*, 141–196.

Zhang, D. K., Jackson, P. J., & Vuthaluru, H. B. (1999). Low-rank coal and advanced technologies for power generation. *Proceedings of the engineering foundation conference on mineral matter in fuels: The impact of mineral impurities in solid fuel combustion*. New York: Kluwer Academic.

# Flue-gas desulfurization products and other air emissions controls

# 3

*K.J. Ladwig**, *G.M. Blythe*†
*Electric Power Research Institute, Palo Alto, CA, United States, †AECOM, Blythe, CA, United States

## 3.1 Introduction

Flue-gas desulfurization (FGD) systems have been used to limit the release of sulfur dioxide ($SO_2$) from coal-fired power plants since the late 1960s. The solids produced by FGD systems represent the second-largest coal combustion product (CCP) stream by volume, exceeded only by fly ash. In this chapter the various types of FGD systems in use and the solids they produce are described.

More recently, additional air emission controls have been employed at power plants that can also impact the characteristics of the high-volume CCPs. These include controls for sulfur trioxide ($SO_3$), hydrochloric acid (HCl), nitrous oxides ($NO_X$), and mercury. This chapter will also provide an introduction to these technologies and their possible impacts on CCPs.

Note that this chapter is largely updated from an Electric Power Research Institute report prepared by the authors (EPRI, 2008a), and is used with permission from EPRI.

## 3.2 FGD for $SO_2$ control

In general, FGD systems for $SO_2$ control can be categorized as "wet" or "dry," with wet systems being more common. Wet FGD systems are often called scrubbers and contact the flue gas with an alkaline slurry or solution. The solid produced is typically in the form of slurry that must be dewatered. The most common type of wet FGD system uses forced oxidation to produce a calcium sulfate dihydrate (gypsum) solid. Older and less common systems use inhibited oxidation to produce a calcium sulfite hemihydrate solid. There are few natural oxidation FGD systems (neither inhibited nor forced), and they can produce either (or both) gypsum or calcium sulfite hemihydrate as a solid by-product.

Dry FGD systems produce a nearly dry product that does not require dewatering. The primary dry FGD technologies employ either a spray drying process or a circulating fluid bed (CFB) process. The spray drying process typically uses slaked lime ($Ca(OH)_2$) slurry as the reagent, while the CFB processes typically use dry hydrated lime (also $Ca(OH)_2$) powder as the reagent. There are several variations on spray drying and CFB absorber processes, but all produce solids that are very similar. True dry

**Coal Combustion Products (CCP's).** http://dx.doi.org/10.1016/B978-0-08-100945-1.00003-4

injection processes, which generally use powdered sodium-based alkalis or hydrated lime as a reagent, are less commonly used for $SO_2$ control, but they are sometimes used for the removal of $SO_3$ and/or HCl from flue gas.

Both wet and dry FGD systems and the products they produce are described in the following sections of this chapter.

### 3.2.1 Wet FGD systems

Wet FGD systems consist of an absorber vessel typically located downstream of the particulate collection device (electrostatic precipitator (ESP) or baghouse). Fig. 3.1 illustrates a typical layout for a power plant with a wet FGD system. An aqueous slurry or solution containing the reagent, usually slaked lime or finely ground limestone, along with recirculated reaction products, is sprayed into the absorber and comes in contact with the flue gas. Some FGD systems use lime with a high magnesia (MgO) content, which leads to an increased liquid-phase alkalinity in the scrubber and can enhance $SO_2$ removal. Magnesia-enhanced lime is often called Mg-lime.

The calcium in the lime/limestone reacts with the sulfur scrubbed from the flue gas to produce calcium sulfite hemihydrate ($CaSO_3 \cdot ½H_2O$), gypsum ($CaSO_4 \cdot 2H_2O$), or a mixture of the two. Table 3.1 shows the primary sorbents and products for wet and dry FGD systems. The solids are collected in a slurry in a reaction tank at the bottom of the absorber. The slurry typically contains 10%–30% suspended solids.

The design and operation of the wet FGD system determine which type of solid is formed. Calcium sulfite would be the only solid product formed in the absence of oxygen in the flue gas as well as without forced oxidation. However, since all flue gases have some oxygen content, a portion of the sulfite is oxidized to the sulfate form. If the oxidation is <15%, all of the sulfate gets incorporated into the calcium sulfite crystal lattice. So even though the solids might contain up to 15% sulfate, they look and

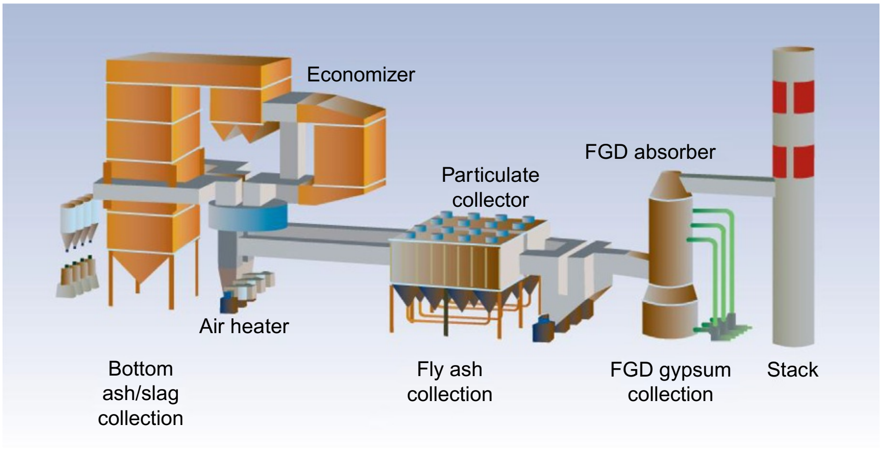

**Fig. 3.1** Typical coal-fired power plant layout.

**Table 3.1** Sorbents and products of wet and dry FGD systems

| Process | Wet | | | Dry (spray dryer or circulating fluid bed absorbers) |
|---|---|---|---|---|
| Oxidation mode | Inhibited oxidation | Natural oxidation | Forced oxidation | Natural oxidation |
| Primary sorbents | Lime, Mg-lime, limestone | Lime, Mg-lime, limestone | Limestone, lime (some low-sulfur-coal systems) | Slaked or hydrated lime, alkaline fly ash, sodium alkali (less commonly) |
| Primary products | Calcium sulfite hemihydrate + typically <20% FGD gypsum<br>$CaSO_3 \cdot \frac{1}{2}H_2O + CaSO_4 \cdot 2H_2O$ | Calcium sulfite hemihydrate + FGD gypsum (gypsum percentage ranges from <20% to 100%, depending on natural oxidation level)<br>$CaSO_3 \cdot \frac{1}{2}H_2O + CaSO_4 \cdot 2H_2O$ | FGD gypsum<br>$CaSO_4 \cdot 2H_2O$ | Calcium sulfite hemihydrate + gypsum + fly ash + unspent sorbent<br>$CaSO_3 \cdot \frac{1}{2}H_2O + CaSO_4 \cdot 2H_2O$ + fly ash<br>or sodium sulfate + fly ash |

behave as 100% calcium sulfite hemihydrate. As the oxidation exceeds 15%, gypsum begins to form as a separate solid phase.

FGD systems tend to be most reliable if they operate in such a way that they produce either all calcium sulfite hemihydrate (including up to 15% sulfate) or all gypsum. Thus it is most desirable to control the sulfite oxidation at 15% or less, or otherwise near 100%. Some FGD systems naturally operate in these regimes, but most require that the oxidation percentage be controlled, either by employing forced or inhibited oxidation. Both oxidation approaches are discussed below.

Some wet FGD systems use performance additives to enhance the amount of liquid-phase alkalinity available in the scrubbing slurry. Typical additives include adipic acid, dibasic acid (i.e., DBA, a by-product that is a mixture of adipic, glutaric, and succinic acids), formic acid, sodium formate, and magnesium oxide or carbonate. Most of these additives can be used in either inhibited or forced oxidation FGD systems, but magnesium (e.g., Mg-lime) is generally used only in inhibited or low natural oxidation systems, as magnesium sulfite is the alkaline species formed in the FGD liquor at high magnesium concentrations. In a forced oxidation system, this sulfite would all become oxidized to the sulfate form, and there would be no benefit from the magnesium. These performance additives can impact the solid by-products from a wet FGD system, either directly through their presence (e.g., organic material content of the dewatered by-product) or by potentially modifying the solid by-product crystal habit and/or dewatering properties (Radian International LLC, 1997).

### 3.2.1.1 Forced oxidation systems

Forced oxidation wet systems are by far the most common type of FGD units at coal-fired power plants. Forced oxidation systems pump air into the absorber reaction tank (sometimes called the mix tank or recycle tank) through distribution devices, typically called spargers. This increases the effective oxygen-to-$SO_2$ ratio and is controlled to achieve essentially 100% sulfite oxidation. Some very low-sulfur coal FGD systems also achieve 100% or nearly 100% oxidation without forced oxidation.

The product resulting from forced oxidation systems is a relatively pure gypsum, referred to as FGD gypsum. FGD gypsum settles and dewaters much more effectively than calcium sulfite hemihydrate. Forced oxidation systems generally have hydrocyclones for primary dewatering, as well as centrifuges, vacuum drums, or most commonly vacuum belt filters for secondary dewatering. A typical forced oxidation wet FGD dewatering system is shown in Fig. 3.2. FGD gypsum that will be used for wallboard is subjected to a water spray wash during the second dewatering step to remove soluble species, such as chloride, from the gypsum product.

FGD gypsum can be dewatered to produce a moist (7%–12% moisture) but free-flowing solid that is easily handled. FGD gypsum is fine-grained, with particle sizes <100 μm and a mass mean of 25–50 μm.

Limestone forced oxidation has been the dominant SO2 control technology installed in the last 20 years, and the production of FGD gypsum has nearly tripled over the past 10 years. FGD gypsum is chemically equivalent to mined gypsum and can therefore be used in many of the same applications. FGD gypsum is relatively

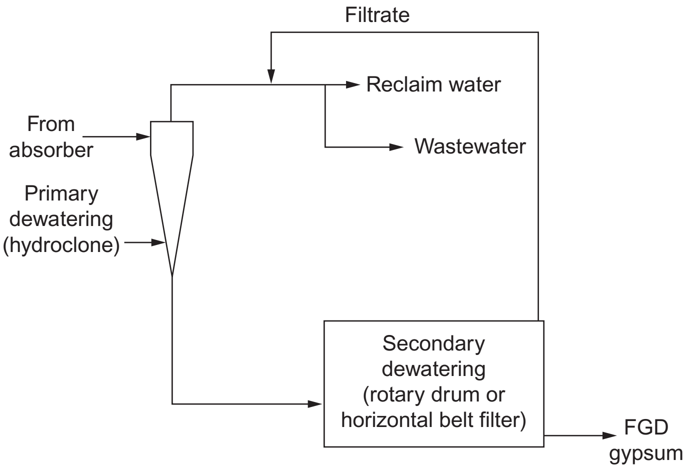

**Fig. 3.2** Typical dewatering system for forced oxidation wet FGD.

**Table 3.2** Statistical summary of FGD gypsum total composition data

| | Count | % BDL | Min | Median | 95th percentile | Max | Normal | Lognormal |
|---|---|---|---|---|---|---|---|---|
| Al | 32 | 0 | 61.1 | 209 | 1120 | 1610 | No | Yes |
| As | 32 | 0 | 1.98 | 2.86 | 8.57 | 11.1 | No | No |
| B | 32 | 0 | 2.67 | 13.2 | 123 | 387 | No | Yes |
| Ba | 32 | 0 | 0.91 | 6.38 | 29.5 | 55.2 | No | Yes |
| Be | 32 | 28 | BDL | 0.020 | 0.098 | 0.127 | No | No |
| Ca | 32 | 0 | 199,000 | 237,000 | 264,000 | 268,000 | Yes | Yes |
| Cd | 32 | 0 | 0.006 | 0.066 | 0.234 | 0.369 | No | Yes |
| Co | 32 | 19 | BDL | 0.230 | 0.578 | 0.716 | No | No |
| Cr | 32 | 0 | 0.45 | 2.19 | 8.64 | 14.8 | No | Yes |
| Cu | 32 | 0 | 0.25 | 1.16 | 2.61 | 3.17 | Yes | Yes |
| Fe | 32 | 0 | 130 | 811 | 1740 | 1820 | Yes | No |
| Hg | 31 | 0 | 0.007 | 0.194 | 0.917 | 1.41 | No | Yes |
| K | 32 | 0 | 29.0 | 197 | 540 | 744 | No | Yes |
| Li | 32 | 9 | BDL | 0.23 | 1.47 | 2.01 | No | Yes |
| Mg | 32 | 0 | 50.3 | 1090 | 2960 | 5860 | No | No |
| Mn | 32 | 0 | 0.83 | 9.18 | 62.4 | 129 | No | Yes |
| Mo | 32 | 0 | 0.044 | 0.560 | 2.24 | 4.00 | No | Yes |
| Na | 32 | 0 | 10.2 | 24.0 | 720 | 1300 | No | No |
| Ni | 32 | 3 | BDL | 1.11 | 2.41 | 2.86 | Yes | Yes |
| P | 32 | 0 | 4.47 | 32.3 | 126 | 180 | No | Yes |
| Pb | 32 | 16 | BDL | 0.98 | 1.95 | 8.30 | No | No |
| S | 32 | 0 | 156,000 | 188,000 | 206,000 | 208,000 | Yes | Yes |
| Sb | 32 | 0 | 0.051 | 0.151 | 1.44 | 4.97 | No | No |
| Se | 32 | 0 | 1.44 | 5.24 | 26.8 | 32.0 | No | Yes |
| Si | 32 | 0 | 69.0 | 252 | 589 | 1050 | No | Yes |
| Sr | 32 | 0 | 70.5 | 170 | 369 | 405 | No | Yes |
| Tl | 31 | 3 | BDL | 0.011 | 0.035 | 0.062 | No | Yes |
| V | 32 | 0 | 0.32 | 1.61 | 5.87 | 8.57 | No | Yes |
| Zn | 32 | 0 | 1.76 | 5.84 | 17.0 | 23.3 | No | Yes |

*Notes*: (1) All concentrations in mg/kg; (2) *BDL*, below method detection limits; (3) Hg was not analyzed in sample 260. There was one Tl outlier that was not included in the analysis; and (4) normality was determined using the Shapiro-Wilk test.

From EPRI. (2011). *Composition and leaching of FGD gypsum and mined gypsum*. Palo Alto, CA: EPRI. 1022146.

pure, with a median $CaSO_4{\cdot}2H_2O$ content of 97%, compared with 88% for raw mined gypsum (EPRI, 2011). Table 3.2 contains composition data for 32 FGD gypsum samples reported in EPRI (2011).

In 2015, 32.7 million tons of FGD gypsum were produced, and 17.0 million tons (52%) were used (ACAA, 2016). FGD gypsum is a high-value product that is most often used as feedstock for wallboard production (11.3 million tons in 2015).These products typically have relatively strict product specifications imposed by the wallboard manufacturers, including free moisture content, gypsum purity, particle size distribution, and maximum combustibles, chloride, total soluble salt, mercury, and/

or ammonia content. Washing is often required during the secondary dewatering step at the power plant to meet chloride and ammonia specifications.

Other applications that used between 0.8 and 1.6 million tons of FGD gypsum in 2015 were cement production, agricultural applications, structural fills, and mining applications. Agricultural applications are a fast-growing area, due to the positive effect of gypsum on soil properties and crop yield (Ladwig, 2016). More recently, research has focused on the role of gypsum in mitigating phosphorus release from agricultural fields.

Gypsum that cannot be used may be landfilled after dewatering, or it may be "stacked." FGD systems that use a gypsum stack typically do not have primary or secondary dewatering, and instead sluice their absorber blow down to a diked area where the solids settle to a relatively low free-moisture content; the water is reclaimed and returned to the FGD system, or is treated and discharged. This area is managed so that with time, the settled gypsum level raises above grade, producing a stack of settled gypsum solids that drains to a water content of about 25%. Stacking or segregated management in a landfill allows the possible reclaiming of the gypsum for later use.

### *3.2.1.2 Inhibited- or low-natural oxidation FGD systems*

Inhibited- or low-oxidation systems are typically older systems, and there has been a decreasing number in operation because of plant retirements and forced oxidation conversions. Inhibited-oxidation systems generally add sodium thiosulfate or elemental sulfur (which reacts with sulfite to form thiosulfate) to the FGD system. The thiosulfate ion acts as a sulfite oxidation inhibitor. Some high-sulfur FGD systems naturally operate at low-sulfite oxidation percentages. The ratio of sulfur dioxide to oxygen in the flue gas is important in controlling oxidation percentages, so high-sulfur systems tend to operate at lower natural oxidation percentages than low-sulfur systems.

Low-oxidation systems produce calcium sulfite hemihydrate mixed with a small amount of excess lime or limestone and some inert material (fly ash and inert minerals from the dissolved lime or limestone) in the absorber slurry. Most of the slurry is recirculated in the FGD system, but a portion called the blowdown or absorber bleed is removed to maintain proper chemistry within the system. The blowdown slurry from the absorber vessels is usually dewatered in thickeners followed by a centrifuge or vacuum filter, although some systems blow down directly from the absorbers to a pond. In plants that have dewatering equipment, the water separated from the solids is usually returned to the FGD absorbers.

The calcium sulfite solids are very difficult to dewater. Even though many inhibited (or low natural oxidation) systems have two stages of dewatering, the by-product still contains 30%–55% moisture. The resulting wet sludge is thixotropic and difficult to handle, so it is often mixed with fly ash, lime, and sometimes other additives in a pug mill to produce a relatively dry, stabilized material. This stabilized mixture, sometimes referred to as fixated scrubber sludge, is often landfilled, but can also be used as structural fill or mine fill. A typical low-sulfite oxidation dewatering system is shown in Fig. 3.3.

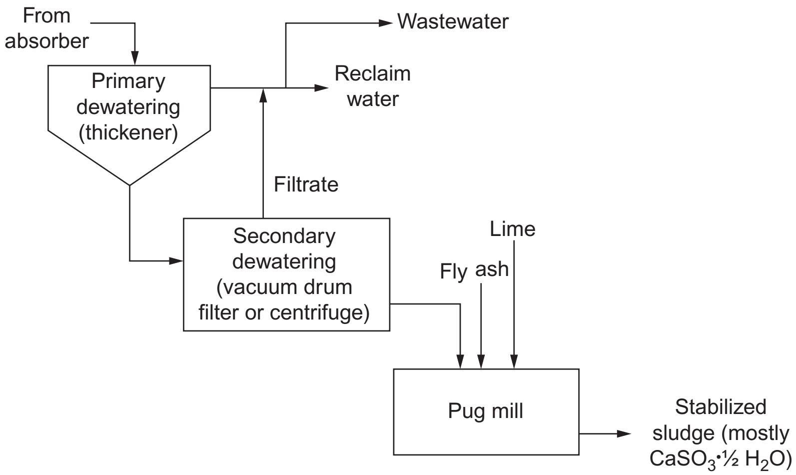

**Fig. 3.3** Typical dewatering system for low-oxidation FGD system.

There are relatively few established beneficial uses for calcium sulfite hemihydrate. In 2015, 11.3 million tons of calcium sulfite hemihydrate by-products were produced by wet FGD systems, and only 1.2 million tons (11%) were used (ACAA, 2016). It is unlikely that new inhibited or low natural oxidation systems will be installed, and many of the existing units have been converted to forced oxidation. In the last 10 years, the production of calcium-sulfite solids has decreased by about 35% (ACAA, 2016). However, the 2015 US EPA Effluent Limitations Guidelines (ELGs) have placed strict limits on the concentrations of mercury, selenium, arsenic, and nitrate/nitrite in FGD wastewater discharged to public surface waters. Since these new regulations, interest has been revived in an inhibited-oxidation FGD operation. As described above, the calcium-sulfite hemihydrate produced does not dewater well, so a considerable amount of water is managed with the solid by-product. Therefore, a separate chloride purge stream (which would be subject to ELG limitations) could possibly be eliminated.

While all modern wet scrubbers are preceded by an ESP or baghouse for primary particulate control, a very few older units built in the 1970s and 1980s are also used for primary particulate control instead of an ESP or baghouse. These scrubbers typically operate at a high-pressure drop (15–25 in $H_2O$) to provide the energy required for efficient particle collection. These units produce a mixture of fly ash and calcium-sulfite hemihydrate and/or gypsum.

### *3.2.2 Dry FGD systems*

Dry FGD technologies include spray drying, which typically uses slaked lime as the reagent, CFB absorbers, which use hydrated lime powder as a reagent, and true dry injection systems, which most often use powdered sodium-based alkalis or hydrated lime as a reagent. These FGD systems produce a dry product that does not require dewatering.

#### *3.2.2.1 Spray dryer absorber and CFB absorber systems*

Spray dryer-based FGD historically has been the most common “dry” FGD technology used in the United States dating back to the early 1980s. However, it is somewhat of a misnomer to call this technology “dry,” as a slaked-lime-based aqueous slurry is actually fed to the spray dryer absorber (SDA). The slurry is finely atomized in the absorber, and heat from the flue gas evaporates all of the moisture to produce a dry (typically $<1\%$ moisture) solid product.

In most SDA FGD systems, the spray dryer vessel is located upstream of the primary particulate control device (fabric filters are most commonly used due to their $SO_2$ removal benefits compared to an ESP). Thus the spray-dried by-product is mixed with the normal fly ash produced by the unit. In recent years, and more commonly in Europe, systems have been built with ESP units upstream of the spray dryer vessels to collect most of the fly ash, thereby retaining the fly ash as a high-value product for use in concrete. In this case the SDA material may contain little or no fly ash. The amount of fly ash mixed with the SDA material is variable, depending on how the ESP is operated.

Most SDA systems have what is called a “two-point” solids discharge, as some solids drop out at the bottom of the spray dryer vessel, while the majority are entrained with the flue gas leaving the absorber vessel and are collected in a downstream fabric filter or ESP. The solid material that drops out at the bottom of the spray dryer tends to be wetter and coarser than the solids collected in the fabric filter or ESP. The two streams are generally combined when sent to disposal or reuse.

The SDA solid is a mixture of calcium-sulfite hemihydrate, gypsum, excess slaked lime, and calcium carbonate. In systems where fly ash is not precollected in an ESP, the solids collected in the particulate control device after the SDA unit contain $\sim$72% fly ash, 15% calcium sulfite, 9% gypsum, 1% unreacted lime, and 3% water (EPRI, 2007a). These percentages vary with the sulfur and ash concentrations in the coal fired, and with the percentage of $SO_2$ removal achieved. The solids generally produce a high pH when wetted due to the excess slaked lime and the alkaline nature of the fly ash when the process is applied to western coal.

Some SDA systems employ a percentage of recycle of the spray-dried solids with the fresh slaked-lime slurry feed to the atomizers. This recycle improves overall lime utilization and improves slurry drying characteristics. In systems that employ recycle, it is generally the fabric filter or ESP catch solids that are recycled, not the spray dryer dropout material, which is more difficult to handle.

In 2015, production of $\sim$1.3 million tons of dry products was reported (ACAA, 2016). The dry product collected from the SDA is mostly landfilled, with less than 20% used, primarily in mining applications. Ongoing research is evaluating the use of SDA material in concrete products (EPRI, 2015). Products low in fly ash content are also being evaluated for use in agricultural applications (EPRI, 2013).

CFB systems take a different approach to introducing water to cool and partially saturate the flue gas, the alkaline reagent, and recycled solids. In this technology the three streams are introduced to the reactor vessel separately. Water is sprayed into the flue gas as it enters the absorber vessel, typically in an up-flow configuration, and the hydrated lime and recycled solids are introduced separately as dry powders. Since the hydrated lime and recycled solids are introduced separately as dry powders rather than as a slurry as in the SDA process, the amount of each that can be added is not limited by the need to avoid flue-gas moisture saturation. This makes the CFB absorber process better suited to higher sulfur coals and to achieving higher $SO_2$ removal percentages, which can potentially produce a by-product with less excess lime content compared to the SDA process. Otherwise, the by-products from the SDA and CFB absorber processes are very similar.

### *3.2.2.2 Dry injection systems*

There are some plants that employ true dry FGD processes for $SO_2$ control by dry injection of finely ground sodium alkali, such as sodium bicarbonate or trona (sodium sesquicarbonate), or hydrated lime into the flue gas upstream or downstream of the air heater and upstream of an ESP or fabric filter. Dry injection processes are sometimes mass-transfer limited for $SO_2$ removal. Thus an excess of the alkali is often injected to increase the particle surface area available for absorbing and reacting with flue gas $SO_2$.

For sodium-based dry injection systems, the dry injection by-product is typically a mixture of sodium sulfate and excess sodium alkali, usually in the form of sodium carbonate. This material is collected along with fly ash in either an ESP or a baghouse. Due to the highly water soluble sodium salts present, sodium-based dry injection solids are mostly landfilled and not reused. Leachates from landfilling of this material can be very alkaline and can have a high dissolved salt content. For systems based on hydrated lime reagent, the by-product is similar to that from the semidry process, such as the SDA process, except the percentage of excess lime is greater and the free moisture content is lower.

Dry injection systems are less commonly used in the United States for $SO_2$ control than wet FGD or semidry FGD technologies. However, they are being used more frequently for $SO_3$ and HCl control, and will be discussed in more detail in a following section.

### *3.2.2.3 Furnace sorbent injection systems*

Another dry FGD technology that was developed in the 1970s and 1980s involves injection of limestone or hydrated lime into the upper furnace; this process is often called furnace sorbent injection, or FSI. The injected sorbent is collected along with the fly ash in the existing ESP or fabric filter. The technology is rarely applied in the United States today. The utilization of the injected calcium-based sorbents is typically low (10%–25%), so a large excess of reagent is required. Thus the technology typically adds a significant amount of calcium sulfate, calcium carbonate, lime (CaO), and/or hydrated lime ($Ca(OH)_2$) to the fly ash stream, resulting in a solid that produces a high pH when wetted. FSI solids are typically landfilled.

## 3.3 $SO_3$ controls

Coal combustion results in the liberation of sulfur primarily as sulfur dioxide ($SO_2$). Sulfur trioxide ($SO_3$) and/or sulfuric acid ($H_2SO_4$) is present in the flue gas from coal firing because of the further oxidation of a small percentage of the coal sulfur (typically 0.5%–1.5%) to $SO_3$ rather than $SO_2$. As the flue gas cools across the air heater, the $SO_3$ combines with flue-gas moisture to form gas-phase sulfuric acid. At the inlet to a wet FGD absorber, a submicron-diameter sulfuric acid mist is formed when the flue gas is humidified and cooled, which causes the gas-phase sulfuric acid to rapidly condense. This submicron acid mist behaves like small particles rather than as a gas in the wet absorber and is not removed at high efficiency. The mist that exits the scrubber very effectively scatters light, which leads to a visible plume opacity (sometimes referred to as blue plume). Other adverse effects can result from having $SO_3$/sulfuric acid in the flue gas, such as ESP and duct corrosion, air heater plugging, or the need to increase air heater outlet gas temperatures to avoid such problems.

The installation of selective catalytic reduction (SCR) controls for nitrous oxides can also increase the $SO_3$ mist. SCR catalysts are oxidation catalysts and can oxidize other flue-gas species, such as $SO_2$ and mercury. Typically, 0.5%–1.5% of the flue gas $SO_2$ is oxidized to $SO_3$ across an SCR catalyst.

As $SO_3$ is formed in the furnace and in downstream SCR systems, $SO_3$ controls can be implemented anywhere in the flue-gas path from the furnace to just upstream of the stack. Control technologies include injected sorbents, fuel additives, and wet ESPs. Each of these technologies is described in the following subsections.

### *3.3.1 Dry sorbent injection*

Dry sorbent injection (DSI) upstream of the ESP is part of the $SO_3$ mitigation measures installed at several plants. In addition to removing $SO_3$, DSI systems can also be used to remove other acid gases, such as HCl. Dry sorbents remove $SO_3$ by a gas-solid reaction. The alkaline sorbent is pneumatically injected upstream or downstream of the air heater and upstream of the existing particulate control device. The reaction products and unreacted sorbent are removed, along with the fly ash by the particulate control device. This section describes both calcium-based (hydrated lime) and sodium-based (trona or sodium bicarbonate) DSI.

#### *3.3.1.1 Hydrated lime powder injection*

In this process, dry hydrated lime powder ($Ca(OH)_2$) is injected into the flue gas upstream of the ESP or baghouse. It can be injected upstream or downstream of the air heater, depending on the application. Another possible approach is to inject hydrated lime directly upstream of a wet FGD system. Fig. 3.4 is a simplified process flow diagram for hydrated lime injection between the air heater and an ESP.

Early tests with hydrated lime injection required high injection rates to achieve $SO_3$ removal, many times higher than the stoichiometric rate (Peterson, Jones, Meserole, & Rhudy, 1993). This resulted in significant amounts of excess sorbent in the fly ash and

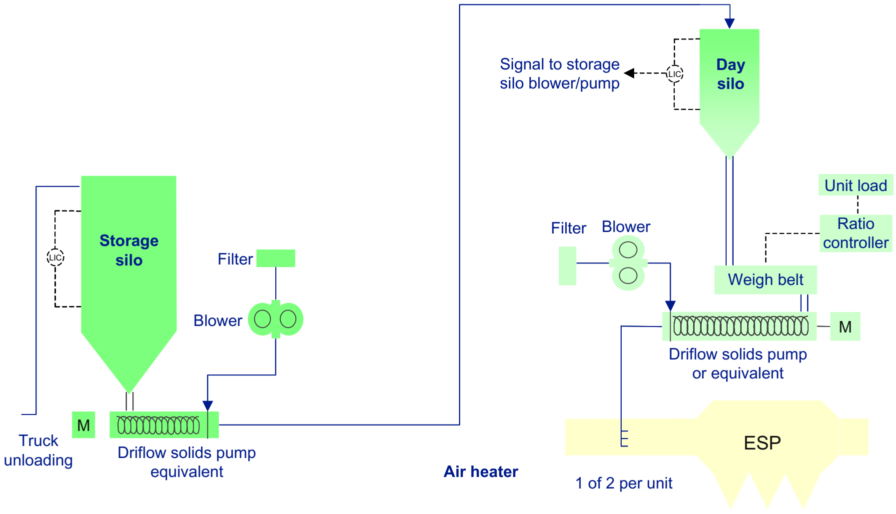

**Fig. 3.4** Simplified process flow diagram for hydrated lime powder injection.

caused the ESP performance to degrade due to increased resistivity. More recent tests on $SO_3$ control using hydrated lime with a high-specific surface area have greatly reduced injection rates compared to conventional hydrated lime (Gale, 2006). Lime companies continue to optimize their hydration products to provide greater performance with lower injection rates for acid gas removal. However, negative impacts on ESP performance are still a drawback associated with lime-based sorbent injection. Some newer coal-fired units and some control technology retrofit configurations avoid this issue by installing a new baghouse downstream of a new or existing ESP and by injecting the hydrated lime between the ESP and baghouse.

Hydrated lime injection upstream of the primary particulate control device increases the quantity of solids collected with the fly ash by the particulate control device. For example, at a sorbent injection rate of 1.5 lb/h/kacfm (0.0004 $kg/m^3/s$), sufficient for about 60%–70% $SO_3$ removal, and for a typical bituminous coal (~8% ash in the coal), the amount of solids removed by the ESP would increase by about 12% compared to normal operation. This additional 12% of material would be a mixture of calcium sulfate, calcium hydroxide, calcium carbonate, and calcium sulfite.

Calcium-based sorbents are expected to have much less impact on fly ash for use in concrete than sodium-based sorbents (SBSs; EPRI, 2014). When calcium-based sorbents are used in low to moderate quantities, the amount of sorbent added may be sufficiently modest in that the reactions in concrete will continue as normal. If calcium-based sorbents are used at high injection rates, the calcium can overwhelm the fly ash and may render it unsuitable for use in concrete. In Portland cement systems, early or flash set can occur if calcium is too dominant in the system. Increased alkalis could also adversely affect the use of the ash in concrete.

EPRI (2014) evaluated the impact of calcium-based sorbent injection on fly ash composition and leaching. Data were limited, but with the exception of the increased calcium and sulfate, other changes in composition and leaching were relatively small. Detailed testing at a plant burning subbituminous coal found only limited impact on leaching of trace constituents. As the native pH of the fly ash was strongly alkaline, the addition of the lime did not increase the fly ash pH significantly in this test. As a result, greater changes in the leaching of trace constituents might be expected for plants burning bituminous coal, which typically have a lower native fly ash pH.

No significant impacts on FGD solids are expected from hydrated lime injection. Any excess lime collected in a wet FGD absorber would tend to be utilized as an FGD reagent, offsetting some of the normal lime or limestone reagent feed to the absorber. Some testing and full-scale operation have been conducted where the hydrated lime is actually injected between the ESP and wet scrubber, rather than upstream of the ESP.

### *3.3.1.2 Sodium-based DSI*

Sodium-based DSI for $SO_3$ and/or HCl removal typically employs either trona or sodium bicarbonate as the alkaline reagent. Trona is a hydrated sodium carbonate-bicarbonate compound ($Na_2CO_3{\cdot}NaHCO_3{\cdot}2H_2O$). It is an evaporite mineral mined principally from the Green River formation in Wyoming and is the primary source of sodium carbonate in the United States. Sodium bicarbonate ($NaHCO_3$) is a commercially produced sodium-based alkali material.

When either reagent is injected into the flue gas at air heater inlet or exit temperatures, they calcine to form soda ash. The soda ash then reacts with $SO_3$ to form sodium sulfate and/or with HCl to form sodium chloride. The excess sodium carbonate, sodium sulfate, and/or sodium chloride are collected along with fly ash in the ESP or baghouse. The process flow diagram for trona or sodium bicarbonate injection looks similar to that shown in Fig. 3.4 for hydrated lime injection, although additional measures may be required to ensure the reagent stays very dry so as to maintain good handling properties. Also, in some cases, trona is ground onsite just prior to injection into the flue gas to improve its effectiveness.

Unlike hydrated lime, injection of sodium-based sorbents can enhance ESP performance. While the benefits of sodium injection are well known for treating sodium depletion in hot-side ESPs, sodium injection can also be used as a resistivity conditioning agent in cold-side ESPs (Peterson et al., 1993; White, 1974).

Similar to hydrated lime, sodium-based DSI increases the quantity of solids collected with the fly ash. Low to moderate injection rates correspond with approximately a 4%–12% increase in fly ash mass for a typical bituminous coal. The extra material in the fly ash would be a mixture of sodium sulfate, sodium carbonate, and possibly sodium chloride, which would add ~1–4 wt% sodium to the fly ash. Higher injection rates result in a greater increase in solids and sodium concentration.

At high injection rates, the concentrations of soluble sodium-sulfur salts and available alkalis will likely preclude the use of the CCP in typical concrete applications. For lower injection rates, it may be possible to use sodium sorbents and maintain fly ash compatible with use in concrete. The existing data do not support defining a clear line that delineates the injection rate that yields an acceptable ash. Some plants report marketing fly ash for use in concrete from a unit using sodium sorbent to control $SO_3$, while other plants report that using sodium sorbents at even low injection rates for $SO_3$

precludes marketing the resultant ash. The high solubility of the sodium sulfate and increased leaching of trace constituents in some cases may also preclude use in structural fills and other applications.

Because the sodium-based dry injection process typically requires a significant excess of the injected alkali reagent to achieve moderate to high $SO_3$ removal levels, there could be a significant excess of alkali added to the fly ash. Thus like hydrated lime, trona or sodium bicarbonate injection could significantly increase the pH of fly ash from bituminous coal. EPRI (2010, 2014) evaluated the impact of SBS injection on fly ash composition and leaching. The primary impacts on the total by-product composition are increases in sodium and sulfur concentrations. However, SBSs have been observed to have a much greater impact on trace constituent leaching than calcium-based sorbents. Leach test concentrations of several trace constituents increased significantly in trona-impacted samples relative to baseline (Dan, Zimmerman, Liu, Shi, & Wang, 2013). The impact on leaching is postulated to be related to association with the highly soluble sodium sulfate salts and is dependent on the ratio of sodium-based reaction products relative to the bulk fly ash.

No impacts on FGD solids would be expected, as excess sodium carbonate and the sodium sulfate formed should be collected by an ESP at high efficiency, due to corresponding improvements in ESP performance during sodium-based DSI.

### 3.3.2 Aqueous SBS injection

The SBS injection process injects a clear, aqueous solution of sodium bisulfite ($NaHSO_3$), sodium sulfite ($Na_2SO_3$), or, more commonly, sodium carbonate ($Na_2CO_3$) into the flue gas. The injection location can be either upstream of the air heater (upstream of an SCR and/or between an SCR and the air heater) or less commonly downstream of the air heater (between the air heater and cold-side ESP). Upstream (of the air heater) injection is preferred by the process developers (Moser, 2007).

The reagent is injected as a solution through an array of air-atomized nozzles and is fed at relatively low molar feed ratios, typically not much more than the theoretical amount required to react with all of the $SO_3$ in the flue gas to form a sodium sulfate salt. Similar to sodium-based DSI, the reaction products are salts containing sodium and sulfate, which are collected along with fly ash in the cold-side ESP, baghouse, or other particulate control device. Fig. 3.5 is a typical process flow diagram for the process.

Initially, it was thought that sodium sulfate ($Na_2SO_4$) was the primary reaction product. However, it is apparent that other sodium species can be formed with sodium to $SO_3$ molar ratios closer to 1:1 [e.g., sodium bisulfate ($NaHSO_4$), which is sticky like ammonium bisulfite (ABS)]. In installations where injection occurs upstream of the air heater, the molar ratio of sodium in the reagent to $SO_3$ in the flue gas is controlled near 2:1. This typically ensures high $SO_3$ removal efficiency and facilitates the formation of sodium sulfate as the primary by-product.

The SBS reagent can consist of commercially available sodium carbonate, sodium bisulfite, or sodium sulfite, the latter of which is a by-product that is typically a mixture of sodium bisulfite and sulfite. The reagent can be received as a clear solution (typically 25–30 wt% dissolved solids) or as a dry powder. The dry powder must

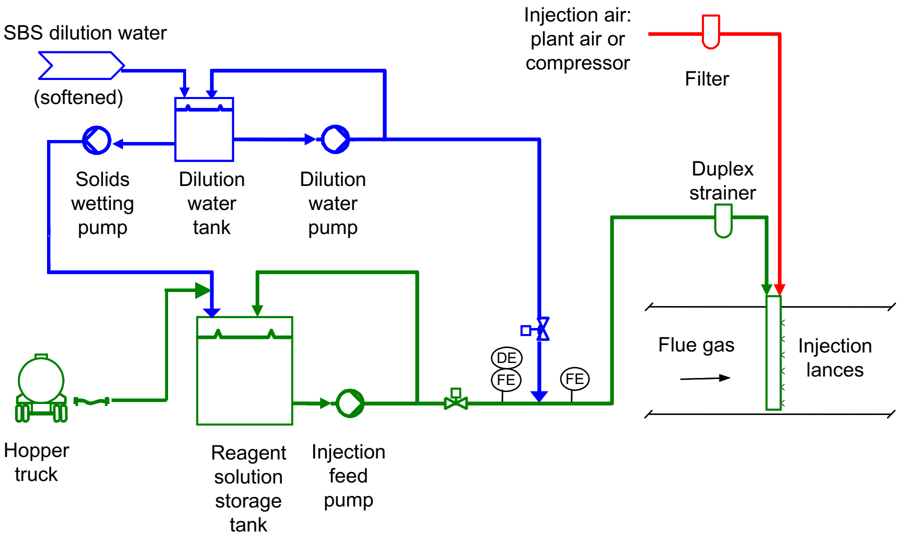

**Fig. 3.5** Simplified process flow diagram for the SBS injection process.

be mixed with softened plant water to obtain the desired reagent concentration before injection.

The impacts to the fly ash are similar to these for trona or sodium bicarbonate injection. However, because the SBS process typically is operated with a high utilization of the injected alkali reagent, there should not be as much excess alkali added to the fly ash. SBS injection process adds about 2–4 wt% to the fly ash mass collected in the particulate control device as sodium sulfate. This corresponds with about 1–2 wt % added to the fly ash when reported as $Na_2O$.

Sodium can be used to condition fly ash resistivity in cold-side ESP applications, so no adverse effects on ESP performance are expected with SBS injection. Therefore no significant impacts of the SBS process are expected downstream of the particulate control device to the FGD solids.

### *3.3.3 Magnesium-based sorbent injection*

Magnesium oxide and magnesium hydroxide have been injected into the furnace and into the flue gas to control $SO_3$. In both cases, the Mg-based sorbents are injected as a slurry and react with $SO_3$ to form magnesium sulfate ($MgSO_4$).

In furnace injection, magnesium hydroxide is typically fed as a slurry into the upper furnace, where temperatures are lower, to prevent dead burning of the sorbent (EPRI, 2002). When magnesium hydroxide slurry is injected into the furnace, the water evaporates and leaves a solid MgO particle. The MgO solid reacts with $SO_3$ in the gas phase to form magnesium sulfate ($MgSO_4$). Magnesium sulfate is water soluble and therefore unlikely to form hard deposits in the boiler. The magnesium sulfate solids are removed along with fly ash in the downstream particulate control device.

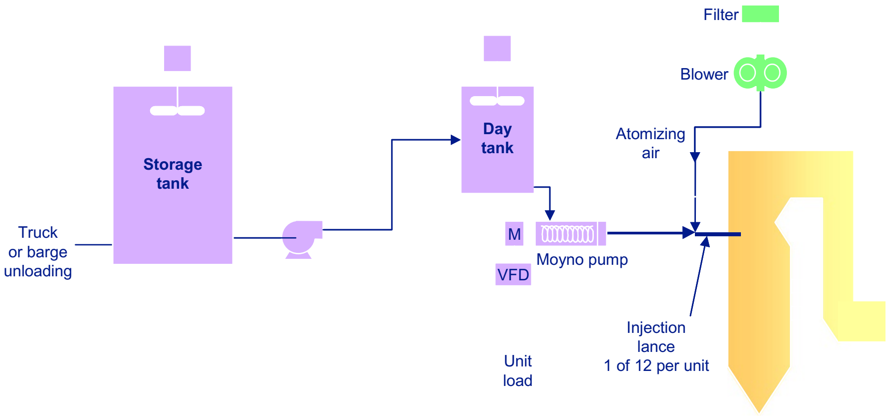

**Fig. 3.6** Example process flow diagram for furnace injection of magnesium hydroxide slurry.

Fig. 3.6 is an example process flow diagram for how a magnesium hydroxide injection in the furnace would typically be implemented. MgO or $Mg(OH)_2$ sorbent can also be injected post combustion in the flue gas, typically downstream of the economizer and/or SCR and upstream of the air heater.

Magnesium hydroxide slurry is available as a commercial product, or it can be produced onsite at plants that are equipped with a Thiosorbic lime FGD system and have a process to convert the calcium sulfite by-product to gypsum. Required sorbent injection rates will depend on the coal sulfur, percent $SO_3$ removal required, and whether the injection locations have been optimized.

Implementation of furnace or flue-gas injection would increase the fly ash mass rate by about 2%–8%. The increased mass in the fly ash would consist of a mixture of magnesium hydroxide, magnesium sulfate, and magnesium carbonate if commercial magnesium hydroxide is used. If by-product magnesium hydroxide is used, the amount in the fly ash would be increased by about one-third. The increased mass would be due to gypsum impurities in the magnesium hydroxide.

Since a considerable excess of the alkaline additive is generally required, the pH of bituminous coal-derived fly ash would be expected to increase. The increased pH and alkali content could affect the solubility of trace constituents and the ability to use the fly ash in concrete. No effects on downstream solids, such as FGD gypsum, are expected.

### 3.3.4 Ammonia injection

Ammonia injection is commonly used along with native or injected $SO_3$ in dual flue-gas conditioning systems for improved cold-side ESP performance due to the cohesive properties of the ammonium salts that form. It has also been tested and/or used commercially for the express purpose of sulfuric acid control at several plants.

Ammonia is injected between the air heater and ESP at $NH_3$:$SO_3$ molar ratios of 1:1 to 2:1 to achieve 90% or more removal of sulfuric acid. Plants that have SCR systems already have a source of ammonia on site. Fig. 3.7 is a simplified process flow diagram

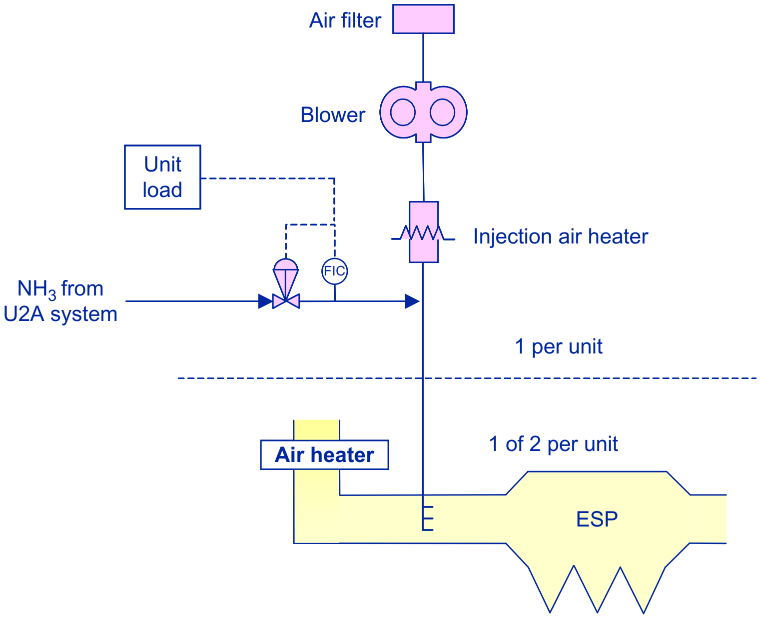

**Fig. 3.7** Simplified process flow diagram for ammonia injection (typical).

for an ammonia injection system. Ammonia/air mixtures are normally piped to an injection manifold where they are introduced into the flue gas duct via injection probes located just downstream of the air heater.

Ammonia reacts very quickly with sulfuric acid vapor at flue-gas temperatures <400°F. Most of the injected ammonia is converted to ammonium bisulfate (ABS) or ammonium sulfate, which is collected along with the fly ash in the particulate control device. Ammonia injection for $SO_3$ control on a plant with an SCR and firing a 3% sulfur coal would increase the fly ash mass rate by about 2%–3%, and it would add 0.5%–1% ammonia to the ash. These are much higher amounts of ammonia than those associated with ammonia slip from SCRs and can increase the amount in fly ash more than 10-fold, compared to slip related to injection of ammonia for SCR operation only. The potential impacts of ammonia on CCP disposal and use are discussed in the next section on $NO_X$ controls.

### 3.3.5 Fuel additives

Fuel additives have long been used as an approach for $SO_3$ mitigation for oil-fired units. The additives typically include some form of magnesium oxide or magnesium hydroxide. In oil-fired units, the magnesium-based additives primarily prevent $SO_3$ formation by tying up vanadium in the ash in the form of unreactive magnesium vanadates. Fuel additives have typically been less effective on coal-fired units, where the primary control mechanism appears to be the removal of $SO_3$ after it is formed through gas-solid reactions. These additives are typically applied to the coal from a storage silo as the coal is conveyed to the bunkers. As the additives are injected into the furnace with the fuel, they can become "dead burned," or sintered, by the high temperatures to which they are exposed, thus they are less reactive with the $SO_3$ formed. The reaction products are collected in the ESP or baghouse along with the fly ash. A portion of the additive may end up in the bottom ash stream.

For a coal with 3% sulfur and 8% ash, and assuming a dry-bottom boiler with 80% of the ash leaving as fly ash, adding ground dolomite ($MgCO_3 \cdot CaCO_3$) at 0.5%–1.0% of the coal feed would correspond with an 8%–17% increase in the amount of fly ash if it all reports to the fly ash rather than the bottom ash. The added material would be a mixture of calcium and magnesium oxides, carbonates, and sulfates. As a considerable excess of the alkaline additive is generally required, an increase in fly ash pH and alkalinity would be expected. The higher pH could also affect the leachability of trace constituents, and the increased alkalis and salts could affect the use of the ash in concrete. No effects on downstream solids, such as FGD gypsum, are expected.

### 3.3.6 Wet ESP

Electrostatic precipitation is a well-established method for collecting fine particulate matter in many different industrial applications; however, sulfuric acid control at coal-fired power plants represents a relatively new application. An ESP works by charging particles in an electric field and moving them to a surface of opposite charge, where they are deposited. In conventional dry ESPs, the deposited particles are removed by mechanical rapping. In wet ESPs the particles collected are sulfuric acid mist aerosols, and the collecting electrodes are irrigated with water to remove the material collected. Wet ESPs are typically located downstream of a wet scrubber, just before the flue gas goes up the stack.

Wet ESP technology solves several limitations on $SO_3$ control encountered by conventional dry ESPs. The wet environment helps ensure that the sulfuric acid is condensed and collectable by electrostatic forces, lowers particle resistivity, and allows high power input levels to enhance the removal of submicron-diameter mist. Wet ESPs can remove other flue-gas components that contribute to plume opacity, including fine fly ash particles, unburned carbon or soot, and wet FGD scrubber carryover. Particle resistivity problems typically encountered with dry ESPs are eliminated with a wet ESP, as the water-saturated condition renders all particles conductive. Wet ESPs have also been demonstrated to remove oxidized mercury from flue gas at a relatively high efficiency and to remove elemental mercury at lower percentages.

Since wet ESPs are typically installed at or near the end of the flue-gas path after the wet scrubber, they generally do not impact other CCPs, with the possible exception of FGD gypsum. A wet ESP generates an aqueous slurry waste that must either be treated separately or, more commonly, added to the FGD system. This slurry waste would include all of the material collected by the wet ESP and washed from the plates, including fine particulate matter that penetrates the upstream particulate collector and wet FGD absorber; sulfuric acid; scrubber carryover slurry; and mercury captured in the wet ESP. If the slurry is treated separately, a filter cake solid waste is generated from the wastewater treatment. The most common practice is to add this slurry stream to the FGD system, which consumes a small amount of FGD reagent to neutralize the acid. In some cases, alkali is added to the wet ESP washwater stream, so little FGD reagent is required for neutralization. The mercury content of the FGD solids and/or liquor would also be increased by adding this stream.

## 3.4 $NO_X$ controls

$NO_X$ control technologies consist primarily of two general technology types: furnace combustion modifications, which include the use of low-$NO_X$ burners, and ammonia (or urea) injection, with or without catalysts. Ammonia injection technologies include rich reagent injection (RRI), which is implemented in the furnace; selective non-catalytic reduction (SNCR), which is implemented in the upper furnace; and SCR that is typically used between the economizer and air heater. SCR is by far the most common of the $NO_X$ controls and uses an ammonia injection.

Fig. 3.8 illustrates where in the flue-gas path each of these technologies would typically be located. The technologies and their impacts on CCPs are discussed below.

### 3.4.1 Combustion modifications/low-$NO_X$ burners

Combustion modifications and/or low-$NO_X$ burners control the formation of $NO_X$ during the fuel combustion process, generally by limiting the availability of oxygen as fuel nitrogen is released. They typically involve some form of staged combustion, wherein certain areas of the furnace operate fuel rich, and then additional air is added to complete combustion. Overfire air (OFA), or separate overfire air, is often added above the burner level to stage combustion conditions.

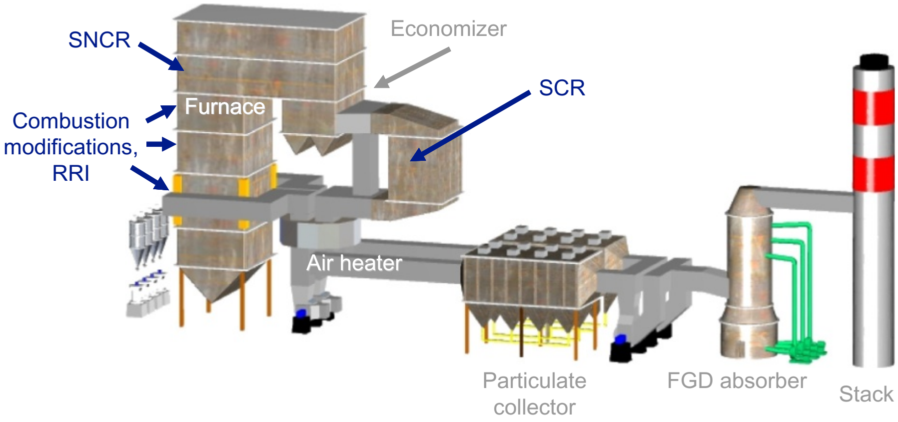

**Fig. 3.8** Illustration of typical locations for $NO_X$ control technologies.

A challenge that sometimes limits the effectiveness of combustion modifications and low-$NO_X$ burners is to lower $NO_X$ emissions while still ensuring complete fuel combustion. Increased flue-gas carbon monoxide (CO) concentrations and/or increased loss on ignition (LOI) in the fly ash can result from low-$NO_X$ firing conditions.

The primary impact of low-$NO_X$ burners to the CCPs is higher LOI levels in the fly ash. A higher LOI adversely affects the air-entraining properties of concrete made with the fly ash, which can in turn adversely affect fly ash sales for concrete, if the LOI exceeds ASTM C-618 specification (6% LOI) or lower contractual limits due to an increased need for air entraining.

As the LOI content of the fly ash increases, it is possible that unburned carbon can penetrate a cold-side ESP because the carbon has a low electrical resistivity and has a tendency to be reentrained. Consequently, this technology could lead to an increase in the amount of carbon captured in the wet FGD system and possibly increase the carbon content of the FGD gypsum.

## 3.4.2 Ammonia injection processes

### 3.4.2.1 Selective catalytic reduction

As noted previously, SCR is by far the most commonly used ammonia-based $NO_X$ control. SCR chemically reduces the $NO_X$ formed in the furnace by oxidation/reduction reactions with ammonia in the presence of a catalyst. The catalyst provides active surface area on which these reactions can take place, so nearly equimolar quantities of ammonia are added compared to the amount of $NO_X$ in the flue gas. The catalysts typically are made of a ceramic material that includes titanium oxide as a carrier and a vanadium oxide as the active species. Some catalysts also use an oxide of tungsten as part of the active species. Catalysts are most commonly installed in a honeycomb or plate configuration.

The catalytic reactions proceed most rapidly at temperatures in the range of 600–750°F, so SCR reactors are typically installed between the economizer and air heater (Fig. 3.8). An ammonia slip refers to excess ammonia in the flue gas that is not utilized in $NO_X$ mitigation. Most modern well-controlled SCR systems limit the ammonia slip to $<2$ ppm in the air heater inlet flue gas, often much less. Ammonia slip tends to increase with the age of the catalyst, and at the end of the catalyst life ammonia slip can greatly exceed 2 ppm in some cases.

### 3.4.2.2 Selective noncatalytic reduction

Like SCR, SNCR is used to chemically reduce $NO_X$ formed in the furnace by oxidation/reduction reactions between ammonia and $NO_X$. However, SNCR does not employ a catalyst. It is typically implemented in the upper furnace, and urea is often used as the ammonia source, as urea decomposes to form ammonia at elevated temperatures. Urea is often preferred over pure ammonia because of health and safety issues associated with handling ammonia, and the fact that the trajectory and penetration of urea injected as an aqueous solution into an upper furnace can be better controlled than when injecting gaseous ammonia.

Because SNCR relies solely on gas-phase reactions, an excess of urea/ammonia is typically required to get higher $NO_X$ reduction levels (e.g., 40%–60% $NO_X$ reduction levels). While most of the excess ammonia is destroyed at the temperatures in the upper part of the furnace, ammonia slip is common with SNCR installations. It is generally desirable to control ammonia slip to 2 ppm or less in the flue gas entering an air heater so as to avoid excessive formation of ABS within the air heater and resulting air heater pressure drop increases. However, many SNCR applications exceed this level of ammonia slip.

### 3.4.2.3 Rich reagent injection

RRI involves injecting urea or ammonia into fuel-rich portions of the furnace to reduce $NO_X$ formation. The technology was originally developed for $NO_X$ control for cyclone-fired coal boilers, but it can be applied to other boiler types. It involves staged combustion and OFA as the means of producing a fuel-rich zone in the furnace. The technology can be combined with low-$NO_X$ burners and/or with SNCR, which was discussed in the previous subsection, to result in greater overall $NO_X$ reduction.

Although the RRI technology also involves injecting urea or ammonia into the furnace similar to SNCR, these are reportedly destroyed at high efficiency within the furnace, so ammonia slip is essentially zero.

### 3.4.2.4 Impacts of ammonia injection on CCPs

The biggest potential issue for ammonia injection is the effect of ammonia slip on fly ash disposal/reuse; it will not affect bottom ash or boiler slag. As noted above, ammonia concentrations in the fly ash are typically well controlled in SCR and RRI systems. Higher levels of ammonia slip (>2 ppm in the flue gas) have been observed for the less-commonly used SNCR technology and for SCR systems that are experiencing catalyst activity problems. Ammonia slip is primarily collected as ammonium bisulfate (ABS), with the fly ash in the downstream particulate control device. At 2 ppm of ammonia slip, the ABS formed would amount to about 300 ppm as ammonia ($NH_3$) if it all reports to the fly ash. Ammonia concentrations in fly ash are typically <100 ppm for SCRs, while concentrations as high as 900 ppm have previously been reported from SNCR systems (EPRI, 2001). In general, fly ashes from subbituminous coals adsorb less ammonia than fly ashes from bituminous coals (EPRI, 1999). Ammonia that is not adsorbed on the fly ash will be absorbed in the FGD absorber; in a plant that has no FGD system, it will exit the unit out the stack.

The ammonia on fly ash can be released in vapor form if the fly ash is contacted with water, especially when the ash pH is naturally alkaline ($pH > 7.0$). Ammonia concentration in the ash may result in odor issues when ashes are wetted in an alkaline environment, particularly for ash concentrations above 100 ppm. To mitigate this potential issue, several methods have been advanced for the beneficiation of ammoniated fly ash for eventual use in concrete (EPRI, 2002, 2005a, 2007b). The impact of ammonia from SCR systems on the use of fly ash in concrete has not proven to be as much of a problem as was initially anticipated.

Ammonia salts are highly soluble and are readily released into the water phase as ammonium ion. As much as 70% of the ammonia adsorbed to the fly ash was released almost immediately on contact with water in batch leaching tests (EPRI, 2001). The presence of the ammonia can also impact the leaching of trace constituents from the fly ash, to some degree, by altering the solution pH or by complexing with some of the metals. However, laboratory testing demonstrated that ammonia complexation is only likely to significantly affect metals concentrations at alkaline pH and very high ammonia levels (>1000 mg/L), not typically observed on fly ash (EPRI, 2005b, 2008b; Wang et al., 2007).

Speciation of mercury has been shown to be affected by the SCR catalyst (Lee, Srivastava, Ghorishi, Hastings, & Stevens, 2004), and other redox sensitive constituents (e.g., As, Cr, Se) may also be affected. Speciation changes may affect their capture and leaching from CCPs. For example, elemental mercury can be oxidized to ionic mercury, increasing its capture in wet FGD systems. The combination of SCR and wet FGD plays a significant role in mercury capture for compliance with the US EPA Mercury and Air Toxics Standards (MATS) in many plants that are so equipped.

## 3.5 Mercury controls

From the standpoint of impacts on CCPs, the most common mercury capture technologies can be grouped as follows, although there is some overlap between the two:

- Sorbent injection and coremoval with fly ash. Activated carbon injection (ACI) is the most commonly used sorbent for coremoval with fly ash.
- Mercury oxidation and coremoval with FGD solids. Cobenefit oxidation by SCR and/or halide addition to the coal (or into the flue gas) are the most commonly used methods to increase mercury oxidation.

Like $SO_3$ control, mercury control can be implemented at a wide range of locations in the flue-gas path, from the furnace to just upstream of the stack.

### *3.5.1 Coremoval with fly ash*

#### *3.5.1.1 Activated carbon injection*

ACI is implemented by pneumatically injecting a fine powder of activated carbon into the flue-gas duct upstream of the particulate device. In most cases the carbon is injected between the air heater and primary particulate control device, although some processes involve carbon injection between the economizer and air heater. An ACI system typically consists of a storage silo, solids feeders, blowers, transport lines, and injection lances. Fig. 3.9 is a photograph of a temporary ACI system installed for a month-long full-scale ACI test.

**Fig. 3.9** Photograph of an ACI system, Showing the activated carbon storage silo (center of photo).

Activated carbon is made from coal, lignite, or other carbon-based material that is processed with heat and steam to produce a highly porous solid powder that has great capacity for adsorption. Mercury in the flue gas can adsorb onto the highly porous carbon particles and be collected along with the carbon in the unit's particulate control device. Several different types of activated carbon are available. Some activated carbons are treated with a bromine addition to improve their performance in flue gas from coals with low chlorine-content and for other applications.

The performance of ACI for mercury control can be very site specific. Factors such as coal type, flue-gas residence time in ductwork, particulate control device type and size, flue-gas temperature, and concentrations of other species in the flue gas such as HCl, nitrogen dioxide ($NO_2$), and $SO_3$ affect the performance of ACI. The type of particulate control device installed on a unit can, in particular, greatly impact the effectiveness of ACI; it is generally more effective with a fabric filter or baghouse than with an ESP and generally less effective with a wet particulate scrubber.

Typical injection rates range from $<1$ lb/MMacf (0.000016 kg/$m^3$) to over 10 lb/MMacf (0.00016 kg/$m^3$). For a typical bituminous coal with about 8% ash, and assuming 75%–80% of the coal ash becomes fly ash, these rates correspond with ~0.5%–5% of the fly ash mass being added as carbon.

The activated carbon captured with the fly ash can significantly impact its use in concrete. Even at the lowest carbon injection rate, fly ash use in concrete admixtures may be adversely affected, due to the effects of the activated carbon on air entrainment in the concrete. Air entrainment is required to give the concrete adequate freeze/thaw resistance. Air entraining agents added to the concrete preferentially attach to the activated carbon, and so they are no longer available to properly entrain air and provide concrete with freeze/thaw protection. As little as 0.5% activated carbon can significantly affect the air entraining characteristics of the concrete (EPRI, 2014). Even small amounts of activated carbon can complicate determining the correct dosage, rendering the fly ash less desirable to concrete producers.

Several proprietary technologies have been demonstrated to “passivate” activated carbon sorbents so they do not significantly impact air entrainment additive requirements (EPRI, 2014). In carbon passivation a sacrificial chemical is applied to the fly ash, and the chemical is adsorbed onto the activated carbon, thereby making the carbon adsorption sites unavailable to attach to air entraining admixtures. In addition, thermal technologies have been offered as a means to eliminate the activated carbon in fly ash. Furthermore, mercury sorbents that are not carbon based and that reportedly do not impact fly ash air entrainment properties are available, as described below.

Numerous studies have shown that mercury captured by activated carbon is relatively stable at ambient temperatures (EPRI, 2004a; Gustin & Ladwig, 2004; US EPA, 2006; UND EERC, 2007). Data indicate that mercury captured by ACI is well retained by the fly ash (EPRI, 2014). Studies designed to look specifically at fly ash in concrete showed that it is not readily released by leaching or volatilization (EPRI, 2006, 2007b; Golightly et al., 2005, 2008). The potential for the release of mercury captured by activated carbon via volatilization or leaching is considered to be low when the fly ash is used or disposed at ambient temperatures and at typical concrete curing temperatures.

Chemically treated (e.g., brominated) carbons are used to enhance the effectiveness of the mercury capture in some applications. Bromide is soluble and can be leached from the fly ash. Laboratory and full-scale testing has shown that brominated activated carbons can thermally desorb bromine into the flue gas upon injection. The amount desorbed varies greatly among powdered activated carbon products, likely because of differences in the amounts of bromine on the products and in the processes by which bromine is added during their production.

The use of fly ash in cement manufacture may also be limited if ACI is used for mercury control. The mercury captured on the activated carbon can be released at the high temperatures found in typical cement kilns (EPRI, 2004b).

#### *3.5.1.2 Other technologies*

Alternative sorbents include both specialty activated carbon and noncarbon sorbents. As described above, these sorbents offer the advantage of preserving the quality of the fly ash to allow its use in concrete. One vendor’s noncarbon sorbent has been applied on numerous units that employ SDA semidry FGD technology, but it has seen limited application for mercury control in other plant configurations.

Toxecon, a modified ACI technology developed to address several shortcomings of conventional ACI, consists of a compact fabric filter installed in the flue-gas path

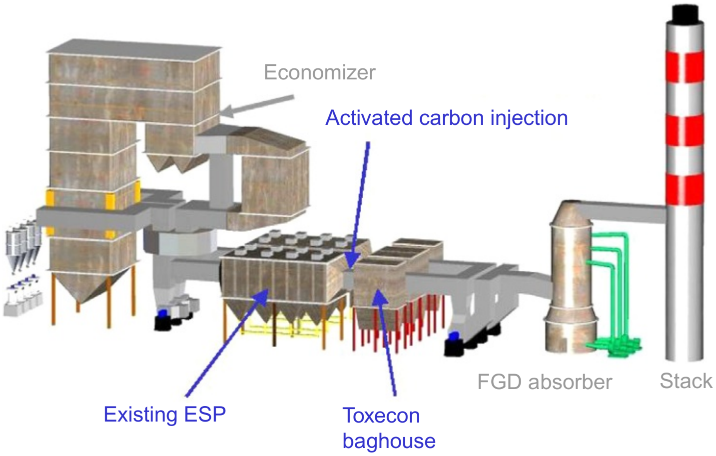

**Fig. 3.10** Illustration of the Toxecon process concept.

downstream of an existing ESP. Activated carbon is injected into the flue gas downstream of the ESP and upstream of this compact fabric filter (Fig. 3.10). This configuration preserves the quality of the ESP ash for use in concrete and produces a small secondary waste stream with a large percentage of activated carbon that must be disposed. As mentioned earlier in this section, some units apply this technology with a conventional pulse-jet fabric filter downstream of the ESP for $SO_3$ control by DSI and mercury control with ACI.

Recently, the injection of activated carbon directly into the FGD absorber has been employed as a mercury control technology. In one version the activated carbon is used to adsorb dissolved mercury from the scrubber slurry liquor as a means of preventing mercury "reemission." Reemission refers to a phenomenon where dissolved, oxidized mercury is chemically reduced by sulfite ion in the scrubber, producing elemental mercury that is insoluble and gets released back into the flue gas. In another version of this technology, activated carbon is injected into the flue gas upstream of the scrubber for an in-flight mercury capture. This is employed in units that have hot-side ESPs for particulate control, where ACI upstream of the ESP would be ineffective, as well as in units that use wet scrubbers as their primary particulate control device.

In forced oxidation systems producing wallboard-grade gypsum, activated carbon particles can increase the combustible percentage in the gypsum product. Wallboard manufacturers typically have very tight limits for combustible content in their gypsum feedstock because much of their output is for "fire code" wallboard. In many cases the hydrocyclones used as the primary gypsum dewatering step remove the bulk of the less dense and smaller activated carbon particles from the gypsum in the overflow stream so as to be returned to the absorber or purged with the scrubber chloride purge stream. However, the impacts of the ACI on FGD gypsum have not been extensively explored to date.

### 3.5.2 Mercury oxidation and coremoval with FGD by-products

The effectiveness of mercury coremoval in an FGD system is generally dependent on the percentage of the mercury in the flue gas that is in an oxidized form. The oxidized form of mercury is water soluble and can be removed in wet or dry scrubbers, while the other predominant form, elemental mercury, is not. Several factors influence the percentage of the coal mercury that is in the oxidized form as the flue gas enters the FGD system. These include

- Coal chloride content—higher coal chloride tends to promote mercury oxidation.
- SCR—SCR catalysts have been observed to oxidize mercury, particularly for coals that have significant chloride levels (typically $>100$ ppm chloride in the coal).
- Type of particulate control device—in some cases, it has been observed that reverse-gas fabric filters can oxidize a significant percentage of the mercury in the flue gas, even for low-chloride subbituminous coals, like those from the Powder River Basin (PRB).

Mercury captured by wet FGD systems can be found in the liquor, in the FGD solids, or both. The factors that control how mercury partitions between phases are not completely understood. In general, mercury in the solid phase tends to be concentrated in fine particles. For wet FGD systems that have hydrocyclones for primary dewatering, the fine solids in the overflow stream can have as much as 10 times the mercury concentration of the larger particles in the underflow (EPRI, 2004a). Since all of the slurry liquor is evaporated in spray dryer-based “dry” FGD systems, in these systems all of the absorbed mercury will be found in the solids stream.

Additional technologies have been developed to enhance the percentage oxidation of mercury in flue gas at the FGD inlet, and to limit reemission of mercury in the absorber. Several technologies are discussed below.

#### 3.5.2.1 Chemical addition

The most common oxidation technology used for mercury control is halogen addition. The effectiveness of this technology is based on increasing the percentage of the mercury in the flue gas that is in the oxidized form. As described previously, eastern coals with a higher chlorine content produce mostly oxidized mercury in their flue gases, while western coals, such as PRB coals, that have a low chlorine content tend to produce mostly elemental mercury. One way to increase the amount of mercury removed by wet scrubbers is to add halogens to the coal to increase the percentage of mercury in the flue gas that is oxidized.

Halogen salts such as calcium chloride ($CaCl_2$), calcium bromide ($CaBr_2$), or potassium iodide (KI) can be added to the coal as a means of supplementing the coal chlorine content. Salts added with the coal or injected into the furnace decompose at furnace temperatures to form vapor-phase acids [HCl, hydrogen bromide (HBr), or hydrogen iodide (HI)] in the flue gas. These vapor-phase halogen acids and/or the small amount of halogens present ($Cl_2$, $Br_2$, or $I_2$) react with elemental mercury to produce oxidized mercury that can be removed by a downstream wet scrubber. Results typically show that calcium bromide can be added at lower rates than calcium chloride to produce equivalent oxidation percentages. In some circumstances, potassium iodide can be added at lower rates than either calcium chloride or calcium bromide to achieve similar oxidation percentages.

For FGD solids, several effects of halogen addition might be expected. One is that higher mercury concentrations may report to the FGD solids. The second is that halogen concentrations will be increased in the FGD liquor. This can increase the amount of halogen material remaining in dewatered products such as gypsum, which may have limitations by the wallboard manufacturer on the amount of dissolved salts allowed. However, washing the FGD gypsum, as is commonly done for wallboard grade gypsum, would remove most of the halogens.

For spray dryer-based dry FGD systems, the presence of elevated halogen levels in the flue gas will alter droplet drying characteristics, due to the deliquescent nature of the calcium salts of these halogen acids. While $SO_2$ removal performance may be improved, droplet drying will slow, and the spray dryer outlet temperature may have to be raised to compensate. The presence of these halogen salts in the FGD solids can alter optimum moisture levels, strength development, permeability, and leachate characteristics (Blythe, 1985).

Halogen addition could also affect fly ash to a lesser degree. The main impact would likely be an increase in the amount of mercury removed with the fly ash, as the higher halogen concentrations in the flue gas would tend to enhance mercury capture by unburned carbon in the fly ash. Halogen concentrations in the fly ash would also increase. However, significant halogen removal with the fly ash would not be expected.

### *3.5.2.2 Scrubber additives*

The net removal of oxidized mercury in wet FGD systems can be limited by a phenomenon called "reemissions," where oxidized mercury absorbed in the scrubber liquor is chemically reduced and converted back to the elemental form. Since the elemental mercury formed is not water soluble, it is released back into the scrubber outlet flue gas. Evidence of reemissions is seen when the elemental mercury concentration in the flue gas at the outlet of a wet scrubber is higher than the inlet elemental mercury concentration.

Additives to the scrubber to limit reemission generally work by rapidly precipitating or adsorbing oxidized mercury from the scrubber liquor to the solid phase, so it will not react with other liquid-phase species and be converted back to the elemental form. Scrubber additives were first used in Europe to prevent reemissions from wet scrubber systems installed on municipal waste burning plants, and they have reportedly been used for this purpose in some European coal-fired plants. Testing of wet scrubber additives began 10 years ago in the United States with varied success (Blythe, 2006, 2007; Ghorishi et al., 2005). Over the past decade, a number of scrubber reemission additives have been developed and demonstrated to be effective, and they are now widely used as part of the mercury control strategy for compliance with the EPA MATS, which went into effect beginning in 2015. Two types of scrubber additives are used. One type is mostly a water-soluble solution that contains some form of reduced sulfur, often sulfides, thiols, or carbamates. These additive types tend to form an insoluble precipitate or complex with dissolved oxidized mercury. Another form of additive is activated carbon, which adsorbs mercury from the FGD slurry liquid phase.

The main impact of scrubber additives will be increased mercury concentrations in the FGD solids, if the additive is effective. The mercury precipitated with the additive should be concentrated in fine particles. For plants with hydrocyclones for the primary dewatering of the FGD by-product, the FGD gypsum mercury content is generally lowered by separating mercury-rich fines for disposal. It is also likely that mercury present in gypsum as a precipitate with a reemissions additive will be more stable than mercury would be in the gypsum with no additive, but this has not been substantiated. In one documented case, gypsum produced from a power plant using a wet scrubber reemissions additive was tested at a commercial wallboard plant, with no noted adverse effects on the wallboard production process (Sanderson, Blythe, & Richardson, 2006).

### 3.5.2.3 Mercury coremoval in wet ESPs

Wet ESP technology was previously discussed as an $SO_3$ control technology. However, wet ESPs have also been documented to remove oxidized mercury and even some elemental mercury from the flue gas treated. The latter is speculated to occur because of the oxidation of elemental mercury due to the corona electrical discharge in the wet ESP. Mercury removed by wet ESPs would be present in the wastewater from the process, and the wastewater is most commonly used as part of the water makeup to the upstream wet FGD system. In this case the wet ESP wastewater would not directly impact CCPs, but it could increase the mercury, selenium, and other trace element concentrations in the FGD wastewater and/or gypsum.

## References

ACAA. (2016). *Coal combustion product (CCP) production and use survey*. American Coal Ash Association. www.ACAA-USA.org.

Blythe, G. M. (1985). *Field evaluation of a utility spray dryer system*. Report no. CS-3954, May. Electric Power Research Institute.

Blythe, G. M. (2006). *Field testing of an FGD additive for enhanced mercury control, task 2 and 4 pilot-scale test results*. Topical report. Cooperative agreement no. DE-FC26-04NT42309, May. Austin, TX: URS Corporation.

Blythe, G. M. (2007). *Field testing of an FGD additive for enhanced mercury control, task 3 full-scale test results*. Topical report. Cooperative agreement no. DE-FC26-04NT42309, May. Austin, TX: URS Corporation.

Dan, Y., Zimmerman, C., Liu, K., Shi, H., & Wang, J. (2013). Increased leaching of As, Se, Mo, and V from high calcium coal ash containing Trona reaction products. *Energy and Fuels*, *27*(3), 1531–1537.

EPRI. (1999). *Investigation of ammonia adsorption on fly ash and potential impacts of ammoniated ash*. Palo Alto, CA: EPRI. TR-113777.

EPRI. (2001). *Characterization of ammonia leaching from coal fly ash*. Palo Alto, CA: EPRI. 1005163.

EPRI. (2002). *Novel ash beneficiation processes for managing unburned carbon and ammonia*. Palo Alto, CA: EPRI. 1004395.

EPRI. (2004a). *Mercury stability in FGD byproducts*. Palo Alto, CA: EPRI. 1004711.

EPRI. (2004b). *Mercury emissions from cement kilns using fly ash as feedstock*. Palo Alto, CA: EPRI. 1011289.

EPRI. (2005a). *Ammonia removal from fly ash: Process review; headwaters Ammonia Slip Mitigation (ASM™) technology*. Palo Alto, CA: EPRI. 1010381.

EPRI. (2005b). *Effects of ammonia on trace element leaching from coal fly ash*. Palo Alto, CA: EPRI. 1010063.

EPRI. (2006). *Mercury emissions from curing concretes that contain fly ash and activated carbon sorbents*. Palo Alto, CA: EPRI. 1012696.

EPRI. (2007a). *A review of literature related to the use of spray dryer absorber material: Production, characterization, utilization applications, barriers, and recommendations*. Palo Alto, CA: EPRI. 1014914.

EPRI. (2007b). *Mercury leachability from concretes that contain fly ashes and activated carbon sorbents*. Palo Alto, CA: EPRI. 1014913.

EPRI. (2008a). *Impact of air emissions controls on coal combustion products*. Palo Alto, CA: EPRI. 1015544.

EPRI. (2008b). *The effect of ammonia on mercury partitioning in fly ash*. Palo Alto, CA: EPRI. 1014014.

EPRI. (2010). *Impacts of sodium-based reagents on coal combustion characteristics and performance*. Palo Alto, CA: EPRI. 1017577.

EPRI. (2011). *Composition and leaching of FGD gypsum and mined gypsum*. Palo Alto, CA: EPRI. 1022146.

EPRI. (2013). *Use of spray dryer absorber product in agriculture—Sulfite oxidation kinetics*. Palo Alto, CA: EPRI. 3002001242.

EPRI. (2014). *Effects of alkaline sorbents and mercury controls on fly ash and FGD gypsum characteristics, and implications for disposal and use*. Palo Alto, CA: EPRI. 3002003766.

EPRI. (2015). *Use of spray dryer absorber material as a replacement for Portland cement in concrete*. Palo Alto, CA: EPRI. 3002006093.

Gale, T. (2006). Hydrated lime for $SO_3$ removal. In: *Paper #128. Megasympsium Conference 2006, Baltimore, MD, August 2006*.

Ghorishi, S., Renninger, S., Farthing, G., Teets, C., Neureuter, J., Hastings, T., et al. (2005). Effects of SCR catalyst and wet FGD additive on speciation and removal of mercury within a forced oxidized limestone scrubber. In *Paper presented at the ICAC clean air technologies and strategies conference 05, Baltimore, MD, March 7–10*.

Golightly, D. W., Sun, P., Cheng, C. M., Taerakul, P., Walker, H. W., Weavers, L. K., et al. (2005). Gaseous mercury from curing concretes that contain fly ash: Laboratory measurements. *Environmental Science and Technology*, *39*(15), 5689–5693.

Golightly, D. W., Cheng, C. M., Sun, P., Weavers, L. K., Walker, H. W., Taerakul, P., & Wolfe, W. E. (2008). Gaseous mercury release during steam curing of aerated concretes that contain fly ash and activated carbon sorbent. *Energy and Fuels*, *22*(5), 3089–3095.

Gustin, M., & Ladwig, K. (2004). An assessment of the significance of mercury release from coal fly ash. *Journal of the Air and Waste Management Association*, *54*, 320–330.

Ladwig, K. (2016). EPRI research on the use of FGD gypsum in agricultural applications. *ASH at Work*. (1), 10–12 ACAA.

Lee, C. W., Srivastava, R. K., Ghorishi, S. B., Hastings, T. W., & Stevens, F. M. (2004). Investigation of selective catalytic reduction impact on mercury speciation under simulated

NOx emission control conditions. *Journal of the Air and Waste Management Association*, *54*, 1560–1566.

Moser, R. E. (2007). SO3's impacts on plant O&M: Part III. *POWER Magazine*, (April).

Peterson, J. R., Jones, A. F., Meserole, F. B., & Rhudy, R. (1993). $SO_3$ removal from flue gas by sorbent injection, EPRI HSTC phase II test results. In *Paper presented at the SO2 control symposium, Boston, MA, 24-27 August*.

Radian International LLC (1997). *High $SO_2$ removal efficiency testing*: (pp. 3–16). Pittsburgh, PA: U.S. Department of Energy Federal Energy Technology Center, Final report for project DE-AC22-92PC91338.

Sanderson, J., Blythe, G. M., & Richardson, M. (2006). *Fate of mercury in synthetic gypsum used for wallboard production*. Topical report, Task 6 Wallboard Plant Test Results, DOE Cooperative agreement no. DE-FC26-04NT42080, Pittsburgh, PA, December.

UND EERC. (2007). *Mercury and air toxic element impacts of coal combustion by-product disposal and utilization*. Grand Forks, ND: UND EERC.

US EPA (2006). *Characterization of mercury-enriched coal combustion residues from electric utilities using enhanced sorbents for mercury control*. EPA-600/R-06/008.

Wang, J., Wang, T., Mallhi, H., Liu, Y., Ban, H., & Ladwig, K. (2007). The role of ammonia on mercury leaching from coal fly ash. *Chemosphere*, *69*(10), 1586–1592.

White, H. J. (1974). Resistivity problems in electrostatic precipitation. *Journal of the Air Pollution Control Association*, *24*(4), 333–334.

# Part Two

# Utilization of coal combustion products

# Introduction to the utilization of coal combustion products

# 4

*R.A. Kruger*
South African Coal Ash Association, Pretoria, South Africa

## 4.1 Introduction

The residues that arise from coal-fired power generation are collectively known as coal combustion products (CCPs). Their nature and characteristics depend upon the properties of the coal, the combustion technology utilized, and the flue gas treatment employed.

The history of CCP utilization is a success story of technical innovation that enabled the development of environmentally sustainable alternatives to nonrenewable resources. Besides reducing the impact of fossil fuel power generation, the use of CCPs as a substitute for mined or manufactured materials in the building, construction, and civil engineering industries lowers costs, conserves resources, decreases energy consumption, and promotes sustainability.

To ensure the establishment of safe and viable technologies, CCPs are utilized in compliance with standards or specified performance criteria applicable to the particular purpose for which they are to be used. Prior to their application, CCPs could require beneficiation or treatment in order to enhance properties, improve performance, reduce contaminants, or ensure compliance to standards.

Depending on the boiler technology and the measures used to restrict environmental impact, a series of CCPs are produced during coal combustion. Firing the boiler with pulverized coal generates cenospheres, fly ash, and bottom ash. In the case of furnaces that operate at very high temperatures, boiler slag rather than bottom ash is formed. Subject to the process employed, flue-gas desulfurization (FGD) produces either dry or semidry absorption product (SDA) or wet FGD gypsum.

Fluidized-bed combustion (FBC) enables the capture of acidic pollutants without resorting to scrubbers. The coal, along with limestone or dolomite, is combusted in a turbulent mix of circulating air, enabling the capture of sulfur within the boiler. However, like pulverized coal combustion, both bottom ash and fly ash are formed. The lower combustion temperature and the presence of the sorbent results in a combustion product with substantially different properties.

By exploiting their appropriate chemical properties and physical features CCPs are used in diverse applications predominantly in the building, construction, and allied industries. Coal ash (i.e., fly ash and bottom ash) is used as a pozzolanic extender for the production blended cements, as a supplementary binder for concrete and grout, and also as a constituent of the feedstock for the manufacture of Portland cement

**Coal Combustion Products (CCP's).** http://dx.doi.org/10.1016/B978-0-08-100945-1.00004-6

clinker. The application of FGD gypsum is meant to be a replacement for the natural gypsum in the manufacture of wallboard, as well as a set retarder for Portland cement and for soil amelioration. FBC ash is extensively used in mine reclamation, where the inherent alkalinity of mitigates the effects of acid mine drainage.

The legal framework under which the CCP market functions varies from country to country. Eliminating ambiguity and establishing a sound regulatory framework is imperative if the market is to develop and flourish. All contingent liabilities that can be attributed to the processing and marketing of CCPs need to be identified and removed to avoid uncertainty and widespread loss of current and future opportunities for beneficial use (Heidrich, 2011).

The commercial use of CCPs is well developed throughout the world. It is driven by a market that appreciates their technical advantages, economic viability, and environmental benefits.

Due to different coal combustion technologies, industrial practices, regulatory issues, taxes, and disposal costs, as well as pricing and availability of competitive alternatives, the characteristic features and trends of utilization differ from country to country; these are discussed in this chapter.

The word "ton" will not be abbreviated when used to refer to a short ton (i.e., 2000 pounds or 907 kg.). A long ton (2000 kg) will be denoted as t, with Mt being one million tons.

## 4.2 Utilization in the United States

The annual report by the American Coal Ash Association (ACAA) on the production and beneficial use of CCPs provides in-depth insight into the CCP industry in the United States. It lists the individual CCPs, along with their specific applications and the amount that is beneficially used.

As benefits became more widely appreciated and utilization increased, it soon became apparent that CCPs perform better, cost less, and offer distinct advantages over other materials commonly used in construction, mining, and agriculture. The role fulfilled by fly ash in improving the quality and durability of concrete while simultaneously reducing its carbon footprint cannot be overestimated. The promulgation of industry standards, specifications, and guidelines for CCP utilization by federal and state agencies, as well as articles and favorable market reports were instrumental in promoting wider CCP use and ensuring their long-term market growth.

A study of the relationship between the usage and production of CCPs in the United States over the last four decades (1974–2013) shows that production grew by 93% from 59.5 to 114.7 million tons. This increase is attributed to a combination of regulatory and market factors reflecting the country's reliance on coal-fired power generation and the need to comply with the Clean Air Act (CAA). With fly ash volume only increasing by 32% from 40.4 to 53.4 million tons, the main contributor to the rise in the volume of CCPs can be ascribed to materials emanating from flue-gas treatment which, in 2013 reached 35.2 million tons (ARTBA, 2015).

CCP utilization was influenced by prevailing macroeconomics, regulatory policies, and particularly the modification of combustion practice, which gave rise to the availability of FGD products. Over the 39-year period, the beneficial use of CCPs increased by nearly 500% from 8.7 to 51.6 million tons annually, marking an improvement in the utilization rate from 14.7% to 44.8%.

A significant contributor to this market growth was attributed to the availability of FGD products, especially FGD gypsum and the emergence of FBC, which provided a new material with unique chemical characteristics to the industry. The market for FGD gypsum grew rapidly due to its extensive use as a substitute for natural gypsum in wallboard manufacture, as well as the benefit of using it as a soil ameliorant in the agricultural sector.

Large volumes of coal ash are used to ameliorate the environmental impact of mining by grouting or backfilling voids in order to stabilize the geological strata. Due to its inherent spherical morphology, the use of fly ash intrinsically enhances flow, allowing the grout to move freely and fill the crevices and voids effectively. Furthermore, the gel precipitating as a result of the pozzolanic reaction reduces permeability, which in turn restricts leaching. By adjusting the fly ash-to-cement ratio, a range of grouts can be prepared to suit specific applications.

The beneficial use of coal ash for coal mine reclamation occurs in varying degrees across the United States. Injection into deep mines has been conducted to provide structural support for subsidence abatement and placement of coal ash, while other CCPs in surface mines have been utilized to reclaim mined land to original grade and to mitigate acid mine drainage. Such practices have been employed at both active and abandoned coal mines. An extensive summary of mine sites where coal ash was utilized is available (Murarka and Erickson, 2006).

A comprehensive investigation into the use of fly ash in formulations for the backfilling of collapsed underground mines was carried out in North Dakota to quantify the benefits and safety of the process (Dodd, 2000). A total of 23 grout formulations were evaluated for flowability, pumpability, cohesion, compressive strength, and leaching potential. It was found that the characteristics of the fly ash played a role in determining the properties of the grout, and its use resulted in improved performance and significant cost savings. Additionally, the concentration of trace elements in the leachates was reduced.

However, care must be exercised in preparing the infill material. A colloidal product that resists dilution by free water is essential. It is therefore recommended to avoid using paddle mixers, mortar mixers, or ready-mix trucks because the ensuing grout will lack homogeneity and require excess water to ensure flowability. Subsequently, more than 85 remediation projects have been carried out in North Dakota, employing pressurized grouting to pump the material directly into mine cavities to stabilize the terrain and prevent further collapse. This technology proved to be far more successful than the gravity filling previously used because a lack of cohesion, the grout tended to wash away or settle prematurely.

After carrying out a detailed study of the rheological and mechanical properties of high-volume fly ash grout (i.e., containing over 55% fly ash) Mirza, Saleh, Roy, and Mirza (1999) confirmed that the addition of fly ash to cement grouts used for filling mines decreases the filling time, improves stability, reduces drying-shrinkage, and attains similar compressive and bond strengths as pure cement grouts.

The highly alkaline nature of FBC ash is exploited as a substitute for lime in mine remediation and the treatment of acid mine drainage (Schueck, Tarantino, Kania, & Scheetz, 2001). More than 80% of the FBC ash was beneficially utilized in 2013.

Because of regulatory uncertainty, as well as the possibility of coal ash being classified a hazardous waste, the market was stagnant between 2009 and 2013. During this period, producers, specifiers and marketers limited the use of coal ash while waiting for the EPA’s decision. In 2014, the EPA indicated that the hazardous waste designation proposal was no longer being considered; that Dec., it finalized the regulations for coal ash disposal under the nonhazardous section (Subtitle D) of the Resource Conservation and Recovery Act (RCRA).

Comparing the CCP markets of 2013 and 2014 illustrates the significance of this ruling (Table 4.1). The amount of CCPs produced increased from 114.7 to 129.7 million tons, most of which was accounted for by desulfurization products. More significantly from a market perspective, 62.4 million tons were beneficially used, setting a new record by exceeding the 2008 peak of 60.6 million tons.

As can be seen in Table 4.1, most of the utilization rates were similar, but the absolute amount of FBC ash and FGD gypsum used was increased by 9.5 million tons. The production of synthetic gypsum increased by 40% and that of dry scrubbers almost doubled. The increase in demand for gypsum was ascribed to the replacement of natural gypsum in wallboard products; in agricultural applications, it is applied to improve soil properties and prevent runoff of fertilizers.

The replacement of coal power plants by renewable energy generation saw a 6% decline in the volume of fly ash produced to 50.4 Mt from 53.4 Mt the year before. However, the restoration of market confidence resulted in a 2% increase in the utilization rate. The diversity of the CCP market and volumes used in the various uses is presented in Table 4.2.

**Table 4.1** **Summary of United States market for CCPs (in million short tons)**

| Category | Fly ash | Bottom ash | Boiler slag | FGD gypsum | FGD wet scrubbers | FGD dry scrubbers | FBC | Total |
|---|---|---|---|---|---|---|---|---|
| **2013** | | | | | | | | |
| Production | 53.40 | 14.45 | 1.36 | 24.40 | 8.51 | 0.68 | 10.33 | 114.69 |
| Used | 23.32 | 5.64 | 0.90 | 11.92 | 0.83 | 0.19 | 8.58 | 51.38 |
| % Use | 44 | 39 | 66 | 49 | 10 | 28 | 83 | 45 |
| **2014** | | | | | | | | |
| Production | 50.42 | 12.48 | 2.69 | 34.14 | 12.60 | 1.26 | 15.77 | 129.68 |
| Used | 23.18 | 6.06 | 1.71 | 16.75 | 1.12 | 0.28 | 13.29 | 62.43 |
| % Use | 46 | 49 | 63 | 49 | 9 | 22 | 84 | 48 |

Table 4.2 **Production and utilization of coal combustion products in the United States (2014)**

| **American Coal Ash Association, 38800 Country Club Drive, Farmington Hills, MI 48331**<br>**Email: info@acaa-usa.org** | | **Phone: 720 870 7897**<br>**Fax: 720 870 7889**<br>**Internet: www.ACAA-USA.org** | **2014 coal combustion product (CCP) production and use survey report** | | | | | | |
|---|---|---|---|---|---|---|---|---|---|
| **Beneficial utilization versus production totals (short tons)** | | | | | | | | | |
| **2014 CCP categories** | **Fly ash** | **Bottom ash** | **Boiler slag** | **FGD gypsum** | **FGD material wet scrubbers** | **FGD material dry scrubbers** | **FGD other** | **FBC ash** | **CCP production/utilization totals** |
| Total CCPs produced by category | 50,422,238 | 12,478,705 | 2,694,705 | 34,123,820 | 12,596,231 | 1,255,775 | 344,551 | 15,768,766 | 129,684,142 |
| Total CCPs used by category | 23,181,723 | 6,063,028 | 1,706,621 | 16,750,990 | 1,163,434 | 275,999 | 0 | 13,285,766 | 62,427,561 |
| 1. Concrete/concrete products/grout | 13,126,930 | 609,558 | 0 | 423,613 | 0 | 0 | 0 | 0 | 14,160,100 |
| 2. Blended cement/feed for clinker | 3,391,272 | 1,197,398 | 0 | 1,308,208 | 120,509 | 0 | 0 | 0 | 6,017,388 |
| 3. Flow able fill | 84,734 | 2672 | 0 | 0 | 0 | 0 | 0 | 0 | 87,406 |

*Continued*

Table 4.2 **Continued**

| **American Coal Ash Association, 38800 Country Club Drive, Farmington Hills, MI 48331**<br>**Email: info@acaa-usa.org** | | **Phone: 720 870 7897**<br>**Fax: 720 870 7889**<br>**Internet: www.ACAA-USA.org** | **2014 coal combustion product (CCP) production and use survey report** | | | | | | |
|---|---|---|---|---|---|---|---|---|---|
| **Beneficial utilization versus production totals (short tons)** | | | | | | | | | |
| **2014 CCP categories** | **Fly ash** | **Bottom ash** | **Boiler slag** | **FGD gypsum** | **FGD material wet scrubbers** | **FGD material dry scrubbers** | **FGD other** | **FBC ash** | **CCP production/ utilization totals** |
| 4. Structural fills/ embankments | 2,805,515 | 1,928,492 | 51,659 | 1,586,234 | 311,183 | 0 | 0 | 0 | 6,683,084 |
| 5. Road base/ sub-base | 365,868 | 306,936 | 12,992 | 0 | 0 | 0 | 0 | 0 | 685,796 |
| 6. Soil modification/ stabilization | 176,112 | 720,791 | 0 | 0 | 0 | 0 | 0 | 0 | 896,903 |
| 7. Mineral filler in asphalt | 68,707 | 0 | 9758 | 5197 | 0 | 0 | 0 | 0 | 83,662 |
| 8. Snow and ice control | 0 | 736,397 | 101,359 | 0 | 0 | 0 | 0 | 0 | 837,756 |
| 9. Blasting grit/ roofing granules | 0 | 127,114 | 1,530,853 | 0 | 0 | 0 | 0 | 0 | 1,657,968 |

| | | | | | | | | | |
|---|---|---|---|---|---|---|---|---|---|
| 10. Mining applications | 1,392,935 | 41,330 | 0 | 813,419 | 578,244 | 229,766 | 0 | 13,151,161 | 16,206,855 |
| 11. Gypsum panel products | 0 | 0 | 0 | 11,221,836 | 0 | 0 | 0 | 0 | 11,221,836 |
| 12. Waste stabilization/ solidification | 279,323 | 475 | 0 | 16,390 | 0 | 0 | 0 | 134,605 | 430,794 |
| 13. Agriculture | 62 | 10 | 0 | 1,332,708 | 0 | 0 | 0 | 0 | 1,332,781 |
| 14. Aggregate | 0 | 181,107 | 0 | 0 | 0 | 0 | 0 | 0 | 181,107 |
| 15. Oil/gas field services | 512,100 | 4708 | 0 | 0 | 0 | 46,233 | 0 | 0 | 563,041 |
| 16. Miscellaneous/ other | 978,165 | 206,039 | 0 | 43,384 | 153,498 | 0 | 0 | 0 | 1,381,086 |

**Summary utilization to production rate**

| CCP categories | Fly ash | Bottom ash | Boiler slag | FGD gypsum | FGD material wet scrubbers | FGD material dry scrubbers | FGD other | FBC ash | CCP utilization total |
|---|---|---|---|---|---|---|---|---|---|
| Totals by CCP type/ application | 23,181,723 | 6,063,028 | 1,706,621 | 16,750,990 | 1,163,434 | 275,999 | 0 | 13,285,766 | 62,427,561 |
| Category use to production rate (%) | 46 | 49 | 63 | 49 | 9 | 22 | 0 | 84 | 48 |
| 2014 cenospheres sold (pounds) | 4,862,361 | Data in this survey represents 189 GWs if name plate rating of the total industry wide approximate 302 GW capacity based on EIA's Jul. 2015 Electric Power Monthly. | | | | | | | |

*Notes*: These are estimates for entire US utility and IPP sectors calculated by dividing the survey respondents data by the portion of the overall industries coal burn they represent, as reported in the Jul. 2015 EIA Electric Power Monthly (58%).

## 4.3 Utilization in Australia

In Australia, coal ash is subject to waste legislation. Despite being faced with the occasional legislative discrepancy between state and federal law, the country has succeeded in creating a proficient coal ash market by taking a pragmatic approach and removing legislative barriers (Heidrich, 2011). This has allowed for the use of coal ash as a resource, provided there is a demonstrable benefit and it is not hazardous in terms of the Basel Convention.

The success of injecting a fly ash slurry into underground bord and pillar coal mine workings to provide support for upgrading the Ipswich motorway and the envisaged extension of this methodology to the adjacent Collingwood Park residential housing area could be the precursor to the widespread use of coal ash in underground stabilization in Australia (Williams et al., 2010).

The coal power stations are primarily located in the east and southeast of the country (Queensland, New South Wales, and Victoria). Approximately 53% of the coal combusted is lignite and produces calcareous ash. The limited and highly centralized processing and distribution capacity at some power station sites requires that coal ash be moved over long distances to supply the market. Shipping fly ash 1000 miles is routine, and road transport of up to 500 miles for specific contracts is not unusual. This movement between states is subject to the Council of Australian Governments Standing Council of Environment and Water.

Based on a survey that included all generators, marketers, and users, Australia produced 12.38 Mt of coal ash (fly ash, bottom ash, and cenospheres) during 2014 compared to 12.26 Mt the year before. The decline from 14.7 Mt in 2008 would therefore seem to have stabilized (Table 4.3).

Due to the low sulfur content of Australian coal, no FGD is produced.

Table 4.3 does not reflect the 22 kilo tons of cenospheres and 50 kilo tons of bottom ash used as mineral fillers or the 10 kilo tons used as a raw feed for cement clinker production.

A total of 5.41 Mt of fly ash (49.3%) was effectively utilized, of which 2.14 Mt directly generated revenue with 1.73 Mt of this attributable to value-added applications, such as cementitious binders and concrete. A total of 2.2 Mt was removed from storage and implemented in projects (e.g., embankments, infill, and haul roads) at the power station. This beneficial use is motivated by cost

**Table 4.3** Utilization of coal ash in Australia (2014) (million tons)

| Application | Fly ash | Bottom ash | Total |
|---|---|---|---|
| Cement and concrete | 1.72 | 0.02 | 1.74 |
| Structural fill and roads | 0.15 | 0.50 | 0.65 |
| Mine backfilling, waste stabilization, and miscellaneous | 0.26 | – | 0.26 |
| Total | 2.13 | 0.52 | 2.65 |

avoidance rather than direct financial benefit. The availability of calcareous fly ash added diversity to the fly ash market by enabling the utilization of 0.25 Mt in mining applications and waste stabilization.

The principle use for fly ash continues to be attributable to size-graded fractions used in cement and concrete. Structural/civil applications and mine site remediation (Table 4.3) mostly utilize ungraded or run-of-station fly ash. With the depletion of sand and gravel resources, there has been a considerable interest from the cementitious industry to supplement supply with CCPs. Demand for fine and coarse aggregates in structural/civil applications is closely tied to economic growth, as well as the future development of both urban and regional infrastructure.

Bottom ash is used as an aggregate in civil construction as well as in agriculture to improve the drainage characteristics of soil. Agricultural use increased from 600 tons in 2012 to over 76,000 tons in 2014.

The figures for the import and export of CCPs (Basel Convention) are included in the data supplied by the ADAA, but sources and destination remain confidential.

## 4.4 Utilization in Europe

The European Coal Combustion Products Association (ECOBA), an association of energy producers representing over 86% of the CCP production in the EU plays a vital role in the promotion, coordination, and development of the CCP industry in Europe.

While one of their responsibilities is to provide annual statistics on CCP production and utilization, they also facilitate research, international collaboration, and disseminate information on CCPs. ECOBA are represented on a number of CEN (Comité Européen de Normalisation) groups, such as the European Committee for Standardization for the development of CCP standards.

The production of CCPs in the EU-15 during 1993–2010 was influenced by the general economy as well as changes in combustion methodology, which was introduced to comply with environmental legislation. It was fairly static around 55–57 Mt from 1993 to 1999, but as the economy grew and more coal-based generation was implemented, it increased rapidly thereafter to reach 64 Mt in 2005. Subsequently, volumes decreased gradually to just over 48 Mt in 2010 due to lower power demand during the economic recession and the introduction of renewable sources of energy. With over 54 Mt of CCPs arising in 2012 and 52 Mt the following year, this continual decline appears to have been halted (Fig. 4.1).

The production of CCPs in Europe in 2012 is given in Table 4.4. In the absence of reliable data, the figures for the EU-28 countries were calculated from the amount of coal consumed and information on operational desulfurization units.

In the majority of cases, CCPs are utilized in the building and construction industry, in civil engineering, and for construction work in underground coal mines (Caldas-Vieira & Feuerborn, 2013). All these applications offer substantial environmental benefits by avoiding the need to quarry or mine natural resources. In the EU-15, about 52% is used for cementitious-related applications and approximately

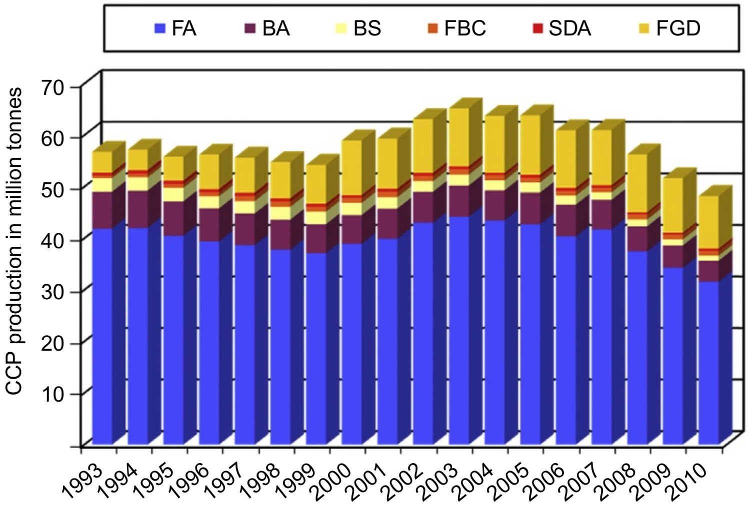

**Fig. 4.1** Production of CCPs in EU-15 (1993–2010).

Table 4.4 **Production of CCPs in Europe (2012)**

| Production Mt/a | | | |
|---|---|---|---|
| Region | EU 15 | EU 28[a] | EU[a] |
| CCPs | 54.64 | >105 | >145 |
| Coal ash | 42.92 | >88 | >124 |
| Desulfurization products | 11.73 | >21 | >21 |

[a] In the absence of reliable statistics, CCP production for EU-28 was calculated from coal consumption and desulfurization figures.

40% is employed for the environmental restoration of open cast mines. About 2% is stockpiled, and 6% is disposed (Caldas-Vieira, 2014).

CCPs are marketed subject to the Registration, Evaluation, Authorisation, and Restriction of Chemicals (REACH) regulation. This requires the products to be registered with the European Chemicals Agency, which by implication means that when traded, CCPs are no longer regarded as waste. Where necessary, CCPs meet any relevant national and European building materials standards and regulations.

Within the EU-15, fly ash represents about 65% of total CCP production. Fly ash is used as a feedstock for the production of cement clinker, as a constituent in concrete, and for the manufacture of various blended cements. In 2013, this accounted for the utilization of 23.24 of the 33.64 Mt (69%) produced. The use of 13.55 Mt of fly ash in concrete accounted for the largest volume. All the boiler slag (0.92 Mt) is used, mainly as blasting grit or in pavement base course. Along with bottom ash, it is also utilized as structural fill and aggregate or binder in road construction. A large portion of the fly ash and bottom ash produced in the EU-15 was used for mine reclamation and restoration.

The FGD product finds wide application in Europe. In 2013, 11.9 Mt were produced, of which Germany accounted for about 65%. FGD gypsum is accepted as a direct replacement for natural gypsum and is used in the manufacture of wallboard, as a set retarder for cement, and to produce gypsum blocks.

Besides the production of wallboard, FGD gypsum is also applied as set retarder for cement, in self-leveling floor screed and in conjunction with fly ash in mine reclamation and restoration. Approximately 90% of the FGD gypsum is beneficially utilized.

## 4.5 Utilization in the United Kingdom

There is a concerted drive in the United Kingdom to increase renewable energy and shut down coal-fired power stations. Less than 15% of the electricity supply in 2015 came from coal-fired power stations. In Nov. 2015, the Secretary of State for Energy and Climate Change announced proposals to close the remaining coal-fired power stations by 2025.

While the planned closures of coal-fired power stations will have a significant impact on the United Kingdom's future energy mix, the UKQAA is confident about the supply of coal ash for construction products both now and in the foreseeable future.

Over the last decade, the coal-fired power stations produced, on average, ~5–6 Mt of fly ash a year. The current annual supply still continues to outstrip demand; on average, 40%–70% was utilized. Should supply become constrained could be imported and there is also around 50 Mt of stockpiled ash that has been amassed over the years. This untapped resource could become a valuable complementary raw material if correctly processed. Extensive investigations into this option are currently underway.

All the bottom ash (0.6–1.0 Mt) is used, primarily as a lightweight aggregate for concrete blocks.

Fly ash-based grouts have long been used to stabilize collapsing and abandoned mines. Recently, this has been extended to include limestone caverns. To remain economically viable, a grout paste containing as little as 2% Portland cement was developed.

The use of coal ash must comply with the European Waste Framework Directive. A material that is considered to be a waste must be recovered and achieve end-of-waste status before it may be utilized. The current use of fly ash is predominantly in cement manufacture and geotechnical engineering (Table 4.5). The figures for the production and use of CCPs in the United Kingdom is included in the EU-15 data. Fly ash is widely referred to as pulverized fuel ash in the United Kingdom, but this terminology is slowly falling into disuse. The United Kingdom has also adopted European Norms since 2007.

Table 4.5 **Fly ash utilization and disposal in the United Kingdom (2014)**

| Fly ash use | Tons | % |
|---|---|---|
| Cement manufacture | 580.85 | 12.5 |
| Concrete | 777.95 | 16.7 |
| Autoclaved aerated concrete | 751.64 | 16.2 |
| Grouting | 163.04 | 3.5 |
| Geotechnical engineering | 833.60 | 17.9 |
| Other applications | 171.97 | 3.7 |
| Disposal | 1367.34 | 29.4 |
| Total fly ash production | 4646.39 | 99.9 |

## 4.6 Utilization in Israel

In the absence of domestic sources, coal-fired power generation in Israel is fully dependant on coal imports, mainly from South Africa and Columbia.

Between 2000 and 2014, Israel imported 13 Mt of washed bituminous coal for power generation per year. On average, this gave rise to 1.1 Mt of fly ash and 0.15 Mt of bottom ash annually.

With disposal at sea being prohibited and limited land available for surface impoundments, it is mandatory that all the coal ash in Israel be beneficially utilized. The Coal Ash Administration, established in 1993 with the objective of coordinating the effort at a national level to solve the problem of ash accumulation at the power plants, chose to deal with the problem by advancing the use of coal ash as an economic resource. The commercial success of this initiative resulted in coal ash being used extensively in cement, concrete, building products, road construction, and agriculture with an average utilization rate of over 99.5% being consistently maintained for the past 14 years.

For the year 2014, cementitious binders (0.46 Mt) and concrete (0.45 Mt) accounted for 96.4% of the fly ash used. The main application for fly ash in concrete is as a partial replacement for dune sand, where it enhances workability. A small (23 Kt) but significant fly ash market has been established by using it to treat (pasteurize) sewage sludge.

Bottom ash utilization was initially delayed due to environmental concerns, but once this application was approved, agricultural applications have been developed especially for soil amelioration, fertility improvement with fly ash stabilized biosolids, modification of its physical properties, and application in reed beds.

Although the volumes are relatively small, a number of innovative applications have been developed. For example, the coarse fraction, $\geq$2 mm, serves as a substrate for plant growth and a soil amendment, as well as in conjunction with lime for the manufacture of fertilizer from municipal sewage sludge. The fine fraction, $\leq$2 mm, is used as a substitute for tuff, for cowshed bedding and as a secretion absorbent in poultry breeding.

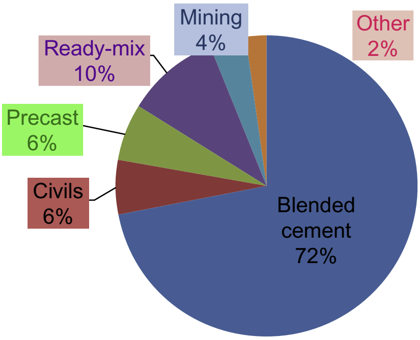

**Fig. 4.2** Breakdown of the 2.5 Mt fly ash market for South Africa in 2014.

With Rotenberg being the only power station equipped with FGD, only modest quantities of gypsum are produced all of which are used in agriculture.

## 4.7 Utilization in South Africa

Coal combustion accounts for 85% of the electrical power generated in South Africa. The state-owned enterprise (Eskom) supplies 95% of the electrical power. A total of 35 Mt of coal ash (29 Mt fly ash and 6 Mt bottom ash) is generated, but only 11.6 Mt (9.9 Mt fly ash and 1.7 Mt bottom ash) are available for sale. Eskom has a zero-effluent discharge policy; therefore it uses the coal ash as a “sink” for their liquid effluents, making it unsuitable for use.

In total, 2.5 Mt (25%) of the available fly ash was sold in 2014. About 1% of the bottom ash is sold. Fly ash is almost exclusively applied in the cementitious market, with 72% used for cement extension and 26% in concrete (Fig. 4.2).

Due to the low sulfur content of the coal, no FGD is currently being produced, but FGD is being fitted to a 600 MW boiler of a power station currently under construction.

## 4.8 Utilization in India

Electricity generation in India is predominantly from low grade high-ash (30%–45%) coal. Due to the volume involved, the management of fly ash has been a matter of concern because of the large area of land require for disposal.

In resolving the problem, the government set up ash utilization initiatives. They removed excise duty on building products using more than 25% fly ash and exempted import duties on equipment acquired for the manufacture of fly ash-based products.

The Indian government established Fly Ash Mission (FAM) as a joint activity between the Department of Science and Technology, Ministry of Power, and Ministry of Environment and Forests as the custodians of the project to increase ash utilization. The FAM set utilization goals, provided appropriate concessions, and actively promoted research, development, and technology transfer so that fly ash could be gainfully utilized instead of being disposed.

The aim of the program was to achieve 100% utilization in a phased manner by implementing new applications and exploiting existing opportunities. Limits were also placed on areas approved for disposal to landfill disposal (Kumar, Mathur, & Sinha, 2005). Progress towards achieving the prescribed goals is monitored by the Central Electricity Authority (CEA; Table 4.6).

Due to the concerted efforts of FAM, these initiatives and policy decisions have led to a large number of technologies applied to the utilization and safe management of fly ash. As a result the market grew significantly over the last 15 years, especially between 2000 and 2010, when utilization increased from 12.0% to peak at 62.6% in 2010. For the last 2 years, the rate has averaged 56%, but the total tonnage utilized has increased consistently, exceeding 100 Mt for the first time in 2014–15 (CEA, 2015).

As a result, the utilization of fly ash increased from 6.64 Mt in 1996–97 to 102.54 Mt in 2014–15, thereby achieving a commendable utilization level of 55.69% for the 182.6 Mt produced at the 145 operational power stations.

Data on fly ash generation and utilization is provided biannually by the power stations. After analysis by the relevant government departments, a comprehensive report on the status of fly ash generation and its utilization is uploaded to the CEA website so that the availability of fly ash at different thermal power stations in the country is easily accessible to anyone interested in using the material. Demonstration projects funded by FAM have also been set up to establish more confidence in promising utilization technologies.

During the 2014–15 year, 42.26% of the fly ash utilized in the manufacture of Pozzolana Cement, 13.00% in mine filling, 11.72% (12 Mt) in bricks and tiles,

**Table 4.6** **Fly ash applications in India (2014–15)**

| | Quantity of fly ash utilized in the mode of utilization | |
|---|---|---|
| **Application** | **Million ton** | **Percentage** |
| Cement | 43.33 | 42.26 |
| Mine filling | 13.33 | 13.00 |
| Bricks and tiles | 12.02 | 11.72 |
| Reclamation of low lying area | 11.04 | 10.77 |
| Ash dyke raising | 9.80 | 9.56 |
| Roads and flyovers | 3.41 | 3.32 |
| Agriculture | 1.97 | 1.93 |
| Concrete | 0.76 | 0.74 |
| Hydropower sector | 0.01 | 0.01 |
| Other | 6.87 | 6.70 |
| Total | 102.54 | 100.00 |

10.77% in reclaiming low lying areas, and 9.56% for ash dykes. Surprisingly, only 0.74% was used in concrete while 3.32% was used in roads & embankments. The 1.97 Mt used in agriculture is applied with great effect as a soil modifier and a source of micro and macronutrients. Demonstration projects indicate that crop yields increase by 15%–30%.

## 4.9 Utilization in China

Coal has been the dominant source of energy driving the rapid economic development of China. The country is the world's largest consumer of coal, with an annual usage surpassing that of the United States, the European Union, and Japan combined. In 2012, coal production was estimated to be 3.47 billion tons.

In 2012, over three billion tons of coal was burned, half of which used to generate electricity. Coal-fired plants account for about 75% of the electrical power used in China (He, Luo, & Hu, 2012). With only about half the coal being washed prior to power generation, a vast amount of ash arises, estimated to be in the region of 500 Mt (Tang et al., 2013). This huge volume presents significant problems for its safe disposal. Coal ash is considered a Class 2 General Industrial Solid Waste and is managed in accordance with the mandatory disposal standard (GB 18599-2001). Wet disposal (90%) dominates, but measures taken do not always suffice to prevent leaching and surface run-off.

China is pursuing a comprehensive utilization policy as the most appropriate way to minimize pollution. The central government has also implemented sustainability guidelines to reduce environmental impact and promote responsible disposal. China is a vast country, (10 million km$^2$) with a diverse geography and various levels of economic development. There are 2386 coal-fired power plants in China; 1642 are independent and 744 are owned by corporations. With so many plants spread over the country, quantifying production can be challenging. Depending on the particular source of information, the annual volume of coal ash produced and mentioned in the literature is divergent, varying from 440 to 540 Mt; for 2015, the estimated volume lies between 570 and 580 Mt (Wei, Wang, Ying, Luo, & Ninomiya, 2015; Yao et al., 2015).

The amount of coal ash utilized is also subject to controversy. The government has set utilization goals and also implemented policies and regulations to provide incentives to achieve these targets. As a result of these measures, the volume of coal ash utilized has increased from 199 Mt in 2005 to 294 Mt in 2012, but with a concomitant increase in fly ash production from 302 to 440 Mt, the utilization rate remained fairly static at about 67%. However, the National Development and Reform Commission of China reported that in 2011, ash generation and utilization was 540 and 367 Mt, respectively (Yao et al., 2015). While the utilization rate (67%) is the same as mentioned above, the volumes quoted are much higher than those from other sources.

Based on an independent 8-month survey of 14 thermal power stations across China, Greenpeace publicly challenged these statistics, stating: "The biggest misconception is the belief that 60% or more of China's coal ash is reused—in reality it is less than 30%."

Currently, fly ash is used in China in the following applications:

- engineering and mine backfill (15%)
- soil amelioration and fertilizers (15%)
- cement extension, clay and cement-bonded bricks, etc. (35%)
- road stabilization, wearing course, and embankments (20%)
- concrete and mortar in construction projects (10%)
- others, including alumina recovery etc. (5%)

New power stations need to have fly ash utilization strategies in place prior to construction, while existing stations are required to upgrade ash handling systems. To facilitate market acceptance and use, power stations may only sell fly ash after processing it in accordance with specific standards. New clay brick and tile production facilities may not be established near power stations, so existing plants are encouraged to use fly ash in their production. Authorities provide incentives (e.g., Shanghai introduced a levy on power stations to support research of new uses of fly ash), but they may also impose penalties on construction projects that do not meet a set target of fly ash utilization.

Although it does not appear to be mandatory, the authorities harbor an expectation that power stations should simplify access for large-scale users of their fly ash. Financial and taxation incentives (e.g., VAT exemption) have been introduced to promote the purchase or application of ash.

There is disparity and imbalance in fly ash utilization rates within China. In the developed coastal regions, especially the Yangtze and Pearl River Delta as well as the Bohai Rim, the utilization-to-production ratio of fly ash could exceed 100% so that customers can compete to secure a fly ash supply, import from other regions, or use ash from storage (Fig. 4.3).

Meanwhile, in the underdeveloped central and western parts of China, the fly ash utilization ratio could be below 30%, although there might be fly ash shortages in certain months because of the cyclical nature of the building material and cement business.

Like elsewhere in the world, fly ash is predominantly used in cementitious and allied applications (Table 4.7). It should be noted that there is a difference in the categories utilized by the three authors to quantify applications. This illustrates the difficulty and uncertainty in characterizing the market.

The Three Gorges dam, which at 22,500 MW is the largest power-producing facility in the world, used 26.4 million $m^3$ of concrete containing 50% fly ash to construct the 2335 m-long, 181 m-high wall. Three Gorges reduces coal consumption by 31 Mt annually, which avoids 100 Mt of greenhouse gas emissions and is an integral part of China's renewable energy policy.

Fly ash utilization is also being diversified and extended beyond the conventional applications in the construction industry. Under a series of preferential policies issued by the state and local government, the recovery of alumina is being undertaken in the Inner Mongolia and Shanxi province. The recovery of magnetite, cenospheres, and gallium is also being pursued.

**Fig. 4.3** Key regions of coal ash use in China (D. Harris, Asian Coal Ash Association).

**Table 4.7** Coal ash utilization in China

| www.asiancoalash.org | % | Tang et al. | % | Jow et al. | % |
|---|---|---|---|---|---|
| Building | 35 | Cement | 38 | Cement | 41 |
| Construction | 10 | Concrete | 14 | Bricks | 26 |
| Roads | 20 | Building | 26 | Roads | 5 |
| Agriculture | 15 | Civil engineering | 20 | Concrete | 19 |
| Backfill | 15 | Other | 2 | Agriculture | 5 |
| Other | 5 | | | Other | 4 |

It is estimated that 10% of the fly ash in China contains more than 30% alumina. Given the limited bauxite reserves of the country, the recovery of alumina either by alkaline or acidic leaching is being studied. An acidic process operating at approximately 130°C achieving a recovery rate of 80% is showing promise. The alkaline sinter process also shows similar recovery rates. For commercialization the most suitable process will be determined by the chemical and mineralogical composition of the ash itself (Tang et al., 2013). Reports indicate that the China Shenka Group are operating a 10,000 pilot plant recovering 80% alumina, along with gallium and silica. A production plant of one million tons may be commercialized in the north of China.

The Chinese Academy of Sciences has developed a technique to chemically extract alumina and then use the residue to produce fibers, which can be used as fillers in the rubber and polymer industries. Initial tests show promise for commercial application.

The National Institute for Clean and Low-carbon Energy (NICE) has developed new and novel application technologies. Their approach of using the resource potential of coal ash has resulted in three new technologies and five new products for specific markets. These include geopolymer foam, polymer fillers and flame retardants (Dong et al., 2015).

The research team at NICE used their dry separation technology to recover two distinct fractions of fine particles, one with a mean size between 2 and 3 μm, as well as a slightly coarser one $<10$ μm. Depending on the specific application envisaged, these particle fractions have been found to exhibit numerous advantages when used to replace $CaCO_3$ in a variety of polyolefin plastics, as well as rubber. They are more amenable to processing and have excellent flame-retardant properties. These results bode well for their commercialization, and the group has developed specific formulations.

The world's first automated fly ash-based ceramic tile manufacturing facility is under construction in China. Compared to the traditional process, the new processing technology is claimed to be 15% cheaper. It saves 80% water and 20% fuel, all while using 20% less energy.

## 4.10 Conclusion

The utilization of CCPs is a success story of technical innovation that enabled the development of environmentally sustainable alternatives to nonrenewable resources. Besides reducing the environmental impact of fossil fuel power generation, the use of CCPs as a substitute for mined or manufactured materials in the building, construction, and civil engineering industries lowers costs and promotes sustainability. The country or regional opportunities in the CCP market are determined by the range of products emanating from the specific coal combustion technology applied and the air pollution abatement equipment fitted. There are a plethora of factors that define the market. The nature of the coal, the combustion practice implemented, environmental regulations and associated incentives, transport logistics, and disposal cost, as well as the pricing and availability of competitive commodities, all play a role in determining the variety CCPs available for commercialization.

Fly ash, bottom ash, and, where the combustion stoichiometry is favorable, cenospheres arise during pulverized coal combustion. Depending on the scrubbing process employed to reduce the environmental impact of using fossil fuels, the desulfurization of the flue gas results in either a dry or SDA or gypsum when wet scrubbing is implemented. FBC enables the capture of acidic pollutants without resorting to scrubbers, although as with pulverized coal combustion, both bottom ash and fly ash are formed the lower combustion temperature, and the presence of the sorbent in the ash results in a product with substantially different properties. With all of these variables, it is not surprising that as described in the preceding sections, the "fingerprint" of CCP utilization is unique to each country. Comparison of applications in various parts of the world highlights how the interplay between technical and economic criteria defines a particular market. In other words, an application in one country does not imply it can be implemented elsewhere. For example, aerated autoclaved concrete is a significant part of the fly ash market in the United Kingdom, but not in other countries.

While the chemical, physical, and mineralogical properties of fly ash are important, the commercial success depends on the cost of accessing and delivering the ash to the market. In instances where the use of fly ash is technically viable but not economically feasible, it may require beneficiation to recover the most reactive or suitable fraction. This not only improves consistency, but also ensures that the fly ash conforms to specific standards and quality criteria, which allows it to compete more effectively with conventional products. Considering all the markets that have been developed throughout the world, coal ash is no longer a waste and should be considered a resource. Currently, and for the foreseeable future, applications in the cementitious sector will dominate the market for fly ash because its pozzolanic and/or hydraulic properties provide significant synergy and technical benefits with Portland cement. Bottom ash is predominantly used worldwide as an aggregate, but in some instances, it can be used in reed beds or serve as a substrate for plant growth.

Obviously the legal framework under which the CCP market functions varies from country to country. Eliminating ambiguity and establishing a sound international regulatory framework is imperative if the market is to develop and flourish. All contingent liabilities attributable to the processing and marketing need to be addressed, and the generally highly emotional and often unjustified connotation of being hazardous requires thorough scientific investigation and should be removed where applicable to avoid uncertainty and cast doubt about future opportunities

Fly ash has an array of attributes that makes it eminently suitable for utilization beyond the building and construction sectors. There are large-volume market opportunities for CCPs for environmental protection, where their unique properties can be exploited to good effect in preference to nonrenewable raw materials The rehabilitation of poor quality or impacted soils is a significant opportunity for fly ash, where its inherent alkalinity and range of trace elements can be exploited to improve soil fertility and agricultural yield. The rheology of fly ash and its synergy with Portland cement can be applied with good effect to backfilling and rehabilitation of mines, as well as mitigating acid mine drainage.

If a paradigm shift can be accomplished by considering coal ash as a mined mineral, it will require processing and beneficiation to increase its value and will encourage the implementation of emerging technologies that could significantly increase the global CCP market. To achieve this, further research and development would be mandatory so that the potential market opportunities can be satisfied by

CCPs with the appropriate properties. This would include pushing the boundaries for current cementitious applications and the development of new binders by improving the knowledge and technological know-how required for the wider use of, for example, geopolymers, as well as novel and composite cements that have a smaller $CO_2$ footprint. In a similar vein, fly ash can serve as a source of aluminum, other trace elements, and rare earth elements.

It is therefore apparent that with all the different types of CCPs available and each possessing unique properties, their future commercial application in one form or another is assured.

## References

ARTBA. (2015). Production and use of coal combustion products in the U.S.: Historical market analysis. Prepared by American Road & Transportation Builders Association for the American Coal Ash Association (ACAA), May.

Caldas-Vieira, F. ECOBA/EDP, Lisbon, Portugal and Feuerborn, J. (2014). Coal combustion products in Europe—A continuous challenge. EuroCoalAsh 2014, Munich, Germany, 14/15 October. ISBN: 978-3-86875-805-4.

Caldas-Vieira, F., & Feuerborn, H. -J. (2013). Impact of political decisions on production and use of CCPs in Europe. In: *World of Coal Ash, April 22-35, Lexington, KY*.

CEA. (2015). Report on fly ash generation at coal/lignite based thermal power stations and its utilization in the country for the year 2014-15. New Delhi: Central Electricity Authority. October.

Dodd, W. E. (2000). *Fly ash use in pressurized grout remote backfilling of abandoned underground mines in North Dakota. In: Third biennial workshop: Interstate Technical Group on Abandoned Underground Mines, Kansas City, MO, April 25-27*. https://www.fhwa.dot.gov/engineering/geotech/hazards/mine/workshops/kdot/kansas04.cfm.

Dong, Y., Jow, J., Zhao, Y., Ding, S., Li, Q., Wang, X., et al. (2015). Fly ash-based technologies and value-added products based on materials science. In: *World of Coal Ash (WOCA) conference, May 5-7, Nashville, TN*.

He, Y., Luo, Q., & Hu, H. (2012). Situation analysis and countermeasures of China's fly ash pollution prevention and control. In: *Procedia Environmental Sciences: Vol. 16. The 7th international conference on waste management and technology* (pp. 690–696).

Heidrich, C. (2011). Legal certainty: Why we need to change the waste paradigm. In: *World of Coal Ash (WOCA) conference, May 9-12, Denver, CO*.

Kumar, V., Mathur, M., & Sinha, S. S. (2005). A case study: Manifold increase in fly ash utilisation in India. In: *Fly ash utilization programme (FAUP)*. New Delhi: TIFAC DST.

Mirza, J., Saleh, K., Roy, V., & Mirza, M. S. (1999). *Use of high volume fly ash in grouting applications*. 12/1/1999. https://www.concrete.org/publications/internationalconcreteabstractsportal.aspx?m=details&ID=6137.

Murarka, I. P., & Erickson, J. (2006). *Use of coal combustion products in mine-filling applications. A review of available literature and case studies*. DOE award no: 99-CBRC. Final report.

Schueck, J., Tarantino, J., Kania, T., & Scheetz, B. (2001). The use of FBC ash for alkaline addition at surface coal mines. In: *International ash utilization symposium 2001, Center for Applied Energy Research, University of Kentucky, Lexington, KY*.

Tang, Z., Ma, S., Ding, J., Wang, Y., Zheng, S., & Zhai, G. (2013). Current status and prospect of fly ash utilisation in China. In: *World of Coal Ash (WOCA) conference, April 22-25, Lexington, KY*.

Wei, Y., Wang, Q., Ying, G., Luo, Z., & Ninomiya, Y. (2015). Characteristics and utilization of fly ash from coal-fired power plants in China. In: *World of Coal Ash (WOCA) conference, May 5-7, Nashville, TN*.

Williams, D., Ramlackhan, M., & Spriggs, D. (2010). *Report on potential for backfilling bord and pillar voids using fly ash slurry*. CSIRO. https://www.dnrm.qld.gov.au/__data/assets/pdf_file/0007/262663/collingwood-park-report-appendix-c.pdf. July.

Yao, Z. T., Ji, X. S., Sarker, P. K., Tang, J. H., Ge, L. Q., Xia, M. S., et al. (2015). Comprehensive review on the application of coal fly ash. *Earth-Science Reviews*, *141*, 105–121.

# Coal fly ash as a pozzolan

# 5

*M. Thomas*[*], *R. Jewell*[†], *R. Jones*[‡]
[*]University of New Brunswick, Fredericton, NB, Canada, [†]University of Kentucky, Lexington, KY, United States, [‡]University of Dundee, Dundee, Scotland

## 5.1 Introduction

The use of pozzolans to produce concrete dates back more than two millennia to the ancient civilizations of Greece and Rome, when volcanic ash was combined with "burned" lime to produce a hydraulic binder. Many of the structures built using such binders still exist today. A prime example of this is the Pantheon in Rome, where volcanic ash was used as a pozzolan in the lightweight concrete dome. Indeed, the village of Pozzuoli near Naples lent its name to the term pozzolan, as it was one of the best sources of volcanic ash due to its proximity to Mount Vesuvius.

Although the potential for using coal fly ash as a pozzolan was realized at the beginning of the last century (Anon, 1914), fly ash did not become widely available until the 1930s. It was the pioneering work of Davis (Davis, Carlson, Kelly, & Davis, 1937) and the University of California, Berkeley that opened the door for its first major use in the construction of the Hungry Horse Dam in Montana (USBR, 1948). Nowadays the use of fly ash as a pozzolan in the production of concrete occurs worldwide. Fly ash is either added directly to concrete as a separate ingredient at the mixer or as a component of blended cement. Fly ash concrete has been used in a great many significant concrete structures; a few notable examples include the Sunshine Skyway (Florida), the San Francisco-Oakland Bay Bridge (California), Channel Tunnel (between England and France), the Three Gorges Dam (China), and what is currently the tallest building in the world, Burj Khalifa (Dubai).

This chapter discusses the use of fly ash as a pozzolan in concrete and how its use affects the properties of concrete. A number of case histories where fly ash has been used in major concrete structures are provided together with information on fly ash specifications. The use of fly ash in other types of cementitious products such as grouts, mortars, flowable fill, and soil cement is also covered briefly. Finally, some information is given regarding the use of coal bottom ash in concrete products and other applications.

## 5.2 Definitions

The following definitions for fly ash and pozzolan are provided by the American Concrete Institute's (ACI CT-13):

***Fly ash*** The finely divided residue that results from the combustion of ground or powdered coal and that is transported by flue gases from the combustion zone to the particle removal system.

**Coal Combustion Products (CCP's).** http://dx.doi.org/10.1016/B978-0-08-100945-1.00005-8

***Pozzolan*** A siliceous or silico-aluminous material that will, in finely divided form and in the presence of moisture, chemically react with calcium hydroxide at ordinary temperatures to form compounds having cementitious properties (there are both natural and artificial pozzolans).

There is no formal (i.e., standardized) definition for coal bottom ash. Like fly ash, *bottom ash* is part of the noncombustible material that forms in a coal furnace, but it comprises larger and heavier particles that settle and accumulate at the bottom of the boiler rather than being carried way with the flue gases.

## 5.3 Origin of fly ash

Coal fly ash and bottom ash are by-products from coal-burning, electricity-generating stations. Ground (pulverized) coal is blown with air into the furnace, where temperatures reach 1500°C (2700°F) and where the combustible materials (e.g., hydrocarbons and oxygen) ignite, and the noncombustible minerals associated with the coal melt and form small liquid droplets. The lighter droplets are carried away from the burning zone with the flue gases and cool rapidly at the surface, where they form glassy spheres. The inside of the larger droplets cools more slowly, allowing the formation of some crystalline phases. These particles are termed fly ash and are collected from the flue gases using mechanical and electrical precipitators, or bag houses. It is this material that is used as a pozzolan in concrete and other cementitious products. Larger and heavier ash particles drop to the bottom of the furnace; this material is termed bottom ash or furnace bottom ash (FBA). Such material is not generally suitable for use as a cementitious material for concrete, but it is used in the manufacture of masonry block and other applications.

## 5.4 Properties of fly ash and bottom ash

### 5.4.1 Fly ash

The physical, chemical, and mineralogical properties of fly ash can vary widely and significantly influence the behavior of the material in concrete. The chemistry and mineralogy of the ash are dependent on the composition of the noncombustible, inorganic components of the coal; these include minerals such as quartz, calcite, gypsum, pyrite, feldspar, and clays in widely varying amounts. The properties of the fly ash also depend on the burning conditions within the furnace and on the collection (and storage) methods.

Table 5.1 shows the chemical composition of two different fly ashes: a low-calcium fly ash produced from burning bituminous coal and a high-calcium fly ash from a subbituminous coal. Fly ashes are commonly encountered in compositions between the two examples shown in the table. Fig. 5.1 shows X-ray diffraction patterns for a low- and high-calcium fly ash, indicating that the mineralogy of the two ashes is very different; typical crystalline compounds are listed in Table 5.2. The broad hump in the diffraction pattern (Fig. 5.1) results from the presence of noncrystalline material

**Table 5.1** **Chemical composition of typical fly ashes**

| | Low-calcium fly ash | Moderate-CaO fly ash | High-CaO fly ash |
|---|---|---|---|
| $SiO_2$ | 56 | 32 | 32 |
| $Al_2O_3$ | 28 | 18 | 18 |
| $Fe_2O_3$ | 6.8 | 5.2 | 5.2 |
| CaO | 1.5 | 30 | 30 |
| $SO_3$ | 0.1 | 2.6 | 2.6 |
| MgO | 0.9 | 5.2 | 5.2 |
| $Na_2O$ | 0.4 | 1.2 | 1.2 |
| $K_2O$ | 2.4 | 0.2 | 0.2 |
| LOI | 2.8 | 0.6 | 0.6 |

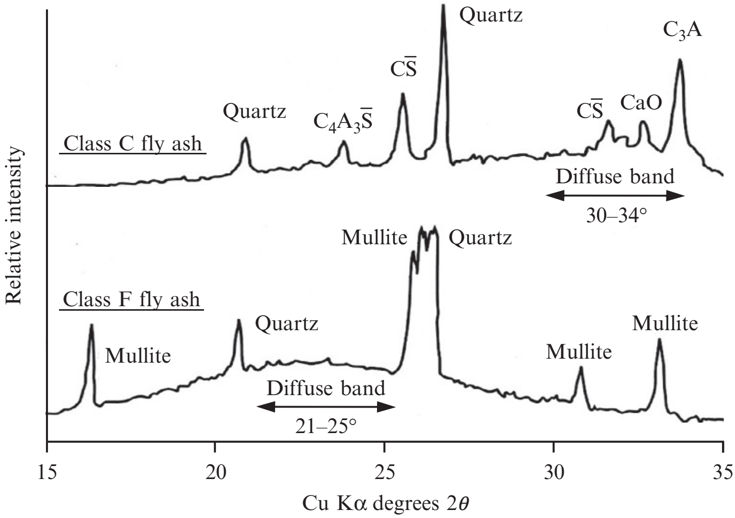

**Fig. 5.1** X-ray diffraction patterns for class F and class C fly ash (Mehta, 1983).

(glass), and its position reflects the composition of the glass. It is evident from these data that low- and high-calcium fly ashes have different chemical compositions and that the crystalline and glassy phases are also quite dissimilar.

Low-calcium fly ash consists principally of aluminosilicate glass and crystalline quartz, mullite, hematite, and magnetite (ACI 232, 2003). The crystalline phases are considered inert in concrete, and the glass will only react in the presence of alkali or lime; such materials are pozzolanic but not hydraulic. High-calcium fly ash, on the other hand, contains a number of crystalline phases that are reactive (hydraulic). This, coupled with the fact that the glass is calcium bearing and more reactive, renders the

**Table 5.2** Crystalline compounds in fly ash

| Mineral name | Chemical formula | Comments |
|---|---|---|
| Quartz | $SiO_2$ | These phases are inert in concrete and are the only crystalline phases in low-calcium fly ash<br>These phases are also present in lesser amounts in high-calcium fly ash |
| Mullite | $Al_6Si_2O_3$ | |
| Hematite | $Fe_2O_3$ | |
| Magnetite | $Fe_3O_4$ | |
| Anhydrite | $CaSO_4$ | Many of these phases react with water to form solid products of hydration<br>The quantity of these phases generally increases as the calcium content of the fly ash increases<br>These phases are not found in fly ashes with low to moderate calcium content ($<15\%$ CaO) |
| Tricalcium aluminate ($C_3A$) | $Ca_3Al_2O_6$ | |
| Dicalcium silicate ($C_2S$) | $Ca_2SiO_4$ | |
| Lime | CaO | |
| Periclase | MgO | |
| Melilite | $Ca_2(Mg,Al)(Al,Si)_2O_7$ | |
| Merwinite | $Ca_3Mg(SiO_4)_2$ | |
| Alkali sulfates | $(Na,K)_2O_4$ | |
| Sodalite | $Ca_2(Ca,Na)_6(Al,Si)_{12}O_{24}(SO_4)_{1-2}$ | |

material both pozzolanic and hydraulic in nature. In other words, high-calcium fly ash will set and harden when mixed with water.

In addition to providing an indication of the mineralogy and reactivity of fly ash, the calcium content also impacts the reactivity of fly ash and how it impacts the rate of hardening, heat evolution, and early-age strength gain, as well as its ability to control expansion due to the alkali-silica reaction (ASR) and damage due to the sulfate attack (Thomas, 2013). Although the calcium content of the fly ash is perhaps the best indicator of how the fly ash will behave in concrete, other compounds such as the alkalis ($Na_2O$ and $K_2O$), carbon [usually measured as loss on ignition (LOI)], and sulfate ($SO_3$) can affect the performance of the fly ash.

Fly ash is comprised predominantly of spherical particles (solid spheres or hollow cenospheres) with a broad size distribution (diameter from $<1$ to $>100$ μm) and median particle in the range from 5 to 20 μm. The spherical shape, broad particle size distribution, and the presence of submicron particles all contribute to the ability of the fly ash to decrease the water demand of concrete (see below). The specific gravity of fly ash depends to a large degree on its iron and carbon content and generally lies in the range from 1.9 to 2.8. Determining the precise value is important for mixture proportioning fly ash concrete. The color of fly ash varies from being almost white to buff colored to light gray. High carbon contents will tend to produce darker gray colors.

### 5.4.2 Bottom ash

Bottom ash and fly ash produced from the same coal will have a similar chemical composition, although the bottom ash will likely contain an increased amount of unburnt coal and hence have an increased carbon content as well as a concomitantly higher loss on ignition, or LOI. Bottom ash differs from fly ash in both particle shape and size as well as mineralogy. As the bottom ash particles fuse during cooling, the material is much coarser than fly ash, ranging in size from fine sand to gravel with a maximum particle size in the order of 12 mm (0.5 in). As a result of the larger fused particles, bottom ash contains more crystalline and less glassy phases than fly ash. It is generally inert showing little pozzolanic reactivity, hence bottom ash is typically not effective as a component of a cementitious binder.

## 5.5 Pozzolanic reaction of fly ash

As defined in Section 5.2 a pozzolan "chemically reacts with calcium hydroxide" to form cementitious compounds. In early Greek and Roman civilizations, volcanic ash was combined with lime (produced from burning limestone in a rudimentary kiln, $CaCO_3 \rightarrow CaO + CO_2$) and water to produce calcium-silicate hydrates. Today's pozzolans, such as fly ash, are usually used in combination with Portland cement (PC), which provides the source of lime. The hydration of the calcium silicate compounds, $C_3S$ (or alite) and $C_2S$ (or belite), in PC can be represented by Eqs. (5.1), (5.2), as follows[1]:

$$2C_3S + 11H \rightarrow C_3S_2H_8 + 3CH \tag{5.1}$$

$$2C_2S + 9H \rightarrow C_3S_2H_8 + CH \tag{5.2}$$

The actual composition of the calcium silicate gel that forms from the hydration of the alite and belite varies, and it is more usual to represent the phase simply as C-S-H, indicating that it has no rigorous stoichiometric composition. C-S-H is the principal cementing compound in PC concrete and is largely responsible for providing strength and other desirable concrete properties. Hydrated PC typically contains somewhere in the range of 50% C-S-H and 20%–25% CH (calcium hydroxide).

The reaction of the CH resulting from Eqs. (5.1), (5.2), with the silica (S) component of a pozzolan that can be represented by Eq. (5.3) (Helmuth, 1987).

$$xCH + yS + zH \rightarrow C_xS_yH_z \tag{5.3}$$

---

[1] Note these equations use "cement-chemists shorthand notation," where $C = CaO$, $S = SiO_2$, $A = Al_2O_3$, $F = Fe_2O_3$, $H = H_2O$.

The alumina present in pozzolans will also react with the CH from PC and may produce a variety of phases, the principal ones including strätlingite or gehlenite hydrate ($C_2ASH_8$) and hydrogarnet ($C_3AH_6$), and calcium aluminate hydrate ($C_4AH_{13}$).

The additional C-S-H that forms as a result of the *pozzolanic reaction* of the silica and alumina from the pozzolan with the calcium hydroxide produced by hydration of the PC is one of the principal mechanisms behind the technical benefits attributed to the use of pozzolans with PC in concrete.

This is an oversimplification of the true chemical path of the pozzolanic reaction as other compounds, such as the alkali hydroxides that reside in the pore solution of PC systems, also serve to accelerate the reactions. However, a detailed treatise of the highly complex series of reactions that do occur is beyond the scope of this text and can be found elsewhere (e.g., Massazza, 1998; Thomas, 2013).

The "pozzolanic activity" of a material defines the ability of that material to react with calcium hydroxide (Thomas, 2013). There are two components to this activity, the first being the total amount of CH with which the material can combine, and the second being the rate at which the reaction with CH occurs. Massazza (1998) states that there is general agreement that the total amount of CH with which a pozzolan can combine is dependent on the following factors:

- nature of the reactive phases in the pozzolan
- content of these phases
- $SiO_2$ content of these phases
- CH/pozzolan ratio of the mix
- duration of curing

On the other hand the rate of the reaction with CH will depend upon

- specific surface area of the pozzolan
- water/solid ratio of the mix
- temperature
- the composition of the PC, in particular its alkali content

Fig. 5.2 presents data from various studies and shows how the quantity of CH in hardened cement pastes changes with varying amounts of different pozzolans; the amount of CH has been normalized on the basis of the amount of PC in the blend. Silica fume and metakaolin, both highly reactive and finely divided pozzolans, consume CH rapidly, and the relative amount is much reduced at 28 days. Low-calcium fly ash, on the other hand, shows relatively little reduction in CH at 28 days, but there is considerable consumption at later ages. In very mature systems (e.g., after 14 years wet curing), 40% fly ash is sufficient to completely consume the calcium hydroxide.

High-calcium fly ashes exhibit both pozzolanic and hydraulic behavior (Thomas, 2013). When mixed with water, some high-calcium fly ashes will harden due to the hydration of crystalline calcium silicate ($C_2S$), the reaction between free lime and some of the glass, and the formation of ettringite. The hydration products in blends of PC and high-calcium fly ash are essentially the same as those that form in PC mixes with the addition of strätlingite and $C_2AH_8$ (Taylor, 1997) and increased quantities of calcium aluminate hydrates.

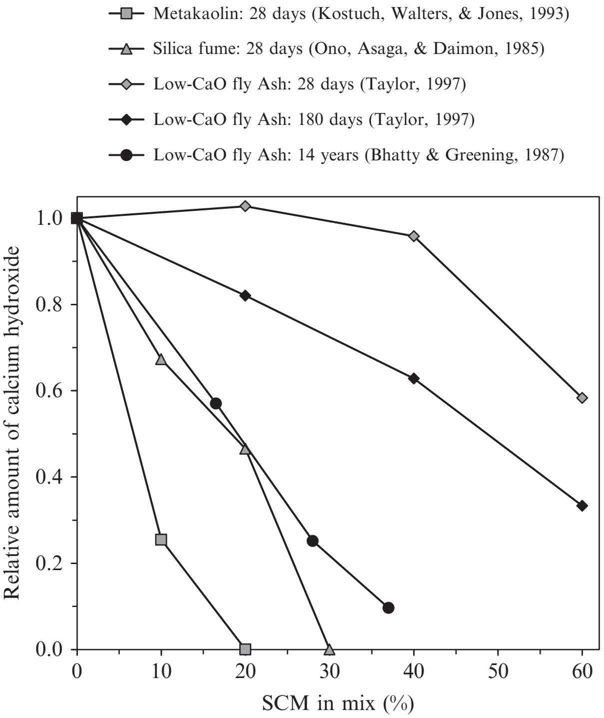

**Fig. 5.2** Consumption of calcium hydroxide by various pozzolans.

## 5.6 Influence of fly ash on the properties of concrete

The incorporation of fly ash in PC concrete influences many parameters including, but not limited to, the following:

- Fresh properties of the concrete including the workability, rheology, air content, pumpability.
- Setting behavior (e.g., time of initial and final set).
- Rate of hydration and heat evolution (including the maximum temperature attained at early ages).
- Evolution of the pore solution chemistry.
- Microstructure, particularly the pore structure (size distribution, connectivity, and tortuosity of the pores) and hence the permeability.
- Mechanical properties (e.g., compressive, tensile, and flexural strength, and modulus of elasticity).
- Volume stability (e.g., shrinkage and long-term or creep behavior).
- Durability including resistance to chloride ingress and corrosion of embedded steel, alkali-aggregate reaction, sulfate attack, cyclic freeze-thaw and salt scaling, and abrasion.

This section provides a brief summary of these effects; more comprehensive information can be found elsewhere (e.g., ACI 232, 2003; Helmuth, 1987; Joshi & Lohtia, 1997; Malhotra & Mehta, 1996; Massazza, 1998; Sear, 2001; Thomas, 2007, 2013).

## 5.6.1 Fresh concrete properties

### 5.6.1.1 Workability and water demand

The water demand of concrete refers to the amount of water required to achieve the desired level of workability or consistency (slump) and is largely controlled by the size, shape, surface texture, and grading of the aggregates, particularly the coarse aggregate. However, it is also a function of the amount and fineness of the cement, as well as the quantity of entrained air present. Good quality fly ash, which is demonstrated by high fineness and low carbon content, generally increases the workability and consistency of concrete, meaning that for a desired level of slump, the water demand is decreased. An approximate rule of thumb is that the water content can be reduced by 3% for each 10% replacement of cement for fly ash (Thomas, 2013). However, coarser fly ashes with higher carbon contents (i.e., high LOI) may lead to increases in water demand; the impact of these parameters on water demand are shown in Figs. 5.3 and 5.4.

The decreased water demand is often attributed to the spherical shape of fly ash particles that lubricate the mix by reducing interparticle friction; this often referred to as the "ball-bearing effect." However, this is somewhat of an oversimplification (Helmuth, 1987), and other contributing factors include an increased paste volume and the presence of submicron fly ash particles with the same surface charge that aids dispersion (Helmuth, 1987; Thomas, 2013).

Well-proportioned concrete mixtures containing fly ash will have improved workability when compared with a PC concrete of the same slump. This means that at a given slump, concrete with fly ash flows and consolidates better than a conventional PC concrete when vibrated. This is especially noticeable at high levels of fly ash. Such

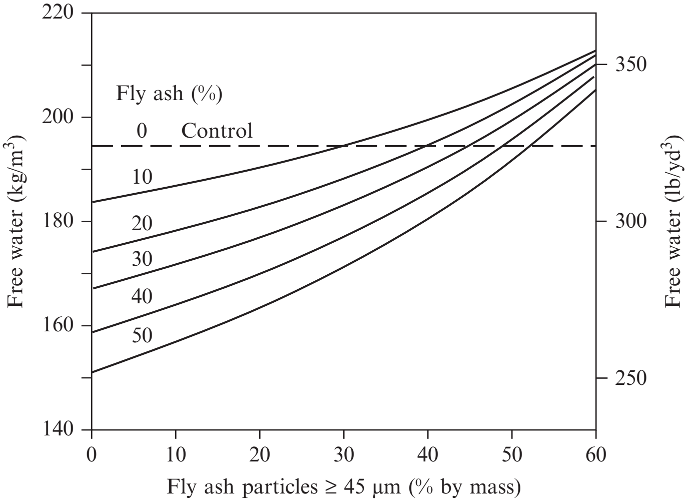

**Fig. 5.3** Effect of fly ash fineness on water demand of concretes proportioned for equal slump (Owens, 1979).

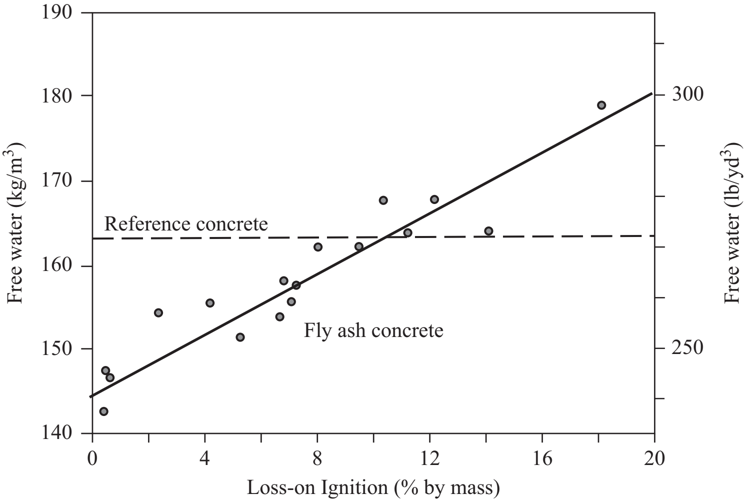

**Fig. 5.4** Effect of fly ash LOI on water demand of concretes proportioned for equal slump. Adapted from Sturrup, V. R., Hooton, R. D., & Clendenning, T. G. (1983). Durability of fly ash concrete. In V. M. Malhotra (Ed.), *Fly ash, silica fume, slag and other mineral by-products in concrete, ACI SP-79*, Vol. 1 (pp. 71–86). Farmington Hills, MI: American Concrete Institute.

concretes are sometimes described as thixotropic. The use of fly ash also improves the cohesiveness and reduces segregation of concrete, and the "lubricating action" renders the concrete easier to pump, reducing wear on equipment (Best & Lane, 1980).

### 5.6.1.2 Bleeding

Fly ash will generally reduce the rate and amount of bleeding[2] in concrete due to the increased volume of paste and increased amount of fines; this is especially noticeable in mixtures with relatively high levels of replacement (e.g., $\geq$30%). However, if advantage is not taken of the reduction in water demand resulting from the use of fly ash, there may be an increase in bleeding.

### 5.6.1.3 Air entrainment

Concrete containing fly ash generally requires a higher dose of air-entraining admixture (AEA) to achieve a satisfactory air-void system. This is mainly due to the presence of unburned carbon in the fly ash that absorbs the admixture. Consequently, higher doses of AEA are required as either the fly ash content of the concrete increases or the carbon content of the fly ash increases. There are a number of technologies for reducing the carbon content of concrete or for reducing its capacity for absorbing AEA. Generally, high-calcium fly ashes require a smaller increase in the air

[2] Bleeding is defined as the upward migration of mixing water in fresh concrete caused by the settlement of the solid materials and results in the development of a layer of water at the surface of newly placed concrete.

entrainment dose compared to low-calcium fly ashes and may, if high in water-soluble alkali, actually require less admixture than mixes without fly ash (Pistilli, 1983).

## 5.6.2 Setting behavior

The influence of fly ash on the setting behavior of concrete is dependent not only on the composition and quantity of fly ash used, but also on the type and amount of cement, the water-to-cementitious materials ratio (w/cm), the type and amount of chemical admixtures, and the concrete temperature. It is fairly well established that low-calcium fly ashes extend both the initial and final sets of concrete; this can be quite significant at low temperature, as shown in Fig. 5.5. Practical considerations may require that the fly ash content is limited during cold-weather concreting, although the use of set-accelerating admixtures and/or high early-strength PC may wholly or partially offset the retarding effect. During hot weather the amount of retardation due to fly ash tends to be small and is likely to be a benefit in many cases.

Higher-calcium fly ashes generally retard setting to a lesser degree than low-calcium fly ashes, probably because the hydraulic reactivity of fly ash increases with increasing calcium content. However the effect of high-calcium fly ashes is more difficult to predict because the use of some of these ashes with certain cement-admixture combinations can lead to either rapid (or even flash) setting or to a severely retarded setting (Roberts & Taylor, 2007; Wang, Qi, Farzam, & Turici, 2006).

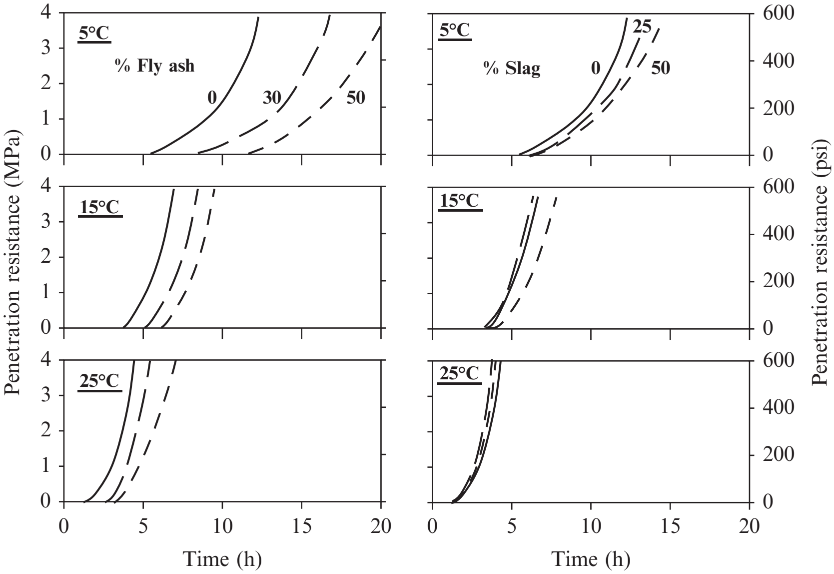

**Fig. 5.5** Effect of fly ash, slag and temperature on the penetration resistance of setting concretes proportioned for equal strength at 28 days and workability (Concrete Society, 1991).

### 5.6.3 Heat of hydration and rise of temperature

The use of fly ash, particularly low-calcium fly ash, reduces the rate of heat evolution and the magnitude of the temperature rise in concrete, especially at high levels of replacement. This is a major incentive for using fly ash in massive concrete pours where very significant temperature rises can occur with potentially damaging consequences for the concrete. Reducing the temperature rise in concrete reduces the potential for thermal cracking and for delayed ettringite formation. Due to their higher reactivity, high-calcium fly ashes are less effective in this role unless they are used at much higher levels of replacement.

Much of the published data on the effect of fly ash on heat evolution has employed isothermal calorimetry, where the amount of heat released is measured on a sample maintained at a constant temperature (typically room temperature). While useful, such studies fail to take account of the considerable impact of temperature on the rate of the pozzolanic reaction (hence the rate of heat release from a system containing pozzolans) and may significantly overestimate the beneficial impact of pozzolans on temperature control.

Numerous workers have measured the impact of fly ash on temperature rise in massive concrete monoliths at close to adiabatic conditions; a number of these studies have been summarized by Thomas (2013). One of the earliest studies of this nature was conducted by Ontario Hydro (Mustard & MacInnis, 1959) during the construction of the Otto Holden Dam. Two elements of the dam, measuring 3.7 × 4.3 × 11.0 m (12 × 14 × 36 ft), were constructed with embedded temperature monitors. One element was constructed using a concrete with 305 kg/m$^3$ (514 lb/yd$^3$) of PC, and the other with a concrete with the same cementitious material content but with 30% of the PC replaced with a Class F fly ash. Fig. 5.6 shows the results from this study, indicating that the use of fly ash reduced the maximum temperature rise over ambient from 47°C to 32°C (85°F to 58°F).

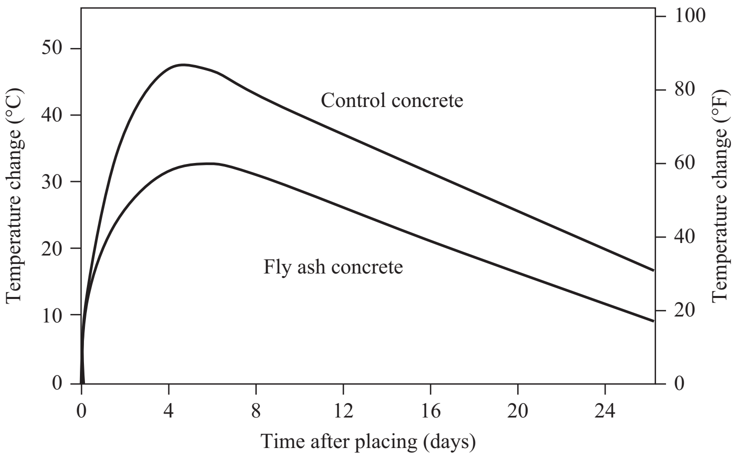

**Fig. 5.6** Effect of fly ash on temperature rise in concrete dams (Mustard and MacInnis, 1959).

### 5.6.4 Pore solution composition

Beyond 24 h or so, the pore solution of concrete is dominated by sodium ($Na^+$) and potassium ($K^+$) ions, which originate principally from the PC, together with hydroxyl ions ($OH^-$) to maintain electroneutrality. The concentration of hydroxyl ions increases with the alkali content of the PC and is generally in the range of 0.2–1.0 mol/L (pH 13.3–14.0). It is the high alkalinity of the pore solution that results in an ASR with certain aggregates (see Section 5.6.8.3) but also helps maintain embedded steel in a passive state. Fig. 5.7 shows how the hydroxyl-ion concentration of hardened cement paste (w/cm = 0.50) produced with a high-alkali cement (0.91% $Na_2Oe$) changes with time with varying amounts of different pozzolan. As previously observed with CH consumption (Section 5.5), high-reactive high fineness pozzolans like silica fume and metakaolin produce a significant reduction in the pore-solution alkalinity at early ages. Low-calcium fly ash (F) takes longer (between 28 and 90 days) to produce significant changes and higher replacement levels (25%–50%) are required to produce the same magnitude decrease as silica fume and metakaolin. High-calcium fly ash (C) is less effective in this role, with 50% C ash producing a similar reduction as 25% F.

The ability of pozzolans to control ASR, discussed in Section 5.6.8.3, is largely attributed to their ability to reduce the alkalinity ($Na^+$, $K^+$, and $OH^-$ concentration) of the pore solution. It is noteworthy that even in mature pastes with a high level of pozzolan (e.g., 20% metakaolin or 50% F fly ash), the pH of the pore solution is still significantly in excess of 13 (0.1 mol/L $OH^-$), which is more than sufficient to maintain the passive layer on embedded steel reinforcement.

### 5.6.5 Pore structure and permeability

Depending on the water-to-cementing-materials ratio (w/cm) and maturity, hardened cement paste typically has a porosity of 20%–30%. Some these pores are associated with the C-S-H and termed "gel pores," which are generally considered to be <10 nm

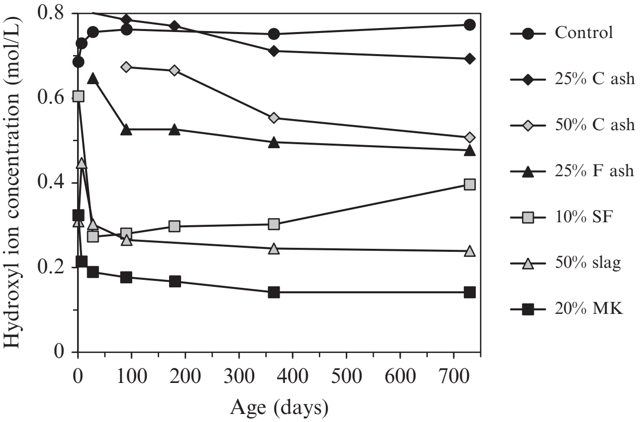

**Fig. 5.7** Pore solution evolution for pastes with high-alkali cement and various SCM's (Thomas, 2011).

and do not contribute to the transport of fluids or ions. Rather, mass transport occurs in the larger “capillary pores,” which range in size from 10 nm to 10 μm. These capillary pores can be subdivided further into large “macropores” (0.05–10 μm), which are mainly responsible for mass transport (movement of fluids and ions) and smaller “mesopores” (10–50 nm), which contribute to transport phenomena in the absence of macropores (Mindess, Young, & Darwin, 2003).

Fig. 5.8 shows the pore size distribution of hardened cement paste with and without fly ash. The data were obtained by mercury intrusion porosimetry, but this technique does not measure the gel pores. At early age (28 days), the capillary porosity, especially the volume of macropores, of the paste containing fly ash is significantly greater than that of the control paste (PC only). However, at a later age (1 year), the volume of macropores is reduced considerably in the fly ash paste and is much lower than that of the control paste.

The ability of pozzolans, like fly ash, to refine the pore structure producing finer and less well-connected pores is well established (Hearn, Hooton, & Nokken, 2006; Manmohan & Mehta, 1981). It is considered to be the main factor in reducing the permeability of concrete containing pozzolans and increasing concrete’s resistance to chloride-ion penetration (see Sections 5.6.5 and 5.6.8.1).

The permeability of concrete to fluids (e.g., water or gas) is generally measured by applying a pressure gradient across a concrete sample and then measuring the rate of fluid flow. The permeability of concrete to water, often termed the hydraulic conductivity, is a function of the volume, size, and connectivity of the pores (i.e., the pore structure). Table 5.3 presents data from an early study on the hydraulic conductivity of concrete pipes (Davies, 1954). At early age (28 days), concrete with fly ash may be many times more permeable than concrete without fly ash, but at a later age (6 months

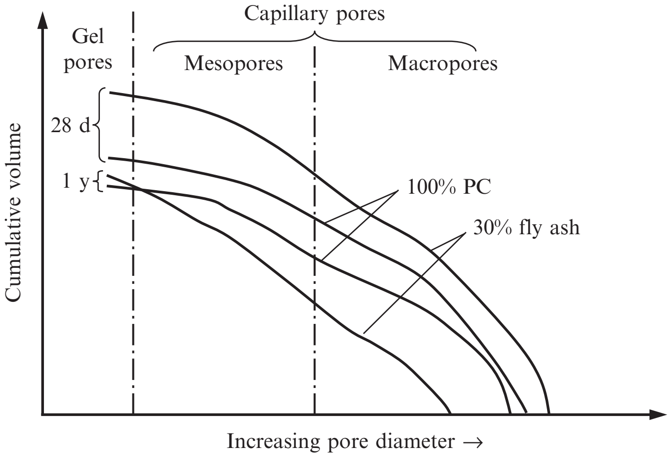

**Fig. 5.8** Effect of fly ash on pore-size distribution at 28 days and 1 year.
Modified from Manmohan, D., & Mehta, P.K. (1981). Influence of pozzolanic, slag, and chemical admixtures on pore size distribution and permeability of hardened cement pastes. *Cement, Concrete & Aggregates, 31*, 63–67.

**Table 5.3** **Effect of fly ash on the permeability of concrete**

| Fly ash | | | Relative permeability | |
|---|---|---|---|---|
| **Source** | **% by mass** | **w/cm** | **28 days** | **6 months** |
| – | 0 | 0.75 | 100 | 26 |
| Chicago | 30 | 0.70 | 220 | 5 |
| | 60 | 0.65 | 1410 | 2 |
| Cleveland | 30 | 0.70 | 320 | 5 |
| | 60 | 0.65 | 1880 | 7 |

Data from Davies, R. E. (1954). *Pozzolanic materials—With special reference to their use in concrete pipe*. Technical Memo. American Concrete Pipe Association.

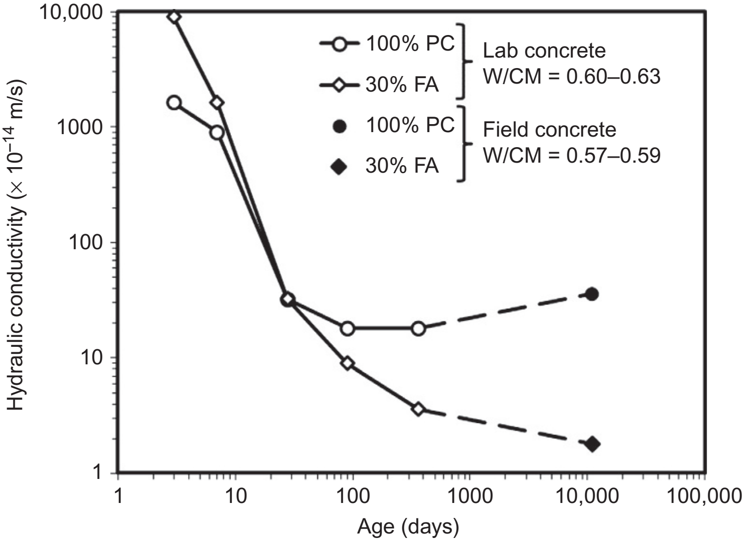

**Fig. 5.9** Effect of fly ash and age on the permeability of concrete.

in this study) the permeability of the fly ash concrete is 5 to 10 times lower. This behavior is consistent with the effect of fly ash on the pore structure previously discussed.

Fig. 5.9 presents unpublished data from the author showing the impact of age on the hydraulic conductivity of concrete with and without fly ash. Data are shown for laboratory-produced concretes (w/cm = 0.60 to 0.63) up to an age of 1 year; for concrete cores extracted from a dam in Northern Ontario, at the age of 30 years. Cores were taken from two different classes of concrete in the dam, namely the "deck" concrete and the "mass exterior" concrete, which had the following properties:

| | Deck concrete | Mass exterior |
|---|---|---|
| Portland cement (kg/m$^3$) | 236 | 147 |
| Fly ash (kg/m$^3$) | – | 63 |
| w/cm | 0.57 | 0.59 |
| 28-day strength (MPa) | 29 | 28 |

At an age of 3 days the fly ash concrete had just over five times the permeability of the PC concrete; the situation was reversed at 1 year. For cores extracted from the 30-year-old dam, the fly ash concrete was 20 times less permeable than the PC concrete.

### 5.6.6 Mechanical properties

The most often measured and specified mechanical property of concrete is the compressive strength. Fig. 5.10 shows the development of compressive strength for standard-cured concrete cylinders (w/cm = 0.45 and 6% air) with and without 25% fly ash. The early-age strength is lower in concrete containing fly ash, especially Class F, but the long-term strength is generally improved. The delayed strength developed is more pronounced at higher levels of replacement and/or colder temperatures. If higher strengths are required at early age, this can be achieved by reducing the w/cm of the concrete, by adding faster reacting pozzolans (e.g., using silica fume in combination with fly ash in a ternary blend cement), and/or the using of set-accelerating admixtures. The impact of w/cm and the use of silica fume on the strength development of fly ash concrete is shown in Fig. 5.11.

The rate of the pozzolanic reaction is accelerated by increases in temperature. The in situ strength of fly ash concrete may be considerably higher at early age than that

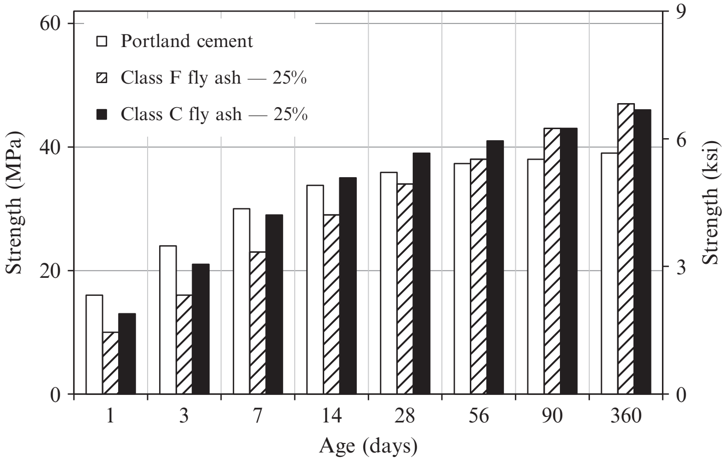

**Fig. 5.10** Strength development of fly ash concrete.

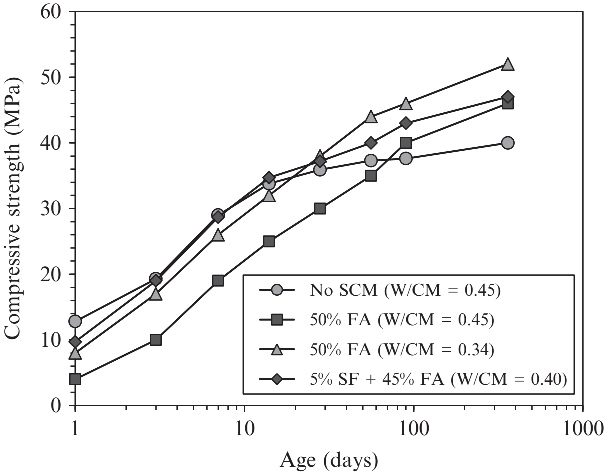

**Fig. 5.11** Effect of w/cm & silica fume on strength of fly ash concrete.

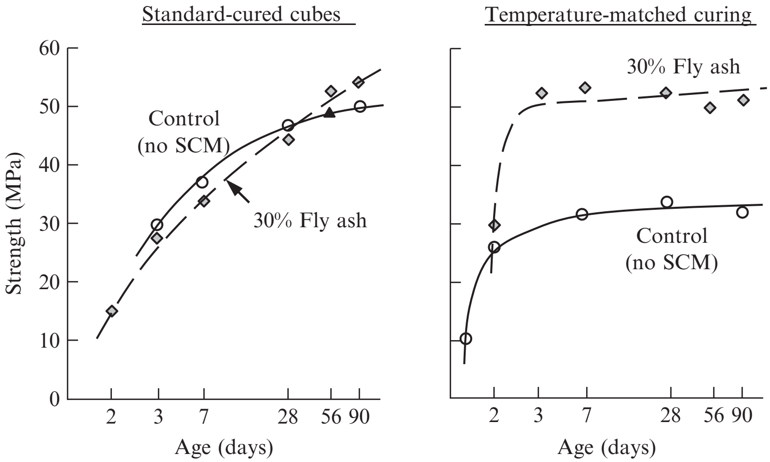

**Fig. 5.12** Strength development of 100-mm cubes subjected to standard laboratory curing and temperature-matched curing (Bamforth, 1980).

predicted by standard-cured cylinders stored at a normal laboratory temperature; this is because of the increase in temperature that occurs within the concrete structure as a result of the heat of hydration of the cement. This was demonstrated by Bamforth (1980) using temperature-matched curing, as shown in Fig. 5.12. The early-age strength of fly ash concrete was greatly enhanced for cubes that were cured at a temperature that matched the internal temperature of a large concrete pour. Conversely, increases in curing temperature can impair the strength of plain PC concrete (without fly ash).

Other mechanical properties, such as the tensile strength, flexural strength, and elastic modulus, are often predicted from the compressive strength using established relationships, such as the formula from the ACI Building Code (ACI 318) for predicting the elastic modulus, $E_c$, from the compressive strength, $f'_c$; the formula is as follows:

$$E_c = 4730\sqrt{f'_c} \tag{5.4}$$

The relationships between these “other properties” and compressive strength are generally not affected by the presence of fly ash (or other SCMs) and can still be used.

## 5.6.7 Volume stability

Concrete undergoes drying and thermal shrinkage as it ages. The amount of thermal shrinkage can be reduced by taking measures to reduce the magnitude of the temperature rise due to hydration, and fly ash can aid that effort. The amount of drying shrinkage is largely a function of the water content of the concrete, the w/cm, and the volume of aggregate. In well-cured and properly-proportioned fly ash concrete, where a reduction in the mixing water content is made to take advantage of the reduced water demand resulting from the use of the fly ash, the amount of shrinkage should be equal to or less than an equivalent PC concrete mix.

Concrete under sustained load will undergo a time-dependent deformation known as creep. The amount of creep is dependent on many factors, including the stress-strength ratio. If fly ash concrete is loaded at early age, it may undergo more creep than PC concrete because of its lower strength (Lane & Best, 1982; Yuan & Cook, 1983). However, if concretes are loaded when they have achieved the same strength, fly ash concrete will creep less because of its improved strength development at later age (Ghosh & Timusk, 1981; Lane & Best, 1982).

## 5.6.8 Durability of concrete

### 5.6.8.1 Chloride resistance

Chloride ions from seawater and antiicing or deicing salts or those present in groundwater can penetrate into porous concrete. If the chlorides can reach the embedded steel in reinforced concrete, they can initiate corrosion of the steel. The refinement in pore structure and reduction in permeability produced by fly ash (see Section 5.6.5) results in an increase in the resistance to chloride penetration. The incorporation of fly ash also increases the capacity of the hydration products to chemically bind chloride ions as they enter the concrete; this further inhibits the progress of the chlorides towards the steel. Fig. 5.13 shows chloride-ion profiles for reinforced concrete samples exposed for various periods of time to the tidal zone at a marine-exposure site located in the Thames Estuary in Essex, United Kingdom (Thomas & Matthews, 2004). The incorporation of 50% fly ash has a dramatic impact on the penetration of chloride ions that is especially noticeable after prolonged periods of exposure.

It is now more common to use indirect measures of concrete permeability and chloride penetrability, such as ASTM C1202, Standard Test Method for Electrical

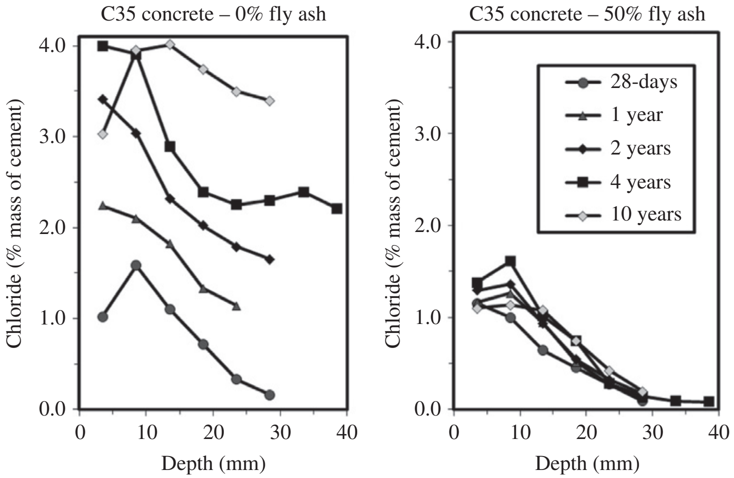

**Fig. 5.13** Chloride profiles for concrete in a marine (tidal) exposure (Thomas and Matthews, 2004).

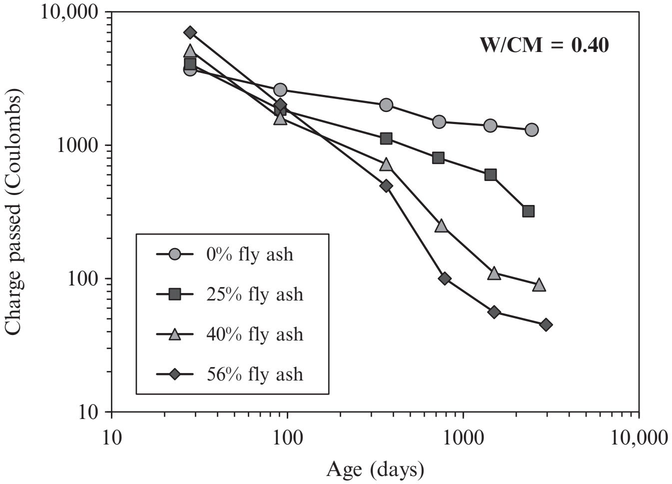

**Fig. 5.14** Effect of fly ash content and age on the "chloride permeability" of concrete (Thomas, 2007).

Indication of Concrete's Ability to Resist Chloride Ion Penetration (often referred to as the Rapid Chloride Permeability Test, or RCPT). Despite the known limitations of this test (it measures electrical conductivity, not permeability or chloride ingress), it does provide a reasonable indication of the ability of concrete to resist chloride penetration. Fig. 5.14 shows RCPT data from the author (Thomas, 2007) for concretes (w/cm = 0.40) with various levels of fly ash continuously moist cured for up to ~7 years. At 28 days, the charge passed increases with fly ash content, with the chloride permeability of the concrete containing 56% fly ash being almost double that of the control concrete without fly ash. However, there is a rapid decrease in the charge passed with time for fly ash concretes, and by 180 days there is a reversal in the trend, with chloride permeability decreasing with increasing fly ash content. After ~7 years, the concretes with 25%, 40%, and 56% fly ash are 4, 14, and 29 times less electrically conductive[3] than the control concrete, respectively.

#### *5.6.8.2 Carbonation*

Carbon dioxide ($CO_2$) present in the atmosphere can also penetrate into porous concrete. As it does so, it reacts with the calcium-bearing hydrates to form calcium carbonate ($CaCO_3$) and reduces the pH of the concrete from above 13 to ~8. This process is known as carbonation, and if the carbonation front can reach the embedded steel in reinforced concrete, it can also initiate corrosion of the steel.

The rate of carbonation of properly proportioned and well-cured concrete is slow. Provided adequate cover is given to embedded steel reinforcement, the carbonation-induced corrosion of the steel is unlikely to occur during the typical service life of a reinforced concrete structure. However, problems with steel corrosion initiated by carbonation are occasionally encountered in concrete structures due to a combination of poor quality concrete, inadequate curing, or insufficient cover.

It has been documented that concrete containing fly ash will carbonate at a similar rate compared with PC concrete of the same 28-day strength (Dhir, 1989; Hobbs, 1988; Lewandowski, 1983; Matthews, 1984; Nagataki, Ohga, & Kim, 1986; Tsukayama, 1980). However, even when concretes are compared on the basis of equal strength, concrete with fly ash (especially at high levels of replacement) may carbonate more rapidly in poorly cured, low-strength concrete (Ho & Lewis, 1983, 1987; Thomas & Matthews, 2000). Consequently, when steel-reinforced[4] concrete with high levels of fly ash is used in areas prone to carbonation (e.g., sheltered outdoor exposure), particular attention must be paid to ensure that the concrete mix proportions, period of moist curing, and depth of cover are adequate for the purpose.

#### *5.6.8.3 Alkali-silica reaction*

An ASR is a reaction between the alkali hydroxides (NaOH and KOH) in the pore solution and certain forms of thermodynamically-unstable silica ($SiO_2$) that are found in some aggregates. The reaction produces an alkali-silica gel that can absorb moisture and swell causing a volume increase in the concrete. If there are sufficient quantities of alkali, reactive silica and moisture available ASR can result in the expansion and cracking of the concrete which, in turn, can make the concrete more vulnerable to other destructive processes, particularly freeze-thaw damage and steel corrosion, resulting in accelerated chloride ingress.

---

[3] Note that the reduction in electrical conductivity is mainly due to the influence of the fly ash on the pore structure; however, some reduction is due because fly ash reduces the alkali and hydroxyl ion concentration of the pore solution (see Section 5.6.4), hence the electrical conductivity of the pore solution.

[4] Note that carbonation is not a concern in nonreinforced concrete or in concrete that is reinforced with corrosion-resistant steels (such as stainless steel) or nonferrous reinforcement.

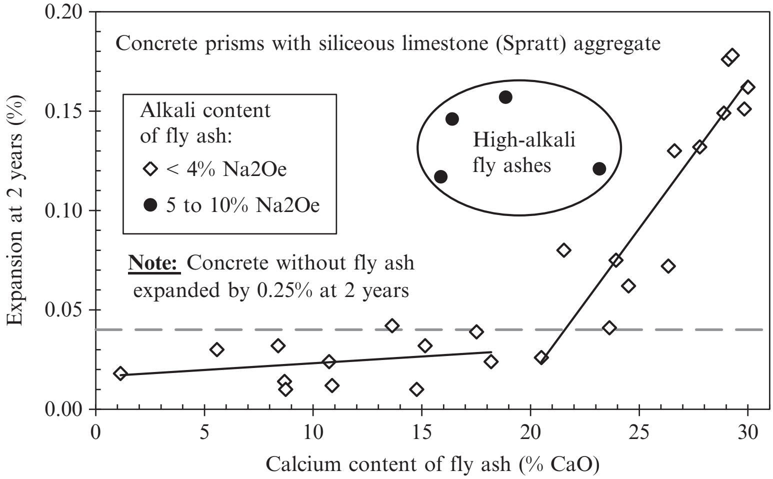

**Fig. 5.15** Effect of fly ash composition on the expansion of concrete with 25% fly ash and highly-reactive spratt aggregates (Shehata and Thomas, 2002; Thomas, 2011).

The main source of alkalis in concrete is the PC, and the risk of damaging ASR can be reduced by limiting the quantity of alkalis supplied by the cement. The risk of damage can be further reduced by using a sufficient quantity of a supplementary cementing material, such as fly ash.

Fig. 5.15 shows the 2-year expansion results from a concrete prism test (CPT; ASTM C1293) containing a highly reactive siliceous limestone and high-alkali cement with 25% replacement with a range of different fly ash; the expansion is plotted against the calcium oxide (CaO) content of the fly ash. Most low-calcium fly ashes ($CaO < 18\%$) are effective at a 25% replacement level in reducing expansion below the typically-used limit of 0.04% at 2 years; these fly ashes would all be classified as Class F fly ashes using the ASTM C618 criteria. As the CaO content of the fly ash increases above about 20%, the material becomes less efficacious in this role; these fly ashes would be classified as Class C by current ASTM criteria. High-alkali fly ashes (in this case, containing between 5% and 10% $Na_2Oe$) are not effective in mitigating expansion at this level of replacement and should generally not be used in concrete containing reactive aggregate without extensive testing. Fig. 5.16 shows the 2-year expansion plotted against the level of fly ash replacement, and the data indicate that Class C fly ashes can be used to control expansion below 0.04%, provided they are used at a sufficient level of replacement. Testing by the author (Shehata & Thomas, 2002) has shown that Class C fly ashes can be used at lower replacement levels to control ASR if they are combined with other SCMs, such as silica fume, in a ternary cement blend.

### *5.6.8.4 Sulfate resistance*

When PC concrete is in contact with soil or groundwater containing soluble sulfates, there is a risk of sulfate attack which manifests itself in the form of expansion, cracking, and spalling of the concrete. In an advanced state, a loss of cohesion as the C-S-H

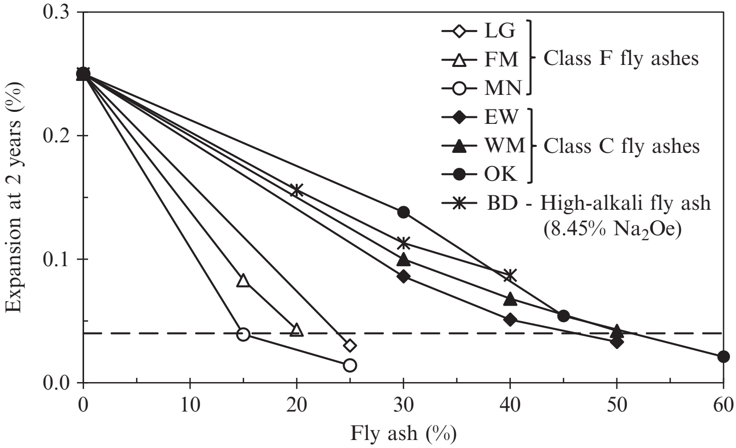

**Fig. 5.16** Effect of fly ash composition on the level of replacement required to suppress ASR expansion (Shehata and Thomas, 2002; Thomas, 2011).

**OPC – 14.1% $C_3A$** **SRPC – 1.2% $C_3A$** **OPC + 20% Fly ash**

100-mm concrete cubes (w/cm = 0.43 to 0.46) after 5 years exposure to $MgSO_4$ solution (1.5% $SO_4$)

**Fig. 5.17** Photographs of 100-mm (4-inch) cubes after 5 years exposure to $MgSO_4$ solution (1.5% $SO_4$).
Photos courtesy of the Building Research Establishment, UK.

is decalcified, becoming gypsum and/or thaumasite. The most vulnerable component of PC is the calcium-aluminate hydrates which, when exposed to sulfates, convert to ettringite resulting in expansion. Research has shown that concrete can be made resistant to sulfate by a combination of low water-to-cementing-materials ratio, low-$C_3A$ (sulfate-resisting) PC, and the use of a sufficient level of suitable SCM; these solutions are reflected in many national codes and specifications for concrete in sulfate exposure conditions.

As with ASR, it is well established that the use of low-calcium (e.g., ASTM Class F) fly ashes is an effective measure for providing sulfate-resistant concrete, but high-calcium (e.g., ASTM Class C) fly ashes are not generally effective. Fig. 5.17 shows the visual condition of three 100-mm cubes after 5 years immersion in a magnesium sulfate solution (1.5% or 15,000 ppm $SO_4$). The cube produced with ordinary

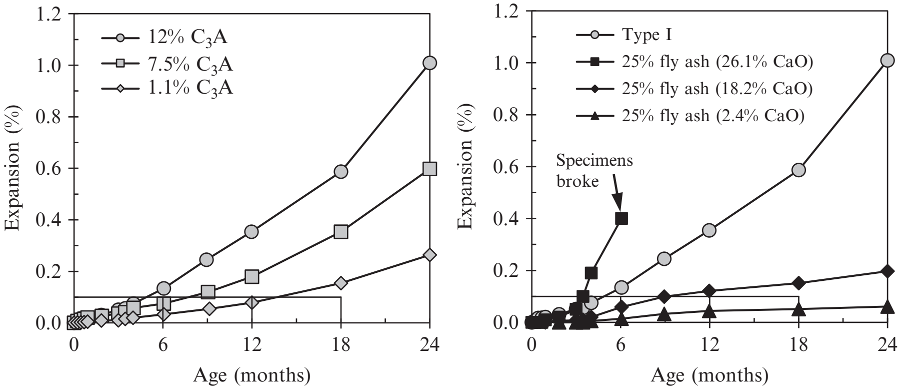

**Fig. 5.18** Effect of SCM on expansion of mortars stored in 5% $Na_2SO_4$ solution as per ASTM C1012.

Portland cement (OPC) with a high $C_3A$ content (14.1%) is in an advanced state of deterioration, whereas cubes produced with sulfate-resisting Portland cement (SRPC with 1.2% $C_3A$) or a blend of OPC with 20% low-calcium fly ash show very little deterioration. Fig. 5.18 shows the expansion data for mortar bars stored in a solution containing 5% sodium sulfate (ASTM C 1012 test method). Generally, expansion $<0.1\%$ at 6, 12, or 18 months is indicative of moderate, high, or very high sulfate resistance, respectively. The figure on the left shows the impact of the $C_3A$ content of straight PC mixtures. The figure on the right shows the impact of blending 25% fly ash with the high-$C_3A$ cement. Very high sulfate resistance is observed in the fly ash with the lowest calcium content; indeed, the performance is better than that for the straight cement mix with low $C_3A$ cement. Mixes with high-calcium fly ash generally perform poorly, with the mortar bars often breaking or sometimes disintegrating within 6 months or so.

### 5.6.8.5 Freeze-thaw and deicer salt scaling

Concrete will be resistant to cycles of freezing and thawing even when saturated, provided that the following conditions are met:

- An adequate air-void system is present (spacing factor, L-bar $\leq$ 230 μm).
- The aggregate is frost-resistant.
- Sufficient strength is attained prior to first freezing ($\geq$3.5 MPa).
- Sufficient strength is attained prior to cyclic freezing and thawing ($\geq$30 MPa).

This is the case regardless of the presence of fly ash. However, concrete surfaces that are exposed to freezing and thawing in the presence of deicing salts can be vulnerable to surface scaling, which is manifested as the peeling or flaking of small pieces of paste or mortar from the surface to expose the fine aggregate or, in severe cases, the coarse aggregate. Accelerating laboratory tests, such as ASTM C 672, indicates that concrete with moderate to high levels (e.g., $\geq$25%) fly ash are more vulnerable to scaling. However, Thomas and Yi (2016) have suggested that is due to the short period of moist curing (14 days) used in the standard test, which results in fly ash concrete having a significantly lower surface strength compared with concrete without fly ash when the freezing commences. A review of field studies (Thomas & Yi, 2016) indicates that the performance of fly ash concrete in the field is generally acceptable, especially for formed and slip-formed surfaces. For hand-finished flatwork (e.g., sidewalks and driveways) improper placing, finishing, or curing can render the surfaces more vulnerable to scaling. In such cases, there is some evidence that concrete with moderate to high levels ($\geq$25%) of fly ash may have increased susceptibility. For hand-finished flatwork where proper placing, finishing, and curing cannot be ensured, it may be prudent to limit the level of fly ash replacement to 25%.

## 5.7 Examples of use in concrete

Initially the incentive for using fly ash in concrete may have been due to cement shortages after WWII, as well as the cost savings in being able to reduce the cement content. However, the ability of fly ash to help control the heat-of-hydration in large pours was soon realized, and this provided additional motivation for using it in large massive structures, such as dams. Nowadays, fly ash is used not just to reduce costs but also because of the many technical benefits associated with its use that are now widely recognized. Wherever fly ash is readily available commercially, it is used in ALL types of concrete including residential, commercial, transportation, marine and high-rise structures, cast-in-place and precast concrete, and various concretes with special properties such as roller-compacted, self-consolidating, high-strength, and high-performance concrete, shotcrete, flowable fill and many other applications.

## 5.8 Specifications for the use of fly ash in concrete

There are a great many national standards and specifications covering the use of fly ash for concrete. Most of these rely on a strict definition of the material with a few limits of physical and chemical composition and performance parameters. For the purposes of this chapter, reference is made to ASTM C 618 as an example.

- ASTM C618 definition: *The finely divided residue that results from the combustion of ground or powdered coal and that is transported by flue gasses*. This definition, combined with the footnote to the definition, specifically prohibits the inclusion (within the specification) of ashes from the combustion of other materials.
- Classification: Two types of fly ash are covered: Class F and Class C.
- Physical properties: A limit is placed on the fineness ($\leq$34% retained on the 45-μm sieve), and there are uniformity requirements based on the fineness and density of the material.
- Chemical requirements: Limits are placed on the (i) sum of the oxides of silica, alumina, and iron ($SiO_2+Al_2O_3+Fe_2O_3$) and these are (sum $\geq$70.0% for Class F and $\geq$50.0% for Class C); (ii) sulfate content ($\leq$5.0% $SO_3$); (iii) moisture content ($\leq$3.0%); and (iv) loss on ignition ($\leq$6.0%).
- Performance requirements: Fly ash must meet a strength activity index when tested in mortars at 7 and 28 days (mortar with 20% fly ash should have a strength no <75% of that of a control mortar without ash); the water requirement of the fly ash mortar must not be >115%

of that of the control. In addition, to protect against unsoundness (due to free CaO or MgO), mortar bars with fly ash are subject to an autoclave test.

- Optional requirements: There are some optional requirements that may be specified by the owner including: (i) drying shrinkage limit; (ii) additional uniformity requirement based on air entrainment; (iii) requirement to control ASR; and (iv) ability to control sulfate attack.

Other national specifications are similar in approach, although the classification criteria may be different. There may be differences in the properties specified and the methods of test used to determine those properties.

## 5.9 High-volume fly ash concrete

Concrete containing a high percentage of fly ash by mass of total cement content has been used in the United Kingdom and elsewhere for over 35 years. This type of concrete has considerable promise in addressing the environmental concerns by minimizing the proportion of PC in a concrete mix and maximizing the proportion of fly ash, thereby reducing the overall $CO_2$ emissions associated with producing concretes. The definition of high-volume fly ash concrete is generally considered to have a minimum of 50% fly ash by mass of the cementitious materials up to a maximum of 85%.

High-volume fly ash (HVFA) concrete has being used for a considerable numbers of years. In the United Kingdom, Didcot Power Station (1981), Mumbles slipways (1983), Grangetown Link (1988), and Wincanton Sewage Works (1984) were subjected to a series of tests (e.g., core compressive strength, carbonation depth, permeability, and chloride and sulfate penetration). The tests showed that these concretes continue performing well after 35 years of exposure to severe environments. In the United States, Canada, and India a wide range of applications covering the full range of structural elements, including columns with 50 MPa concrete, piles, shotcrete, and slabs, have been summarized by Malhotra and Mehta (2008).

The United Kingdom has compiled (MPA) lifecycle data for the most commonly used cementitious materials, as summarized in Table 5.4. Using this data shows that HVFA mixes can have significantly lower embodied $CO_2$ and is typically around 50% lower than the equivalent PC concrete.

**Table 5.4 Embodied CO2e of UK cement, additions, and cementitious material (MPA, 2015)**

| Cement, additions, and cementitious material | Kg $CO_2$e/tonne[a] |
|---|---|
| Portland cement | 913 |
| Ground granulated blastfurnace slag | 67 |
| Fly ash (low lime) | 4 |
| Limestone fines | 75 |

[a] From cradle to leaving the factory gate of the addition manufacturer.

### 5.9.1 Mix constituent proportions

Table 5.5 gives typical mix constituent proportions for a range of cube-compressive strengths, along with a typical range of component materials for different levels of strength in high-performance HVFA concrete.

The cement phase can be preblended or mixer blended, although the former is limited to a maximum of 55% of cementitious content in EN 206 and thus just within the HVFA range. Given the low free water contents and water/cement ratio used with HVFA, super plasticizing chemical admixtures are used to achieve the required workability. Sulfonated, naphthalene-formaldehyde condensate and polycarboxylate-based super plasticizers are used, although the dosage of these varies depending on the characteristics of fly ash used. This does mean that HVFA concrete mixes are very cohesive but do not bleed and are resistant to segregation. Mixes generally have high flowability and pumpability; consequently, their surface finish is usually excellent. Synthetic resin type AEAs are also widely used with HVFA, and the usual care to determine the correct dosage is required (as described in other chapters of this book).

Due to low PC content, the autogenous temperature rise in large volume sections is much lower than equivalent PC content. For example, Malhotra and Mehta reported that at the Hindu Temple on Kauai Island, Hawaii, where the structural slab contained 57% fly ash, the peak temperature was only 40°C.

The high fly ash content makes the material more sensitive to curing conditions, and the setting and hardening rates of HVFA concrete at early age are slower, especially under cold weather conditions. Therefore a relatively longer moist curing or leaving the form work in place for at least a week is essential to achieving the optimum strength and durability characteristics that are possible from HVFA concrete. This is, of course, is beneficial to long-term strength, and typically this can be 50%–80% higher than the standard 28-day strength.

It should be noted that fly ash can be used as a filler aggregate in concrete or to replace part of the fine aggregate phase. While used in this manner, fly ash is not counted towards the cementitious content of the mix, and it still gives the benefits as described.

**Table 5.5** **Typical cementitious contents of HVFA concretes (UKQAA)**

| Mix constituent proportions (kg/m$^3$) | | | |
|---|---|---|---|
| Free water | 120–130 | 115–125 | 100–120 |
| Portland cement | 100–130 | 150–160 | 180–200 |
| Fly ash | 125–150 | 180–200 | 200–225 |
| Water/cement ratio | 0.40–0.45 | 0.33–0.35 | 0.30–0.32 |
| Embodied $CO_2/m^3$ | 108 | 145 | 178 |
| Typical 28-day compressive strength (MPa) | 20 | 30 | 40 |

Particular attention to curing is necessary to achieve the durability potential of this type of concrete and is also important in preventing rapid carbonation, which will, in any case, be generally higher than the equivalent PC concrete.

### 5.9.2 *Use of fly ash as a cementitious material in other applications*

Fly ash and fly ash blends can directly replace a portion of PC in cementitious applications. These materials can be used alone or blended with other materials with cementitious properties to produce a cement or concrete with performance properties different from those produced with only PC. As fly ash resembles PC both chemically and physically, the material may be used in many applications that require binding capabilities, such as soil cements.

Soil cements increase the shear strength and durability (i.e., resistance to swell) of soils, particularly in soils with high clay contents (Rossow, 2003). High clay contents relate to high plasticity soils, which lose shear resistance with increasing moisture content. The need for soil stabilization has led to the development of soil cements or cement modified soil. Traditionally, PC is mixed with soil and water to bond the soil particles together (Horpibulsuk, 2012). Economic drivers have led to the use of industrial by-products to offset the more expensive, energy-intensive manufactured products. To reduce the cost of soil stabilization, Class F fly ash may be blended with lime and soil to create a cement modified soil (Silvani, Braun, Masuero, & Consoli, 2016). Alternatively, a Class C (high calcium) fly ash may be used without the addition of lime because of its self-cementitious properties. Blending high plasticity soils with fly ash and lime allows the moisture present in the soil to react with the added source of reactive silica and lime to form hydrated cementitious compounds which chemically bind the soil particles. Additionally the increased particle size of the bonded particles increase the internal frictional forces, thereby increasing the resistance to shear failure.

## 5.10 Use of bottom ash

As a by-product of coal combustion, bottom ash has found many beneficial uses as an aggregate in civil construction projects as partial replacement of PC or partial replacement of fine aggregates. Bottom ash has the appearance and particle size gradation similar to a natural-fine aggregate, such as river sand. The physical properties of bottom ash include angular particles with a porous surface texture and range in size from a fine sand to a fine gravel; it is usually a well-graded material. Therefore bottom ash most closely resembles a construction aggregate, of which there is a wide variety; some examples include crushed stone, sands, mine waste, and sand-shell mixtures.

When assessing nontraditional materials for the replacement of natural concrete aggregates, testing parameters will include grading or size distribution, porosity, absorption, texture, elastic modulus, and compressive strength (Mehta & Monteiro, 2006). ASTM Standard C 294 provides language that is useful for understanding the terms used to designate aggregate constituents. Most standard or natural aggregates, such as river sand and limestone gravel, have a bulk density of 95–100 lb/ft$^3$ and are used to produce normal-weight concrete with a unit weight of approximately 150 lb/ft$^3$ (Mehta & Monteiro, 2006). Aggregates with bulk densities $<70$ lb/ft$^3$ are referred to as lightweight aggregates (LWAs). Thermally processed materials such as expanded clay and shale are referred to as synthetic aggregates, including bottom ash from coal combustion. Bottom ash is generally an angular and porous material, but it is not uncommon to find the presence of nonporous, crystalline bottom ash that is glassy in appearance. These physical characteristics coupled with the typical particle size ranging from 75 μm to 25 mm make bottom ash an ideal natural aggregate replacement material.

### 5.10.1 Masonry blocks and concrete

Most concrete masonry units (CMUs) are produced with a combination of sand and locally available coarse aggregate, such as limestone. Although bottom ash is weaker than river sand, it also has a considerably lower density and can reduce the weight of concrete. Another advantage to bottom ash is its porosity, which can provide a reservoir of moisture that is available for the internal curing of the concrete binder. Alternatively, the high porosity of most bottom ash aggregates leads to a reduced fresh concrete workability with increased mixing water; or the incorporation of higher dosages of plasticizers to increase flow. The increased water demand of bottom ash, as a coarse aggregate in concrete, leads to a reduction in compressive strength with increased water loss by bleeding; these effects are magnified by increasing the utilization rate of bottom ash (Andrade, Rocha, & Cheriaf, 2009). The negative effects of increased water demand may be countered by high dosages of admixtures.

When used in masonry applications the lower density of bottom ash is crucial to the fabrication of lightweight construction materials, such as standard hollow core units (i.e., 8 × 8 × 16 in blocks), which have a unit weight in the range of 34–40 pounds. Lightweight CMUs (<34 lbs) of similar dimension are also produced for a variety of specialty construction purposes that require the lower weight. ASTM C 90 categorizes CMUs unto three weight classes: normal (heavy) weight (125 lb pcf), medium weight (105–125 lb pcf), and lightweight (<105 lb pcf) (ASTM C90-16, 2016). Lightweight CMUs are commonly produced from manufactured aggregates, such as expanded shales or clays. However, coal-combustion bottom ash can be similar in many ways to manufactured aggregate. During coal combustion, the combination of high temperature and turbulent air flow results in a porous bottom ash with bulk densities of 45–75 lb/ft$^3$, which is similar to manufactured aggregate.

LWA concrete blocks in the density range of 1000–1500 kg/m$^3$ are widely used for a variety of construction purposes. For example, in the United Kingdom, the market for precast CMUs is approximately 8.6 million m$^3$. LWA blocks form cost-effective, general-purpose, load-bearing or nonload-bearing masonry units with a proven track record for use above and below ground level. They can also be used as infill units in beam and block floor systems. Blocks can be produced in a standard face texture suitable for plaster and dry lining, a close-textured finish suitable for direct decoration or "fair face," where no decoration is required.

Although many LWAs are suitable for use in blocks, including sintered fly ash LWA, FBA has been and remains the most commonly used material in the United Kingdom, although the practice does not seem widespread in the rest of the world. The success of FBA and PFA in the United Kingdom may stem from their consistent range of chemical and physical properties. FBA is collected from the base of furnaces within the power station and is usually water cooled and transferred to stockpiles. The material is then either crushed or screened in different size fractions at the station or at the block manufacturer's site. Typical grades used in block production are 14-0, 14-5, and 5-0 mm, depending on the type of block being manufactured.

The density of FBA, in the range 800–1100 kg/m$^3$ depending on the grade used, is ideally suited to achieve the typical LWA block density range and the relevant technical properties. BS 6073 permits the use of FBA in blocks. The limits are suggested in the United Kingdom annex to BS EN 13055-1 and the tests are detailed in BS EN 1744-1.

### 5.10.2 Manufacture

The majority of LWA blocks today are manufactured in modern, highly automated and closely controlled factories using "static" casting machines or mobile "egg-laying" machines. In a static plant cement, fly ash, aggregates, and water are usually batched into and mixed in a horizontal pan-type mixer to an almost "earth-dry" consistency, which is then vibro-compacted into a mold onto a steel or wooden pallet. The blocks are immediately demolded and transferred onto the pallet to a storage area for curing. Often this curing area consists of enclosed chambers that are heated at temperatures up to 80°C, depending on the heat source, to accelerate the cement hydration and strength development to optimize the throughput of the plant. Blocks are then packaged into cubes of various configurations and further stored in a stockyard, if required, to achieve the final strength.

### 5.10.3 Aerated concrete blocks

Of this total market, ~24% were LWA blocks in the density range of 1000–1500 kg/m$^3$, and 31% were autoclaved aerated concrete (AAC) blocks, also known as "Aircrete" within the United Kingdom, in the range 400–800 kg/m$^3$. AAC blocks have high levels of thermal insulation, a high strength/weight ratio, and the ability to meet acoustic and fire insulation requirements. The blocks contribute to an overall cost savings arising from a number of secondary savings. Lighter foundations and structural frames result, and the need for less insulation all produce real benefits. They are easily cut, worked, and laid, with minimum maintenance and low handling costs.

Manufacture of AAC is a lightweight building product used in the construction of domestic dwellings and commercial buildings. It is manufactured as blocks or steel-reinforced panels. Characterized by its fine cellular structure with air pores ranging from 0.1 to 2 mm, AAC has a high ratio of compressive strength to density.

This property allows AAC to be used as a load-bearing unit where efficient thermal insulation is required.

AAC is made by reacting together finely divided calcareous and siliceous raw materials in saturated steam at temperatures above 100°C. The steam curing of specimens within pressure vessels (autoclaves) at several times atmospheric pressure ensures hydrothermal conditions are maintained. The curing process is termed autoclaving. The calcareous raw material is normally quicklime (calcium oxide) or a combination of quicklime and PC. The siliceous component can be finely divided quartz, amorphous silica, or aluminosilicate glass. Fly ash, from coal-burning power stations, is largely composed of aluminosilicate glass and is therefore a suitable raw material for the manufacture of AAC.

There are several advantages associated with the use of fly ash for the manufacture of AAC. Environmental benefits are achieved by using a by-product material as an alternative to a primary aggregate such as sand. The autoclaved matrix that results from the use of fly ash due to the influence of aluminum ions has a high resistance to sulfate attack. A low thermal conductivity can be achieved for AAC made with fly ash due to the low conductivity of the fly ash itself.

The manufacture of AAC is unlike that of conventional concrete or mortar. The raw materials are fine powders, without aggregate particles of any significant size, and the starting point is a water-based slurry. Three aspects of the process differentiate it from other concrete precasting methods. There is an initial "aeration" stage in which the slurry expands to form a stable cellular mass. Once the stiffening of the mix has occurred and sufficient "green strength" achieved, the cellular mass is cut into individual masonry units. Finally, autoclaving at elevated temperatures (180–200°C) promotes hydrothermal reactions, thereby forming a stable, high-strength intercellular matrix.

### 5.10.4 Use of fly ash

Generally unprocessed fly ash, either dry or conditioned with fresh water, is used for the manufacture of AAC. The fineness specifications of BS3892: Part 1 or EN 450 are of limited relevance to autoclaved products. It is possible to use relatively coarse fly ash because of the elevated temperatures and high alkalinity within the autoclaves. These conditions ensure the rapid dissolution of the aluminosilicate particles and increase the availability of silica for the formation of calcium silicate hydrates.

### 5.10.5 Properties of AAC

The thermal conductivity ($\lambda$) of AAC is directly related to density. Typically, $\lambda$ values range from 0.1 to 0.2 W/m K, within the density range of 400–800 kg/m$^3$ commonly produced in the United Kingdom. The high degree of thermal insulation provided by AAC enables the stringent energy efficiency requirements of the new building regulations to be achieved.

The compressive strength of AAC, as tested in accordance with BS 6073, ranges from 2.8 N/mm$^2$ to over 8 N/mm$^2$, depending on density. This satisfies the structural requirements of a wide range of building types. The drying shrinkage of AAC complies with BS 6073.

AAC blocks are resistant to frost damage and sulfate attack and have British Board of Agrément approval for use below DPC level in foundations. Soil or groundwater conditions that are defined by BRE Special Digest 1 and are up to Class DS 4 can be tolerated. AAC is fire resistant because of its calcium silicate hydrate matrix and is classified as noncombustible in accordance with the building regulations.

## 5.11 Road bases

Bottom ash has a successful history of use as a granular base material for roads that are constructed over soft subgrades (Chesner, Collins, & MacKey, 1998). However, the aggregate must satisfy material specifications for gradation, soundness, and abrasion loss. Of the 12 million tons of bottom ash produced in the United States, ~3% was utilized for road base applications in 2015 (ACAA, 2015). Principal criteria governing the use of bottom ash in road base include limiting fines passing the #200 sieve (0.075 mm) and to avoid soft aggregates (i.e., require LA abrasions >50%). When compacted, the highly irregular shape of bottom ash provides a higher angle of shear resistance. Generally standard Proctor compaction, moisture-density, curves for bottom ash typically resemble that of a cohesionless material (Lovell, Ke, Huang, & Lovell, 1991).

## 5.12 Structural pipe bedding

Bottom ash may be used in place of sand or pea gravel. For backfill or compacted fill applications, bottom ash must be close to optimum moisture content and free of pyrites, as the presence of available sulfate may lead to expansion-related issues. Materials used for these applications are often referred to as controlled low-strength materials (CLSM). A CLSM is defined by ASTM D 5971 as a mixture of soil, bottom ash, fly ash, cement, and water that hardens to compressive strengths higher than soil but <8.3 MPa (ASTM D5971, 2013). The low strength of this self-compacting cementitious material provides sufficient support strength as a fill material that may be easily excavated, if needed, with traditional methods due to the low strength (Lini Dev & Robinson, 2015).

## 5.13 Slope stabilization

Materials for slope stabilization must exhibit high shear strength with low compressibility at low-unit weights (Amaya & Amaya, 2007). Materials meeting these parameters will minimize additional loading to foundation soils, reducing the potential for deformation while minimizing differential settlement upon loading. The highly irregular shape of bottom ash increases the angle of shearing resistance under dry conditions. However, wet bottom ash develops a similar range of shear resistance to natural granular soils (Lovell et al., 1991).

## 5.14 Summary

Fly ash has long been a mainstay in the construction industry because it is a versatile and readily available secondary resource that is essential for future construction. The need for fly ash in concrete has never been more important, particularly with respect to client demands to reduce embodied energy and contribute to more sustainable construction. Typically the use of 30%–50% fly ash will result in a reduction in embodied $CO_2$ between 25% and 40%, depending on the type of concrete mix specified. There is also an increased investment in the use of fly ash to produce LWAs, which minimizes the use of primary aggregates. The use of fly ash in concrete has a long track record and has become ever more widespread since the 1930s. In terms of durability, fly ash brings a wide range of improvements to concrete; in particular, it also significantly increases resistance to ASR, sulfate attacks, and chloride ingress.

Although many countries are reducing or even phasing out coal-fired power stations, the importance of and need for fly ash has already sparked international trade in the material; the genesis and current extent of that trade is described in another chapter of this book. In addition, there are significant quantities of fly ash available in stockpiles and ponds. While these have not yet been exploited and are likely to require some form of beneficiation, there is a wealth of research showing the potential of these unused resources.

## References

ACAA. (2015). *Coal combustion product (CCP) production & use survey report*. American Coal Ash Association. *http://www.acaa-usa.org*.

ACI 232. (2003). *Use of fly ash in concrete*. ACI Committee 232 report, ACI 232.2R-03. Farmington Hills, MI: American Concrete Institute.

Amaya, P. J., & Amaya, A. J. (2007). The use of bottom ash in the design of dams. In: *Proceedings of the 2007 World of Coal Ash (WOCA)* May 7–10, Covington, KY, Proceedings CD.

Andrade, L. B., Rocha, J. C., & Cheriaf, M. (2009). Influence of coal bottom ash as fine aggregate on fresh properties of concrete. *Construction and Building Materials*, *23*(2), 609–614.

Anon. (1914). An investigation of the pozzolanic nature of coal ashes. *Engineering News*, *71* (24), 1334–1335.

ASTM C90-16. (2016). *Standard specification for loadbearing concrete masonry units*. West Conshohocken, PA: ASTM International. *www.astm.org*.

ASTM D5971. (2013). *Standard practice for sampling freshly mixed controlled low-strength material*. West Conshohocken, PA: ASTM International. *www.astm.org*.

Bamforth, P. B. (1980). In situ measurement of the effect of partial Portland cement replacement using either fly ash or ground granulated blast-furnace slag on the performance of mass concrete. *Proceedings, Institution of Civil Engineers (London), Part 2*, *69*(September), 777–800.

Best, J. F., & Lane, R. O. (1980). Testing for optimum pumpability of concrete. *Concrete International*, *2*(10), 9–17.

Bhatty, M. S. Y., & Greening, N. R. (1987). Some long-time studies of blended cements with emphasis on alkali-aggregate reaction. In: *Proceedings of 7th international conference on alkali-aggregate reaction*. Ottawa: Noyes.

Chesner, W., Collins, R., & MacKey, M. (1998). *User guidelines for waste and by-product materials in pavement construction*. Washington, DC: Federal Highways Administration FHWA-RD-97-148, 683 p.

Davies, R. E. (1954). *Pozzolanic materials—With special reference to their use in concrete pipe*. Technical Memo. American Concrete Pipe Association.

Davis, R. E., Carlson, R. W., Kelly, J. W., & Davis, H. E. (1937). Properties of cements and concretes containing fly ash. *Journal of the American Concrete Institute*, *33*, 577–611.

Dhir, R. K. (1989). Near—Surface characteristics of concrete: Prediction of carbonation resistance. *Magazine Concrete Research*, *41*(148), 137–143.

Ghosh, R. S., & Timusk, J. (1981). Creep of fly ash concrete. *ACI Materials Journal*, *78*(5), 351–357.

Hearn, N., Hooton, R. D., & Nokken, N. R. (2006). Pore structure, permeability, and penetration resistance characteristics of concrete. In J. F. Lamond & J. H. Pielert (Eds.), *Significance of tests and properties of concrete and concrete making materials*. West Conshohocken, PA: ASTM STP 169D. American Society for Testing and Materials [chapter 23].

Helmuth, R. (1987). *Fly ash in cement and concrete*. Skokie, IL: Portland Cement Association. 203 p.

Ho, D. W. S., & Lewis, R. K. (1983). Carbonation of concrete incorporating fly ash or a chemical admixture. In: *Proceeding of the first international conference on the use of fly ash, silica fume, slag, and other by-products in concrete*. ACI SP-79, Vol. 1 (pp. 333–346). Farmington Hills, MI: American Concrete Institute.

Ho, D. W. S., & Lewis, R. K. (1987). Carbonation of concrete and its prediction. *Cement and Concrete Research*, *17*(3), 489–504.

Hobbs, D. W. (1988). Carbonation of concrete containing PFA. *Magazine Concrete Research*, *40*(143), 69–78.

Horpibulsuk, S. (2012). Strength and microstructure of cement stabilized clay. In V. Kazmiruk (Ed.), *Scanning electron microscopy*. Rijeka, Croatia: InTech.

Joshi, R. C., & Lohtia, R. P. (1997). *Fly ash in concrete: Production, properties and uses*. Boca Raton, FL: CRC Press. 128 p.

Kostuch, J. A., Walters, G. V., & Jones, T. R. (1993). High performance concretes incorporating metakaolin—A review. In: R. K. Dhir & M. R. Jones (Eds.), *Proceedings of concrete 2000: Vol. 2* (pp. 1799–1811). Dundee: University of Dundee.

Lane, R. O., & Best, J. F. (1982). Properties and use of fly ash in Portland cement concrete. *Concrete International*, *4*(7), 81–92.

Lewandowski, R. (1983). Effect of different fly-ash qualities and quantities on the properties of concrete. *Betonwerk and Fetigteil-Technik*. Nos 1–3.

Lini Dev, K., & Robinson, R. G. (2015). Pond ash based controlled low strength flowable fills for geotechnical engineering applications. *International Journal of Geosynthetics and Ground Engineering*, *1*(4), 32.

Lovell, C., Ke, T. -C., Huang, W. -H., & Lovell, J. (1991). Bottom ash as a highway material. In *Transportation Research Record 1310* (pp. 106–116). Washington, DC: National Academy Press.

Malhotra, V. M., & Mehta, P. K. (1996). *Pozzolanic and cementitious materials, advances in concrete technology: Vol. 1*. Amsterdam: Gordon and Breach Publishers. 191 p.

Malhotra, V. M., & Mehta, P. K. (2008). *High performance, high volume fly ash concrete for building sustainable and durable structures* (3rd ed.). Ottawa: Supplementary Cementing Materials for Sustainable Development Inc.

Manmohan, D., & Mehta, P. K. (1981). Influence of pozzolanic, slag, and chemical admixtures on pore size distribution and permeability of hardened cement pastes. *Cement, Concrete & Aggregates*, *3*(1), 63–67.

Massazza, F. (1998). Pozzolana and pozzolanic cements. In P. C. Hewlett (Ed.), *Lea's chemistry of cement and concrete* (pp. 471–631). London: Arnold [chapter 10].

Matthews, J. D. (1984). Carbonation of ten-year old concretes with and without PFA. In: *Procedings 2nd international conference on fly ash technology and marketing, London, Ash Marketing, CEGB, 398A*.

Mehta, P. K. (1983). Pozzolanic and cementitious byproducts as mineral admixtures for concrete—A critical review. In: *Proceedings of the first international conference on fly ash, silica fume, slag and other mineral by-products in concrete*, ACI SP-79, Vol. 1 (pp. 1–46). Detroit, MI: America Concrete Institute.

Mehta, P. K., & Monteiro, P. J. M. (2006). *Concrete, microstructure, properties and materials*. New York, NY: McGraw-Hill.

Mindess, S., Young, J. F., & Darwin, D. (2003). *Concrete* (2nd ed.). Prentice-Hall.

Mineral Products Association. (2015). Fact Sheet 18: Embodied CO2e of UK cement, additions and cementitious material.

Mustard, J. N., & MacInnis, C. (1959). The use of fly ash in concrete by Ontario hydro. *Engineering Journal*, (December), 74–79.

Nagataki, S., Ohga, H., & Kim, E. K. (1986). Effect of curing conditions on the carbonation of concrete with fly ash and the corrosion of reinforcement in long term tests. In *Fly ash, silica fume, slag and natural pozzolanas in concrete*, ACI-SP91, Vol. 1 (pp. 521–540). Farmington Hills, MI: American Concrete Institute.

Ono, K., Asaga, K., & Daimon, M. (1985). Hydration in the system of cement and silica fume. In: *Cement Association of Japan, Review of the 39th general meeting, Technical session, Tokyo* (pp. 40–43).

Owens, P. L. (1979). Fly ash and its usage in concrete. *Concrete Magazine*, (July), 22–26.

Pistilli, M. F. (1983). Air-void parameters developed by air-entraining admixtures as influenced by soluble alkalis from fly ash and Portland cement. *ACI Journal, Proceedings*, *80*(3), 217–222.

Roberts, L. R., & Taylor, P. C. (2007). Understanding cement-SCM-admixture interaction issues: Staying out of the safety zone. *Concrete International*, (January), 33–41.

Rossow, M. (2003). *Fly ash facts for highway engineers*. New York, NY: Continuing Education and Development. 82 p.

Sear, L. K. A. (2001). *The properties and use of coal fly ash*. London: Thomas Telford. 261 p.

Shehata, M. H., & Thomas, M. D. A. (2002). Use of ternary blends containing silica fume and fly ash to suppress expansion due to alkali-silica reaction in concrete. *Cement and Concrete Research*, *32*(3), 341–349.

Silvani, C., Braun, E., Masuero, G. B., & Consoli, N. C. (2016). Behavior of soil–fly ash–lime blends under different curing temperatures. *Procedia Engineering*, *143*, 220–228.

Taylor, H. F. W. (1997). *Cement chemistry* (2nd ed.). London: Thomas Telford. 459 p.

Thomas, M. D. A. (2007). *Optimizing the use of fly ash in concrete*. PCA IS548 Skokie, IL: Portland Cement Association. 24 p.

Thomas, M. D. A. (2011). The effect of supplementary cementing materials on alkali-silica reaction: A review. *Cement and Concrete Research*, *41*, 1224–1231.

Thomas, M. D. A. (2013). *Supplementary cementing materials in concrete*. Boca Raton, FL: CRC Press. 210 p.

Thomas, M. D. A., & Matthews, J. D. (2000). Carbonation of fly ash concrete. In: *Proceedings of the 4th ACI/CANMET international conference on the durability of concrete*, ACI SP-192, Vol. 1 (pp. 539–556). Farmington Hills, MI: American Concrete Institute.

Thomas, M. D. A., & Matthews, J. D. (2004). Performance of PFA concrete in a marine environment—10-year results. *Cement and Concrete Composites*, *26*, 5–20.

Thomas, M. D. A., & Yi, H. (2016). Deicer-salt scaling of concrete containing fly ash. In: M. T. Hasholt, K. Fridh, & R. Doug Hooton (Eds.), *Proceedings of the international RILEM conference materials, systems and structures in civil engineering 2016 segment on frost action in concrete, Proceedings PRO 114*. Paris: RILEM.

Tsukayama, R. (1980). Long term experiments on the neutralization of concrete mixed with fly ash and the corrosion of reinforcement. In: *Vol.III. Proceedings of the seventh international congressional on the chemistry of cement, Paris* (pp. 30–35).

USBR. (1948). *Physical and chemical properties of fly ash—Hungry Horse Dam*. Laboratory Report CH-95. US Bureau of Reclamation.

Wang, H., Qi, C., Farzam, H., & Turici, J. (2006). Interaction of materials used in concrete: Effects of fly ash and chemical admixtures on Portland cement performance. *Concrete International*, (April), 47–52.

Yuan, R. L., & Cook, R. E. (1983). Study of a class c fly ash concrete. In: *Proceeding of the first international conference on the use of fly ash, silica fume, slag, and other by-products in concrete*. ACI SP-79, Vol. 1 (pp. 307–319). Detroit, MI: American Concrete Institute.

# The utilization of flue-gas desulfurization materials

# 6

*T. Butalia**, *W. Wolfe**, *P. Amaya*†
*The Ohio State University, Columbus, OH, United States, †American Electric Power, Columbus, OH, United States

## 6.1 Introduction

Chapter 3 of this book outlines the various types of flue-gas desulfurization (FGD) materials generated at power plants. In general, postcombustion desulfurization includes wet processes, which generate stabilized sulfite FGD ($CaSO_3$) or the sulfate ($CaSO_4$) FGD gypsum, and dry processes, which generate spray dryer (SD), duct injection (DI), or circulating fluidized bed (CFB) materials. Desulfurization during the combustion cycle generates solid by-products, such as fluidized bed combustion (FBC) ash.

In the United States, the main types of FGD materials generated are sulfite, FGD gypsum, and dry FGD. FGD gypsum generated from wet forced oxidation processes and the anhydrite by-products such as FBC are sulfate-rich FGD materials. The material generated in wet limestone or lime nonforced oxidation systems, as well as SD, DI, and CFB processes, result in FGD materials that are also rich in sulfites. These "sulfite" CCPs (sometimes called scrubber sludge) are typically too wet to process, and so they are often mixed with fly ash to reduce water content and improve handling characteristics. This fly ash modified sulfite FGD is then referred to as "stabilized sulfite FGD."

In 2014, a total of about 120 million metric tons of coal combustion by-products (CCBs) were generated in the United States (American Coal Ash Association, 2014 CCP Survey). Of this, about half (59 million metric tons) were FGD materials, and about half the FGD material generated in the United States was beneficially utilized, as seen in Table 6.1. The leading beneficial uses for FGD materials were mine reclamation (about 13 million metric tons) and wallboard manufacturing (about 10 million metric tons). Cement manufacturing, structural fills, and agricultural applications accounted for 1–2 million metric tons, while all other beneficial uses were less than 0.5 million metric tons for 2014.

Comprehensive and detailed studies of FGD materials and their potential uses for mine reclamation, highway applications, and agricultural uses were conducted at The Ohio State University, with support from the electric power industry and the Ohio Coal Development Office (Stehouwer et al., 1995, 1996, 1998; Dick et al., 1999a, 1999b; Butalia & Wolfe, 2000, 2010).

**Coal Combustion Products (CCP's).** **http://dx.doi.org/10.1016/B978-0-08-100945-1.00006-X**

**Table 6.1 2014 FGD material production and beneficial use**

| | FGD gypsum | Stabilized FGD | Dry FGD material | Totals |
|---|---|---|---|---|
| Production (MST) | 34.12 | 12.60 | 17.37 | 64.09 |
| Beneficial use (MST) | 16.75 | 1.16 | 13.56 | 31.47 |
| *% Beneficial use* | *49.1* | *9.2* | *78.1* | *49.1* |
| Concrete/grout (MST) | 0.42 | 0 | 0 | 0.42 |
| Cement manufacturing (MST) | 1.31 | 0.12 | 0 | 1.43 |
| Structural fills (MST) | 1.59 | 0.31 | 0 | 1.90 |
| Mining applications (MST) | 0.81 | 0.58 | 13.38 | 14.77 |
| Wallboard (MST) | 11.22 | 0 | 0 | 11.22 |
| Waste stabilization (MST) | 0.02 | 0 | 0.13 | 0.15 |
| Agriculture (MST) | 1.34 | 0 | 0 | 1.34 |
| Other uses (MST) | 0.04 | 0.15 | 0.05 | 0.24 |

*MST*, million short tons (1.0 million short tons = 0.9 million metric tons).
From American Coal Ash Association, (2014). *Coal combustion product* (*CCP*) *production and use survey report*. https://www.acaa-usa.org/Portals/9/Files/PDFs/2014ReportFinal.pdf Accessed 31.03.16.

Cordoba (2015) reports on utilization of FGD in Europe while Su et al. (2015), through collaborative research and demonstration projects, identified a number of practical markets for dry FGD by-product in China. In this chapter information is presented from that research, as well as additional work performed at a number of research institutions regarding the beneficial utilization potential for fly ash stabilized sulfite FGD, FGD gypsum, and dry FGD materials for the applications listed above.

## 6.2 Highway applications

The existing and potential highway uses of FGD materials can be classified into six general categories:

1. Structural fills
2. Stabilized road bases/subbases
3. Flowable fills
4. Subsidence control and remediation
5. Manufactured aggregate
6. Additive in asphalt pavement

The use of FGD materials in highway applications can be limited by the swell potential of the particular FGD material under consideration. Some dry FGD materials rich in residual calcium oxide that are well compacted with little or no overburden stress can be susceptible to swell when first exposed to water infiltration. Two distinct episodes of free swelling have been observed (Adams, 1992; Adams & Wolfe, 1993; Dick et al., 1999a, 1999b; Stehouwer et al., 1995, 1996, 1998). The first swell episode corresponds to the initial hydration of the sample, and the second episode of the swell corresponds to mineralogical changes in the material. In most cases the amount of swell in the second episode is larger than the first. The percent free swell generally increases with curing time but at a decreased rate with time. It is recommended that the one-dimensional swell potential of FGD materials should be carried out per ASTM D4546 for a minimum of 30 days, or until the mineralogical swell stabilizes, whichever is longer. In general, FGD materials generated from wet processes (e.g., stabilized sulfite FGD and sulfate FGD gypsum) and some of dry processes (e.g., SD, DI, or CFB) show small amounts of free swell. On the other hand, FBC ash that is rich in calcium oxide content can exhibit significant swell when first exposed to water. In such cases, preconditioning the FBC ash with water can alleviate some of the swell potential.

### 6.2.1 Structural fills

FGD materials offer several advantages over natural soils in the construction of highway embankments and structural fills including:

- Availability of material in sufficient quantities to accommodate any appropriate design,
- Typically higher slope stability factors of safety compared to naturally occurring soils,
- Suitability for construction on low-bearing strength foundation soils because of their lower unit weights compared to soil,
- High shear strength-to-unit weight ratio resulting in ideal placement under foundations,
- Availability of free draining materials, such as bottom ash.

The design and construction of FGD structural fills is carried out according to procedures detailed in ASTM E2277. However, some dry FGD materials rich in residual calcium oxide that are well compacted with little or no overburden stress can be susceptible to swell when first exposed to water infiltration. Therefore all FGD materials intended for use in structural fill applications should be tested for one-dimensional swell, as outlined in ASTM D4546, for a minimum of 30 days or until the mineralogical swell stabilizes, whichever is longer.

To evaluate the field handling and compaction characteristics of a dry FGD (SD) ash, approximately 100 $m^3$ were used to construct a truck ramp at The Ohio State University to provide a location for unloading hard trash collected around campus (Wolfe & Beeghly, 1993). The ash was placed to within about ±5% of the optimum moisture content and greater than a 90% Standard Proctor density, as determined in laboratory density tests (ASTM D698). After a year of service, properties testing conducted on the samples cored from the ramp showed that the in situ water content was considerably higher than the as-placed water content. Although unconfined compressive strength tests conducted on the sample cores exhibited lower strengths than those achieved for samples stored in the laboratory for the same amount of time, the ramp has performed well with no evidence of failures during use by university vehicles.

A slide in a fill section supporting Ohio State Route 541 west of Coshocton, Ohio, closed the highway in both directions in the fall of 1993. To reopen the roadway, the failed section was stabilized using FBC ash. Reconstruction consisted of removing approximately 9000 $m^3$ of soil in order to expose the failure surface. Half the excavated soil was stockpiled onsite for later use, while the rest was transported offsite and reused in other ODOT construction projects. Underdrains were constructed to divert groundwater away from the embankment. FBC ash from the AEP Tidd demonstration facility was transported to and stockpiled at the project site. Self-loading scrapers delivered the material stocked onsite, as bulldozers spread it evenly over an area 12 m wide and 30 m long. The first lift was approximately 0.6 m thick and was placed and compacted on the first day. Subsequent lifts ranging between 0.4 and 0.6 m in thickness were placed until the FGD embankment was constructed to a design height ranging from 4 to 6 m. The thicknesses of individual layers and the amount of water added to the FGD at compaction were field monitored. It was observed during placement that this FGD material (FBC ash) remained highly workable over a wide range of moisture contents. The original embankment material was placed on top of the FGD fill in controlled lifts. A final layer of the FBC ash was placed and compacted as the driving surface, so the roadway could be opened during the winter. The permanent paved road surface was constructed the following spring. Regular monitoring of the water quality upstream and downstream of the project was done throughout construction and for several years after the repairs were completed. The variations in pH and the total dissolved solids were within the acceptable range of fluctuations associated with the nearby stream. However, water samples taken from underdrains showed a significant rise in sulfates and total alkaline measured as $CaCO_3$. The volume of stream flow was so much greater than the volume of water in the underdrains that the total system appeared unaffected by the increase in measured sulfates and $CaCO_3$ in the leachate. Inclinometers, piezometers, and deformation measuring gauges were installed at the site and monitored by ODOT personnel for several years. A more detailed description of the project was presented by Nodjomian (1994), Kim (1994), Nodjomian and Wolfe (1994), and Kim, Nodjomian, and Wolfe (1995).

A second highway embankment repair project involved the stabilization of a portion of Ohio State Route 83 south of Cumberland, Ohio. A section of the roadway damaged and repeatedly patched due to continuing downslope movement over several years was reconstructed in 1994 using FBC ash from the AEP Tidd plant. Approximately 11,000 $m^3$ of embankment soil were excavated. Fabric drain boards were installed in a trench dug along the hillside to divert groundwater away from the embankment. The trench was backfilled with compacted FGD in approximately 0.3-m thick lifts using a small bulldozer for spreading and a sheepsfoot roller for compaction.

The embankment was divided into four test sections. Control sections were established at the two ends of the site, and they were repaired according to standard ODOT procedures by drying, replacing, and compacting the stockpiled soil. One test section consisted of a field mixture of FBC ash and on-site soil. The fourth section was constructed using 100% FBC ash. The blended ash/soil section was compacted in lifts of about 0.2 m, while the ash-only section was compacted in thicker lifts ranging from 0.3 to 0.6 m. Strict control was kept over the moisture content and compacted density for all four sections. Approximately 95% of the Standard Proctor compaction density was achieved. The embankment construction was completed in Dec. 1994. However, because asphalt plants had closed down for the season, half of the road was constructed with a 0.5 m compacted dry FGD wearing course, while the other half was made with a 0.5 m layer of stone aggregate. The road was opened to traffic in late December. The ash and the ash/soil sections have performed well and have not needed repairs. Water around the embankment has shown no indication of metals leaching into the surrounding environment. More details on the Ohio SR83 project can be found in Payette (1996) and Payette, Wolfe, and Beeghly (1997).

Savings from the two highway repair projects were estimated by ODOT engineers to be between 25% and 40% compared to the cost of using conventional methods and materials. Site visits 20 years after construction and 10 years after the end-of-slope monitoring showed no visible distress in the FGD sections at either site.

Stabilized FGD materials have also been used in Pennsylvania (Brendel & Glogowski, 1989) for structural fills. However, the volumes of stabilized FGD materials used in highway embankment or structural fill applications is rather limited in the United States due to increased regulatory uncertainty for these large volume fills placed over natural areas (Hardin & Daniels, 2011).

### 6.2.2 Stabilized bases/subbases

Stabilized FGD materials have been used successfully for road base construction at a number of different sites in the United States, including Florida, Pennsylvania, Ohio, and Texas (Amaya, Booth, & Collins, 1997; Prusinski, Cleveland, & Saylak, 1995; Smith, 1985, 1989; Jackson, Schultz, Sander, & Schopp, 2009), as well as in China (Jiang, Wu, Su, Lu, & Lin, 2011; Su et al., 2015).

The swelling potential of a wide variety of FGD materials was studied by Adams (1992) and Adams and Wolfe (1993) by conducting long-term laboratory swell tests on more than a dozen samples from four power plants representative of different dry FGD processes. They observed two distinct swelling episodes, the first of which occurred almost immediately after water was supplied to the specimens. This corresponds with the time period during which naturally occurring soils typically experience greater increases in volume due to hydration reactions. The start of the second episode of swelling was observed after 10 or more days had elapsed. A study of the occurrence of swell along with mineralogical changes in FGD material is presented in Stehouwer et al. (1998).

In regions subject to large temperature variations, the effects of freeze-thaw cycling on the engineering properties of FGD can be significant. Hargraves (1994) and Chen, Wolfe, and Hargraves (1997) investigated the effect of thermal cycling on the strength of compacted stabilized FGD material. Higher water content samples exhibited greater reduction in compressive strength due to freeze-thaw cycling. It was observed that satisfactory strengths could be maintained under freeze-thaw cycling if at least 5% lime (dry weight basis) was added to the FGD before compaction, and the material was allowed to cure for a minimum of 60 days before being exposed to freeze-thaw. These observations are now included in the guidelines that have been issued for the structural use of FGD in the midwestern United States.

Freeze-thaw cycling also affects the resilient modulus. Roy (1994) and Wolfe, Butalia, and Meek (1997) subjected compacted FGD samples to alternating cycles of freeze and thaw. They found that in highway construction applications, FGD products could be used satisfactorily as a subgrade material in the construction of low-volume roads, and the moduli of FGD materials subjected to laboratory freeze-thaw cycling moduli compared favorably with published values for materials commonly used in road base construction.

Hua et al. (2010) produced a satisfactory road base material by stabilizing FGD gypsum from a Chinese power plant with lime and sodium silicate (water glass). Their results are particularly interesting because the study originated with a pavement failure resulting from the inadvertent use of unamended FGD gypsum instead of fly ash in the construction of the base and subbase of several highways in the Jiangsu province of China.

In Amaya et al. (1997) investigated various mixes of stabilized FGD material and bottom ash with addition of 4%–10% cement. The unconfined compressive strength and durability characteristics of the mixes were evaluated in the laboratory. Durability was tested by subjecting compacted FGD samples to freeze-thaw cycling while given free access to water. The unconfined compressive strength was measured initially after 7 days of curing and then after 12 cycles of freeze and thaw. Based on results of the laboratory testing, a mix consisting of 60% FGD by weight and 40% by weight bottom ash, to which an additional 7% by weight cement was added was selected for field implantation. The FGD, bottom ash, and cement were mixed in a pug mill and placed on a 100 m long section of a proposed truck haul road in the summer of 1995. The base layer was placed in one 0.3 m thick loose lift and compacted using pneumatic and tandem vibratory rollers to a final thickness of about 0.2 m. The base layer was cured for 7 days with free access to water and then surfaced with 50 mm thick asphalt concrete before being opened to traffic. Amaya et al. (1997) reported no distress or failures for the haul road section underlain by the FGD base layer after more than 1 year of heavy off-road truck traffic at the power plant. In fact, it is now two decades later, and the FGD base section is still performing well without a need for significant repairs. Based on this work by Amaya et al. (1997), it is recommended that stabilized FGD bases and subbases are designed so as to minimize the reduction in strength when subjected to freeze-thaw cycling along with free access to water. Recent research by Amaya et al. (2015) has shown the potential of using dry FGD materials for soil stabilization.

### 6.2.3 Flowable fills

Flowable fill is defined by the American Concrete Institute (1994) as a self-compacting cementitious material that is in a flowable condition at time of placement and has a compressive strength of 1200 psi or less at 28 days. Most flowable fill mixes are designed to have strengths of 150–200 psi for ease of excavation at a later time. Flowable fill typically consists of a mixture of fine aggregate or filler, cementitious material, and water. Flowable fills are also commonly known by several other terms, including controlled density fill (CDF), controlled low-strength material (CLSM), flowable mortar, plastic soil-cement slurry, K-Krete, Flash Fill, etc. The performance criteria for flowable fills is outlined in ACI 229R-94 (American Concrete Institute, 1994). The material can be used to fill voids in an irregular excavation and hard-to-reach places, such as under and around pipes in trenches. The material is self-leveling, does not need compaction, and hardens in a couple of hours after placement. The material can be placed in freezing temperatures, requires no compactive effort, and improves job safety and labor costs because no workers are needed in the trench as it is filled. A significant benefit of flowable fill is that it does not need compaction, resulting in reduced excavation and equipment costs. Typically, most ready-mix concrete producers can provide flowable fills using fly ash, as the ash is used as an admixture in concrete.

Many FGD materials have low unit weight (lower than natural soil fills) and good shear strength characteristics (typically equal to or greater than select granular fill); hence they hold promise for flowable fill applications. Research conducted at The Ohio State University (Lee, 1998; Lee, Butalia, & Wolfe, 1999) has investigated the potential of using two types of FGD (SD and fly ash-stabilized FGD) in a flowable fill as a replacement for conventional fly ash. Several design mixes were studied as part of that program. The mixes consisted of varying amounts of FGD, cement, lime, and water. The mixes were tested in the laboratory for their flow characteristics, unit weight, moisture content, unconfined compressive strength, resistance to erosion, set-time, penetration, and long-term strength characteristics. Tests were conducted for up to 90 days of curing. FGD flowable fills without any additives were observed to have properties comparable to those measured or reported for regular (i.e., normal set) flowable fill in terms of flow and strength, and FGD flowable fills containing additives and admixtures compared favorably with the characteristics of conventional quick set-flowable fills. However, there remain some concern, including the anchoring of pipes and confinement prior to initial set of material and the potential for long-term corrosion of buried pipe. Procedures to alleviate these concerns need further laboratory and field investigations.

### 6.2.4 Subsidence control and remediation

Subsidence can result when underground mining activity causes a collapse of overlying rock and unconsolidated materials. When the collapse reaches the ground surface, mine subsidence can damage public infrastructure and private property, therefore it presents a danger to the public's safety (Crowell, 2010).

In 1994, Indiana Power and Light (Meiers, 2006) began research to develop a technology that would reduce surface mine subsidence using fixated FGD material. Over 16,000 cubic yards of the sulfite FGD material was successfully injected into an abandoned underground mine complex, achieving good roof contact and unconfined compressive strengths greater than 100 psi (700 kPa).

In March 1995, mine subsidence caused the collapse of the eastbound lanes of I-70 in Ohio, resulting in the closure of a portion of that main east-west artery for several months. Repairs of subsidence events often involve injection grouting the voids. The I-70 repair, as well as most similar repairs, have involved standard grout mixes containing as much as 85% fly ash and 15% Portland cement. However, research has shown that several FGD materials can play a role in mine subsidence remediation. In 2011, OSU researchers demonstrated that an FGD gypsum grout mix could be

**Fig. 6.1** Grout containing FGD gypsum placed at field trial.

designed to stabilize auger holes at previously mined sites (Kirch, 2011; Warden et al., 2014). Fig. 6.1 shows a grout mix as placed in a 2012 field trial. This work showed that an FGD gypsum based grout mix could be satisfactorily field blended and placed, and design strengths necessary for void filling and overburden support could be achieved. However, further research is needed to demonstrate full-scale applicability in subsidence remediation. FBC ashes that exhibit swell could also be good candidates for the abatement of underground mine subsidence.

### *6.2.5 Manufactured aggregate*

Synthetic aggregates made of sulfite-rich FGD and Class F fly ash can be an economic alternative to conventional natural aggregates particularly for high-volume road construction or repair.

Consol Energy investigated the potential use of synthetic FGD aggregate for several years (Wu, 2005). The FGD used in the CONSOL studies process involved mixing sulfite-rich filter cake with Class F fly ash, as well as subsequent pelletization and curing in a specially designed temperature vessel (United States Department Of Energy Project Facts, 1999). In Oct. 1998 in Warren, Ohio, a 23 m long by 3.5 m wide by 40 mm thick test patch of asphalt paving material was constructed as part of a bench-scale project sponsored by the Ohio Coal Development Office. The test patch was made of manufactured FGD aggregate meeting the AASHTO specifications for Class A road aggregates. The coarse aggregate in the asphalt mix was prepared by mixing equal parts by weight of FGD aggregate and natural stone. An adjacent control test patch was constructed using only natural coarse aggregates.

A scale-up of the technology presented above was carried out by Universal Aggregate (Wu & Yuran, 2007) in the design, construction, and operation of a lightweight aggregate manufacturing plant at the Birchwood power plant in King George County, Virginia, using SD FGD ash generated at the facility. This full-scale commercial demonstration supported by USDOE successfully produced lightweight aggregate from SD FGD material. Tests to measure the durability of the aggregate were conducted by Wu (2005).

### 6.2.6 *Additive in asphalt pavement*

Jiang et al. (2011) reported on collaborative research conducted in China and the United States to identify practical uses of Dry FGD in China as asphalt filler in highway construction. Chen, Xiao, Pang, Zeng, and Wu (2014) conducted a series of tests that demonstrated that fatigue life, as measured in indirect tensile tests, improved when FGD and steel slag were included in the asphalt mix design. Although it appears the bulk of the improvement could be attributed to the addition of the slag, the addition of FGD positively affected fatigue life at lower stress levels (<300 kPa).

## 6.3 Wallboard

The American Coal Ash Association estimated that 31 million metric tons of FGD gypsum were produced at US power plants in 2014, but slightly less than half that amount (15 million metric tons) was used beneficially (see Table 6.1). Of the amount reused, more than 10 million metric tons were applied in the wallboard industry. While these numbers represent the single largest beneficial use of FGD gypsum, the Gypsum Association estimates that FGD gypsum wallboard makes up about only half of all the wallboard manufactured in the United States.

According to the Gypsum Association, FGD gypsum is chemically indistinguishable from mined (natural) gypsum. Since the two sources of gypsum behave the same way, FGD gypsum has been used to make wallboard for nearly as long as wallboard has been manufactured (Burkard, 1985). Nevertheless, there have been questions raised over the potential for heavy metal contamination from the FGD gypsum. Most trace contaminants that have been observed in coal ash occur in the fly ash component. Since its usage began in the United States, FGD gypsum is separated from the fly ash and then dewatered, heavy metals have been reported at much lower levels than those typically reported for fly ash (Su, Jiang, Lu, Chen, & Wu, 2013; Su et al., 2015). However, mercury, which vaporizes during combustion, can be in the form of oxidized mercury in the flue gas. High percentages of mercury removal (70% or more) from the flue gas can be accomplished with current scrubbing technologies. However, the mercury must stay in the FGD for these methods to be successful. The presence of Hg in FGD gypsum has been studied by several investigators (Hassett, Heebink, & Pflughoeft-Hassett, 2004; Heebink & Hassett, 2005; Pasini & Walker, 2012; Pekney, Martello, Schroeder, & Granit, 2009; Xin, Gustin, & Ladwig, 2006). Marshall, Blythe, and Richardson (2005) investigated the fate of the mercury present in samples of FGD gypsum during the manufacturing of wallboard, over the life of the finished wallboard product, and after the wallboard's disposal in construction waste streams.

Lee, Bradshaw, Edil, and Benson (2012) quantified the benefits of using FGD gypsum in wallboard production from a sustainability perspective. Their research showed that annual cumulative savings for energy expenditure, water consumption, greenhouse gas emissions, and financial expenses for replacing virgin gypsum with FGD gypsum in wallboard were significant.

## 6.4 Agricultural applications

As a source of both sulfur and calcium, the benefits of gypsum as a soil conditioner have long been known. Mined gypsum has been used to increase crop yields for over 250 years (https://www.gypsum.org). In a comparison of the chemical properties of an FGD gypsum and a natural (mined) gypsum, Chen and Dick (2011) showed the two to be similar in their behavior and effects on the studied crops, but the FGD gypsum was typically finer grained and possessed a higher degree of purity than natural gypsum.

In 2014, about 1.34 million tons of FGD gypsum were used as an agricultural soil amendment (see Table 6.1). There are three general uses of gypsum in agricultural applications (US EPA, 2008):

1. as a source of nutrients for plants,
2. to improve the physical and chemical properties of soil,
3. to modify the soil structure so as to reduce the movement of nutrients, sediment, pesticides, and other contaminants.

### 6.4.1 Source of Nutrients

Chen, Dick, and Nelson (2005) observed that alfalfa and soybean yields increased with the application of FGD gypsum. The application of FGD gypsum to alfalfa crops was also studied by Stout and Priddy (1996), who found that yields on soils with acid subsoils increased without influencing heavy metals concentrations. However, sulfur concentrations were increased in plant tissues to the point that it raised concerns about animal health. Plant growth experiments were conducted by Álvarez-Ayuso, Giménez, and Ballesteros (2011) on two acidic soils. Samples of the soils were then mixed with different amounts of FGD gypsum (1%, 2%, 5%, and 10% gypsum plus control) and planted with ryegrass or alfalfa. After 90 days the alfalfa yield appeared to be unaffected by the FGD, while the ryegrass biomass was less than the ryegrass grown without added FGD gypsum. When FGD was applied to the acid soils in the study, fluoride concentrations in the plant mass were reduced, imparting "an important reduction of health risks for animals feeding on (these) plants." Sumner (1993) reviewed gypsum treatments for acid subsoils and observed that substantial yield increases were reported in a wide variety of crops. He observed that these increases were usually the result of an increased supply of $Ca^{2+}$ and the detoxification of $A1^{3+}$. He cautioned that the use of gypsum in very sandy soils could increase the rate at which Mg and K moved through the soil column, potentially leading to deficiencies in these nutrients.

A study by Nan et al. (2016) illustrated the benefits of applying FGD gypsum and humic acid for improving the physical and chemical properties of soil and increasing the productivity of rapeseed yield.

Alva (1994) reported that combining FGD gypsum with fly ash or chicken manure to soil in which citrus rootstock seedlings planted produced significantly improved growth. However, when the FGD gypsum was applied in higher rates with both fly ash and chicken manure, growth was lower than the control (no amendments), likely because the overall dosage was too high. Sloan, Dowdy, Dolan, and Rehm (1999) also examined the behavior of a fly ash-amended FGD. In their study, Sloan et al. applied a calcium sulfate-sulfite FGD containing approximately two-thirds fly ash to a potentially boron- and sulfur-deficient silt loam. Tissue sulfur concentrations increased as a result of the FGD applications. They concluded that FGD can be a ready boron and sulfur source for alfalfa production, particularly later in the season when availability of native soil boron may become limiting. One year after application, the FGD-supplied boron had not leached below 0.15 m, thereby minimizing any environmental threat to ground water quality (Sloan et al., 1999).

Rhoton and McChesney (2011) examined the effects of a surface application of FGD gypsum to no-till cotton. The study site was a highly erodible soil in the loess uplands of Mississippi. Rhoten and McChesney documented significant improvements in several physical and chemical properties of the soil over three growing seasons. Data showed statistically significant increases in Ca and S concentrations in the soil through the profile within 1 year following the initial application.

### 6.4.2 Improvement of soil physical and chemical properties of soil

Gypsum is helpful in treating sodic and other soils that experience crusting. Clark, Ritchey, and Baligar (2001) observed that although limestone ($CaCO_3$ and/or $CaMg(CO_3)_2$) has been commonly used as an amendment to increase soil pH, FGD can be successfully applied. Because FGD is more soluble than limestone, it moves through the soil column more easily. The calcium ions promote the aggregation of clay particles, which increases water infiltration and storage in soil, therefore reducing runoff and erosion. Limestone is most effective at the site of incorporation in soil and not readily leached. Thus soils treated with limestone must be cultivated/disturbed to distribute the calcium within the profiles and to make it available in deeper profiles. Tilling soil has been common for the production of cultivated crops, but not for pasture, perennial, and shrub/tree plants. Truman, Nuti, Truman, and Dean (2010) studied the effect on water retention, runoff, and sediment loss of applying FGD gypsum to silty, sandy soils. They treated the soil with several different rates of FGD and subjected the treated plots to different intensities of simulated rainfall. They found that for all levels of FGD applied to the soil, runoff decreased and infiltration increased. They also observed that runoff continued to decrease and infiltration increase as the application rate increased up to the maximum rate studied. They also found that the infiltration increases translated directly into decreased demand for irrigation during the growing season, resulting in “a positive and significant impact on natural resource conservation, producer profit margins, and environmental quality” (Truman et al., 2010). Chen et al. (2009) applied stabilized FGD to the soil surface. The major active constituent in the FGD used after oxidation was $CaSO_4 \cdot 2H_2O$ (gypsum) and $CaSO_4 \cdot ½\ H_2O$, which are considerably more soluble than $CaCO_3$, and therefore have the potential to leach into lower soil profiles. The FGD promoted soil aggregation, increased water infiltration rates and movement through the soil profile, and mitigated subsoil acidity and Al toxicity. A key finding was that at an application rate (1.12 Mg $ha^{-1}$), similar to the minimum rate (1.1 Mg $ha^{-1}$) reported by Truman et al. (2010), the benefits of adding $CaSO_3$ to the soil surface were seen as similar to the benefits reported when using gypsum, provided planting is delayed at least 3 days to as much as several weeks after the application of the FGD-$CaSO_3$. Chen, Dick, and Nelson (2001) observed that the treatment of an acidic soil with FGD by-products lowered the soluble concentrations of potentially toxic metals in the soil, thus reducing their uptake into alfalfa and improving the quality of the alfalfa for animal consumption.

Kost et al. (2014) studied the effects of gypsum applications in two field experiments, one on hay and the other on corn. In these tests, the effects of gypsum applications were mixed. Although corn yields were influenced by the amount of gypsum applied, there was no clear effect, and the yields were not significantly different from the control (no applied FGD gypsum). On the hay fields, high rates of application resulted in increases in Ca and S, but there were decreases in Mg when compared to the control. Kilpatrick (2012) observed that FGD gypsum had no effect on Miscanthus growth 18 months after application, even though the FGD application resulted in higher total and extractable sulfur levels in the soil. The metal content of feedstock was unaffected by the application of FGD gypsum.

Buckley and Wolkowski (2012, 2014) reported that for the FGD gypsum application rates used, corn yield was unaffected during the year of application. Soybean yield was increased for application rates of up to 1.2 tonnes/hectare but above that rate, yields dropped to the yields seen on the control (unamended) plots.

Li, Mao, and Liu (2015) examined the effectiveness of applications of FGD gypsum in the treatment of tidal lands undergoing reclamation. They showed that significant doses of FGD gypsum could be used to accelerate the processes of desalination and vegetation of reclaimed land.

Sakai, Matsumoto, and Sadakata (2004) evaluated the use of FGD gypsum as an alkali soil amendment in China. They studied the effects of both wet and semidry FGD gypsums applications on the soil pH, exchangeable sodium production (ESP), and corn yield. Nineteen plots were included in the study. The authors found that soil pH and ESP decreased in the treated soil when compared to the control, while corn yields increased. Metal content in the corn in the treated plots was compared with the control; most of the metal content in the amended soil decreased over the values measured in the untreated soil.

### *6.4.3 Reduction in the transport of nutrients, sediment, pesticides, and other contaminants*

FGD gypsum application can reduce the solubility of nutrients, such as phosphorus, in livestock and poultry manure, as well as soils treated with manure. Gypsum converts readily soluble phosphorus to less-soluble forms, which can reduce the runoff of phosphorus into adjacent streams, lakes, or groundwater.

By improving the soil's workability and its ability to retain water, Chen et al. (2005) found that the FGD gypsum did not increase the concentrations of potentially toxic metals in the examined plant tissues.

Yang et al. (2016) studied the feasibility of using FGD gypsum to remove Cd and Pb from the upper root zone in a reclaimed tidal flat in Southern China. The heavy metal removal rate correlated with the amount of FGD gypsum and leaching water that was applied. Multiple applications of FGD gypsum also increased observed removal rates.

Similarly, Chen et al. (2005) observed that the FGD gypsum may have other benefits for crop growth due to the availability of trace nutrients, but with lower levels of the elements that Chen and Dick (2011) identified as "elements of concern" (As, Ba, Cd, Pb, and Se). Gypsum (FGD and mined) can also improve the physical properties of the soil by reducing the dispersion of individual particles and increasing flocculation and water infiltration and movement (Chen et al., 2005; Chen & Dick, 2011; Watts & Dick, 2014)

Feldhake and Ritchey (1996) studied the leachate from an acid Appalachian subsoil that had been treated with FGD gypsum. The data collected showed reduced aluminum saturation, resulting in greater root growth and increased water uptake. The authors suggest that because the plants possess greater root depth and density, the plant would be more drought tolerant. Measurements taken by Stout, Sharpley, and Weaver (2003) over multiple growth cycles showed that leachable phosphorus was reduced when FGD gypsum was applied to high P soils. In a study in which FGD gypsum was used to stabilize soil treated with poultry litter, Schomberg, Fisher, Endale, Franklin, and Jenkins (2011) and Endale, Schomberg, Fisher, Franklin, and Jenkins (2014) observed significant reductions in runoff each of the two years the area was monitored. However, after making allowances for the severe changes in the climate during the test, they were unable to definitively attribute this reduction to the effects of the FGD gypsum. In contrast to Schomberg et al. and Endale et al., Torbert and Watts (2014) applied FGD gypsum at different rates to a sandy loam soil to evaluate the effectiveness of the applications in reducing runoff of soluble reactive phosphorus. Their data showed a greater than 50% reduction during a simulated rainfall event. At the same time the concentrations of heavy metals in the runoff were all below detection limits. In greenhouse studies, Adeli, Sheng, Jenkins, and Feng (2015) were able to observe that the addition of FGD gypsum to soil fertilized with poultry litter reduced phosphorous runoff (leachate). The measured reductions were substantial: >50% for first leaching event and >90% in the second for the fresh litter samples, and 47% and 81% for the first and second leaching events in soil samples treated with composted litter. Watts and Torbert (2015) demonstrated FGD gypsum's effectiveness in reducing phosphorus loss in pastures fertilized with poultry litter over the span of a complete growing season. Phosphorous loss in runoff was reduced by as much as 35% in rainfall simulations for as long as 6 months after being treated.

In a study of 16 applications of FGD and mined gypsum on three soils, Briggs, Fine, Markee, and Gustin (2014) examined the release of mercury (Hg) from the amended soils into the atmosphere and into leachate. They sought to observe the amount of Hg in the environment that could be attributed to application of gypsum. They found the amount of Hg in the FGD gypsum treated soils was low. Measured values were comparable to the amounts measured in the untreated soil, but that tilling the FGD gypsum into the soil did result in a lower release of Hg into the air than did placing the FGD gypsum on the surface. They speculated this observation might have implications for use of FGD gypsum in no-till applications.

### 6.4.4 Summary

Gypsum is an excellent soil amendment, supplying readily available Ca and S that all plants need for nutrition. Gypsum is considered moderately soluble in soil, therefore sulfur may be released over multiple years. Agronomists are predicting that crop deficiencies will become common due to a shift away from sulfur in fertilizers and pesticides. Increasing crop yields will continue to result in increases in sulfur demand, while decreased atmospheric deposition reduces the sulfur in soil. Clark et al. (2001) summarized the benefits and constraints for use of FGD gypsum on agricultural land. They concluded that when used appropriately, FGD gypsum benefits agricultural land without causing contamination or other detrimental effects.

## 6.5 Cement manufacturing

The use of FGD materials in cement manufacturing can be divided into two main types and purposes:

1. FGD gypsum is commonly used as a set retarder in Portland cement production.
2. CFBC and some other dry FGD materials are used as hydraulic cements.

As recorded in Table 6.1, in 2014, cement manufacturing in the United States used about 1.43 million tons (1.3 metric tons) of FGD material (almost all FGD gypsum). Another 0.4 million tons (0.36 metric tons) of FGD gypsum was utilized in other concrete products.

Jewell, Rathbone, Duvallet, Robl, and Mahboub (2015) investigated the use of fluidized bed combustor ash as a potential hydraulic cement in the manufacture of low-energy cements. They showed that both the spent bed materials (i.e., coarse bottom ash and finer fly ash) were high in calcium, hence they could act as hydraulic cements. Their work focused on the production of a cement to maximize the amount of CFBC ash in it while achieving adequate strength values comparable to those commercially produced.

Bin, Fang, Ren, Gao, and Zhu (2009) showed that FGD and granulated blast furnace slag could be added to cement for structural applications. Their test data show slight declines in both flexural and compressive strength with increasing FGD content. However, strengths remained adequate as the decreases were seen to be small in mixes containing less than 19% FGD. Therefore, Bin et al. recommended an FGD content of 19% be considered for optimal usage.

Zhong, Ni, and Li (2012) combined FGD gypsum with ground granulated blast furnace slag and fly ash replacing cement to make a grout suitable for a variety of low strength concrete applications.

Gypsum blocks have been used in China for many years. Although gypsum is suitable for interior work, it has not proved satisfactory for exterior construction because of its slight solubility in water. FGD gypsum has been shown to be a suitable substitution for natural gypsum in block construction, but the poor water resistance of gypsum blocks in general has limited the number of uses. Zhao, Liu, Hao, and Li (2012) investigated the water absorbance characteristics and consequent strength loss associated with an FGD gypsum block modified by a granulated blast furnace slag/high calcium fly ash mixture. They found that blocks made from FGD gypsum when combined with an appropriate amount of ground blast furnace slag and fly ash, retained over 80% of their initial (i.e., dry) strength.

## 6.6 Livestock feeding and hay storage pads

In high rainfall areas, yield can be improved in livestock operations by paving feedlot and feeding areas with a durable material (traditionally, concrete or rock aggregates) to reduce the amount of unproductive energy the animals expend. Strength and durability testing has shown that compacted FGD could be an inexpensive and reliable technique for stabilizing feedlots and other high animal traffic areas. The site chosen to demonstrate this application was the OSU bull breeding and research facility at the Eastern Ohio Resource Development Center (EORDC) in Belle Valley, Ohio.

First, dry cyclone ash from AEP's Tidd plant was used to stabilize the saturated organic in-place soil by blending the ash into the top 0.5 m of the soil and then compacting the mixture to produce a stabilized base. Next, a 0.5–0.8 m thick layer of compacted ash was placed on top of the stabilized base. Farm personnel using standard farm equipment performed all the construction activities. Some minor failures were observed when the first cohort of cattle was brought onto the feedlot; however, repairs were made and the feedlots now perform well. Additional livestock feeding and hay storage pads were constructed at the EORDC farm in Sep. 1993 using stabilized FGD from AEP's Conesville plant. These feedlots have performed very well, experiencing an approximately 6–12 mm annual wear. The Ohio EPA was satisfied with the performance of the FGD feeding and hay storage pads, and American Electric Power currently has a state-wide blanket permit to install (PTI) FGD livestock feedlot and hay storage pads using lime-enriched FGD material from its Conesville and Gavin power plants. As long as the conditions in the PTI are met and the thickness of FGD layer is less than 0.4 m, no additional approval from the Ohio EPA is necessary. The construction of FGD feedlots does not require any special equipment. The cost of an FGD feedlot can be up to 25% lower than the cost of purchasing and using aggregate, as well as 65% less than an equivalent concrete pad. AEP's plants have generally provided the material free of charge at the plant, with farmers paying for hauling costs. In some cases the plant has been willing to truck the material to the site if it is in vicinity of the plant. To date, more than 150 such feeding and hay storage FGD pads have been constructed in over 12 Ohio counties. OSU has published a fact sheet to assist in the planning, construction, and maintenance of these stabilized FGD feeding and hay storage pads (Wolfe & Cline, 1995; Butalia, Dyer, Stowell, & Wolfe, 1999).

## 6.7 Waste stream pollutant fixation

Research has shown that FGD by-products have the potential to solidify/stabilize hazardous wastes or sludge. Spray dryer and fixated FGD material can work as solidification agents by turning hazardous waste or sludge into a monolithic solid. The fixation of hazardous sludge and wastes with FGD by-products uses the pozzolanic and sulfo-pozzolanic nature of the by-products to develop chemical cementation bonds to bind the materials together (Smith, 1987). The presence of calcium sulfite/sulfate minerals, the major solids in FGD by-products, can accelerate the strength development of the stabilized waste under alkaline conditions (Poon, Kou, Lam, & Lin, 2001) by forming secondary minerals, such as ettringite (Cheng, Bigham, & Walker, 2007). Phillips (1979) studied the workability of calcium-based dry FGD material and demonstrated that the material can undergo a pozzolanic reaction similar to that obtained with lime and fly ash.

Weeter (1981) investigated the feasibility of using dry FGD material to stabilize/fixate hazardous waste and sludge. Weeter reported that fixating hazardous sludge, such as cadmium waste, with the calcium-based dry FGD material could reduce the leachate concentrations. The leaching characteristics of the sludge and wastes evaluated by the toxicity characteristic leaching procedure (TCLP) in his study became nonhazardous after being fixated by dry FGD material.

Qiao, Poon, and Cheeseman (2006) investigated the performance of using coal fly ash and FGD gypsum in the solidification and stabilization (S/S) of waste from an electroplating plant, with respect to the resulting unconfined compressive strength and leaching characteristic. In that study, coarse fly ash with low pozzolanic reactivity was used. Although cement was added to provide adequate strength, the research showed the addition of FGD gypsum could reduce the porosity of the waste and promote the strength development. Results from their leaching studies suggested that the mobility of heavy metals in the waste was effectively reduced after solidification.

Solem-Tishmack et al. (1995) used four high calcium CCBs, including calcium sulfite FGD material, to mobilize boron and selenium. They found that after 91 days of curing, all of the tested CCBs developed enough strength to be used for solidification and stabilization. They reported a measured unconfined compressive strength of an FGD/fly ash mixture (2:1 ratio) of 670 psi (4600 kPa) after curing, which is many times greater than the stated threshold of 50 psi (350 kPa) for stabilization/solidification applications. The leaching of Se and boron showed a generally positive correlation with the amount of ettringite formed after curing.

## 6.8 Landfill liner and cap

One potential use of FGD material is in the creation of low-permeability liners (Butalia & Wolfe, 1997, 1999; Butalia, Wolfe, & Walker, 2005). Low-permeability liners are constructed for a number of applications, including storage ponds, wetlands, and landfills. Utilization of stabilized FGD material as a liner would lower the amount of FGD entering landfills, as well as reduce the mining and consumption of clay and other naturally occurring low-permeability materials. Both laboratory and field data have indicated that stabilized FGD material is an adequate replacement for clay in low-permeability liner and cap applications.

The suitability of dry and wet FGD materials for applications as low-permeability liners in place of commonly used clay and synthetic liners was investigated by Kim, Wolfe, and Wu (1992a) and Butalia and Wolfe (1997). Characterization of stabilized FGD showed that laboratory samples could be compacted to achieve permeability coefficients equal to or lower than the value typically required by EPA for lining waste containment facilities ($1 \times 10^{-7}$ cm $s^{-1}$). These low permeabilities were measured for samples with high fly ash to filter cake ratio (2:1) and high lime percentage (8%).

Butalia et al. (2005) used stabilized FGD material as a liner for a livestock manure storage facility, constructed at The Ohio State University's Ohio Agriculture Research Development Center (OARDC)'s Western Branch in South Charleston, Ohio (Cheng, Walker, Butalia, & Wolfe, 2007). The livestock manure storage facility was constructed with a double-liner design in which stabilized FGD material was used for the primary inner liner, while on-site clay was used as an outer (secondary) liner. The facility was rectangular in shape (46 m × 61 m) and had a design storage capacity of 4000 $m^3$ (a six month capacity). A leachate collection system was installed between the FGD liner and the in situ natural clay. Approximately 2500 metric tons of lime-enriched stabilized FGD material was used in the construction of the primary liner. The lime-enriched stabilized FGD material consisted of a mixture of fly ash, dewatered filter cake from wet lime scrubbers, and additional lime. Water quality monitoring data at the facility showed that the concentration levels of most detectable elements in the leachate increase immediately upon the introduction of water into the FGD liner facility. However, the concentration levels of these constituents decreased sharply after the initial spike. As livestock manure was added to the facility with time replacing the water, the level of several parameters (i.e., Si, Mg, As, Ba, P, and B) showed a generally increasing trend. Except for Ba and nitrate, all detectable potential pollutants (As, B, Cr, Cu, Zn, phosphate, and ammonium), were retained in the stabilized FGD liner as the pond liquid passed through. Sorption was proposed as the likely dominant removal mechanism. The thermodynamic geochemical speciation modeling suggested that the precipitation of Fe- and Ca-containing phosphate solids could also contribute to the retention of trace elements within the FGD material (Cheng, Bigham, et al., 2007).

## 6.9 Land reclamation

The beneficial use of CCBs (e.g., FGD materials and fly ash) at coal mines has been an area of continued research. Federal, academic, and industrial organizations have all carried out studies to promote the use of CCBs in land reclamation. Potential beneficial uses include:

1. Agricultural supplements to create productive artificial soils on abandoned mine lands (AMLs) where native soils are not available,

2. Seals to contain acid-forming materials and prevent the formation of acid mine drainage (AMD),
3. Flowable fills to seal and stabilize abandoned underground mines, therefore limiting subsidence and the production of AMD,
4. Fill materials for final highwall and pits and within the spoil area,
5. Solidification/stabilization reagents for hazardous sludge and wastes.

Among all of the various beneficial uses of FGD materials in the United States (see Table 6.1), mine reclamation applications are the leading type of use of about 13.5 metric tons per year. Accordingly, the remainder of this chapter will focus on land reclamation applications.

CCBs have been used in mine reclamation in a number of states, including Arizona, Delaware, Maryland, Massachusetts, Michigan, Minnesota, Missouri, Ohio, Oklahoma, Pennsylvania, Virginia, West Virginia, and Wisconsin (Vories & Harrington, 2006).

The USEPA has stated (Federal Register, 2010) that there is no evidence showing adverse environmental effects when CCBs are used at coal mine sites. OSMRE is working with USEPA to develop effective federal regulations to ensure that the placement of coal ash in mine fill operations is adequately controlled at both active and abandoned unreclaimed mine lands. Beneficial use of FGD materials can be divided into two categories: (1) incorporation into the mine reclamation process at active SMCRA permitted sites, and (2) incorporation into the design and remediation of AML sites. Both of these categories will be discussed in more detail below.

Pasini (2009) carried out a life cycle impact assessment for five different abandoned mine land reclamation scenarios, including the dangerous remains of past surface mining; e.g., highwalls (i.e., vertical or near-vertical surface cuts made to reach the coal seam), and highwall pits (i.e., a highwall with impounded water at its base), as well as underground mines and openings and coal refuse piles. The environmental impacts associated with these reclamation scenarios, such as air pollutant emissions, total toxic release, global warming potential, and energy consumption, were compared to landfilling. The results of Pasini's work showed that using FGD material for abandoned mine land reclamation is a better option than landfilling in terms of the overall negative environmental impact. It also showed that there are only slight differences in impacts, whether as a result of reclaiming abandoned highwalls and highwall pits or underground mine entranceways. The FGD material exhibited low-leaching availability of mercury and other environmentally hazardous constituents, relatively inexpensive transportation and earthwork unit costs, and reliable material production by coal combustion power plants.

### 6.9.1 Reclamation of abandoned and active mined lands

Abandoned mine lands can pose risks to the public and the environment by disrupting the flow of nearby surface water streams, discharging highly acidic and metal-enriched AMD, creating dangerous highwalls, and degrading habitat and threatening animal species.

Yet full reclamation and restoration of AML is rarely undertaken due to the high costs, which includes the cost of materials. Only where these unreclaimed sites pose a clear threat to the health and safety of residents are they repaired by the state.

However, reclaiming AMLs using FGD materials, including sulfate-rich FGD gypsum and stabilized sulfite-rich FGD has been shown to be effective and economically viable (Butalia & Wolfe, 2010; Dick, 2006; Stehouwer et al., 1996). FGD can improve the physical (e.g., landscape, soil texture, and water-holding capacity), and chemical (e.g., alkalinity and nutrients) characteristics of AMLs. Using FGD instead of the conventional natural material (e.g., nearby sand, aggregate, and clay) in mine reclamation also can reduce the consumption of natural resources and costs associated with the handling and disposal of the CCBs. The cost savings associated with the utilization of FGD materials enables the reclamation of abandoned and active coal mine lands, often without the use of public AML reclamation funds.

In Butalia and Wolfe (2010) issued a report titled "FGD By-product Utilization at Ohio Coal Mine Sites: Past, Present, and Future." The objective of this effort was to identify large volume reclamation applications in which FGD materials could be used beneficially. The study examined potential sites within a 25 km radius of the five coal-fired power plants in Ohio that produce FGD material. The study also reviewed the engineering and chemical leaching characteristics of FGD materials (e.g., stabilized FGD and FGD gypsum). The report concluded that the FGD material produced at Ohio's power plants was suitable for use in reclamation projects for both abandoned and active mine sites.

### 6.9.2 Elimination of dangerous highwalls

The use of FGD materials for highwall reclamation follows ASTM E2243.

The Midwestern Mine Reclamation site, located in Pike County, Indiana, consisted of approximately 225 ha of previously surface mined land and abandoned underground workings. Due to the limited supply of low-permeability soil in this area, the reclamation plans for this site included the use of about 600,000 $yd^3$ (460,000 $m^3$) of stabilized sulfite FGD material. It was used to create a low-permeability cover over the exposed coal refuse and as a backfill for existing abandoned highwalls. Locally available mine spoil was used to establish a vegetative cover. The Indiana Geological Survey monitored the chemical qualities of both the groundwater and surface water for a 2-year period (1997 and 1998). The intent of the reclamation project was to improve site safety conditions by backfilling or removing dangerous highwalls, to lessen the potential for AMD, and to reduce erosion by regrading and revegetating the disturbed areas (Bryenton et al., 2006). A follow-up study was conducted by researchers at Indiana University that examined the impacts of FGD materials placed in the field, as well as examined the chemical phases that contain trace elements and characterized the morphology subject to ambient leaching processes (Zhang et al., 2015).

In 2011, construction was begun at a demonstration project near AEP's Conesville Power generating station. Initially, stabilized FGD material was used to encapsulate a core of FGD gypsum and stabilized FGD fill (Phase A). In a subsequent activity (Phase B), FGD gypsum, stabilized FGD material, and fly ash were all used to

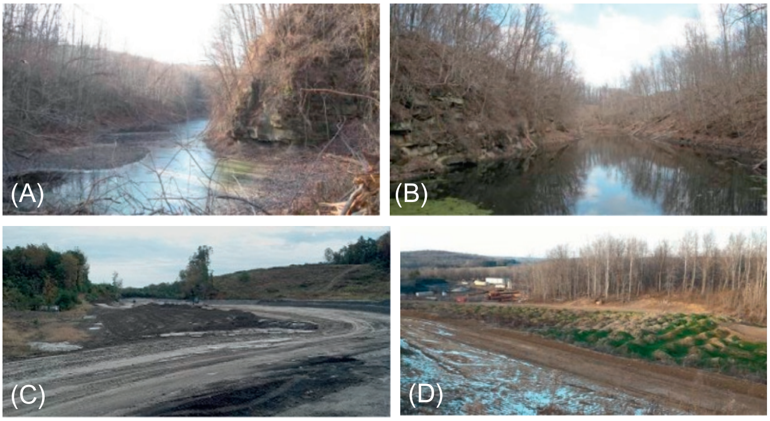

**Fig. 6.2** Progression of reclamation at the Conesville Five Point Site. (A) Phase A project area before reclamation. (B) Phase B project area before reclamation. (C) Backfilling Oct. 2014. (D) Capping and vegetation Jan. 2016.

eliminate a highwall. By Mar. 2016, over 1.5 million metric tons of CCBs had been placed at the project reclamation site (Fig. 6.2). By the end of 2016, over 750 m of highwall will be eliminated, and about 45 ha of abandoned mined lands will be reclaimed by end of 2016.

Approximately 0.4 million metric tons of FGD gypsum from the AEP Cardinal Power plant were used to eliminate 250 linear meters of AML highwall, and almost 200 m of active mining highwall at the Star Ridge site in Jefferson County in eastern Ohio (Fig. 6.3).

**Fig. 6.3** Progression of reclamation at the Cardinal Star Ridge Site. (A) Site before reclamation. (B) Water in pit before reclamation. (C) Placement of FGD gypsum Sep. 2013. (D) Resoil Aug. 2015.

### 6.9.3 AMD mitigation

FGD by-products can be used as sealing materials or neutralization agents to remediate AMD (Lamminen et al., 2001; Rudisell, Stuart, Novak, Payne, & Togni, 2001).

Acid mine drainage occurs when surface and groundwater come in contact with geologic strata containing sulfide minerals exposed by mining. In the presence of ferric iron, the accelerated oxidation of iron pyrite ($FeS_2$) produces sulfuric acid (Evangelou, 1998; Johnson, 2003):

$$FeS_2 + 3H_2O \rightarrow Fe^{2+} + S_2O_3{}^{2-} + 6H^+$$

$$8Fe^{3+} + S_2O_3{}^{2-} \rightarrow 8Fe^{3+} + 10H^+ + 2SO_4{}^{2-}$$

Another possible geochemical process, which suggests that the oxidation of pyrite depends on the presence of oxygen in the water, can be expressed as:

$$2FeS_2 + 7O_2 + 2H_2O \rightarrow 2Fe^{2+} + 4SO_4{}^{2-} + 4H^+$$

$$4Fe^{2+} + O_2 + 4H^+ \rightarrow 4Fe^{3+} + 2H_2O$$

$$4Fe^{3+} + 12H_2O \rightarrow 4Fe(OH)_3 + 12H^+$$

A similar oxidation process can occur for other sulfide minerals, such as copper, zinc, cadmium, lead, and arsenic, and produce elevated concentrations of these constituents in the receiving streams.

At the Broken Aro complex in Coshocton County, Ohio, stabilized FGD was used to seal an abandoned underground mine complex. The FGD material was used to seal the groundwater inside the mine to inundate the voids left by the mining operations. The FGD seal limits the amount of oxygen present in the mine, thereby minimizing the oxidation reaction within the underground mine. Improvements in water quality were observed after reclamation (Fig. 6.4).

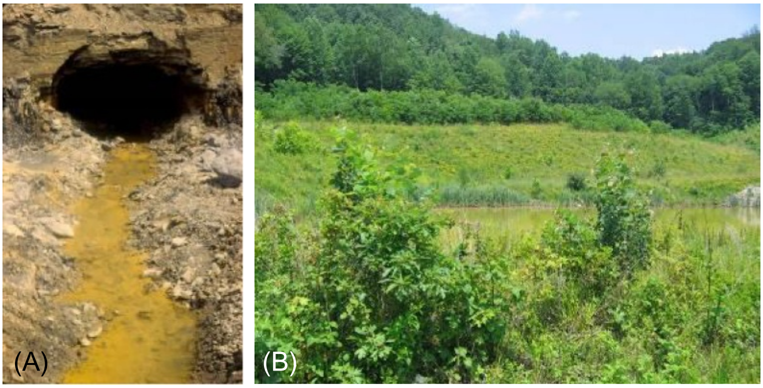

**Fig. 6.4** Broken aro site reclamation. (A) Before reclamation. (B) Post reclamation in 2008.

### 6.9.4 Refuse and mine spoil reclamation

Coal refuse piles are comprised mainly of the coal shales that encased the coal seam prior to the coal extraction. At the time the coal was mined, these wastes, which have a lower thermal value than the coal, were discarded onsite. Water percolating through the piles produces the same type of acidic leachate present in the unreclaimed mines discussed in the last section, but low-permeability stabilized FGD has been shown to be an effective capping material, providing a barrier to the salt and acid migration from the toxic coal refuse to the surface and to limit the surface water infiltration into the pile. Once the FGD cap is constructed, the site can be resoiled and revegetated.

An example of stabilized FGD as a cap material is the Rehoboth refuse pile, which was a 24 ha coal waste site located in Perry County, Ohio. Prior to reclamation the runoff from the site caused flooding along roadways and waterways in the general area of the coal refuse material. Drainage from the site was highly acidic, and unstable slopes were eroding into a local creek. Approximately 0.6 m of stabilized FGD were placed and compacted to form an impermeable cap over the regraded site. A 0.6 m layer of an artificial soil consisting of approximately 50% coal refuse mixed with 50% stabilized FGD was placed over the FGD cap. Finally a 0.2 m growing medium consisting of composted yard waste, spoil, and FGD covered the site. This mix of materials became problematic at the site following completion of the project when the vegetation at the site became distressed exhibiting chlorosis. Investigations showed that the incorporation of coal refuse into the resoil mix probably had a greater impact than expected, and boron toxicity resulted when the FGD material placed above the cap came in contact with the low pH coal refuse material. An application of lime to the overall site at a rate of 55 metric tons/hectare was completed in 2004. A 2008 site review found the site to be in excellent overall condition, with only a few small areas exhibiting erosion features (Butalia et al., 2010; see Fig. 6.5).

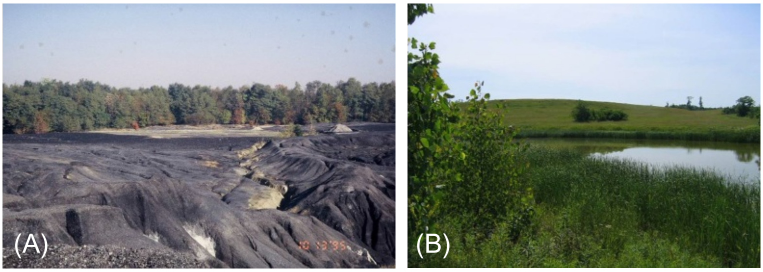

**Fig. 6.5** Rehoboth reclamation site. (A) Prior to reclamation. (B) Reclaimed site with FGD pond liner.

## 6.10 Conclusions

This chapter has focused on the beneficial utilization of three types of commonly generated FGD materials: stabilized FGD (sulfite) and FGD gypsum from the wet scrubbing processes, and dry FGD materials (primarily SD and fluidized bed) from the dry processes. In 2014, mine reclamation activities accounted for approximately half the volume of FGD used beneficially, which is about 13.5 million metric tons per year. Wallboard manufacturing utilized about 10 million metric tons per year with cement manufacturing, structural fill, and agricultural applications combining to account for about 1–2 million metric tons each per year. FGD gypsum usage in wallboard manufacture appears to be on the rise after nearly a decade of constant demand/use, and the use of FGD gypsum as a soil amendment in agricultural applications has increased approximately 10 fold in the last decade; this trend is expected to continue. The overall utilization of stabilized FGD materials at mine sites is currently rather low, but it is expected to increase with regulatory clarity on the use of these materials at mine sites. Highway application markets for FGD materials are expected to continue to remain stable, while cement manufacturing may increase slightly. The current utilization of FGD material, which is about 50%, is expected to increase incrementally over the next decade.

## References

Adams, D. A. (1992). *Swelling characteristics of dry sulfur dioxide removal waste products* [M.S. thesis]. Columbus, OH: The Ohio State University.

Adams, D. A., & Wolfe, W. E. (1993). The potential for swelling in samples of compacted flue gas desulfurization by-products. In *Tenth American Coal Ash Association Symposium, Orlando, FL*.

Adeli, A., Sheng, J., Jenkins, J. N., & Feng, G. (2015). Composting and gypsum amendment of broiler litter to reduce nutrient leaching loss. *Journal of Environmental Quality*, *44*, 676–683. http://dx.doi.org/10.2134/jeq2014.04.0144.

Alva, A. K. (1994). Possible utilization of flue-gas desulfurization gypsum and fly ash for citrus production: evaluation of crop growth response. *Waste Management*, *14*(7), 621–627.

Álvarez-Ayuso, E., Giménez, A., & Ballesteros, J. C. (2011). Fluoride accumulation by plants grown in acid soils amended with flue gas desulphurisation gypsum. *Journal of Hazardous Materials*, *193*(3), 1659–1666.

Amaya, P. J., Booth, E. E., & Collins, R. J. (1997). Design and construction of roller compacted base courses containing stabilized coal combustion by-product materials. In *Vol. 1. Proceedings of the 12th international symposium on management and use of coal combustion by-products*. Palo Alto, CA: Electric Power Research Institute. Report No. TR-107055.

Amaya, M., Cheng, C., Butalia, T., Yongrui, L. M., Wu, M., & Wolfe, W. E. (2015). *Beneficial utilization of Chinese dry flue gas desulfurization materials for stabilization of weak soils*. Nashville, TN: World of Coal Ash.

American Coal Ash Association. (2014). *Coal combustion product (CCP) production and use survey report*. https://www.acaa-usa.org/Portals/9/Files/PDFs/2014ReportFinal.pdf. Accessed 31.03.16.

American Concrete Institute. (1994). *Controlled low strength materials (CLSM).* American Concrete Institute Committee 229, Report No. 229R Detroit, MI: American Concrete Institute.

ASTM D4546. *Standard test methods for one-dimensional swell or collapse of soils*. ASTM Book of Standards Volume 04.08.

ASTM D698. *Standard test methods for laboratory compaction characteristics of soil using standard effort*. ASTM book of standards volume 04.08.

ASTM E2243. *Standard guide for use of coal combustion products* (*CCPs*) *for surface mine reclamation*: *Re-CONTOURING and highwall reclamation*. ASTM Book of Standards Volume 11.05.

ASTM E2277, *Standard guide for design and construction of coal ash structural fills*. ASTM Book of Standards Volume 11.05.

Bin, G., Fang, Z., Ren, A., Gao, Q., & Zhu, T. (2009). The preparation of eco-cementing materials in utilization of semidry desulphurization ash with steel slag and mineral materials. In *2009 International conference on energy and environmental technology, October 16–18, Guilin, Guangxi, China* (pp. 441–444).

Brendel, G. F., & Glogowski, P. E. (1989). *Ash utilization in highways: Pennsylvania demonstration project*. Palo Alto, CA: Electric Power Research Institute. Report No. GS-6431.

Briggs, C. W., Fine, R., Markee, M., & Gustin, M. G. (2014). Investigation of the potential for mercury release from flue gas desulfurization solids applied as an agricultural amendment. *Journal of Environmental Quality*, *43*, 253–262.

Bryenton, D. L., et al. (2006). *Design and construction guidelines for CCB utilization in an AML setting—A case study CCB associated with coal mining.* A Technical Interactive Forum—USDOI Office of Surface Mining and Coal Research Center Carbondale, IL: Southern Illinois University. pp. 105–109.

Buckley, M. E., & Wolkowski, R. P. (2012). Effect of land application of FGD gypsum on plant yield and crop nutrient concentration. *Crop Management*. http://dx.doi.org/10.1094/CM-2012-0925-01-RS.

Buckley, M. E., & Wolkowski, R. P. (2014). In-season effect of flue gas desulfurization gypsum on soil physical properties. *Journal of Environmental Quality*, *43*, 322–327.

Burkard, E. A. (1985). Manufacture of gypsum board from FGD gypsum. US Patent No. 4502901 A.

Butalia, T., Dyer, P., Stowell, R., & Wolfe, W. (1999). *Construction of livestock feeding and hay bale storage pads using FGD material*. The Ohio state extension fact sheet, AEX-332-99, Columbus, OH: The Ohio State University.

Butalia, T. S., & Wolfe, W. E. (1997). Re-use of clean coal technology by-products in the construction of impervious liners. In *1997 Ash utilization symposium, Lexington, KY*.

Butalia, T. S., & Wolfe, W. E. (1999). Evaluation of permeability characteristics of FGD materials. *Fuel*, *78*, 149–152.

Butalia, T. S., & Wolfe, W. E. (2000). *Market opportunities for utilization of Ohio flue gas desulfurization (FGD) and other coal combustion products (CCPs), volume 1—executive summary, volume 2—findings, recommendations, and conclusions*. Columbus, OH: The Ohio State University.

Butalia, T., & Wolfe, W. (2010). *FGD by-product utilization at Ohio coal mine sites: past, present, & future*. Columbus, OH: The Ohio State University.

Butalia, T. S., Wolfe, W. E., & Walker, H. (2005). Use of coal combustion by-products as low permeability liners for manure storage facilities. In L. N. Reddi (Ed.), *ASCE manuals and reports on engineering practice no. 105. Animal waste containment in lagoons*. Reston, VA: American Society of Civil Engineers.

Chen, L., & Dick, W. A. (2011). *Gypsum as an agricultural amendment: general use guidelines*. Bulletin 945 Columbus, OH: Ohio State University Extension. 35p.

Chen, L., Dick, W. A., & Nelson, S. (2001). Flue gas desulfurization by-products additions to acidic soil: Alfalfa productivity and environmental quality. *Environmental Pollution*, *114*, 161–168.

Chen, L., Dick, W. A., & Nelson, S., Jr. (2005). Flue gas desulfurization products as sulfur sources for alfalfa and soybean. *Agronomy Journal*, *97*, 265–271.

Chen, L., Ramsier, C., Bigham, J., Slater, B., Kost, D., Lee, Y. B., et al. (2009). Oxidation of FGD-CaSO3 and effect on soil chemical properties when applied to the soil surface. *Fuel*, *88*, 1167–1172.

Chen, X., Wolfe, W. E., & Hargraves, M. D. (1997). The influence of freeze-thaw cycles on the compressive strength of stabilized FGD sludge. *Fuel*, *76*, 755–759.

Chen, Z. W., Xiao, Y., Pang, L., Zeng, W. -B., & Wu, S. P. (2014). Experimental assessment of flue gas desulfurization residues and basic oxygen furnace slag on fatigue and moisture resistance of HMA. *Fatigue and Fracture of Engineering Materials and Structures*, *37*, 1242–1253. http://dx.doi.org/10.1111/ffe.12205.

Cheng, C. -M., Bigham, J., & Walker, H. (2007). Influence of pH on the leaching kinetics of fixated flue gas desulfurization (FGD) material. *Journal of Environmental Quality*, *36*, 874–886.

Cheng, C. -M., Walker, H., Butalia, T., & Wolfe, W. (2007). Beneficial reuse of FGD material in the construction of low permeability liners: impacts on inorganic water quality constituents. *Journal of Environmental Engineering*, *133*(5), 523–531.

Clark, R. B., Ritchey, K. D., & Baligar, V. C. (2001). Benefits and constraints for use of FGD products on agricultural land. *Fuel*, *80*, 821–828.

Cordoba, P. (2015). Status of flue gas desulphurisation (FGD) systems from coal-fired power plants: overview of the physic-chemical control processes of wet limestone FGDs. *Fuel*, *144*, 274–286.

Crowell, D. L. (2010). *GeoFacts # 12, mine subsidence*. Columbus, OH: ODNR, Division of Geological Survey.

Dick, W. (2006). *Flue gas desulfurization (FGD) product as a soil amendment for mine reclamation*. Wooster, OH: The Ohio State University, School of Environment and Natural Resources.

Dick, W., Bigham, J., Forster, L., Hitzhusen, F., Lal, R., Stehouwer, R., et al. (1999a). *Land application uses of dry FGD by-product: phase 3 report*. Palo Alto, CA: Electric Power Research Institute, EPRI.

Dick, W., Bigham, J., Forster, L., Hitzhusen, F., Lal, R., Stehouwer, R., et al. (1999b). *Land application uses of dry flue gas desulfurization by-products: executive summary*. Columbus, OH: The Ohio State University.

Endale, D. M., Schomberg, H. H., Fisher, D. S., Franklin, D. H., & Jenkins, M. B. (2014). Flue gas desulfurization gypsum: implication for runoff and nutrient losses associated with broiler litter use on pastures on ultisols. *Journal of Environmental Quality*, *43*(1), 281–289. http://dx.doi.org/10.2134/jeq2012.0259.

Evangelou, V. P. (1998). Pyrite chemistry: the key for abatement of acid mine drainage. In A. Geller, H. Klapper, & W. Salomons (Eds.), *Acidic mining lakes: acid mine drainage, limnology and reclamation* (pp. 197–222). Berlin: Springer.

Federal Register, Part II, EPA 40 CFR, Parts 257,61,264, et al. Disposal of CCR from electric utilities—proposed rule, 2010.

Feldhake, C. M., & Ritchey, K. D. (1996). Flue gas desulfurization gypsum improves orchardgrass root density and water extraction in an acid subsoil. *Plant and Soil*, *178*, 273–281.

Gypsum Association. Gypsum builds the economy. https://www.gypsum.org Accessed April 2016.

Hardin, C. D., & Daniels, J. L. (2011). Preserving structural fills and mine reclamation as acceptable beneficial use of CCR's. In *World of Coal Ash Conference, Denver, CO*.

Hargraves, M. D. (1994). *The effect of freeze-thaw cycles on the strength of flue gas desulfurization sludge* [M.S. thesis]. Columbus, OH: The Ohio State University.

Hassett, D. J., Heebink, L. V., & Pflughoeft-Hassett, D. F. (2004). Potential for mercury vapor release from coal combustion by-products. *Fuel Processing Technology*, *85*(6–7), 613–620.

Heebink, L. V., & Hassett, D. J. (2005). Mercury release from FGD. *Fuel*, *84*(11), 1372–1377.

Hua, M., Wang, B., Chen, L., Wang, Y., Quynh, V. M., He, B., et al. (2010). Verification of lime and water glass stabilized FGD gypsum as road sub-base. *Fuel*, *89*(8), 1812–1817. http://dx.doi.org/10.1016/j.fuel.2009.11.02.

Jackson, N. M., Schultz, S., Sander, P., & Schopp, L. (2009). Beneficial use of CFB ash in pavement construction applications. *Fuel*, *88*(7), 1210–1215.

Jewell, R. B., Rathbone, R. F., Duvallet, T. Y., Robl, T., & Mahboub, K. C. (2015). Fabrication and testing of low-energy calcium sulfoaluminate-belite cements that utilize circulating fluidized bed combustion by-products. *Coal Combustion and Gasification Products*, *7*, 9–18.

Jiang, Y., Wu, M. -C. M., Su, Q., Lu, M., & Lin, C. (2011). Dry CFB-FGD by-product utilization—international perspectives. In *2011 World of coal ash (WOCA) conference, Denver, CO, May 9–12*.

Johnson, D. B. (2003). Chemical and microbiological characteristics of mineral spoils and drainage waters at abandoned coal and metal mines. *Water, Air, and Soil Pollution*, *3*, 47–66.

Kilpatrick, L. A. (2012). Impacts of biosolids and FGD gypsum application on marginal soil quality and production of miscanthus as a bioenergy crop. In *Thesis presented in partial fulfillment of the requirements for the degree master of science in the Graduate School of The Ohio State University*.

Kim, S. H. (1994). *A decision support system for highway embankment design using FGD by-products* [Ph.D. dissertation]. Columbus, OH: The Ohio State University.

Kim, S. H., Nodjomian, S., & Wolfe, W. E. (1995). Field demonstration project using clean coal technology by-products. In *Vol. 1. Proceedings of 11th international symposium on use and management of coal combustion by-products (CCBs), Orlando, FL, January 15–19* (pp. 1–15): American Coal Ash Association and Electric Power Research Institute. EPRI TR-104657.

Kim, S. H., Wolfe, W., & Wu, T. (1992). Permeability of FGD by-products. In *Proceedings of the 9th annual Pittsburgh coal conference, Pittsburgh, PA, October 12–16* (pp. 218–223).

Kirch, J. P. (2011). *Potential use of flue gas desulfurization gypsum in a flowable grout for re-mining of abandoned coal mines* [M.S. thesis]. Columbus, OH: The Ohio State University.

Kost, D., Chen, L., Guo, X., Tian, Y., Ladwig, K., & Dick, W. A. (2014). Effects of flue Gas desulfurization and mined gypsums on soil properties and on Hay and corn growth in eastern Ohio. *Journal of Environmental Quality*, *43*, 312–321. http://dx.doi.org/10.2134/jeq2012.0157.

Lamminen, M., Wood, J., Walker, W., Chin, Y. -. P., He, Y., & Traina, S. (2001). Effect of flue gas desulfurization (FGD) by-product on water quality at an underground coal mine. *Journal of Environmental Quality*, *30*, 1371–1381.

Lee, J. W. (1998). *Beneficial use of FGD by-products as flowable fill* [M.S. thesis]. Columbus, OH: The Ohio State University.

Lee, J. C., Bradshaw, S., Edil, T., & Benson, C. (2012). Quantifying the benefits of using flue gas desulfurization gypsum in sustainable wallboard production. *Coal Combustion and Gasification Products*, *4*, 17–20.

Lee, J. W., Butalia, T. S., & Wolfe, W. E. (1999). Potential use of FGD as a flowable fill. In *1999 International ash utilization symposium, Lexington, KY, October 18–20*.

Li, X., Mao, Y., & Liu, X. (2015). Flue gas desulfurization gypsum application for enhancing the desalination of reclaimed tidal lands. *Ecological Engineering*, *82*, 566–570.

Marshall, J., Blythe, G. M., & Richardson, M. (April 2005). *Fate of mercury in synthetic gypsum used for wallboard production*. Topical report: task 1 wallboard plant test results, cooperative agreement no: DE-FC26-04NT42080 USG Corporation. 33p.

Meiers, J. R. (2006). *Fluid placement of fixated scrubber sludge in abandoned underground coal mines to reduce surface subsidence and abate AMD*. A Technical Interactive Forum—USDOI Office of Surface Mining and Coal Research Center Carbondale, IL: Southern Illinois University. pp. 210–216.

Nan, J., Chen, X., Wang, X., Lashari, M. S., Wang, Y., Guo, Z., et al. (2016). Effects of applying flue gas desulfurization gypsum and humic acid on soil physicochemical properties and rapeseed yield of a saline-sodic cropland in the eastern coastal area of China. *Journal of Soils and Sediments*, *16*, 38–50. http://dx.doi.org/10.1007/s11368-015-1186-3.

Nodjomian, S. M. (1994). *Clean coal technology by-products used in a highway embankment stabilization demonstration project* [M.S. thesis]. Columbus, OH: The Ohio State University.

Nodjomian, S. M., & Wolfe, W. E. (1994). Field demonstration projects using clean coal technology by-products. In *Second annual great lakes geotechnical/geoenvironmental conference, West Lafayette, IN*.

Pasini, R. (2009). *An evaluation of flue gas desulfurization gypsum for abandoned mine land reclamation* [MS thesis]. Columbus, OH: The Ohio State University.

Pasini, R., & Walker, H. W. (2012). Estimating constituent release from FGD gypsum under different management scenarios. *Fuel*, *95*, 190–196.

Payette, R. M. (1996). *Landslide remediation using clean burning coal technology by- products* [MS thesis]. Columbus, OH: The Ohio State University.

Payette, R. M., Wolfe, W. E., & Beeghly, J. (1997). Use of clean coal combustion by-products in highway repairs. *Fuel*, *76*, 749–753.

Pekney, N. J., Martello, D., Schroeder, K., & Granit, E. (2009). Environmental chamber measurements of mercury flux from coal utilization by-products. *Fuel*, *88*(5), 890–897.

Phillips, H. L. (1979). *An evaluation of the waste product from a calcium based Dry flue Gas desulfurization system* [M.S. thesis]. Knoxville, TN: The University of Tennessee.

Poon, C. S., Kou, S. C., Lam, L., & Lin, Z. S. (2001). Activation of fly ash/cement using calcium sulfate anhydrate (CaSO4). *Cement and Concrete Research*, *31*, 873–881.

Prusinski, J. R., Cleveland, M. W., & Saylak, D. (1995). Development and construction of road bases from flue gas desulfurization material blends. In *Vol. 1. Proceedings of the 11th international ash utilization symposium*. Palo Alto, CA: Electric Power Research Institute. Report No. TR-104657.

Qiao, X. C., Poon, C. S., & Cheeseman, C. (2006). Use of flue gas desulfurization (FGD) waste and rejected fly ash in waste stabilization/solidification systems. *Waste Management*, *26*, 141–149.

Rhoton, F. E., & McChesney, D. S. (2011). Influence of FGD gypsum on the properties of a highly erodible soil under conservation tillage. *Communications in Soil Science and Plant Analysis*, *42*, 2012–2023.

Roy, B. L. (1994). *The effect of freeze-thaw cycling on the resilient modulus of clean coal technology by-products* [M.S. thesis]. Columbus, OH: The Ohio State University.

Rudisell, M. T., Stuart, B. J., Novak, G., Payne, H., & Togni, C. S. (2001). Use of flue gas desulfurization by-product for mine sealing and abatement of acid mine drainage. *Fuel*, *80*, 837–843.

Sakai, Y., Matsumoto, S., & Sadakata, M. (2004). Alkali soil reclamation with flue gas desulfurization gypsum in China and assessment of metal content in corn grains. *Soil and Sediment Contamination*, *13*, 65–80. http://dx.doi.org/10.1080/10588330490269840.

Schomberg, H. H., Fisher, D. S., Endale, D. M., Franklin, D., & Jenkins, M. B. (2011). Evaluation of FGD-gypsum to improve forage production and reduce phosphorus losses from piedmont soils. In *World of coal ash conference, May 9–12*.

Sloan, J. J., Dowdy, R. H., Dolan, M. S., & Rehm, G. W. (1999). Plant and soil responses to field applied flue gas desulfurization residue. *Fuel*, *78*(2), 169–174.

Smith, C. L. (1985). FGD sludge C coal Ash road base: seven years of performance. In *Proceedings of the 8th international coal and solid fuels utilization conference, Pittsburgh, PA*.

Smith, C. L. (1987). Lime-based fixation of flue gas desulfurization waste. In K. A. Gutschick (Ed.), *Lime for environmental uses, ASTM STP 931* (pp. 52–69). Philadelphia, PA: American Society for Testing and Materials.

Smith, C. L. (1989). The first 100,000 tons of stabilized scrubber sludge in roadbase construction. In *Proceedings of the Power-Gen 89 conference, New Orleans, LA*.

Solem-Tishmack, J. K., McCarthy, G. J., Docktor, B., Eylands, K. E., Thompson, J. S., & Hassett, D. J. (1995). High-calcium coal combustion by-products: engineering properties, ettringite formation, and potential application in solidification and stabilization of selenium and boron. *Cement and Concrete Research*, *25*, 658–670.

Stehouwer, R., Dick, W., Bigham, J., Forster, L., Hitzhusen, F., McCoy, E., et al. (1995). *Land application uses for dry FGD by-products: Phase 1 report*. Electric Power Research Institute. EPRI TR-105264.

Stehouwer, R., Dick, W., Bigham, J., Forster, L., Hitzhusen, F., McCoy, E., et al. (1996). *Land application uses for dry FGD by-products. Phase II report. OCDO-96010697*. Columbus, OH: The Ohio State University.

Stehouwer, R., Dick, W., Bigham, J., Forster, L., Hitzhusen, F., McCoy, E., et al. (1998). *Land application uses for dry FGD by-products: phase 2 report*. Electric Power Research Institute. EPRI TR-109652.

Stout, W. L., & Priddy, W. E. (1996). Use of flue gas desulfurization (FGD) by-product gypsum on alfalfa. *Communications in Soil Science and Plant Analysis*, *27*(9–10), 2419–2432. http://dx.doi.org/10.1080/00103629609369712.

Stout, W. L., Sharpley, A. N., & Weaver, S. R. (2003). Effect of amending high phosphorus soils with flue-gas desulfurization gypsum on plant uptake and soil fractions of phosphorus. *Nutrient Cycling in Agroecosystems*, *67*, 21–29.

Su, Q., Jiang, Y., Lu, M., Chen, Y., & Wu, M. -C. M. (2013). Development of dry FGD by-product utilization as building materials in China. In *World of coal ash (WOCA) conference, Lexington, KY, May 22–25*.

Su, Q., Robl, T. L., Jewell, R. B., Wolfe, W. E., Butalia, T. S., Zhao, Z., et al. (2015). Development of key technologies for dry FGD by-product resource comprehensive utilization: a project history. In *2015 World of coal ash (WOCA) conference, Nashville, TN, May 5–7*.

Sumner, M. E. (1993). Gypsum and acid soils: the world scene. *Advances in Agronomy*, *51*, 1–32.

Torbert, H. A., & Watts, D. B. (2014). Impact of flue gas desulfurization gypsum application on water quality in a coastal plain soil. *Journal of Environmental Quality*, *43*, 273–280.

Truman, C. C., Nuti, R. C., Truman, L. R., & Dean, J. D. (2010). Feasibility of using FGD gypsum to conserve water and reduce erosion from an agricultural soil in Georgia. *Catena*, *81*(3), 234–239. http://dx.doi.org/10.2134/jeq2012.0422.

United States Department Of Energy Project Facts. (1999). *Production of construction aggregate from flue gas desulfurization sludge*. Washington, DC: United States Department of Energy.

US EPA. (2008). Agricultural uses for flue gas desulfurization (FGD) gypsum, EPA530-F-08-009.

Vories, K. C., & Harrington, A. (Eds.), (2006). *Proceedings of flue gas desulfurization by-products at coal mines & responses to the National Academy of Sciences Final Report "managing coal combustion residues in mines": a technical interactive forum*. Carbondale, IL: USDOI Office of Surface Mining and Coal Research Center, Southern Illinois University.

Warden, R. W., et al. (2014). *Beneficial use of FGD materials in reclamation of abandoned and active coal mines field trial*. Columbus, OH: Department of Civil, Environmental, and Geodetic Engineering, The Ohio State University.

Watts, D. B., & Dick, W. A. (2014). Sustainable uses of FGD gypsum in agricultural systems: introduction. *Journal of Environmental Quality*, *43*, 246–252.

Watts, D. B., & Torbert, H. A. (2015). Influence of flue gas desulfurization gypsum on reducing soluble phosphorus in successive runoff events from a coastal plain bermudagrass pasture. *Journal of Environmental Quality*. http://dx.doi.org/10.2134/jeq2015.04.0203.

Weeter, D. W. (1981). Utilization of dry calcium based flue gas desulfurization waste was a hazardous waste fixation agent. *Journal of the Air Pollution Control Association*, *31*, 751–753.

Wolfe, W. E., & Beeghly, J. H. (1993). Truck ramp construction from clean coal technology waste products. In *Symposium on recovery and effective reuse of discarded materials and by-products for construction of highway facilities, Denver, CO*.

Wolfe, W. E., Butalia, T. S., & Meek, B. L. (1997). Influence of freeze thaw cycling on resilient modulus of clean coal technology by-products. In *1997 Ash utilization symposium, Lexington, KY, October 20–22* (p. 1997).

Wolfe, W. E., & Cline, J. H. (1995). A field demonstration of the use of wet and dry scrubber sludges in engineered structures. In *Vol. 1. Proceedings of 11th international symposium on use and management of coal combustion by-products (CCBs), Orlando, FL, January 15–19*: American Coal Ash Association and Electric Power Research Institute. pp. 17(1-10), EPRI TR-104657.

Wu, M. (2005). *Durability evaluation and promotion of manufactured aggregates from coal combustion by-products*. Final Report for DE-FC26-00NT40910 Universal Aggregates, LLC.

Wu, M., & Yuran, P. (2007). *Commercial demonstration of the manufactured aggregate processing technology utilizing spray dryer ash*. Final Report for DE-FC26-02NT41421 Universal Aggregates, LLC.

Xin, M., Gustin, M. S., & Ladwig, K. (2006). Laboratory study of air–water–coal combustion product (fly ash and FGD solid) mercury exchange. *Fuel*, *85*(16), 2260–2267.

Yang, P., Li, X., Tong, Z. -J., He, B. -Y., Wang, L. L., Guo, S. -H., et al. (2016). Use of flue gas desulfurization gypsum for leaching Cd and Pb in reclaimed tidal flat soil. *Environmental Science and Pollution Research International*, *23*(8), 7840–7848. http://dx.doi.org/10.1007/s11356-016-6058-x.

Zhang, Q., et al. (2015). *Geochemical characterization of CCB and numerical simulations of their long-term effects as capping materials at coal mine reclamation sites*. Nashville, TN: World of Coal Ash.

Zhao, F. -Q., Liu, H. -J., Hao, L. -X., & Li, Q. (2012). Water resistant block from desulfurization gypsum. *Construction and Building Materials*, *27*, 531–533. http://dx.doi.org/10.1016/j.conbuildmat.2011.07.011.

Zhong, S., Ni, K., & Li, J. (2012). Properties of mortars made by uncalcined FGD gypsum-fly ash-ground granulated blast furnace slag composite binder. *Waste Management*, *32*, 1468–1472. http://dx.doi.org/10.1016/j.wasman.2012.02.014.

# Fly ash-based geopolymer chemistry and behavior

# 7

*R.V.R. San Nicolas**, *B. Walkley*†, *J.S.J. van Deventer**
*The University of Melbourne, Melbourne, VIC, Australia, †The University of Sheffield, Sheffield, United Kingdom

## 7.1 Introduction

With demand driven by environmental protection and waste utilization, several innovative and advanced uses for coal fly ash have been developed and adapted depending on the ash characteristics and the chosen application. The alkali activation of fly ash has been studied extensively in recent decades; however, progression towards large-scale manufacture of alkali-activated fly ash (AAFA) geopolymer materials remains slow due to many regulatory obstacles (described later in the chapter) (Duxson, Fernández-Jiménez, et al., 2007; Provis & van Deventer, 2014a). This issue is complicated further by the fact that the composition and physiochemical characteristics of fly ashes vary dramatically both between sources and as a function of time, even when sourced from the same power station (Duxson, Fernández-Jiménez, et al., 2007; Duxson, Provis, Lukey, & van Deventer, 2007). These variations create significant differences in performance, and the parameters controlling this are difficult to extract (Criado, Fernández-Jiménez, Palomo, Sobrados, & Sanz, 2008; Duxson, Mallicoat, Lukey, Kriven, & van Deventer, 2007; Pacheco-Torgal, Castro-Gomes, & Jalali, 2008). Nevertheless, ashes showing value in alkali-activation processes are not solely the result of traditional combustion of black coal; ash sources including some low-Ca brown coal fly ashes (Škvára, Kopecký, Šmilauer, & Bittnar, 2009) and fluidized bed coal combustion ash (Topçu & Toprak, 2011; Xu, Li, Shen, Zhang, & Zhai, 2010) as well as the silica-rich ash resulting from the combustion of rice husk and bark (Songpiriyakij, Kubprasit, Jaturapitakkul, & Chindaprasirt, 2010) have all shown potential value in this area.

A strong relationship between mix design parameters and the performance of fly ash cements is not as readily predictable as is the case for Portland cement (PC)-based systems. Additionally, there still needs to be extensive laboratory testing prior to the use of any particular AAFA mix design, meaning that ongoing quality control throughout a production run is essential. Nevertheless, this chapter intends to provide an overview of current trends, an explanation of the current knowledge of this system, and recommendations for future improvement and methods of development of these products.

**Coal Combustion Products (CCP's).** **http://dx.doi.org/10.1016/B978-0-08-100945-1.00007-1**

## 7.2 Fly ashes used as precursors for alkali activation

### *7.2.1 Composition of fly ash*

Fly ash composition varies depending on the type of coal used and the incineration process in place at the power plant. The crystalline phases in fly ash particles, usually mullite, quartz, and magnetite, remain relatively inert throughout the early stages of alkaline dissolution and geopolymerization; only the glassy phases are dissolved and participate in the reaction process during this time. Consequently, the use of molar ratios based on bulk chemical composition provides very limited information. The direct use of glassy phase composition, rather than the overall bulk ash composition, to formulate AAFA binders is considered to give more appropriate descriptions of the gel chemistry, and this principle has now been adopted (Fernández-Jiménez & Palomo, 2005; Swanepoel & Strydom, 2002).

Silica is both the main component of every fly ash and the main component of the structural network in AAFA. The amount of glassy/reactive silica is closely linked to the reactivity of the ash and some authors (Fernández-Jiménez, Palomo, Sobrados, & Sanz, 2006; Fernández-Jiménez, Puertas, Sobrados, & Sanz, 2003) have proposed a minimum of 40% of glassy silica is necessary to qualify the fly ash as reactive. It is important, however, to consider all the reactive species in the glassy component of the ash to qualify its reactivity, not just the sufficient amount of glassy/reactive silicon.

The amount of Al available in the glassy phase is also crucial in the proper formulation of AAFA, as it is the main constituent responsible for the cross-linked chemically stable nature of the aluminosilicate gel. Fly ash with large amounts of reactive Al ($Si/Al < 1.5$) can generate large amounts of reaction products (Valcke, Sarabèr, Pipilikaki, Fischer, & Nugteren, 2013), but according to Němeček et al. (2011), it does not lead to improvement in mechanical properties. Other factors, including activator and solid precursor chemistry, dissolution kinetics and the porosity of hardened gels must be considered.

The role of Ca in AAFA has been investigated (Lloyd, Provis, Smeaton, & van Deventer, 2009; Oh, Monteiro, Jun, Choi, & Clark, 2010), and while there has been extensive discussion around this, results are often contradictory. Some researchers report high Ca AAFA samples present higher strength development, while others report the opposite. Consequently, it is not possible to predict the AAFA binder strength based on Ca content of the fly ash precursor.

The alkali metals (mainly Na and K in fly ash, denoted M) and alkali earth metals (mainly Ca and Mg, denoted Me) present in fly ashes can act as network modifiers in AAFA, which, if present at high enough concentrations, form non-bridging oxygen sites (Stebbins & Xu, 1997) and reduce the degree of polymerization of the aluminosilicate glass. Glasses with charge-balanced compositions ($(M_2O + MeO)/Al_2O_3 > 1$) show a higher reactivity of the glassy phase in AAFA systems (Diaz, Allouche, & Eklund, 2010), similar to PC systems (Durdziński, Dunant, Haha, & Scrivener, 2015).

While Fe and Ti are usually present in the glassy phase of fly ashes, their presence in the resulting binding phase seems to be low (Rickard, Williams, Temuujin, & van

Riessen, 2011; Ward & French, 2006). A high concentration of Fe in the glassy phase of fly ashes can result in a high amount of fivefold coordinated $Fe^{2+}$ and $Fe^{3+}$, which decreases the polymerization degree of the glass and thus increases the reactivity of fly ash. On the other hand, $Ti^{4+}$ is expected to act as a four-coordinated network former acting as charge compensators for Al and Fe tetrahedra (Henderson & Fleet, 1997; Zhang, Provis, Zou, Reid, & Wang, 2016), which may increase glassy phase polymerization and decrease fly ash reactivity.

## 7.2.2 Morphology of fly ash

The morphology of fly ash is characterized by hollow spheres, consisting essentially of a vitreous phase and a few minority crystalline phases, such as quartz (5%–13%), mullite (8%–14%) and magnetite (3%–10%) (Fernández-Jiménez et al., 2003). A key morphological characteristic of fly ash is its fineness, with a lower particle size giving better mechanical and durability performance for some AAFA (Ivan Diaz-Loya, Allouche, & Vaidya, 2011; Kumar, Kumar, & Mehrotra, 2007; Lee & van Deventer, 2002; Rickard et al., 2011). Class F and Class C fly ashes comply with ASTM C618 (30% retained at 45 μm). In the AAFA mixing process the activating solution wets the fly ash particles, forming a layer of liquid on the surface. The volume of this surface layer is directly proportional to the surface specific area, if it is assumed that the thickness is uniform for all particles. The surface specific area is thus an important property governing the activating liquid requirement of fly ash, and it is also an important physical property affecting the dissolution of fly ash in geopolymerization, thus influencing the compressive strength of the derived geopolymers (Kumar & Kumar, 2011). This phenomenon is observed in both AAFA and fly ash/PC blends. AAFA produced from fly ashes exhibiting high specific surface areas do not necessarily exhibit high compressive strengths, however, and several other parameters need to be considered. These include the interparticle distance and the interparticle volume, two parameters that also play a key role in strength development of AAFA (Fig. 7.1). The interparticle volume is used in the recently developed calculation of the activity index for fly ash (Zhang et al., 2016).

The surface chemistry of fly ash is known to be essential in determining reactivity in the early stages of the alkali activation process (Lee & van Deventer, 2002), and although the influence of mechanochemical processing on chemistry (as opposed to particle size and shape modification) has been discussed, its influence in fly ash chemistry is still not well understood and requires further analysis.

## 7.2.3 Activators

In AAFA systems, both the nature and dosage of the activator used have profound effects on the reaction kinetics, composition, and strength of the final AAFA product (Komljenović, Baščarević, & Bradić, 2010; Phair & van Deventer, 2002a, 2002b; Provis, Lukey, & van Deventer, 2005; Rowles & O'Connor, 2003; van Jaarsveld & van Deventer, 1999; van Riessen, Jamieson, Kealley, Hart, & Williams, 2013;

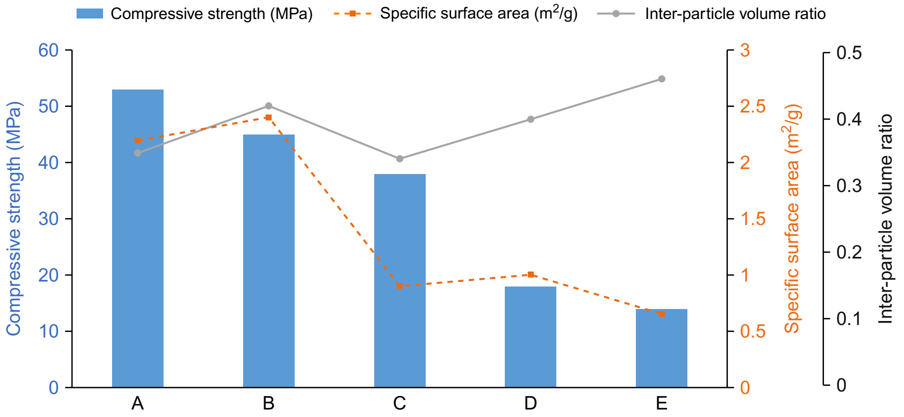

**Fig. 7.1** Relationship between fly ash specific surface area, interparticle volume ratio and compressive strength of AAFA pastes after 28 days of curing.
Based on Zhang, Z., Provis, J. L., Zou, J., Reid, A., & Wang, H. (2016). Toward an indexing approach to evaluate fly ashes for geopolymer manufacture. *Cement and Concrete Research, 85*, 163–173.

Wastiels, Wu, Faignet, & Patfoort, 1994). Several activators can be used, with alkali silicates and alkali hydroxides being the most common. These activators lead to AAFA with higher strength (up to 80 MPa at 28 days), lower porosity (Criado, Fernández-Jiménez, de la Torre, Aranda, & Palomo, 2007; Duxson, Provis, Lukey, Mallicoat, et al., 2005; Lloyd, Provis, Smeaton, et al., 2009), and a modulus (molar ratio $SiO_2/M_2O$) between 1 and 2, where the optimum modulus value depends on the nature of the fly ash precursor. Increasing the concentration of the activator generally leads to an increase in compressive strength. Optimum strength also seems to be observed at a binder Na/Al ratio (i.e., not including Al in an unreacted precursor) of around 1, although this also depends to some extent on the binder Si/Al ratio (Komljenović et al., 2010; Provis, Lukey, & van Deventer, 2005; Rowles & O'Connor, 2003). The strength of AAFA can be enhanced by increasing the initial Si/Al ratio (Wastiels et al., 1994), which increases the number of strong Si—O—Si bonds in the final product. The amount of $Al_2O_3$ in the reagent system is also known to play an important role in reaction kinetics due to thermodynamically favorable dissolution of Al species (Wastiels et al., 1994).

The use of a highly concentrated activating solution can also bring advantages in terms of reducing the water/binder ratio necessary to supply a given alkali content to the binder, while dilution of the activator reduces its alkalinity and thus its effectiveness (Phair & van Deventer, 2002a). The influence of the nature of the alkali cation is similar for both silicate- and hydroxide-based activators. It has been noted that there are different blends of Na and K that give optimal performance when combined with different fly ashes (van Jaarsveld & van Deventer, 1999), depending on the composition, glass content and structure, and particle size of the fly ash.

Sodium aluminate solutions from the aluminum processing industry have been tested as potential activators (van Riessen et al., 2013), and produced binders with strengths exceeding 40 MPa (Phair & van Deventer, 2002b). However, Oh, Moon, Oh, Clark, and Monteiro (2012), show that the incorporation of sodium aluminate into Class C fly ash activated with 10 M NaOH solution reduced the compressive strength. Both alkali carbonate- and sulfate-based activators have also been tested, and slow strength development was observed (Criado et al., 2007; Fernández-Jiménez & Palomo, 2005). The addition of a calcium source such as CaO (Shi & Day, 1995) or cement clinker is commonly suggested to accelerate strength development in AAFA systems (Nath & Sarker, 2015).

The addition of alkali sulfate salts to AAFA binders with hydroxide (Criado, Jiménez, & Palomo, 2010) or silicate (Criado et al., 2010; Provis, Walls, & van Deventer, 2008) activators appears to negatively influence setting rates and strength development, with the sulfate not participating to any notable extent in the gel formation processes.

The nature of the main AAFA reaction products (a sodium, potassium) aluminosilicate hydrate ((N,K)–A–S–H, where $N=Na_2O$, $K=K_2O$, $A=Al_2O_3$, $S=SiO_2$, and $H=H_2O$) gel framework and zeolite precipitates) are dictated not only by the chemical characteristics of the solid precursors but also by the nature of the activator (Criado et al., 2007; Duxson, Provis, et al., 2007). Silica in sodium silicate activators is highly soluble and consequently readily taken up into the (N, K)–A–S–H gel. The degree of polymerization in such sodium silicate-activated fly ashes depends directly on the $SiO_2/Na_2O$ ratio of the binder and determines the structural evolution of the gel described in the following section.

### 7.2.4 Life-cycle analysis of AAFA

Several life-cycle analysis (LCA) studies have been performed on AAFA materials to evaluate their $CO_2$ savings compared to PC-based products. These studies show very different outcomes, from more than 80% $CO_2$ reduction for AAFA compared with PC (Duxson, Fernández-Jiménez, et al., 2007; Habert & Ouellet-Plamondon, 2016; van Deventer, Provis, & Duxson, 2012) to nil (Habert, d'Espinose de Lacaillerie, & Roussel, 2011), with other values in between (Buchwald, Dombrowski, & Weil, 2005; McLellan, Williams, Lay, van Riessen, & Corder, 2011; Provis & van Deventer, 2009; Stengel, Heinz, & Reger, 2009; Tempest, Sansui, Gergely, Ogunro, & Weggel, 2009). Differing methods of production of the alkaline activators result in very different amounts of $CO_2$ emissions, and are the primary cause of the variation in $CO_2$ savings in the LCA. For example, the production of sodium silicate based on $Na_2CO_3$ can be obtained by furnace or hydrothermal routes, with $CO_2$ emissions varying by a factor of 2–3, while other emission categories in a complete LCA could vary by a factor of 800 (Fawer, Concannon, & Rieber, 1999). The case of NaOH is similar, and varying production methods utilised in different parts of the world will alter the LCA outcomes substantially.

Many of the published mix designs for AAFA involve a high activator addition, usually in an attempt to accelerate dissolution and binding phase formation. In contrast, proprietary mix designs for AAFA used at commercial scale have involved very low levels of activator. Such activator has been sourced from industrial waste streams, with negligible $CO_2$ emissions. This has been made possible by using proprietary reagents to accelerate dissolution and phase formation reactions interactively. The resultant AAFA then results in a $CO_2$ saving of 80%–90% compared with most PC blends. These commercial mix designs using low activator addition have also resulted in substantial cost reduction compared with PC blends, which has been the key driver for their adoption, rather than just $CO_2$ reduction.

## 7.3 AAFA materials: (N,K)–A–S–H gel framework

The ability to form cementitious materials by alkali activation of silica-rich precursors such as fly ash has been known for decades; however, both academia and industry have shown increasing interest in this system recently due to the abundance and underuse of fly ash in many parts of the world, including China, Australia, and the United States.

### 7.3.1 AAFA nanostructure

The main reaction product of the alkali activation of silica-rich precursors such as fly ash is a three-dimensional alkali aluminosilicate hydrate gel network consisting of cross-linked $AlO_4^-$ and $SiO_4$ tetrahedra linked via shared oxygen atoms (denoted "bridging oxygen") with terminal hydroxyl groups forming at the gel surface (Criado et al., 2008; Davidovits, 1994; Duxson, Fernández-Jiménez, et al., 2007; Duxson, Mallicoat, et al., 2007; Fernández-Jiménez et al., 2006; Ikeda, 1997; Palomo, Alonso, Fernandez-Jiménez, Sobrados, & Sanz, 2004; Phair, Smith, & van Deventer, 2003; Provis & van Deventer, 2014b). The nanostructure of alkali aluminosilicate gels is dictated by the alkali and alkaline earth cations present within the mix formulation, most commonly sodium or potassium, and consequently primarily consists of a (sodium, potassium) aluminosilicate hydrate ((N,K)–A–S–H) gel framework with a highly cross-linked disordered pseudozeolitic structure (Provis, Lukey, & van Deventer, 2005; Provis, Palomo, & Shi, 2015).

Al and Si are present in tetrahedral coordination, with Si existing in $Q^4(m\text{Al})$ environments where $m$ is between 1 and 4, depending on the Al/Si ratio of the gel, and Al predominantly in $q^4(4\text{Si})$ environments due to the energetic penalty associated with Al—O—Al bonding (Provis, Duxson, Lukey, & van Deventer, 2005). The negative charge associated with Al substitution for Si is balanced by the alkali cations and is thought to be delocalized across all oxygen atoms, with the oxygen atom closest to the charge-balancing alkali cation carrying the majority of this delocalized negative charge (Duxson, 2006; Duxson, Mallicoat, et al., 2007). Cationic Al species have been observed to charge balance $AlO_4$ tetrahedra in zeolites (Katada et al., 2005; Yu et al., 2010) and provide thermal stability for these materials (Habert & Ouellet-Plamondon, 2016; Provis et al., 2008; van Deventer et al., 2012). Recent $^{27}$Al triple quantum magic angle spinning (MAS) nuclear magnetic resonance (NMR) studies of alkali aluminosilicate gels have revealed the presence of a charge-balancing cationic extra-framework Al species (Brus, Kobera, Urbanová, Koloušek, & Kotek, 2012; Walkley, 2016).

While (N,K)–A–S–H gels are generally described as amorphous, nanocrystalline zeolite phases have been observed within the gel framework (Provis, Lukey, & van Deventer, 2005). Studies utilizing solid state $^{29}$Si and $^{27}$Al MAS NMR spectroscopy

(Bernal et al., 2013; Duxson, Provis, Lukey, Separovic, & van Deventer, 2005; García-Lodeiro, Fernández-Jiménez, Palomo, & Macphee, 2010; Lodeiro, Fernández-Jimenez, Palomo, & Macphee, 2010) and X-ray and neutron pair distribution function analysis (Provis & van Deventer, 2007; White, Bloomer, Provis, Henson, & Page, 2011; White, Provis, Llobet, Proffen, & van Deventer, 2011; White, Provis, Proffen, & van Deventer, 2010) have determined that (N,K)–A–S–H gels possess a short-range order of at least two to three nearest neighbors; however, the extent of this ordering on a larger scale is unclear.

Alkali metal cations and alkaline earth metal cations can also be present within coal fly ash and can act as network modifiers within the geopolymer gel framework. The level of network-modifying cations present has been observed to affect the compressive strength of the geopolymer binder formed upon alkali activation, with strength generally increasing along with an increase in network modifying cation content (Duxson & Provis, 2008; Provis & van Deventer, 2009). This is likely due to faster dissolution rates during the alkali activation of precursors containing high amounts of network modifying cations (Provis & van Deventer, 2009). Other factors also influence compressive strength, including fly ash particle size distribution and the glassy phase content (Gomes et al., 1999; Kumar et al., 2007; van Jaarsveld, van Deventer, & Lukey, 2003; Zhang et al., 2016). Some of the alkali and alkaline earth metal cations may also form additional phases, particularly sulfates or carbonates, or are included in Fe-rich phases as substituents (Gomes et al., 1999).

Embedded within the disordered aluminosilicate geopolymer gel are unreacted solid aluminosilicate precursor particles, as well as a complex network of pores containing water originally supplied by the activating solution that is not an integral part of the chemical structure of the gel (Provis & van Deventer, 2009). The pore structure of AAFA is dependent on the activating solution and activation conditions on a scale where the pores are approximately $>100$ nm; below this limit the nanopore structure has been believed to be independent of the type of activator solution (Škvára et al., 2009). More recent investigations have shown that the pore size, shape, and distribution in alkali-activated metakaolin geopolymers are dependent on the alkali activator (Kutchko & Kim, 2006; Melar et al., 2015; Steins, Poulesquen, Diat, & Frizon, 2012), with potassium-based activators resulting in geopolymers with smaller pores and a greater pore network surface area than sodium-based activators (Steins et al., 2012).

Magnesium content of coal fly ashes ranges from negligible to approximately 2 wt.% (Zhang et al., 2016), and therefore does not significantly influence the reaction product formation during alkali activation.

Iron is a significant constituent of many coal fly ashes, generally accounting for up to 14 wt.% of the ash (Zhang et al., 2016). Iron oxides are present primarily as heterogeneous distributions of FeO, $Fe_2O_3$, and $Fe_3O_4$ in both fourfold and fivefold coordination states (Provis & van Deventer, 2009; Wang, Scrivener, & Pratt, 1994) in both the glassy phase of the ash as well as in crystalline hematite, magnetite, and maghemite phases; the amount of each phase is dictated by thermal processing conditions and the composition of the ash (Barbosa, MacKenzie, & Thaumaturgo, 2000; Cormier, Calas, & Cuello, 2010; Kutchko & Kim, 2006; Zhang et al., 2016). These oxides are largely insoluble and are generally considered to not participate

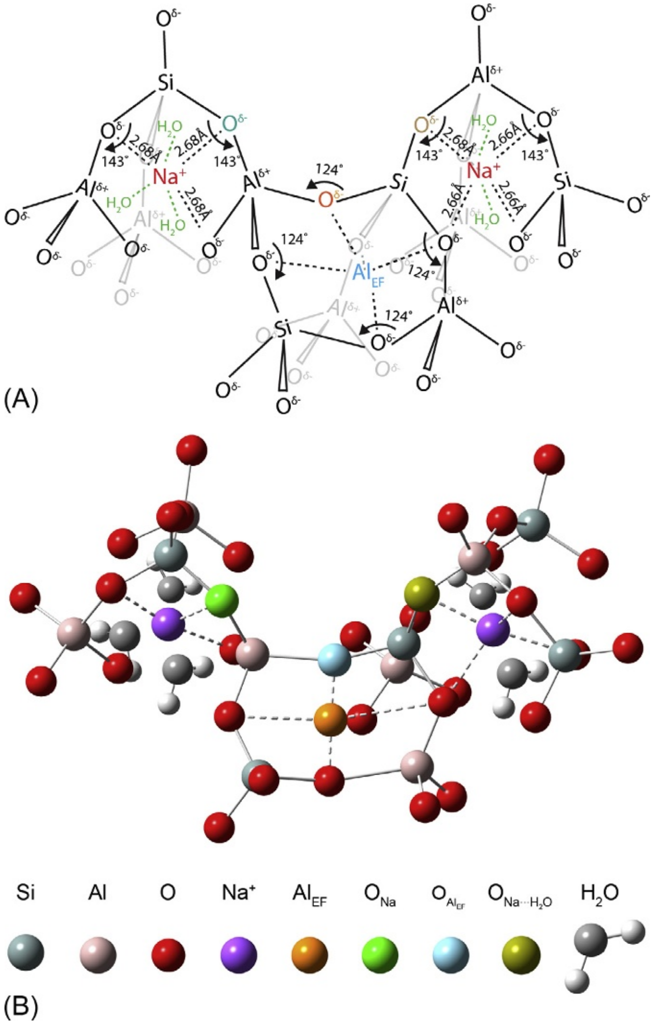

**Fig. 7.2** (A) Structural model proposed by Walkley (2016) showing a polymerized section of N–A–S–H with charge-balancing sodium (*red*), charge-balancing extra-framework Al ($Al_{EF}$) (*blue*), bridging oxygen charge balanced by $Na^+$ and three associated $H_2O$ molecules (*teal*), bridging oxygen charge balanced by $Al_{EF}$ (*orange*) and bridging oxygen charge balanced by $Na^+$ and two associated $H_2O$ molecules (*brown*) and (B) 3D representation of a polymerized section of the N–A–S–H gel showing each species as marked.

significantly in the formation of reaction products during alkali activation (Lloyd, Provis, & van Deventer, 2009a, 2009b; Provis, Rose, Bernal, & van Deventer, 2009; van Deventer, Provis, Duxson, & Lukey, 2007); however, some studies have shown their presence has a negative impact on reaction product formation due to reduced ash reactivity (Fernández-Jiménez, Palomo, Macphee, & Lachowski, 2005; Lloyd et al., 2009b).

### 7.3.2 Structural models

Despite extensive academic focus on alkali aluminosilicate gels based on coal fly ash, few structural models have been proposed. Early structural models describing the N–A–S–H gel formed in sodium silicate-activated aluminosilicate precursors are primarily limited to average cation coordination spheres and bulk gel composition (Barbosa et al., 2000; Davidovits, 1994; Rowles, Hanna, Pike, Smith, & O'Connor, 2007). A recent investigation applying $^{29}$Si MAS NMR and $^{27}$Al, $^{23}$Na, and $^{17}$O multiple quantum MAS NMR to synthetic alkali aluminosilicate gels has revealed important information about individual chemical sites, the distribution of bond angles, or interatomic distances present within this gel (Walkley, 2016; Walkley, San Nicolas, Sani, Rees, et al., 2016; Walkley, San Nicolas, Sani, Gehman, et al., 2016). The structural model developed from these data (Fig. 7.2; Walkley, 2016) reveals six distinct structural sites that assemble to form the N–A–S–H gel. Three of these sites are $Q^4$(4Al) Si units, in which the negative charge due to tetrahedrally coordinated Al is balanced by $Na^+$ ions coordinated by any of the following: three framework (bridging) oxygen atoms and three $H_2O$ molecules, $Na^+$ ions coordinated by four framework oxygen atoms and two $H_2O$ molecules, or by extraframework Al atoms ($Al_{EF}$) coordinated by six framework oxygen atoms. Increasing the Si/Al ratio reduces the amount of charge-balancing $Al_{EF}$ species within the gel, as well as increasing the number of $Si^{IV}$—O—$Si^{IV}$ linkages (due to the presence of $Q^4(m\mathrm{Al})$ Si units, $1 \leq m \leq 3$). Extra-framework Al species have been observed previously in zeolites and aluminosilicate gels (Brus et al., 2012; Katada et al., 2005; Li et al., 2007; Yu et al., 2010). N–A–S–H described by this model contains a significant distribution of $Si^{IV}$—$O^-$—$Al^{IV}$ bond angles, with an average value of 143.4 and 124.4 degrees in the $Na^+$ and $Al_{EF}$ balanced $Q^4$(4Al) Si units, which is consistent with the absence of any long range order.

The relative proportions of $Si^{IV}$—O—$Si^{IV}$ and $Si^{IV}$—$O^-$—$Al^{IV}$ bonds and of $H_2O$ molecules associated with charge-balancing $Na^+$ ions are dependent on the Si/Al of the aluminosilicate precursor (Kumar & Kumar, 2011). Higher water content within N–A–S–H is associated with an increased Al content of the gel. Water has previously been shown to be primarily physiosorbed to the surface of the N–A–S–H gel or mobile within the gel pores (Duxson, Lukey, Separovic, & van Deventer, 2005; Duxson, Lukey, & van Deventer, 2007; Provis & Bernal, 2014). The association of water molecules with charge-balancing $Na^+$ and an increase in the proportion of water molecules with increasing Al content has significant implications for alkali aluminosilicate gel durability, as the ability to retain water within N–A–S–H is a key factor in determining binder resistance to thermal stresses and microcracking.

### 7.3.3 Dissolution and reaction mechanisms

The (N,K)–A–S–H gel nanostructure is significantly affected by kinetic limitations on the silica and alumina release from the precursors (Hajimohammadi, Provis, & van Deventer, 2010, 2011), and consequently evolves over time as the alkali activation reaction proceeds.

Alkali activation of an aluminosilicate precursor can be considered to consist of three distinct stages: the dissolution of the precursor material, gel nucleation and formation, and solidification and hardening (Provis et al., 2015; Provis & van Deventer, 2009, 2014b; Swanepoel & Strydom, 2002). Alkaline hydrolysis and dissolution of the precursor aluminosilicate material are largely dependent on the activating conditions, particularly the pH of the activating solution, with higher activating solution pH leading to increased rates of dissolution (Duxson, Provis, et al., 2007; Fernández-Jiménez, Palomo, & Criado, 2005; Provis & van Deventer, 2009).

Alkali cations and hydroxyl ions are provided by the activating solution, and the hydroxyl ions attack the Si—O—Si and Si—O—Al bonds, forming $Si(OH)_4$ and $Al(OH)_4^-$ intermediate complexes, as well as oligomeric anionic species containing $Si—O^-$ bonds (Provis et al., 2015; Provis & van Deventer, 2009). The negative charge on these anionic species is balanced by the alkaline metal cations, and the formation of $Si—O^-Na^+$ and $Al—O^-Na^+$ bonds slightly hinders the formation of Si—O—Si and Si—O—Al bonds via the reverse reaction (Provis & Bernal, 2014; Provis & van Deventer, 2009).

After dissolution of the precursor aluminosilicate material, the aqueous phase quickly becomes supersaturated with aluminosilicate species (due to the high rate of dissolution of the amorphous aluminosilicate material at high pH), inducing coagulation to form new Si—O—Si and Si—O—Al bonds via the condensation of $Si(OH)_4$. After the initial dimers have formed, these dimers and other $Si(OH)_4$ species begin to react, and three-dimensional polycondensation occurs (Provis & van Deventer, 2009).

The composition of the (N,K)–A–S–H gel framework evolves over time as the reaction proceeds. Dissolution of the Al species from the aluminosilicate precursor is thermodynamically preferential over the dissolution of the Si species, and consequently during the early stages of reaction a high proportion of Al—O—Si bonds form (Provis et al., 2015). As the reaction progresses the Si species continue to dissolve from the precursor and are incorporated into the (N,K)–A–S–H gel framework via condensation between Si—OH groups, increasing the proportion of Si—O—Si bonds (Duxson, Provis, et al., 2007; Provis et al., 2015; Provis & van Deventer, 2009). It has been suggested that the transition in Si/Al ratios between the two phases occurs gradually as the Si species dissolve from the aluminosilicate precursor at later ages and leads to an increased formation of Si—O—Si bonds (Provis & van Deventer, 2014b), which has been observed to exhibit improved mechanical properties (Duxson, Fernández-Jiménez, et al., 2007; Fernández-Jiménez, Palomo, & Criado, 2005; Palomo et al., 2004). The addition of soluble silica (e.g., in the alkaline activator) affects the composition, microstructure and growth mechanism of the early-age Al-rich gel, but it does not alter the composition or microstructure of the final stable Si-rich (N,K)–A–S–H gel (Criado et al., 2008; White, Provis, Proffen, & van Deventer, 2012).

As the reaction progresses, further polymerization of these reactive species occurs, driving the precipitation of a solid phase and crystallization of a three-dimensional gel network. Water that was consumed during alkaline hydrolysis is released via the condensation reactions previously discussed and resides in the pore network of the three-dimensional aluminosilicate gel framework. The three-dimensional aluminosilicate network continues to polymerize and rearrange, evolving over time into a highly connected three-dimensional network. A hardened binder is generally formed within approximately 24 h, but an effective equilibrium in these systems can take over six months to reach. It should be noted that effective equilibrium can be considered the point at which the rate of reaction in the system is slow enough to be considered negligible, while true equilibrium would occur when a crystalline state is achieved. Reaction kinetics are affected by many parameters relating to the curing conditions and raw materials, particularly the temperature of curing and the nature of the alkaline activator (Bakharev, 2005; Criado, Palomo, & Fernández-Jiménez, 2005; Fernández-Jiménez & Palomo, 2005; Palomo et al., 2004; Provis & van Deventer, 2009).

The crystalline phases present in coal fly ash such as quartz or mullite (which form at high temperatures from the molten clay) are generally considered to be unreactive, because the rate of reaction of these materials is extremely slow when compared with the amorphous aluminosilicate phases present in coal fly ash; these crystalline phases are often observed in both the coal fly ash and geopolymer binder in similar quantities (Criado et al., 2005; Fernández-Jimenez et al., 2006; Lee & van Deventer, 2002). The difference in the rate of reaction is due to the highly strained bonds between the Si and O atoms and defects that weaken the amorphous material, making it more susceptible to attacks from water and alkaline solutions (Provis & van Deventer, 2009). $Fe_2O_3$ is also present within many fly ashes and is largely insoluble. Consequently, it is not expected to participate in the alkali activation reactions (Lloyd et al., 2009b; Provis et al., 2009).

The dissolution mechanisms of the coal fly ash during alkali activation, the subsequent effect of these mechanisms on the final structure, and therefore the mechanical properties of the hardened binder are still poorly understood (Provis & van Deventer, 2009). One major factor contributing to this lack of understanding is that most studies of these materials are performed on just one type of fly ash (Provis & van Deventer, 2009). Those few that do study a number of coal fly ash types often do not account for the presence of impurities or the effect that these impurities have on the dissolution and reaction mechanisms or the final structure and properties of the hardened binder. Structural reorganization determines the final composition of the binder, as well as pore microstructure and distribution in the material, two characteristics that are instrumental in the development of many physical properties of the resulting cement. Recent work examining the effects of varying physical and chemical characteristics of silica-rich precursors on the nanostructure of synthetic analogues of AAFA (Walkley, San Nicolas, Sani, Rees, et al., 2016; Walkley, San Nicolas, Sani, Gehman, et al., 2016), as well as the development of an indexing approach to evaluate the suitability of fly ashes for production of tailored AAFA (Zhang et al., 2016), has opened a new line of inquiry into fundamental dissolution and reaction mechanisms that ultimately govern AAFA performance.

## 7.4 Tailored mix design for targeted properties (activators, class of ash, chemistry trends)

The properties of AAFA are strongly dependent on many parameters including mix design and the type of fly ash and activators. These are parameters that need to be carefully chosen in accordance with the application.

### 7.4.1 Curing

Reaction kinetics governing the formation of AAFA depends on many parameters (Duxson, Fernández-Jiménez, et al., 2007; Wang, Pu, Scrivener, & Pratt, 1995). The curing temperature affects the degree of gel polymerization and consequently the formation of a dense molecular structure (Criado et al., 2005; Shi & Day, 1995; Swanepoel & Strydom, 2002). It also affects the transport properties and durability of the final product (Duxson, Fernández-Jiménez, et al., 2007; Provis & van Deventer, 2014b). The compressive strength and elastic modulus of AAFA depend on the heat curing regime and increase with increasing curing temperature (up to 75°C) and increasing curing duration (up to 24 h) (Provis & van Deventer, 2009, 2014b). AAFA cured at ambient temperature (i.e. 23°C) typically exhibit very low compressive strengths at early ages due to the very slow rate of strength development. Consequently, it appears that ambient curing is not a suitable nor a practical option for low-calcium AAFA concrete. For curing temperatures lower than 75°C and curing durations shorter than 18 h, samples do not reach their full densification capacity, hence they exhibit larger porosity compared to samples cured for longer at higher temperatures up to 90°C (Pacheco-Torgal, Labrincha, Leonelli, Palomo, & Chindaprasit, 2014). It has been suggested that it is possible to overcome this issue by blending the fly ash with a small amount of PC (about 5%) prior to activation in order to develop a concrete of normal strength under ambient curing conditions. This approach also allows up to a 40% reduction in the amount of activator used (Nath & Sarker, 2015).

A recent study demonstrated that it is possible to use direct electric current (rather than elevated temperatures) to provide energy to the system during curing of AAFA, providing economic advantages (Kovtun, Ziolkowski, Shekhovtsova, & Kearsley, 2016). It has been reported that the resistivity of AAFA is lower than cement-based concrete, and therefore this method of curing is more efficient than curing under traditional ambient conditions. A strong linear correlation between compressive strength and resistivity has been observed for geopolymer concrete (Kovtun et al., 2016).

### 7.4.2 Setting

Alkali-activated Class C fly ash exhibits shorter setting times, while alkali-activated Class F fly ash exhibits extended setting times. Setting times can be manipulated by blending the fly ash with other pozzolans, such as ground-granulated blast furnace slag (GGBFS), and selecting suitable activators. To adjust the setting characteristic of AAFA, the use of accelerators and retarders is also common. Lee and van Deventer (2002) examined the effect of an inorganic salt addition on the setting characteristics of $KOH/Na_2O{\cdot}SiO_2$-activated Class F fly ash pastes. The setting was accelerated by Ca and Mg salts through solid dissolution. The authors also found that K salts delayed setting only when the initial activating solution was low in soluble silicate. Furthermore, the right composition of Cl, $CO_3^{2-}$ and $NO_3^-$ salts could retard the setting. Some accelerators and retarders used for PC systems are also applicable to Class C fly ash-based geopolymer systems. Addition of gluconate efficiently delays the setting time of Class C fly ash paste with no adverse effect on strength. An addition of 1% and 2% sucrose could delay final setting time from 130 min to 210 and 230 min, respectively (Rattanasak, Pankhet, & Chindaprasirt, 2011). The addition of 1% and 2% $CaCl_2$ to the system can also accelerate setting, with a reduction of final setting times from 130 min to 60 and 45 min, respectively.

## 7.5 Structural behavior of AAFA

### 7.5.1 Engineering properties

Very few studies have focused on analysis of the structural behavior of AAFA to date. Some early studies compared the failure mode and deflection of steel-reinforced AAFA concrete and PC-based concrete beams and columns, concluding that each exhibited similar behavior (Dattatreya, Rajamane, Sabitha, Ambily, & Nataraja, 2011; Sumajouw, Hardjito, Wallah, & Rangan, 2007; Sumajouw & Rangan, 2006). On the contrary, other studies (Fernandez-Jimenez, Palomo, & Lopez-Hombrados, 2006; Nguyen, Ahn, Le, & Lee, 2016; Sofi, van Deventer, Mendis, & Lukey, 2007) demonstrated that at equivalent compressive strength, an AAFA concrete will have a lower elastic modulus than PC-based concrete using the current standards AS 3600 and ACI 363. As Duxson et al. proposed in 2005 (Duxson, Provis, Lukey, Mallicoat, et al., 2005), the elastic modulus of AAFA is related to the microstructure of the binder which is in turn dependent on binder composition, the nature of the alkali-silicate activating solution and the reaction conditions. This is different from normal concrete, for which the elastic modulus also depends on the properties of the aggregate (Hirsch, 1962; Hobbs, 1971; Silva, de Brito, & Dhir, 2016). Using nanoindentation, it was shown that N–A–S–H gels seem to have an intrinsic elastic modulus of around 17–18 GPa, much lower than that of C–A–S–H (approximately 43 GPa) (Ivan Diaz-Loya et al., 2011; Němeček et al., 2011). Wongpa, Kiattikomol, Jaturapitakkul, and Chindaprasirt (2010) also showed that the elastic modulus of fly ash-based geopolymers decreases with increasing curing time. The measured deflections of the beam and the predicted deflection using a finite element model agree with values obtain by Nguyen et al. (2016).

Poisson’s ratio of AAFA concrete with compressive strength in the range of 45–58 MPa is from 0.16 to 0.21. These values are similar to the values of PC concrete. The stress-strain relations of AAFA concrete in compression match those of PC concrete (Nguyen et al., 2016). Diaz et al. (2010) measured a wider range of Poisson’s ratio between 0.07 and 0.23 for AAFA concretes, which were observed to increase at higher compressive strengths.

Similar trends also appear to hold for relationships describing splitting tensile strengths of AAFA concretes (Temuujin, Williams, & van Riessen, 2009) when compared to those commonly used for PC concretes. However, it is necessary to develop a theoretical and mechanistic understanding of the likely deviations from the “expected” (i.e., PC-like) behavior in an engineering context and also potentially in terms of parameters which could better reflect the mechanical behavior of the AAFA.

### 7.5.2 Shrinkage

Shrinkage of AAFA is an important engineering property, influencing the cracking probability of the AAFA under restrained conditions. Investigations focusing on AAFA shrinkage, particularly autogenous shrinkage, are limited. Nevertheless, drying shrinkage of heat-cured AAFA seems to be lower than PC, while the drying shrinkage of AAFA samples cured under ambient conditions seems larger (Pacheco-Torgal et al., 2014; Wallah & Rangan, 2006). Contrary to PC-based materials, AAFA under restrained conditions did not cause cracking of the samples at early ages, due to a lower total shrinkage. The mechanism of AAFA shrinkage is still not fully understood and several parameters play a large role, including curing temperature and humidity. For PC-based materials, autogenous shrinkage is dependent on the chemical reactions occurring, microstructure development, and internal relative humidity of the material. Mechanisms governing autogenous shrinkage in AAFA and PC systems differ significantly due to differing reaction mechanisms and microstructure between the two systems. (Pacheco-Torgal et al., 2014) It has been shown that increasing the sodium and silica content of AAFA increases autogenous shrinkage (Hardjito & Wallah, 2002; Hardjito, Wallah, Sumajouw, & Rangan, 2004a, 2004b). The continuous reorganization and polymerization of the gel structure induces autogenous shrinkage of AAFA paste, which contrasts with the self-desiccation process occurring in PC paste. A finer pore size distribution in AAFA specimens causes larger autogenous shrinkage. Drying shrinkage of different AAFA mixtures is not proportional to weight loss (as occurs in PC-based systems) due to differences in capillary pressure in the AAFA pore structure (Bazant & Chern, 1984). Therefore the pore structure is an important factor in determining the drying shrinkage of AAFA mixtures. During the production of AAFA concrete, most of the water released during the chemical reaction may evaporate during the high-temperature curing process. Because the remaining water contained in the micropores of the hardened concrete is small, the induced drying shrinkage is also very low (Sumajouw, Hardjito, Wallah, & Rangan, 2005; Wallah & Rangan, 2006).

### 7.5.3 Creep

The phenomena affecting the magnitude of the creep behavior of AAFA concrete and its rate of development can be classified as either intrinsic or extrinsic factors (Bazant & Chern, 1984). Similar to shrinkage, the creep strain of AAFA concrete is dependent on the time and condition of loading. A higher compressive strength results in lowering of the creep strain in AAFA concrete, similar to PC concrete (Gilbert, 1988). Consequently, a minimum of 3 days curing at 40°C or 1 day curing at 80°C is required to obtain final drying shrinkage strains similar to or less than those adopted by Eurocode 2 for PC concrete (Wallah, 2010). Recent research relates the creep response of PC to the packing density distribution of calcium-silicate-hydrate. However, it has been suggested by Davidovits (2005) that the smaller creep strains of

AAFA concrete may be due to a "block-polymerization" concept. According to this concept the Si and Al atoms in the fly ash are not entirely dissolved by the alkaline liquid. "Polymerization" that takes place is only on the surface of the particles and is sufficient to form the "blocks" necessary to produce the geopolymer binder. Therefore the bulk of the inner part of the fly ash particles remain undissolved, such that they act as "microaggregates" in the system. Further research needs to be done to confirm this theory. An increase in the proportion of capillary pores within the AAFA pore network has also been observed to increase AAFA creep (as well as shrinkage). Despite these advances, the underlying mechanisms governing creep in AAFA concrete are yet to be fully understood.

### *7.5.4 Durability*

The service life of a construction material is linked to its transport properties and chemical composition. Transport properties of AAFA can be very different depending on the properties of the fly ash used (nature, size, and chemistry) and also the formulation and curing conditions used to generate the AAFA system. The ability to design tailored AAFA materials for unique aggressive environments by manipulating these parameters is a significant advantage of AAFA systems.

#### *7.5.4.1 Pore size and porosity*

The pore structure of a material is important in determining the transport properties and thus the durability characteristics. Sorptivity provides an indication of the pore structure and connectivity (capillary network), which is a major factor influencing the penetration of aggressive ions into the concrete when exposed to severe environments (e.g. marine environment). Lower sorptivity delivers a higher resistance of concrete towards water absorption. A high sorptivity coefficient indicates the existence of a highly connected porous structure or low tortuosity of the pore network. Important factors that impact the pore structure of AAFA binders include fly ash properties, activator type and dosage, and curing conditions. The pore structure in AAFA binders varies substantially when different fly ashes are used. The pores in AAFA binder are mostly in a range of 10–50 nm, which is significantly smaller than that for PC (20–200 nm), even though the total porosity is similar. The amount of water in the activator is one of the most important factors that affect the porosity of AAFA binders. However, the particle size and packing density of fly ash are also important. It is well known that in AAFA systems, only a fraction of fly ash particles (usually between 5% and 30%, Chindaprasirt, Rattanasak, & Jaturapitakkul, 2011; Rattanasak et al., 2011) and at most 60% (Fernández-Jiménez et al., 2006) can be dissolved by the alkali activator and react to form alkali aluminosilicate gels. These gels fill the space between residual particles to reduce the porosity in the final binder. A high packing density is critical in achieving a compact and strong binder. The activator type also affects the pore size and porosity of AAFA binders to a large degree. AAFA activated by NaOH solution exhibited higher porosity than AAFA activated by a KOH/$K_2SiO_3$ solution with a modulus ($SiO_2/K_2O$ ratio) of 0.63 (Palomo, Grutzeck, & Blanco, 1999). The AAFA binder activated by $Ca(OH)_2$ produced typical C–A–S flocculation microstructure, and the pores are larger than in NaOH activated binders. The pore sizes are reduced from several micrometers in $Ca(OH)_{2^-}$, NaOH-, and $2Na_2O{\cdot}SiO_2$-activated binders to $<1$ nm in $Na_2O{\cdot}1.5SiO_2$-activated binders (Chi & Huang, 2013; Criado, Jiménez, Sobrados, Palomo, & Sanz, 2012; Fernández-Jiménez & Palomo, 2005; Komljenović et al., 2010). Liquid transportation in concrete also occurs via capillary water absorption. Capillary water absorption of AAFA binders is much higher than for PC binders across various liquid/solid ratios. The porosity of AAFA binders is consistent with the water absorption ratio; however, the porosity of the PC binders is much lower than the water absorption ratio. This is due to the complex pore network and increased tortuosity in PC, which makes it difficult for fluid to intrude. Capillary absorption has a close relationship with porosity and is influenced less by pore size distribution. The high porosity and high capillary absorption of the AAFA binder are expected to lead to a low resistance to chloride diffusion. Regardless of external conditions, such as chloride concentration and liquid pressure, the permeability and water absorption properties of AAFA binders strongly depend on their formulation. The liquid requirement is a critical factor in determining the final porosity. When a coarse fly ash (such as Class F Grade II or III fly ash according to GB/T 1596–2005) is used as the single solid material, the high liquid requirement usually leads to a high porosity. Moreover, as the pore size in AAFA binders ranges between 20 and 100 nm, the capillary absorption force is very high. These properties may lead to the fast penetration of chloride and other harmful ions in AAFA concrete (Wongpa et al., 2010). Therefore the utilization of fly ash in alkali-activated binder manufacturing needs to consider the pore size and porosity of the final products, in addition to the possibility of high capillary absorption, permeability, and ion diffusion rate (Adam, 2009).

### 7.5.4.2 Freeze/thaw resistance

Several accelerated tests have been used to evaluate the freeze-thaw resistance of the AAFA; however, accelerated tests do not always model what occurs in real systems (e.g. as is the case for carbonation), and research in this area is ongoing. Further work developing mathematical models for freeze-thaw behavior of the AAFA should complement existing models developed for PC-based materials. Such models would contribute to the understanding and prediction of AAFA durability.

### 7.5.4.3 Passivation and corrosion of carbon steel reinforcement

Corrosion of steel reinforcement embedded within AAFA cements is one of the major durability issues facing this material. Few investigations have directly investigated the corrosion of steel reinforcement in AAFA systems; however, many studies focused on carbonation and chloride migration, which are two phenomena that lead to corrosion.

A recent direct corrosion measurement study on low-calcium AAFA concrete showed that these systems behave comparably to PC concrete systems, exhibiting comparable passivation and similar electrochemical performance when used in chloride-contaminated environments (Babaee & Castel, 2016). Another study showed that AAFA corrosion durability was inferior to PC-based materials (Monticelli et al., 2016), despite the fact that the measured chloride content in the AAFA systems was much lower than in the PC-based materials, which usually indicates a better resistance to corrosion. The limited total chloride concentrations are due to the formation of highly soluble alkali metal salts, so that the external chlorides can easily penetrate but can also be easily leached out during the exposure to chloride cycles. However, under these conditions, a relatively high fraction of free aggressive chlorides is likely present and available to stimulate the rebar corrosion attack.

### *7.5.4.4 Carbonation*

AAFA corrosion can also be caused by carbonation, and many studies investigate carbonation behavior in these materials. AAFA-based binders carbonate mainly through the precipitation of alkali bicarbonate salts (nahcolite) (Bernal et al., 2013; Criado et al., 2005) from the pore solution with almost no change to the binder gel. Some fly ash-based binders also show indications of a diffuse carbonation reaction zone, particularly in samples with an immature gel when exposed to a high $CO_2$ concentration. Under accelerated carbonation exposure, both N-A-S-H and calcium aluminosilicate hydrate (C-A-S-H) gels in alkali-activated fly ash/slag blends are affected, leaving a cross-linked remnant silicate phase derived from the decalcification of the C–A–S–H gel and coexisting with the largely unaltered N–A–S–H gel resulting from activation of fly ash, as well as various alkali and alkali-earth carbonate precipitates. The need to develop a standard methodology to assess the carbonation performance of alkali-activated materials is evident. The availability of such a method is essential to developing better understanding of the factors governing degradation mechanisms in these materials. The relatively low natural carbonation rates identified in alkali-activated concretes suggest that these materials have good resistance to carbonation during their service life, and accelerated carbonation tests are not replicating what is likely to take place in the long term. This suggests that further research in developing methods for measuring the progress of the carbonation front in alkali-activated materials needs to be conducted. Efforts in this area are being led and coordinated through the RILEM Technical Committee TC 247-DTA (durability testing of alkali-activated materials).

### *7.5.4.5 Alkali aggregate reaction*

Another major parameter dictating durability is the alkali aggregate reaction (AAR) between the aggregate and the binder used for concrete. A number of studies (Davidovits, 2005; Davidovits, Davidovits, & Davidovits, 1994; Fernández-Jiménez, Garcia-Lodeiro, & Palomo, 2007; García-Lodeiro, Palomo, & Fernández-Jiménez, 2007) show that AAFA involves less abnormal swelling due to AAR, even with very reactive aggregates. A series of studies comparing AAR behaviors of PC and AAFA are present in the literature; however, resistance of AAFA systems to AAR swelling is inconclusive (Davidovits, 2005; Davidovits et al., 1994; Fernández-Jiménez et al., 2007; García-Lodeiro et al., 2007). Some AAFA mortars show unusual behavior. In AAFA the formation of the gel structure typical of AAR was observed, but crystalline phases of zeolites such as hydroxysodalite, herschelite, and zeolite P were found using scanning electron microscopy (SEM)/energy dispersive X-ray spectroscopy (EDX) and X-ray diffraction (XRD) (García-Lodeiro et al., 2007). The increased zeolite concentration due to the AAR would not be harmful because zeolites normally form as a precipitate in the preexisting pores in the matrix, so their growth would not cause stress that could lead to the formation of cracks. However, it must be kept in mind that more common natural conditions of curing at ambient temperature (compared with 85°C in 1 M NaOH solution) still need to be tested to confirm the behavior of AAFA systems. Cracking patterns resembled those of AAR-affected PC concrete, but no gel was observed using SEM. This could be because of insufficient calcium in the system. It is possible that a low-viscosity gel formed and dispersed through the pore structure and did not cause internal stresses sufficient to drive substantial expansion.

## 7.6 Fly ash for lightweight materials

The potential of AAFA binders to provide enhanced fire resistance is significant compared to PC-based lightweight concrete. The aluminosilicate AAFA binding phases are important in providing high-temperature stability. Several techniques can be used to generate lightweight AAFA; for example, via the addition of an aluminum powder blowing agent (Wang, Wu, & Zhang, 2013), which releases $H_2$ gas upon reaction with water. The performance of AAFA foam generated by this procedure has been compared to traditionally autoclaved PC-based material (using a mix of cement, quartz sand and aluminum powder at a rate of 0.05%–0.08% by volume, autoclaved for around 12 h at 190°C at pressures between 8 and 112 bar). The AAFA foam exhibited a closed-pore network, exceptional fire resistance, and demonstrated that high chemical durability that can be achieved at curing temperatures below 80°C without the need for autoclaving (Wang et al., 2013). Experiments and micromechanical simulations show that the bulk densities lie in the range of 400–800 kg/$m^3$. However, standardization of feedstocks and control of efflorescence are two key challenges facing the development of commercially mature AAFA foam concrete technology; detailed exploration of the chemistry of raw materials and the microstructural development of AAFA materials is required. AAFA foam concrete is usually used for non-structural purposes and consequently some durability phenomena are not of concern. The introduction of this new construction material into the market will also open new avenues for AAFA use in niche applications. AAFA products contain much higher soluble alkali content than conventional PC products, and different pore structures (from the nanoscale upwards) when compared with hydrated PC, and efflorescence could be a significant issue when the products are exposed to humid air or in contact with water. Shrinkage of AAFA binders has not been reviewed for foam applications and may be another challenge for AAFA foam concrete production.

Higher-strength (more than 20 MPa at 28 days) lightweight AAFA-based materials have also been studied. Unlike mixing with PC concrete, AAFA-based materials did not exhibit poor distribution, floating, and segregation. This is due to the viscous and cohesive properties of the fresh AAFA (Abdullah et al., 2012).

## 7.7 Commercial adoption of geopolymer concrete

The correct commercial drivers must be in place to enable the adoption of a new construction material. Usually, a substantial reduction in $CO_2$ emissions can be a driver for demonstration projects, or for inclusion as an innovation component as part of a larger project, but in general it is not a sufficient driver for widespread adoption. The strongest driver is usually cost reduction, but improved technical performances, such as enhanced resistance to aggressive media and fire or utilization of waste precursors to create a new value chain, may also be drivers. In Europe, there is overall a shortage of newly produced fly ash, but there remains an abundance of landfilled fly ash that can be utilized and will require innovative use of activation technology. In countries like India, Australia, and South Africa, there remains sufficient fly ash as a source material, but often regulatory restrictions, transport cost, or control over the supply chain constrain the utilization of fly ash in blended concrete.

Despite the aforementioned drivers and the favorable $CO_2$ emissions of correctly designed geopolymer concrete, it is essential to gradually build industry confidence in geopolymers from a technical and commercial perspective. There are only a few examples of geopolymers in long-term structural applications that can demonstrate the long service life of this emerging construction material (Provis & van Deventer, 2014b), but confidence has been strengthened by recent large-scale structural applications in Australia and especially South Africa, where Murray & Roberts Construction has built structures containing 90% fly ash using activation technology. The implementation of new advances in geopolymer technology is often dependent on scale and hence availability in the supply chain, so close collaboration is required between technology providers, materials suppliers, concrete manufacturers, contractors, asset owners, consulting engineers, and regulatory authorities to build market confidence, achieve wider adoption, and guide further research.

In the United Kingdom, Publicly Available Specification (PAS 8820) for alkali-activated cementitious material and concrete, published in May 2016, will hopefully facilitate the commercial adoption of AAFA. Regulatory progress has also been made in Australia by the roads authority, VicRoads, that has recognized geopolymer concrete as being equivalent to PC-based concrete for a range of applications. In South Africa, major advances have been made in the approval of large structures using activation technology and high fly ash content by adopting a performance-based approach (Alexander & Thomas, 2015; Beushausen et al., 2016). Nevertheless, geopolymer cement is not recognized as a binder in its own right in the Australian standards for structural concrete or in most other international standards frameworks. Beside the challenge associated with relating accelerated durability testing data to in-service life predictions, there is also the question as to whether existing structural engineering design methods calibrated for Portland-based concrete are applicable to geopolymer concretes. These questions often arise from a lack of insight by the general concrete community into the microstructure of geopolymer-type materials. Although research results have given some comfort and have supported commercial adoption, it is rather the success of in-service construction applications that has given the confidence to early adopters to continue with the technology. It is essential that research continues, not just on phase assemblage and durability, but that the industry should collaborate more with researchers in developing appropriate structural design methods and working toward the prediction of service life.

Although it is a tedious task, it is necessary to build confidence in geopolymer concrete from scratch in each new market, as consumers wish to see success under local conditions. Moreover, fly ash has a complex phase chemistry that is source specific, which means that new mix designs must be developed to suit each fly ash. Small "low risk" projects, where the cost of replacement is low if performance is not met, must first be completed to build confidence before more complex projects are tackled. This has been achieved in Australia and South Africa, and it is now being contemplated in India. The key challenge is often the availability of suitable precursors at the right price for demonstration projects in a new location, which is a more challenging situation technically and commercially than when there is a suitable supply chain at scale. This is the equivalent of building a car from components compared with delivery from an assembly line.

Contemporary concrete technology does not allow for an ultra-high replacement of PC by supplementary cementitious materials (SCM), including fly ash, owing to their low reactivity, hence there is slow strength development. The early strength of the concrete results mainly from binding phases formed from the PC, with the SCM dissolving more gradually when sufficient portlandite has been formed by the PC. Increased levels of SCM also cause a higher water demand, which means that excessive levels of superplasticizer are required to reduce water demand, as in normal concrete technology a higher water addition results in higher permeability and hence decreased durability. Consequently, the high admixture requirement of high slag or ash concrete leads to high-cost mix designs. Geopolymer technology usually accelerates the dissolution of SCM by the addition of strong alkalis to accelerate dissolution. This approach increases the cost of the mix design and may lead to the formation of undesirable phases resulting in poor durability.

An alternative approach that has been used successfully at commercial scale (Engineering News, 2016) is to tailor a series of proprietary activators and catalysts to suit the reaction profile of SCM in order to accelerate dissolution reactions and at the same time catalyze the formation of binding phases. This methodology ensures that desirable phases are formed at the right time along the reaction pathway, while the formation of deleterious phases is avoided. This exploits the reaction of binding gel with aggregate particles, which reduces the amount of cementitious material required. Moreover, it has been demonstrated that if the mix design enables the formation of stable crystalline phases, a higher than usual water/cement ratio can give a matrix with very low permeability and exceptional durability, contrasting conventional wisdom.

## 7.8 The case for performance-based standards

It is evident that the mainly prescriptive cement and concrete standards in most jurisdictions are a key hurdle to the adoption of an innovative binder design, as previously mentioned. The general perception is that these standards allow innovation, but in practice, they prescribe PC to be the key binder that is only aided by SCM. Only a few standards do not prescribe the minimum level of PC content of the cementitious materials, but most standards, such as the European framework standard EN 206-1 (Müller, 2012), prescribe a minimum PC content for different applications or exposure classes. This prescription is highly inhibitive to innovation and presents a formidable challenge to the commercial adoption of new cementitious binders, including geopolymers.

The underlying assumptions in most existing standards are (a) For a higher strength concrete the addition of fly ash must be reduced, as the reactivity is too slow to give adequate strength development; (b) A minimum cementitious content per $m^3$ is prescribed, which assumes that binding phases do not result from the aggregate particles; (c) A maximum water/cement ratio is prescribed, which assumes that too much water leads to higher permeability and hence low durability; (d) Only fly ash and GGBFS are usually approved as SCM, which prevents the use of other reactive materials. Although such restrictions are well intended regarding existing concrete technology, they necessarily prevent the adoption of more advanced concrete technology, especially if such assumptions no longer apply.

Unfortunately, prescriptive standards give structural engineers, concrete specialists, contractors, asset owners, and insurance companies a false sense of security. Despite claims to the contrary, vested interests are served by the current prescriptive PC-based framework. If the construction industry is serious in migrating to a performance framework of standards, it will allow the wider adoption of geopolymer concrete and enable the industry to reduce its $CO_2$ footprint significantly.

It is important to ask which performance and durability testing methods should be used in order to specify performance criteria. The discussion above shows the challenge of developing testing methods for durability that are independent of initial binder phase assemblage. In a critical review of performance-based approaches (Alexander & Thomas, 2015), it was explained that it is possible to relate service-life prediction models to durability testing, even when it is known that the diffusion parameters in concrete are complicated by several factors, including interaction between the diffusing species and the matrix and the reduction of diffusion coefficients with age. It is noteworthy that South Africa has developed a suite of durability index tests (e.g., oxygen permeability, sorptivity, and chloride conductivity) that are linked to service life models for the relevant deterioration mechanisms in reinforced concrete structures.

## 7.9 Conclusions

Fly ash-based geopolymers have progressed from a laboratory research phase to an industrial application phase in various structures and in different countries. Although building market confidence will be an ongoing endeavor, geopolymer concrete now offers a high-volume, affordable, and low-$CO_2$ alternative to PC. Progress on the modification of existing accelerated durability testing methods and the development of methods to predict service life should lead to the development of a performance standards framework, which is essential for the wider utilization of fly ash-based geopolymer cement. Such a framework will greatly enhance market adoption, as it will simplify material specification for use by structural engineers and reduce perceived risk, which will expand the scale of the supply chain.

Much progress has been made on the characterization and phase modeling of fly ash-based geopolymers at the nanoscale. Nevertheless, more work is required on the link between the nanostructure, microstructure, and macroscopic/engineering behavior of these materials. This is a very challenging task due to the heterogeneous nature of AAFA at every length scale. Additional insight into the phase assemblage and nanostructure of fly ash-based geopolymers of industrially relevant composition will underpin the further development of accelerated durability testing methods and service life prediction, which will help to build further confidence in the market. There is a need to generate more data to describe the engineering behavior of geopolymer concrete under different ambient conditions so that existing structural design methods can be recalibrated.

## References

Abdullah, M. M. A. B., Hussin, K., Bnhussain, M., Ismail, K. N., Yahya, Z., & Abdul Razak, R. (2012). Fly ash-based geopolymer lightweight concrete using foaming agent. *International Journal of Molecular Sciences*, *13*(6), 7186–7198.

Adam, A. A. (2009). *Strength and durability properties of alkali activated slag and fly ash-based geopolymer concrete* (Thesis). Melbourne: RMIT University Melbourne.

Alexander, M., & Thomas, M. (2015). Service life prediction and performance testing—Current developments and practical applications. *Cement and Concrete Research*, *78*(Part A), 155–164.

Babaee, M., & Castel, A. (2016). Chloride-induced corrosion of reinforcement in low-calcium fly ash-based geopolymer concrete. *Cement and Concrete Research*, *88*, 96–107.

Bakharev, T. (2005). Geopolymeric materials prepared using Class F fly ash and elevated temperature curing. *Cement and Concrete Research*, *35*(6), 1224–1232.

Barbosa, V. F., MacKenzie, K. J., & Thaumaturgo, C. (2000). Synthesis and characterisation of materials based on inorganic polymers of alumina and silica: Sodium polysialate polymers. *International Journal of Inorganic Materials*, *2*(4), 309–317.

Bazant, Z. P., & Chern, J. -C. (1984). Bayesian statistical prediction of concrete creep and shrinkage. *ACI Journal*, *81*(4), 319–330.

Bernal, S. A., Provis, J. L., Walkley, B., San Nicolas, R., Gehman, J. D., Brice, D. G., et al. (2013). Gel nanostructure in alkali-activated binders based on slag and fly ash, and effects of accelerated carbonation. *Cement and Concrete Research*, *53*, 127–144.

Beushausen, H., Alexander, M. G., Basheer, M., Baroghel-Bouny, V., d'Andréa, R., Gonçalves, A., et al. (2016). Principles of the performance-based approach for concrete durability. In H. Beushausen & L. Fernandez Luco (Eds.), *Performance-based specifications and control of concrete durability: State-of-the-art report RILEM TC 230-PSC* (pp. 107–131). Dordrecht: Springer.

Brus, J., Kobera, L., Urbanová, M., Koloušek, D., & Kotek, J. Í. (2012). Insights into the structural transformations of aluminosilicate inorganic polymers: A comprehensive solid-state NMR study. *The Journal of Physical Chemistry C*, *116*(27), 14627–14637.

Buchwald, A., Dombrowski, K., & Weil, M. (2005). Evaluation of primary and secondary materials under technical, ecological and economic aspects for the use as raw materials in geopolymeric binders. In V. Bilek & Z. Kersner (Eds.), *2nd international symposium on non-traditional cement and concrete, Brno, Czech Republic* (pp. 32–40).

Chi, M., & Huang, R. (2013). Binding mechanism and properties of alkali-activated fly ash/slag mortars. *Construction and Building Materials*, *40*, 291–298.

Chindaprasirt, P., Rattanasak, U., & Jaturapitakkul, C. (2011). Utilization of fly ash blends from pulverized coal and fluidized bed combustions in geopolymeric materials. *Cement and Concrete Composites*, *33*(1), 55–60.

Cormier, L., Calas, G., & Cuello, G. (2010). Structural study of Ca-Mg and K-Mg mixing in silicate glasses by neutron diffraction. *Journal of Non-Crystalline Solids*, *356*(44), 2327–2331.

Criado, M., Fernández-Jiménez, A., de la Torre, A. G., Aranda, M. A. G., & Palomo, A. (2007). An XRD study of the effect of the $SiO_2/Na_2O$ ratio on the alkali activation of fly ash. *Cement and Concrete Research*, *37*(5), 671–679.

Criado, M., Fernández-Jiménez, A., Palomo, A., Sobrados, I., & Sanz, J. (2008). Effect of the $SiO_2/Na_2O$ ratio on the alkali activation of fly ash. Part II: $^{29}Si$ MAS-NMR survey. *Microporous and Mesoporous Materials*, *109*(1–3), 525–534.

Criado, M., Jiménez, A. F., & Palomo, A. (2010). Effect of sodium sulfate on the alkali activation of fly ash. *Cement and Concrete Composites*, *32*(8), 589–594.

Criado, M., Jiménez, A. F., Sobrados, I., Palomo, A., & Sanz, J. (2012). Effect of relative humidity on the reaction products of alkali activated fly ash. *Journal of the European Ceramic Society*, *32*(11), 2799–2807.

Criado, M., Palomo, A., & Fernández-Jiménez, A. (2005). Alkali activation of fly ashes. Part 1: Effect of curing conditions on the carbonation of the reaction products. *Fuel*, *84*(16), 2048–2054.

Dattatreya, J., Rajamane, N., Sabitha, D., Ambily, P., & Nataraja, M. (2011). Flexural behaviour of reinforced geopolymer concrete beams. *International Journal of Civil and Structural Engineering*, *2*(1), 138.

Davidovits, J. (1994). Properties of geopolymer cements. In: *First international conference on alkaline cements and concretes, scientific research on binders and materials* (pp. 131–149). Kiev, Ukraine: Kiev State Technical University.

Davidovits, J. (2005). Geopolymer, green chemistry and sustainable development solutions. In: *Proceedings of the world congress geopolymer*. Saint-Quentin, France: Geopolymer Institute.

Davidovits, J., Davidovits, M., & Davidovits, N. (1994). *Process for obtaining a geopolymeric alumino-silicate and products thus obtained*. Google Patents.

Diaz, E. I., Allouche, E. N., & Eklund, S. (2010). Factors affecting the suitability of fly ash as source material for geopolymers. *Fuel*, *89*(5), 992–996.

Durdziński, P. T., Dunant, C. F., Haha, M. B., & Scrivener, K. L. (2015). A new quantification method based on SEM-EDS to assess fly ash composition and study the reaction of its individual components in hydrating cement paste. *Cement and Concrete Research*, *73*, 111–122.

Duxson, P. (2006). *The structure and thermal evolution of metakaolin geopolymers* (Ph.D. thesis). Melbourne: Chemical and Biomolecular Engineering, The University of Melbourne.

Duxson, P., Fernández-Jiménez, A., Provis, J. L., Lukey, G. C., Palomo, A., & van Deventer, J. S. J. (2007). Geopolymer technology: The current state of the art. *Journal of Materials Science*, *42*(9), 2917–2933.

Duxson, P., Lukey, G., Separovic, F., & van Deventer, J. (2005). Effect of alkali cations on aluminum incorporation in geopolymeric gels. *Industrial & Engineering Chemistry Research*, *44*(4), 832–839.

Duxson, P., Lukey, G., & van Deventer, J. J. (2007). Physical evolution of Na-geopolymer derived from metakaolin up to 1000°C. *Journal of Materials Science*, *42*(9), 3044–3054.

Duxson, P., Mallicoat, S. W., Lukey, G. C., Kriven, W. M., & van Deventer, J. S. J. (2007). The effect of alkali and Si/Al ratio on the development of mechanical properties of metakaolin-based geopolymers. *Colloids and Surfaces A: Physicochemical and Engineering Aspects*, *292*(1), 8–20.

Duxson, P., & Provis, J. L. (2008). Designing precursors for geopolymer cements. *Journal of the American Ceramic Society*, *91*(12), 3864–3869.

Duxson, P., Provis, J. L., Lukey, G. C., Mallicoat, S. W., Kriven, W. M., & van Deventer, J. S. J. (2005a). Understanding the relationship between geopolymer composition, microstructure and mechanical properties. *Colloids and Surfaces A: Physicochemical and Engineering Aspects*, *269*(1–3), 47–58.

Duxson, P., Provis, J. L., Lukey, G. C., Separovic, F., & van Deventer, J. S. (2005b). $^{29}$Si NMR study of structural ordering in aluminosilicate geopolymer gels. *Langmuir*, *21*(7), 3028–3036.

Duxson, P., Provis, J. L., Lukey, G. C., & van Deventer, J. S. J. (2007). The role of inorganic polymer technology in the development of 'green concrete'. *Cement and Concrete Research*, *37*(12), 1590–1597.

Engineering News. (2016). First carbon-friendly pour for Khobab wind farm foundations. *Engineering News (South Africa)*, *6 July*.

Fawer, M., Concannon, M., & Rieber, W. (1999). Life cycle inventories for the production of sodium silicates. *The International Journal of Life Cycle Assessment*, *4*(4), 207.

Fernández-Jimenez, A., De La Torre, A., Palomo, A., López-Olmo, G., Alonso, M., & Aranda, M. (2006). Quantitative determination of phases in the alkali activation of fly ash. Part I. Potential ash reactivity. *Fuel*, *85*(5), 625–634.

Fernández-Jiménez, A., Garcia-Lodeiro, I., & Palomo, A. (2007). Durability of alkali-activated fly ash cementitious materials. *Journal of Materials Science*, *42*(9), 3055–3065.

Fernández-Jiménez, A., & Palomo, A. (2005). Composition and microstructure of alkali activated fly ash binder: Effect of the activator. *Cement and Concrete Research*, *35*(10), 1984–1992.

Fernández-Jiménez, A., Palomo, A., & Criado, M. (2005a). Microstructure development of alkali-activated fly ash cement: A descriptive model. *Cement and Concrete Research*, *35*(6), 1204–1209.

Fernandez-Jimenez, A. M., Palomo, A., & Lopez-Hombrados, C. (2006). Engineering properties of alkali-activated fly ash concrete. *ACI Materials Journal*, *103*(2), 106–112.

Fernández-Jiménez, A., Palomo, A., Macphee, D. E., & Lachowski, E. E. (2005b). Fixing arsenic in alkali-activated cementitious matrices. *Journal of the American Ceramic Society*, *88*(5), 1122–1126.

Fernández-Jiménez, A., Palomo, A., Sobrados, I., & Sanz, J. (2006). The role played by the reactive alumina content in the alkaline activation of fly ashes. *Microporous and Mesoporous Materials*, *91*(1–3), 111–119.

Fernández-Jiménez, A., Puertas, F., Sobrados, I., & Sanz, J. (2003). Structure of calcium silicate hydrates formed in alkaline-activated slag: Influence of the type of alkaline activator. *Journal of the American Ceramic Society*, *86*(8), 1389.

García-Lodeiro, I., Fernández-Jiménez, A., Palomo, A., & Macphee, D. E. (2010). Effect of calcium additions on N–A–S–H cementitious gels. *Journal of the American Ceramic Society*, *93*(7), 1934–1940.

García-Lodeiro, I., Palomo, A., & Fernández-Jiménez, A. (2007). Alkali-aggregate reaction in activated fly ash systems. *Cement and Concrete Research*, *37*(2), 175–183.

Gilbert, R. I. (1988). Time effects in concrete structures. In: *Developments in civil engineering*. vol. 23. Amsterdam, The Netherland: Elsevier.

Gomes, S., François, M., Abdelmoula, M., Refait, P., Pellissier, C., & Evrard, O. (1999). Characterization of magnetite in silico-aluminous fly ash by SEM, TEM, XRD, magnetic susceptibility, and Mössbauer spectroscopy. *Cement and Concrete Research*, *29*(11), 1705–1711.

Habert, G., d'Espinose de Lacaillerie, J. B., & Roussel, N. (2011). An environmental evaluation of geopolymer based concrete production: Reviewing current research trends. *Journal of Cleaner Production*, *19*, 1229–1238.

Habert, G., & Ouellet-Plamondon, C. (2016). Recent update on the environmental impact of geopolymers. *RILEM Technical Letters*, *1*, 7.

Hajimohammadi, A., Provis, J. L., & van Deventer, J. S. (2010). Effect of alumina release rate on the mechanism of geopolymer gel formation. *Chemistry of Materials*, *22*(18), 5199–5208.

Hajimohammadi, A., Provis, J. L., & van Deventer, J. S. (2011). The effect of silica availability on the mechanism of geopolymerisation. *Cement and Concrete Research*, *41*(3), 210–216.

Hardjito, D., & Wallah, S. (2002). *Study on engineering properties of fly ash-based geopolymer concrete*.

Hardjito, D., Wallah, S. E., Sumajouw, D. M., & Rangan, B. V. (2004a). On the development of fly ash-based geopolymer concrete. *ACI Materials Journal-American Concrete Institute*, *101*(6), 467–472.

Hardjito, D., Wallah, S. E., Sumajouw, D., & Rangan, B. (2004b). Properties of geopolymer concrete with fly ash as source material: Effect of mixture composition. *Special Publication*, *222*, 109–118.

Henderson, G. S., & Fleet, M. E. (1997). The structure of titanium silicate glasses investigated by Si K-edge X-ray absorption spectroscopy. *Journal of Non-Crystalline Solids*, *211*(3), 214–221.

Hirsch, T. J. (1962). Modulus of elasticity of concrete affected by elastic moduli of cement paste matrix and aggregate. *Journal Proceedings*, *59*(3), 427–452.

Hobbs, D. W. (1971). The dependence of the bulk modulus, Young's modulus, creep, shrinkage and thermal expansion of concrete upon aggregate volume concentration. *Matériaux et Construction*, *4*(2), 107–114.

Ikeda, K. (1997). Preparation of fly ash monoliths consolidated with a sodium silicate binder at ambient temperature. *Cement and Concrete Research*, *27*(5), 657–663.

Ivan Diaz-Loya, E., Allouche, E. N., & Vaidya, S. (2011). Mechanical properties of fly-ash-based geopolymer concrete. *ACI Materials Journal*, *108*(3), 7.

Katada, N., Nakata, S., Kato, S., Kanehashi, K., Saito, K., & Niwa, M. (2005). Detection of active sites for paraffin cracking on USY zeolite by $^{27}$Al MQMAS NMR operated at high magnetic field 16 T. *Journal of Molecular Catalysis A: Chemical*, *236*(1–2), 239–245.

Komljenović, M., Baščarević, Z., & Bradić, V. (2010). Mechanical and microstructural properties of alkali-activated fly ash geopolymers. *Journal of Hazardous Materials*, *181*(1–3), 35–42.

Kovtun, M., Ziolkowski, M., Shekhovtsova, J., & Kearsley, E. (2016). Direct electric curing of alkali-activated fly ash concretes: A tool for wider utilization of fly ashes. *Journal of Cleaner Production*, *133*, 220–227.

Kumar, S., & Kumar, R. (2011). Mechanical activation of fly ash: Effect on reaction, structure and properties of resulting geopolymer. *Ceramics International*, *37*(2), 533–541.

Kumar, R., Kumar, S., & Mehrotra, S. P. (2007). Towards sustainable solutions for fly ash through mechanical activation. *Resources, Conservation and Recycling*, *52*(2), 157–179.

Kutchko, B. G., & Kim, A. G. (2006). Fly ash characterization by SEM-EDS. *Fuel*, *85*(17), 2537–2544.

Lee, W. K. W., & van Deventer, J. S. J. (2002). Structural reorganisation of class F fly ash in alkaline silicate solutions. *Colloids and Surfaces A: Physicochemical and Engineering Aspects*, *211*(1), 49–66.

Li, S., Zheng, A., Su, Y., Zhang, H., Chen, L., Yang, J., et al. (2007). Brønsted/Lewis acid synergy in dealuminated HY zeolite: A combined solid-state NMR and theoretical calculation study. *Journal of the American Chemical Society*, *129*(36), 11161–11171.

Lloyd, R. R., Provis, J. L., Smeaton, K. J., & van Deventer, J. S. J. (2009). Spatial distribution of pores in fly ash-based inorganic polymer gels visualised by Wood's metal intrusion. *Microporous and Mesoporous Materials*, *126*(1–2), 32–39.

Lloyd, R., Provis, J., & van Deventer, J. (2009a). Microscopy and microanalysis of inorganic polymer cements. 2: The gel binder. *Journal of Materials Science*, *44*(2), 620–631.

Lloyd, R. R., Provis, J. L., & van Deventer, J. S. (2009b). Microscopy and microanalysis of inorganic polymer cements. 1: Remnant fly ash particles. *Journal of Materials Science*, *44*(2), 608–619.

Lodeiro, I. G., Fernández-Jimenez, A., Palomo, A., & Macphee, D. (2010). Effect on fresh CSH gels of the simultaneous addition of alkali and aluminium. *Cement and Concrete Research*, *40*(1), 27–32.

McLellan, B. C., Williams, R. P., Lay, J., van Riessen, A., & Corder, G. D. (2011). Costs and carbon emissions for geopolymer pastes in comparison to ordinary Portland cement. *Journal of Cleaner Production*, *19*, 1080–1090.

Melar, J., Renaudin, G., Leroux, F., Hardy-Dessources, A., Nedelec, J. M., Taviot-Gueho, C., et al. (2015). The porous network and its interface inside geopolymers as a function of alkali cation and aging. *Journal of Physical Chemistry C*, *119*(31), 17619–17632.

Monticelli, C., Natali, M., Balbo, A., Chiavari, C., Zanotto, F., Manzi, S., et al. (2016). A study on the corrosion of reinforcing bars in alkali-activated fly ash mortars under wet and dry exposures to chloride solutions. *Cement and Concrete Research*, *87*, 53–63.

Müller, C. (2012). Use of cement in concrete according to European standard EN 206-1. *HBRC Journal*, *8*(1), 1–7.

Nath, P., & Sarker, P. K. (2015). Use of OPC to improve setting and early strength properties of low calcium fly ash geopolymer concrete cured at room temperature. *Cement and Concrete Composites*, *55*, 205–214.

Němeček, J., Šmilauer, V., & Kopecký, L. (2011). Nanoindentation characteristics of alkali-activated aluminosilicate materials. *Cement and Concrete Composites*, *33*(2), 163–170.

Nguyen, K. T., Ahn, N., Le, T. A., & Lee, K. (2016). Theoretical and experimental study on mechanical properties and flexural strength of fly ash-geopolymer concrete. *Construction and Building Materials*, *106*, 65–77.

Oh, J. E., Monteiro, P. J. M., Jun, S. S., Choi, S., & Clark, S. M. (2010). The evolution of strength and crystalline phases for alkali-activated ground blast furnace slag and fly ash-based geopolymers. *Cement and Concrete Research*, *40*(2), 189–196.

Oh, J. E., Moon, J., Oh, S. -G., Clark, S. M., & Monteiro, P. J. M. (2012). Microstructural and compositional change of NaOH-activated high calcium fly ash by incorporating Na-aluminate and co-existence of geopolymeric gel and C–S–H(I). *Cement and Concrete Research*, *42*(5), 673–685.

Pacheco-Torgal, F., Castro-Gomes, J., & Jalali, S. (2008). Alkali-activated binders: A review: Part 1. Historical background, terminology, reaction mechanisms and hydration products. *Construction and Building Materials*, *22*(7), 1305–1314.

Pacheco-Torgal, F., Labrincha, J., Leonelli, C., Palomo, A., & Chindaprasit, P. (2014). *Handbook of alkali-activated cements, mortars and concretes*. Cambridge: Elsevier.

Palomo, A., Alonso, S., Fernandez-Jiménez, A., Sobrados, I., & Sanz, J. (2004). Alkaline activation of fly ashes: NMR study of the reaction products. *Journal of the American Ceramic Society*, *87*(6), 1141–1145.

Palomo, A., Grutzeck, M., & Blanco, M. (1999). Alkali-activated fly ashes: A cement for the future. *Cement and Concrete Research*, *29*(8), 1323–1329.

Phair, J., Smith, J., & van Deventer, J. (2003). Characteristics of aluminosilicate hydrogels related to commercial "Geopolymers" *Materials Letters*, *57*(28), 4356–4367.

Phair, J. W., & van Deventer, J. S. J. (2002a). Effect of the silicate activator pH on the microstructural characteristics of waste-based geopolymers. *International Journal of Mineral Processing*, *66*(1–4), 121–143.

Phair, J. W., & van Deventer, J. S. J. (2002b). Characterization of fly-ash-based geopolymeric binders activated with sodium aluminate. *Industrial & Engineering Chemistry Research*, *41*(17), 4242–4251.

Provis, J. L., & Bernal, S. A. (2014). Geopolymers and related alkali-activated materials. *Annual Review of Materials Research*, *44*, 299–327.

Provis, J. L., Duxson, P., Lukey, G. C., & van Deventer, J. S. (2005). Statistical thermodynamic model for Si/Al ordering in amorphous aluminosilicates. *Chemistry of Materials*, *17*(11), 2976–2986.

Provis, J. L., Lukey, G. C., & van Deventer, J. S. J. (2005). Do geopolymers actually contain nanocrystalline zeolites? A reexamination of existing results. *Chemistry of Materials*, *17*(12), 3075–3085.

Provis, J. L., Palomo, A., & Shi, C. (2015). Advances in understanding alkali-activated materials. *Cement and Concrete Research*, *78*, 110–125.

Provis, J. L., Rose, V., Bernal, S. A., & van Deventer, J. S. (2009). High-resolution nanoprobe X-ray fluorescence characterization of heterogeneous calcium and heavy metal distributions in alkali-activated fly ash. *Langmuir*, *25*(19), 11897–11904.

Provis, J. L., & van Deventer, J. S. (2007). Direct measurement of the kinetics of geopolymerisation by in-situ energy dispersive X-ray diffractometry. *Journal of Materials Science*, *42*(9), 2974–2981.

Provis, J. L., & van Deventer, J. S. J. (2009). *Geopolymers: Structures, processing, properties and industrial applications*. Abingdon, UK: Woodhead Publishing.

Provis, J. L., & van Deventer, J. S. J. (2014a). Alkali activated materials. State-of-the-art report, RILEM TC 224-AAM. In: In J. L. Provis & J. S. J. van Deventer (Eds.), *vol. 13. RILEM state-of-the-art reports*. New York, NY: Springer

Provis, J. L., & van Deventer, J. S. (2014b). *Alkali activated materials*. New York, NY: Springer.

Provis, J. L., Walls, P. A., & van Deventer, J. S. J. (2008). Geopolymerisation kinetics. 3. Effects of Cs and Sr salts. *Chemical Engineering Science*, *63*(18), 4480–4489.

Rattanasak, U., Pankhet, K., & Chindaprasirt, P. (2011). Effect of chemical admixtures on properties of high-calcium fly ash geopolymer. *International Journal of Minerals, Metallurgy, and Materials*, *18*(3), 364–369.

Rickard, W. D. A., Williams, R., Temuujin, J., & van Riessen, A. (2011). Assessing the suitability of three Australian fly ashes as an aluminosilicate source for geopolymers in high temperature applications. *Materials Science and Engineering A*, *528*(9), 3390–3397.

Rowles, M. R., Hanna, J. V., Pike, K. J., Smith, M. E., & O'Connor, B. H. (2007). $^{29}$Si, $^{27}$Al, $^{1}$H and $^{23}$Na MAS NMR study of the bonding character in aluminosilicate inorganic polymers. *Applied Magnetic Resonance*, *32*(4), 663–689.

Rowles, M., & O'Connor, B. (2003). Chemical optimisation of the compressive strength of aluminosilicate geopolymers synthesised by sodium silicate activation of metakaolinite. *Journal of Materials Chemistry*, *13*(5), 1161–1165.

Shi, C., & Day, R. L. (1995). Acceleration of the reactivity of fly ash by chemical activation. *Cement and Concrete Research*, *25*(1), 15–21.

Silva, R. V., de Brito, J., & Dhir, R. K. (2016). Establishing a relationship between modulus of elasticity and compressive strength of recycled aggregate concrete. *Journal of Cleaner Production*, *112*(Part 4), 2171–2186.

Škvára, F., Kopecký, L., Šmilauer, V., & Bittnar, Z. (2009). Material and structural characterization of alkali activated low-calcium brown coal fly ash. *Journal of Hazardous Materials*, *168*(2–3), 711–720.

Sofi, M., van Deventer, J., Mendis, P., & Lukey, G. (2007). Engineering properties of inorganic polymer concretes (IPCs). *Cement and Concrete Research*, *37*(2), 251–257.

Songpiriyakij, S., Kubprasit, T., Jaturapitakkul, C., & Chindaprasirt, P. (2010). Compressive strength and degree of reaction of biomass- and fly ash-based geopolymer. *Construction and Building Materials*, *24*(3), 236–240.

Stebbins, J. F., & Xu, Z. (1997). NMR evidence for excess non-bridging oxygen in an aluminosilicate glass. *Nature*, *390*(6655), 60–62.

Steins, P., Poulesquen, A., Diat, O., & Frizon, F. (2012). Structural evolution during geopolymerization from an early age to consolidated material. *Langmuir*, *28*(22), 8502–8510.

Stengel, T., Heinz, D., & Reger, J. (2009). Life cycle assessment of geopolymer concrete—What is the environmental benefit? In: *Concrete solutions 09, Sydney, Australia*.

Sumajouw, D. M., Hardjito, D., Wallah, S. E., & Rangan, B. V. (2005). Fly ash-based geopolymer concrete: An application for structural members. In: *Proceedings of the geopolymer 2005 world congress: Green chemistry and sustainable development solutions* (pp. 149–152).

Sumajouw, D., Hardjito, D., Wallah, S., & Rangan, B. (2007). Fly ash-based geopolymer concrete: Study of slender reinforced columns. *Journal of Materials Science*, *42*(9), 3124–3130.

Sumajouw, M., & Rangan, B. V. (2006). Low-calcium fly ash-based geopolymer concrete: Reinforced beams and columns. In: *Proceedings of the 31st conference on our world in concrete and structures*. Singapore.

Swanepoel, J. C., & Strydom, C. A. (2002). Utilisation of fly ash in a geopolymeric material. *Applied Geochemistry*, *17*(8), 1143–1148.

Tempest, B., Sansui, O., Gergely, J., Ogunro, V., & Weggel, D. (2009). Compressive strength and embodied energy optimization of fly ash based geopolymer concrete. In: *World of Coal Ash 2009, Lexington, KY*.

Temuujin, J., Williams, R., & van Riessen, A. (2009). Effect of mechanical activation of fly ash on the properties of geopolymer cured at ambient temperature. *Journal of Materials Processing Technology*, *209*(12), 5276–5280.

Topçu, İ. B., & Toprak, M. U. (2011). Properties of geopolymer from circulating fluidized bed combustion coal bottom ash. *Materials Science and Engineering A*, *528*(3), 1472–1477.

Valcke, S. L. A., Sarabèr, A. J., Pipilikaki, P., Fischer, H. R., & Nugteren, H. W. (2013). Screening coal combustion fly ashes for application in geopolymers. *Fuel*, *106*, 490–497.

van Deventer, J. S. J., Provis, J. L., & Duxson, P. (2012). Technical and commercial progress in the adoption of geopolymer cement. *Minerals Engineering*, *29*, 89–104.

van Deventer, J., Provis, J., Duxson, P., & Lukey, G. (2007). Reaction mechanisms in the geopolymeric conversion of inorganic waste to useful products. *Journal of Hazardous Materials*, *139*(3), 506–513.

van Jaarsveld, J. G. S., & van Deventer, J. S. J. (1999). Effect of the alkali metal activator on the properties of fly ash-based geopolymers. *Industrial & Engineering Chemistry Research*, *38*(10), 3932–3941.

van Jaarsveld, J. G. S., van Deventer, J. S. J., & Lukey, G. C. (2003). The characterisation of source materials in fly ash-based geopolymers. *Materials Letters*, *57*(7), 1272–1280.

van Riessen, A., Jamieson, E., Kealley, C. S., Hart, R. D., & Williams, R. P. (2013). Bayer-geopolymers: An exploration of synergy between the alumina and geopolymer industries. *Cement and Concrete Composites*, *41*, 29–33.

Walkley, B. (2016). *Understanding geopolymers through synthetic gel systems* (Thesis).

Walkley, B., San Nicolas, R., Sani, M. -A., Rees, G. J., Hanna, J. V., van Deventer, J. S., et al. (2016). Phase evolution of C-(N)-A-S-H/N-A-S-H gel blends investigated via alkali-activation of synthetic calcium aluminosilicate precursors. *Cement and Concrete Research*, *89*, 120–135.

Walkley, B., San Nicolas, R., Sani, M. -A., Gehman, J. D., van Deventer, J. S. J., & Provis, J. L. (2016). Phase evolution of $Na_2O$-$Al_2O_3$-$SiO_2$-$H_2O$ gels in synthetic aluminosilicate binders. *Dalton Transactions*, *45*(13), 5521–5535.

Wallah, S. (2010). Creep behaviour of fly ash-based geopolymer concrete. *Civil Engineering Dimension*, *12*(2), 73–78.

Wallah, S., & Rangan, B. V. (2006). *Low-calcium fly ash-based geopolymer concrete: Long-term properties*. Res. Report-GC2 (pp. 76–80). Bentley: Curtin University.

Wang, S. -D., Pu, X. -C., Scrivener, K. L., & Pratt, P. L. (1995). Alkali-activated slag cement and concrete: A review of properties and problems. *Advances in Cement Research*, *7*(27), 93–102.

Wang, S. -D., Scrivener, K. L., & Pratt, P. (1994). Factors affecting the strength of alkali-activated slag. *Cement and Concrete Research*, *24*(6), 1033–1043.

Wang, C., Wu, J. -Z., & Zhang, F. -S. (2013). Development of porous ceramsite from construction and demolition waste. *Environmental Technology*, *34*(15), 2241–2249.

Ward, C. R., & French, D. (2006). Determination of glass content and estimation of glass composition in fly ash using quantitative X-ray diffractometry. *Fuel*, *85*(16), 2268–2277.

Wastiels, J., Wu, X., Faignet, S., & Patfoort, G. (1994). Mineral polymer based on fly ash. *Resource Management Technology*, *22*(3), 6.

White, C., Bloomer, B., Provis, J. L., Henson, N. J., & Page, K. (2011). *The synergy between total scattering and advanced simulation techniques: Quantifying geopolymer and gel evolution*. New Mexico: Los Alamos National Laboratory (LANL).

White, C. E., Provis, J. L., Llobet, A., Proffen, T., & van Deventer, J. S. (2011). Evolution of local structure in geopolymer gels: An in situ neutron pair distribution function analysis. *Journal of the American Ceramic Society*, *94*(10), 3532–3539.

White, C. E., Provis, J. L., Proffen, T., & van Deventer, J. S. (2010). The effects of temperature on the local structure of metakaolin-based geopolymer binder: A neutron pair distribution function investigation. *Journal of the American Ceramic Society*, *93*(10), 3486–3492.

White, C. E., Provis, J. L., Proffen, T., & van Deventer, J. S. (2012). Molecular mechanisms responsible for the structural changes occurring during geopolymerization: Multiscale simulation. *AIChE Journal*, *58*(7), 2241–2253.

Wongpa, J., Kiattikomol, K., Jaturapitakkul, C., & Chindaprasirt, P. (2010). Compressive strength, modulus of elasticity, and water permeability of inorganic polymer concrete. *Materials & Design*, *31*(10), 4748–4754.

Xu, H., Li, Q., Shen, L., Zhang, M., & Zhai, J. (2010). Low-reactive circulating fluidized bed combustion (CFBC) fly ashes as source material for geopolymer synthesis. *Waste Management*, *30*(1), 57–62.

Yu, Z., Zheng, A., Wang, Q., Chen, L., Xu, J., Amoureux, J. P., et al. (2010). Insights into the dealumination of zeolite HY revealed by sensitivity-enhanced 27Al DQ-MAS NMR spectroscopy at high field. *Angewandte Chemie International Edition*, *49*(46), 8657–8661.

Zhang, Z., Provis, J. L., Zou, J., Reid, A., & Wang, H. (2016). Toward an indexing approach to evaluate fly ashes for geopolymer manufacture. *Cement and Concrete Research*, *85*, 163–173.

# Part Three

# The beneficiation of coal combustion materials

This page intentionally left blank

# Ash beneficiation, quality, and standard criteria

# 8

*T. Robl*
University of Kentucky, Lexington, KY, United States

## 8.1 Introduction

This section of the book revolves around a review of technologies for the beneficiation of coal ash. Beneficiation transforms coal ash from a byproduct to a product. Changes in burner configurations and other environmental controls have impacted quality, and beneficiation is needed for many sources of ash just to meet the minimum national standards. Chapters written by technical experts on air classification, electrostatic separation, thermal beneficiation, and chemical passivation are offered. A chapter on the recovery of ponded and landfilled ash also includes the review of wet technologies, such as hydraulic classifiers, hydrocyclones, and screening.

The primary reason for beneficiating fly ash is to improve its quality to meet or exceed national standards for use in concrete and mortar. To complicate matters, there are multiple national standards that differ significantly. These standards greatly affect the choice of beneficiation technology, thus a review of them is relevant.

## 8.2 National ash standards

Perhaps the oldest standard for fly ash in concrete is the American Society for Testing and Materials ASTM C-618 (ASTM C618—12, 2012). Many national standards follow the lead of this well-established approach to some degree. For example, the Indian Standard, IS 3812-1 and IS 3812-2 (Bureau of India Standards, 2003a, 2003b), the Chinese standard, GB/T 1596 (People's Republic of China National Standard GB/T, 2005) and the Canadian Standard (CAN/CSA, A3001-13, 2013) uses criteria and test methods that are like ASTM but also includes additional grades of ash. The European Standard EN 450 differs in both classification and test methodology (BS EN 450-1, 2012). In addition to these, there are also well-established standards in Japan (Standards Association, 1999), the Russian Federation (GOST 25818-91, n.d.), and Australia (Australian Standard AS3582.1, 2007), which are somewhat different.

### 8.2.1 Fly ash classification

Under ASTM guidelines, if the $SiO_2+Al_2O_3+Fe_2O_3$ content of the ash is greater than 70%, then it is designated Class F; if it is less than 70% but not less than 50%, then it is designated as Class C. ASTM, somewhat strangely, does not address what the other

**Coal Combustion Products (CCP's).** http://dx.doi.org/10.1016/B978-0-08-100945-1.00008-3

component might be. This convention is followed by the Indian IS 3812, which refers to a "siliceous" and "calcareous" fly ash corresponding to Classes F and C. The Chinese GB/T 1596 refers directly to Classes C and F, based on $SiO_2 + Al_2O_3 + Fe_2O_3$.

The Canadian standard uses classifications based on CaO and defines a Class F, (<8% CaO), Class CI, (8%–20% CaO) and Class CH > 20%. The Russian Federation recognizes an acidic (CaO < 10%) and alkaline (CaO > 10%) classification. The European EN 450 does not define a Class C type of fly ash at all and limits the calcium oxide content to no more than 10% by weight. Therefore much of the most commonly utilized fly ash in the United States would not meet European standards, nor would fly ash from many Asian coals.

### 8.2.2 Carbon or loss on ignition

Perhaps the most common problem with fly ash is the high concentrations of carbon char, typically measured as loss on ignition (LOI). Carbon interferes with air entrainment in the concrete, which is important for freeze-thaw resistance. At higher levels, carbon also contributes to darkening the concrete, which is undesirable in many applications. LOI is primarily a function of the type of coal burned and the design and operation of the boiler. The use of activated carbon for mercury control exacerbates this problem due to the high air adsorption affinity of the activated carbon.

The ASTM C618 limits the LOI to no more than 6%, but it does allow for higher levels in Class F ash with appropriate testing. However, in practice this limit may be lower as other organizations, such as state highway departments or national transportation authorities, which may require limits such as 3% or 4% As in the case of fineness, most other national standards have various levels of LOI associated with ash grades. For example, EN 450 lists three categories of LOI (A, B, and C) with maximums of 5%, 7%, and 9%, respectively. The Chinese standard includes values of 5%, 8%, and 15%, for Grades I, II, and III. The Canadian limits LOI at 8% for Class F and 6% for Class CL and CH, respectively.

### 8.2.3 Particle size or fineness

Fineness affects the reactivity of the ash. Finer fly ash particles are more reactive due to their larger surface area, improved particle packing, and flowability of the mortar or concrete. The ASTM criteria for fineness specifies that no more than 34% of the fly ash may be retained on a 325 mesh (i.e., 45 μm) wet screen. All other standards recognize additional levels or grades of fly ash based on fineness. For example, EN 450 recognizes two, a Category N at less than 40% retained on a 325-mesh screen, and a Category S with less than 12%. China recognizes three grades (I, II, III): less than 12%, less than 25%, and less than 45% retained on a 325-mesh screen. India recognizes particle sizes based on the Blaine test with two different levels of fineness, as does the Japanese standards, which uses both Blaine and fineness based sieve retention. The finer ash is, of course, more valued. This would also affect the beneficiation strategy, making technologies (e.g., air classification) more cost effective in some countries than others.

### 8.2.4 Uniformity

The consistency of the fly ash is important, as it is relatable to the quality and reliability of the product in the market place. For example, inconsistent properties create problems at the ready-mix plants with the application of air entrainment admixture dosages. Uniformity criteria are commonly ascribed in national standards. These range from the simple ASTM C 618 standard, which requires no more than 5% variation on fineness or density in 10 consecutive samples; to the complex EN 450, which sets criteria for a host of parameters with minimum frequency of sampling, with prescribed complex statistical methods to follow, and targets that must be met.

### 8.2.5 Strength activity index

Strength activity indexing is a measure of the effectiveness of the fly ash in concrete, although the test is typically performed on mortars primarily for the sake of simplicity. Some specifications for strength activity or strength index are present in most national standards. Typically, it is measured and reported as a ratio of the strength of a mortar mix with a prescribed level of ash substituted for Portland cement to that with a mortar mix with Portland cement only. It is also measured in some prescribed time period, typically 28 days.

Unfortunately, due to the variations in test methodology, these data are not comparable among the various national standards. To illustrate: ASTM requires that a strength index of 75% be achieved as measured at 7 or 28 days. EN 450 prescribes an activity index of 75% be achieved at 28 days or 85% at 90 days. These requirements seem similar or at least comparable; however, this is not the case. ASTM uses a flow table to set the water in the tests; that is, the samples are prepared at constant flow, and the water variation is measured as water demand. EN 450 sets the test samples at constant water, and for Category S measures the flow separately to determine water demand.

Fly ash has both a physical and chemical impact on concrete. Setting the tests to constant flow typically results in the reduction of water with a resultant gain in strength. Thus this test is emphasizing the physical or rheological properties of the mortar, which shows up quickly, hence the allowable measurement at 7 days. The European test, at constant water, is more of a measurement of the chemical activity of the fly ash, which generally is slower, hence the measurements at 28 days and 90 days.

There are other test differences as well. ASTM specifies a standard mortar sand (ASTM C778) that has a narrow size range, while EN 450 uses a mortar sand with a broader size range (EN 196-1) (ASTM C778—13, 2013; CEN EN 196-1, n.d.). These differences affect the relative packing and strength development of the mix. Thus variations in both materials and methods among the national standards suggest that strength index values be compared only judiciously.

### 8.2.6 Other standard criteria

There are several additional parameters that appear in the national standards for fly ash. These include: sulfate, phosphate, alkali, chloride, magnesium, free lime and reactive lime contents, set time criteria, soundness testing (expansion), and moisture.

These are all important, but they show significant variations among the standards. These variations lend credence to recent proposals that a common international standard should be developed for fly ash (Kelly, 2015).

# 8.3 Beneficiation technologies

## 8.3.1 *Caveat emptor*

All the ash beneficiation technologies reviewed in this section of the book are solid and credible solutions to solving or improving ash quality. These are discussed by experts who have worked with them over extended periods of time, so they reflect certain opinions and views that are associated with a long-term familiarity. There is no technical panacea or best choice, however. Each approach has advantages and may or may not be appropriate for any given ash. Choices need to be made based upon a specific ash composition, weighed against a backdrop of national standards, market size and area, and economics. The discussion of the technologies proceeds from the simplest to the more complex and includes a discussion of the authors' opinions on the strengths and disadvantages of each.

### *8.3.1.1 Selective collection*

The least expensive method for ash beneficiation is enhanced quality control at the power plant; this is accomplished by monitoring the various ash streams for LOI and/or fineness and segregating the ash. The LOI in the ash is sometimes found to vary as a function of the load; that is, the lowest LOI produced during a constant load and higher LOI during periods of an increasing or decreasing load. Large power plants typically consist of 2–6 individual furnaces that may vary in age and design, resulting in variation in ash quality. By selectively collecting and segregating ash from selected units or electrostatic precipitator fields, a higher quality ash can sometimes be recovered for sale.

Selective collection has been successfully employed at power plants in the United States, but may not be a widespread practice. Modifying operations at the plant can yield a substantial return for even the smallest investment, particularly if the infrastructure for selective collection and storage is already in place. As selective collection recovers only a fraction of the ash produced, it may be best suited for plants in small ash markets. Costs for this approach can vary widely, from a tens of thousands of dollars for the routine monitoring of ash quality to millions of dollars if separate ash handling equipment, silos, and load-out equipment must be added.

Depending on plant operations, a selective collection may still leave a large percentage of the ash requiring disposal. The capital costs for installing equipment for selectively recovering ash can be high if new silos and collection systems are needed and integrated with other operations at the plant. Instituting operational changes to improve ash for sale are sometimes met with resistance, due to concerns that they may negatively affect the plant performance.

#### 8.3.1.2 Chemical passivation

Chemical passivation uses chemicals to reduce the activity of the carbon in the ash. This reduces the need to add large or variable amounts of air entraining agents to the concrete mix. Several passivation methods have been developed, and a few are commercially available from large concrete marketers. One approach has been to add low dosages of a "sacrificial chemical" to the ash, which will react with the active sites on the carbon, thereby neutralizing them. Another approach uses chemicals to encapsulate the carbon.

Chemical passivation systems have been installed at many power plants in the United States. They are a cost-effective solution for marginal ash. This equipment is typically installed at the load-out silo, and the installation is inexpensive and quick. Operating costs are in the range of a few dollars per ton of ash for chemicals. This approach can improve a problematic ash and make it more acceptable in the market place. Some systems also indicate that chemical passivation can be used on activated carbon (Hill, Zhang, & Shaw, 2009; Howard, Kabis, & Farrington, 2013). Although passivation does not lower LOI, it can be used in cases where specifications allow performance standards in lieu of numerical standards.

Early systems suffered from inconsistent distribution of chemicals on ash, which appear to have been largely corrected over time. This approach has a limited LOI range, as it does not directly reduce the LOI in the ash but rather lowers its activity. Thus an ash may still be out of spec for LOI content even after treatment. It also does not improve the physical uniformity of the ash.

#### 8.3.1.3 Air classification

Air classification systems are installed at many power plants to control the fineness of the fly ash by rejecting coarse ash particles. It uses centrifugal force to selectively separate the coarser fractions of the ash from the finer fractions. This is a well-established technology with many equipment manufacturers. Fly ash is a mixture of coarser, lighter particles (carbon) and smaller, denser particles (glassy silicates), which have different separation profiles; thus air classification is not always effective for reducing LOI.

Air classification is a very successful technology with a long history of ash improvement. Air classification equipment has relatively low capital costs, but installation costs can vary widely, and integration into the collection system can still run into the millions of dollars, but maintenance costs should be low. By improving the fineness of fly ash, this simple and relatively inexpensive technology can make a marginal ash into a high-performing pozzolan with greatly improved uniformity, marketability, and economic value.

Air classification is not consistent or predictable for LOI reduction. If the carbon in the ash is very coarse, which is sometimes the case, some LOI reduction will occur. However, if the carbon is fine, it may increase LOI in the product. Air classification produces a coarse reject stream, which can be high in carbon with the potential for being recycled, but often must be landfilled.

### 8.3.1.4 Electrostatic separation

The first successful commercial application of electrostatic separation to fly ash was developed by Separation Technologies, Inc. (STI), now ST Equipment and Technologies (STET) in the 1990s (Vasiliauskas, Shilling, & Willauer, 1999). In this approach, particle charging is accomplished by interparticle contact or "tribocharging," whereby charges are transferred between particles by differences in electron affinity.

The technology works by feeding ash from the raw ash silo through a vibrating screen to distribute the ash uniformly into a thin gap between two parallel plane electrodes. The particles are then swept up by a moving open-mesh belt and conveyed in opposite directions, depending on their charge. The moving belt is the key to this technology, as it continuously wipes off the plates as it moves, refreshing the attraction of the plates.

The STET process has a long-proven track record of producing large quantities of consistent pozzolan from high LOI fly ash. It has a modest capital cost relative to thermal beneficiation. The unit is relatively small with modest installation requirements, and it is well suited for smaller power plants. Early versions of the technology were reported to require frequent belt changes, but maintenance issues appear to have been largely addressed. Once it is installed the process appears to be reliable and simple to operate. This technology is not targeted for fineness but may improve this parameter as well as particle size uniformity as well if the reject stream is coarse.

Ash sources with significant quantities of very fine carbon may diminish yield and limit applicability. It produces a reject stream of 25% or more, typically requiring disposal. The process does little to improve the fineness of the noncarbon portion of the ash. Also, as is the case of all electrostatic technologies, the efficiency can be affected by humidity and the feed to the process must be dry.

### 8.3.1.5 Thermal beneficiation

Thermal beneficiation is the use of combustion to reduce the level of carbon in the ash. Thermal beneficiation also eliminates ammonia issues and can improve fineness and uniformity. Successful thermal beneficiation technologies have been commercially deployed since 1999 (Keppeler, 2001). This technology produces more than a million tons of marketable fly ash per year in the eastern United States. There are two technologies that can be considered proven: the first is PMI's Carbon Burnout (CBO) system, based on dense phase fluidized bed combustion; and the second is SEFA Group's STAR technology, based on dilute or entrained fluidized bed combustion.

The ability of thermal beneficiation to improve ash quality is truly impressive. It is a proven, highly flexible technology that can operate on a variety of ash types with a very wide range of carbon concentrations and sizes. It produces an ash that is low or even free of carbon. It also eliminates ammonia from fly ashes impacted by nitrous oxide controls or opacity treatments. The process may improve fineness by eliminating coarse carbon and liberating ash trapped within.

Thermal beneficiation is a combustion process and may require additional air emission permitting. If not integrated into the power plant, it will also require its own emission control system. It is by far the most expensive of all the technologies considered. A facility can cost tens of millions of dollars, which suggests that it would be more attractive for larger power plants with access to large and stable markets. The construction of a thermal beneficiation facility may require significant plant modifications and systems integration; however, it does not specifically target ash fineness and uniformity.

## *8.3.2 Beneficiation and recovery of landfilled and ponded ash*

The recovery of ash from ponds and landfills has a history of application mostly in road base or structural fill. The beneficiation of these materials for application in the concrete and other added value applications has not been a common practice. The recovery of ash from ponds or landfills is inevitable based on two contravening forces. The first is the large number of coal power plant closings. This reduces the number of point sources of ash and increases transportation costs overall, affecting the economics of the market. Secondly, there is an increasing need for supplementary cementitious materials to reduce the carbon footprint of Portland cement-based concrete; this need will only increase in the future.

Ponded and landfilled ash represents a processing challenge that is more like a natural resource recovery operation. The ponds have often operated for several decades, and the materials are highly variable; some contain bottom ash, coal mill rejects, and/or scrubber by-products that are codisposed with fly ash. Sedimentation also affects particle size distribution, and a careful and thorough assessment of the ash deposit is needed to determine the amount of ash that can be recovered and the level of beneficiation required.

### *8.3.2.1 Integrated wet ash processing technologies*

Applicable technologies for the recovery and processing of wet ash can readily be found in the mineral processing industries. In many respects the processing of wet ash is like sand and gravel or coal cleaning operations. The recovery of ponded ash will include ashrecovery, requiring a truck and shovel or dredge operation. Ash separation to improve the particle size distribution of the product, could include coarse screening, followed by a hydraulic classification of some verity and, if needed, froth flotation to reduce LOI. A product dewatering step is needed that might including product thickening and/or filtration and/or stacking and dewatering. Finally, thermal drying will allow for the conventional handling of the product.

There are many potential advantages for recovering stored ash. These include: the advantage of operating “on demand,” thereby minimizing storage requirements and reducing capital costs; production from large known reserves that are in or near high-priced and underserved markets; the potential to produce highly beneficiated ash with superior performance at competitive costs; and finally, the potential to produce multiple products, including aggregates from a single source.

There are also substantial disadvantages. As discussed, these deposits are heterogenous and will require substantial planning and resource assessment. Recovery systems must be designed, tailored to the deposit, and implemented. Products must be evaluated and tested. Finally, although there are plans in progress, no large recovery operation is currently in place, representing a substantial unknown for investors.

## References

ASTM C618—12. (2012). *Standard specification for coal fly ash and raw or calcined natural pozzolan for use in concrete*. West Conshohocken, PA, USA: American Society for Testing and Materials.

ASTM C778—13. (2013). *Standard specification for standard sand*. West Conshohocken, PA, USA: American Society for Testing and Materials.

Australian Standard AS3582.1. (2007). *Supplementary cementitious materials for use with portland and blended cement—Part 1: Fly ash*. Standards Australia International.

BS EN 450-1. (2012). *Fly ash for concrete: Definition, specifications and conformity criteria*. London, UK: British Standards Institution.

Bureau of India Standards. (2003a). IS 3812-1: Specification for pulverized fuel ash, Part 1: For use as Pozzolana in cement, cement mortar and concrete, New Delhi.

Bureau of India Standards. (2003b). IS 3812-2: Specification for pulverized fuel ash, Part 2: For use as admixture in cement mortar and concrete, New Delhi.

CAN/CSA. (2013). *A3001-13 cementitious materials for use in concrete*. Canadian Standards Association, Toronto British Standards Institution.

CEN EN 196-1. Specification for Standard sand (also ISO 679).

GOST 25818-91. Thermal plant fly-ashes for concretes. http://gostexpert.ru/data/files/25818-91/f0e477bffb4cb1657b52d8e7050a8c41.pdf.

Hill, R., Zhang, Z., & Shaw, B. (2009). *A fly ash carbon treatment for producing a marketable product for activated carbon contaminated fly ash*. World of Coal Ash. www.flyash.info.

Howard, C., Kabis, S., & Farrington, S. A. (2013). *Advances in chemical beneficiation of fly ashes containing natural carbon or powdered activated carbon*. World of Coal Ash www.flyash.info.

Kelly, R. P. (2015). *Parallels and non-conformities in worldwide fly ash classification: The need for a robust, universal fly ash classification system for fly ash*. World of Coal Ash. www.flyash.info.

Keppeler, J. G. (2001). Carbon burn-out an update on commercial applications. In: *International ash utilization symposium*. www.flyash.info.

People's Republic of China National Standard GB/T 1596—2005. (2005). Fly ash used for cement and concrete.

Japanese Standards Association. (1999). Fly ash for concrete uses, JIS A 6201.

Vasiliauskas, A., Shilling, M., & Willauer, C. S. (1999). Successful fly ash beneficiation at Carolinas Power and Light's Roxboro station. In: *International ash utilization symposium*. www.flyash.info.

# Assessing ash quality and performance

# 9

*L.L. Sutter*[*], *D.P. Bentz*[†]
[*]Michigan Technological University, Houghton, MI, United States, [†]NIST, Gaithersburg, MD, United States

## 9.1 Introduction

Fly ash for use in concrete is typically specified according to ASTM C618 *Standard Specification for Coal Fly Ash and Raw or Calcined Natural Pozzolan for Use in Concrete* (ASTM C618, 2015) and characterized/evaluated using test methods for sampling and testing provided in ASTM C311 *Standard Test Methods for Sampling and Testing Fly Ash or Natural Pozzolans for Use in Portland-Cement Concrete* (ASTM C311, 2013). Both documents are overseen by the ASTM C09.24 Subcommittee on Supplementary Cementitious Materials. Internationally, other material specifications and tests are used with the purpose of characterizing the same properties discussed in this chapter. References to specific ASTM standards are provided for context.

Within ASTM C618, usable fly ash materials are identified as either Class F or Class C. ASTM C618 also specifies a Class N, which describes natural pozzolan materials. Class F fly ash is historically obtained from burning anthracite or bituminous coal, while Class C from burning lignite or subbituminous coal. However, modern combustion processes utilize coal blends to optimize burner operations with respect to efficiency, cost, and air quality. Therefore, tracing an ash class to a specific coal type is less meaningful. The ASTM C618 specification lists both chemical and physical requirements that the fly ash must meet or exceed. Chemical requirements include a minimum value for the "sum of the oxides" (SUM), which is the sum of the $SiO_2$, $Al_2O_3$, and $Fe_2O_3$ contents, and maximum values for the $SO_3$ content, moisture content, and loss on ignition (LOI) of the fly ash. The latter three values are the same for Class F and Class C fly ashes, making SUM the primary distinction between the two classes. The sum of oxides has a minimum value of 70% for Class F ash and 50% for Class C fly ashes. This separation means the CaO content of Class C fly ashes usually exceeds that found in Class F fly ashes, but once again there can be exceptions to this comparison. Specified physical requirements include: fineness (i.e., maximum amount retained on a 45 μm sieve), strength activity index (SAI) at 7 days and 28 days, water requirement relative to an ordinary Portland cement control mortar, soundness as evaluated using autoclave expansion, and limits on the maximum variations in measured density and fineness. Finally, the user of the specification may elect to include optional physical requirements that test mixtures with fly ash and Portland cement and

**Coal Combustion Products (CCP's).** http://dx.doi.org/10.1016/B978-0-08-100945-1.00009-5

consider drying shrinkage, variability in air content, control of alkali-silica reaction (ASR), and sulfate resistance. In most of these optional tests, performance is measured relative to a control mixture prepared using cement only for the cementitious component.

ASTM C618 specifies the minimum physical and chemical requirements for a fly ash, while ASTM C311 provides the test methods used to evaluate fly ash performance with respect to these requirements. Procedures are provided for determining moisture, LOI, available alkali, and ammonia contents, the oxide composition, the physical properties of density and fineness, and specific performance tests to assess drying shrinkage, soundness, air entrainment in mortar, SAI, water requirement, and effectiveness at mitigating alkali silica reactions (ASR) and sulfate attacks. Overall, the ASTM C618 and C311 standards have provided an adequate quality control system for fly ash, but they provide little insight into the projected performance of a specific fly ash in a specific concrete mixture. This shortcoming has been recognized for many years, and efforts continue to improve the existing standards and develop more discerning and pertinent test procedures. Some examples of recent efforts in this area will be provided in the sections on LOI (i.e., carbon content) and air entrainment issues and test methods that will be discussed next. The SAI will be considered in more detail at the end of this chapter, where alternates will also be discussed.

## 9.2 Carbon content and loss on ignition

### 9.2.1 Carbon in fly ash

An important characteristic of fly ash is the presence of various forms of carbon intermixed with the fly ash. The carbon resulting from combustion is present in different forms broadly classified as char particles that are typically 5–50 μm, or soot and carbon black particles that are typically a micrometer or less in diameter. More recently, an additional external source of carbon has been introduced into fly ash. Specifically, in many power plants powdered activated carbon (PAC) is commonly added to the combustor exhaust stream to adsorb mercury and other constituents whose emissions are limited by air quality standards.

The combustion of coal is a two-step process where initially gases and highly volatile components are driven out of the coal structure, leaving behind a carbon char that burns as a second step. These chars either burn in the combustor or are carried out of the furnace as unburnt carbon intermixed in the fly ash (Bailey, Tate, Diessel, & Wall, 1990). These char particles exhibit a wide range of morphologies depending on the coal maceral from which they originated. The texture, porosity, and specific surface area of these chars vary with changes in particle morphology. The other class of carbon (i.e., soot and carbon black) condenses out of the exhaust stream of the combustor as the stream cools in the exhaust path. It is more difficult to characterize the morphology of these submicron soot particles.

The general problem with carbon in fly ash is twofold. The lesser problem is one of adding color, which affects architectural applications, but is generally not a concern for most structures. The far more serious problem is that carbon can readily adsorb organic chemicals, such as air entraining admixtures (AEAs), on to its surface. To develop this idea, a brief review of the air entrainment mechanism is provided in the following section.

### 9.2.2 Air entrainment in concrete

Air bubbles are purposefully entrained in concrete to provide resistance to cyclic freeze-thaw (F-T) exposure. A detailed discussion of air entrainment and F-T protection is beyond the scope of this discussion, and the reader is directed to the numerous textbooks and publications that address the issue. Suffice it to say that in order to provide protection from F-T exposure, a system of properly spaced and sized air bubbles is required in the hardened cement paste matrix. This is accomplished through the use of AEAs. An AEA is an organic compound made from natural sources, such as wood resins or tall oil, or synthetic chemicals. The AEA has an anionic, hydrophilic "tail" and a nonionic, hydrophobic "head," as shown schematically in Fig. 9.1A. As shown schematically in Fig. 9.1B, the hydrophilic, anionic polar groups (i.e., head) sorb strongly to the ionic cement particles while the hydrophobic, nonpolar portion of the surfactants (i.e., tail) orient towards the solution and stabilize, or entrain, air bubbles, and prevent the smaller bubbles from coalescing into larger ones (Bruere, 1955).

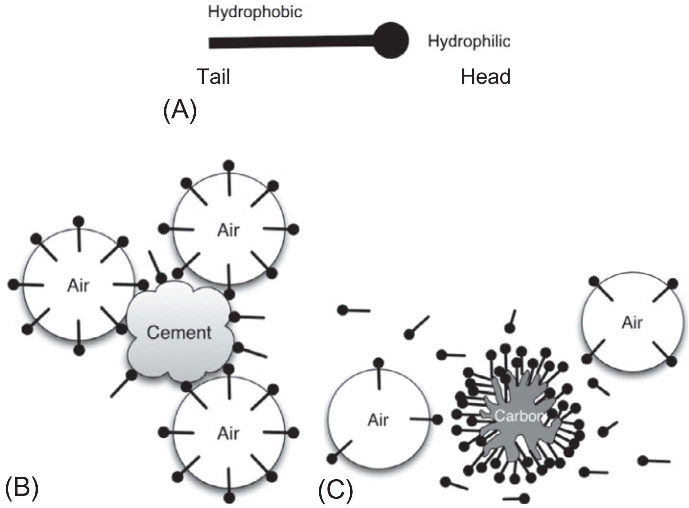

**Fig. 9.1** Schematic representation of (A) an air entraining admixture (AEA) molecule, (B) AEA stabilizing air in a concrete system, and (C) carbon preferentially adsorbing AEA and rendering the chemical ineffective at entraining air.
From Sutter, L. L., Hooton, R. D., & Schlorholtz, S. (2013). *Methods for evaluating fly ash for use in highway concrete, NCHRP report 749* [54 pp.]. Washington, DC: National Cooperative Highway Research Program, Transportation Research Board of the National Academies, with permission.

### 9.2.3 Effect of carbon on air entrainment

When adsorbent carbon is present, it preferentially adsorbs the AEA, diminishing the residual AEA concentration in the mixture water to a point where effective air bubble stabilization does not occur. This is shown schematically in Fig. 9.1C. To offset this adsorption, a higher quantity of AEA must be added to a concrete mixture containing fly ash to ensure the desired air-void structure formation. However, with variation in carbon content in fly ash, it is difficult to specify the proper amount of air entrainment required, and often the AEA dosage is either inadequate or excessive.

The adsorption potential of carbon is a function of the porosity, surface texture, surface chemistry, and specific surface area of the carbon particles. These properties all vary as the combustion conditions vary. PAC is, by design, highly adsorbent and potentially presents a significant problem when included in a concrete mixture.

### 9.2.4 Loss on ignition test

Under current specifications, the abundance of carbon in fly ash is determined by means of a LOI test, and there are specified maximum limits for LOI in fly ash (i.e., 6% LOI in ASTM C618). The LOI procedure is provided in ASTM C311, which in turn refers to ASTM C114 *Standard Test Methods for Chemical Analysis of Hydraulic Cement*. In the LOI test, a dry sample of fly ash is ignited at 750°C until a constant mass is achieved; the percentage loss of mass is calculated and reported as the LOI.

The LOI test is a reasonable predictor of total carbon content when the only volatile phases in the fly ash are unburned, residual carbon. However, materials combusted along with the coal or stack additives can affect the results (Schlorholtz, 2006, chap. 43). Other tests for carbon are sometimes used instead of LOI because in addition to being more accurate for total carbon content, they are typically much faster. These include dedicated carbon determination units that work on a LOI principal but selectively analyze only volatilized carbon.

Although the LOI test effectively limits the total carbon in fly ash, it does so without consideration for the type of carbon or its adsorption capacity. Not all carbon forms will exhibit the same adsorption behavior; identifying the carbon form, or more specifically identifying the adsorption capacity, is far more useful than simply specifying the total carbon through limiting the LOI.

## 9.3 Adsorption-based tests for characterizing carbon in fly ash

### 9.3.1 Foam index test

The foam index test is used as a quick screening test to estimate the effect of a particular fly ash on the air entrainment of concrete. The test requires observing the stability of the foam produced when the fly ash, or fly ash and cement, and diluted AEA are combined with water and agitated. The test provides a quick indication of possible changes in the amount of AEA required when using the same materials combination in concrete. The foam index test procedure is currently not standardized and numerous variations of the test are reported in the literature. A review of the various published procedures was provided by Harris, Hover, Folliard, and Ley (2008).

In general, the procedure involves adding diluted AEA solution to the test slurry, agitating the mixture after the addition of the AEA, then visually monitoring the slurry surface for formation of a "stable foam." If the foam is determined to not be stable after a "cycle" (i.e., addition of the AEA solution, agitation, and observation), another cycle is performed. The AEA solution is added drop by drop, usually one drop per cycle, using either a laboratory syringe or a micropipette capable of dispensing individual drops of a prescribed size. This incremental process is continued until a stable foam is observed, which is defined as one that covers the entire surface of the slurry in the test container and persists for a prescribed observation time without dissipating (e.g., 15–60 s, depending on the method used).

How the foam index is expressed varies among users. Many express the foam index simply as the number of AEA solution drops required to achieve a stable foam. Using this approach, a constant AEA solution concentration is used, and as will be discussed, a single solution concentration is not the optimum for a range of ash types. However, for a consistent fly ash, cement, and AEA materials combination, the number of drops is a measure that can identify variation in that combination. In some cases the total amount of undiluted AEA, known as the absolute volume of AEA, is determined by a variety of approaches, such as weighing the syringe before and after the test and calculating the volume of AEA based on the mass consumed, the solution concentration, and the AEA specific gravity. A more common approach is to simply calculate the absolute volume of AEA, as shown in Eq. (9.1).

$$\text{Absolute volume AEA} = N_{\text{D}} \times V_{\text{D}} \times C_{\text{S}} \tag{9.1}$$

where absolute volume AEA is the volume of undiluted AEA added, mL; $N_{\text{D}}$ is the number of drops; $V_{\text{D}}$ is the volume of each drop, mL (typically 0.02–0.05 mL, determined experimentally); and $C_{\text{S}}$ is the concentration of the AEA solution, mL undiluted AEA per mL solution.

Another useful form of the foam index is the relative foam index, which is the ratio of the foam index using cement and fly ash to that of a cement-only test sample, expressed as a percentage. When testing combined fly ash and cement samples, the typical ratio of cement to fly ash is 4:1, although a range of replacement levels are reported, depending on the specific method used.

The foam index test, because of the short contact time and constantly changing solution concentration, does not determine the AEA adsorption at equilibrium; therefore using the test to predict absolute changes in AEA dosage requires considerable experience with the specific materials being tested. The foam index test is an empirical test and provides an estimate of the instantaneous adsorption capacity of a fly ash. A variation in performing any aspect of the procedure may cause variation in the results. Also, the test is subjective; determination of a "stable foam" varies by operator, as does the agitation energy. However, it is still a useful tool, particularly for simple measurements in the field or ready-mix operation.

Changes to the foam index test have been suggested to improve reproducibility and precision. One suggested change is to select an optimum AEA solution concentration for the fly ash being tested (Sutter, Hooton, & Schlorholtz, 2013). In terms of proportions for an adsorption test, the optimum balance of adsorbent (i.e., fly ash) and adsorbate (i.e., AEA solution) occurs when the lowest possible AEA solution concentration can be used to achieve a stable foam layer in the prescribed time. The best accuracy and reproducibility, as well as the lowest degree of subjectivity, is achieved when an incremental addition represents a small change in the total AEA added. That is, if after some number of cycles the technician performing the test believes the foam to be stable, the least subjective test is one where another increment of AEA can be added and another cycle performed to verify that a stable foam has been achieved; the addition of that extra increment is only a small percentage of the total AEA added. Conversely, if the AEA solution is too dilute, the time required to achieve the end of the test could literally be hours, therefore making the test impractical. High solution strengths increase the error associated with the incremental AEA addition, but reduce total analysis time. Increased quantities of fly ash in the slurry will require a commensurate increase in AEA addition, leading to the problems previously described.

Research on optimal conditions for the foam index test indicate that 12–18 min is the optimal test duration in terms of practicality and AEA addition rate (Sutter et al., 2013). To achieve a foam index result in this time period, the recommended solution strengths are 2%, 6%, 10%, and 15% AEA by volume (Sutter et al., 2013), although any concentration can be used. It is necessary to experiment with the different solutions to establish the correct choice by discarding test results that take less than 12 or more than 18 min and by using a lower or higher solution concentration, respectively (Sutter et al., 2013).

Likewise, the agitation time and energy is important; longer agitation times lengthen the test, while shorter agitation times may lead to insufficient initial contact between the AEA and the fly ash. Use of a mechanical agitator has been proposed to reduce the subjectivity of the shaking intensity and length (Sutter et al., 2013).

The foam index test is an assessment of instantaneous adsorption, not the adsorption that occurs at equilibrium. Additionally, the foam index test is not quantitative; it does not directly provide the amount of AEA adsorbed. Therefore direct measurement of the adsorption isotherm is often more useful for predicting AEA adsorption and performance.

### *9.3.2 Adsorption isotherms*

The fundamental tool for understanding adsorption capacity of organic chemicals onto carbon is the adsorption isotherm. An adsorption isotherm is used to describe the equilibrium between the solid phase and liquid phase concentration of an adsorbate. Determining the adsorption isotherm is a relatively straightforward test than can be performed with conventional laboratory equipment (e.g., flasks, beakers, or stir plates). To measure an adsorption isotherm, a mass of adsorbent is mixed with a solution of adsorbate, with initial concentration $C_0$, for a prescribed period of time sufficient for adsorption to occur and reach equilibrium. After the prescribed time, the reduction in solution concentration of adsorbate is determined. This process is repeated for a number of different quantities of adsorbent. Alternatively, the quantity of adsorbent can remain constant with each test, and the solution concentration can be varied. The results of this series of tests are plotted on a log-log scale, and the data is fit with a power law fit; the slope and intercept of this fit determine the constants for the Freundlich equation shown in Eq. (9.2). The driving force for adsorption is the concentration gradient between the solution and the adsorbate on the adsorbent surface; therefore as shown in Eq. (9.2), the adsorption capacity ($q$) is a function of the solution concentration. This is one reason why the foam index test does not achieve a true equilibrium; the solution concentration is constantly being altered by the addition of more AEA solution.

$$q = K \times C^{1/n} \tag{9.2}$$

where $q$ is the mass of adsorbate adsorbed per unit mass of adsorbent, mg/g; $K$ is the Freundlich isotherm capacity parameter, (mg/g) $(\text{L/mg})^{1/n}$; $C$ is the solution concentration, mg/L; and $1/n$ is the Freundlich isotherm intensity parameter, dimensionless.

An example isotherm is shown in Fig. 9.2 for an iodine solution adsorbed by fly ash.

### 9.3.3 Determination of fly ash iodine number

The fly ash iodine number is based on tests developed in the water treatment industry for measuring the adsorption capacity of activated carbon. ASTM D4607 *Standard Test Method for Determination of Iodine Number of Activated Carbon* is designed

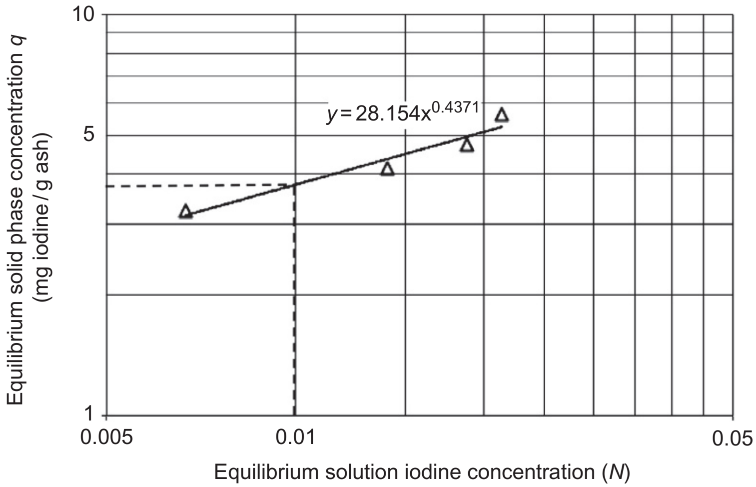

**Fig. 9.2** Example of iodine adsorption isotherm for coal fly ash.
From Sutter, L. L., Hooton, R. D., & Schlorholtz, S. (2013). *Methods for evaluating fly ash for use in highway concrete, NCHRP report 749* [54 pp.]. Washington, DC: National Cooperative Highway Research Program, Transportation Research Board of the National Academies, with permission.

to quantitatively characterize the adsorption capacity of activated carbons that have a high adsorption capacity. The test serves as a good indication of the microporosity of carbon, as an iodine molecule is very small (Sontheimer, Crittenden, & Summers, 1988). The results of an ASTM D4607 test are shown in Fig. 9.2. A standard iodine solution ($C_0$) is contacted with four different masses of fly ash. The ash-treated solutions are filtered to separate the ash from the solution, and the iodine remaining in the filtrate is measured by titration. The amount of iodine adsorbed per gram of fly ash is determined for each mass of fly ash and plotted versus the residual solution concentration on a log-log scale. From the resulting plot, the amount of iodine adsorbed (mg iodine/g fly ash) at a residual iodine solution concentration of 0.01 N is reported as the iodine number of the fly ash. Because a standard solution is used (i.e., iodine), the test provides a relative measure of adsorption capacity that can be used to compare the different adsorption capacities of fly ash materials.

For use with fly ash, the ASTM D4607 test was modified to use a lower initial solution concentration ($C_0$) than recommended for activated carbon (i.e., 0.025 N as compared to 0.1 N), and a lower residual concentration for determining the iodine number (i.e., 0.01 N as compared to 0.02 N). The contact time was also increased (5 min as compared to 30 s) to account for the slower rate of reaction with a more dilute initial concentration.

Treatment of the fly ash is required prior to performing the fly ash iodine number test. The purpose of the treatment is to acidify the fly ash and remove any sulfur from the material. Iodine converts to iodide in a basic environment. Therefore acidifying the fly ash is necessary to ensure that all observed reduction in iodine concentration results from iodine adsorption rather than conversion to iodide. For the developed method, the ash was treated with one cycle of boiling in 5 wt.% HCl.

Although the iodine number test based on a modified version of ASTM D4607 demonstrates well the basic principal of iodine adsorption, the test itself is more rigorous than required for measuring fly ash adsorption. The four-point isotherm approach is useful for accurately determining the adsorption capacity of highly activated carbon. More recent research has been performed to adopt a single-point isotherm method for use with fly ash, based on ASTM D1510 *Standard Test Method for Carbon Black-Iodine Adsorption Number*. The test uses the same ash pretreatment as described for the modified ASTM D4607 test. However, the ash is contacted with a 0.025 N iodine solution and the amount adsorbed at that concentration is taken as the iodine number for the ash (Sutter, Vruno, Anzalone, & Dong, 2014).

### *9.3.4 Determination of direct adsorption isotherm*

An adsorption isotherm for a specific materials combination provides the equilibrium relationship between the solid and liquid phase concentrations of the adsorbate. For the case of fly ash and AEA, the solid phase concentration represents the mass of AEA sorbed per mass of ash, while the liquid phase concentration represents the residual adsorbate concentration of the solution. To achieve a specific solution concentration, extra AEA must be added to satisfy the adsorption capacity of the fly ash. An adsorption isotherm is unique for the combination of materials; with a given adsorbent, the amount of adsorbate sorbed on the solid is dependent on the properties of the adsorbent as well as the solid. Therefore to fully characterize the adsorption properties of a system of materials, the isotherm must be established using those specific materials. The iodine number test will characterize the adsorption properties of the solid phase (i.e., fly ash) with iodine, but the actual adsorption of AEA will be affected by the AEA used as well as the presence of the cement.

A standard test for determining the adsorption isotherm for activated carbon is ASTM D3860 *Standard Practice for Determination of Adsorptive Capacity of Activated Carbon by Aqueous Phase Isotherm Technique*. This procedure determines the adsorptive capacity of activated carbon for a specific adsorbate species by contacting an aqueous solution of the adsorbate with activated carbon, determining the amount of the constituents removed from solution, and calculating the adsorptive capacity from a Freundlich isotherm plot. This standard procedure cannot be applied directly to the case of AEA adsorption by fly ash because chemisorption by the cement and physical adsorption by the fly ash are taking place at the same time. Therefore to be applied to fly ash, modifications to the existing standard test are required.

The first modification is to use a mixture of cement and fly ash as the adsorbent. The cement reduces the solution concentration of AEA, as shown in Fig. 9.3. When the cement comes in contact with the AEA solution, a portion of the AEA chemisorbs

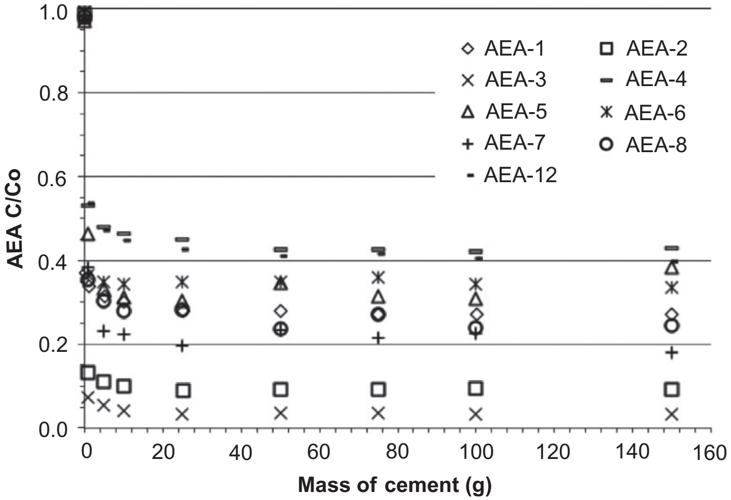

**Fig. 9.3** The result of chemisorption of AEA by cement. The AEA concentration in solution after contact is shown as the ratio $C/C_0$, where $C$ is the residual solution concentration after contact and $C_0$ is the initial solution concentration. The amount of chemisorption is dependent on the AEA type and independent of the cement type.

From Sutter, L. L., Hooton, R. D., & Schlorholtz, S. (2013). *Methods for evaluating fly ash for use in highway concrete, NCHRP report 749* [54 pp.]. Washington, DC: National Cooperative Highway Research Program, Transportation Research Board of the National Academies, with permission.

onto the cement almost instantaneously. The amount of chemisorption is independent of the amount of cement above a certain quantity of cement (i.e., 20 g cement) and is independent of the cement type (Sutter et al., 2013). Because the physical adsorption by fly ash is dependent upon the solution concentration, it is required to account for the impact of the cement on the initial solution concentration. Beyond the chemisorption demonstrated, cement shows no appreciable physical adsorption (Sutter et al., 2013).

The second modification is to establish how the solution concentration of AEA is determined. ASTM D3860 does not specify an analytical method, and generally the adsorbate is a simple organic chemical and the solution concentration is determined by standard analytical methods. Measuring AEA concentration is more difficult because AEAs are a mixture of complex organics. The chemical oxygen demand (COD) test is often used in water treatment to measure the dissolved organics in water. The test uses extreme oxidation conditions through a strong oxidizing agent (i.e., potassium dichromate $K_2Cr_2O_7$), strong acid (i.e., sulfuric acid $H_2SO_4$), and high temperature (i.e., 150°C). Nearly all organic compounds are oxidized to $CO_2$ and measured as milligrams of oxygen consumed per liter of water. Commercially available kits are available to measure COD; this approach provides a reliable and accurate method for determining AEA concentration in solution (Sutter et al., 2013).

To measure the direct adsorption isotherm, at least three samples of fly ash and cement (40 g fly ash/20 g cement for each test) are contacted with three AEA solutions of varying concentrations for 60 min. The residual AEA concentration is measured, and the adsorbed AEA concentration is then calculated. The results are plotted in the same manner as those shown in Fig. 9.2, and the Freundlich isotherm parameters are determined. To use the isotherm, the desired solution concentration ($C_s$) is calculated based on the AEA dosage and the volume of mixing water. The adsorption capacity ($q$) is calculated or read from the graph and is provided in units of mL/g fly ash. The sum of $C_i$ and $q$ is the estimated dosage of AEA required to achieve the desired solution concentration (Sutter et al., 2013).

### 9.3.5 Methylene blue

Other sorption-based methods have been investigated. In research by McCarthy, Islam, Csetenyi, and Jones (2012), the adsorption capacity of fly ash was determined by a colorimetric method. A solution of Acid Blue 80 (AB80) was contacted with fly ash and filtered; the filtrate was then analyzed with a spectrophotometer to measure the concentration of residual AB80. The blue dye was selected because its molecular size is similar to that of AEAs. A good correlation was found between measured adsorption capacity and increases in AEA dosage to produce a target air content in lab-scale mortar and concrete mixtures in which the tested fly ashes partially replaced the cement. The adsorption capacity results obtained also correlated well with $N_2$ adsorption surface area measurements (BET).

Subsequent work with blue dye was reported by Islam, McCarthy, Csetenyi, and Jones (2012) investigating AB80 and methylene blue adsorbates. The methylene blue test was derived from a British test method used to evaluate sand for clay content and is noninstrumental, relying on a subjective measure of color intensity. Both methods were found to correlate well with $N_2$ surface area measurements, and a relationship was found with increased AEA demand when the fly ashes studied were employed in laboratory concrete mixtures. The referenced British test method is similar to ASTM C1777 *Standard Test Method for Rapid Determination of the Methylene Blue Value for Fine Aggregate or Mineral Filler Using a Colorimeter*, except the latter employs a spectrophotometer for measuring the concentration of methylene blue. Both papers discussing blue dye adsorbates reported better correlation between adsorption capacity and measured surface area than between the adsorption capacity and LOI.

## 9.4 Particle size measurement

The particle size distribution of fly ash is specified as fineness in ASTM C618. The test method used to measure fineness is ASTM C430 *Standard Test Method for Fineness of Hydraulic Cement by the 45-µm (No. 325) Sieve*. In this test method, the fly ash sample is wet sieved on a 45-µm sieve. To meet ASTM C618, a fly ash must have a maximum of 34% retained on the 45-µm sieve. The amount of material retained on the 45-µm sieve provides a general indicator of the total amount of fine material present, but this fraction is not indicative of the total material that contributes to the hydration reaction in concrete.

Fineness of fly ash (i.e., particle size distribution) affects the water demand for a given level of concrete workability, as well as the reactivity of the fly ash in concrete mixtures. Fly ash particles have a greater distribution of smaller particles as compared to Portland cement. Because of this, fly ash has a greater specific surface area when compared to cement, and the replacement of cement by fly ash may result in increased water demand to wet the additional surface area. Reactivity is also affected by particle size. It is well known that a finely divided material will react with a solution faster than a coarser material. Therefore control of particle size will also impact properties such as strength, rate of strength gain, and ASR mitigation, all of which are dependent on the fly ash particle reacting with the mixing water of the concrete.

In addition to a sieve analysis, the fineness of fly ash can be determined using an air-permeability method, which provides a measure of specific surface area. ASTM C618 does not currently have a specific surface area requirement, but this requirement had been included in older versions of the standard along with the determination of fineness. The specific surface area can be estimated by using ASTM C204 *Standard Test Methods for Fineness for Hydraulic Cement by Air-Permeability Apparatus*, commonly referred to as the Blaine fineness. A Blaine fineness apparatus is used to draw air through a packed powder sample, and the specific surface area is calculated knowing the density and air flow versus time. This method can be used to provide a rapid indication of the average specific surface, which is affected by the particle size distribution. However, it does not provide a direct measure of particle size distribution.

Direct measurement of the particle size distribution for a fly ash is possible using sedimentation, or particle size analyzers based on laser diffraction or X-ray transmission (i.e., X-ray sedigraph). Sedimentation and particle size analyzers require the material to be analyzed while settling in water or another fluid of known viscosity and density. For Class C ash, this can present special problems due to its cementitious properties. When tested in water, Class C ash will begin to react during the test. Using an organic liquid (e.g., isopropanol) as the carrier fluid can avoid this problem. Laser-based particle size analyzers can also analyze material in air and these can be directly applied. Some sedimentation-based techniques require an extended duration to perform the analysis, whereas rapid tests that can determine the quality and usability of fly ash in minutes are desired. The wide range in particle composition and the presence of porosity in the fly ash (e.g., censospheres) affects the settling time and skews the particle size distribution. Particle size determination is still an area that needs more research to establish an effective method of determination.

## 9.5 Analysis for incompatibilities

Proper design of a concrete mixture containing fly ash requires compatibility of the cement, fly ash, and other powders, and any chemical admixtures being combined. An improper combination of materials can lead to mixtures that flash set, or conversely, it may sit for hours without setting; the latter case is due to excessive retardation of the hydration reactions. As will be shown in the examples that follow, one powerful tool for examining materials' compatibility is isothermal calorimetry, as outlined in the ASTM C1679 *Standard Practice for Measuring Hydration Kinetics of Hydraulic Cementitious Mixtures Using Isothermal Calorimetry* (ASTM C1679, 2014); a similar standard based on semiadiabatic calorimetry has been recently published by ASTM as ASTM C1753 *Standard Practice for Evaluating Early Hydration of Hydraulic Cementitious Mixtures Using Thermal Measurements* (ASTM C1753, 2015).

### *9.5.1 Sulfate optimization*

As many fly ashes provide a significant source of aluminate phases and/or their own source of (calcium) sulfates, sulfate optimization can be an issue in producing high-volume fly ash (HVFA) concretes that have desired constructability properties (Niemuth, Barcelo, & Weiss, 2012). The properties affected by sulfate imbalance include setting time and early-age strength development. Portland cements are generally optimized with respect to sulfate content based on measured compressive strengths at a specific target age, such as 7 days or 28 days. This "sulfate optimization" is commonly performed, assuming the material will be subsequently employed in a 100% Portland cement concrete mixture. The incorporation of relatively large quantities of fly ash into a concrete can thus result in systems that are either undersulfated, oversulfated, or in fortuitous cases, still properly sulfated.

As examples, Figs. 9.4 and 9.5 show the influence of additional gypsum (calcium sulfate dihydrate) on the hydration reactions in two different blended cement/fly ash mixtures prepared using the same highly reactive and retarding Class C fly ash (Bentz,

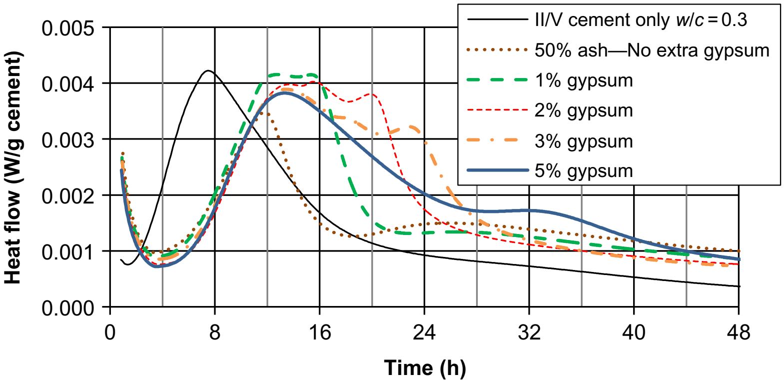

**Fig. 9.4** Isothermal calorimetry curves for Type II/V cement/Class C fly ash blends ($w/cm = 0.3$) with various addition levels of gypsum (Bentz, 2010).

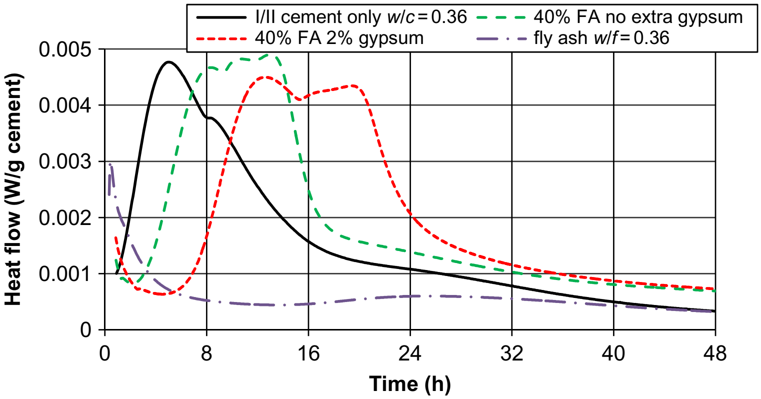

**Fig. 9.5** Isothermal calorimetry curves for Type I/II cement/Class C fly ash (FA) blends ($w/cm = 0.36$) with and without additional gypsum (Bentz, Ferraris, & Snyder, 2013).

2010; Bentz, Sato, De la Varga, & Weiss, 2012). In Fig. 9.4, an ASTM C150 Type II/V cement (2.5% $SO_3$ content by mass) was used, while in Fig. 9.5, the mixtures used an ASTM C150 Type I/II cement (3.27% $SO_3$ content by mass). As can be seen in Fig. 9.4, for the first cement blended with the fly ash on a 50:50 mass basis, the addition of supplemental gypsum had a pronounced positive effect on the hydration reactions, restoring the shape of the isothermal calorimetry curve to its expected form, but still not eliminating the excessive retardation produced by the use of Class C fly ash. While both the 1% and 2% addition levels of gypsum produce reasonable calorimetry curves, with distinct silicate and aluminate hydration peaks, 2% was selected as the optimum value for subsequent mixtures, based on those mixtures providing a slightly higher cumulative heat release value at 24 h (Bentz, 2010). This higher heat release should correspond to a higher 1-day strength as well (Niemuth et al., 2012). Conversely, as shown in Fig. 9.5, when the same fly ash is used with a Type I/II cement of higher sulfate content, at a 40:60 fly ash:cement ratio (by volume), a 2% addition of gypsum only results in a further unwanted retardation of the hydration reactions without significantly altering the shapes of the hydration peaks. Fig. 9.5 also shows the calorimetry results for a paste prepared from just the Class C fly ash and water, indicating its high initial reactivity. The prepared paste generates heat in a noticeable manner, and flash sets in a matter of minutes, though it does not develop any significant strength beyond that setting point. In both cases the influences of additional gypsum on the hydration reactions can be observed by using small samples and standardized isothermal calorimetry experiments on paste specimens, as opposed to the more labor-intensive conventional employment of strength testing (Niemuth et al., 2012).

## 9.5.2 High range water reducer incompatibilities

While the previous section focused on incompatibilities due to sulfate imbalance in simple cement/fly ash mixtures without chemical admixtures, additional issues often arise when a high range water reducer (HRWR) is included in the concrete mixtures, along with other admixtures. As shown previously by Roberts and Taylor (2007), excessive retardation can also be produced by the improper selection of an HRWR; in their particular study, a lignin-carbohydrate water-reducing admixture was used. A further example of this influence of HRWR on performance is provided in Fig. 9.6, showing the difference in hydration response depending on the selection of HRWR employed in a Type II/V cement/Class F fly ash blended paste (50:50 on a mass basis). While both HRWRs are observed to increase retardation, the performance of HRWR-B would almost certainly be unacceptable from a practical concrete construction viewpoint. In addition to dramatically lengthening the duration of the so-called "induction period," HRWR-B has also modified the basic shape of the peak in the calorimetry curve. The Class F fly ash by itself produced no retardation, so any

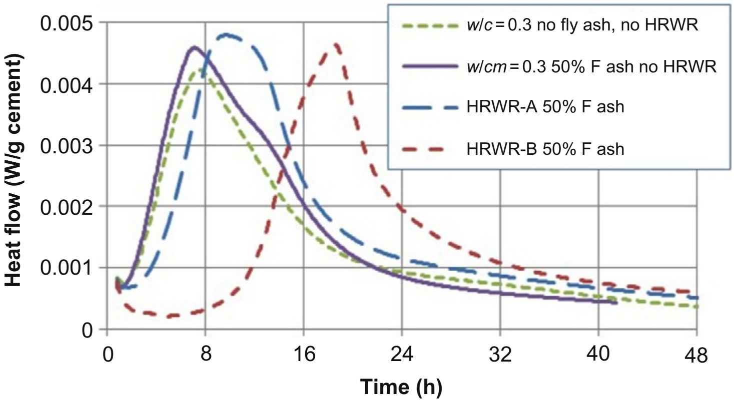

**Fig. 9.6** Isothermal calorimetry curves for a Type II/V cement/Class F fly ash blend with (two different) and without an HRWR (Bentz, Ferraris, et al., 2013).

delays in setting time for a blended paste without HRWR would be simply due to a dilution effect (e.g., the blended mixture containing only 50% of the cement present in the control mixture).

The above examples clearly indicate that calorimetry can be a useful tool in developing HVFA mixtures as it provides diagnostic information about the hydration reactions occurring in the paste. As complete and useful as this measurement technique is, it cannot readily predict all the important early-age performance issues of cement-fly ash mixtures such as false setting, early stiffening, etc. A more complete picture of how these mixtures will perform will often require additional test methods, such as modified versions of the ASTM C359 *Standard Test Method for Early Stiffening of Hydraulic Cement (Mortar Method)* (ASTM C359, 2013), a mini-slump test (currently under ASTM ballot), and rheometer tests based on the guidance provided in the ASTM C1749 *Standard Guide for Measurement of the Rheological Properties of Hydraulic Cementitious Paste Using a Rotational Rheometer* and elsewhere (ASTM C1749, 2012; Roberts & Taylor, 2007; Tanesi, Ardani, Meininger, & Nicolaescu, 2012).

## 9.6 Setting time delays and their mitigation

As cited in the 2012 NRMCA survey (Obla, Lobo, & Kim, 2012), an issue commonly encountered with HVFA concrete mixtures is their delayed setting, with corresponding delays in finishing and other construction operations.[1] Due to a substantial research effort in recent years, several viable mixture proportioning options have been developed to mitigate excessive delays in setting for fly ash concrete mixtures.

As with conventional Portland cement concretes, nonchloride accelerators can be effectively employed to reduce setting times of fly ash concrete mixtures (Cost, 2011; Keith & Schindler, 2012). Especially for HVFA concretes, higher dosages may be required to attain target setting times, such as that of a comparable 100% Portland cement concrete mixture. The dosage will also depend on the characteristics of the fly ash, the replacement level, and the expected curing temperatures. In general, lower curing temperatures and higher CaO contents in Class C fly ashes require higher dosages and, in some cases, acceptable setting behavior of a 50% HVFA mixture may not be achievable with this approach (Cost, 2011; Keith & Schindler, 2012). Nonchloride accelerators also can be fairly expensive, so economic considerations may sometimes dictate their use in a proposed cement/fly ash mixture.

As will be shown in the section to follow, one convenient method that has been already employed in practice for increasing the early-age strength of HVFA concrete mixtures, particularly during the winter construction season, is to switch to an ASTM C150 Type III (i.e., finer particle size) Portland cement. In practice, such a change typically has a significantly greater impact on early-age strength development than

---

[1] Low early-age strengths that also influence the timing of construction operations, such as formwork removal, will be considered as a separate issue in a subsequent section of this chapter.

on initial and final setting times. For example, one recent study (Bentz, Ferraris, De la Varga, Peltz, & Winpigler, 2010) indicated that switching to a Type III cement reduced the setting time delays by only about 1 h for two HVFA mortars, one with a Class C fly ash and the other with a Class F fly ash. The mixtures originally exhibited a 3- to 4-h delay in setting relative to a corresponding 100% Portland cement control mortar. However, for these same two HVFA mortars, this switch to Type III cement increased their 1-day compressive strengths by an impressive 60% on average. If Type III cement is being used to enhance early-age strengths, it is always a good idea to take into consideration its potential contributions to reducing setting time delays as the mixture proportions are being developed and optimized.

Different additions have been investigated for their ability to restore setting times of HVFA mixtures to values typical of those achieved for corresponding 100% Portland cement control mixtures. One study screened numerous candidate powders and identified calcium hydroxide and a rapid set cement as the two most promising candidates (Bentz, 2010). Table 9.1 provides representative setting times resulting from these additions in HVFA pastes prepared with either a Class C or a Class F fly ash (Bentz & Ferraris, 2010). For both fly ashes, a 5% calcium hydroxide addition by mass restored the initial and final setting times to be nearly identical to those of the control cement paste (i.e., no fly ash). For the rapid set cement, while a 5% addition was adequate for the Class F fly ash mixture, a 10% addition was required for the Class C fly ash. One additional consideration when employing these powder additions is their subsequent influence on compressive strength. While the rapid set cement addition has produced mortars with similar or superior long-term (28 days or 91 days) strengths, as compared to those of the control 100% Portland cement mortar, a significant decrease in 28-day strength on the order of 15% has been observed for HVFA mortars prepared with Class F fly ash and a 5% calcium hydroxide addition (Bentz, 2010; Bentz et al., 2010). Still, calcium hydroxide additions have been recently used in practice to produce HVFA concretes (e.g., 70% replacement of Portland cement) that exhibited greater bonding to reinforcing steel when compared to 100% Portland cement control concrete mixtures (Looney, Arezoumandi, Volz, & Myers, 2012),

**Table 9.1** Setting times for HVFA paste mixtures (Bentz & Ferraris, 2010)

| Paste mixture | Vicat initial set (h) | Vicat final set (h) |
|---|---|---|
| Type II/V cement, 0.67% HRWR | 5.1 | 5.9 |
| 50% C ash, 2% gypsum, 0.33% HRWR | 8.2 | 8.8 |
| 50% C ash, 2% gypsum, 5% CH, 0.33% HRWR | 5.3 | 6.0 |
| 50% C ash, 2% gypsum, 10% rapid set cement, 0.33% HRWR | 3.1 | 4.5 |
| 50% F ash, 0.87% HRWR | 8.6 | 10.2 |
| 50% F ash, 5% CH, 0.87% HRWR | 5.2 | 5.9 |
| 50% F ash, 5% rapid set cement, 0.87% HRWR | 3.3 | 4.5 |

although the measured compressive strengths of the HVFA mixtures were indeed about 20% lower than that of the control concrete.

In the initial screening study described above, a relatively coarse limestone powder, with a modal particle diameter of about 27 μm, had basically no effect on the early-age hydration response as assessed using isothermal calorimetry (Bentz, 2010). However, subsequent investigations have indicated that limestone powder additions can indeed be quite effective for mitigating setting time delays and increasing early-age strengths in HVFA mixtures when finer limestone particles are employed (Bentz, Sato, et al., 2012; Cost & Bohme, 2012; Gurney, Bentz, Sato, & Weiss, 2012). Results when using a fine limestone with a median particle diameter on the order of 1 μm have been particularly promising (Bentz, Tanesi, & Ardani, 2013; Gurney et al., 2012). The fine limestone particles provide additional surface area for the precipitation and growth of calcium silicate hydrate gel and other products from the cement hydration and pozzolanic reactions. Additionally, the fine limestone particles can also participate in these reactions leading to the formation of stable carboaluminate phases, as opposed to conventional sulfoaluminates. The carboaluminate phases may be stiffer than the sulfoaluminate phases that would be formed in the absence of limestone, further contributing to strength enhancements (Moon et al., 2012).

A study employing four different modal diameters of limestone powders has indicated the reduction in setting time for a fixed set of mixture proportions is directly proportional to the provided limestone surface area, as quantified by BET surface area measurements (Gurney et al., 2012). Fig. 9.7 illustrates this linear relation for mixtures with either a Class C or a Class F fly ash, where in some mixtures a portion of the fly ash has been replaced by limestone powder. In this study, titanium dioxide (anatase), with a surface area similar to that of one of the limestone powders, was also included as an inert material to confirm that both the size and chemical natures of the powder material are critical to its ability to accelerate early-age reactions in cement-based materials. While a nano-limestone provided the most significant reduction in setting times, the performance of a fine limestone powder with a 0.7 μm median particle diameter was also quite acceptable.

As another example, the same 0.7 μm fine limestone has been subsequently employed in a series of HVFA concrete mixtures (Bentz, Tanesi, et al., 2013), whose mixture proportions are provided in Table 9.2. As indicated in Fig. 9.8, the replacement of a portion of the fly ash with a fine limestone powder markedly reduces setting time delays in these more sustainable concretes. In addition to their improvement of setting times, the fine limestone powder additions also provided substantial benefits to mechanical (strength) and transport (electrical resistivity) properties (Bentz, Tanesi, et al., 2013).

## 9.7 Strength development issues and their mitigation

The classical approach to increasing concrete strengths, at all ages, is to reduce the water-to-cement ratio (*w/c*) in a Portland cement concrete, or equivalently the *w/cm* in a concrete containing fly ash. The advent of HRWRs, also known as

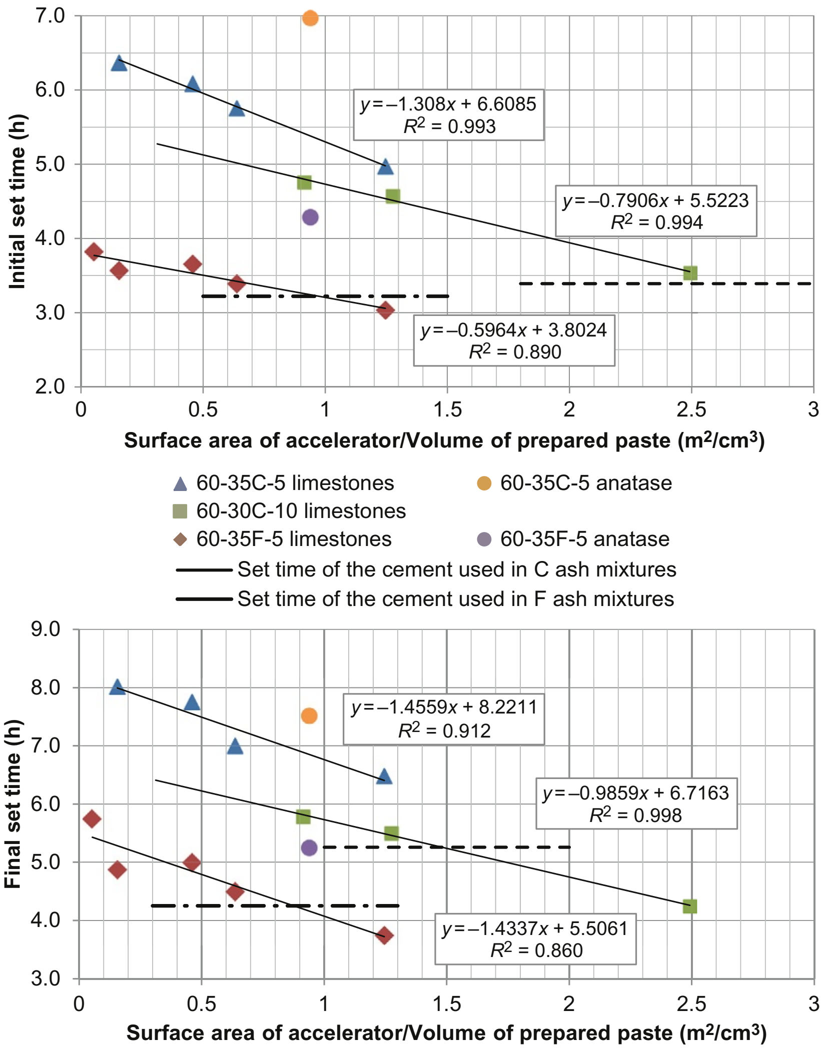

**Fig. 9.7** Correlation between initial *(top)* and final *(bottom)* setting times and surface areas of the accelerating powders.

Taken from Gurney, L., Bentz, D. P., Sato, T., & Weiss, W. J. (2012). Reducing set retardation in high volume fly ash mixtures with the use of limestone: Improving constructability for sustainability. Transportation Research Record, Journal of the Transportation Research Board, No. 2290. *Concrete Materials, 2012*, 139–146.

superplasticizers in their early days, has permitted substantial reductions in *w*/*c* or *w*/*cm* without a significant loss of slump or workability. Thus decreasing *w*/*cm* of an HVFA mixture to obtain more acceptable early-age and 28 days strengths is common practice. For a 100% Portland cement target concrete, with a *w*/*c* in the range of

**Table 9.2** **Concrete mixture proportions for study of HVFA with fine limestone (Bentz, Tanesi, et al., 2013)**

| Mix ID | Cementitious (kg/m$^3$) [(lb/yd$^3$)] | Type I/II cement (kg/m$^3$) [(lb/yd$^3$)] | Class F fly ash (kg/m$^3$) [(lb/yd$^3$)] | Class C fly ash (kg/m$^3$) [(lb/yd$^3$)] | Limestone 0.7 µm (kg/m$^3$) [(lb/yd$^3$)] | Coarse aggreg. (kg/m$^3$) [(lb/yd$^3$)] | Fine aggreg. (kg/m$^3$) [(lb/yd$^3$)] | Water content (kg/m$^3$) [(lb/yd$^3$)] | *w/cm* | HRWR (fl oz/ cwt) |
|---|---|---|---|---|---|---|---|---|---|---|
| PC | 335 [564] | 335 [564] | | | | 1040 [1750] | 858 [1444] | 134 [226] | 0.40 | 7.7 |
| 40F | 291 [491] | 201 [338] | 91 [153] | | | 1040 [1750] | 858 [1444] | 134 [226] | 0.46 | 3.8 |
| 30F10L | 297 [499] | 201 [338] | 68 [114] | | 28 [47] | 1040 [1750] | 858 [1444] | 134 [226] | 0.45 | 3.8 |
| 40C | 310 [522] | 201 [338] | | 109 [183] | | 1040 [1750] | 858 [1444] | 134 [226] | 0.43 | 3.0 |
| 30C10L | 311 [523] | 201 [338] | | 82 [138] | 28 [47] | 1040 [1750] | 858 [1444] | 134 [226] | 0.43 | 3.0 |
| 60F | 270 [454] | 134 [226] | 136 [229] | | | 1040 [1750] | 858 [1444] | 134 [226] | 0.50 | 3.8 |
| 45F15L | 278 [467] | 134 [226] | 102 [172] | | 41.6 [70] | 1040 [1750] | 858 [1444] | 134 [226] | 0.48 | 3.8 |
| 60C | 298 [501] | 134 [226] | | 163 [275] | | 1040 [1750] | 858 [1444] | 134 [226] | 0.45 | 3.0 |
| 45C15L | 298 [502] | 134 [226] | | 122 [206] | 41.6 [70] | 1040 [1750] | 858 [1444] | 134 [226] | 0.45 | 3.0 |

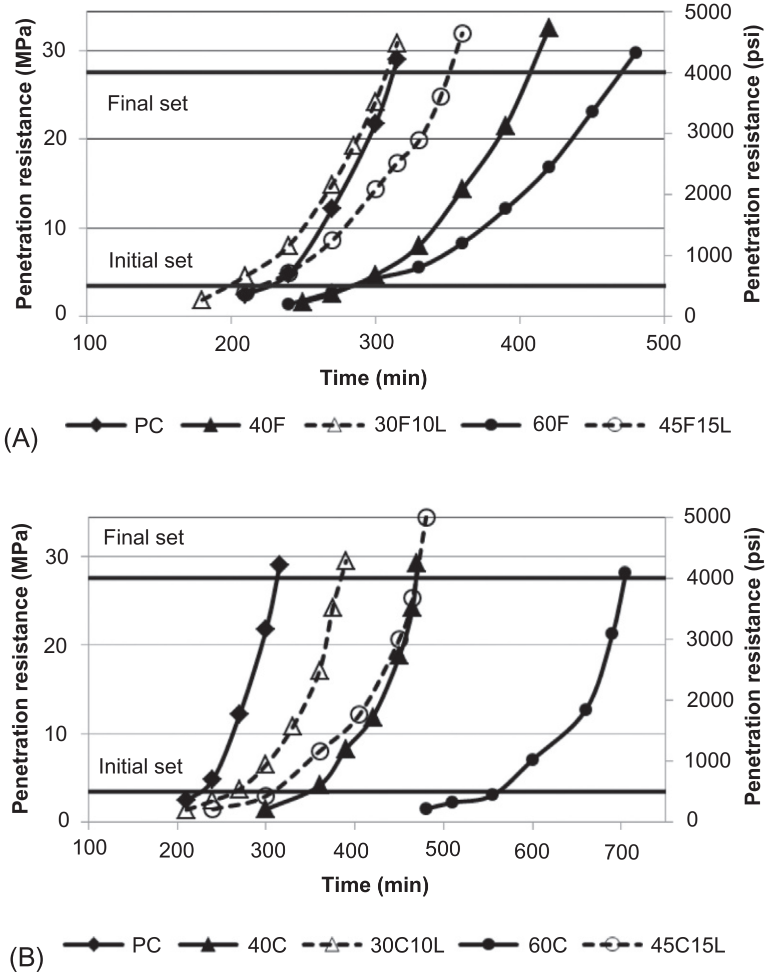

**Fig. 9.8** Setting development: (A) Portland cement mixture and mixtures containing Class F fly ash (45F15L indicates a mixture with 45% Class F fly ash and 15% limestone by volume); (B) Portland cement mixture and mixtures containing Class C fly ash (30C10L indicates a mixture with 30% Class C fly ash and 10% limestone by volume).
Taken from Tanesi, J., Bentz, D. P., & Ardani, A. (2013). Enhancing high volume fly ash concretes using fine limestone powder. In *ACI SP-294: Advances in Green Binder Systems*, Minneapolis, MN, October.

0.40–0.45, typical reductions in *w*/*c* when transitioning to a HVFA mixture are on the order of 0.05–0.10 (Bentz et al., 2010; Bentz, Tanesi, et al., 2013; Keith & Schindler, 2012). However, when the starting *w*/*cm* of the target concrete is on the order of 0.3 (e.g., for a high-performance concrete), the *w*/*cm* of a HVFA mixture that performs similarly may require little or no reduction. For some cement-fly ash combinations, the reduction in *w*/*cm* necessary to meet targeted 28-day strength levels will still be insufficient to provide adequate early-age strength for timely formwork removal and other construction operations. In these cases, further measures to specifically increase early-age strengths may be necessary.

One such measure that has been employed in practice in HVFA concretes is the use of an ASTM C150 Type III cement, which is more finely ground and may have an increased sulfate content by comparison with an ASTM C150 Type I/II/V cement. Some representative compressive strength results from a study on HVFA mortars are provided in Fig. 9.9 (Bentz et al., 2010). Using the strengths of the $w/c = 0.40$, 100% Portland cement mortar as the target values, the original HVFA mixtures (50:50 by mass) prepared with a reduced *w*/*cm* of 0.30 fail to achieve the target strengths at 1 day. Only the Class C fly ash mixture reached the target strength at 7 days. However, switching to a Type III cement brought both fly ash mixtures to an acceptable strength level at 1 day and provided strengths that exceeded the target values at ages of 28 days and beyond. Fig. 9.9 is also informative because the 365-day strength values of the HVFA mixtures are approaching the levels of a 100% Portland cement $w/c = 0.3$ mortar that itself exhibits a minimal strength increase beyond 28 days. This illustrates the propensity of the longer term pozzolanic reactions to make a significant contribution to later age strength development in these HVFA systems, and supporting the transition

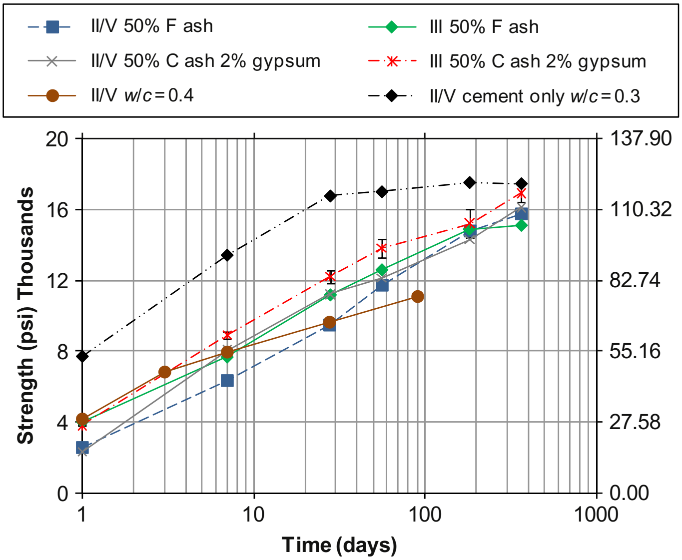

**Fig. 9.9** Measured mortar cube compressive strengths versus age. For the mixtures with fly ash, $w/cm = 0.3$ in every case. Error bars (one standard deviation among three specimens) are provided for the III 50% C ash 2% gypsum data to provide an indication of variability. Taken from Bentz, D. P., Ferraris, C. F., De la Varga, I., Peltz, M. A., & Winpigler, J. (2010). Mixture proportioning options for improving high volume fly ash concretes. *International Journal of Pavement Research and Technology, 3*(5), 234–240.

from the 28-day testing usually employed for Portland cement concretes to later ages (i.e., 56 days or 91 days) for compliance strength testing of HVFA mixtures.

In addition to mitigation of excessive setting time delays, replacement of a portion of the fly ash in an HVFA concrete mixture with a fine limestone powder will also have a beneficial influence on compressive strength values. Fig. 9.10 provides measured compressive strengths for HVFA concretes with and without 1 μm limestone replacing a portion of the fly ash on a volume-for volume-basis (Tanesi, Bentz, & Ardani, 2013). All mixtures were prepared with constant volume fractions of water, powders (including cement, fly ash, and limestone), and fine and coarse aggregates. As shown previously in Fig. 9.8, these limestone replacements reduced the setting times of the HVFA mixtures

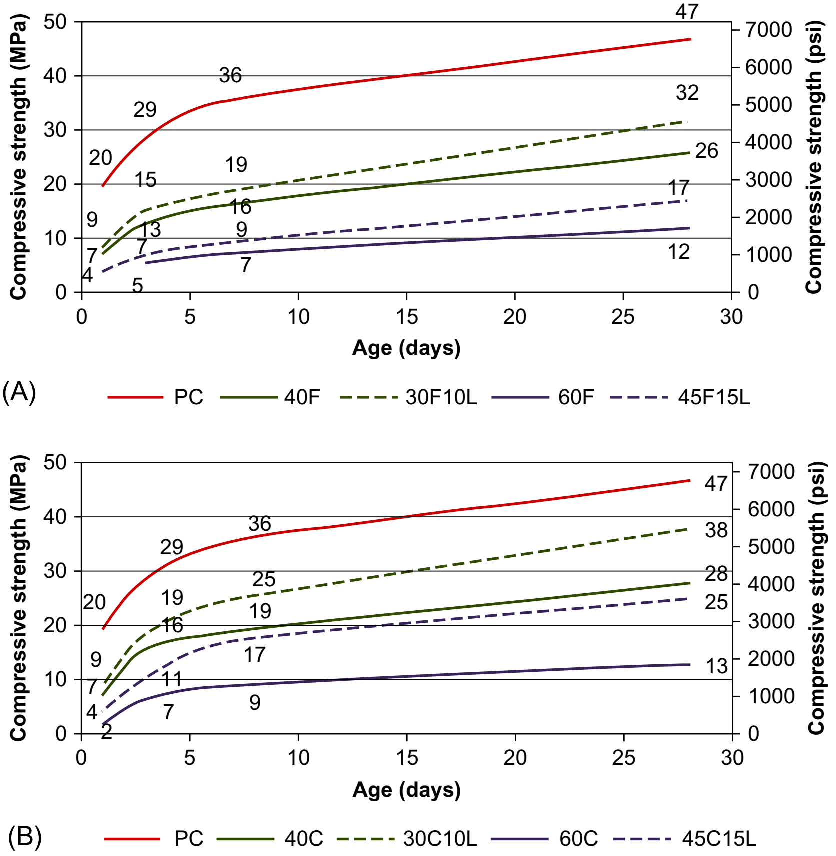

**Fig. 9.10** Compressive strength development for concrete mixtures (see Table 9.2) containing: (A) Class F fly ash and (B) Class C fly ash. Coefficients of variation for three replicate specimens varied from 0.67% to 2.5% for the various mixtures. Numbers above lines indicate strengths obtained at testing ages of 1 days, 3 days, 7 days, and 28 days.

Taken from Tanesi, J., Bentz, D. P., & Ardani, A. (2013). Enhancing high volume fly ash concretes using fine limestone powder. In *ACI SP-294: Advances in Green Binder Systems*, Minneapolis, MN, October.

to be nearly equal to those of the control Portland cement mixture. With respect to strength at early ages, for both the Class F and the Class C fly ash studied, the fine limestone increases strengths by about 2 MPa (about 300 psi). By 28 days, these strength enhancements have increased significantly, and in the best case, a Class C fly ash HVFA concrete with an initial 28-day strength of 13 MPa (1900 psi) has nearly doubled to 25 MPa (3600 psi) with the incorporation of the fine limestone powder. This strength improvement is likely due to a combination of the acceleration provided by the fine limestone powder (i.e., increased specific surface) and the enhanced formation of stiffer carboaluminate phases (Moon et al., 2012) in this particular cement/Class C fly ash/fine limestone ternary blend. While significant, these increases still failed to achieve the target strengths of the Portland cement concrete. Thus other measures such as a *w/cm* reduction and/or substitution of a Type III cement would need to be employed, along with the fine limestone replacements for fly ash (Bentz, Tanesi, et al., 2013).

## 9.7.1 Strength activity index testing

Some of the issues with the current ASTM C311 SAI test have been presented in a recent study (Bentz, Duran-Herrera, & Galvez-Moreno, 2012). According to the test procedure, for the test mortar, 20% of the cement is replaced with fly ash on a mass basis and the water content of the mixture is adjusted to give a flow equivalent to the 100% Portland cement control mortar. Because the density of fly ash and cement are quite often substantially different, by as much as 30% or more in extreme cases, a mass-based replacement alters the volume fractions of water and cementitious materials contained in each mixture subsequently used for strength testing. An adjustment of the water level to provide the same flow as the control mortar further alters these volume fractions. As water content has a large impact on strength, any beneficial or detrimental impact of the fly ash on strength is confounded with these changes in volume fractions. As has been shown in a recent study (Bentz, Duran-Herrera, et al., 2012), the test could be easily corrected by performing the replacement of cement with fly ash on a volume basis and keeping the water volume content constant. Any changes in flow of the fly ash mortar relative to the control mortar could be measured or compensated for with a water reducer. Pursuing this option in the standards committee has been a slow process. Within ASTM, consistency on this testing is lacking as the Annex A1 of ASTM C595 performs its activity index testing with a 35% volumetric replacement of cement by pozzolan, but still recommends testing at constant flow conditions. An alternate approach to modifying ASTM C311 would be to develop new test methods for evaluating the activity of fly ash and other pozzolans, such as the Keil Hydraulic Index (KHI) test, which will be described next.

## 9.7.2 Keil Hydraulic Index test

The existing SAI test has long been criticized for not effectively evaluating the pozzolanic and cementitious properties of a fly ash. As previously stated, the test involves replacing with fly ash, 20% by mass of the Portland cement in a test sample mixture, preparing mortar cubes, and then comparing the strength of those mortar cubes to control samples prepared with 100% Portland cement. Sutter et al. (2013) demonstrated that replacing 20% of the cement with an inert filler material actually produces samples that pass the SAI test. Table 9.3 presents data from their study where three different cements were used and in the case of the test samples, a fine quartz powder was used. The quartz powder had a fineness of 3.2% and an average particle size of 7.3 μm. As can be seen, at both 7 days and 28 days, the samples with inert filler exceeded the ASTM C618 SAI specification limit of 75% of the control.

An alternative to the SAI test is the KHI test (Keil, 1952) that was originally developed for strength activity testing of slag. In this test, the control sample is prepared with a replacement of inert material equal to the replacement of fly ash used in the test sample. For a 20% replacement of fly ash, the KHI is calculated as shown in Eq. (9.3).

$$\text{Keil Hydraulic Index} = \frac{a-c}{b-c} \times 100 \tag{9.3}$$

where $a$ is the strength of 20% fly ash/80% Portland cement at time $t$; $b$ is the strength of 100% Portland cement at time $t$; $c$ is the strength of 20% ground quartz/80% Portland cement at time $t$.

The difference between this method and the standard SAI test is the KHI test allows for separation of the pozzolanic and hydraulic effects from the physical filler effects. The Keil Activity can range from 0% for an inert material to over 100% if the SCM material develops more strength than the Portland cement mixture. A negative value of the KHI indicates the fly ash did not perform as well as the inert filler. Results for the KHI with 8 different fly ash sources are shown in Table 9.4 (Sutter et al., 2013).

As can be seen in Table 9.4, the Class F ash sources demonstrated very little to no contribution to strength at 7 days, but they did demonstrate a measurable increase at 28 days. Conversely, the Class C ash sources demonstrated a significant strength contribution at 7 days and a measurable increase at 28 days. The results of the KHI test align with the known properties of fly ash and provide a clear indication of strength gain, separate of any contributions from a filler effect.

**Table 9.3** **Results of the strength activity index test with three different cements and a quartz powder**

| | | 100% cement | 20% replacement | |
|---|---|---|---|---|
| **Cement type** | **Age (days)** | **Strength (psi)** | **Strength (psi)** | **SAI** |
| PC-1 | 7 | 4554 | 3829 | 84 |
| PC-2 | 7 | 4293 | 3408 | 79 |
| PC-3 | 7 | 4090 | 3539 | 87 |
| PC-1 | 28 | 5715 | 4815 | 84 |
| PC-2 | 28 | 5526 | 4235 | 77 |
| PC-3 | 28 | 5134 | 4351 | 85 |

From Sutter, L. L., Hooton, R. D., & Schlorholtz, S. (2013). *Methods for evaluating fly ash for use in highway concrete, NCHRP report 749* [54 pp.]. Washington, DC: National Cooperative Highway Research Program, Transportation Research Board of the National Academies, with permission.

**Table 9.4 Results of the Keil Hydraulic Index test with eight fly ash sources, four Class F and four Class C at a 20% replacement level. The inert filler used was a quartz powder with a fineness of 3.2% and an average particle size of 7.3 μm. The results are for tests using three different Portland cements**

| | KHI—7 days (%) | | | KHI—28 days (%) | | |
|---|---|---|---|---|---|---|
| ID-% replace. | PC-1 | PC-2 | PC-3 | PC-1 | PC-2 | PC-3 |
| Class F #1 | −31 | 4 | −43 | 71 | 91 | 66 |
| Class F #2 | 7 | 28 | 26 | 119 | 55 | 34 |
| Class F #3 | 10 | −6 | −24 | 7 | 73 | 39 |
| Class F #4 | 53 | 44 | 26 | 135 | 102 | 109 |
| Class C #1 | 121 | 40 | 84 | 184 | 75 | 171 |
| Class C #2 | 115 | 101 | 80 | 96 | 30 | 72 |
| Class C #3 | 122 | 46 | 110 | 184 | 99 | 153 |
| Class C #4 | 203 | 83 | 41 | 138 | 119 | 130 |

From Sutter, L. L., Hooton, R. D., & Schlorholtz, S. (2013). *Methods for evaluating fly ash for use in highway concrete, NCHRP report 749* [54 pp.]. Washington, DC: National Cooperative Highway Research Program, Transportation Research Board of the National Academies, with permission.

Another issue highlighted by this research is the dependence on the cement type with regards to the KHI test. The same dependence is seen with the standard SAI test. The results of the SAI and KHI tests using the three different cements, plotted against measured compressive strength, are shown in Figs. 9.11 and 9.12, respectively.

In both tests, PC1 resulted in higher strengths and higher SAI and KHI values as compared to the same ash sources tested with PC2 and PC3. The problem of cement type can now be addressed with the development of the Cement and Concrete Reference Laboratory (CCRL—www.ccrl.us) reference cement, which can be used as a common cement for all strength testing of supplementary cementitious materials.

## 9.8 Summary

Fly ash is a heterogeneous material that results from the combustion of coal, primarily to produce electrical power. The process of combustion and the composition of the fuel stream, which is predominately coal, affects the quality and performance of the ash. Because power producers are generating power as a primary product and fly ash as a residual product, the characteristics of fly ash will change as burning conditions change to affect power production. This variability in ash characteristics presents a challenge in using fly ash in concrete.

A key constituent of fly ash is unburnt carbon resulting from the combustion process. Also, carbon is added in the form of powder activated carbon to help power producers meet emission standards. The carbon is an issue primarily when the concrete produced is air entrained. Air entrainment is accomplished through the use of an AEA

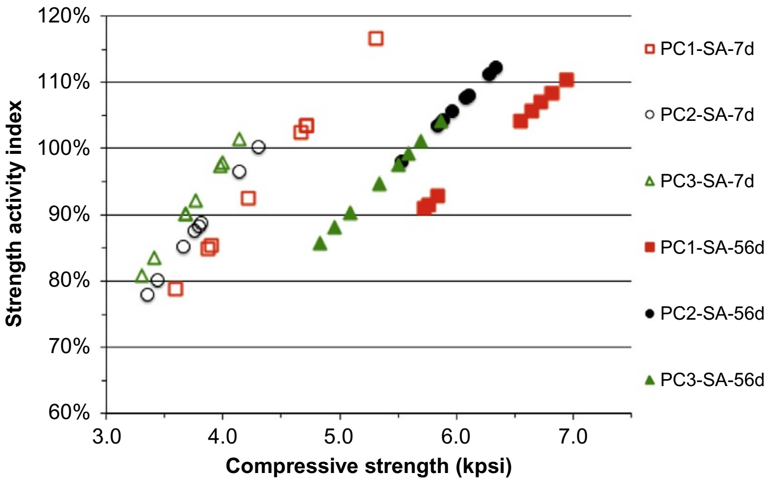

**Fig. 9.11** SAI versus compressive strength for a 20% replacement level for eight fly ash sources, four Class F, and four Class C at a 20% replacement level. The inert filler used was a quartz powder with a fineness of 3.2% and an average particle size of 7.3 μm. The results are for tests using three different Portland cements.
From Sutter, L. L., Hooton, R. D., & Schlorholtz, S. (2013). *Methods for evaluating fly ash for use in highway concrete, NCHRP report 749* [54 pp.]. Washington, DC: National Cooperative Highway Research Program, Transportation Research Board of the National Academies, with permission.

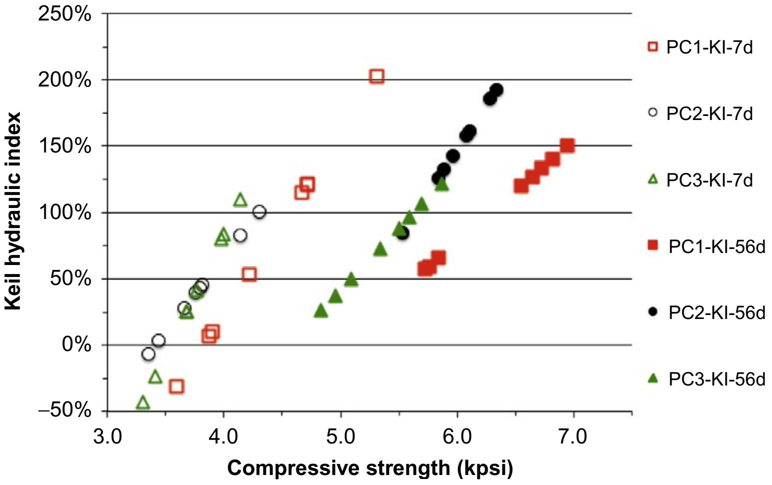

**Fig. 9.12** KHI versus compressive strength for a 20% replacement level for eight fly ash sources, four Class F, and four Class C at a 20% replacement level. The inert filler used was a quartz powder with a fineness of 3.2% and an average particle size of 7.3 μm. The results are for tests using three different Portland cements.
From Sutter, L. L., Hooton, R. D., & Schlorholtz, S. (2013). *Methods for evaluating fly ash for use in highway concrete, NCHRP report 749* [54 pp.]. Washington, DC: National Cooperative Highway Research Program, Transportation Research Board of the National Academies, with permission.

and produces concrete that is resistant to cyclic freezing and thawing. Residual carbon in the ash can adsorb the AEA from the concrete mixture water and thereby render them ineffective at entraining air.

The amount of carbon in fly ash has historically been determined by a LOI test. Although this test can accurately predict the total amount of carbon present, it does not characterize the adsorption capacity of the carbon. Adsorption capacity can vary widely, and it is especially significant when PAC is introduced. Two ash sources with the same LOI can have markedly different adsorption properties.

New tests have been developed to assess adsorption, but they have yet to be implemented in any standards or materials specifications. The principal tests currently available are the foam index test, iodine number test, the direct determination of the adsorption isotherm for a specific ash/AEA combination, and the methylene blue-based adsorption tests. The foam index test provides a simple means of evaluating AEA adsorption, but is not quantitative in terms of the amount of AEA adsorbed; also, it does not evaluate the cementitious system with AEA at equilibrium. Still, it is a useful quick diagnostic test. The iodine number test is an adsorption isotherm-based test that determines the mass of iodine adsorbed from the solution-per-unit mass of fly ash. It is an excellent test for assessing the adsorption capacity of an ash, but it does so using iodine; the adsorption capacity will vary with changes in the adsorbate properties. Nonetheless, it is extremely useful for simply evaluating an ash adsorption or monitoring changes in ash adsorption on a temporal basis. The direct adsorption isotherm provides a quantitative measure of the volume of AEA adsorbed per unit mass of fly ash in the presence of cement. The cement strongly impacts the system and affects adsorption of AEA by fly ash. The methylene blue adsorption test is relatively new and potentially offers many advantages in terms of simplicity. It provides the same basic information attained from the iodine number test (i.e., it characterizes only the ash).

Particle size is critical to fly ash performance. The smaller particles are more reactive and therefore performance in terms of strength development, ASR mitigation, and sulfate attack mitigation all vary significantly. Current ASTM specifications rely only on a sieve analysis to establish the amount of fly ash finer than 45 μm. Other tests exist for measuring particle size distribution but to date, these tests have not been adopted in any fly ash specifications.

One of the performance properties most influenced by fly ash replacement for cement is setting time, particularly for HVFA concretes. Generally, setting times are increased, sometimes dramatically, due to cement dilution, sulfate imbalance, incompatibilities with admixtures such as HRWRs, and/or detrimental influences of fly ash components on early-age hydration reactions. A variety of effective mitigation strategies for these setting time delays have been investigated, including additions of calcium hydroxide or a rapid set cement and the replacement of a portion of the fly ash by a fine limestone powder. In the latter case, not only are setting times reduced, but also early and later age properties (strength and durability) are generally improved.

The contribution to strength development is an important property of fly ash. Current ASTM tests assess this property based on a comparison of a control sample prepared with 100% Portland cement to a test sample with 20% fly ash/80% Portland cement. This SAI has been criticized because given the specification limits, an inert material can pass the test. Modifications to the SAI test are needed. One proposed modification is the KHI that compares a control sample prepared with 20% inert material/80% Portland cement to a test sample with 20% fly ash/80 Portland cement. By doing so, the filler effect of the replacement material is eliminated, and the true cementitious and pozzolanic nature of the ash can be measured. Both the SAI and KHI tests are affected by the cement used, therefore any modifications should consider the use of a standard cement. Two other deficiencies of the existing SAI test are: (a) it is conducted at constant flow conditions resulting in different values of *w*/*cm* for the test and control samples, and (b) by replacing cement with fly ash on a mass basis the volume fraction of water in the test and control samples is further altered. These two factors confound any determination of how a given fly ash influences strength.

## Acknowledgments

The use of information published by the Transportation Research Board of the National Academies, Washington, DC does not necessarily indicate acceptance by the National Academies, the Federal Highway Administration, or by the American Association of State Highway Officials of the findings, conclusions, or recommendations either inferred or specifically expressed herein.

## References

ASTM International. (2012). *ASTM C1749-12 standard guide for measurement of the rheological properties of hydraulic cementitious paste using a rotational rheometer* [4 pp.]. West Conshohocken, PA: ASTM International.

ASTM International. (2013). *ASTM C359-13 standard test method for early stiffening of hydraulic cement (Mortar Method)* [4 pp.]. West Conshohocken, PA: ASTM International.

ASTM International. (2013). *ASTM C311/C311M-13 standard test methods for sampling and testing fly ash or natural pozzolans for use in Portland-cement concrete* [10 pp.]. West Conshohocken, PA: ASTM International.

ASTM International. (2014). *ASTM C1679-14 standard practice for measuring hydration kinetics of hydraulic cementitious mixtures using isothermal calorimetry* [15 pp.]. West Conshohocken, PA: ASTM International.

ASTM International. (2014). *ASTM D3860-98(2014) standard practice for determination of adsorptive capacity of activated carbon by aqueous phase isotherm technique* [4 pp.]. West Conshohocken, PA: American Society for Testing and Materials.

ASTM International. (2014). *ASTM D4607-14 standard test method for determination of iodine number of activated carbon* [5 pp.]. West Conshohocken, PA: American Society for Testing and Materials.

ASTM International. (2015). *ASTM C114-15 standard test methods for chemical analysis of hydraulic cement* [32 pp.]. West Conshohocken, PA: American Society for Testing and Materials.

ASTM International. (2015). *ASTM C150/C150M-15 standard specification for Portland cement* [9 pp.]. West Conshohocken, PA: ASTM International.

ASTM International. (2015). *ASTM C430-08(2015) standard test method for fineness of hydraulic cement by the 45-μm (No. 325) sieve* [3 pp.]. West Conshohocken, PA: American Society for Testing and Materials.

ASTM International. (2015). *ASTM C618-15 standard specification for coal fly ash and raw or calcined natural pozzolan for use in concrete* [5 pp.]. West Conshohocken, PA: ASTM International.

ASTM International. (2015). *ASTM C1753-15 standard practice for evaluating early hydration of hydraulic cementitious mixtures using thermal measurements* [19 pp.]. West Conshohocken, PA: ASTM International.

ASTM International. (2015). *ASTM C1777-15 standard test method for rapid determination of the methylene blue value for fine aggregate or mineral filler using a colorimeter* [4 pp.]. West Conshohocken, PA: American Society for Testing and Materials.

ASTM International. (2016). *ASTM C204-16 standard test methods for fineness of hydraulic cement by air-permeability apparatus* [10 pp.]. West Conshohocken, PA: American Society for Testing and Materials.

ASTM International. (2016). *ASTM D1510-16 standard test method for carbon black-iodine adsorption number* [10 pp.]. West Conshohocken, PA: American Society for Testing and Materials.

Bailey, J. G., Tate, A., Diessel, C. F. K., & Wall, T. F. (1990). A char classification system with applications to coal combustion. *Fuel*, *69*(2), 225–239.

Bentz, D. P. (2010). Powder additions to mitigate retardation in high volume fly ash mixtures. *ACI Materials Journal*, *107*(5), 508–514.

Bentz, D. P., & Ferraris, C. F. (2010). Rheology and setting of high volume fly ash mixtures. *Cement and Concrete Composites*, *32*(4), 265–270.

Bentz, D. P., Ferraris, C. F., De la Varga, I., Peltz, M. A., & Winpigler, J. (2010). Mixture proportioning options for improving high volume fly ash concretes. *International Journal of Pavement Research and Technology*, *3*(5), 234–240.

Bentz, D. P., Duran-Herrera, A., & Galvez-Moreno, D. (2012). Comparison of ASTM C311 strength activity index testing vs. testing based on constant volumetric proportions. *Journal of ASTM International*, *9*(1). 7 pp.

Bentz, D. P., Sato, T., De la Varga, I., & Weiss, J. (2012). Fine limestone additions to regulate setting in high volume fly ash mixtures. *Cement and Concrete Composites*, *34*(1), 11–17.

Bentz, D. P., Ferraris, C. F., & Snyder, K. A. (2013a, September). Best practices guide for high-volume fly ash concretes: Assuring properties and performance. NIST Technical Note 1812, U.S. Department of Commerce.

Bentz, D. P., Tanesi, J., & Ardani, A. (2013). Ternary blends for controlling cost and carbon content. *Concrete International*, *35*(8), 51–59.

Bruere, G. M. (1955). Air entrainment in cement and silica paste. *Journal of the American Concrete Institute*, *26*(9), 905–919.

Cost, V. T. (2011). Concrete sustainability versus constructability—Closing the gap. In *Proceedings of the 2011 international concrete sustainability conference, Boston, MA*. Available at: http://www.nrmcaevents.org/?nav=display&file=189.

Cost, V. T., & Bohme, P. (2012). Synergies of Portland-limestone cements and their potential for concrete performance enhancement. In: *Proceedings of the 2012 international concrete sustainability conference, Seattle, WA*.

Gurney, L., Bentz, D. P., Sato, T., & Weiss, W. J. (2012). Reducing set retardation in high volume fly ash mixtures with the use of limestone: Improving constructability for sustainability. Transportation Research Record, Journal of the Transportation Research Board, No. 2290. *Concrete Materials*, *2012*, 139–146.

Harris, N. J., Hover, K. C., Folliard, K. J., & Ley, M. T. (2008). The use of the foam index test to predict AEA dosage in concrete containing fly ash: Part I—Evaluation of the state of practice. *Journal of ASTM International*, *5*(7).

Islam, G. S., McCarthy, M., Csetenyi, L., & Jones, M. (2012). Investigating techniques for evaluating fly ash behaviour in air-entrained concrete. In *Proceedings EuroCoalAsh*.

Keil, F. (1952). Slag cements. In *Proceedings of the 3rd international symposium on the chemistry of cements* (pp. 530–571). London: Cement and Concrete Association.

Keith, K. P., & Schindler, A. K. (2012). Phase II—Task 3 setting and temperature development. Final report for project BAA No. DTFH61-08-R-0034 greatly increased use of fly ash in Hydraulic Cement Concrete (HCC) for pavement layers and transportation structures.

Looney, T. J., Arezoumandi, M., Volz, J. S., & Myers, J. J. (2012). An experimental study on bond strength of reinforcing steel in high-volume fly-ash concrete. *Advances in Civil Engineering Materials*, *1*(1). 17 pp.

McCarthy, M., Islam, G. S., Csetenyi, L., & Jones, M. (2012). Colorimetric evaluation of admixture adsorption by fly ash for use in air-entrained concrete. *Materials and Structures*, *45*(12), 1793–1803.

Moon, J., Oh, J. E., Balonis, M., Glasser, F. P., Clark, S. M., & Monteiro, P. J. M. (2012). High pressure study of low compressibility tetracalcium aluminum carbonate hydrates $3CaO \cdot Al_2O_3 \cdot CaCO_3 \cdot 11H_2O$. *Cement and Concrete Research*, *42*, 105–110.

Niemuth, M. D., Barcelo, L., & Weiss, J. (2012). Effect of fly ash on optimum sulfate levels measured using heat and strength at early ages. *Advances in Civil Engineering Materials*, *1*(1). 18 pp.

Obla, K. H., Lobo, C. L., & Kim, H. (2012). The 2012 NRMCA supplementary cementitious materials use survey. *Concrete Infocus*, *Summer*.

Roberts, L. R., & Taylor, P. C. (2007). Understanding cement-SCM-admixture interaction issues. *Concrete International*, *29*(1), 33–41.

Schlorholtz, S. M. (2006). Supplementary cementitious materials. In J. Lamond & J. Pielert (Eds.), *Significance of tests and properties of concrete and concrete-making materials* (pp. 495–511). West Conshohocken, PA: ASTM STP 169D, American Society for Testing and Materials.

Sontheimer, H., Crittenden, J. C., & Summers, S. (1988). *Activated carbon for water treatment* [p. 102]. Karlsruhe: DVGW-Forschungsstelle and American Water Works Association, ISBN: 3-922671-20-9.

Sutter, L. L., Hooton, R. D., & Schlorholtz, S. (2013). *Methods for evaluating fly ash for use in highway concrete, NCHRP report 749* [54 pp.]. Washington, DC: National Cooperative Highway Research Program, Transportation Research Board of the National Academies.

Sutter, L. L., Vruno, D., Anzalone, G. C., & Dong, J. (2014). *Laboratory study for comparison of Class C versus Class F fly ash for concrete pavement, Final report 0092-12-04* [153 pp.]. Madison, WI, USA: Wisconsin Highway Research Program.

Tanesi, J., Ardani, A., Meininger, R., & Nicolaescu, N. (2012). *Evaluation of high-volume fly ash (HVFA) mixtures (paste and mortar components) using a dynamic shear rheometer (DSR) and isothermal calorimeter, Report No. PB2012-112546*. Springfield, VA: National Technical Information Service.

Tanesi, J., Bentz, D. P., & Ardani, A. (2013). Enhancing high volume fly ash concretes using fine limestone powder. In *ACI SP-294: Advances in Green Binder Systems, Minneapolis, MN, October*.

# Air classification

# 10

*J. Jow*
National Institute of Clean-and-Low-Carbon Energy (NICE), Beijing, China

## 10.1 Introduction

Coal combustion products (CCP) have three types of solid wastes: fly ash, bottom ash (or boiler slag), and flue-gas desulfurization (FGD) gypsum. The typical particle-size range of fly ash is 0.1–600 μm. There is a specific size requirement for fly ash to replace the cement used in building materials. The weight of particles with a size greater than 45 μm cannot be greater than 34% according to ASTM C618-12a (ASTM C618-12a, n.d.), and cannot be greater than 45%, 25%, or 12% by weight, classified as Class III, Class II, or Class I fly ash, respectively, according to the GB/T 1596–2005 specifications (GB/T, 1596–2005). Of course, not all fly ash initially produced from the coal-fired power plant can meet these size requirements; air classification, milling, or sieving is typically used to process fly ash to meet those requirements.

Bottom ash is too heavy to be carried up in the flue gas and collected at the bottom of the combustion chamber. Bottom ash has a similar chemical composition to fly ash but a higher LOI. The typical particle size of bottom ash is much coarser than fly ash, ranging from 75 μm to 50 mm.

Bottom ash in some boilers, such as slag tap or cyclone furnaces, becomes molten before cooling into dense granules called boiler slag. Bottom ash or boiler slag is typically used as the raw material for clinker production, aggregates, and skid control on icy roads. Except for lightweight aggregates used in concrete, no specific particle size is required.

Due to the environmental requirements on sulfur emissions, sulfur from the flue-gas stream is typically removed via a chemical reaction with limestone ($CaCO_3$) through the scrubber emission control system to produce FGD gypsum. The primary chemical composition of FGD gypsum is $CaSO_4$ $2H_2O$. It is a fine-grain material with an average particle size of 42–45 μm with less than 2% particles greater than 200 μm due to the usage of very fine limestone powder. The typical applications for FGD gypsum include wallboard, plaster, structural fill, mining applications, soil or agricultural applications, glass making, set retarder for Portland cement, and pigments and/or fillers. Most of these applications do not require size classification.

In general, the coal-fired power plant produces fly ash six to seven times more than bottom ash and five to six times more than FGD gypsum. Due to the large quantity and application needs, size classification is often required for fly ash, but it is rarely used for bottom ash (boiler slag) or FGD gypsum. Besides milling for size reduction and

**Coal Combustion Products (CCP's).** http://dx.doi.org/10.1016/B978-0-08-100945-1.00010-1

sieving for size separation, air classification is a commonly used separation process to obtain two or more fly ash materials with desired particle size distributions.

Air classification is a mechanical separation process that uses air as the dispersion agent for particulate materials, separating them into two or more size classes by a combination of mechanical forces such as centrifugal, drag, gravity, or collision. This separation process has three steps: the utilization of air to disperse the particulate materials to form an air-solid mixture flowing into the separation device, the separation of the air-solid mixture into two or more fractions by a mechanical force in the device, and the collection of fine and coarse fractions out of the air stream.

For a particulate material with a particle size distribution from $d_{\min}$ to $d_{\max}$, it can be ideally classified into two fractions: the fine fraction from $d_{\min}$ to $d_c$ and the coarse fraction from $d_c$ to $d_{\max}$. The diameter $d_c$ that separates both fractions is called the cut size. The sieving process is an ideal classification and has its sieve aperture close to its $d_c$. However, air classification is not an ideal classification. There are always some particles with the size smaller than $d_c$ in the coarse fraction and the size larger than $d_c$ in the fine fraction. Therefore the cut size is the particle size which has the same amount (by weight) in the fine and coarse fractions under the overlapped particle size range. For example, fly ash can be separated into the fine and coarse parts by air classification; their accumulated volumes are shown in Fig. 10.1. The average particle size $D_{50}$ is 51.2 μm for the coarse part and 8.3 μm for the fine part, while the average particle size for the feed is 24.5 μm.

The mass at each given particle size for the feed, fine and coarse parts is calculated and shown in Fig. 10.2. The cut size is around 26 μm.

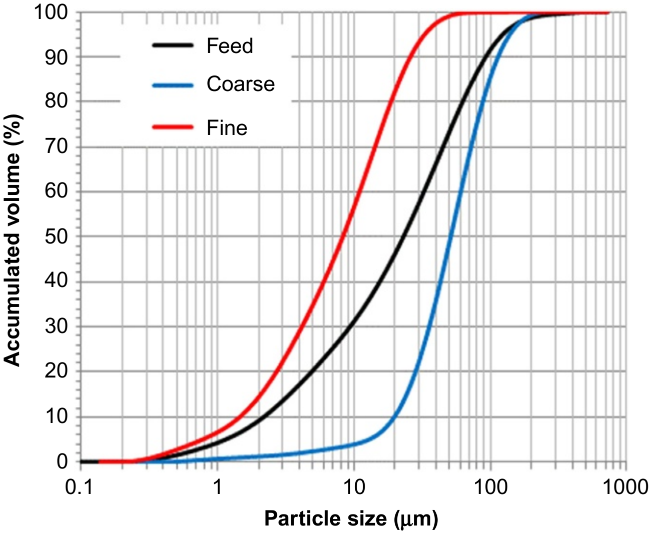

**Fig. 10.1** An example of accumulated volume for feed, fine, and coarse parts by air classification.

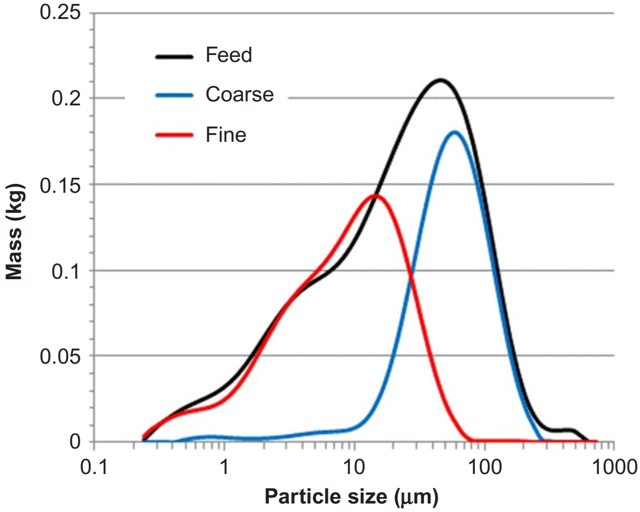

**Fig. 10.2** An example of cut size by air classification.

## 10.2 Purposes and beneficiation

From a materials science perspective, CCP have three fundamental properties: chemical composition, mineral composition, and particle size distribution. Fly ash has the largest volume and the most significant variations in these fundamental properties due to the differences in the operational conditions at the coal-fired power plants, such as the coal types, coal pretreatment, combustion processes, ash collection system, and environmental control unit. Chemical compositions depend on coal types, combustion process, and environmental control systems. Mineral compositions depend on coal types and combustion process. The variation in particle size distribution depends on the coal pretreatment, combustion process, and ash collection system. Coal types can be anthracite, bituminous coal, subbituminous coal, or lignite, which affects ash chemical and mineral compositions. The specific geographic location of coals can also affect their chemical and mineral compositions. Different combustion processes include fluidized bed, fixed bed, pulverized bed, or integrated gasification combined cycle, and affect these fundamental properties. Environmental control units used to reduce or eliminate Hg, Sulfur, or $NO_x$ concentration affect specific chemical compositions. Any variations in these operations will produce fly ash with different values in its fundamental properties.

Below are the examples used to compare the chemical compositions, mineral compositions, and particle size distributions of three fly ash samples, identified as SH, JJ, and ZG, produced from three different power plants from the Guohua Power Company (a subsidiary of Shenhua Group, the largest coal producer in the world). For chemical compositions, six key compositions and their levels of these three fly ashes are listed in Table 10.1. Fly ash with $Al_2O_3 > 35\%$ is called high Al fly ash which can be used for

**Table 10.1** Key chemical compositions of three fly ashes

| Compositions | SH | JJ | ZG |
|---|---|---|---|
| $SiO_2$ | 45.1 | 53.3 | 33.9 |
| $Al_2O_3$ | 30.0 | 18.1 | 55.7 |
| CaO | 10.5 | 12.9 | 1.0 |
| $Fe_2O_3$ | 6.5 | 5.5 | 2.2 |
| $SO_3$ | 1.1 | 1.0 | 1.6 |
| LOI | 3.1 | 0.7 | 0.8 |
| Other oxides | 3.7 | 8.5 | 4.8 |
| f-CaO | 0.9 | 1.5 | 0.3 |
| $SiO_2/Al_2O_3$ | 1.5 | 3.1 | 0.6 |

aluminum extraction. Fly ash is also classified into Class C or F based on its CaO content.Class C fly ash has a CaO content $>10\%$, while Class F fly ash has a CaO content $\leq 10\%$. All fly ash has pozzolanic reactivity. These three fly ashes have lower sulfur content (not higher than 3% or 5%) and LOI (not higher than 5%, 8%, 15%, or 6%). Therefore they meet the requirements specified in GB/T 1596–2005 or ASTM C618-12a for concrete use.

The mineral compositions of these three fly ashes are listed in Table 10.2. The glassy content is the reactive phase containing amorphous aluminosilicates, while the crystal phase consists of many stable crystal minerals. The glassy content of these fly ashes ranges from 42% to 58%. ZG has the lowest glassy content, but it has the highest mullite (51.1%) and corundum (6.4%) content without any quartz. SH and JJ have a similar glassy content, while JJ has a higher quartz content and more Ca-containing minerals but a lower mullite content.

For particle size distributions, Fig. 10.3 shows significant variations for these three fly ashes. The particle size range is very wide from 0.2 to 650 μm. Their particle size range, $D_{50}$, $D_{90}$, and wt% $>$ 45 μm of these three different fly ashes are listed in Table 10.3.

Among these three fundamental properties of fly ash samples, particle size has the widest variation. This can be controlled in order to eliminate the variations and obtain the desired particle size distributions. The mineral and chemical compositions of fly ash are not controllable, except for LOI, which can be controlled via electrostatic separation or reduced by a carbon burn-out process.

Finer fly ash has a higher surface area and is expected to have a higher reactivity, resulting in a higher utilization value. The dry separation methods commercially available for producing finer fly ash products are air classification via cyclone and centrifugal separation, sieving, or milling. Generally, the lowest particle size filtered by cyclonic-based separation is about 10 μm, while sieving separation can only filter particle size down to 20 μm (635 mesh). Milling is a process that breaks down the large fly ash particles into smaller particles, but it requires significant energy to obtain particle sizes less than 10 μm. Air classification is the most cost effective dry separation method for obtaining fly ash with a finer particle size distribution.

**Table 10.2** Mineral compositions of three fly ashes

| ID | % Glass | Mullite | Quartz | Corundum | Lime | Anhydrite | Gehlenite | Anorthite | Hematite | Magnetite |
|---|---|---|---|---|---|---|---|---|---|---|
| SH | 52.9 | 29.9 | 10.2 | – | 1.2 | 1.8 | – | 1.7 | 2.1 | 0.2 |
| JJ | 58.2 | 7.5 | 21.8 | – | 9.0 | 1.0 | – | 0.8 | – | 1.7 |
| ZG | 42.0 | 51.1 | – | 6.4 | – | – | – | 0.5 | – | – |

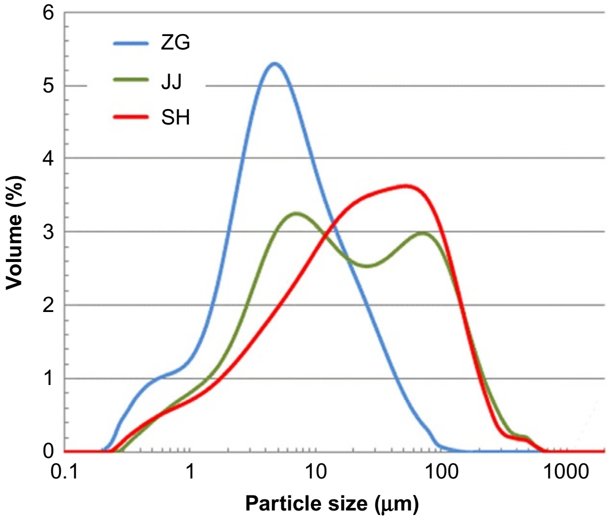

**Fig. 10.3** Particle size distributions of three different fly ash samples.

**Table 10.3 Particle size range, $D_{50}$, $D_{90}$, and wt% > 45 μm of three fly ash samples**

| Sources | Range (μm) | $D_{50}$ (μm) | $D_{90}$ (μm) | wt% > 45 μm |
|---|---|---|---|---|
| ZG | 0.2–140 | 5 | 23 | 2 |
| JJ | 0.2–650 | 15 | 112 | 21 |
| SH | 0.2–650 | 22 | 112 | 21 |

Original fly ash always has a wide range of particle sizes with significant variation of particle size distribution, even from batches produced from the same plant. The purpose of using air classification is to increase its utilization value and rate by further filtering the fly ash to obtain batches with finer, consistent, and desired particle size distributions for higher value applications.

Two other Guohua's coal-fired power plants, identified as CD and SZ, have produced fly ash with similar chemical and mineral compositions as SH. However, there are significant differences in their particle size distributions due to using cyclone separation. The cyclone separation system produces fine and coarse fly ash, identified as CD-f and CD-c vs. SZ-f and SZ-c, as shown in Fig. 10.4. CD produces much finer and coarser fly ashes than SZ.

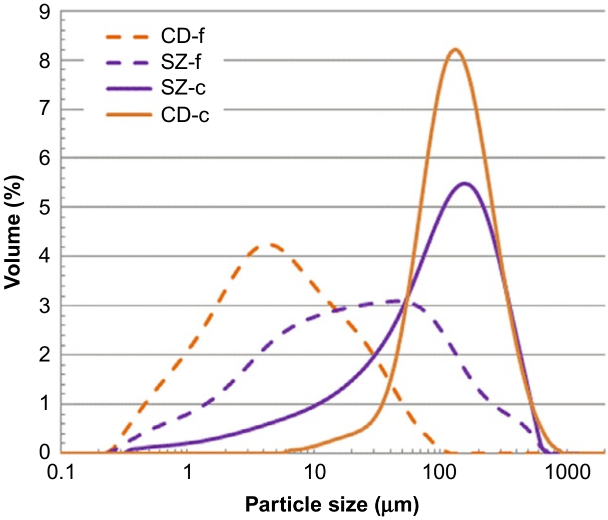

**Fig. 10.4** Particle size distributions of fine and coarse fly ash collected from the same plant.

## 10.3 Theory and fundamental parameters

Air classification, also known as air elutriation, uses air as the medium to carry and separate solid particles into two or more groups with different particle sizes by a combination of mechanical forces, such as centrifugal, drag, gravity, or collision (Holdich, n.d.). An air classifier typically consists of a vertical tube that moves air at a controlled velocity. The original particles are typically introduced through a side tube. Smaller particles will be separated out through the top of the air classifier because their terminal velocities are lower than the airflow velocity, while the larger particles with higher terminal velocity fall down to the bottom of the device. This is a size classification.

Air classification is based on airflow rates and the characteristics of particles, such as density and size. At each airflow rate, the original particulate material is separated into two groups: fine and coarse particles. The fine particles obtain their terminal velocities below the velocity of the air stream flowing along with it, while coarser particles that have terminal velocities higher than the air velocity will fall down to the tube. The airflow rates can be increased to separate much finer particles with narrower size ranges. Further size fractions can be achieved by allowing the overflow from the first tube to pass through additional tubes arranged in series.

For fly ash, finer particles are obtained through various commercially available processes, such as air classification, sieving, or milling. Air classification is the most important and efficient dry process to separate the fine and coarse particles from the original fly ash particles. Two basic types of air classification are cyclonic and centrifugal classifications.

### 10.3.1 Cyclonic classification

Cyclonic classification is a method of removing solid particles from a gas or liquid stream through vortex separation without the usage of filters. The rotational effect and the force of gravity are used to separate mixtures of solids and fluids. Cyclonic air classification uses air as the medium. A swirling flow field is formed when the air-solid mixture rushes into the vortex-shaped cyclone inlet. A high-speed rotating flow of the air-solid mixture is established within a cylindrical or conical container. The air-solid mixture flows in a helical pattern, beginning at the top (wide end) of the cyclone and ending at the bottom (narrow end). In this conical system the rotational radius of the stream is gradually reduced as the rotating flow moves towards the narrow end of the cyclone to further separate smaller and smaller particles. The air stream is expected to contain smaller (or lighter) particles exiting the cyclone in a straight stream through the center of the cyclone and out the top. On the other hand, the larger (or heavier) particles in the rotating air stream have too much inertia to follow the tight curve of the air stream. These larger particles will strike the wall, falling to the bottom of the cyclone, where they are removed and collected.

For a particle circling at distance of a rotational radius of r from the central axis, the centrifugal, drag, and buoyant forces exerted on the particle are shown in Fig. 10.5.

If the air velocity is moving in a spiral, the velocity has a tangential velocity $V_t$ and an outward radial velocity. Based on Stokes' law, the drag force $F_R$ creates an inward radial velocity $V_r$, which opposes the outward velocity on the particle with the particle size $d_p$, as described here:

$$F_R = -3\pi\eta d_p V_r$$

where $\eta$ is the viscosity of the air-solid mixture (Pa s); $d_p$ is the particle size (m); and $V_r$ is the radial velocity (m/s).

The centrifugal force on the particle in the outward radial direction is described here:

$$F_C = \pi d_p^3 \rho_p V_t^2 / 6r$$

where $V_t$ is the tangential velocity (m/s); $\rho_p$ is the particle density (kg/m$^3$); and $r$ is the particle at the radius of a circle (m).

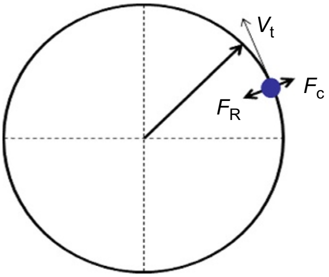

**Fig. 10.5** Forces on a particle moving in a circle with $r$ radius.

The buoyant force, where the fluid exerts its force in the inward radial direction opposite to the centrifugal force exerted on the particle, can be described thus:

$$F_B = -\pi d_p^3 \rho_f V_t^2 / 6r$$

where $\rho_f$ is the fluid density (kg/m$^3$).

To determine the outward radial motion of the particle with a mass of w, we take the sum of these forces by Newton's second law of motion, as described here:

$$w(\partial V_r / \partial t) = F_R + F_C + F_B$$

When the particle reaches the "terminal velocity," which is $\partial V_r / \partial t = 0$ at the radius $r_t$, the radial velocity will cause enough drag force to counter the centrifugal and buoyancy forces. The equation here shows all forces at balance:

$$F_R + F_C + F_B = 0$$

$$3\eta d_p V_r = d_p^3 (\rho_p - \rho_f) V_t^2 / 6r$$

When the forces are at the balance, $r$ equals $r_t$ at the balance and $d_p$ is equivalent to the cut size $d_c$, which is determined by Eq. (10.1):

$$r_t = d_p^2 (\rho_p - \rho_f) V_t^2 / (18\eta V_r)$$

$$d_c^2 = (18\, r_t \eta V_r) / \left[ (\rho_p - \rho_f) V_t^2 \right] \tag{10.1}$$

where $r_t$ is the radius when the forces are at balance for the cut size $d_c$.

The cut size $d_c$ is the desired particle size, where the original particle size distribution is divided into the coarse and fine particle size distributions. The basic assumption is that particles in the outward swirling part would be collected onto the cyclone wall, and those in the inward swirling part would escape through the cyclone exit tube. If a particle at a given size in a state of perfect balance is located at the interface of inward and outward swirling parts, it has a 50% probability of escaping and 50% probability of being collected. This particle size is the cut size $d_c$. For those collected from the cyclone wall as a coarse particle distribution, particles larger than the cut size will be collected with a probability of >50% while particles smaller than the cut size have a probability of <50% of being collected on the cyclone wall. On the other hand, for particles collected from the cyclone exit tube as a fine particle distribution, particles larger than the cut size will be collected with a probability <50% but particles smaller than the cut size have a probability of >50%. One original particle size distribution is then divided into two overlaid particle size distributions at $d_c$.

Several variables that influence its cut size, shown by Eq. (10.1), are discussed below:

- A cyclone with a smaller diameter tends to have a small balanced radius, resulting in a smaller $d_c$ for a finer size distribution. However, the handling capacity (productivity) will be also lower.

- The higher particle density has a smaller $d_c$ value under the same conditions.
- The $d_c$ value becomes smaller when the solid-air mixture has lower viscosity. For given particles, a lower solid concentration has a lower viscosity, which can obtain smaller particles but will lower productivity.
- Increasing the airflow also increases the tangential velocity, which will reduce the $d_c$ value. This is the most important operational parameter needed to produce finer particles while maintaining high productivity.

### 10.3.2 Centrifugal classification

The solid particles are carried into the classifier by the airflow stream through the primary inlet. Internal impellers apply centrifugal forces to the particles while allowing air to pass through them for the separation of the fine particles. The coarse particles are discharged through the valve after they drop to the bottom of the classifier. Prior to discharge a secondary air stream enters into the bottom of the classifier and passes through the particle material. Particles near the cut size are returned to the classifier chamber. The two air streams combine and enter a cyclonic separator for the final recovery of the fine particles.

For a particle with density $\rho_p$, the equation of the resistance force ($F_R$) and centrifugal force ($F_C$) are given here. The particle density $\rho_p$ needs to be much greater than the fluid density in a rotating flow field to prevent the gravitational effect:

$$F_R = 3\pi\eta d_p v_r$$

$$F_C = \pi d_p^3 \rho_p v_t^2/(6r)$$

where $\eta$ is the viscosity of the air-solid mixture (Pa s); $d_p$ is the particle size (m); $V_r$ is the radial velocity (m/s); $V_t$ is the tangential velocity (m/s); $\rho_p$ is the particle density (kg/m$^3$); and $r$ is the particle at the radius of a circle (m).

When $F_C > F_R$ the particles fly to the inner wall to be collected as coarse particles. When $F_C < F_R$ the particles will come out of the chamber along with air to be collected as fine particles. The particles at the cut size ($d_c$) can be obtained when $F_C = F_R$:

$$d_c^2 = 18\eta r v_r/\left(\rho_p v_t^2\right)$$

$V_t$ and $V_r$ are also related to airflow, and the radius at the balance as described here:

$$v_r = Q/(2\pi r h) \quad (\mathrm{m/s})$$

$$v_t = 2\pi r n/60 \quad (\mathrm{m/s})$$

where $Q$ is air flow (m$^3$/s); $r$ is the radius at the balance (m); $n$ is the rotational revolution of the impeller (1/s); and $h$ is the height of the centrifugal unit (m).

Eq. (10.2) shows that the key effects of equipment, materials, or operational parameters on the cut size and productivity are as follows:

$$d_c^2 = \left(9{*}30^2/\pi^3\right)\eta Q/\left(h\rho_p r^2 n^2\right) \approx 261.6\eta Q/\left(h\rho_p r^2 n^2\right) \tag{10.2}$$

- A larger diameter or longer height of the centrifugal unit will produce a smaller particle size and higher productivity due to the larger capacity of the separation unit.
- The higher particle density can have a finer particle size without negatively influencing productivity.
- A lower viscosity of the air-solid mixture due to a lower solid concentration gives a finer particle size, but a lower productivity.
- A higher airflow rate produces the larger cut size and higher productivity.
- Increasing the rotational revolution of impellers increases the tangential velocity, which results in the production of a finer particle size. This is the most effective approach to obtaining a lower particle size without affecting productivity.

## 10.4 Air classifiers

Air classifiers have two basic types: simple expansion chambers, such as cyclones; and centrifugal force-based air classifiers, such as the Mumford-and-Moodie type patented in 1885 or the Whirlwind-type separator. Cyclonic air classifiers use a high-speed rotating airflow to create the force fields within a cylindrical or conical container, while the centrifugal force-based air classifiers use a rotating distributor plate to impart a centrifugal force. Centrifugal force air classifiers can be further categorized as internal or external fan types. Internal fan types do not require cyclones or a filtration bag to collect the fine fraction, but external the fan ones do. The cyclonic and centrifugal forced air classifiers are available commercially and are offered, for example, by Metso and Sturtevant, respectively. A schematic diagram follows of the Whirlwind Air Classifier offered by Sturtevant Inc., USA, as shown in Fig. 10.6. The speed of the selector blades, the velocity of the airflow, and the feed rate control the fineness.

The cyclonic air classifier, as shown in Fig. 10.7, is owned by Salt River Materials Group, located at the San Juan Generating Station in Waterflow, New Mexico. It has been used for more than 20 years. The similar cyclonic air classification systems are also used at the Four Corners Power Plant at Fruitland and the Cholla Power Plant in Joseph City, New Mexico. The capacity of these systems is up to 85 tons/h. The rate of producing fine fly ash from raw fly ash ranges from 75% to 90% depending on its fineness. These systems can even produce fine fly ash having no more than 6% by weight with its particle sizes larger than 325 mesh to meet Class I or Class S fly ash, according to the Chinese standard GB/T 1596 or European standard EN 450 for high value applications, respectively.

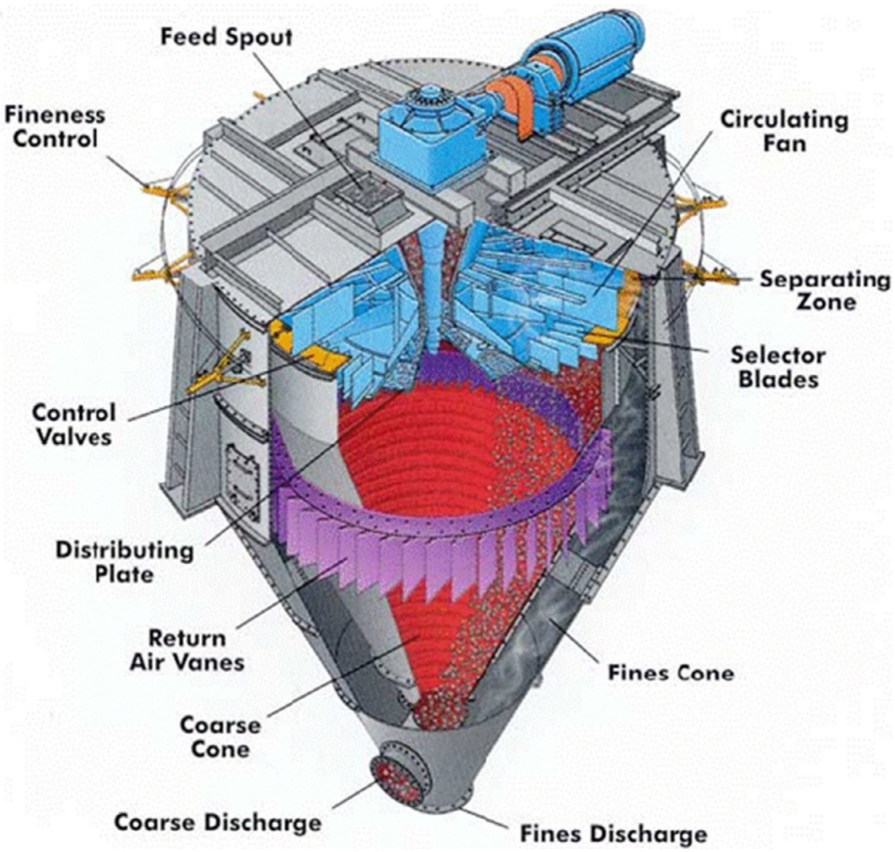

**Fig. 10.6** Whirlwind air classifier.

## 10.5 Practical uses

A lab-scale air classification system set up at the National Institute of Clean-and-Low-Carbon Energy in Beijing, China, is shown in Fig. 10.8 (Dong, Jow, Su, & Lai, 2013).

It consists of a feeder (identified as 1), which has an adjustable screw speed to control the feeding rate of the particulate material; an air blower to control the airflow rate; a centrifugal separator (identified as 2) with an adjustable fan speed; a cyclone separator (identified as 3); a filter bag; and an induced draft fan. The speed of the centrifugal fan is in a tunable range from 200 to 3000 rpm. The diameter of the centrifugal separator is about 0.3 m. The diameter of the cyclonic separator is 0.2 m. The airflow for the whole system is in the range from 500 to 1400 $m^3$/h. The processing capacity is about 20 kg/h of fly ash particulate materials according to the design specifications. The energy consumption of this air classification system is estimated to be 45–50 kWh/ton.

**Fig. 10.7** Cyclonic air classifier.

**Fig. 10.8** Centrifugal force-based air classifier.

The cut size or average particle size of the separated particle size distribution can be tuned by different centrifugal fan speeds, feeding rates, and airflows. A higher fan speed (rpm) produces finer fly ash under the given feeding speed and airflow. A higher feeding rate produces a higher solid-gas concentration, resulting in a higher viscosity and larger cut size, while a higher air flow also increases the cut size; both increase the productivity. A higher centrifugal fan speed at optimal feeding and airflow rates is used to achieve a good balance of the desired particle size and productivity.

Here is an example of the original fly ash with a particle size range of 0.20–478 μm and $D_{50}$ of 23 μm, which is run through this air classification system at the fan speed of 2900 rpm using the airflow of 1000 $m^3$/h to produce three separated fly ash materials: coarse fly ash (from centrifugal separator), fine fly ash (from cyclone separator), and ultrafine fly ash (from filter bag), as listed in Table 10.4. The particle size distributions of the original and the separated fly ashes are shown in Fig. 10.9.

The same original fly ash sample was run at different centrifugal fan speeds of 500, 1000, 2000, and 2900 rpm, respectively, while the airflow was kept at about 1000 $m^3$/h. Their particle size distributions are shown in Fig. 10.10.

**Table 10.4** $D_{50}$, **range, percent weight of original and separated fly ash materials**

| Sample ID | $D_{50}$ (μm) | Range (μm) | Weight (%) | Weight (kg) |
|---|---|---|---|---|
| Original | 23 | 0.2–478 | 100 | 15.54 |
| Coarse | 30 | 0.2–200 | 84 | 12.99 |
| Fine | 2.7 | 0.3–30 | 14 | 2.21 |
| Ultra-fine | 1.2 | 0.1–20 | 2 | 0.34 |

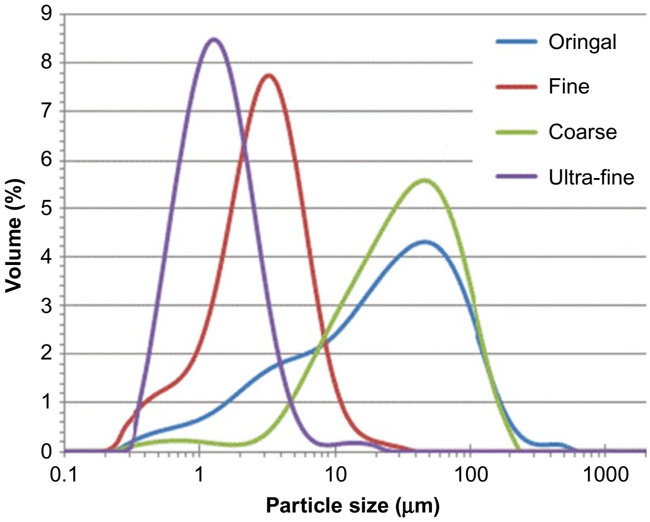

**Fig. 10.9** Particle size distribution of the original and three separated fly ash samples.

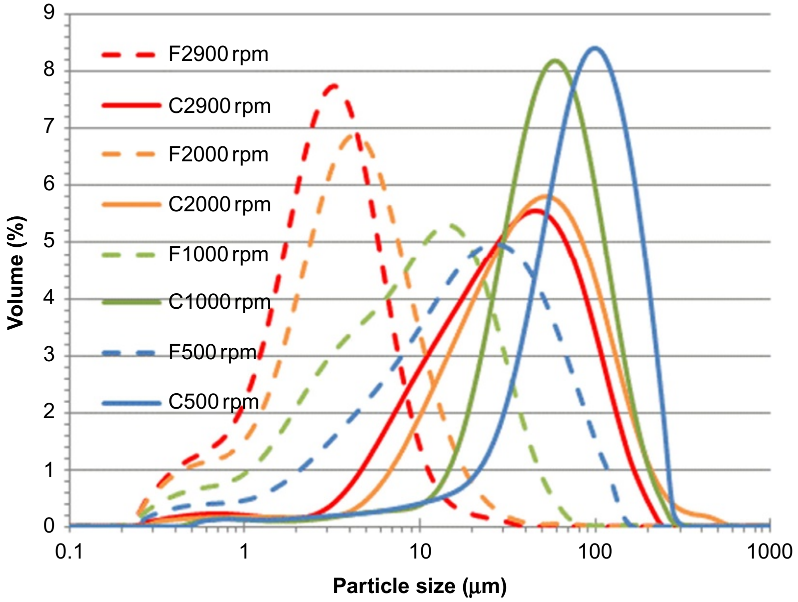

**Fig. 10.10** Particle size distributions of the original and separated fly ash at different fan speeds.

**Table 10.5 Average particle sizes and amounts of coarse and fine parts at different fan speeds**

| Fan speed (rpm) | Coarse kg | Coarse $D_{50}$ (µm) | Fine kg | Fine $D_{50}$ (µm) |
|---|---|---|---|---|
| 500 | 0.9 | 79.4 | 4.1 | 17.5 |
| 1000 | 2.2 | 51.2 | 2.7 | 8.3 |
| 2000 | 3.7 | 38.9 | 1.3 | 3.6 |
| 2900 | 3.6 | 30.1 | 0.7 | 2.7 |

The results achieved by different fan speeds are summarized in Table 10.5. The average particle size and the amount of fine fly ash are decreased from 17.5 to 2.7 µm as the centrifugal fan speed is increased. The average particle size of coarse fly ash is also decreased from 79.4 to 30.1 µm, but the amount is increased as the fan speed is increased. It clearly shows that a centrifugal force-based air classifier can produce the fine fly ash particle size distribution with $D_{50}$ between 2 and 3 µm.

## 10.6 Alternative technologies

The hydraulic classifier process is another separation technology. This process can also separate out fine fly ash with $D_{50}$ of 2–3 μm, but it is a wet process;drying fine fly ash is required for dry applications. Sieving and milling are two other competing alternative technologies to air classification. Sieving is the closest to an ideal size classification, performing much better than air classification, but it has a limitation in the lowest cut size, as it is very difficult to go down below 20 μm using a 635 mesh size. Sieving is also less efficient for separating large quantities of particulate materials. Milling can easily grind down the large particle sizes to the desired fine particle size for single particle size distribution, but it is a very energy-intensive process to grind down below 10 μm.

### *10.6.1 Sieving*

A sieve is a device for separating particulate materials into various desired particle size ranges through woven screens, such as meshes or nets, or by mechanical forces, such as shaking, tapping, or vacuum. Sieve sizes are regulated by various commonly used sieve standards, including US ASTM E11:01 standard, European EN 933-1 standard, and International ISO 565:1990 and ISO 3310-1:2000 standards. Commercial sieve mesh dimensions are listed in Table 10.6. Sieves are commonly used in a series, in which each member sieve is selected to pass particles for a desired particle size range, such as 70–140 mesh using 70 and 140 mesh sizes.

Sieving is a supplementary separation process from air classification. For example, coarse fly ash obtained from an air classifier, as shown in Fig. 10.8, can be further separated by the sieving equipment offered by SWECO to obtain three fractions using 140, 70, and 40 mesh screens. Fig. 10.11 is coarse fly ash (BJ-C2900rmp) and its three sieved samples.

### *10.6.2 Milling or grinding*

Milling or grinding can reduce coarse fly ash particles to fine particle size in a similar range as particles separated out from air classification. But milling does not directly compete with air classification, as milling is not a filtration technique. Milling reduces the fly ash particle size by breaking up large spherical particles into smaller irregularly shaped particles that can have a negative impact on rheology. Milling also consumes more energy than air classification to obtain the fine particle size distribution and has a size limitation, as it is difficult to reduce the particle sizes down to less than 10 μm. The advantage of milling is that the entire milled quantity will consist of only one defined particle size distribution instead of fine and coarse particle size distributions.

Milling breaks solid materials into smaller pieces by grinding, crushing, or cutting by attrition, collision, or compressive forces. For particles less than 50 μm, the energy needed to grind the material down to the desired size follows the Von Rittinger

## Table 10.6 Commercial sieve mesh dimensions

| Sieve size | Opening | | Standard mesh | | Sieve size | Opening | | Standard mesh | |
|---|---|---|---|---|---|---|---|---|---|
| (mm) | (in) | (µm) | US | Tyler | (mm) | (in) | (µm) | US | Tyler |
| 5.6 | 0.22 | 5600 | 3.5 | – | 0.3 | 0.012 | 300 | 50 | 48 |
| 4.75 | 0.187 | 4750 | 4 | – | 0.25 | 0.01 | 250 | 60 | 60 |
| 4 | 0.157 | 4000 | 5 | – | 0.21 | 0.008 | 212 | 70 | 65 |
| 3.35 | 0.132 | 3350 | 6 | – | 0.18 | 0.007 | 180 | 80 | 80 |
| 2.8 | 0.11 | 2800 | 7 | – | 0.15 | 0.006 | 150 | 100 | 100 |
| 2.36 | 0.093 | 2360 | 8 | – | 0.13 | 0.005 | 125 | 120 | 115 |
| 2 | 0.079 | 2000 | 10 | – | 0.11 | 0.004 | 105 | 140 | 150 |
| 1.7 | 0.066 | 1700 | 12 | 10 | 0.09 | 0.004 | 90 | 170 | 170 |
| 0.85 | 0.033 | 850 | 20 | 20 | 0.07 | 0.003 | 74 | 200 | 200 |
| 0.71 | 0.028 | 710 | 25 | 24 | 0.06 | 0.002 | 63 | 230 | 250 |
| 0.6 | 0.023 | 600 | 30 | 28 | 0.05 | 0.002 | 53 | 270 | 270 |
| 0.5 | 0.02 | 500 | 35 | 32 | 0.04 | 0.002 | 44 | 325 | 325 |
| 0.425 | 0.017 | 425 | 40 | 35 | 0.04 | 0.002 | 37 | 400 | 400 |
| 0.355 | 0.014 | 355 | 45 | 42 | 0.03 | 0.001 | 25 | 500 | – |

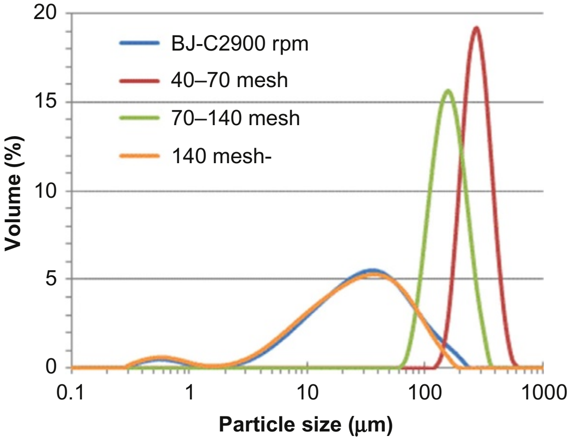

**Fig. 10.11** Coarse fly ash with its three sieved samples.

grinding law, while the particle sizes less than 50 mm but greater than 50 μm follows the Bond grinding law, as listed here:

For the particle size <50 μm,

$$W_R = C_R(1/d_E - 1/d_A)$$

For the particle size <50 mm but >50 μm,

$$W_B = C_B\left(1/\sqrt{d_E} - 1/\sqrt{d_A}\right)$$

$W_R$ or $W_B$ is grinding work (kJ/kg). $C_R$ or $C_B$ is grinding coefficient. The size of the source material is $d_A$. The size of the ground material is $d_E$.

Three types of millings have been used to grind fly ash to smaller particle size: ball milling, vibration milling, and plate (pan or plane) milling. Ball milling is typically loaded with particulate materials at its 30%–40% capacity. A higher rotation speed, longer processing time, greater ball density, or greater impact force produces finer particle size distribution. The accumulated volumes of Class II fly ash, which has no more than 25% by weight higher than 45 μm, and its ball-milled samples at different times of 15, 30, 45, 60, 90, and 120 min are shown in Fig. 10.12. A longer grinding time produces finer particle size. After 15 min of grinding, all milled fly ashes become Class I fly ash, which is no more than 12% by weight greater than 45 μm, according to fly ash classification under the Chinese standard, GB/T 1596–2005.

Vibration milling is the core technology for energetically modified cement (EMC) technology, which was patented in 1993 by Dr. Vladimir Ronin. Plate milling was introduced in 2015 at the World of Coal Ash conference by Professor Li Hui from Xi'an University of Architecture and Technology. Her paper showed the energy consumption to grind down fly ash with $D_{50}$ of 21.57 μm down to 3 μm is 1019, 1323, and 120 kWh/ton for ball, vibration, and plate milling, respectively.

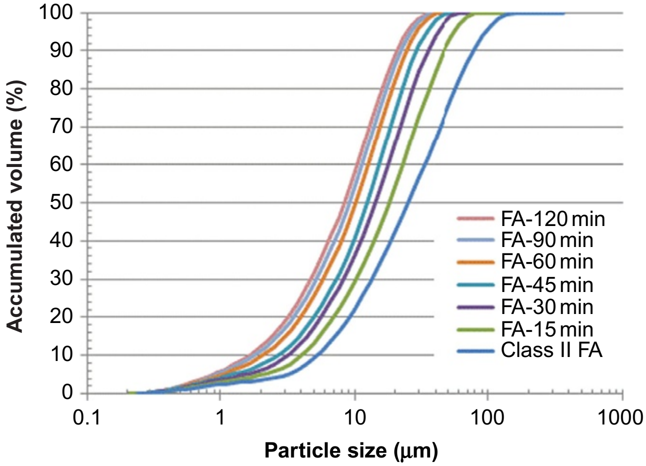

**Fig. 10.12** Class II fly ash with its ball-milled samples at different times.

## 10.7 Future trends

The issues of fly ash utilization (or beneficiation) are due to its massive volume, significant variations in its fundamental properties, and location relative to marketable value and demands. Three fundamental properties of fly ash are chemical composition, mineral composition, and particle size and its distribution, all of which affect its utilization. Fly ash with a consistent and specific quality in chemical composition, mineral composition, and particle size distribution is needed as the raw material for the high value applications. It is expected that industry standards will be established to classify fly ash with consistent fundamental properties for different value-added applications, particularly high-value utilizations.

In China, fly ash produced near the city or the east coast is fully utilized due to massive building and construction needs, while fly ash is still being over supplied in the remote regions due to low utilization. It is still good to pursue as a technology development or a business opportunity how to fully utilize fly ash and achieve its maximum utilization value without any negative environmental impact.

Original (unrefined and unfiltered) fly ash produced from the coal-fired power plant has very low commercial value and is difficult to utilize, particularly in the remote areas. Any commercial application of fly ash requires a consistent raw material quality, including its particle size distribution.

Conventional wisdom states that finer fly ash can be collected by more electrostatic precipitators at each coal-fired power plant. Fig. 10.13 shows five fly ashes collected from each precipitator at the same power plant, identified as SH-1, SH-2, SH-3, SH-4, and SH-5. Indeed, SH-3, SH-4, and SH-5 have finer average particle size than SH-1 and SH-2, but they still have a very wide range of particle size distributions. Since a finer particle size is typically needed for high-value applications, fly ash from

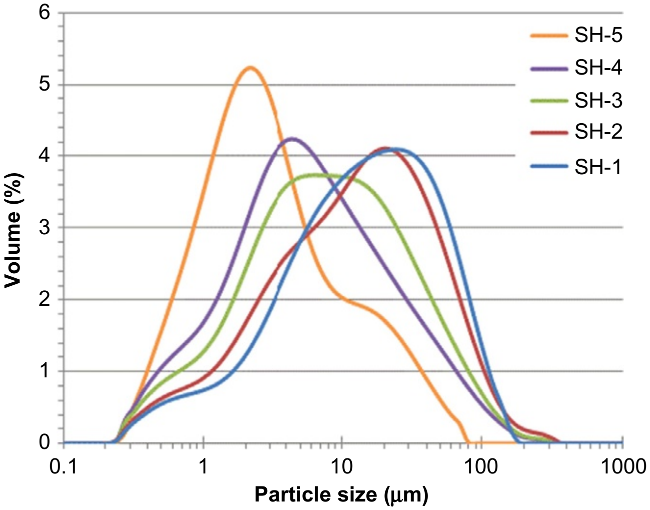

**Fig. 10.13** Particle size distributions for fly ashes from different precipitators.

different electrostatic precipitators should not be mixed all together but instead stored in different storage tanks, particularly SH-1 and SH-2 vs. SH-3, SH-4, and SH-5.

## 10.8 Summary and conclusions

The role of air classification for the beneficiation of fly ash is to classify its broad particle size distribution into two or more desired particle size fractions for the applications where specific particle size requirements are needed, such as filler applications (e.g., 2500, 1250, 800, 400 mesh, etc.) or classification for mortar or concrete uses (no more than 12%, 25%, or 45% by weight greater than 45 μm for Class I, II, or III). Air classification can be used not only to obtain fly ash with the desired particle size distributions, but also to obtain fly ash raw materials with the consistent quality needed to eliminate the variation in particle size distributions from plant to plant or even batch to batch from the same plant for further utilization or product development.

Air classification can produce a much finer fly ash than milling without destroying its spherical shape by using less processing energy. Air classification can also produce much finer particles at a more efficient rate than sieving for obtaining two or more desired and consistent particle size distributions. It is recommended that fly ash from different electrostatic precipitators at each coal-fired power plant shall be collected separately to increase its efficiency and reduce its cost of obtaining the finer fly ash particles for high value-added applications.

## References

ASTM C618-12a. (n.d.). Standard specification for coal fly ash and raw or calcined natural pozzolan for use in concrete.

Dong, Y., Jow, J., Su, J., & Lai, S. (2013). Fly ash separation technology and its potential applications. In *2013 WOCA, Lexington, Kentucky*.

GB/T (1596–2005): Fly ash technical requirements used for cement and concrete.

Holdich, R. G. (n.d.). *Fundamentals of particle technology*. Department of Chemical Engineering Loughborough University, Midland Information Technology and Publishing: Leichesterhsire, UK.

# Electrostatic beneficiation of fly ash

# 11

J.D. Bittner*, F.J. Hrach†
*Orca Technical Interests LLC, Tacoma, WA, United States, †ST Equipment & Technology LLC, Needham, MA, United States

## 11.1 The benefits and challenges of electrostatic separation

Electrostatic separation processes have been used for beneficiating minerals since the early 20th century (Ralston, 1961). The advantages of electrostatic separation for separating unburned carbon from fly ash to produce a concrete quality pozzolana are many when compared to wet beneficiation processes or combustion-based thermal processes. Electrostatic separation is a dry process that requires no water, and the recovered ash product does not require dewatering and drying. The process also does not generate wastewater contaminated with flotation chemicals. It requires very little energy, <2 kwh/tonne. The unburned carbon separated from the raw feed ash is returned to the utility boiler to recover the fuel value. The electrostatic process does not generate combustion-related pollutants, such as nitrogen oxides, sulfur oxides, or mercury. However, the separation of unburned carbon from fly ash by electrostatics has presented many challenges.

Historically, electrostatic separation processes have been used commercially to separate mineral particles >100–150 μm (Brands, Beier, & Stahl, 2005). In a typical fly ash generated from pulverized coal combustion, particles range in size from 1 to >200 μm, with most of the mass below 20 μm. As we will discuss, this has presented a fundamental challenge for the design and operation of electrostatic separation equipment.

Pulverized coal-fired boilers typically range in electrical output from 500 to 1000 MW. A single power station usually has several generating units with a generating capacity of up to 4000 MW. By burning a typical bituminous coal with 10% ash content and assuming 15% of the ash fired in the coal goes to bottom ash, a single 500 MW unit can generate 16 tonnes per hour of fly ash at maximum load, which averages 11 tonnes per hour at a 70% utilization rate. For a 1500 MW station, the relevant numbers are 48 tonnes per hour at maximum load and 33 tonnes per hour on average. Therefore high feed rates (i.e., 10–50 tonnes per hour), are required for commercial operations that separate unburned carbon from fly ash. This has been a challenge for conventional electrostatic separation equipment and many concepts that have been applied to fly ash.

**Coal Combustion Products (CCP's).** http://dx.doi.org/10.1016/B978-0-08-100945-1.00011-3

## 11.2 The importance of fly ash properties in electrostatic separation

Fly ash is composed of spherical glassy mineral particles that are electrically nonconductive, irregularly shaped, and sometimes porous and lacy unburned carbon particles that are conductive. The difference in conductivity is important for causing and/or preventing electrostatic separation depending on the design of the equipment.

Fly ash particles are very fine compared to other minerals that are separated by electrostatics. Measured by dry ultrasonic sieving, fly ash from pulverized coal-fired boilers typically has only 10%–30% of the mass >325 mesh (+45 μm). The median particle diameter is typically 15–20 μm. The median size of the unburned carbon particles is generally larger than the mineral particles. The 95th percentile particle size can be 150–300 μm. A typical particle size distribution measured by laser light scattering and ultrasonic sieving is shown in Fig. 11.1. The laser light scattering measures larger particles than ultrasonic sieving due to the poorer dispersion of agglomerates by the dry dispersion method of the laser system.

The unburned carbon content is measured by loss on ignition (LOI). Feed ash LOIs depend on coal type, boiler design, and operating conditions. They range from 3% to 25%, but are mostly 5%–15%. The target product LOIs range from 2% to 5% depending upon the market requirements; European requirements are on the high end, and US and Japanese requirements are on the low end.

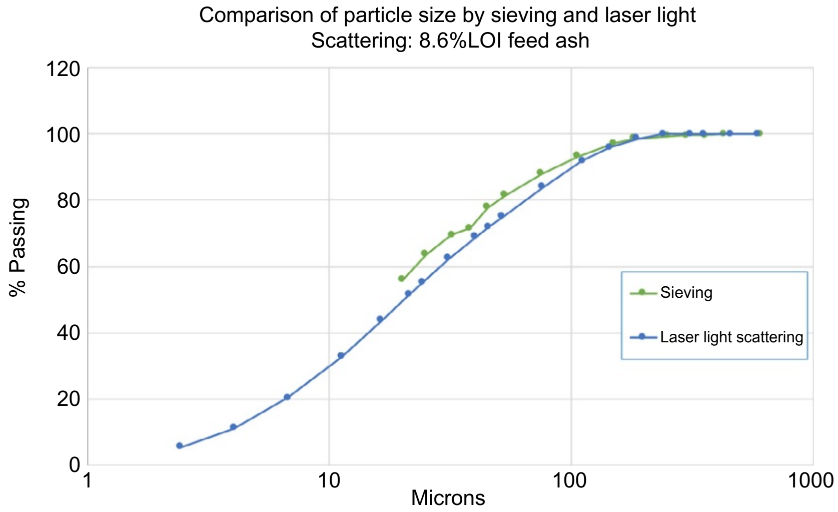

**Fig. 11.1** Fly ash particle size distribution.

## 11.3 Fundamentals of electrostatics

### 11.3.1 Particle charging mechanisms

There are three mechanisms by which particles can acquire charges in commercial electrostatic separation equipment: corona charging, induction charging, and triboelectric charging (Fig. 11.2).

#### 11.3.1.1 Corona charging

In corona charging, particles are bombarded by either positive or negative ions generated in a corona discharge in a high electric field. A negative corona, where negative ions are created by electron attachment to oxygen atoms, is generally preferred because it allows a more intense corona to be produced in air. All particles are charged with the same polarity in the corona by the ions, which are accelerated toward the particles in the electric field. In the case of fly ash, both the nonconductive mineral and conductive carbon are charged negative (Kelly & Spottiswood, 1989b).

#### 11.3.1.2 Induction charging

Induction charging occurs when uncharged particles enter an electric field and come in direct contact with a conducting electrode. A nonconducting particle will become and remain polarized. The charge will not drain to the electrode, and it will remain with a net-zero charge. When a conducting particle comes in contact with the conducting electrode, it will acquire charge of the same sign as the electrode by conduction. The force of the applied field will repel it from the electrode it has contacted and toward the electrode of opposite polarity (Manouchehri, Hanumantha Roa, & Forssberg, 2000).

#### 11.3.1.3 Triboelectric charging

Triboelectric charging occurs when two particles of dissimilar materials come into contact. Dissimilar materials, whether they are conductors, semiconductors, or nonconductors, have different electron work functions. The work function is defined as the energy required to remove the most loosely held electron from the surface in a vacuum. The work function is not a bulk property of the material but a property of the surface that depends upon the crystal face and surface contamination. When dissimilar particles collide, electrons flow from the surface of the material with the lower work function to the surface of the material with the higher work function. The amount of charge that is created is a function of the velocity of contact and the number of contacts. The maximum charge density created by triboelectric charging in air is limited to about $2.66 \times 10^{-5}$ Coul/$m^2$ by the electrical breakdown of air as the contacting particles move apart. However, such high-charge densities are not achieved in practice (Kelly & Spottiswood, 1989b; Manouchehri et al., 2000).

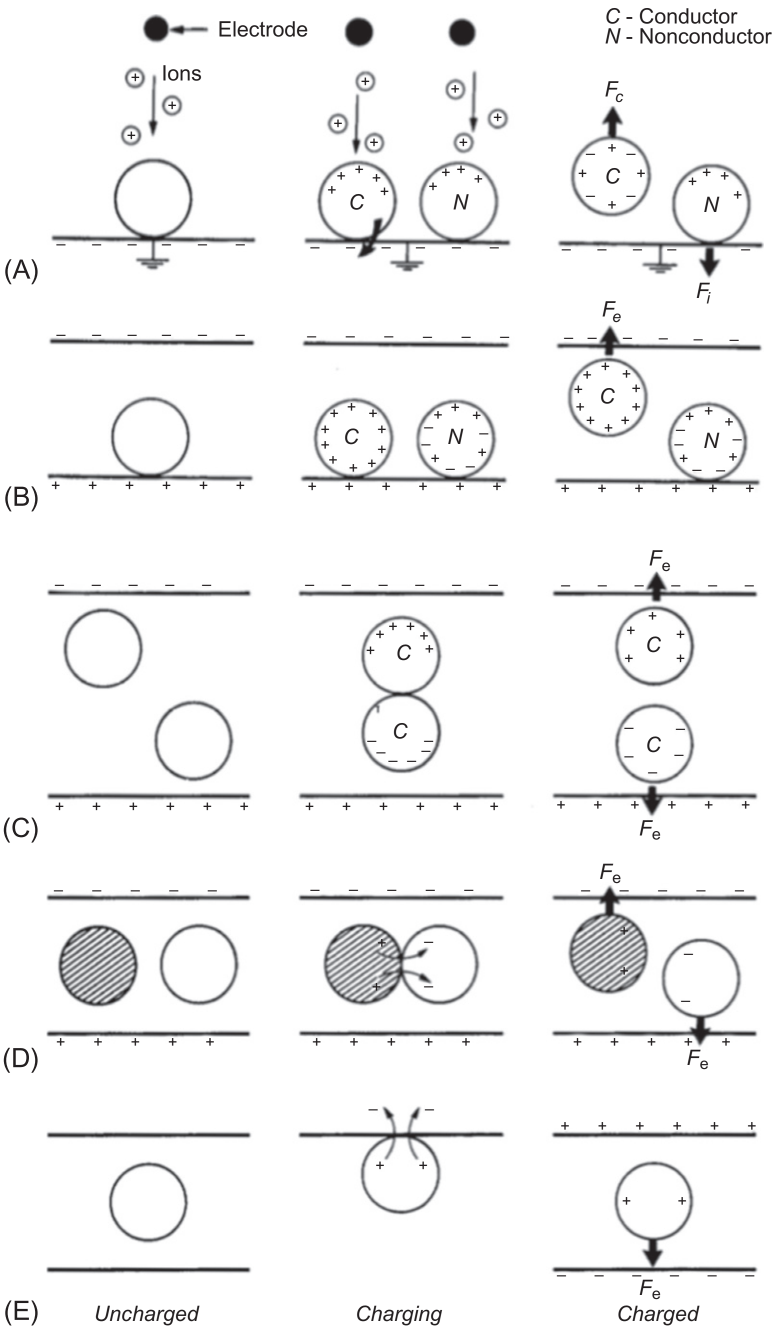

**Fig. 11.2** Particle charging processes: (A) corona charging, (B and C) induction charging, (D) particle/particle tribocharging, and (E) particle/surface tribocharging (Kelly & Spottiswood,1989b).
From Kelly, E., & Spottiswood, D. (1989). The theory of electrostatic separations: a review, Part II. Particle charging. *Minerals Engineering*, *2*(2), 193–205.

Particles can also be charged triboelectrically by their contact with a third surface, such as a plate or the inner surface of a pipe or cyclone. The material of the third surface is generally chosen to have a work function between that of the mineral and that of the carbon particles; thus contact with the third surface will charge the mineral particle and the carbon particles with opposite polarities.

Humidity and other adsorbed surface species can have a significant effect on the charge density created by tribo-charging. In fly ash that has been kept dry in a low-humidity environment, such as storage in an ash collection silo at a power plant with minimum exposure to ambient air, the glassy mineral oxide particles charge negative while the carbon particles charge positive. However, when exposed to high relative humidity, the charge decreases and can go to zero, making electrostatic separation impossible. In a situation where the fly ash has been wetted with water and then dried, the charge can reverse; the carbon particles will charge negative and the mineral particles charge positive (Cangialosi, Notarnicola, Liberti, & Stencel, 2009; Cangialosi et al., 2006). Although not completely understood, it is hypothesized that the redistribution of water soluble ions between carbon and mineral occurs on contact with liquid water.

## 11.3.2 Forces acting on charged particles

In any design of electrostatic separation equipment and its operation, there are at least three forces acting on the particles: the electrostatic force under the influence of an electric field, gravity, and aerodynamic drag (Fig. 11.3).

The electrostatic force on a particle in an electric field is

$$F_e = Q \cdot E$$

where $Q$ is the charge on the particle in Coul, and $E$ is the electric field strength in V/m.

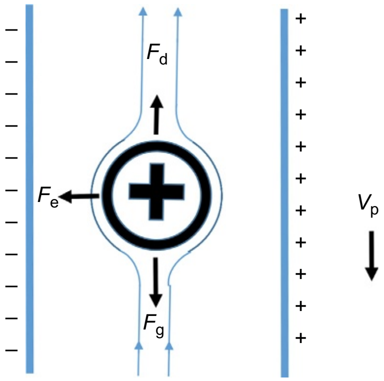

**Fig. 11.3** Forces on a particle in free fall in an electric field.

For a spherical particle of diameter $D$ in m,

$$F_\mathrm{e} = \sigma \pi D^2 E$$

where $\sigma$ is the charge density on the surface of the particle in Coul/m$^2$.

The force of gravity on a spherical particle is

$$F_\mathrm{g} = (\pi/6) D^3 \rho_\mathrm{p} g$$

where $\rho_\mathrm{p}$ is the particle density and $g$ is the acceleration of gravity.

The drag force on a spherical particle is

$$F_\mathrm{d} = (\pi/8) \rho_\mathrm{f} v_\mathrm{p}^2 C_\mathrm{d} D^2$$

where $\rho_\mathrm{f}$ is the fluid density, $v_\mathrm{p}$ is the particle velocity, and $C_\mathrm{d}$ is the drag coefficient. The drag coefficient is determined from a relationship with the Reynolds number ($\mathrm{Re} = \rho_\mathrm{f}\, D\, v_\mathrm{p}/\mu_\mathrm{f}$) for a sphere, where $\mu_\mathrm{f}$ is the viscosity of the fluid (Tilton, 2008).

These model relationships have been used to estimate the forces acting on particles over the size range of fly ash in a typical free fall separator. Particles are charged triboelectrically in a charging device (e.g., fluidized bed, cyclone or curved pipe tribocharger, etc.) above two vertical parallel plate electrodes to which high voltage is applied to achieve electric field intensities of 100–150 kV/m. For the purposes of illustration, charge densities of $2 \times 10^{-6}$ Coul/m$^2$ are assumed. This is significantly below the maximum cited above, but is in line with experimental measurements on several particle-tribocharger material combinations (Manouchehri, Hanumantha Rao, & Forssberg, 2002). The particles fall under the force of gravity in the gap between the electrodes. Particles move horizontally towards the electrode of the opposite polarity. The vertically flowing stream is split into two or three streams at the exit of the gap between the electrodes. Positively charged particles are collected exiting near the negative electrode and negatively charged particles are collected near the positive electrode. The results of these model calculations are summarized in Table 11.1.

The first observation is that gravitational forces vary by more than four orders of magnitude over the particle size range in a typical fly ash feed (<10 up to 300 μm). Accordingly, the terminal velocities (calculated from the balance of drag and gravitational forces) of the particles as they fall under the force of gravity also vary widely. As the charge on the particles is proportional to their surface area, the electrical forces that cause the particles to move horizontally from the center of the electric field towards the electrodes also decreases with particle size. From the balance between the electrical forces and the aerodynamic drag forces, the horizontal velocity of each particle size fraction can be estimated. The ratio of the horizontal velocity to the vertical terminal velocity determines the particle trajectories in the absence of other flow disturbances.

From the variation of the velocity ratio $v_\mathrm{h}/v_\mathrm{t}$ from 0.41 for 300 μm particles to 8.0 for 10 μm particles, the trajectory of the finer particles will tend to take them to the electrode surfaces, while the larger particles may barely move far enough horizontally

**Table 11.1** Calculated forces on particles in electrostatic separation

**$E$ (V/m) 1.50E+05**
**$Q/A$ (Coul/m$^2$) 2.00E−06**

| | **Gravitational** | | **Electrical** | | | **Drag** |
|---|---|---|---|---|---|---|
| | | **Terminal velocity** | | **Horizontal velocity** | | **$v = 0.1$ m/s** |
| **$D$ (μm)** | **$F_g$ (N)** | **$v_t$ (m/s)** | **$F_e$ (N)** | **$v_h$ (m/s)** | **$v_h/v_t$** | **$F_d$ (N)** |
| 300 | 3.24E−07 | 1.8 | 8.46E−08 | 0.74 | 0.41 | 7.11022E−09 |
| 100 | 1.20E−08 | 0.25 | 9.40E−09 | 0.43 | 1.72 | 1.85888E−09 |
| 50 | 1.50E−09 | 0.113 | 2.40E−09 | 0.23 | 2.07 | 9.2944E−10 |
| 20 | 9.60E−11 | 0.027 | 3.76E−10 | 0.11 | 4.00 | 3.50213E−10 |
| 10 | 1.20E−11 | 6.80E−03 | 9.40E−11 | 0.054 | 7.95 | 1.75106E−10 |

to be effectively separated. The collection of fine particles (<100 μm) on the electrodes is a problem in free-fall separators (Brands et al., 2005). In fly ash separation, the nonconductive mineral particles which collect on the positive electrode build up insulating deposits which decrease the effective electric field between the electrodes, causing poor separation. When the positively charged conductive carbon particles contact the negative electrode, they exchange charges by induction with the electrode surface. The resulting negatively charged carbon is then attracted to the positive electrode along with the mineral particles, thus decreasing the separation efficiency.

As already noted the majority of the fly ash particles are below 50 μm, with more than 50% or 60% <20 μm. The terminal velocities of the particles >50 μm are 4–65 times greater than those particles <20 μm. These larger particles moving at 0.1–1.8 m/s will create flow disturbances as they pass through the much more slowly moving fine particles. It is not unreasonable to assume that these disturbances in the air flow will be of similar velocity to the particles causing them (>0.1 m/s). The drag forces on particles buffeted by 0.1 m/s air currents are shown in the last column of Table 11.1. The drag forces for particles 50 μm and below are the same order to and a factor of 10 higher than both the gravitational and electrical forces, thus flow disturbances caused by the faster falling large particles will dominate the trajectories of the finer particles, making the effective separation of the finer particles impossible. On the other hand, the drag forces on the particles >100 μm are much less than the gravitational or electrical forces. Gravity and electrical forces will control the trajectories and separation of the larger particles with minimal effect from air currents of the order 0.1 m/s.

These insights gained from this simple analysis about the difficulty in separating particles <100 μm electrostatically are consistent with experience in the separation of other minerals by free-fall separation, where it is necessary to carefully control the particle size distribution of the feed for effective separation, and it is typically necessary to remove all fine particles <100 to 150 μm prior to free-fall separation.

## 11.4 Electrostatic separator concepts to separate unburned carbon from fly ash

As already noted the conventional free-fall electrostatic separator is severely limited in its ability to separate particles as fine as fly ash. There have been many concepts proposed for equipment design and operation in order to address these limitations and separate unburned carbon from fly ash.

### *11.4.1 Vertical parallel plate separators*

Two research groups have used ambient air as a carrier gas rather than gravity to control the flow of particles through the electric field in attempts to overcome the shortcomings of traditional vertical free-fall separators in separation of particles finer than 50 μm. A group at the University of Kentucky Center for Applied Energy Research patented a vertical separator that transports the fly ash in laminar flow conditions

(Stencel, Schaefer, Ban, & Neathery, 1999; Stencel et al., 1999). A group at the Korea Electric Power Research Institute (KEPRI) has applied for a patent for a tribocharger for a vertical parallel plate separator that utilizes turbulent flow (Kim & Lee, 2011).

#### *11.4.1.1 University of Kentucky laminar flow separator*

In the University of Kentucky system, laminar flow is used to reduce the transport of fine particles by turbulent eddies that reduce the separation efficiency. A key feature of this device is the clean curtain gas that flows next to the electrodes and surrounds the particle-laden gas in an attempt to prevent particles from colliding with the electrodes, causing a build-up of insulating mineral particles or a charge reversal of the conducting carbon particles. A charge reversal of carbon particles causes them to be attracted to the positive electrode with the mineral particles.

The flow diagram of the University of Kentucky process consists of a feed system, a tribocharging section, and a separation zone (Fig. 11.4). The feed system includes an eductor, in which the particles to be separated are entrained in ambient air at a ratio of ~1/1 solid/gas mass ratio. The velocity of the particle-laden turbulent flow is >10 m/s through a feed pipe (20) lined with a dielectric material with an electron work function that is between that of the carbon and mineral particles. Charging occurs by particle contact with the wall and other particles, with particle-particle contact dominating at high solid loadings. The separation chamber consists of two parallel electrode plates separated by 100 mm with an applied voltage of 10–15 kV, creating an applied electric field of 100–150 kV/m.

Prior to entering the electric field, the high velocity particle laden turbulent flow is expanded through a diffuser and a flow straightener with a grid-like structure to reduce the turbulence and transition to laminar flow (Fig. 11.5). The design includes a curtain of clean air flowing next to the electrodes on both sides of the entrained particle flow. This curtain flow is created by flow straighteners to ensure laminar flow parallel to the plates. Its velocity is adjusted to match the velocity of the particle-laden flow as both enter the electric field. Under laminar flow conditions with electrode length of ~760 mm, residence time is approximately 3 s for bench scale unit described in the patent.

The charged particles entering the electric field are attracted to the electrode of opposite polarity. As they move towards their respective electrodes, they will enter the curtain flow near the electrode. The exit of the separation chamber is divided into three channels, which collect the negative particles near the positive electrode and the positive particles near the negative electrode, as well as those particles flowing in the center that have not traversed sufficiently horizontally. These "middlings" can be recycled to the feed or processed in a subsequent electrostatic separation stage.

Although the University of Kentucky group has published many papers, this technology was developed at the bench scale. When scaled up to a pilot scale unit (250–500 kg/h), there is only limited data to evaluate the technology (Ban, Li, Hower, Schaefer, & Stencel, 1997; Stencel et al., 1999). The data included in the original patent are shown in Table 11.2 (Stencel, Schaefer, et al., 1999).

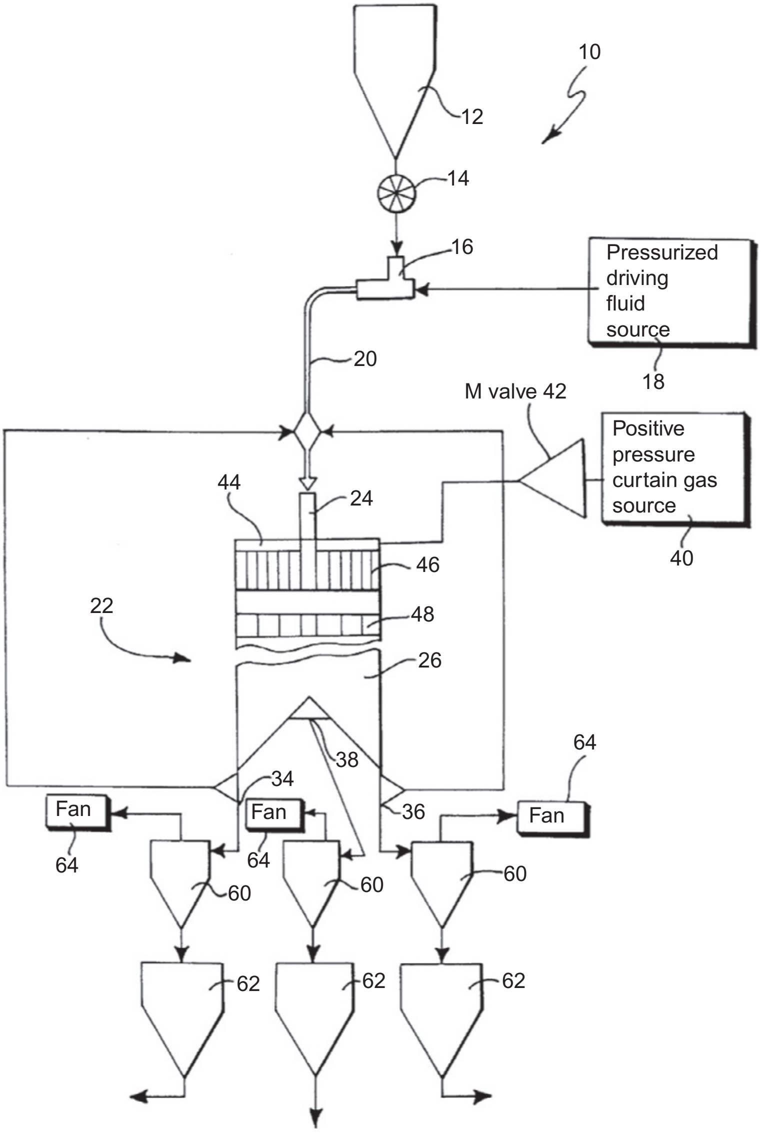

**Fig. 11.4** University of Kentucky pneumatic transport triboelectrostatic carbon/ash separator. From Stencel, J., Schaefer, J., Ban, H., & Neathery, J. (1999). *Apparatus and method for triboeletric separation*. US Patent No. 5,938,041.

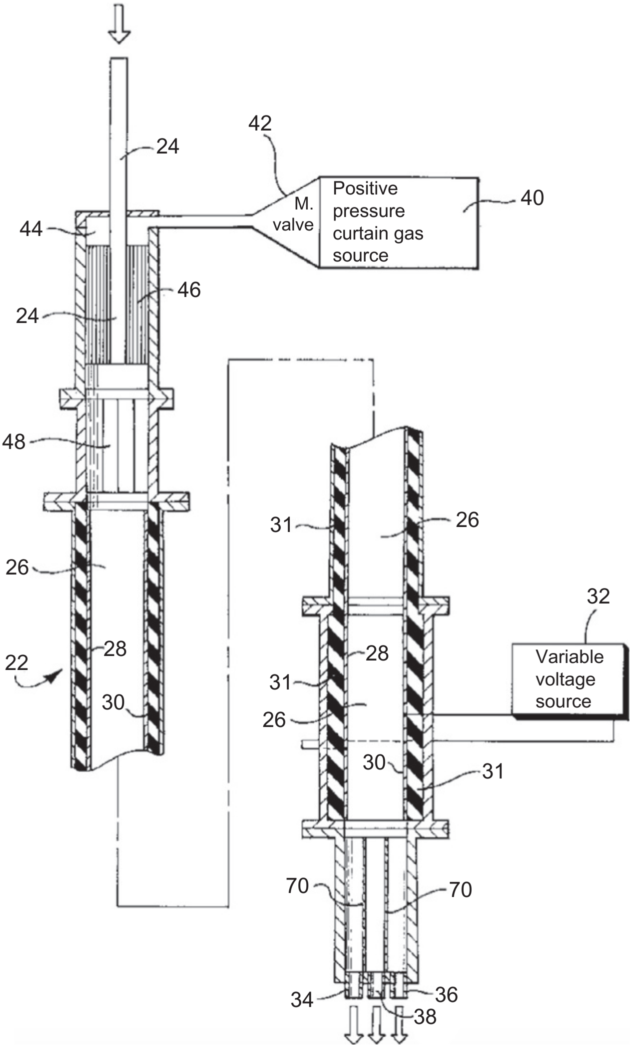

**Fig. 11.5** University of Kentucky laminar flow vertical plate electrostatic separator.
From Stencel, Schaefer et al. (1999). *Apparatus and method for triboelectric separation*. US Patent 5,938,041.

This data shows the effect of the feed rate and applied voltage on the separator performance. However, there is no information on whether middlings were collected or their LOIs. Without this information, it is difficult to assess separation performance. However, this data does provide some insight into the scalability of the technology.

The data in the patent is from a bench scale unit with 100 mm wide electrodes separated by a 100 mm gap, and the length of the electrodes is about 760 mm. The data are reported for feed rates from ~0.91–9.1 kg/h (2–20 lb/h).

**Table 11.2** Data from University of Kentucky bench scale pneumatic transport triboelectric separator

| Feed ID | kV | Lb/h | Feed LOI | Prod LOI | Carbon LOI |
|---|---|---|---|---|---|
| 1 | 7.5 | 4.83 | 10.45 | 3.24 | 24.26 |
| 1 | 10 | 4.79 | 10.45 | 3.87 | 23.54 |
| 1 | 12.5 | 1.87 | 10.45 | 4.12 | 20.24 |
| 1 | 12.5 | 4.82 | 10.45 | 4.11 | 19.7 |
| 2 | 10 | 4.09 | 11.68 | 2.26 | 32.62 |
| 2 | 10 | 11.76 | 11.68 | 2.77 | 29.64 |
| 2 | 10 | 16.32 | 11.68 | 3.09 | 28.6 |
| 2 | 10 | 20.22 | 11.68 | 3.22 | 24.7 |
| 2 | 10 | 4.92 | 12.06 | 2.34 | 34.39 |
| 3 | 10 | 3.5 | 8.87 | 2.2 | 36.7 |
| 4 | 10 | 4.79 | 9.94 | 3.87 | 23.54 |

Data from Stencel, J., Schaefer, J., Ban, H., & Neathery, J. (1999). *Apparatus and method for triboeletric separation*. US Patent No. 5,938,041.

A factor that limits the throughput of all electrostatic separators is the effect of the charges on the particles on the effective electric field in the separation zone. This is known as the space charge effect. When charged particles are introduced between the electrode plates, the charges on the particles interact with the charges on the plates and reduce the local electric field. As one moves away from the surface of one of the electrodes, the field is reduced by the charge on particles in the space between the point of interest and the surface of the electrode. When the charge in the space between the electrodes is equal to the charge on the surface of the electrodes, there is no electric field between the electrodes, even though voltage is applied to the electrodes. The charges between the electrode set up a field that is equal and opposite to the applied field, resulting in a net-zero field.

The charge on the surface of the electrodes is determined by the following relationship for a parallel plate capacitor,

$$Q = CV = (A \cdot \varepsilon)/d \cdot V$$

where $Q$ is the charge on the plates, $C$ is the capacitance of a parallel plate capacitor, $A$ is the area of the electrode, $\varepsilon$ is the permittivity of free space, $8.85 \times 10^{-12}$ Farads/m, $d$ is the gap between the plates, and $V$ is the applied voltage.

By rearranging the relationship,

$$Q/A = \varepsilon \cdot V/d = \varepsilon \cdot E$$

where $E$ is the applied field.

When the charges on the particles between the electrodes are equal or greater than this value, which is determined by the applied electric field, no separation occurs.

There is an optimum charge between the electrodes where the throughput of the high-purity products is maximized. With very few charged particles between the plates, the effective field is the applied field (i.e., the maximum) but the throughput rate is very low. At higher throughput rates (i.e., more charges between the plates) the effective field decreases, and the particle movement toward the electrode is eventually reduced to zero. It can be shown that the optimum charge (i.e., the point where the throughput is maximized) is one-half the charge required to drive the field to zero.

Returning to Table 11.2 and noting the series with Feed ID 2 at 10 kV applied voltage, the separation deteriorates in three steps as the feed rate is increased from 4 to 20 lb/h. The product LOI monotonically increases from 2.3% to 3.2% while the carbon LOI decreases from 32.6% to 24.7%. Thus, at 10 kV this separator is operating near or past the optimum point for charge density.

One might consider increasing the applied voltage to increase the optimum charge density and thus improve the separation at higher throughput. Again referring to the data in Table 11.2, with Feed ID 1 the voltage was increased from 7.5 to 10 to 12.5 kV at a constant feed rate of 4.8 lb/h, yet the separation deteriorated. The product LOI increased from 3.2% to 3.9% to 4.1%, while the Carbon LOI decreased from 24.3% to 23.5% to 19.7%. This unexpected result indicates one (or both) of two things are occurring. Firstly, the separator is operating near the high-voltage limit, with the corona discharge increasing as the voltage is increased. The electrons and ions generated by the corona attach to the triboelectrically charged particles and neutralize them, thus reducing the separation efficiency. Alternatively, as the applied voltage is increased, more carbon particles are colliding with the negative electrode, reversing their charge, and are being attracted towards the positive electrode, which also reduces separation efficiency.

Thus, with respect to the charge density (rate) and voltage (electric field), the separator in the example of US Patent 5,938,041 is operating near its optimum. The options for increasing throughput for this device are very limited. Increasing the charge on the particles by improved tribocharging is not effective if the device is already operating at the optimum point for charge density. Likewise, increasing the gap between the electrodes while maintaining electric field strength is also not effective because the optimum charge point is unchanged. Optimum charge density depends on the electric field, not on the electrode gap.

The only method for a scale-up of the vertical parallel plate separator is to increase the electrode area by increasing the width of the electrodes. For this approach the feed rate is directly proportional to the electrode area. If 100 mm wide electrodes with a 100 mm gap can process 9.1 kg/h (20 lb/h), then a 10 m wide electrode with a 100 mm gap can process 910 kg/h (2000 lb/h). In fact, this is the approach proposed in the patent, as seen in Fig. 11.6 (Stencel, Schaefer, et al., 1999). The capacity would be increased by assembling an array of 1 m (40 in) wide electrode pairs with parallel feed distribution and product collection systems with a parallel curtain gas distribution system. Mechanically, this is a difficult design task that must provide a uniform distribution of feed, carrier gas, and curtain gas, as well as a collection of a minimum of two product streams and perhaps a middling stream for recycle or a subsequent stage of separation. The complexity of such a device is illustrated by a subsequent patent, shown in Fig. 11.7 (Stencel et al., 2001).

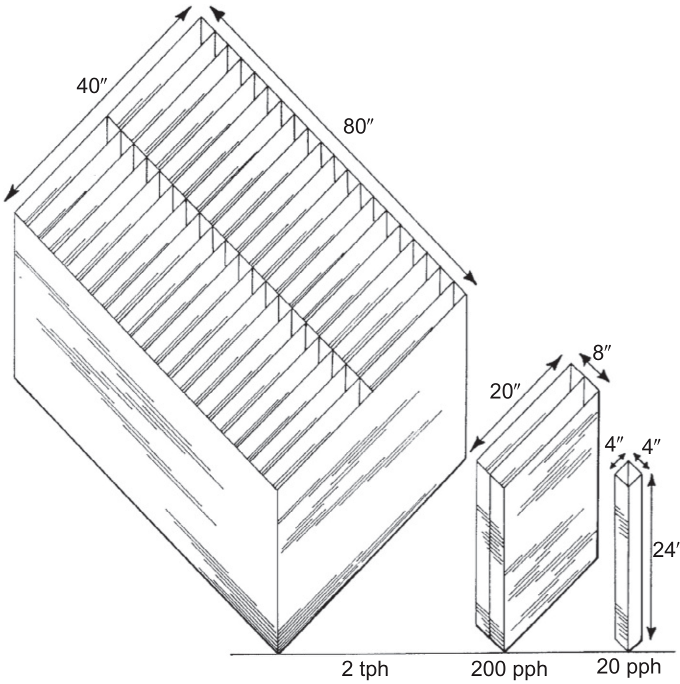

**Fig. 11.6** Scale-up concept for University of Kentucky laminar flow vertical plate electrostatic separator.
From Stencel, Schaefer et al. (1999). *Apparatus and method for triboelectric separation.* US Patent 5,938,041.

This mechanically complex system was scaled to a pilot unit with a 250 kg/h feed rate. A unit to demonstrate the technology at 1000 kg/h was installed in 2001 at the Jack McDonough Plant of Georgia Power in 2001 (Lockert, Lister, & Stencel, 2001). This unit was a single-stage separation from which three streams were collected: a low LOI product, a high LOI product, and a middling product similar to the feed. There is no published data on the performance of either the 250 kg/h pilot unit or the 1000 kg/h demonstration unit. Subsequent to the installation of the 1000 kg/h unit at the Georgia Power Plant, a larger commercial scale unit of unknown capacity was installed at Colorado Springs Utilities' Nixon Plant. This unit was not successful and was therefore dismantled.

### *11.4.1.2 KEPRI turbulent flow separator*

The research group at the KEPRI also used a carrier gas to control the downward velocity between two vertical parallel plate electrodes (Kim, Cho, & Kim, 2001; Kim & Lee, 2009). However, rather than using laminar flow and relatively long residence times (on the order of seconds), they used a high velocity (16.8 m/s) turbulent

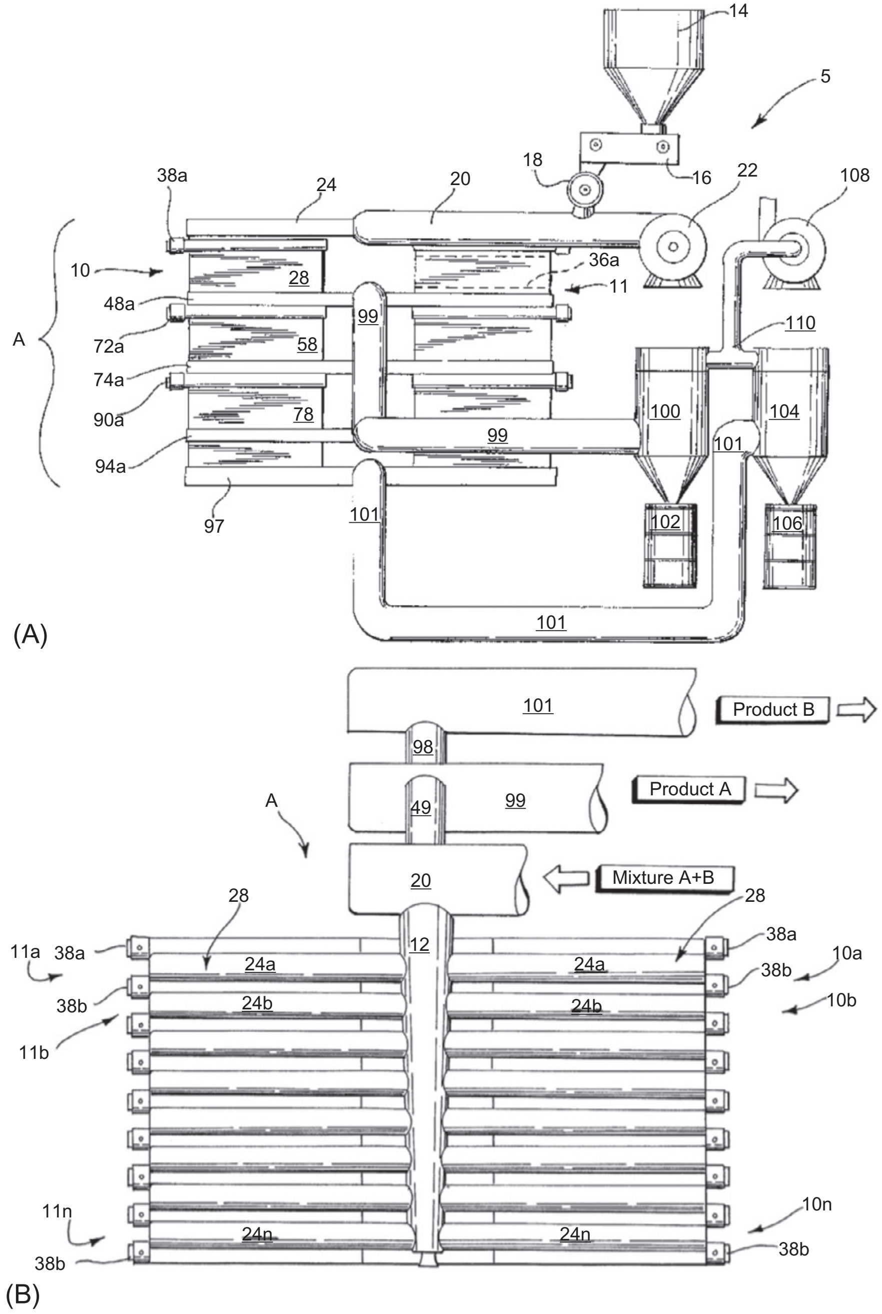

**Fig. 11.7** (A) Concept for parallel multistage electrostatic separators—side view and (B) concept for parallel multistage electrostatic separators—top view.
From Stencel, J., et al. (2001) *Particle separation system using parallel multistage electrostatic separators*. US Patent 6,323,451 B1.

slot jet and shorter (150 mm) effective electrode lengths that gave residence times of 10's of milliseconds. A schematic of the KEPRI process in shown in Fig. 11.8 (Kim & Lee, 2009).

From a bench scale batch system, KEPRI scaled the technology to a 50 kg/h continuous laboratory system (Kim et al., 2001), and then to a 300 kg/h pilot plant (Kim & Lee, 2009). The pilot scale system utilized 200 mm long (effective length was less due to positioning of the splitter) by 900 mm wide electrodes separated by a 100 mm gap. The applied voltage was 50 kV (500 kV/m). A single splitter was used to collect two products, a low carbon and high carbon product. No middlings were collected, and the system included rappers to remove ash deposits from the electrodes. All of the system variables, such as ash feed rate, air rates, splitter position, diffuser exit slit dimensions, and ambient air relative humidity were optimized. The best performance was demonstrated by reducing a 9% LOI feed ash to a 4.5% product LOI at mass yield of 66.7% (ash mineral recovery of 70%) at 300 kg/h. From this study, a scale-up factor was determined to be 830 kg/h $m^2$ of the total electrode area (including both positive

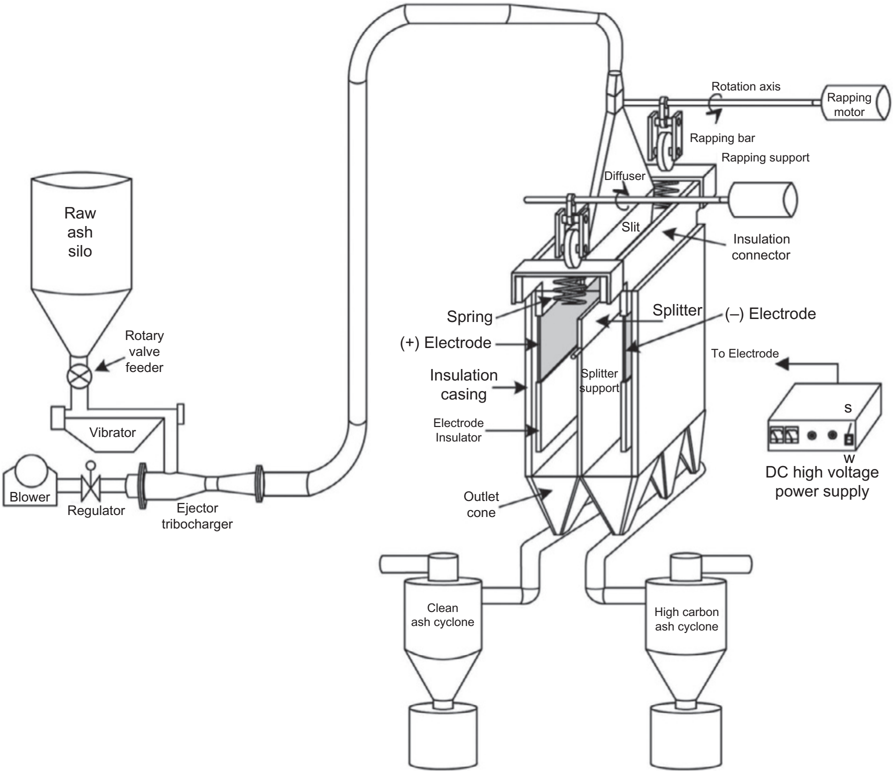

**Fig. 11.8** KEPRI pilot scale electrostatic separation system.
From Kim, J.K, & Lee, H.D. (2009). Design variables of pilot scale electrostatic separator for removing unburned carbon from coal fly ash. *Journal of Chemical Engineering of Japan, 42*(7), 471-477. Copyright Society of Chemical Engineers of Japan.

and negative electrodes), or based on one electrode, 1660 kg/h m$^2$. The increased electrode area must come from wider electrodes, not increased length. KEPRI observed that increasing the electrode length (diffuser-splitter distance) beyond 150 mm resulted in increased low-carbon product LOIs and lower high-carbon product LOIs due to the impingement of carbon particles on the negative electrode, which reversed charge and were attracted to the positive electrode with the mineral particles.

KEPRI has paid special attention to increasing the tribocharging in their process and have developed an electrostatic induction ejector tribocharger. As shown in Fig. 11.9, this device is an eductor with electrode plates (24a and 24b) in the throat (22), with ~10 kV applied. Dimensions of the scaled-up model, which can process 105–330 kg/h, are an 18.5 mm diameter high-pressure motive air inlet (29) and a 10 mm gap between the electrodes, which are 17.4 mm wide and 35 mm long. The electrode plates are made of 304 SS, which has an electron work function between carbon and the aluminosilicate ash mineral. Charging is both by induction on particle contact with the charged plates and particle-particle contact. The impact of the high voltage plates on the net charge, as measured by a Faraday cage (Kim & Kim, 2001), is shown in Fig. 11.10 (Kim & Lee, 2011). Over the range of injection rates, the measured net negative charge is four to eight times higher with the induction ejector tribocharger than with the conventional ejector tribocharger. Furthermore, the charge produced by the induction tribocharger does not decrease as rapidly with increasing solids rate as the conventional ejector. With this improved tribocharger, a 9% LOI feed was reduced to a 3% LOI product at a 68% mass yield at a rate of about 300 kg/h.

Although quite different from the University of Kentucky vertical parallel plate technology in velocity (~0.3 vs ~17 m/s), residence time (~3 vs ~0.15 s), and

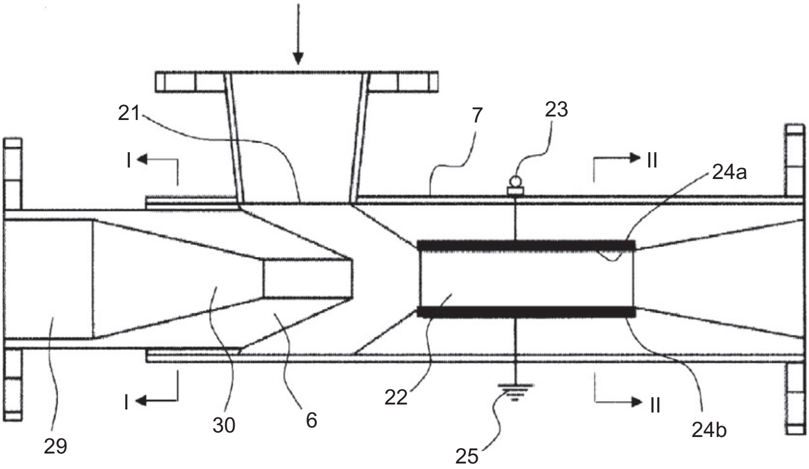

**Fig. 11.9** KEPRI induction ejector tribocharger.
From Kim, J., & Lee, H. (2011). *Electrostatic separator for unburned carbon from coal ash using induction type ejector tribocharger*. US Patent 2011/0036758.

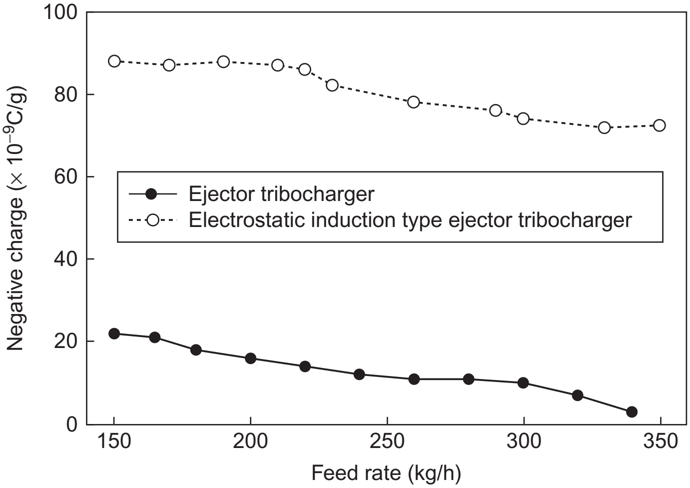

**Fig. 11.10** Effect of induction ejector tribocharger on ash net charge density.
From Kim, J., & Lee, H. (2011). *Electrostatic separator for unburned carbon from coal ash using induction type ejector tribocharger*. US Patent 2011/0036758.

electric field (~150 vs 500 kV/m), the KEPRI technology has the same scale-up limitations. The only way to scale up from the optimized pilot plant results is to increase the width of the electrodes. Using the KEPRI scale-up factor, 30 m of electrode pairs by 200 mm length would be required to process 10,000 kg/h of material. To scale to 40,000 kg/h, an array of 120 m wide electrode pairs would be required operating in parallel. In either case the complexity and cost of tribocharging, feed distribution, and product collection would be great.

### 11.4.2 Inclined vibrating electrode separators

In the late 1990s and early 2000s, two groups patented and made significant efforts to develop fly ash separators based on inclined vibrating electrodes with counter electrodes placed above them to attract the unburned carbon.

#### 11.4.2.1 Minerals and Coal Technologies/Korea Fly Ash Company vibrating electrode separator

Minerals and Coal Technologies (MCT) of Blacksburg Virginia worked with the Korea Fly Ash Company (KFAC) to develop the inclined vibrating electrode separator shown in Fig. 11.11 (Yoon, Han, Yan, & Park, 2001; Yoon, Yan, Han, & Park, 2001)

In this device the bottom plate (2) of the inclined trough is an electrode. The electric field is created by applying a positive voltage to the v-shaped troughs (3) spaced 32 mm off and parallel to the solid inclined electrode. In some examples the effects are reported of applying voltage to a screen (8) placed in the plane of the trough

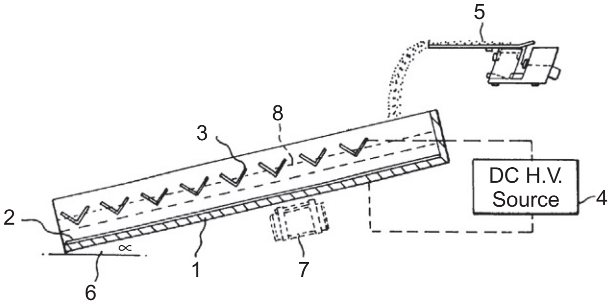

**Fig. 11.11** MCT/KFAC inclined vibrating electrode separator.
From Yoon, R.H., et al. (2001). *Electrostatic method of separating particulate materials*. US Patent No. 6,320,148 B1.

electrodes. A positive 30 kV was applied to the troughs relative to the negative plate electrode. The theory of operation is that as the particles bounce and slide down the inclined vibrating electrode, the conductive carbon particles acquire a negative charge by contact with the negative plate electrode, while the nonconductive mineral particles do not acquire a charge by induction, though they remain close to the plate electrode as they are attracted by image forces in their polarized state. The forces of the electric field propel the negative carbon particles toward and into the positive trough electrodes from which they are collected.

Most experiments were conducted on small batch runs using 100 g of feed ash on a 250 mm wide by 900 mm long electrode. Because residence times were short, three, four, or five stages of separation were used. The most impressive results were those obtained on the +200 mesh (+75 μm) fraction of ash that had been screened. With five passes through the device, a 26.6% LOI feed was reduced to 1.3% LOI with a 49% mass yield. However, the +75μm fraction is of little practical importance as only 10%–15% of fly ash is in this fraction, and this coarse ash is the least reactive in pozzolanic reactions in concrete. On the −75 μm fraction, a 4.3% LOI feed was reduced to only a 2.9% LOI with an 89% mass yield after five stages of processing. These results highlight the diminishing effectiveness of this approach as the particle size decreases. It was noted that the finer mineral particles become “entrained” with the carbon particles and end up in the troughs. This is likely because as the particle size decreases, the aerodynamic drag forces become much higher than the electrostatic forces.

The process was sensitive to humidity, and all experiments were done at <40% relative humidity. An unusual finding that was not explained was that the separation was very poor when the polarity was reversed and the bottom plate electrode was positive. Normally if fly ash has been collected from the power plant and stored without exposure to high humidity, the carbon charges positive and the mineral charges negative in particle-to-particle contact tribocharging. If particle-to-particle contact tribocharging were a significant contributor to the charging of the carbon, one would expect that operation with the bottom plate positive would give a better separation, as it would augment the induction positive charging of carbon on contact with the plate electrode. These unusual results indicate that either the feed ash had been exposed to high humidity, and therefore the particle-to-particle contact charges of the carbon and mineral were reversed, as discussed in Section 11.3.1.3 or the induction charging of the carbon on contact with the bottom electrode is indeed the dominant charging mechanism.

The scale-up of such a process can be very challenging. If the theory is correct and each carbon particle must contact the negative bottom plate electrode, perhaps several times to accumulate enough charge to be attracted to the positive collection troughs, then as the particle size decreases, the required electrode area becomes larger. The processing rate is then proportional to electrode area. An estimate of this scale-up challenge can be made from results reported in the patent on continuous experiments in which the feed rate was varied. At the highest feed rate, 300 g/min, a 4.0% LOI feed ash was reduced to a 2.1% LOI product at 94.4% mass yield (96.3% mineral recovery) after three passes through the separator. Given the electrode area of the bench scale device of 0.225 $m^2$, the scale-up factor would be 27 kg/h $m^2$. For 10,000 and 40,000 kg/h, respectively, 375 and 1500 $m^2$ would be required. Nevertheless, the developers constructed and tested a 500 kg/h pilot facility and declared their intentions to build a 3000 to 5000 kg/h facility at the KFAC (Yoon, Yan, et al., 2001). No results have been reported on these two larger units, neither of which are in operation now.

### 11.4.2.2 Kawasaki inclined vibrating electrode separator

A team at Kawasaki Plant Systems worked to develop a similar inclined vibrating electrode separator between 2000 and about 2006. The challenges of developing this type of separator and the Kawasaki innovations are discussed in three US patents (Takikawa, Masamoto, Fukumoto, & Mayumi, 2011; Takikawa, Mashio, Masamoto, & Mayumi, 2014; Yoshiyama, Shibata, & Kinoshita, 2006). The initial concept is shown in Fig. 11.12.

This device is comprised of an inclined (25 degrees to the horizontal) bottom electrode that is constructed of a porous sintered metal plate (34), through which dehumidified aeration air (−4°C dew point) passes at a superficial velocity of 10 mm/s. Parallel to this bottom electrode is a series of one or more metal mesh (1 mm) electrodes (36a–36d) that are offset by 20 mm from the bottom electrode and each other. The bottom electrode (34) and alternating mesh electrodes (36b and 36d) are grounded and positive relative to a negative 13 kV applied to the mesh electrodes 36a and 36c. The entire apparatus is then vibrated (32) at an amplitude of 1.5 mm and a frequency of 25 Hz. Fly ash containing unburned carbon is introduced to the device at the top of the inclined electrode. The combination of dehumidified air and vibration causes the ash to become fluidized and move down across the positively charged bottom electrode. According to the inventors, when the conductive carbon particles (18) come in contact with the positive bottom electrode, they are charged positive by induction. The particles are repulsed by the bottom positive electrode and attracted to the upper negative electrode. The insulating mineral particles, which become polarized in the electric field and especially on contact with either electrode, are attracted to both the positive and negative electrodes, but they do not exchange charges with either electrode. Thus they remain electrically neutral and stay between

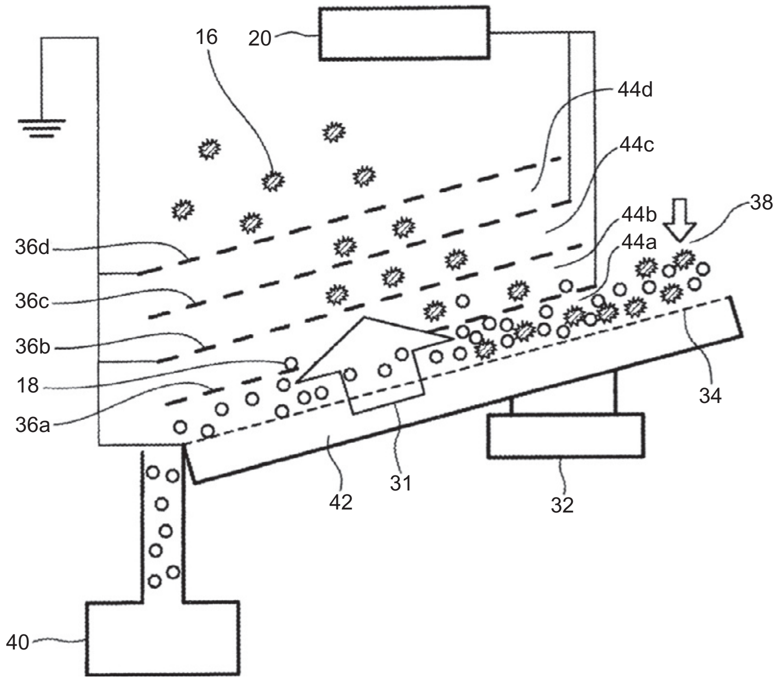

**Fig. 11.12** Kawasaki inclined vibrating electrode separator—initial concept.
From Yoshiyama, E., Shibata, Y., & Kinoshita, T. (2006). *Method for electrostatically separating particles, apparatus for electrostatically separating particles, and processing system*. US Patent No. 7,119,298 B2.

the electrodes. Some of the positively charged carbon particles that are moving towards the negative mesh electrode pass though the openings in the mesh. Others collide with the metal mesh, reversing charge through induction to become negative, and are then drawn by the electric field back to the positive electrode, where the process starts over until they pass through an opening in the metal mesh electrode.

The performance of this system on a 1 kg/h scale is presented in a number of examples in the earliest patent (Yoshiyama et al., 2006). All examples used a feed ash with an LOI of 4.2%. The best results were achieved with ash treated with calcium stearate to help disperse and fluidize it. In the best case a 4.2% LOI feed was reduced to a 1.1% LOI product with a 70% mass yield. No dimensions were given for the bottom electrode, nor were any rate experiments completed to allow an estimate of a scale-up factor. However, if the charging mechanism works as the inventors describe, then the scale-up is proportional to the bottom electrode area.

Subsequent patents by Kawasaki show the difficulties and limitations in this initial design (Takikawa et al., 2011, 2014). At higher than 5% feed LOI, it was found that sparks were generated between the metal mesh electrode and the bottom plate electrode. The sparking phenomenon is worse at high LOIs and high electric fields. A corona discharge is generated wherever an electric field is high enough to cause the electrical breakdown of air. Eventually a thin discharge plasma (commonly called a streamer) is formed, which then short circuits between the upper and lower electrodes. Even prior to the formation of streamers, the separation deteriorates due to the attachment of the electrons of the corona discharge to both mineral and carbon particles, wiping out the induction and triboelectric charging. The locally high electric fields were caused by powder that adhered to the lower surface of the upper side electrode. A number of counter measures were developed, with the most practical one implemented in the design shown in Fig. 11.13.

A single upper electrode (2) made of a high dielectric strength resin was used. To dislodge the layer of adhered particles, annular weights (11) were placed around high dielectric strength resin rods that acted as high voltage leads and supported the resin mesh electrode. From the vibration (5) of the whole device, the weights bounced up and down to impact the mesh electrode and remove the powder deposits. Results from the operation of such a device at 100 kg/h are given in the patent. The mesh electrode dimensions were 0.2 m width by 1.6 m length (total area 0.32 $m^2$). They were offset from the bottom plate electrode by 80 mm, and about −20 kV was applied (250 V/m). Feeds with LOIs ranging from 24% to 30% were reduced to 8%–9% LOI products at 65%–74% mass yield. To get an idea of the ability to scale this device to commercial rates, a scale-up factor of 312 kg/h $m^2$ of mesh electrode area can be calculated from these examples. To scale to 10,000 kg/h, 32 $m^2$ of electrode area would be required. For 40,000 kg/h, 128 $m^2$ would be required. Of course this only produces a factor of three reduction of LOI. A similar scaling factor would probably apply for reducing a 9% LOI feed to a 3% LOI product. This factor of three reduction of LOI from the feed to the product at a 70% product mass yield was advertised by Kawasaki Plant Systems on their website in 2005 (Kawasaki Plant Systems & Ltd., 2005). This technology is no longer promoted on the Kawasaki website, and there are no commercial operations using this technology.

Note that the scale-up factor for the Kawasaki technology is a factor of 10 greater than that for the Korea Fly Ash inclined vibrating electrode technology. This is probably due to the use of aeration air by Kawasaki and perhaps a positive voltage on the bottom plate electrodes rather than a negative voltage. The aeration air allows for a

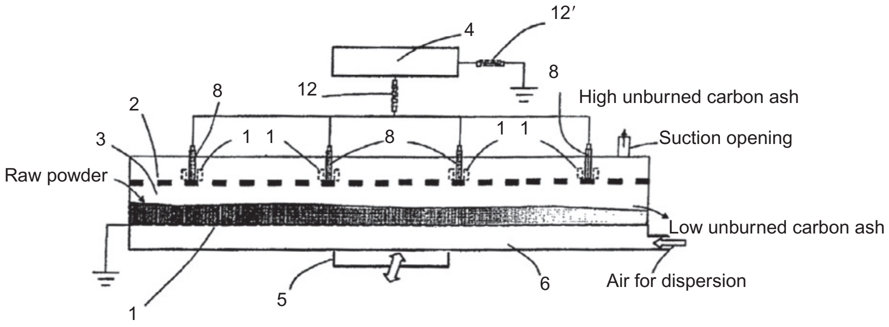

**Fig. 11.13** Kawasaki inclined vibrating electrode separator—improved design.
From Takikawa, N., Mashio. K., Masamoto, M., & Mayumi, Y. (2014). *Electrostatic separator method and electrocstatic separation device*. US Patent 8,653,394 B2.

thin fluidized bed of ash on the bottom electrode, which enhances contact of the carbon particles with the positive electrode over that of a nonaerated bed or individual particles sliding down a vibrating electrode. The fluidized bed increases the particle-to-particle contact; this can result in positive tribocharging of the carbon that augments rather than works against the induction charging on the bottom electrode, as it would in the case of a negative bottom electrode.

### 11.4.3 High-tension roll separator with magnets

The Claudius Peters Projects GmbH, in cooperation with STEAG Power Minerals, has recently developed a unique high-tension roll separator for the separation of unburned carbon from fly ash (Garbe, 2015). This technology applies a combination of electrostatic separation and magnetic separation on a rotating roll. The details of the design are shown in Fig. 11.14 from the German patent (Claudius Peters Project GmbH, 2014).

In this device, fly ash is deposited on the top of a metal drum (2) rotating such that its peripheral speed (20) at the surface is 2–20 m/s. Within the drum is a high-intensity electromagnet (3) fixed to provide a magnetic field over the arc 30. A negative high voltage corona electrode (5) generates negative ions and an electric field between the corona electrode and the grounded drum. The negative ions collide with both the conductive carbon and the nonconductive mineral particles, charging them

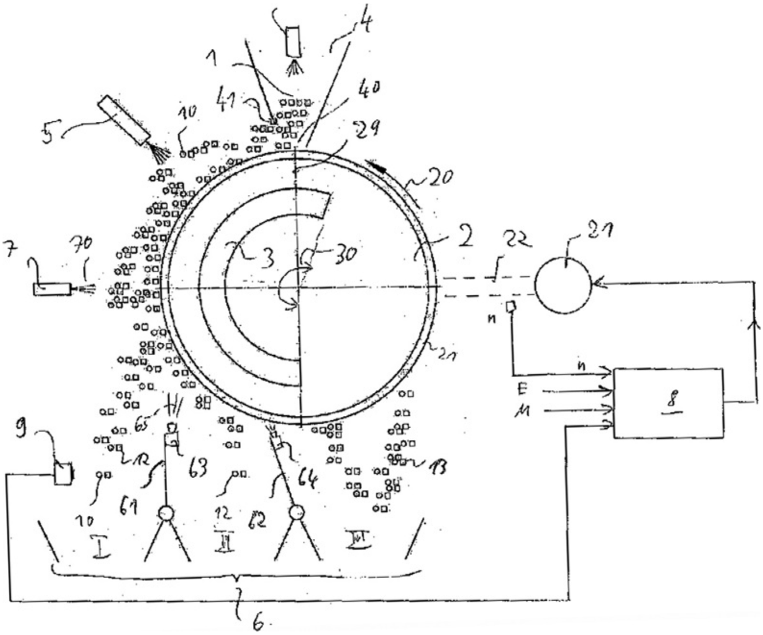

**Fig. 11.14** Claudius Peters Projects high-tension roll separator with magnet.
From Cladius Peters Project GmbH. (2014) *Roll separator for separating fly ash.* Germany Patent DE 202012010543U1.

negative. Both conductive and nonconductive particles are attracted to the drum. The conductive particles lose their negative charge to the drum; through induction, they become charged positive and are repelled by the drum.

In a conventional high-tension roller designed to separate conductive from nonconductive particles, there are normally one or more negative field electrodes placed in space off the surface of the drum, after the corona electrode and in the direction of rotation of the drum. The purpose of these field electrodes is to set up an electric field that pins the nonconductive particles to the drum. Through centrifugal forces and electrostatic forces, the conductive carbon particles are thrown from the drum surface. There are serious limitations for conventional high-tension roll separators, including the fact that every particle must come in contact with the drum surface in order for charge to be transferred for conductive particles and for non-conductive particles to be pinned to the drum. Because every particle must come in contact with the drum, the mass rate per unit drum length is directly proportional to the particle size and the drum speed. A simple model illustrates the limitation encountered when processing fine particles using conventional high-tension roll separators. For a system where each particle must contact the drum surface, the feed rate can be expressed as:

$$\dot{m} = \pi * D_\mathrm{r} * W * \omega * \text{surface particle density}$$

If one assumes there to be uniformly sized spherical particles where each particle is hexagonally packed across the drum width, then the maximum particle surface density is

$$\text{Max surface particle density} = \frac{\pi}{3\sqrt{3}} * \rho_\mathrm{p} * d_\mathrm{p} * t$$

where

$m$ is the feed rate, kg/h
$D_\mathrm{r}$ is the drum roll diameter, m
$W$ is the drum width, m
$\omega$ is the drum rotational speed
$V_\mathrm{r}$ is the drum speed, typically 5 m/s for high-tension roll separators
$\rho_\mathrm{p}$ is the particle density, assume 2300 kg/m$^3$ for fly ash
$d_\mathrm{p}$ is the particle size, assume 20 μm for fly ash
$t$ is the surface film thickness, assume 1 for number of particles

Simplified, it is

$$\frac{\dot{m}}{W} = \frac{\pi}{3\sqrt{3}} * V_\mathrm{r} * \rho_\mathrm{p} * d_\mathrm{p}$$

For typical values used in high-tension roll operation for minerals, the maximum predicted scale-up factor for fly ash particles is estimated to be only 500 kg/h/m of drum width. Furthermore, the relatively large aerodynamic drag forces disturb the trajectories of the fine fly ash particles thrown from the drum, which smears the separation. Thus conventional high-tension roll separators have not been effective at industrially significant rates for particles below 50 μm.

The Claudius Peters Group has significantly improved the performance for fly ash with the addition of magnets in the drum. As the iron content of ash increases, the fraction of magnetic and paramagnetic particles increases. In the improved device, magnetic forces act to help pin the mineral particles to the rotating drum. This apparently allows the drum speed and throughput to be increased over what could be achieved using a conventional high-tension roll separator when processing fly ash.

Returning to Fig. 11.14, the coarsest and conductive particles are thrown from the drum first. Their separation from the drum and collection in compartment I is assisted by air jets 65 and 70. After the coarse and conductive particles are removed, the weakly magnetic nonconductive particles are collected in compartment II and assisted by air nozzle 64. Lastly the highly magnetic nonconductive particles are collected in compartment III after the drum has rotated out of the magnetic field past the end of the magnet. Given the importance of aerodynamic drag on the particles $<20$ μm, these air jets would have a large influence on the trajectories of the particles removed from the drum, making their capture in the correct compartment difficult.

Claudius Peters currently has a pilot machine at their test center in Germany, with a capacity up to 850 kg/h using what appears to be about a 1 m long roll. Results from a number of ashes are reported in Table 11.3. Results for the mass yields of the products are not given for each test; however, the general comment is made that they are between 50% and 85% (Garbe, 2015). The fineness (i.e., residue on +45 μm wet screen) of the feed and products are also shown. There is a striking reduction in the +45 μm fraction, which is a beneficial property. Because all of the reduction in the +45 μm fraction cannot be due to the removal of the small amount of carbon, a considerable amount of coarse mineral must also be removed, suggesting a particularly low mass yield of the products for the amount of carbon removal achieved.

**Table 11.3** **Claudius Peters results on high-tension electrostatic/magnetic roll separator**

| LOI (%) | | Residue, +45 μm (%) | |
|---|---|---|---|
| **Feed** | **Product** | **Feed** | **Product** |
| 8.8 | 5.1 | 21.6 | 1.6 |
| 6.8 | 2.3 | 20.4 | 11.7 |
| 6.2 | 2.7 | 3.8 | 0 |
| 11.2 | 3.4 | 21 | 1 |
| 14.4 | 6.4 | 27.3 | 16.3 |
| 7.6 | 3.48 | 27.5 | 12.6 |
| 10.7 | 4.74 | 21.4 | 8 |
| 6.5 | 3.41 | 14.3 | 8.6 |

From Garbe (2015). Ash Trade Europe conference presentation. Reproduced with permission from Claudius Peters Projects GmbH.

**Table 11.4** **Iron oxide in coal ash for six US power plants**

| | Plant 1 | Plant 2 | Plant 3 | Plant 4 | Plant 5 | Plant 6 |
|---|---|---|---|---|---|---|
| Average (%) | 3.07 | 9.39 | 7.43 | 7.39 | 5.33 | 17.68 |
| Minimum (%) | 2.51 | 6.26 | 5.88 | 5.57 | 0.82 | 15.5 |
| Maximum (%) | 5.03 | 12 | 10.33 | 8.67 | 8.29 | 19.64 |

The performance improvement of this technology over the conventional high-tension roll separator is due to the high-intensity magnetic field acting on the magnetic properties of the nonconducting mineral particles. Therefore one might suspect that the separation performance and rate would depend upon the amount of iron in the ash; this can vary widely for coal. For example, the amount of iron in ash (reported as $Fe_2O_3$) generated at six different power plants over an extended period is shown in Table 11.4. The question remains as to whether this technology can handle this wide variation in iron and the presumably magnetic properties of the ash.

### 11.4.4 Triboelectric belt separator

ST Equipment & Technologies LLC (STET) has developed an electrostatic separator for the separation of unburned carbon from fly ash at high rates (Bittner, Dunn, & Hrach, 2000; Cerullo, Bozman, & Dunn, 1999; MacKay & Sert, 2013; Whitlock, 1989, 1998; Whitlock & Sert, 2005, 2008). The principles of operation of the STET separator are illustrated in Figs. 11.15 and 11.16. The separator is comprised of a continuous loop belt, both sections of which run at high speed (4–20 m/s) through a narrow gap (10–18 mm) between two parallel planar electrodes to which a high voltage is applied (+ and −5 kV). The belt, which is made of a nonconducting plastic, is a large mesh with about 60% open area. The particles can easily pass through the openings in the belt. The particles are charged by the triboelectric effect through particle-to-particle collisions in the air slide feed distributor and within the gap between the electrodes.

The flow patterns and particle-to-particle contact within the electrode gap that are established by the moving belt are key to the effectiveness of the separator. Upon entry into the gap between the electrodes the negatively charged mineral particles are attracted to the bottom positive electrodes by the electric field forces. The positively charged carbon particles are attracted to the negatively charged top electrode. The geometry of the belt cross-direction strands serves to sweep the particles off the electrodes, moving them toward the proper end of the separator and back into the high-shear zone between the oppositely moving sections of the belt. Because the particle number density is so high within the gap between the electrodes (approximately one-third of the volume is occupied by particles) and the flow is vigorously agitated (relative velocities more than 20 m/s), there are many collisions between particles; optimal charging occurs continuously throughout the separation zone. The counter-current flow induced by the oppositely moving belt sections and the continual recharging and reseparation creates a counter-current multistage separation within a

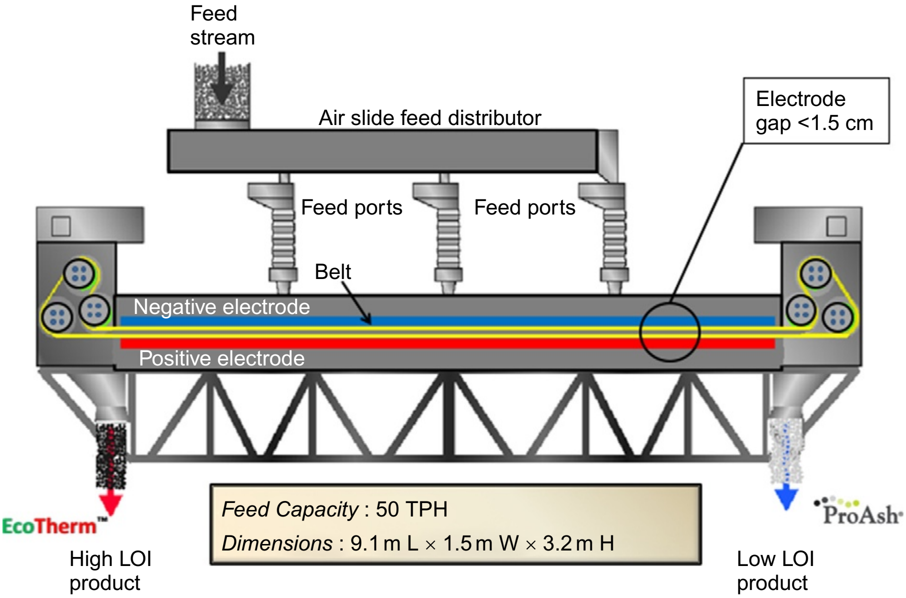

**Fig. 11.15** Schematic of STET triboelectric belt separator.

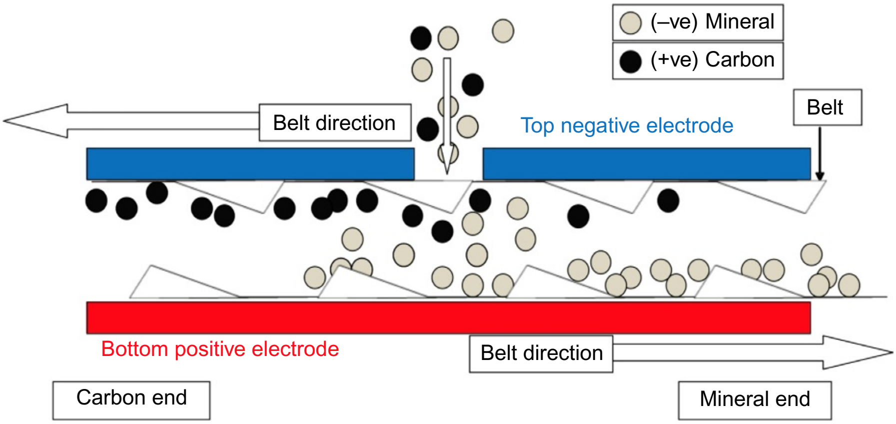

**Fig. 11.16** Electrode gap of STET belt separator.

single apparatus. This continuous charging and recharging of particles within the separator eliminates the need for any tribocharging system prior to introducing material to the separator, thus removing a serious limitation on the capacity of electrostatic separation. This internal recharging also allows operation at very high electric fields in which corona and streamers would degrade particle charging and performance in other devices. The output of this separator is two streams, a low LOI product and a high LOI product, without a middlings stream. The efficiency of this separator has been shown to be equivalent to approximately three stages of free-fall separation with middlings recycle.

The STET separator has many process variables that enable the optimization of the trade-off between product purity and recovery that is inherent in any beneficiation process. The coarse adjustment is the feed port through which the feed is introduced to the separation chamber. The port furthest from the discharge hopper of the desired product gives the best grade (i.e., lowest LOI products) but at the expense of a lower recovery. Finer adjustments are the speed of the belt, and the electrode gap which is adjustable between 9 and 18 mm. The pretreatment of feed material by the precise control of trace moisture content (as measured by feed relative humidity) is vital to achieving optimum separation results.

The STET separator has feed rates for fly ash separation as high as 50,000 kg/h. The active electrode dimensions are 6.1 m long by 1.1 m wide, thus the feed rate per unit total electrode area is 5960 kg/h $m^2$ (one electrode). This is 4–220 times greater than the technologies discussed above. There is a combination of factors that account for the high rate capability. The high electric field (1000 KV/m) allows a higher space charge (higher number of particles and/or higher charge per particle) between the electrodes before space charge effects decrease the effective field and the separation deteriorates. The high speeds (typically >10 m/s) that the belt moves the ash through the electrode gap keep the particle number density down even at high mass throughput rates, which allows higher number of charges per particle. Because the belt carries particles by mechanically induced turbulent flows toward the shear layer between the oppositely moving sections of the belt, the distance that a particle has to be moved from the "wrong" stream to the "correct" stream under the force of the electric field is on the order of a millimeter or less. The force and the velocity with which the particles move is proportional to the field strength. The combination of the high electric field and short distance make separation times very short.

The STET separator is designed for separating mixtures with a particle size ranging from <1 μm to about 500 μm. The median particle size for fly ash produced in a pulverized coal boiler is typically 15–20 μm with an average top size (P95) of 150–300 μm, which makes this technology particularly well suited for fly ash processing. Because a large portion of the unburned carbon particles is larger than the mineral particles, the fly ash particle size is slightly reduced by STET carbon separation. For example, when processing a feed fly ash with 8.6% LOI and 22.2% +45 μm size fraction, a product fly ash product was produced with 1.0% LOI with 12.5% retained on 325 mesh.

The STET separator's separation capabilities are illustrated in Table 11.5. These are single pass results from commercial plants processing siliceous fly ash (ASTM Class F) generated from bituminous coals and blends of bituminous coal and petroleum coke. The STET separator has successfully processed fly ash generated from bituminous coals from the central and northern Appalachian regions, Colombia, Indonesia, Australia, Russia, Poland, and South Africa, as well as from anthracite coal from the United Kingdom.

Table 11.5 **STET separator results from commercial plants**

| Feed LOI (%) | Product LOI (%) | Carbon LOI (%) | Mass yield (%) | Mineral recovery (%) |
|---|---|---|---|---|
| 6.3 | 1.8 | 29.9 | 84 | 88 |
| 11.2 | 2.1 | 40.6 | 76 | 84 |
| 19.3 | 2.9 | 49.7 | 65 | 78 |
| 23.1 | 3.4 | 55.2 | 62 | 78 |

Table 11.6 **Properties of feed and recovered low-LOI ash: fresh and landfilled**

| Separator feed | Feed LOI (%) | Low carbon product LOI (%) | Product fineness (%) +45 μm | Product mass yield (%) | High carbon product LOI (%) |
|---|---|---|---|---|---|
| Fresh A | 10.20 | 3.60 | 23 | 84 | 39 |
| Landfill A | 9.80 | 3.30 | 20 | 75 | 28 |
| Fresh B | 5.30 | 2.80 | 17 | 91 | 28 |
| Landfill B | 6.90 | 4.50 | 24 | 86 | 26 |

The STET separator has also been successfully tested for the removal of powdered activated carbon from high-calcium content fly ash (ASTM Class C) generated from subbituminous coals in the Western United States.

As discussed in Section 11.3.1, the triboelectric charging behavior of ash that has been wetted and stored in a landfill, then recovered and dried, is the reverse of that of freshly generated ash stored without exposure to ambient humidity. Whatever the fundamental mechanism, it does not appear to degrade the practical application of triboelectric separation to reduce the carbon content of the ash. The properties of the low LOI fly ash recovered using the STET process for both ash freshly collected from the boiler and ash recovered from the landfill is summarized in Table 11.6. The results show that the STET process efficiency for the recovered landfill ash is within the range expected for ash freshly collected from the utility boiler (Baker, Gupta, & Gasiorowski, 2015).

## 11.5 Commercial electrostatic separation of unburned carbon from fly ash

Of the many electrostatic separation technologies proposed and developed over the last 20 years, only one is now operating commercially: STET's tribolectrostatic belt separator. Over the last 20 years, 22 STET belt separators have been installed and operated in 15 power plants in five countries, including Canada, United Kingdom, Poland, South Korea and the United States. More than 16 million tonnes of low-carbon (1.5%–4% LOI) product have been produced. The low carbon product has been used as a pozzolanic admixture for concrete and an additive for blended cements. At three of these power plant sites, the fly ash can be contaminated with ammonia from the power plant emission control systems. The STET separator processes fly ash containing ammonia, which is removed after carbon separation.

To provide a 100% solution to the fly disposal problem, the high-carbon product is used as a fuel for its heating value in power plants and cement kilns. Systems have been installed at seven power plants to return the high-carbon product to the boiler to capture the fuel value. The high carbon product from four STET plants is being used as feed for cement kilns to capture the fuel value and the mineral value of the alumina. The fuel value of the unburned carbon in the high LOI product is 30,200 kJ/kg (13,000 Btu/lb) of carbon, close to that of pure carbon. When it is burned in the boiler, its fuel value is converted to energy at the same efficiency as coal, about 35%.

The capabilities and reliability of the STET are highlighted by the experience at the Zaklad Gospodarki Popiolami plant in Janikowo, Poland. This greenfield plant was commissioned in July 2010 (Bittner, Gasiorowski, & Lewandowski, 2011). In November 2015, it processed its one millionth tonne of feed ash. In 2013, ZGP processed 200,912 tonnes of feed ash at an average LOI of 9.6%, producing 170,615 tonnes of 4.5% LOI product at a mass yield of 85% for use in blended cement and 30,297 tonnes of 41% LOI product for cement kiln feed. The plant operated for 7680 hours in 2013 with only 23 hours of downtime due to separator maintenance and 335 hours of downtime for balance of plant maintenance (Grobelny, 2016).

## 11.6 Summary and conclusion

Electrostatic processes are very attractive for separating mixtures of particles because they are dry processes, have low energy requirements, and have minimal environmental emissions. However, conventional electrostatic processes for industrial minerals are not able to separate fine particles such as fly ash, where most particles are well below 100 μm. These fine particles present some fundamental limits on electrostatic separation processes.

Over the past 20 years, there have been many concepts developed to separate unburned carbon from fly ash using electrostatic methods. Although many of these concepts have worked at low rates on a laboratory or pilot plant scale, most of them have fundamental limitations that prevent scaling up to commercial rates (10,000 to 50,000 kg/h) both practically and economically. Many of them can only be scaled by increasing the electrode area by operating multiple units in parallel.

Only one technology is currently in commercial use: STET's tribo-electrostatic belt separator has been in commercial operation since 1995. More than 20 units have been installed worldwide, processing ash from a wide range of coals. A single STET separator can process up to 50,000 kg/h.

## References

Baker, L., Gupta, A., & Gasiorowski, S. (2015). *Triboelectric beneficiation of landfilled fly ash.* Lexington, KY: ACAA and CAER.

Ban, H., Li, T., Hower, J. C., Schaefer, J. L., & Stencel, J. M. (1997). Dry triboelctrostatic beneficiation of fly ash. *Fuel*, *76*(8), 801–805.

Bittner, J., Dunn, T., & Hrach, F., Jr. (2000). *Method and appratus for separation of unburned carbon from fly ash*. US Patent No. 6,074,458.

Bittner, J., Gasiorowski, S., & Lewandowski, W. (2011). *Polish chemcial plant utilizes separation technologies' carbon removal process.* Lexington, KY: ACAA and CAER.

Brands, L., Beier, P., & Stahl, I. (2005). *Electrostatic separation.* Weinheim: Wiley-VCH Verlag, GmbH.

Cangialosi, F., Notarnicola, M., Liberti, L., & Stencel, J. (2009). The role of weathering on fly ash charge distribution during electrostatic beneficiation. *Journal of Hazardous Materials*, *164*, 683–688.

Cangialosi, F., et al. (2006). Significance of surface moisture removal on triboelectrostatic beneficiation of fly ash. *Fuel*, *85*, 2286–2293.

Cerullo, T., Bozman, C., & Dunn, T. (1999). *Belt separator having improved belt geometry*. US Patent No. 5,904,253.

Claudius Peters Project GmbH. (2014). *Roll separator for separating ash*. Germany Patent No. DE 202012010543U1.

Garbe, J. (2015). *Fly ash separation.* Frankfurt: GMI Global LLC.

Grobelny, P. (2016). *Premium plant manager*, *ZGP Plant* [Interview] (4 February 2016).

Kawasaki Plant Systems, Ltd. (2005). *Kawasaki plant systems—Environmental protection facility: Unburned content separation facility*. Available at: www.global.kawasaki.com (Accessed 25 March 2008).

Kelly, E., & Spottiswood, D. (1989a). The theory of electrostatic separations: A review part III separation of particles. *Minerals Engineering*, *2*(3), 337–349.

Kelly, E., & Spottiswood, D. (1989b). The theory of electrostatic separations: A review, part II. Particle charging. *Minerals Engineering*, *2*(2), 193–205.

Kim, J. -K., Cho, H. -C., & Kim, S. -C. (2001). Removal of unburned carbon from coal fly ash using a pneumatic triboelectric separator. *Journal of Environmental Science and Health, Part A*, *36*(9), 1709–1724.

Kim, J. -K., & Kim, S. -C. (2001). Tribo-electrostatic beneficiation of fly ash for ash utilization. *Korean Journal of Chemical Engineering*, *18*(4), 531–538.

Kim, J. -K., & Lee, H. -D. (2009). Design variables of pilot scale electrostatic separator for removing unburned carbon from coal fly ash. *Journal of Chemical Engineering of Japan*, *42*(7), 471–477.

Kim, J., & Lee, H. (2011). *Electrostatic separator for unburned carbon from coal ash using induction type ejector tribocharger*. US Patent No. US 2011/0036758.

Lockert, C., Lister, R., & Stencel, J. (2001). *Commericalization status of a pneumatic transport, triboelectrostatic system for carbon/ash separation.* Lexington, KY: Center for Applied Research, University of Kentucky.

MacKay, B., & Sert, B. (2013). *Electrostatic separation control system*. US Patent No. 8,552,326 B2.

Manouchehri, H., Hanumantha Rao, K., & Forssberg, K. (2002). Triboeletric charge, electrophysical properties and electrical beneficiation potential of chemically treated feldspar, quartz and wollastonite. *Magnetic and Electrical Separation*, *11*(1–2), 9–32.

Manouchehri, H. R., Hanumantha Roa, K., & Forssberg, K. S. E. (2000). Review of electrostatic separation part 1: Fundamental aspects. *Minerals and Metallurgical Processing*, *17*(1), 23–36.

Ralston, O. (1961). *Electrostatic separation of mixed granular solids* (1st ed.). Amsterdam: Elsevier Publishing Company.

Stencel, J., Schaefer, J., Ban, H., & Neathery, J. (1999). *Apparatus and method for triboeletric separation*. US Patent No. 5,938,041.

Stencel, J., et al. (1999). *Technology development for carbon-ash beneficiation by pneumatic transport triboelectric processing*. Lexington, KY: Center for Applied Energy Research, University of Kentucky.

Stencel, J., et al. (2001). *Particle separation system using parallel multistage electrostatic separators*. US Patent No. 6,323,451 B1.

Takikawa, N., Masamoto, M., Fukumoto, K., & Mayumi, Y. (2011). *Electrostatic separation method and electrostatic separation device*. US Patent No. 8,071,904 B2.

Takikawa, N., Mashio, K., Masamoto, M., & Mayumi, Y. (2014). *Electrostatic separation method and electrostatic separation device*. US Patent No. 8,653,394 B2.

Tilton, J. (2008). *Perry's chemical engineers' handbook* (8th ed.). New York, NY: McGraw-Hill.

Whitlock, D. (1989). *Separating constituents od a mixture of particles*. US Patent No. 4,839,032.

Whitlock, D. (1998). *Method and apparatus for electrostatic separation*. US Patent No. 5,829,598.

Whitlock, D., & Sert, B. (2005). *Method of forming a continuous belt for a belt-type separator device*. US Patent No. 6,942,752 B2.

Whitlock, D., & Sert, B. (2008). *Continuous belt for a belt-type separator device*. US Patent No. 7,467,709 B2.

Yoon, R.-H., Han, O.-H., Yan, E., & Park, B.-W. (2001). *Electrostatic method of separating particulate materials*. US Patent No. 6,320,148 B1.

Yoon, R. -H., Yan, E., Han, O. -H., & Park, B. -W. (2001). *Pilot scale testing of a vibrating electrostatic separator for fly ash decarbonization*. Pittsburgh, PA: US Department of Energy NETL.

Yoshiyama, E., Shibata, Y., & Kinoshita, T. (2006). *Method for electrostatically separating particles, apparatus for electrostatically separating particles, and processing system*. US Patent No. 7,119,298 B2.

# Thermal processing

# 12

*J. Castleman*
The SEFA Group, Inc., Lexington, SC, United States

## 12.1 Background

Over the last several decades, there has been a considerable amount of research and development intended to create technologies and processes that increase the benefit of fly ash in particular applications. These processes are generically referred to as "fly ash beneficiation."

The three most prevalent commercial technologies that beneficiate fly ash when used as supplementary cementitious material in concrete are chemical treatment, triboelectric separation, and thermal beneficiation. This chapter discusses the key elements of thermal beneficiation and its advantages, as well as the two commercially available thermal processes.

In the simplest terms, thermal beneficiation involves the processing of fly ash at elevated temperatures, typically between 1200°F and 1800°F (650–980°C), in order to alter the chemical and/or physical characteristics of the ash to improve performance in concrete and other mineral filler applications. As a part of this type of technology it is critical that the process be able to sustain itself without any supplemental fuel or energy. For this reason the only commercially viable thermal processes are those that rely on the combustion of the unburned carbon in the fly ash in order to elevate the temperatures and reach self-sustaining operation.

Although there are several thermal beneficiation processes that have been attempted in the past, only two have proven to be commercially viable. These are the carbon burnout (CBO) process and the staged turbulent air reactor (STAR) process.

## 12.2 Effects of thermal beneficiation

*Reduces LOI*: In order to market fly ash as pozzolan, the fly ash must meet the requirements of the relevant specifications for pozzolan-grade fly ash. The most commonly discussed specification for fly ash used as pozzolan in concrete is loss on ignition (LOI). LOI is the test method and metric used in the industry to infer the amount of unburned carbon remaining in the fly ash. Both commercial thermal beneficiation processes meet this criteria.

*Greenhouse Gas Reduction*: Cement manufacture produces significant $CO_2$ emissions, mostly from calcination of limestone (calcium carbonate) to drive off carbon (~60%), but also from the combustion of fossil fuels (~40%). It is well known that

**Coal Combustion Products (CCP's).** http://dx.doi.org/10.1016/B978-0-08-100945-1.00012-5

one ton of $CO_2$ is produced for every ton of cement produced at a cement mill. For example, the Environmental Protection Agency (EPA) quantifies this $CO_2$ reduction in its waste reduction model (WARM) as $-0.87$ $MTCO_2E$ per short ton of fly ash recycled in concrete (USEPA, 2003). Of course, carbon is burned, and $CO_2$ is emitted as part of any thermal process where combustion of carbon takes place. However, even at the most extreme case of 25% LOI fly ash the actual net benefit ($CO_2$ equivalency) will be less.

*Adapts to Changes in Coals/Chemistry*: Fly ashes from high-calcium coals, such as subbituminous or lignite, that produce Class C fly ash are particularly problematic since these fly ashes "experience significant glass devitrification that could result in reductions in pozzolanic activity" (Fox, 2005). In the case of CBO, differences in coal ash chemistry (especially CaO content) can dramatically affect the process and the finished product, thereby limiting the temperature of the operating regime to less than 700°C to avoid sintering and/or glass devitrification. To date, no CBO has demonstrated the ability to process Class C fly ash. The operating regime for the STAR process is totally different than that of the CBO fluid bed. The STAR process is more similar to a tangentially fired, pulverized coal-fired unit, therefore it can be adapted to a wide variety of coal sources (including high calcium coals) and can operate at different temperatures. Both Class C and F fly ashes have been successfully processed on STAR facilities.

*Increased Landfill Life*: Since there is no solid or liquid waste generated by thermal beneficiation processes, the volume of landfill space saved through the use of these processes is directly related to the volume of raw feed fly ash introduced into the plant. All of the product from the process is beneficially used. Further, the net volume is reduced due to the carbon reduction taking place in the process. Thus the net yield of beneficiated ash is 100%.

*Heat Recovery from Combustion*: In order to cool the fly ash and flue gases, hot water, steam, or other fluid media can be produced and used on a variety of applications. These include returning hot water to the power plant, power generation, ash drying, and industrial process steam, among others.

*Ammonia Removal*: During selective noncatalytic reduction (SNCR) operations—and, in some cases, during selective catalytic reduction (SCR) operations—or when ammonia or urea is used for the postcombustion treatment of flue gas and/or coal fly ash, ammonium sulfate salts are deposited on the surface of the collected fly ash. These salts are considered a "contaminant" in the fly ash, and when fly ash containing these ammonium salts is incorporated in plain cement concrete, ammonia gas is liberated. The resulting odor is unacceptable in the marketplace and negatively impacts the marketability of the fly ash.

Both of the thermal beneficiation processes (CBO and STAR) remove the ammonia without any additional costs. The ammonium salts will decompose into nitrogen and water vapor at the operating temperatures of the thermal beneficiation processes and become part of the flue gas (USEPA, 2003). The operating temperatures of the CBO are high enough to thermally decompose 94 to 98% of the ammonia vapor into nitrogen and water vapor.[3] Due to the higher operating temperatures of the STAR process, ammonia content in STAR fly ash is below the detection limit of the test methods used to date.

*Mercury Sequestration*: Coal fly ash typically contains a trace amount of mercury. Mercury measurements made at power plants have shown that as much as 20% of the mercury in the flue gases is adsorbed by the fly ash. It is commonly believed that the primary mechanism for mercury sorption derives from the partially pyrolyzed coal char, which creates a low-grade activated carbon (Huggins, 1999).

These unburned carbon particles are entrained in the flue gases, and depending on the speciation of the mercury in the flue gas, can serve as an efficient sorbent. In fact, it has been suggested that unburned carbon from fly ash could be separated from the mineral matter and used as an economical sorbent to remove mercury from flue gases at coal burning power plants (IMP).

Although most of the mercury contained in power plant fly ash is adsorbed on the unburned carbon particles, some mercury is also deposited on the mineral matter fraction of the fly ash. Regardless, the total mercury level in fly ash is low enough so that it does not negatively impact the marketability of fly ash used in plain cement concrete. The eventual fate of mercury deposited on fly ash used in concrete is to be encapsulated in the cement matrix of the concrete (Knowles & The SEFA Group, 2009).

The thermal beneficiation processes will vaporize all the mercury during thermal processing. The heated fly ash is entrained in the mercury-laden flue gases and pneumatically transported through a shell and tube heat exchanger, where the entire mass flow is cooled to temperatures below the condensation temperature of mercury. Testing has shown that 99.98% of the vaporized mercury recondenses on the low-carbon fly ash (Giampa, 2003).

*Flue-Gas Emissions*: Since thermal beneficiation involves a combustion process, carbon and any other volatiles that remain on the fly ash can be part of the process flue gas. In particular, both the CBO and STAR processes produce flue gas that contains $SO_2$, $NO_x$, CO, $CO_2$, VOCs, mercury, and ammonia, as discussed above. Since the CBO and STAR have significantly different emissions and approaches toward control of these, the emissions will be discussed in more detail in the sections below.

## 12.3 Commercial thermal beneficiation

A variety of potential fly ash beneficiation processes have been investigated and even tested on small-scale pilot plant units. However, only two processes have been demonstrated on a large operating scale. The two commercially available technologies, the carbon burnout (CBO) process and the staged turbulent air reactor (STAR) process, are discussed in detail below.

### 12.3.1 Carbon burnout process

In 1992, Progress Materials Inc. (PMI) began development of the carbon burnout (CBO) fly ash beneficiation technology under a program funded by Electric Power Research Institute (EPRI) and EPRI members. In the early CBO research, two types of transport reactors were tested, with residence times on the order of 1 to 15 seconds. A transport reactor is a reactor in which all of the reactants travel together at more or less the same speed. In this early work the large volume of air necessary to provide sufficient oxygen for carbon burnout was used to transport the reacting fly ash from the inlet to discharge points. However, no substantial carbon burnout was detected.

In contrast, fluidized-bed reactors are well known for their ability to provide extended residence time for certain reactions. There are two primarily types of fluidized beds—the bubbling fluidized bed (BFB) and the circulating fluidized bed (CFB). In the BFB, the solid material stays substantially in place in the bed while the gaseous material travels at relatively low velocities upward through the bed. In the CFB, the velocity of the gas is greatly increased so that the bed becomes very dilute. Most or all of the solid material is elutriated with the gas, then it is separated from the fluid and reinjected into the bed. At the time of the CBO development, CFBs were thought to be undesirable for very fine solids (such as fly ash) due to the economic difficulty of repeatedly separating fine solids from the fluid stream.

Therefore PMI focused its attention on using the BFB technology as the basis for the CBO development. It was not known at the time, however, whether a dry bubbling bed reactor using fly ash particles could be used to reduce fly ash carbon. One problem was that the expected allowable velocity would be on the order of 0.003 m/s, the single-particle terminal-settling velocity expected for the fine fly ash particles to prevent excess transport of material from the bubbling bed. A reactor using this velocity would have a huge plan area to pass the required air quantity and would therefore be uneconomical.

After several years of research, PMI discovered a method in which the bed velocity could be increased by approximately two orders of magnitude without departing significantly from the bubbling bed regime. Use of the higher bed velocity allows reduction of a bed plan area by a factor of approximately 100 with obvious economic benefits (Cochran & Kirkconnell, 1995).

In 1992 a one-tph CBO pilot plant was constructed and operated as a "proof of concept." This plant, which operated in a continuous mode, proved to be extremely useful in characterizing appropriate carbon combustion conditions for a wide range of ash sources. Generalizing, operations have shown that ash from any coal that can be successfully combusted in a dry-bottom (i.e., non-slag-tap) pulverized coal furnace may be successfully processed in a CBO fluid bed. The product ash is then tested for concrete application properties. As expected, all ash sources tested to date have fully met specifications after the residual carbon was combusted (Huttenen, 2005). As of this publication, the CBO has only processed Class F fly ash and no high lime Class C ashes (Cochran & Kirkconnell, 1995).

#### *12.3.1.1 Process description*

Fig. 12.1 shows a schematic of the CBO process. The main component is the fully refractory lined combustor that contains the bubbling fluidized bed. The process starts with a specific amount of bed material, typically that spent in a previous operation. A forced draft fan provides combustion air to the bed through a distributor plate, which is a combination of many smaller plates with very small air supply holes. This air distributor is a proprietary design of the CBO technology. It is one of the keys to the

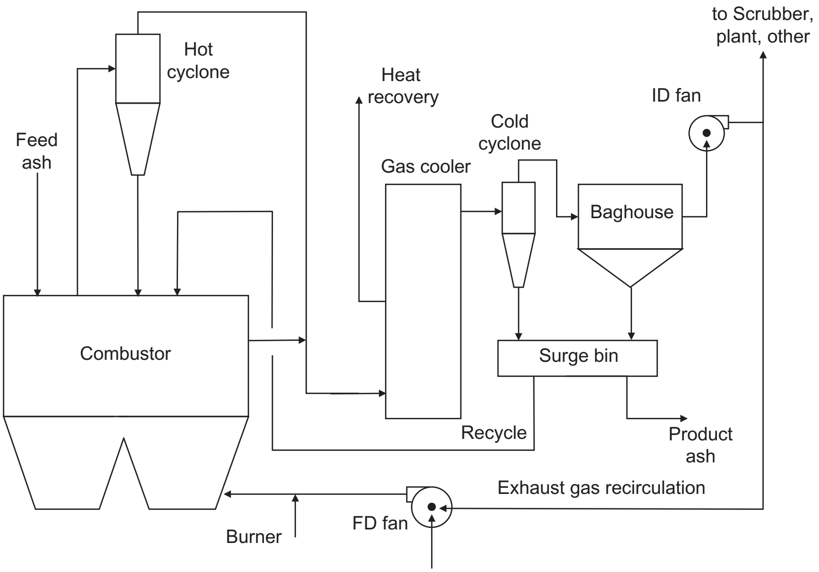

**Fig. 12.1** Carbon burnout process.

process as it provides optimum fluidization of the small ash particles. The typical CBO operates with bed velocity in the 0.15-0.5 m/s range.

For cold startups the air is preheated by an alternate heat source, typically oil or gas, to raise the bed temperature to the ignition temperature of the carbon in the bed. Once the bed combustion rate is stable, the startup fuel is removed and the process will self sustain. The high carbon raw fly ash is fed by gravity through the roof at one end of the combustor. The raw feed mixes with the existing hot bed, and combustion takes place. The heat from the combustion of the carbon in the ash is absorbed by the bed material and the combustion gases. Due to the low fluidizing velocity, the vast majority of the low-carbon product exits the combustor via an overflow weir at the opposite end of the combustor. The combustion gases and few elutriated solids exit through the roof of the combustor. This gas/solid mixture flows through hot cyclones, where most of the solids are separated and returned to the combustor. The gas and solids that exit the hot cyclones combine with the solids from the overflow weir. This hot gas and solids stream is cooled in a gas cooler and possibly an air preheater before entering a cold cyclone and then a baghouse for the final particulate collection. The solids captured in the cold cyclone and baghouse are combined in a surge bin below. Some of the now cooled solids are recycled back to the combustor to help control the temperatures in the bed. The remaining solids are transported to a product silo. The heat recovered from the process at the gas cooler can be used for various applications.

In addition, an Exhaust Gas Recirculation (EGR) system has been added to the process in which a controlled quantity of flue gas downstream of the induced draft fan is returned to the inlet of the forced draft fan. This low-oxygen flue gas reduces the CBO combustion rate while maintaining proper fluidization in the bed. The degree of combustion reduction is determined by the percentage of recirculated gas as compared to the outside air. With EGR the CBO process has the enhanced ability to "follow load" based on the incoming carbon content of the feed ash (Frady, Carolina Electric, & Gas, 1999).

As the process is based on a dense bubbling bed with very high rates of particle-to-particle contact, it is likewise very sensitive to ash sintering and agglomeration. Therefore the bed temperature must be controlled to well under the ash fusion temperature, which can be relatively low for many fly ashes. At the same time, if the bed is too cold, adequate carbon burnup cannot be achieved. Results from actual CBO operation has shown this range to be 667–732 C. As mentioned above, one of the key components of the process is the use of recycled product solids to keep the bed temperature within this range. Given the relatively low operating velocity and temperatures, it is critical that adequate time is available for the combustion process to take place. This residence time for a typical CBO is on the order of minutes, sometimes as high as 100 minutes (Cochran & Kirkconnell, 1995).

This residence time and the desired amount of carbon to be burned define the size of the CBO combustor, as the time is a direct function of the feed rate (and carbon content) and total bed mass in the combustor. It should also be noted that because the operating temperature is not much higher than the ignition temperature, some amount of combustion must exist in all parts of the bed at all times, or the temperatures could decrease rapidly and stop the combustion process in the entire bed. This condition is referred to as burnout. Commercial operating experience has shown that the bed must always contain at least 1.5% carbon to keep the process self sustaining.

Given the economics and practical applications of the technology, the CBO process is designed to burn raw feed ash of 8%–25% LOI. Since the process is a thermal one, the design is based on the amount of carbon burned in the unit. Therefore the amount of raw feed ash processed is in direct proportion to the LOI of the raw feed ash. For example, if the raw feed ash LOI is 10% the plant can process approximately twice the ash as compared to a raw feed LOI of 20%. It should be noted that due to the carbon burnout condition, the process is not able to sustain itself below eight percent; product LOIs are typically around two percent (Frady et al., 1999).

*Waste Disposal*: With respect to waste streams, the CBO has minimal impact. There is no solid or liquid waste stream from the CBO process; all incoming high-carbon ash exits as a combination of product ash and flue gas. Further, the CBO process removes all of the ammonia contained in fly ash. The ammonia is decomposed to nitrogen and water, resulting in ash that contains no ammonia residue. As stated previously, the CBO process will vaporize all the mercury during thermal processing. The heated fly ash is entrained in the mercury-laden flue gases and pneumatically transported through a shell and tube heat exchanger where the entire mass flow is cooled to temperatures below the condensation temperature of mercury (Giampa, 2003).

*Emissions*: With regard to other flue-gas constituents from the combustion of the fly ash, such as $SO_2$, CO, $CO_2$, and VOCs, there is no data publically available on the CBO process, because all of the CBO facilities to date vent their flue gas back to the main power plant. These emissions are not measured specifically from the CBO process; however, Tampa Electric Company submitted an air construction permit

**Table 12.1** CBO emission rates—95 mmbtu/h (28 MWth) unit (ECT, 2005)

| Pollutant | lb/mmbtu | Control efficiency |
|---|---|---|
| $NO_x$ | 0.949 | 0.0 |
| CO | 0.244 | 0.0 |
| SO2 | 5.000 | 95.0 |
| VOC | 0.018 | 0.0 |
| PM10 | 0.048 | 50.0 |

application in 2005, which included a CBO (ECT, 2005). Table 12.1 shows the estimated emission rates, and the CBO heat input is 95 mmbtu/hr.

*Hot Restart*: Another operating advantage of the CBO process involves the hot restart of the unit after a forced or unforced shutdown. Shutdown of the fluid bed involves stopping the ash feed and then the flow of fluidization air. Absent of air, the combustion of the carbon in the bed immediately ceases. The bed loses fluidization and "slumps." In this slumped condition, the temperature profile degrades very slowly, because ash is a good insulator, and the fluid bed is heavily insulated. This heat retention enables "hot starts" –a startup in which no supplemental fuel is required. Hot-start capability has been demonstrated at up to 16 hours of downtime. With hot-start capability, steady-state operations can be reached within 10 minutes of rolling the fans. Product quality is not affected, as only on-spec product ash leaves the fluid bed. The hot-start benefit is invaluable during periods of low feed ash availability. The CBO plant can intentionally cease combustion operations for several hours until sufficient feed ash is available, and then quickly come back online (Huttenen, 2005).

*Reclaimed Ash*: With regard to reclaimed ash application, the CBO has certain limitations. Fly ash is a reactive glass is therefore metastable, which is to say that fly ash will chemically react with other substances whenever possible and convert into a more stable and less reactive, state. For example, when fly ash gets wet, reactive sites on the surface of the amorphous glass phase of the fly ash particles react with the water. Calcium-silicate-hydrate gels, hydroxyl groups, and other reaction products can form on these surface sites, which stabilize the metastable glass surface and lower the entropy of the fly ash, which therefore reduces the pozzolanic reactivity of the fly ash. Consequently, for coal ashes that have lost pozzolanic reactivity, the most important issue to be addressed is how to restore the reactivity and therefore the strength-producing character of fly ash after prolonged exposure to water.

As CBO operating temperatures are lower than the calcining temperatures needed to make SCMs from nonreactive minerals, it is unlikely that CBO processing would significantly increase the reactivity of wet fly ash. Regardless, there is a couple of issues that would need to be addressed in order to be able to process ash from a landfill through a CBO plant: 1) the CBO process is not designed to accept wet feed material, and 2) if the landfilled coal ash has coarser coal ash particles, such as bottom ash, comingled with the fly ash, then the coarsest and/or heaviest particles will accumulate near the bottom of the combustor during CBO processing. Therefore the CBO process would need to be modified, or more likely, the landfilled coal ash would need to be preprocessed in order to dry and remove coarse particles before introducing the material into the combustor (Progress Materials & Inc.).

### 12.3.1.2 Example commercial applications

In 1997, high carbon fly ash from the South Carolina Electric & Gas (SCE&G) Wateree Station, a two-unit, 772 MW plant southeast of Columbia, SC. were processed in the CBO pilot plant. Data acquired during the test program on the Wateree ash provided the major design parameters for a full-scale CBO plant. These data included optimal fluidization velocities, combustion rates, appropriate temperature regimes, and heat exchange coefficients.

The CBO product ash carbon content was less than two percent. Test results demonstrated that concrete mixes made with CBO fly ash replacing varying percentages of Portland cement had nearly identical plastic and hardened characteristics to control mixes containing only cement. In short, the CBO fly ash provided significant benefits to the concrete mixes without undesirable "side effects." The determination of the air-entraining characteristics of the CBO fly ashes was given special emphasis. Laboratory concrete testing showed that CBO fly ash had consistently superior air entraining characteristics. Field testing confirmed the laboratory results (Frady et al., 1999).

Following the pilot plant tests, SCE&G contracted with The SEFA Group (with a technology license from PMI) to provide a CBO facility at Wateree Station. The CBO plant was owned SCE&G. The SEFA Group was contracted to operate the plant and provide the product marketing services. Initial site work began in December 1997 on a plant designed to process 180,000 tpy of ash. Start-up activities began in mid-1998, and the first commercial CBO plant began operations in early 1999. The plant was designed to process 12.5% LOI feed ash with a product LOI of 2.0%–2.5%. Higher throughputs have been achieved at lower feed LOIs without compromising the product, but as noted above, the minimum limit is around eight percent (Keppeler et al., 2001; Keppler, 2003).

An important feature of the Wateree CBO is heat recovery from the residual carbon's combustion is returned to Wateree Station by heating a portion of the power plant's condensate stream. This portion of the condensate stream bypasses two existing feedwater heaters, thereby reducing the amount of extraction stream required (Frady et al., 1999).

The Wateree CBO fly ash product is finer in particle size than the high-carbon feed ash, and it is very similar to the fineness of low-carbon fly ash produced by the Wateree units before low NOx burners. The CBO product fly ash shows no signs of agglomeration. The fly ash has performed very well in the concrete marketplace and is viewed as a premium product (Keppler, 2003). By the end of 2015, over 2 million tons of fly ash had been processed in the Wateree CBO plant.

After the Wateree project, there were three more commercial CBO plants constructed and operated.

Santee Cooper Winyah Station CBO was placed in service September 2002 and designed to process approximately 225,000 tons of fly ash per year. In contrast to the Wateree CBO, this plant was built, owned, operated, and ash marketed by The SEFA Group.

Dominion Energy Brayton Point Station CBO was placed in service August 2006 and designed to process approximately 310,000 tons of fly ash per year.

Dominion Virginia Power Chesapeake Energy Center CBO was placed in service November 2006 and designed to process approximately 180,000 tons of fly ash per year.

As of January 2016, only two of these units remain in operation. The Wateree and Brayton Point CBO plants operate intermittently as demand requires, although the Brayton Point CBO is scheduled to be decommissioned in 2017 due to the closure of the host utility plant. The Winyah CBO plant was partially demolished in 2015 and replaced with a new STAR fly ash beneficiation plant in order to also reclaim and beneficiate pond ash.

### 12.3.2 Staged turbulent air reactor (STAR)

In 2004 the SEFA Group began development of a new thermal beneficiation process in order to create a technology that would incorporate all of the same benefits of the CBO process while removing many of the limitations; chief among them were feed ash flexibility and product quality. This new process, called the Staged Turbulent Air Reactor (STAR), provides all the benefits and functionality of the CBO plus many additional enhancements.

While the CBO process is based on the bubbling fluidized-bed technology, the STAR process is entirely different. It is essentially a hybrid of the circulating fluidized-bed and transport reactor processes. It operates in a completely different regime as compared to a BFB. It has been well known for many years that the CFB is much more efficient in burning high carbon low volatile fuels. However, PMI determined this type of process would never be a feasible alternative to the CBO. Instead, SEFA took a different design approach and was able to successfully demonstrate this design.

The STAR technology offers many new advantages/opportunities not formerly available with other beneficiation processes. Further, the STAR has demonstrated the ability to provide a range of products that can be applied across a wide variety of new markets not previously open to by-product fly ash or other beneficiation processes.

The STAR process is specifically designed and operated to reduce the heterogeneity of fly ash by eliminating or lowering the amount of unburned carbon and other contaminants, including unburned organics from alternative fuels, such as biomass or other “opportunity” fuels. The process operates at temperatures that are high enough to burn off residual organics comingled in the fly ash, including coal char particles. Plant operation can be varied to either reduce or remove all carbon from fly ashes. It can also be operated to reduce some types of agglomerates, thereby improving particle size distribution, as well as to blend various coal fly ashes in order to reduce variations in ash chemistry or to optimize the performance of coal ash for particular ash utilization opportunities/markets. Further, The STAR process has successfully demonstrated sustained operation with both Class C and Class F fly ash.

The STAR process is designed to burn fly ash with LOIs ranging from 6% to over 25%. In addition, typical commercial operation removes any ammonia and can also reduce other contaminants. The STAR process lowers the amount of residual unburned carbon, reducing the LOI to under the maximum LOI limit of all relevant specifications. STAR-processed fly ash is typically around 1% LOI or less; however, operating conditions can also be adjusted to change/control the LOI of the finished product to meet the expectations of the marketplace.

In fact the STAR process can remove all of the carbon when desired (Knowles, Fedorka, & Castleman, 2013). Typically, when the LOI of fly ash is around 0.5%, there is effectively no carbon left in the fly ash and/or the remaining amount of residual carbon is encapsulated inside the glass particles of the fly ash and, therefore, it no longer has any negative impact. And the remaining fly ash particles would be very homogeneous. This fly ash would be pure mineral matter that had been melted and cooled while suspended in the flue gas. It would be comprised primarily of glass spheres, would have uniform density, particle shape and texture and would be an excellent mineral filler (Hwang, 1999).

#### *12.3.2.1 Process description*

Figure 12.2 shows an overall process flow diagram of the STAR process. Combustion air is supplied to the main combustion chamber, or reactor, through two separate systems. Primary air is supplied through an air distributor at the bottom of the reactor. Secondary air is supplied through ports along the vertical wall of the reactor. Each of these air supplies utilizes a dedicated forced draft fan. The primary air is heated using an air pre-heater prior to entering the reactor. Raw feed ash is pneumatically conveyed from existing storage silos to a process feed bin. The reactor is heated to combustion temperature using a supplemental fuel, such as propane. There is typically a primary air in-duct burner and burners located on the walls of the reactor. Once the reactor reaches adequate combustion temperature raw ash is pneumatically fed through injection ports on the wall of the reactor. The carbon in the ash ignites immediately and temperatures begin to rise. The ash feed is gradually increased and startup fuel decreased until the entire reactor is well above the carbon ignition temperature and combustion process can be self-sustained without the supplemental fuel.

Depending on the source of the raw ash or the LOI, the carbon in the feed ash can react differently, which can result in a wide range of temperatures throughout the reactor. In order to balance these temperatures, a large portion of the hot ash leaving the reactor is collected in a hot cyclone and re-injected into the bottom of the reactor via a nonmechanical valve called a J-valve. This recycled hot ash acts much like a thermal flywheel for the process, as such a large portion of the heat entering the reactor is now supplied by the recycle ash and not just the combustion of the carbon in the raw feed. Water can be injected at specific locations along the wall of the reactor to help control and balance temperatures as well.

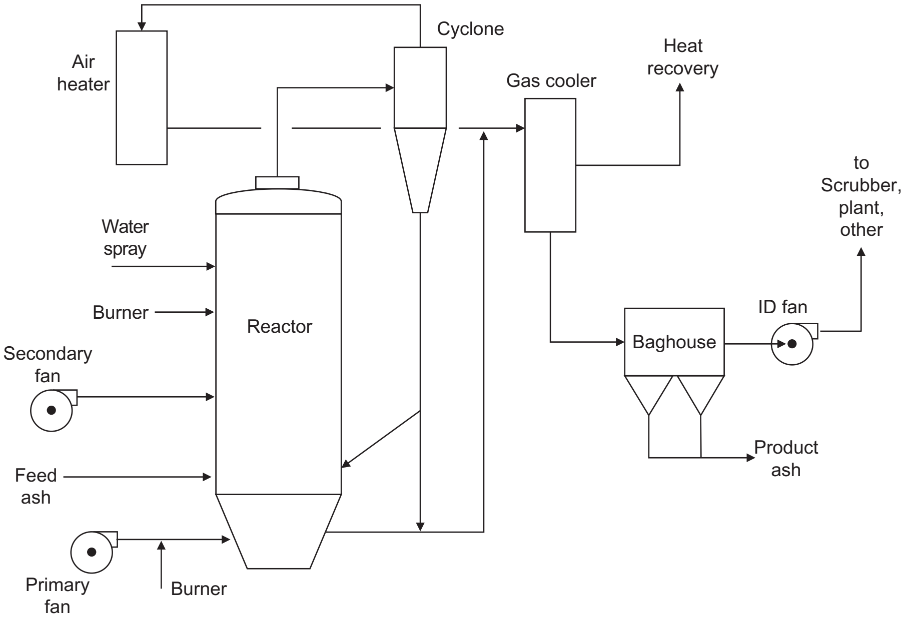

**Fig. 12.2** Staged turbulent air reactor.

The uncollected ash and flue gas exiting the cyclone pass over two heat exchangers, the primary air pre-heater and a flue-gas cooler, which cool the gas/solids mixture to an acceptable temperature. Ash can also exit the system at the bottom of the reactor or J-valve. Solids from the reactor drain mix with the cyclone exit gas and solids prior to the air preheater. Solids drained from the J-valve mix at the inlet to the APH or gas cooler, depending on the application. The removal of these solids from the system allows for optimum control of the amount of solids in, or recycled to, the reactor. After the gas cooler, the cooled gas/ash pass through a baghouse where the ash is separated from the flue gas. The processed fly ash collected by the baghouse is transported via enclosed pneumatic conveyors to product storage dome and silo via diverter valves. The fly ash is discharged from the dome to the silo and then to a truck tank loadout station. The ash-free gas exits to an induced draft fan and then, if ash-sulfur levels are high enough, to a scrubber to reduce sulfur dioxide ($SO_2$) emissions.

The system has two control systems that monitor and regulate system operation: a burner management system and a distributed control system. The burner management system (BMS) has all combustion-related safeguards that must be satisfied to permit combustion within the incinerator chamber. The distributed control system (DCS) monitors and controls the rate at which the system operates.

Like the CBO process, the STAR process is a thermal processing unit and therefore designed based on the amount of carbon burned. The amount of raw feed ash processed is in direct proportion to the LOI of the raw feed ash. If the raw feed ash LOI is six percent the plant can process approximately twice the ash as compared to a raw feed LOI of 12%. All STAR plants are designed to operate at 90% availability. In addition, given the heat release characteristics of any STAR plant, most plants are designed with a turndown ratio of 2:1 from the nominal design capacity.

The steady state reactor operating temperature can vary between 800°C and 1000°C depending on the raw ash feed rate, feed LOI, desired product LOI, and other desired product characteristics. Temperatures below this range can result in loss of adequate combustion to sustain the process and the initiation of gas burners to maintain operation. Temperatures exceeding this range can result in agglomerations in the reactor, cyclones, or J-valves, thus forcing a unit shut down.

One of the critical components is the air distribution system. The pressure drop across the fluidizing air pipes is a function of the hole size, air mass flow, temperature, and pressure. This proprietary system provides the optimum fluidizing velocity across the range of load and operating conditions. The superficial velocity must be maintained at a level well above the minimum fluidizing velocity for all of the particles in the process in order to avoid potential areas of agglomeration.

*Emissions*: Due to the high operating temperature and the use of water spray to control temperatures, flue-gas emissions such as NOx, CO, and VOCs, are inherently controlled by the process and do not require any additional treatment. In certain cases, where the ash sulfur content is high enough, flue-gas desulfurization equipment must be added to control SO2. Of course, if the flue gas is routed back to the host utility plant, no additional control is necessary as the STAR SO2 is negligible compared to the plant. Table 12.2 shows the estimated emissions for a 140 mmbtu/hr STAR Unit (SEFA, 2011). As shown, these are significantly lower than the CBO emission rates.

*Mineral Filler*: Typically, when the LOI of fly ash is around 0.5%, there is effectively no carbon left in the fly ash, and/or the remaining amount of residual carbon is encapsulated inside the glass particles of the fly ash; therefore it no longer has any negative impact. The STAR process has demonstrated the ability to achieve LOIs around 0.5% and lower. This effectively removes all the residual carbon and the remaining fly ash particles are very homogeneous. This fly ash is pure mineral matter that has been melted and cooled while suspended in the flue gas.

**Table 12.2 STAR emission rates—140 mmbtu/h (41 MWth) unit (SEFA, 2011)**

| Pollutant | lb/mmbtu | Control efficiency |
|---|---|---|
| $NO_x$ | 0.036 | 0.0 |
| CO | 0.114 | 0.0 |
| SO2 | 0.295 | 95.0 |
| VOC | 0.011 | 0.0 |
| PM10 | 0.006 | 90.0 |

Having additional market sectors into which fly ash can be sold reduces the risk of partially or completely losing the opportunity to beneficially utilize fly ash in the event specifications and/or regulations change in the future. Developing additional markets for fly ash, such as high-value mineral filler will diversify a utility's fly ash utilization program, creating a more sustainable ash utilization paradigm for the utility.

*Enhanced Strength Properties*: Further, efficient operation of the STAR can actually increase the amount of glass surface area in the product fly ash, freeing the mineral matter from the carbon char and thereby enhancing the strength-producing characteristics of the fly ash. Table 12.3 shows typical test results for STAR product concrete strengths. Coal fly ash produced by low-NOx combustion practices will typically have less glass than coal fly ash produced before the advent of low-NOx combustion practices. Therefore creating increasing the surface area of glass with the STAR process may be vitally important in order for some fly ashes to maintain their value in the marketplace.

*Waste Disposal and Heat*: Of course as with the CBO, there is no solid or liquid waste generated by the CBO or STAR processes, the volume of landfill space saved through the use of these processes is directly related to the volume of raw feed fly ash introduced into the plant. Also, similar to the CBO process, there is a significant amount of heat available for recovery and beneficial use. These include returning hot water to the power plant, power generation, ash drying, and industrial process steam, among others.

*Reclaimed Ash*: One of the key advantages of the STAR process is the ability to process reclaimed fly ash from landfills and ponds. As discussed previously, fly ash that cannot be recycled when produced at a power plant is commonly disposed in a landfill designated for that purpose. Fly ash may be segregated and disposed by itself in large monofills, or the fly ash may be combined with coarser coal ashes, such as bottom ash and/or "economizer ash." When coal ash is placed and compacted in a landfill using standard geotechnical practices, water is added to obtain the predetermined optimum moisture content required for compaction of that particular coal ash, typically around 20% water by weight.

Tests conducted at the McMeekin STAR Plant were conducted by blending certain percentages of reclaimed material with normal dry ash, as well as with 100% reclaimed ash. Table 12.4 shows the Concrete Strength test results. The processed reclaim ash was as good, or better, than the STAR-processed dry ash concrete, and the compressive strengths for the concretes containing STAR-processed ashes were higher than the concretes made with the by-product fly ashes.

The STAR process can be designed to handle both wet and dry feed material and coarser feed ashes, and reclaimed coal ashes from both landfills and ash ponds have been STAR-processed with good results. The STAR process will dry and size-classify coal ash in the reactor, producing two separate product ash outflows: the finer fly ash for concrete comes out of the top of the reactor, and a larger particle size ash for other beneficial uses flows out of the bottom of the reactor. STAR plants are specially designed and built to not only process high-LOI, dry fly ashes, but also to reclaim coal ashes from landfills and/or ash ponds so as to produce pozzolan-grade fly ash (Knowles et al., 2013).

**Table 12.3** STAR product strength test results (Knowles & The SEFA Group, 2009)

| Concrete materials | Low-LOI class F by-product fly ash | Source A class F STAR ash | Source B class F STAR ash | Class C by-product fly ash | Class C STAR ash | 50/50 Blend source A class C STAR ash |
|---|---|---|---|---|---|---|
| Giant (Holly Hill) cement (kg) | 181.4 | 181.4 | 181.4 | 181.4 | 181.4 | 181.4 |
| Fly ashes (kg) | 54.4 | 54.4 | 54.4 | 54.4 | 54.4 | 54.4 |
| Total cementitious material (kg) | 235.8 | 235.8 | 235.8 | 235.8 | 235.8 | 235.8 |
| % Fly ash | 23% | 23% | 23% | 23% | 23% | 23% |
| MM Garner #67 (kg) | 816.5 | 816.5 | 816.5 | 816.5 | 816.5 | 816.5 |
| Matthews Sand (kg) | 558 | 563 | 562 | 567 | 569 | 566 |
| City Water (l) | 146.1 | 145.4 | 141.2 | 140.4 | 144.2 | 146.1 |
| w/cm Ratio | 0.62 | 0.62 | 0.60 | 0.59 | 0.61 | 0.62 |
| BASF Polyheed 977 (l) | 1.23 | 1.23 | 1.23 | 1.23 | 1.23 | 1.23 |
| ***Trial batch results*** | | | | | | |
| Slump (cm) | 15.9 | 12.1 | 14.0 | 8.9 | 12.7 | 10.2 |
| % Air | 1.6 | 2.4 | 3.0 | 2.5 | 4.6 | 2.3 |
| Relative yield (%) | 0.997 | 1.002 | 1.006 | 1.001 | 1.024 | 1.000 |
| Concrete temp (°C) | 17.2 | 17.2 | 16.1 | 16.1 | 16.7 | 16.1 |
| Air temp (°C) | 16.1 | 17.2 | 15.6 | 16.1 | 16.1 | 15.6 |
| ***Compressive strength results (MPa)*** | | | | | | |
| 7-Day average | 21.6 | 25.3 | 24.4 | 28.5 | 28.9 | 28.2 |
| 7-Day average w/ slump adjustment | **21.9** | **25.4** | **24.6** | **28.5** | **29.0** | **28.2** |
| 28-Day average | 25.6 | 30.8 | 32.6 | 35.7 | 35.1 | 35.4 |
| 28-Day average w/ slump adjustment | **28.7** | **31.8** | **34.6** | **35.0** | **36.4** | **35.4** |

Table 12.4 **STAR-reclaimed product strength test results (Knowles et al., 2013)**

| **Cubic meter mix proportions (kg)** | **Mix 1 control**[a] | **Mix 2 blend**[b] | **Mix 3 100%**[c] | **Mix 4 100%**[d] | **Mix 5 Plant A**[e] | **Mix 6 Plant B**[f] |
|---|---|---|---|---|---|---|
| Type I cement | 249 | 249 | 249 | 249 | 249 | 249 |
| Fly ash | 83 | 83 | 83 | 83 | 83 | 83 |
| Loss on ignition (%) | 0.9 | 1.7 | 1.2 | 1.9 | 3.5 | 2.6 |
| Total cementitious material | 332 | 332 | 332 | 332 | 332 | 332 |
| % SCM | 25% | 25% | 25% | 25% | 25% | 25% |
| #57 Stone | 1098 | 1098 | 1098 | 1098 | 1098 | 1098 |
| Natural sand | 746 | 746 | 746 | 746 | 746 | 746 |
| City water (l) | 121.7 | 122.2 | 119.1 | 122 | 121.6 | 124.9 |
| w/cm Ratio | 0.48 | 0.48 | 0.47 | 0.48 | 0.48 | 0.49 |
| Water reducer (ml) | 496.8 | 496.8 | 496.8 | 496.8 | 496.8 | 496.8 |
| Air entrainer (ml) | 59.6 | 59.6 | 59.6 | 86.1 | 265 | 364.3 |
| ***Trial batch results*** | | | | | | |
| Slump (cm) | 12.1 | 12.1 | 11.4 | 12.1 | 12.1 | 12.7 |
| Air % | 4.4 | 4.4 | 4.5 | 4.4 | 4.5 | 5.2 |
| Unit weight (kg/$m^3$) | 2362 | 2370 | 2360 | 2365 | 2364 | 2346 |
| Relative yield % | 98.83% | 98.54% | 98.77% | 98.74% | 98.77% | 99.71% |
| Concrete temp (°C) | 13 | 13 | 15 | 16 | 17 | 18 |
| Air temp (°C) | 14 | 15 | 10 | 16 | 16 | 16 |
| ***Compressive strength results (MPa)*** | | | | | | |
| 7-Day average | 24.41 | 25.3 | 25.23 | 24.34 | 27.1 | 20.41 |
| 28-Day average | 32.06 | 33.99 | 32.61 | 33.23 | 33.09 | 24.34 |
| 7–28-Day gain | 7.65 | 8.69 | 7.38 | 8.89 | 6 | 3.93 |

[a] STAR-processed dry fly ash for a control mix.
[b] STAR-processed blend of dry fly ash (75%) and reclaimed ash (25%).
[c] 100% STAR-processed reclaimed ash (morning run).
[d] 100% STAR-processed reclaimed ash (afternoon run).
[e] By-product fly ash—Source A.
[f] By-product fly ash—Source B.

### 12.3.2.2 *Commercial operating experience*

There are currently three commercial STAR facilities in operation. These are:

A 140,000 tpy unit located at the South Carolina Electric and Gas (SCE&G) McMeekin Station in Columbia, SC. This plant is owned and operated by The SEFA Group, who also provide the product marketing and sales.

A 400,000 tpy unit located at the NRG Morgantown Station in Morgantown, MD. This plant is owned by NRG but is operated by The SEFA Group; SEFA also provides the product marketing and sales.

A 350,000 tpy unit located at the Santee Cooper Winyah Station in Georgetown, SC. This plant is designed to process both the dry by-product ash from the operating generation plants but also the ash reclaimed from the disposal ponds. This is the first beneficiation plant of any technology to process reclaimed ash.

*McMeekin STAR Facility*: In 2006, SEFA began construction on the first STAR plant. The McMeekin STAR Plant would be owned operated by SEFA, who would also market the product ash. This plant was designed to process 140,000 tpy of the raw fly ash from the McMeekin units, as well as ash from other SCE&G facilities. The plant started commercial operation in 2008. During typical operation the McMeekin STAR Plant processes bituminous coal fly ash. However, some subbituminous coal fly ash and various blends of bituminous and subbituminous coal fly ashes have been processed. The LOI of the raw feed fly ashes processed through the STAR plant have ranged from slightly over 20% LOI to slightly under six percent LOI. STAR product ash is typically around one percent LOI; however, STAR plant operating conditions can be adjusted to change/control the LOI of the finished product to meet the expectations of the marketplace. For example, at times the STAR plant has been operated to consistently produce fly ash with LOIs less than 0.5% and at other times it has been operated to consistently produce fly ashes having LOIs near three percent (Knowles & The SEFA Group, 2009).

Since startup the McMeekin STAR Plant has processed around 600,000 tons of fly ash.

*Morgantown STAR Facility*: In February 2011, construction began on a STAR plant at the NRG Morgantown Generating Station. The plant started commercial operation in September 2012.

The Morgantown plant is the second-generation application of the STAR process. At almost three times the capacity of the McMeekin plant, significant time was spent in reducing the risk of such a large scale up. The plant contains enhancements to several systems such as a reactor, cyclones, J-valves, and an air distribution system.

Fly ash used in the process includes that from the Morgantown Station and that transported from the NRG Chalk Point Station. The plant is designed to process approximately 240,000 tons/year of fly ash from the Morgantown facility and approximately 156,000 tons/year of fly ash from the Chalk Point facility. Since startup the Morgantown STAR plant has processed over 400,000 tons of ash (Knowles, Fedorka, & Castleman, 2013).

*Winyah STAR Facility*: Currently there are hundreds of millions of tons of previously disposed coal ash sitting idly in ponds all over the country. The industry was in need of a beneficiation technology that could not only process poor-quality fly ash into a high-quality additive for concrete, but could also transform previously disposed coal ash, such as pond ash, into a quality product for concrete.

In 2013, SEFA first successfully demonstrated the commercial-scale beneficiation of pond ash at its McMeekin STAR Plant. The following year, SEFA decommissioned its currently existing carbon burnout beneficiation plant at the Winyah generating station and replaced it with a STAR plant that could interchangeably beneficiate both freshly-produced fly ash and previously disposed coal ash reclaimed from ponds.

The Winyah STAR Plant routinely operates using only reclaimed coal ash from ponds and yet is able to switch its feed source at a moment's notice to process 100% dry fly ash as it is produced at WGS.

The Winyah STAR Plant also routinely processes coal ash with residual carbon contents ranging from 5% to over 25%. Because this plant is a stand-alone solution, it does not depend on WGS in any way and will operate normally even when all the WGS units are offline. In fact, even if any or all of the WGS units are decommissioned in the future, the plant could continue operating at full capacity for decades, limited only to processing the on-site pond ash.

Uninterrupted supply and consistent quality always translate to more fly ash being used. Customers lose confidence in fly ash when they cannot rely on it being available when needed or if the quality of the fly ash causes problems with their production and processes. The Winyah STAR Plant allows Santee Cooper to maximize the annual amount of coal ash used from WGS by providing a continuous supply of quality product to its customer base.

Unless reclaimed pond ash is used at Winyah to augment the feed material, the supply of STAR fly ash would never keep up with demand. Like most coal-fired power plants, the recent trend at WGS has been for less coal to be burned, especially during the spring and fall months, when customer demand for fly ash is at its highest. Reclaimed coal ash from ponds provides continuous feed material for the Winyah STAR Plant and ensures continuous supply for customers (Knowles et al., 2013).

## 12.4 Summary

Thermal beneficiation has been demonstrated to be a commercially viable method for improving the quality of fly ash which previously was unfit for market applications. Further, there are two distinctly different technologies commercially available and have been proven at multiple locations and range of production capacity. In addition, both of these processes, the CBO and STAR, offer a wide range of flexibility and performance that exceeds the capabilities of many nonthermal processes.

## References

Cochran, J. W., & Kirkconnell, F. (1995). Electric Power Research Institute. Method of Fly Ash Beneficiation and Apparatus for Same, March 1995, US Patent 5399194.

ECT, (2005). Big Ben Station Carbon Burnout—Application for Air Construction Permit.

Fox, J. M. (2005). *Changes in Fly Ash with Thermal Treatment, 2005 World of Coal Ash Conference*. Kentucky: Lexington. http://www.flyash.info/2005/132fox.pdf.

Frady, W. T., South Carolina Electric & Gas, Keppeler, J.G., Progress Materials, Inc., Knolwes, Jimmy, The SEFA Group, 1999. South Carolina Electric & Gas—Successful Application of Carbon Burn–Out at the Wateree Station, 1999 International Ash Utilization Symposium, Center for Applied Research, University of Kentucky, Paper #99, www.flyash.info.

Giampa, V. M. (2003). Progress Materials, Inc., “The Fate of Ammonia and Mercury in the Carbon Burn Out Process”.

Giampa, V. M. Ammonia Removal from Coal Ash by Carbon Burnout Out, http://www.netl.doe.gov/publications/proceedings/01/scr/giampa.pdf.

Huggins, Y. (1999). In *Huffman, University of Kentucky, Senior, Physical Sciences Inc. Definition of Mercury Species in Unburned Carbon from Pulverized Coal Combustion, Air and Waste Management Meeting*. http://www.psicorp.com/pdf/library/sr-0977.pdf.

Huttenen, A. (2005). Electric Power Research Institute, Technical Brief—Design, Operation, and Performance of a Commercial Scale Carbon Burn-Out Facility, June 2005, TB-114328.

Hwang, J. Y. (1999). Beneficial use of fly ash. In *Proceedings*: *13th U.S./Korea joint workshop on energy and environment* (pp. 373–396).

(http://www.imp.mtu.edu/jmmce/issue1-1/Jim_JMMCE.pdf; http://www.imp.mtu.edu/jmmce/issue1-2/mercury_JMMCE.pdf).

Keppeler, J. G. (2001). Carbon Burn-out—An Update on Commercial Applications. International Ash Utilization Symposium, Lexington, Kentucky. University of Kentucky Center for Applied Energy Research, 2001, Paper #61, www.flyash.info.

Keppler, J. G. (2003). Progress Materials, Inc., Carbon Burn Out—A Commercially Proven Solution for Fly Ash Woes, March 2003.

Knowles, J., Fedorka, W., & Castleman, J. (2013). Staged Turbulent Air Reactor Beneficiation Process—Commercial Update, http://www.flyash.info/2013/157-Fedorka-2013.pdf

Knowles, J., & The SEFA Group. (2009). *New Commercial Beneficiation Process Staged Turbulent Air Reactor (STAR)"*. World of Coal Ash Conference. http://www.flyash.info/2009/049-knowles2009.pdf.

Progress Materials, Inc., Carbon Burn-Out Frequently Asked Questions, http://www.pmiash.com/cboFAQs.asp.

SEFA. (2011). *Morgantown Generating Station STAR—Application for Air Construction Permit*.

USEPA. (2003). *Background Document for Life-Cycle Greenhouse Emission Factors for Fly Ash.* http://www3.epa.gov/climatechange/wycd/waste/downloads/fly-ash-chapter10-28-10.pdf.

# Chemical passivation

# 13

*R. Minkara*
Headwaters Incorporated, Kennesaw, GA,
United States

## 13.1 Introduction

The Clean Air Act Amendments of 1990 regulated NOx emissions from coal-fired utility boilers. NOx is an acid rain precursor and a contributor to atmospheric ozone formation. Some NOx emission reduction can be achieved by boiler combustion control using low NOx burners (LNBs). The basic principle of LNB involves decreasing the amount of air into the primary combustion zone to create a fuel-rich environment and lower combustion temperature, thus reducing NOx formation. LNBs have led to increased amounts of unburned fuel resulting in elevated levels of residual unburned carbon (UBC) in fly ash. The adsorptive surface of UBC is shown in Fig. 13.1. Fig. 13.2 shows how the surface area of UBC contributes to the total surface area of fly ash containing UBC.

### *13.1.1 Effect of carbon on the use of fly ash*

The marketability of fly ash for concrete use is limited by its carbon content due to interference with air entrainment in concrete (History of the CAER, 1995). ASTM and State Department Of Transportation (DOT) specifications control the level of UBC in ash for concrete use by limiting the loss on ignition (LOI) of fly ash. LOI is used as a proxy for carbon content in ash. ASTM C 618 limits the LOI for ash to 6%. AASHTO M295 limits the LOI for ash to 5%. A list of State DOT LOI limits is shown in Table 13.1 illustrates that although ASTM C 618 and AASHTO are the most widely accepted specifications for fly ash across the US, DOTs (the largest consumers of fly ash in the United States), establish even more stringent limits to avoid interference with AEAs used in concrete.

Concrete is a composite material made of stone and sand bonded together by a hydraulic binder. The hydraulic binder consists of Portland cement, fly ash, water, and performance-enhancing admixtures. Fly ash is considered a mineral admixture that is used to enhance the rheology of fresh concrete and the durability and strength of hardened concrete (Teixeira et al., 2016). Other admixtures include air entrainment agents (AEAs), which are liquid reagents added to concrete in very small dosages of a few ounces per 100 lbs of cement weight (or few hundreds of mL per 100 kg of cement weight) for the purpose of inducing and stabilizing microscopic air voids in concrete during mixing.

These stabilized air voids play an essential role in providing long-term freeze-thaw durability and scaling resistance for concrete structures in cold regions. Concrete is a

**Coal Combustion Products (CCP's).** **http://dx.doi.org/10.1016/B978-0-08-100945-1.00013-7**

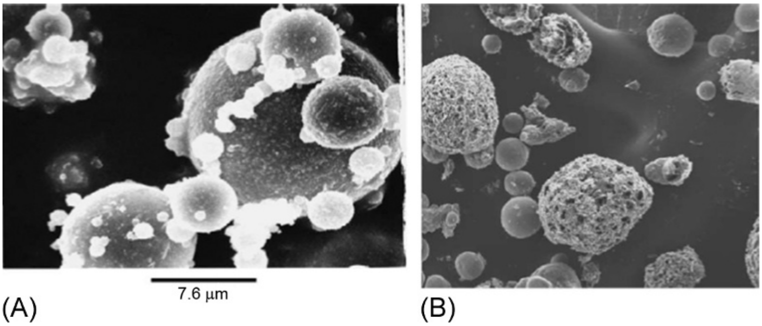

**Fig. 13.1** SEM fly ash in (A) and unburned carbon (UBC) in (B) (Wang & Hongwei, 2006).

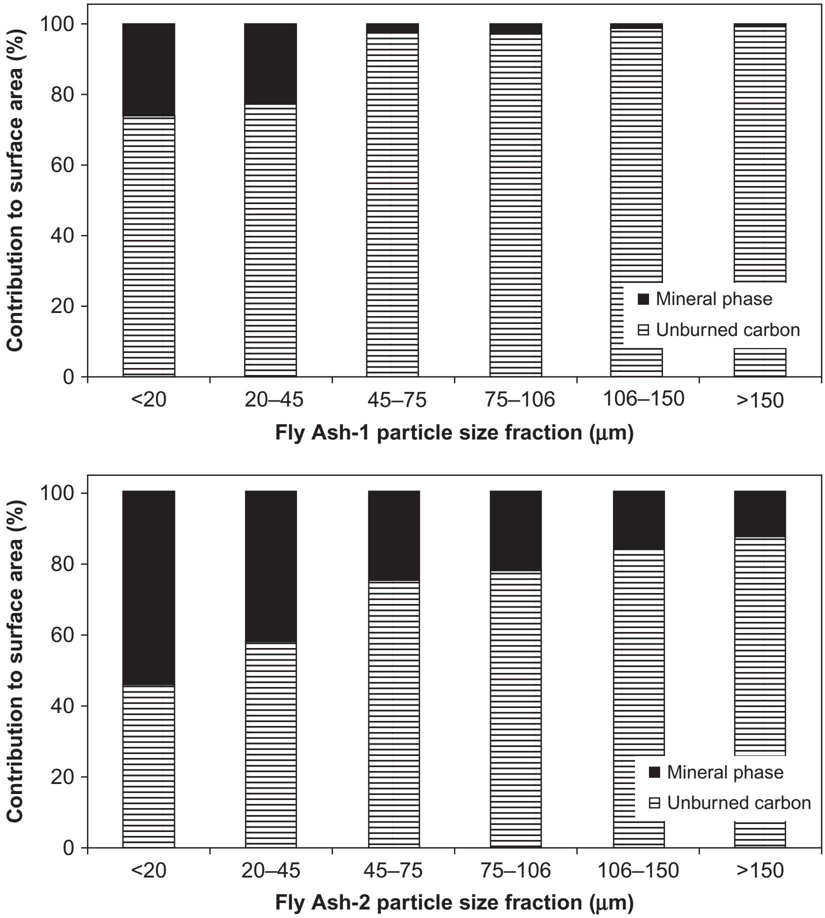

**Fig. 13.2** Particle size contribution from unburned carbon compared to fly ash (Zhu, Wang, Dai, Huang, & He, 2013).

Table 13.1 **Limits on LOI adopted by selected state DOT agencies**

| Maximum allowable LOI in ash | |
|---|---|
| Maine, Mississippi, Nebraska, Pennsylvania, Texas, Utah, Virginia, West Virginia, Wisconsin, Wyoming | 6% |
| Alabama, Arkansas, California, Florida, Georgia, Illinois, Iowa, Louisiana, Maryland, Massachusetts, Michigan, Montana, Nevada, New Hampshire, Oklahoma, South Carolina, Tennessee, Vermont | 5% |
| Connecticut, Delaware, New York, North Carolina, Rhode Island | 4% |
| Minnesota | 3.5% |
| Arizona, Colorado, Indiana, Kansas, Kentucky, New Jersey, Ohio | 3% |
| North Dakota, South Dakota | 2% |
| Idaho, Missouri, Oregon, Washington | 1.5% |

porous material that holds water in interconnected microscopic pore channels. When concrete temperature drops below freezing, pore water turns into ice and expands by about 9% in volume. The pressure buildup from the expanding ice is relieved by the presence of air voids, which allow for movement and expansion of pore water during freeze-thaw cycles. About 6% ± 1% air void is desired in concrete to allow for movement and expansion of pore water during freeze-thaw cycles to prevent cracking (Hill et al., 2006).

The practice of entraining air into concrete mixtures has other profound positive effects on the characteristics and performance of both fresh and hardened concrete. In fresh concrete, the entrained microscopic air bubbles improve the rheology of the slurry by acting as a lubricant to enhance workability and increase slump, therefore allowing for reduced water content, which results in less shrinkage and higher strength. Bleeding and its adverse impact on the surface of slabs are also reduced by the lower water content made possible by entrained air. The lower water content also results in less segregation and more cohesive concrete.

In hardened concrete, other cobenefits include enhanced sulfate resistance and reduced salt scaling. These enhanced durability characteristics are primarily the result of lowering the water/cement ratio to compensate for the loss of strength due to the air content.

AEAs that are typically used in concrete can be divided into a small number of chemical groups, which are shown in Table 13.2. Carbon in ash adsorbs AEAs preventing concrete from entraining the desired level of air voids. Very high levels of carbon in ash can darken concrete and create the undesirable “black bleed,” where carbon floats to the top of concrete slab during finishing, causing strength and esthetic degradation.

### *13.1.2 Mitigation of carbon in fly ash*

LNBs installed in the 1990s on units burning bituminous coal resulted in unacceptable levels of UBC in fly ash and created early opportunities for carbon mitigation technologies (Pflughoeft-Hassett, 2010). Fly ash containing unacceptable levels of

**Table 13.2** **Common air entrainment agent groups**

| |
|---|
| Salts of wood resins |
| Synthetic detergents |
| Salts of sulfonated lignin |
| Salts of petroleum acids |
| Salts of proteinaceous materials |
| Fatty and resinous acids and their salts |
| Organic salts of sulfonated hydrocarbons |

carbon can be beneficiated by carbon removal or passivation. Carbon removal can be accomplished by the separation of the carbon-rich fraction using triboelectrostatic separation, froth flotation processes, or by igniting the UBC in a post-collection combustion process.

There is no one solution for mitigation of carbon in ash. Coal-fueled power plants consume a range of coal types in boiler and emissions control configurations that vary widely from facility to facility. Market demand, supply conditions, and value of beneficiated ash in the local market, as well as utility incentives, play a role in selecting carbon beneficiation technologies. Carbon removal processes are covered in other chapters.

The most common carbon mitigation processes are the postcollection combustion of carbon and electrostatic separation. These technologies are useful for high UBC content. Unfortunately, Powedered Activated Carbon (PAC) is usually less than 2%, which can be a challenge for processes that involve the removal of carbon.

### 13.1.3 Chemical passivation

Chemical passivation is achieved without removal of the carbon, which makes it ideal for PAC mitigation and can be used in concrete with high LOI (Plunk, 2015). The systems are capable of treating high LOI ashes (ASTM C 618 requires LOI of less than 6%). The concept takes advantage of carbon's ability to adsorb organic compounds. Patents have included ethers, esters, carboxylic acids, aromatic sulfonates, surfactants, and a large variety of other organic compounds (Hill et al., 2006). Carbon passivation consists of adding organic compounds as sacrificial agents to fly ash in order to passivate the adsorptive capacity of carbon.

First generation passivation systems had some issues that needed improvement in order for the technology to be effective. The first thing that had to be overcome was the inability of older systems to evenly treat the ash. Fly ash was frequently either underdosed or overdosed due to the potent sacrificial agents used (Minkara & Kelley, 2015). A small dosage change had the potential to overwhelm the ash, leaving too much of the sacrificial agent in the ash. If overdosed, these agents can generate air in concrete, which is not their intended purpose. Second generation reagents have been formulated to reduce its activity and decrease the possibility of overdosing the ash (Minkara & Kelley, 2015). Another idea that has been patented includes processing the ash in the presence of ozone to neutralize the surface of carbon. The use of ozone as an oxidation agent eliminates the undesirable effect of carbon on air entrainment in concrete (Chen et al., 2005).

The ash treatment system itself had to be improved upon by designing a better application method to deliver a more uniform distribution of product to ash. Specialized nozzles have been included to treat the ash uniformly without clogging. Lastly, some plants have carbon contents that vary more than others. Traditional test methods of foam index (FI) and LOI proved insufficient. They were not accurate or representative enough to ensure proper dosing. Some adsorption tests were adopted from the activated carbon industry, such as the methylene blue and iodine number (IN) tests. However, a more representative and accurate adsorption test method has recently been developed to determine the carbon in ash affinity to adsorb AEAs (Minkara, Yeboah, Nordman, Rhodes, & Kelley, 2015). The new test method is based on fluorescence spectroscopy and has the potential to be automated for continuous monitoring of ash quality.

Recently, due to the EPA Maximum Achievable Control Technology (MACT) rule (EPA, 2016), a PAC injection in flue gas has become a widely practiced solution to control mercury emissions from power plants (Plunk, 2015). Typical PAC injection systems are designed to introduce activated carbon ahead of particulate control systems to allow enough residence time for mercury capture and collect the PAC with the fly ash in existing electrostatic precipitators or baghouses (Scala, Chirone, & Lancia, 2011). PAC-contaminated fly ashes are more challenging than UBC in ash for use in air-entrained concrete due to their significantly higher absorption capacity caused by their extremely high surface area. Examples of surface areas for UBC, activated carbon, and fly ash are provided in Table 13.3.

Very low concentrations of activated carbon in ash can render an ash unsuitable for air-entrained concrete. Although ash with UBC content as high as 6% measured as LOI can be acceptable according to ASTM C 618 for use in air-entrained concrete, activated carbon content of less than 1% can be troublesome for air entrainment in concrete. The European standard EN 450, on the other hand, has three categories of acceptable LOI levels, less than 5%, 2%–7%, and 4%–9%. Nonetheless, the issue remains that activated carbon, even in very small quantities, can have a significant interference with AEAs.

**Table 13.3** Surface areas of fly ash, UBC, and PAC

| Sample type | Fly ash | Unburned carbon | Activated carbon |
|---|---|---|---|
| Specific surface area ($m^2/kg$) | 170–1000 (User guidelines, 2016) | 50,000–400,000 (Kulaots, Hurt, & Suuberg, 2002) | 500,000–1,500,000 (HAYCARB, 2016) |

## 13.2 Limitations of traditional testing

Variability in coal-fired unit configurations, ash composition, and powdered activated carbon (PAC) characteristics are not the only challenges facing first-generation carbon mitigation technologies. Imprecise test methods for determining carbon impact on ash also complicates quality control (QC) in assuring consistent quality fly ash.

Traditionally, there are three methods of assessing residual carbon in fly ash and evaluating its impact when used in concrete, LOI, FI testing, and air in mortar testing. LOI testing is used to determine the mass percentage of carbon that remains in an ash sample. FI testing is used to determine the amount of air entraining agents needed to satisfy the adsorption capacity of ash to generate a stable foam, while air in mortar testing gives information on how well fresh mortar with an elevated AEA dosage is expected to hold entrained air over time.

### 13.2.1 Loss on ignition

For LOI, a small amount of fly ash is dried to a constant weight to eliminate water interference. The dried sample is placed into an uncovered porcelain crucible and ignited in a muffle furnace at a temperature ranging from 750°C (ASTM C 618) to 925°C (EN 450), depending on the test method. Unfortunately, LOI does not differentiate for the decomposition of substances other than carbon that are lost during heating (Chan, Weber, & Brown, 2005). For instance, water adsorbs easily onto the surface of carbon and may not be evaporated during the drying step. As the carbon is lost, the water is also removed (Sarker, 2013). Some elements may also be prone to oxidize or reduce in the muffle furnace environment, therefore skewing the results of the test. LOI is usually a higher measurement than the actual amount of UBC in the fly ash. In addition to UBC the combustion of the fly ash causes an expulsion of all water (free and bound), unburned fuel, volatiles (hydrates and hydroxyl compounds), the loss of carbon dioxide from carbonates, the conversion of metal sulfides into metal oxides, metal sulfates, and sulfur oxides, along with other chemical species.

### 13.2.2 Foam index testing

The FI test was developed by V.H. Dodson and soon was adopted by many as a rapid method to determine the amount of AEAs needed to form a bubble microstructure in concrete that allows water to expand during freeze and thaw cycles without cracking the concrete. In addition to determining the dosage of AEA needed to entrain air in concrete, the FI test is currently used to determine the impact of carbon in ash on the dosage of AEA. The higher the dose of AEA required, the higher the adsorption capacity of the carbon. Although this method is widely used in the fly ash and concrete industries, there is no standard version of it currently published by any standardization body. Therefore there are several different versions of the test which makes the results highly variable and hard to obtain interlaboratory reproducibility. Nonetheless, attempts are currently being made at ASTM to standardize the test.

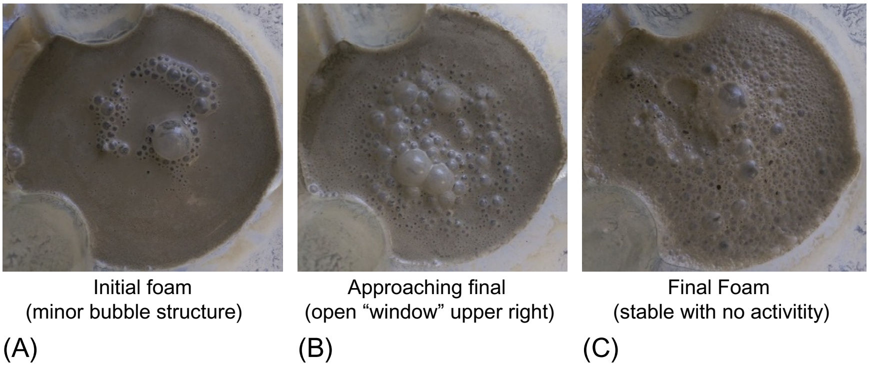

**Fig. 13.3** Example of the development of stable foam as a foam index test progresses.

One way to perform the FI test is by mixing 40 or 80 g of ash (depending on whether the ash is Class C or Class F) with 200 mL of water. The slurry is then mixed (either in a blender, a jar, or with an automated shaker) for a 10-second cycle. Drops of the desired AEA are added to the slurry, and the mix cycle is repeated. This continues until a stable foam is formed on the top of the slurry (Fig. 13.3C). Once a stable foam is covering the entire surface of the aqueous phase of the slurry, the technician visually inspects to ensure there is no activity (i.e., popping bubbles) for at least 10 seconds, which determines the endpoint. The FI is recorded as the number of drops of AEA necessary to achieve the stable foam.

Use of the FI test frequently results in imprecise measurements due to its inherent variability and subjectivity. These factors can easily result in inadequate Quality Assurance (QA) and Quality Control (QC) practices. This method is designed to measure the adsorption potential or total adsorption of AEA in an ash.

### *13.2.3 Air in mortar (ASTM C-185)*

A more comprehensive approach to evaluating the ability of fresh mortar to hold entrained air over a period of time is described by ASTM C-185 Standard Test Method for Air Content in Hydraulic Cement Mortar. The process is more cumbersome and less suited to identifying the variability of ash performance day by day and hour by hour in the field due to the high volume of ash needing to be tested in an operational setting and the length of time the test requires. In addition to the time demands of the test, cement hydration, mixture rheology, and the manual handling of the fresh mortar specimens can affect the results.

According to ASTM C-185, sand, cement, fly ash, AEA, and a sufficient amount of water to produce the prescribed flow are mixed. The amount of the desired AEA is to be sufficient to achieve a particular volume of air in the mortar. The air volume is calculated by weighing the resulting mixture in a calibrated volumetric vessel to obtain the mass per unit volume the mixture, then, this value is divided by the

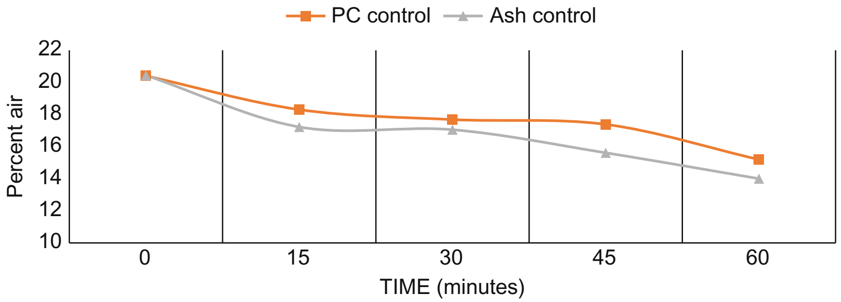

**Fig. 13.4** Air content versus time from an ASTM C-185 test.

theoretical mass per unit volume (calculated using the mass and specific gravity of each material). In order to monitor prolonged AEA adsorption by carbon, the mixing and weighing cycles are repeated every 15 minutes for a total of 1 hour to determine the air content at each time interval. The AEA levels can also be varied to obtain AEA dosage information (Fig. 13.4).

The air content gives information on how well fresh concrete will hold air over time and provides an indication of how adsorptive the carbon is in the fly ash. As the adsorptive capacity of carbon increases, the air content decreases over time.

### 13.2.4 Air in concrete

Air-entrained concrete contains stable, well-uniformed bubbles of microscopic air, which relieve internal pressure on the concrete by providing tiny chambers for water to expand into when it freezes. The stability of the bubble structure is needed throughout the process of mixing, placement, and final hydration of the concrete. The impact of PAC in ash on air content and stability can be evaluated on both fresh concrete using ASTM C 231 and hardened concrete using ASTM C 457.

#### 13.2.4.1 Air content of fresh concrete (ASTM C 231)

Air content in concrete is typically measured at the ready-mix concrete plant using an air pressure meter as specified in ASTM C 231 (Fig. 13.5). This calibrated vessel with a separate air chamber is connected through a valve to the test bowl that is filled with freshly mixed concrete. With the valve closed, the separate chamber is pressurized to a predetermined operating pressure. When the valve is opened, the air expands into the test chamber, and the pressure drops in proportion to the air contained within the concrete sample. The pressure gauge is read in units of percent air content.

#### 13.2.4.2 Air in hardened concrete (ASTM C 457)

The air-void system in hardened concrete can be analyzed according to ASTM C 457. This test is used to determine the susceptibility of concrete to damage due to freezing and thawing or to forensically determine why it has occurred. A petrographic cross section of hardened concrete used in ASTM C 457 is shown in Fig. 13.6.

Fig. 13.5 Air pressure meter used in ASTM C 231M.

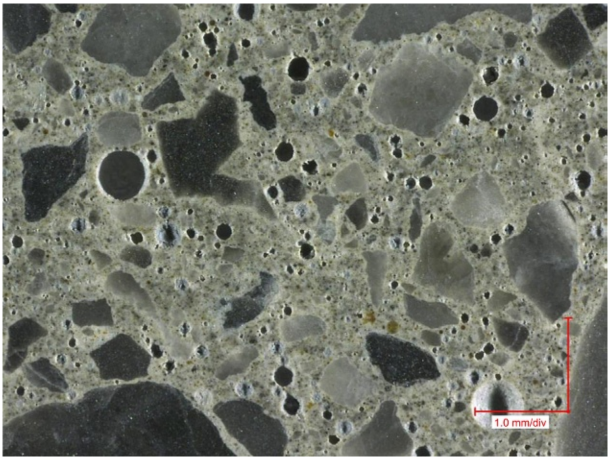

Fig. 13.6 Petrographic cross section of hardened concrete.

## 13.3 Adsorption tests

PAC added for mercury control presents different challenges for ash use in concrete. Activated carbon is much more adsorptive than unburned coal with a high affinity to adsorb AEAs that are used in concrete production. These characteristics are the result of activated carbon's complex pore structure (Fig. 13.7). Mercury is sequestered in very small portions of the carbon structure, but there remain ample pores and surface area available to adsorb other compounds, including AEAs from fresh concrete mixtures.

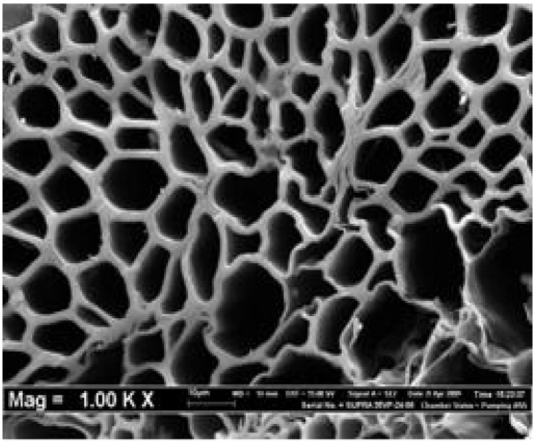

**Fig. 13.7** Micrograph of activated carbon particle.

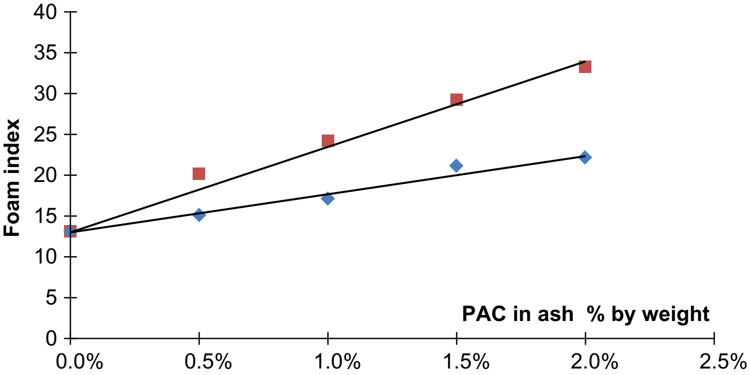

**Fig. 13.8** Number of drops of AEA needed to reach stable foam in ash/water slurry containing two different PACs.

Additionally, PACs used for mercury control can have different effects on ash quality for use in concrete. Fig. 13.8 shows high variability in the impact of two different PAC samples (identified by red and blue markers) on potential air entrainment demand as measured by FI testing.

The increased variability of content, type, and adsorption capacity of carbon in fly ash has raised the need to develop more accurate adsorption test methods for determining the impact of activated carbon on ash. There are several test methods working toward utilizing existing activated carbon adsorption tests to measure the adsorption capacity of ash and its impact on concrete. For example, IN, which has been traditionally used to determine the adsorption capacity of carbon black, is now being considered as a potential test method to determine the adsorption capacity of fly ash. In this test method, carbon black/fly ash is first boiled in a 5% HCl solution to remove any sulfur that may interfere with the results. After drying and filtering (and crushing, if necessary), a known amount of carbon black (or fly ash, as may be the case) is mixed with a standard iodine solution. Subsequently, the solution is filtered to separate the solids. Lastly, the concentration of the remaining iodine in the filtrate is measured by titration. The results are expressed in grams of iodine adsorbed per kilogram of carbon black/fly ash (Ahmed, David, Sutter, & Watkins, 2014). Although the IN test provides a relative indication of surface area, it may not measure the capacity of fly ash to adsorbed other chemical species.

## 13.4 Automated methods

New automated adsorption-based systems have been developed to provide more accurate, dependable, and less labor-intensive measurements of ash quality than FI testing (Fig. 13.9). This referenced system utilizes adsorption and fluorescence principles to analyze ash samples and determine the AEA adsorption potential for QA as well the optimum passivation reagent dosage.

**Fig. 13.9** Adsorption potential instrument.

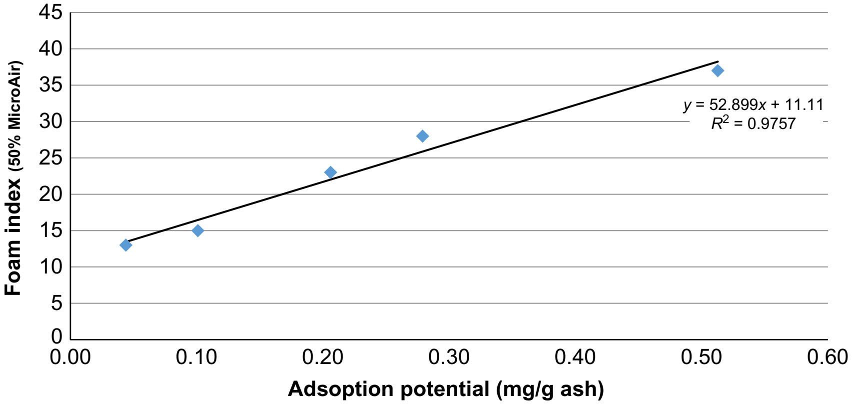

**Fig. 13.10** Adsorption potential as measured by automated fluorescence spectroscopic technique.

Automated fluorescence spectroscopic techniques overcome the variability inherent in FI testing by eliminating operator subjectivity and providing more accurate measurements of AEA adsorption potential. Like many surfactants, AEAs contain conjugated bonds, and the electrons are promoted to an excited state when they absorb ultraviolet radiation. The wavelength used to excite the electrons can vary depending upon which compound is being analyzed. After excitation, the electrons fall back to the ground state, fluorescing and emitting light of a different wavelength that can be detected by optical sensors. The fluorescence intensity is proportional to the concentration of the organic compound being analyzed.

Fluorescence spectroscopic techniques can determine the adsorption potential of ash samples by mixing fly ash with a prescribed volume of surfactant solution with a known (initial) concentration. During mixing, a finite amount of surfactant is adsorbed by the carbon particles leaving the rest in solution. Subsequently, an aliquot of solution is filtered, and the concentration of remaining surfactant in solution (final) is measured. The difference between the initial and the final concentration is the adsorption capacity of the fly ash, given in milligrams of surfactant adsorbed per gram of fly ash. When needed, computer outputs can be correlated to calculate the traditional FI numbers commonly used in the trade (Fig. 13.10).

## 13.5 Chemical passivation

The latest generation of chemical passivation technologies have made significant improvements to key factors for effective carbon mitigation. Second-generation reagents have been reformulated to improve dispersion and have a greater affinity to adsorb onto activated carbon, thereby neutralizing its effects. When applied to fly ash, the reagent saturates the activated carbon surfaces with a sacrificial agent to prevent the carbon from attracting AEAs used in concrete (Minkara & Kelley, 2015).

In-line ash treatment systems have been developed to provide an accurate and uniform distribution of reagent as it is applied to fly ash. The next generation systems can also be fully automated, significantly reducing the potential for operator error.

Although these type of systems can treat fly ashes with high contents of native UBC, they are especially suited to beneficiate fly ash sources containing relatively small amounts of highly adsorptive carbon that are not otherwise treatable by carbon removal (i.e., either by burning or separation).

In most cases, these systems are customizable to address specific power plant configurations and conditions. The systems typically consist of ash handling components that can easily fit between the bottom of the ash silo and existing load-out. This facilitates the ash treatment as trucks or rail cars are being loaded. New ash handling systems include aerated slides that fluidize fly ash to increase its contact surface with the reagent from the treatment system, providing a distribution of reagent on treated ash. Ash handling equipment and components are customized to fit the silo space and match the site needs (Minkara & Kelley, 2015).

Table 13.4 shows different fly ashes containing various amounts of PAC and UBC and the reagent dosages needed to partially neutralize the adsorption capacity to acceptable levels. The effect of the reagent is captured by measuring the FI of fly ash before (initial FI) and after (final FI) treatment. The results show how fly ash with high FI and thus high adsorption can be treated to obtain fly ash with a low FI and thus low adsorption, making it acceptable for its use in concrete. Performance of an operational field-installed treatment system is shown in Fig. 13.11. It also shows in-line treatment systems that can be highly effective in uniformly neutralizing AEA adsorption in fly ash.

The performance of treated fly ash in concrete is shown in Table 13.5. Concrete with treated fly ash entrained virtually the same amount of air (measured according to ASTM C 231) as concrete with untreated fly ash, but with less than half of the dosage of AEA, proving the AEA adsorption capacity of the fly ash was effectively mitigated by chemical passivation.

**Table 13.4** **Reagent dosages for various ashes with powdered activated carbon (PAC) and/or unburned carbon (UBC)**

| Material | Carbon (%) | Initial FI | Reagent dosage (lb/ton) | Final FI |
|---|---|---|---|---|
| C-Ash (PAC) | 0.1 | 37 | 0.4 | 9 |
| C-Ash (PAC) | 0.8 | 37 | 1.0 | 12 |
| C-Ash (PAC) | 0.5 | 27 | 1.9 | 7 |
| C-Ash (PAC & UBC) | 1.4 | 78 | 1.9 | 7 |
| F-Ash (PAC & UBC) | 2.9 | 28 | 1.0 | 15 |
| F-Ash (UBC) | 0.5 | 30 | 1.3 | 9 |
| F-Ash (UBC) | 1.8 | 25 | 1.9 | 7 |
| F-Ash (PAC & UBC) | 3.5 | 61 | 2.3 | 6 |

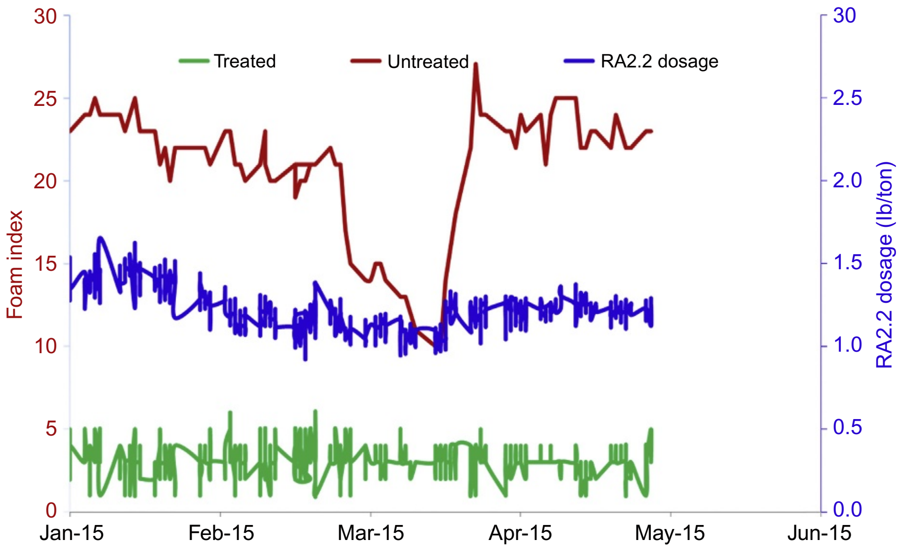

**Fig. 13.11** Chemical passivation system performance results (Minkara & Kelley, 2015).

**Table 13.5** **Chemically passivated fly ash performance in concrete**

| | **Control** | **Ash with PAC** | |
|---|---|---|---|
| **Concrete testing parameter** | **Cement** | **Untreated** | **Treated** |
| Foam index (MBVR) | – | ***18*** | ***5*** |
| AEA (MBVR) dosage (oz./cwt) | ***1.2*** | ***4.2*** | ***1.7*** |
| Air content (6%±1%) | **7.0%** | **6.3%** | **5.8%** |
| Water/cement ratio | 0.53 | 0.49 | 0.49 |
| Slump, inches (6±1) | 6.25 | 6.25 | 5.75 |
| 7 days (psi) | 3433 | 3592 | 3918 |
| 28 days (psi) | 4594 | 4764 | 4908 |

## 13.6 Summary

Residual UBC in fly ash has long been the most common barrier to utilizing ash in high-value concrete applications, mainly because the AEAs added to concrete to create an air-void system resistant to freezing and thawing cycles have great affinity to carbon surfaces. Therefore when UBC is present, AEAs tend to adsorb into these carbon surfaces instead of generating air voids, resulting in premature concrete failures. For this reason, fly ash sources with high amounts of residual carbon are rendered unusable in concrete. Technologies to remove residual carbon or neutralize its effects have been developed and deployed for nearly two decades to provide fly ash that would not interfere with air entrainment in concrete (Harris & Wheelock, 2008; Hill et al., 2006; Kabis, 2015; Xinkai, Tao, & Stencel, 2003).

Chemical passivation is an effective way to neutralize the effects of residual unburned and activated carbon in ash. The concept involves adding a sacrificial agent to the ash to mitigate carbon adsorption properties. In addition to the sacrificial agent the technology also requires accurate reagent dosing equipment, testing, and diagnostic methods for determining appropriate reagent dosage and QC. Passivation reagents are selected for their great affinity to adsorb on activated carbon and to minimize their impact on ash use in concrete. When applied to fly ash the reagent saturates the activated carbon surfaces with a sacrificial agent to prevent the carbon from attracting AEAs used in concrete. The treatment process, typically installed at the power plant, provides an accurate and uniform distribution of reagents to assure consistent treatment of fly ash. Automating the treatment system can reduce the potential for operator error. Robust testing methods to measure the adsorption potential of ash containing PAC are needed to determine reagent dosage as well as for QC and QA of treated ash.

## References

Ahmed, Z. T. H., David, W., Sutter, L. L., & Watkins, M. K. (2014). Fly ash iodine number for measuring adsorption capacity of coal fly ash. *Materials Journal*, *111*(4), 383–390.

Chan, K. -S., Weber, R. J., & Brown, R. C. (2005). Characterization of unburned carbon content in coal fly ash with dielectric constant measurement. *AIP Conference Proceedings*, *760*(1), 1523–1530.

Chen, X., et al. (2005). United States Patent 6890507. Ozone Treatment of Fly Ash.

EPA. (2016). *Mercury air toxics standards*. Available from: https://www.epa.gov/mats/regulatory-actions-final-mercury-and-air-toxics-standards-mats-power-plants.

Harris, T., & Wheelock, T. D. (2008). Process conditions for the separation of carbon from fly ash by froth flotation. *International Journal of Coal Preparation and Utilization*, *28*(3), 133–152.

HAYCARB. (2016). *Activated carbon basics [cited 2016 June 16, 2016]*. Available from: http://www.haycarb.com/activated-carbon.

Hill, R., et al. (2006). *Sacrificial agents for fly ash concrete*. Google Patents.

History of the CAER. (1995). http://www.caer.uky.edu/about/history.shtml.

Kabis, S. (2015). Carbon blocker: Waste management's patented solution to preserving fly ash quality and use. *Ash at Work*, *69*(2).

Kulaots, I. H., Hurt, R., & Suuberg, E. M. (2002). Size distribution of unburned carbon in coal fly ash and its role in foam index. *Fuel Chemistry Division*, *47*(2).

Minkara, R., & Kelley, J. M. (2015). Second generation carbon passivation agent with tamed dosing response for treatment of carbon containing fly ash. *World of Coal Ash*, *24*(2).

Minkara, R., Yeboah, Nordman, R., Rhodes, D., & Kelley, J. (2015). *A novel method for determining adsorption capacity of carbon containing fly ash*. Nashville, TN: WOCA.

Pflughoeft-Hassett, D. (2010). Preserving the beneficial uses of coal combustion products. *Electric Perspectives*, *35*(2), 68–75.

Plunk, G. C. (2015). How PACT was used to avoid 5 million tons of landfilled fly ash. *Ash at Work*, *69*(2).

Sarker, P. K. (2013). *Fly ash: Sources, applications, and potential environments impacts*. Hauppauge, New York: Nova Science Publishers, Inc.

Scala, F., Chirone, R., & Lancia, A. (2011). Elemental mercury vapor capture by powdered activated carbon in a fluidized bed reactor. *Fuel*, *90*, 2077–2082.

Teixeira, E. R., et al. (2016). Comparative environmental life-cycle analysis of concretes using biomass and coal fly ashes as partial cement replacement material. *Journal of Cleaner Production*, *112*(Part 4), 2221–2230.

User guidelines for waste and byproduct materials in pavement construction. (2016). [cited 2016 June 19, 2016]. Available from: http://www.fhwa.dot.gov/publications/research/infrastructure/structures/97148/cfa51.cfm.

Wang, S. W., & Hongwei, W. (2006). Environmental-benign utilisation of fly ash as low-cost adsorbents. *Journal of Hazardous Materials*, 482–501.

Xinkai, J., Tao, D., & Stencel, J. M. (2003). Enhancement of dry triboelectric separation of fly ash using seed particles. *Coal Preparation*, *23*(1/2), 67.

Zhu, Z., Wang, X., Dai, S., Huang, B., & He, Q. (2013). Fractional characteristics of coal fly ash for beneficial use. *ASCE Journal of Materials in Civil Engineering*, *25*(1), 63–69.

# Recovery, processing, and usage of wet-stored fly ash

# 14

*M.J. McCarthy**, *T. Robl*†, *L.J. Csetenyi**
*University of Dundee, Dundee, United Kingdom, †University of Kentucky, Lexington, KY, United States

## 14.1 Introduction

Recent figures indicate that 780 Mt of coal combustion residues are produced globally on an annual basis (Heidrich, Feuerborne, & Weir, 2013). Much of the fly ash from this is used beneficially; for example, utilization in the European Union was about 43% in 2010 (European Coal Combustion Products Association, 2016), which is comparable to levels in the United States of around 40%–50% over the last few years (American Coal Ash Association, 2016). Quantities of ash taken up in China, the largest producer, were high during the peak construction years, but they are now slowing. The surplus that cannot be used has to be managed, typically onsite by the generators themselves. Frequently the ash is stored wet, either in stockpiles or ponds (lagoons).

At the same time, power generation by coal is reducing due to environmental concerns and competition from other fuels, primarily natural gas, with renewables also playing a role. Indeed, the United Kingdom is likely to see its remaining coal-fired power stations taken out of service by 2025 (British Broadcasting Corporation, 2015), while there have been 200 closures (about 40%) across the United States over the last 5 years (Sierra Club, 2015). These have led to a reduction in local availability of standard-compliant fly ash.

The effects that fly ash has on concrete and its use in this application are well known (Concrete Society, 2011; Sear, 2001; Thomas, 2013). As pressure mounts for reducing the carbon footprint of Portland cement (PC) concrete, fly ash as a pozzolana and supplementary cementitious material is likely to play an increasingly important role.

The drop in geographic density of coal power plants, which are the sources of fly ash, is increasing its delivery costs and changing its pricing and cost structure. These disruptions in supply are already creating changes in the fly ash market, with continued increases in the seaborne trade of fly ash likely (Duve, 2015). The recovery of stockpile and ponded ash is also expected to become more attractive (Groppo & Robl, 2001; McCarthy, Jones, Zheng, Robl, & Groppo, 2013).

It is estimated in the United Kingdom that levels of up to 50 Mt of stockpile material are available in ash fields (Carroll, 2015), while it has been noted in the United States that there are 1425 wet-storage ponds and landfills in 37 states (Cooper, 2015),

**Coal Combustion Products (CCP's).** **http://dx.doi.org/10.1016/B978-0-08-100945-1.00014-9**

and as much as a billion tonnes of stored ash. It is probable that a combination of imported and recovered ash will be needed in some regions to meet future demand.

The Authors have worked with stockpile and ponded ash at power plants over the past 30 years. These have been located throughout the United Kingdom, in parts of the Eastern United States (Kentucky, Alabama, Tennessee, West Virginia, Ohio, New York, Florida, Georgia, and North and South Carolina), and more recently in China. With this background, we can safely state that each ash deposit is unique and would need a tailored approach to recover the resource efficiently. Nevertheless, there are generalities that can still be drawn.

This chapter is concerned with the characterization and recovery of stockpile and ponded ash, specifically the effects of wet storage, its influence on reactivity, and possible options for using fly ash as a product of beneficiation or directly in wet form.

## 14.2 Storage of fly ash

Fly ash is commonly recovered by electrostatic precipitators; however, smaller plants may use mechanical devices such as baghouses (Khambeker & Barnum, 2012; Sear, 2001). On its collection and removal, fly ash is generally treated in one of the following ways (American Coal Ash Association, 2003; Sear, 2001), depending on the handling system and application requirements:

*Dry handling*. This is typical for ash that is to be sold for use in concrete. Dry ash is mainly kept in silos or other large-volume containers. Much of it is then transported by powder tanker, but some may also be bagged for use in smaller quantities.

*Moistened or conditioned fly ash*. The fly ash is combined with relatively low levels of water (typically 10%–20% by mass) which reduces dusting. Examples of use in this form include fill or grout; the material may also be stored in stockpiles. Many power plants in the United States have or will be converted to dry handling and ash conditioning systems.

*Slurried fly ash*. This involves the combination of ash with significant quantities of water (solids-to-water ratios by mass of about 10%–20% (Sear, 2001)). The ash is pumped along pipelines to ponds, where it will naturally settle. This can continue until these areas fill up. It has been a common handling/storage method for many years, as it is simple, dustless, and energy efficient. However, the ash dam failure at the Kingston Power plant in Tennessee in 2008, along with concerns about groundwater contamination, have brought pressure to end this practice in the United States.

*Combined systems*. A common practice at some plants has been to dredge ponds when full, stack the ash to drain, and then transfer it to a stockpile. In many cases, this is a more expedient option than trying to expand a pond. The ash is likely to be different from that conditioned and stored directly at the power plant, as it has been effectively washed.

There is no prohibition in international standards for the use of fly ash recovered from stockpiles or ponds. However, both the United States and European standards cover the moisture condition of fly ash when it is used in concrete. This is given in terms of a limit on the moisture content of fly ash [e.g., 3.0% in ASTM C618 (American Society for Testing and Materials, 2015)], or else reference to drying as a method of processing before use [EN 450-1 (British Standards Institution, 2012)]. These seem likely to relate to handling issues, rather than potential effects on performance.

## 14.3 Wet-storage effects on fly ash

### *14.3.1 Stockpile vs. ponded ash*

At least when broadly considered, stockpile and ponded ash have different properties. Conditioned and stockpile ash may be relatively homogeneous, but they are often found to have agglomerated, at least to some degree, which can affect their performance when used in concrete. The agglomerates show varying degrees of induration and may be cemented by sulfate or carbonate deposition, or by self-cementing or pozzolanic processes, including the formation of silicate gel-like materials. The presence of higher levels of free lime in the fly ash tends to increase these effects (McCarthy, Tittle, & Dhir, 1999).

All fly ashes have some level of soluble salts that may include alkali-chlorides, nitrates, or sulfates. If not washed from the ash, these will most likely contribute to the formation of agglomerates. Undoubtedly, the compaction of the ash in stockpiles also plays an important role.

Ash is typically moved to ponds in a dilute slurry. Since many older ponds did not have liners, the washing processes may continue over a longer period of time as rainwater percolates through the ash substrate. As the ash flows into the pond, it sorts and stratifies, resulting in a heterogeneous body of material. Overcoming this heterogeneity and producing a consistent material is a challenge for the recovery of ash from ponds.

The storage of fly ash in an excess of water has been found to give similar effects to those at lower moisture levels, with agglomeration occurring (McCarthy, Tittle, & Dhir, 1998). However, with high water levels, the development of cementing structures can be affected and there may be dispersion, although the presence of sulfate-based products has been noted. It appears that the loss of fine particles (through agglomeration) and chemical changes to particle surfaces may affect the reactivity potential of the material (McCarthy et al., 1998). Variations have been observed between some UK and US pond ashes; further work is needed to examine this, but it may be due to compositional differences between ashes and local storage conditions.

The codisposal of scrubber materials also has an impact on ash agglomeration. In a recent study of a large ash pond in China (Duvallet, Robl, Henke, Zhou, & Harris, 2016), it was found that even a small amount of codisposed gypsum ($Ca_2SO_4 \cdot 2H_2O$) resulted in higher levels of sulfate in the ponded ash, as well as particle sizes that were much coarser compared to dry fly ash collected from the plant.

## 14.3.2 Case studies: Stockpile ash

*Geotechnical*. Early research on wet-stored fly ash mainly related to its use as fill, where compaction characteristics and the development of strength properties were of interest. With the recognition of fly ash recovery potential, these effects have received increasing attention, since they may influence the material's use in other applications.

In a paper from the 1960s, an early example of the effects of combining water with fly ash was noted during a survey of storage areas in northwestern England, where hardening had occurred (Raymond, 1961). Laboratory tests quantified property development in moist compacted ash, and it was suggested that the reaction was pozzolanic, initiated by free lime present in the ash. It was later found (Raask, 1982) that with limited water in fly ash compacts, the precipitation of gypsum, ettringite ($Ca_6Al_2(SO_4)_3(OH)_{12}{\cdot}26H_2O$, aka AFt), and calcium silicate hydrates may occur, giving a cementing structure. The water present and its passage through the material were considered important with regard to the resulting bond strength.

In fill applications, it appears that a combination of effects occur with the addition of water to fly ash (Clarke, 1992; Sear, 2001). Initially with compaction, there are cohesive forces in the material. Thereafter, strength develops with sulfate-based products forming; in the longer term, there are potential enhancements in this with pozzolanic reactions (in the presence of sufficient free lime).

*Cement and concrete*. Early tests (Dhir, Jones, Munday, & Hubbard, 1985) (see Table 14.1) examining fly ash for use in concrete indicated that material with low moisture contents (up to 6.0%) tended to be coarse, with high loss-on-ignition (LOI) and water requirements, and reduced reactivity. However, the influence of the moisture condition/storage on these was not considered. Research (Yasuda, Niimura, Iizawa, & Shimada, 1991) using short-term wet storage (3 months) found small changes in the above properties and compliance with the relevant national standard, suggesting potential for use in concrete. Other tests on wet ash made during the study gave some loss in mortar strengths (compared to newly generated ash) after

**Table 14.1** **Selected fly ash properties from early UK study (Dhir et al., 1985)**

| Source | PFA ref no. | Moisture content (%) | LOI (%) | Fineness (%)[a] | Water requirement (%) | Pozzolanic activity index (%) |
|---|---|---|---|---|---|---|
| South West | P13[b] | 6.0[c] | 13.1[c] | 19.5[c] | 97[c] | 74[c] |
|  | P14 | 0.2 | 5.3 | 17.6[c] | 94 | 88 |
| Midland | P22[b] | 5.0[c] | 9.3[c] | 30.8[c] | 103[c] | 64[c] |
|  | P24 | 0.1 | 3.7 | 16.5[c] | 93 | 84[c] |
| Scotland | P31 | 1.3[c] | 4.2 | 33.7[c] | 98[c] | 72[c] |

[a] Residue on 45-μm sieve.
[b] Conditioned fly ash.
[c] Exceeds particular standard limit.

7 years of storage. In the development of artificially agglomerated high-calcium [Class C to ASTM C618 (American Society for Testing and Materials, 2015)] moistened fly ash to replace cement and aggregate (Kilgour, 1991), reaction products including ettringite, monosulfate,[1] and strätlingite ($Ca_2Al_2(SiO_2)(OH)_{10}{\cdot}2.5(H_2O)$) were found. Micronized fly ash from the agglomerated product (with $\approx$30% >45 μm by laser particle size analysis) gave reductions in 28-day compressive strengths compared to dry ash produced at the power plant, when it was used as a cement component in concrete.

Research (McCarthy et al., 1999) investigating wet-stored fly ash at a range of moisture levels (also covering those found in stockpiles; between 1% and 40% by mass of fly ash) and its potential as a cement component, confirmed several of the above findings and identified a number of effects. The fly ashes were siliceous [Class F to ASTM C618 (American Society for Testing and Materials, 2015)] with total CaO < 5.0% [and free lime contents ranging from <0.1% to 0.9%, using the BS EN 451-1 (British Standards Institution, 1994) test method]. With the addition of water and sealed storage in the laboratory (20°C), fly ash particles agglomerated, as shown in Fig. 14.1, with most changes tending to occur during the initial 6 months of storage.

Agglomeration was generally greatest at moisture contents of 10%–20%, with lower levels (1%) appearing to give insufficient water for reaction and higher levels (40%) causing dispersion. The effects of added moisture tended to occur more rapidly and to a greater degree when the free lime content of fly ash was higher (see Fig. 14.1).

LOI was found to increase slightly with time, moisture level and free lime content. For example, LOI increases of up to 1.0% were obtained by 6 months for the materials/moisture condition shown in Fig. 14.1. Thermogravimetric analysis data suggests that this reflects combined water. Other work on externally stored ash has also detected carbonation from atmospheric carbon dioxide. The water requirement increased as reactivity reduced with greater effects for high free lime ash. As with some of the work described above, the presence of gypsum and bassanite ($2Ca_2SO_4{\cdot}H_2O$) that formed during storage and pretest treatment was noted, while ettringite and strätlingite occurred in some high free lime ash. The effects of wet-storage on fly ash morphology compared to dry material are also illustrated in the scanning electron microscope (SEM) images shown in Fig. 14.2 (McCarthy et al., 1998; Dhir, McCarthy, & Tittle, 1999).

### 14.3.3 Case studies: Fly ash in ponds

Several studies have been carried out to investigate the recoverability of fly ash stored in ponds (Groppo & Robl, 2001; McCarthy et al., 2013; Robl, Groppo, Jackura, & Tapp, 2006; Robl, Groppo, Rathbone, Marrs, & Jewell, 2008) and considered methods for sampling and mapping material in these areas (Jewell, Robl, & Groppo, 2005; Tyra, Groppo, Robl, & Minster, 2003). The equipment shown in Fig. 14.3 was

---

[1] Or AFm—a family of minerals that, like AFt, accept substantial elemental substitution and have variable composition. An example of an end member is Kuzelite $Ca_4Al_2(OH)_{12}(SO_4){\cdot}6(H_2O)$.

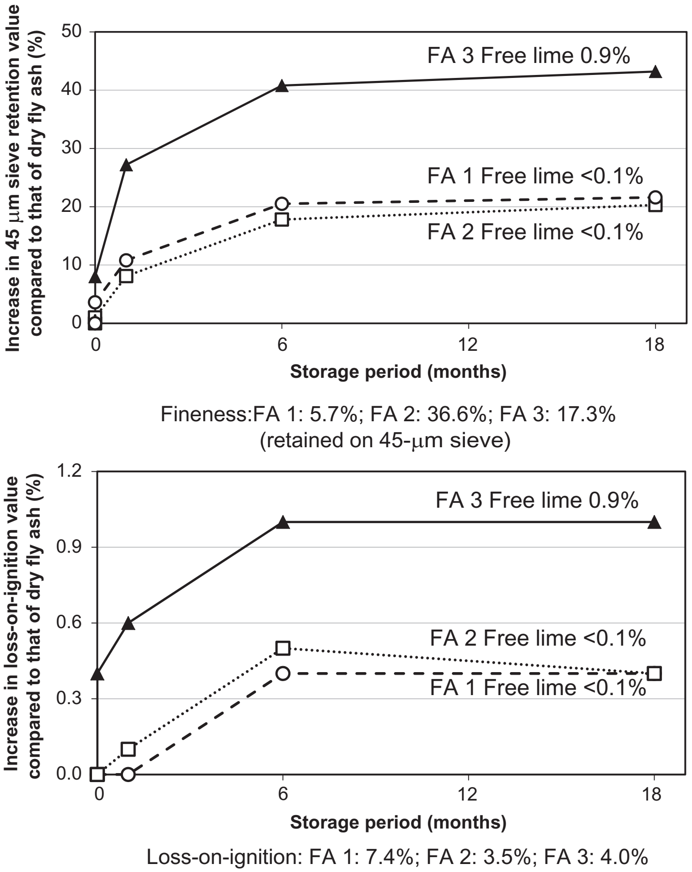

Fineness:FA 1: 5.7%; FA 2: 36.6%; FA 3: 17.3%
(retained on 45-μm sieve)

Loss-on-ignition: FA 1: 7.4%; FA 2: 3.5%; FA 3: 4.0%

**Fig. 14.1** Effect of wet-storage period on changes in fineness *(upper)* and LOI *(lower)* of fly ash (laboratory-stored in sealed bags, 20°C, moisture content 10%).

developed for obtaining material samples and comprises an amphibious vehicle with drilling and vibracoring equipment. Site investigations have enabled material distribution and an understanding of sedimentation behavior to be established.

A detailed survey of a pond at Kentucky Utilities Ghent power plant, following 20 years of service, found that of the 13 cores taken (~124 m of core and 381 samples), nearly 90% of the material was <150 μm, with average particle sizes between 13 and 99 μm. These were influenced by sample location relative to the pond inlet and their depth. The majority of carbon was in the coarse fraction of ash. The LOI values for the <150 μm fraction were between 2.4% and 4.6%.

Oxide analysis data corresponding to the different sample colors are shown in Table 14.2. The ash was siliceous (Class F), with the sum of the main oxides ($SiO_2 + Al_2O_3 + Fe_2O_3$) > 70% and CaO < 5.1%. The main components detected were quartz, aluminosilicate glass, hematite, magnetite, anhydrite, and mullite.

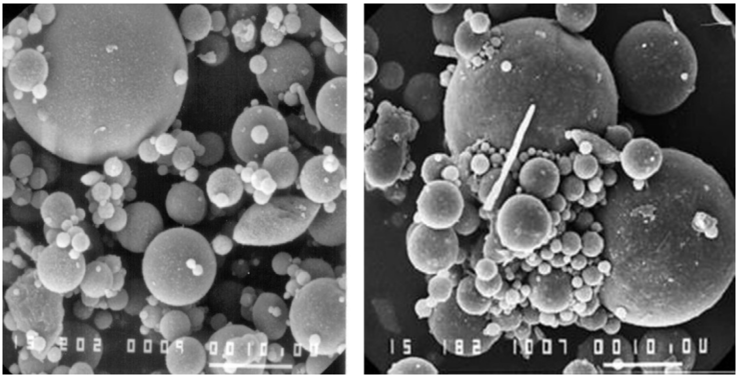

**Fig. 14.2** Scanning electron microscope images of dry- *(left)* and wet-stored *(right)* fly ash (FA 2 in Fig. 14.1; laboratory-stored in sealed bags, 20°C, moisture content 10%, 18 months) (McCarthy et al., 1998; Dhir et al., 1999).

Petrographic analysis indicated an abundance of smooth glassy spheres in the <150 μm material. It was estimated that ~1.6 Mt of <10 μm fly ash was available from the pond, with 1.4 Mt of coarse carbon also present (Jewell et al., 2005).

Processing circuitry for ash recovery was also conducted on the ash pond. Processes that were tested included two levels of screening, teeter bed and lamellae classifiers, and froth flotation and thickening (Fig. 14.4). The cross-flow lamellae

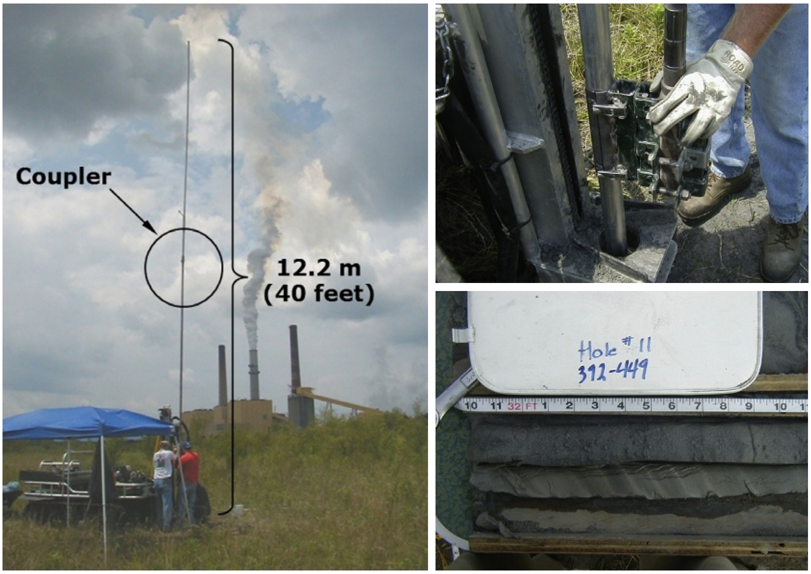

**Fig. 14.3** Sampling vehicle and vibracoring unit used in US ponds.

**Table 14.2** **XRF data corresponding to pond-stored fly ash color (Jewell et al., 2005)**

| Chemical composition (%) | Color | | | |
|---|---|---|---|---|
| | **Brown** | **Tan** | **Dark gray** | **Light gray** |
| $SiO_2$ | 40.85 | 51.13 | 53.97 | 53.27 |
| $Al_2O_3$ | 18.68 | 27.23 | 26.73 | 27.41 |
| $Fe_2O_3$ | 21.80 | 7.27 | 5.08 | 4.84 |
| CaO | 5.05 | 1.61 | 1.35 | 1.30 |
| MgO | 1.02 | 0.84 | 1.02 | 1.02 |
| $Na_2O$ | 0.54 | 0.46 | 0.26 | 0.35 |
| $K_2O$ | 2.45 | 1.81 | 2.47 | 2.65 |
| $P_2O_5$ | 0.23 | 0.26 | 0.20 | 0.21 |
| $TiO_2$ | 1.11 | 1.91 | 1.77 | 1.76 |
| $SO_3$ | 0.80 | <0.01 | 0.02 | <0.01 |
| LOI | 3.7 | 1.8 | 7.2 | 2.6 |
| Total ($SiO_2$, $Al_2O_3$, $Fe_2O_3$) (%) | 81.33 | 85.63 | 85.78 | 85.52 |

classifier was further developed (Robl & Groppo, 2011) and a commercial-scale unit was demonstrated in 2015.

Data from tests investigating ash in a UK pond are given in Table 14.3 (McCarthy et al., 2013). As shown, a range of properties were found, which had greater variability than similar tests on stockpile ash (from another plant). The main oxides were typical of those for UK fly ashes, while chloride present may correspond to the use of seawater to wet the

**Fig. 14.4** Field demonstration circuitry for recovery of ash from a pond in Northern Kentucky. Flotation cells were housed in the trailer.

**Table 14.3 Characteristics of recovered fly ashes from UK pond and stockpile sites (McCarthy et al., 2013)**

| Fly ash[a] characteristics | | Storage area | |
|---|---|---|---|
| **Storage type (No. of samples)** | | **Pond (34)** | **Stockpile (45)** |
| LOI (%) | | 3.8–20.2 (8.2) | 11.2–25.4 (15.3) |
| Particle size distribution, µm | $d_{10}$ | 3.2–14.3 (6.2) | 3.7–7.1 (4.9) |
| | $d_{50}$ | 13.4–100.5 (43.7) | 27.4–43.6 (34.8) |
| | $d_{90}$ | 54.1–521.5 (153.0) | 96.5–208.5 (127.5) |
| 45 µm ret. (%) | | 12.0–61.9 (39.8) | 31.1–42.3 (36.7) |
| **Chemical composition (%)** | | | |
| CaO | | 2.0–4.3 (2.7) | 1.2–3.5 (2.2) |
| $SiO_2$ | | 40.0–52.5 (47.4) | 35.8–45.8 (40.4) |
| $Al_2O_3$ | | 24.3–31.4 (28.5) | 19.5–23.6 (21.5) |
| $Fe_2O_3$ | | 3.3–6.8 (4.9) | 5.3–8.5 (6.7) |
| MgO | | 1.1–2.8 (1.6) | 0.7–1.5 (1.2) |
| $TiO_2$ | | 1.2–1.6 (1.4) | 1.0–1.7 (1.1) |
| $K_2O$ | | 0.7–1.6 (1.1) | 1.7–3.1 (2.6) |
| $Na_2O$ | | 0.3–3.8 (1.1) | 0.3–2.0 (0.6) |
| $P_2O_5$ | | 0.5–1.5 (0.9) | 0.5–0.8 (0.6) |
| $Cl^-$ | | 0.4–6.4 (1.8) | 0.0–3.0 (0.3) |
| $SO_3$ | | 0.2–1.2 (0.6) | 0.2–1.8 (0.7) |
| **Main mineral composition[b] (%)** | | | |
| Quartz | | 3.0–13.9 (8.3) | 2.4–4.7 (3.2) |
| Mullite | | 13.9–32.3 (22.3) | 5.0–7.9 (6.5) |
| Noncrystalline[c] content | | 47.3–72.3 (59.1) | 60.7–72.6 (67.2) |

[a] Results given as range (mean).
[b] For stockpile ash, results are from nine measurements.
[c] By difference. *Note*: This does not necessarily equal the pozzolanically reactive "glass" content.

fly ash or proximity to the coast. Examples of SEM images for the material are shown in Fig. 14.5, with the presence of agglomeration/reaction products noted. These are compared with ash recovered from a US pond, which highlights the need to consider storage areas individually in relation to recovery. Indeed, exploitation requires the geographic and stratigraphic distribution of the quality and nature of the resource to be assessed.

## 14.4 Processing of stockpile and ponded ash

### 14.4.1 Approaches

There do not appear to be any processing plants that are operating exclusively on stored fly ash. However, the thermal processing unit (SEFA's STAR process, discussed in this volume) operating at the Winyah power station in South Carolina is

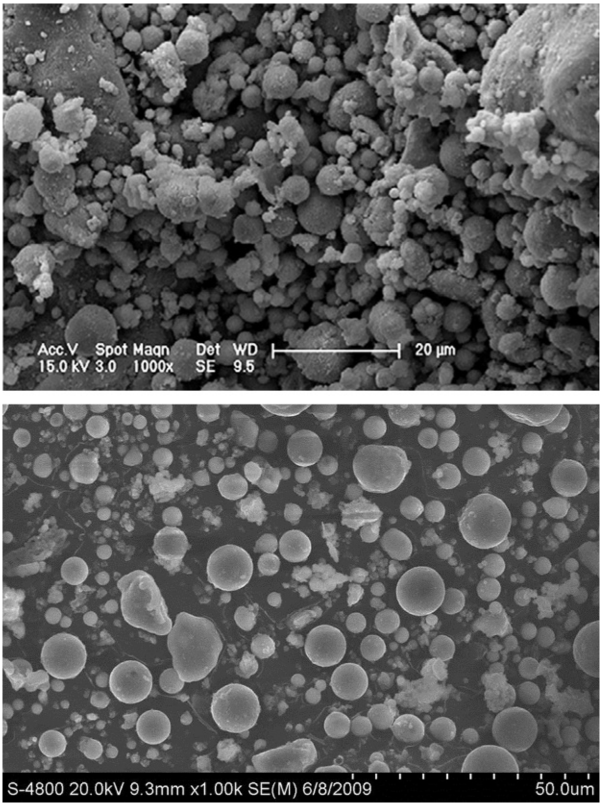

**Fig. 14.5** Scanning electron microscope images of fly ash recovered from a UK pond *(upper)* (McCarthy et al., 2013) and US pond *(lower)* showing differences in aggregation.

currently processing ponded ash along with fresh ash from the plant. A full-scale production unit is based at the Fiddler's Ferry power plant in the UK (RockTron process), but it is not currently in use (Carroll, 2015).

Strategies for the recovery of wet-stored fly ash for use in concrete are different from the processing of dry fly ash. Typically, these are single-process steps, such as air classification to increase fineness, or electrostatic separation to reduce LOI. The recovery of ash from a stockpile or pond is closer to a mining or quarry operation. The raw ash needs to be removed, slurried, and separated by particle size, then thickened and dried. If appropriate, steps may also be required for the separation of carbon and de-agglomeration.

There are two approaches that are used in ash recovery. The first involves traditional truck and shovel operations. Even if the ash is agglomerated, it can be readily recovered from stockpiles and ponds with a backhoe or front-end loader. For wet active ponds, a long-armed backhoe or a dredge is typically employed. Recent work has used a dredge to feed a classifier during a demonstration in Ohio. The dredge delivered a slurry, which ranged in solids content from essentially 0% up to 35%, averaging about 15%. The large variation in solids content was due to the relatively small size of ash ponds, which required frequent starts and stops. Nonetheless, the dredge proved capable of delivering large volumes of ash cheaply and efficiently.

### 14.4.2 Preliminary stages

Slurrying of fly ash for processing at water-to-solids ratios of up to 15% is used to provide the medium for particle separation; it also enables washing and de-agglomeration of the material (Smalley, Michael, & Watt, 2006). Thereafter, screening can be carried out to remove coarser particles, including unburned or unwanted components, such as vegetation (Mensa-Biney & Marten, 2007; Robl et al., 2006), prior to using other processes.

Typical screen sizes for preliminary treatment (i.e., "trash screens") are of the order of several millimeters (i.e., 3/8″ to 1/2″). A ~10 mm screen (Robl et al., 2006) was adopted in a field demonstration unit. For laboratory and bench/pilot-scale work, 5 mm (McCarthy et al., 2013) and 3.3 mm (Mensa-Biney & Marten, 2007) screens have been used. In these cases, further particle separation by various means was carried out to reduce the range of particle sizes before applying other treatment processes, such as carbon removal.

### 14.4.3 Froth flotation

If required by the ash composition, froth flotation is a well-established technique that can be effective for separating carbon char from fly ash. Froth flotation is used for processing many types of ores, including cleaning coal fines (Harris & Wheelock, 2008). The process is based on differences in the "wettability" of materials. Nonwettable materials are more susceptible to bubble attachment, the mechanism of separation, which is achieved by the addition of a frothing agent and injection of air (Eisele & Kawatra, 2002).

Unburned carbon in fly ash is mainly present as partially oxidized coke particles (Drzymala, Gorke, & Wheelock, 2005). The oxidation reduces their wettability compared to, for example, that of fresh coal. Thus, an oily collector is often added for ash separation. The collector partitions to the surface of the char, providing an improved interface for bubble attachment. Work at the University of Kentucky since the early 1990s (Groppo & Brooks, 1995) has also used a surfactant to help disperse the oily collector and improve the rate of flotation.

Flotation release analyses (to examine fly ash suitability for the process) using a batch flotation cell indicated differences in carbon reduction/yield for fly ashes from the same and different sources (Robl et al., 2008). For most ashes, this approach achieves both good separation and high product yields. However, the process is less effective with some ashes (about one in five of those tested). Fly ash from co-combustion of coal and petroleum coke, along with the presence of unusually fine carbon particles (e.g., abundant carbon char-ash agglomerated particles) can greatly diminish the effectiveness of this approach.

The efficacy of carbon separation is influenced by various factors, including the carbon concentration, dose and type of reagents, and flotation procedure (Drzymala et al., 2005; Eisele & Kawatra, 2002; Harris & Wheelock, 2008; Walker & Wheelock, 2006). Flotation systems adopted with fly ash include mechanical (Robl et al., 2008) and pneumatic (Smalley et al., 2006) devices, as well as columns (Li et al., 2015), which have been trialed or used at field- or industrial-scale levels. Of these, mechanical flotation (e.g., Denver Cells) has received the widest coverage in the literature. Mechanical flotation uses an impeller and can include multiple cells; it has been effective in reducing the LOI of fly ash to low levels. A laboratory study using both column and mechanical flotation systems (McCarthy et al., 2013) found the latter achieved greater carbon reductions. Agglomeration with wet storage may also affect carbon particle distribution in the material, potentially influencing separation (McCarthy et al., 2013).

### 14.4.4 Screening

Depending on the characteristics of the ash, wet vibratory repulping screens can be a reasonable choice in size separation. Due to its shape, fly ash causes the excessive blinding of woven screens, known as the "egg crate" effect. Thus slotted screens are best employed, which are made from steel wedge wire or polymers such as urethane. Screening provides a sharp cut that is only dependent on particle size. However, the proportion of screen openings decreases with their size, reducing separation efficiency and throughput. Although both polymer and wedge wire as fine as 45 μm are available, the lower practical range for screening ash is probably between 75 and 150 μm.

### 14.4.5 Hydraulic classification

Hydraulic classification involves the separation of particles by differential settling. The forces involved are best described by Stokes' Law, which states that:

$$V = 2\left(\rho_{\mathrm{p}} - \rho_{\mathrm{f}}\right)/9\mu \cdot gR^2$$

where $V$ is the velocity of the particle, $\rho_{\mathrm{p}}$ is the density of the particle, $\rho_{\mathrm{f}}$ is the density of the fluid, $\mu$ is the dynamic or kinematic viscosity of the fluid, $g$ is the gravitational constant, and $R$ is the diameter of the particles. Stokes' Law assumes laminar flow and round particles with no particle-particle interactions.

Using this formula, 1-, 10-, and 45-μm-diameter particles with a density of 2.4 g $\mathrm{cm}^{-1}$ will have fall velocities of 0.005, 0.5, and 9.2 cm $\mathrm{min}^{-1}$, respectively. Otherwise, the 45-μm particle will drop at a rate that is more than 2000 times faster than the 1-μm particle and 20 times faster than the 10-μm particle. To drop 1 cm, it will take the 1-μm particle 3.6 hours, the 10-μm particle about 2 minutes, and the 45-μm particle 6 seconds. This suggests the removal of 45 μm and larger particles should be relatively straightforward for hydraulic classification, as they will literally drop like "rocks," and for the most part, this applies to many ponded fly ashes.

In general, there are two approaches for hydraulic classifiers. One uses an upward flow of water to separate particles. The flow will elutriate particles with a lower fall velocity than that of the flow. These are sometimes referred to as teetered bed classifiers; a good example of this is the McLanahan Hydrosizer (Fig. 14.6). Work at the University of Kentucky has focused on the use of inclined plates or lamellae in a crossflow classifier, which was developed specifically for fly ash (Robl & Groppo, 2011). The lamellae provide a surface for the particles to settle and flow downward as a densified slurry. The spacing of the lamellae has an effect on the cut point of the slurry. For a lamellae spacing of 10 cm, 10-μm particles would require a retention time of 20 minutes, to ensure they all have time to settle (i.e., drop 10 cm).

**Fig. 14.6** McLanahan Hydrosizer (*upper left*), SWECO hydrocyclone (*upper right*), and Louisville Dryer Corp. rotary gas unit (*lower*).

Of course in practice, none of the above is true. Many ash particles are not round, they have a range of densities, and there is considerable particle-particle interaction. The latter results in hindered movement and blanket settling. In addition, the smallest ash particles have such low mass that they don't follow Stokes' Law, and effects such as Brownian motion become factors. These particles partition with water and not the other solids.

Unlike most minerals produced by crushing and milling, fly ash is formed from a molten state and has a low surface charge. This, plus storage in fresh water with low conductivity and near neutral pH, produces a surface with low zeta ($\zeta$) potential. As a result, there is a strong tendency for the ash to form flocs, which can significantly affect separation efficiency. It has been found that sulfonate, carboxylate, and melamine-based dispersants (Robl & Groppo, 2003) are useful in breaking down flocs and improving efficiency at a higher slurry density. Their adoption has its benefits in concrete applications, as these chemicals are also used as high-range water reducers.

Another approach to hydraulic classification is the hydrocyclone, which looks like a miniature pneumatic cyclone. The slurry is spun around an axis, sweeping large particles to the outside wall. Thus centrifugal forces are added to that of gravity to achieve the separation. Given that the density contrast between the particle and fluid is much smaller in water and cyclones only provide seconds of retention time, hydrocyclones that operate on silt-size particles have small diameters, with lower throughput compared to their pneumatic relatives. For this reason, multiple hydrocyclones are often grouped together, for example the SWECO company offers both manifold and packed vessel configurations that group up to 300 individual cyclones (Fig. 14.6). Although hydrocyclones cannot make separations at as small a particle diameter as hydraulic classifiers, they are relatively compact, inexpensive, and reliable; they are worth consideration when planning a pond recovery circuit.

### 14.4.6 Magnetic separation and other methods

Another process that has gained interest over time is the recovery of magnetite from ash ponds. Magnetite is a useful product with an attractive value; it is surprising that there has not been more success with it. There may be two reasons for this: first, although the efficiency of the magnetic separating and materials recovery is high, the yield is low, as typically there is a very small percentage of magnetite in ash. Thus a lot of ash must be processed for a modest amount of product. Second, the product itself is not pure magnetite ($Fe_3O_4$) and often contains fused particles with silicate ash and internal impurities caused by ionic substitution (e.g., $Mg^{2+}$ for $Fe^{2+}$). A recent study on recovered magnetite at a power plant in Kentucky combined spiral concentration with magnetic separation. The spiral concentrator provides a more concentrated feed to the magnet and therefore increases process efficiency (Groppo & Honaker, 2009).

### *14.4.7 Thickening and drying*

Particle separation by hydraulic methods generally results in a product with a high water content that requires further processing. There are several choices for this including conventional thickeners/clarifiers that use a round tank, therefore providing settling time. The solids concentrate at the bottom of the tank, where rakes move them to a central discharge point and they are pumped out, while clarified water discharges from the top of the tank. Another approach is adopted in deep cone thickeners, which use a tall vessel that narrows towards the bottom. Here the weight of the solids helps in the dewatering, as do stirrers. Both approaches work well and can be assisted by the addition of flocculating chemicals.

It has been found that classified fly ash slurries with solids densities over 60% can still be readily pumped. Further water reduction can be achieved with vacuum filtration, or if space and time permits, simple stacking and draining, a potentially lower-cost approach. Moisture levels of 20%–25% are readily achievable with these approaches.

Standards and conventional handling equipment would indicate that drying is necessary. In the United States the current price of natural gas makes attractive the selection of a proven rotary direct-fired natural gas dryer, like that manufactured by the Louisville Dryer Company (Fig. 14.6). In some climates, solar dryers may be of use. In addition, indirectly heated dryers that use waste heat are available; however, these trade fuel savings for increased complexity and capital costs.

### *14.4.8 Beneficiated ash in mortar and concrete*

A number of studies have been carried out (e.g., McCarthy, Jones, Zheng, & Dhir, 2008; Robl et al., 2008) to investigate the use of processed wet-stored fly ash in different applications to evaluate performance, with both UK and US ash. Work investigating the behavior of fly ash recovered from a UK stockpile has shown that finer fractions gave water-reducing properties. Similarly, they met requirements for reactivity according to the relevant standard. Satisfactory performance has also been found for materials used in precast concrete components (McCarthy et al., 2008). However, with some tests on concrete there appeared to be little benefit to strength with finer fractions compared to directly recovered material.

The initial approach taken in the United States was to produce a highly beneficiated ash that could offer superior performance. The strategy was that the added cost of beneficiation would have to be offset by a premium price. Using a pilot-scale lamellae classifier, as described above, ponded ash samples from the Ghent and Kingston power plants in Kentucky and Tennessee were produced. The ashes from these ponds appeared to have little or no agglomeration and were not difficult to beneficiate. Dispersants were used for both materials; the median ($d_{50}$) particle sizes were $\sim$6 μm for samples from the Ghent ash pond and $\sim$8 μm for samples from the Kingston ash pond. This translated to product yields of 50%–75%.

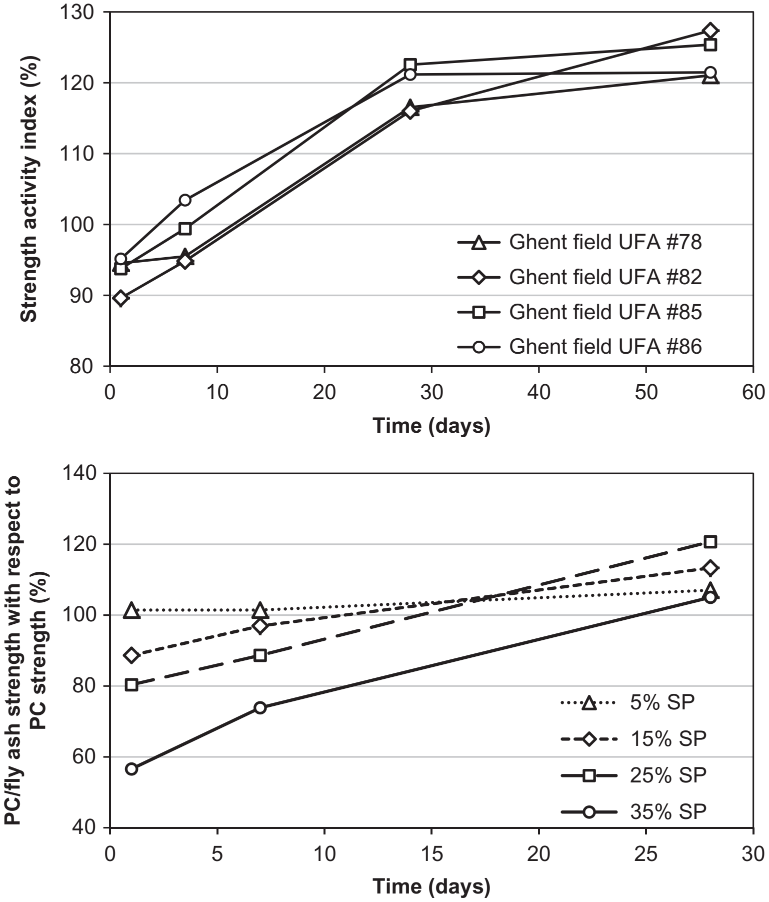

**Fig. 14.7** Relative strength gain of mortar *(upper)* and concrete *(lower)* for beneficiated ponded ash from Ghent power plant.

Strength activity index testing of these samples (by ASTM methods) achieved levels that exceeded 100% within the first week and reached as high as 120% in 28 days (Fig. 14.7). Similar testing of concrete (at equal slump) achieved equivalent strengths to PC controls at around 14 days with 25% fly ash in cement and 28 days when the level was increased to 35%.

Durability testing also indicates good performance. For example, data from rapid chloride tests (American Society of Testing and Materials, 2014) on concrete (w/c ratio 0.45) with 20 and 40% levels of the Ghent material in cement, gave 420 and 150 coulombs (very low), respectively. This was in comparison to 1200 coulombs (low) for 20% of conventional fly ash and 2420 coulombs (moderate) for the control PC concrete.

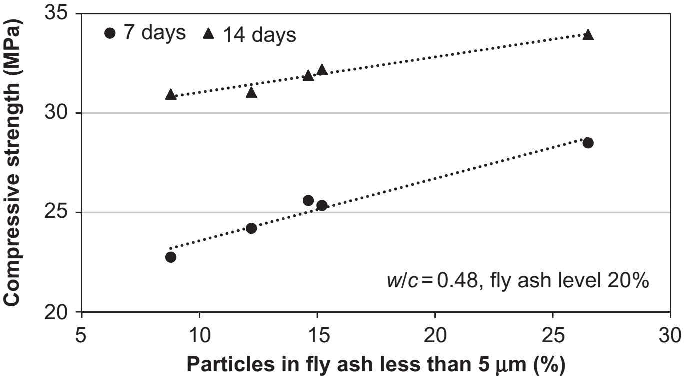

**Fig. 14.8** Relationship between sub 5 μm content in fly ash and 7- and 14-day mortar strengths.

To date, the work on stored ash suggests the restoration of gradation is important in maintaining a high level of activity in the recovered ash. This is illustrated in Fig. 14.8, which shows the relationship between the sub 5 μm size fraction of five different stockpile and ponded ash samples and early mortar strength (7 and 14 days). These were prepared at constant water content (w/c ratio 0.48) and with 20% fly ash in the cement. The strength improvement with fine particle content is evident from the figure.

## 14.5 Direct use of stockpile ash in concrete

Stockpile fly ash may be comparatively homogeneous, and although it can undergo changes affecting performance, it may have the potential for recovery and direct use in concrete. Several projects have been carried out to examine this (Dhir, McCarthy, & Halliday, 2004; Dhir, McCarthy, Tittle, & Kii, 2000; McCarthy, Dhir, Halliday, & Wibowo, 2006; McCarthy, Tittle, & Dhir, 2000; McCarthy, Tittle, Dhir, & Kii, 2001; McCarthy et al., 1999); these considered siliceous (Class F) fly ashes with total CaO mainly < 5.0% (and free lime contents ranging from <0.1% to 0.9%) and included laboratory studies and full-scale concrete production trials.

A reasonable approach for using wet fly ash from stockpiles in concrete is to take account of the moisture condition during the batching stage, much like wet aggregates. This involves:

**(i)** Measuring the moisture content of fly ash
**(ii)** Taking the water content of concrete as that batched plus that in the fly ash
**(iii)** Adjusting the fly ash content to allow for water present in the material

The moisture in fly ash is therefore assumed to contribute to the mix water in concrete. This method was followed in the work described below, which considers laboratory-stored ash, unless noted otherwise.

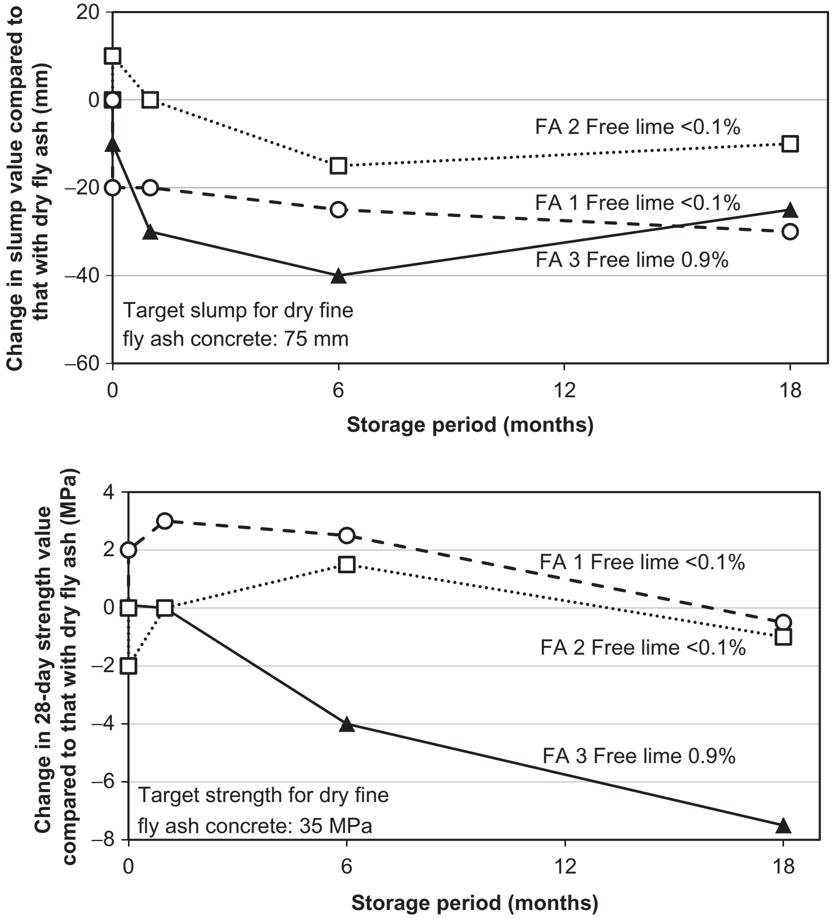

Fineness: FA 1: 5.7%; FA 2: 36.6%; FA 3: 17.3% (retained on 45-µm sieve)

Loss-on-ignition: FA 1: 7.4%; FA 2: 3.5%; FA 3: 4.0%

Concrete: *w*/*c* ratio 0.5; 30% fly ash level

**Fig. 14.9** Effect of wet-storage period on changes in workability (slump; *upper*) and 28-day strength *(lower)* of concrete with fly ash (laboratory stored in sealed bags, 20°C, moisture content 10%).

### 14.5.1 Fresh properties

Measurements of workability (in terms of slump) on concretes of equal w/c ratio (0.5), with 30% ash and no admixture are shown in Fig. 14.9. In general, there was a gradual reduction in slump with wet-stored fly ash that was moistened at 10%. The greatest effects tended to occur during the period of storage up to about 6 months. Similar type behavior was noted for ashes of different fineness, with little influence of moisture contents (10%–20%). As indicated, more noticeable effects were found for high free lime ash (McCarthy et al., 2000).

While the action of the concrete mixer may break down some agglomerates, the results appear to relate to the effects that wet storage has on some of the water-reducing properties of ash and increased water requirement due to rough particle surfaces. This may be expected to influence superplasticizing admixture requirements with regard to controlling workability. The bleeding of the concrete (relevant to the material's stability) tended to reduce with wet-storage period and for high free lime ash.

### 14.5.2 Engineering properties

Results from tests for compressive (standard cube) strength on the above concretes are shown in Fig. 14.9. For material, wet stored (moistened at 10%) for up to 6 months only slight effects on concrete strength up to 28 days were noted. In general, reductions tended to increase with storage period and for longer-term strength. While the fineness and moisture content of the fly ash did not noticeably influence behavior, the effects tended to be greater for high free lime ash in concrete, with reductions in strength of 7.5 MPa after 18 months' storage (McCarthy et al., 2000).

Engineering properties of wet-stored ash (free lime $< 0.1\%$) concrete, tested at 28 days, that cover flexural strength, elastic modulus, drying shrinkage, and creep are shown in Table 14.4 (McCarthy et al., 2001). These were compared at equal slump (75 mm) and 28-day compressive strength (35 MPa), requiring small changes in w/c ratio/superplasticizer dose between wet-stored and dry fly ash concretes. The results suggest that there was little difference in properties between them.

**Table 14.4 Engineering properties of dry- and wet-stored fly ash concretes (laboratory-stored in sealed bags, 20°C, moisture content 10%) (McCarthy et al., 2001)**

| | (i) Flexural strength (MPa) | | (ii) Elastic modulus (GPa) | | (iii) Drying shrinkage ($\% \times 10^{-3}$) | | (iv) Creep coefficient | |
|---|---|---|---|---|---|---|---|---|
| **FA** | **Dry** | **6 m**[a] | **Dry** | **6 m**[a] | **Dry** | **6 m**[a] | **Dry** | **6 m**[a] |
| FA 4 | 3.4 | 3.7 | 22.5 | 21.5 | 123 | 104 | 1.15 | 1.22 |
| FA 5 | 3.6 | 3.5 | 22.5 | 21.0 | 114 | 88 | 1.40 | 1.30 |

[a] Fly ash storage period (months).
FA 4: fineness 4.8% (retained on 45-μm sieve), loss-on-ignition 5.2%.
FA 5: fineness 29.6% (retained on 45-μm sieve), loss-on-ignition 3.7%.
Concrete: slump 75 mm; equal 28-day strength, 35 MPa; 30% fly ash level.
Specimens water cured (20°C) to 28 days, except (iii).
(i) BS 1881: Part 118—third-point loading.
(ii) BS 1881: Part 121—cyclic loading to $0.33 \times f_{cu,28}$.
(iii) After removing from molds, 2 days curing in water at 20°C, then in air at 20°C/55% RH for 48 weeks.
(iv) Sustained load $0.5 \times f_{cu,28}$ for 24 weeks.

### 14.5.3 Durability

Measurements of water/air transport rates into concrete can provide an indication of potential durability. Data from tests (Dhir et al., 2000) for water absorption (initial surface absorption at 10 minutes, ISA-10) (British Standards Institution, 1996) and intrinsic (air) permeability (Dhir, Hewlett, & Chan, 1989) in concretes compared at equal slump (75 mm) and strength (35 and 60 MPa), are shown in Fig. 14.10. The

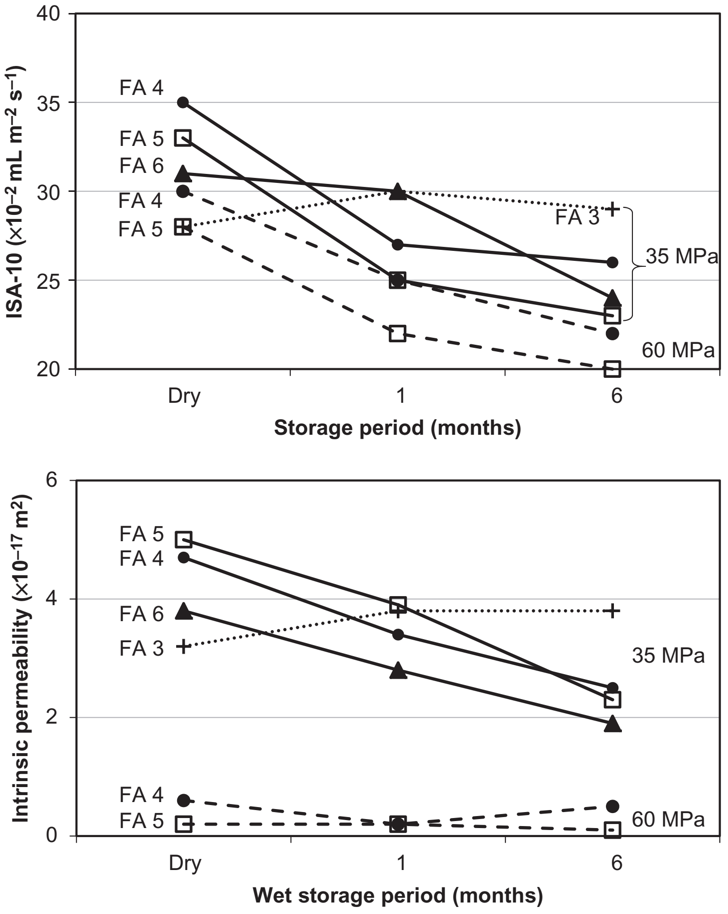

Fineness: FA 4: 4.8%; FA 6: 14.6%; FA 5: 29.6%; FA 3: 17.3% (retained on 45-μm sieve)

Loss-on-ignition: FA 4: 5.2%; FA 6: 7.5%; FA 5: 3.7%; FA 3: 4.0%

Concrete: slump 75 mm; equal 28-day strength; 30% fly ash level

**Fig. 14.10** Water absorption *(upper)* and intrinsic (air) permeability *(lower)* of dry- and wet-stored fly ash concrete (free lime of fly ash <0.1%, except FA 3, which is 0.9%) (laboratory stored in sealed bags, 20°C, moisture content 10%) (Dhir et al., 2000).

results indicate similar or slightly improved (lower) values for these properties with wet storage.

The effects of conditioned/stockpile ash on most aspects of concrete durability have been investigated, including carbonation, chloride diffusion, freeze-thaw scaling, and abrasion (Dhir et al., 2000). In general, these also indicate that for dry and wet-stored fly ash compared at equal slump/28-day strength, similar properties are obtained. Limited testing for alkali-aggregate reaction in concrete suggests the use of moistened ash also has little influence on this process compared to that with dry ash (McCarthy et al., 2006). Further investigation under normal exposure conditions is needed to confirm these findings.

### *14.5.4 Trials with stockpile fly ash in concrete*

In general the effects of stockpile fly ash on concrete are relatively small compared to dry material and can be dealt with by adjustments to the concrete mix. However, moistening of the material may introduce certain effects that could affect handling during concrete production. Trials (Dhir et al., 2004) using site-stored ash have been carried out to investigate these at both ready-mix and precast concrete production plants. The trials mainly involved (i) consideration of the handling and storage plant, (ii) identification of suitable concrete mixes or products, (iii) laboratory support work to establish mix proportions, (iv) the trial where production of concrete was carried out at the site, and (v) testing of samples taken.

In some cases, it was possible to feed wet-stored ash through the hopper and transport system at these plants. Where this was carried out, aggregate hoppers were used to store the material (generally introduced in small quantities, shortly before use), which was then transferred to the concrete mixer. Laboratory tests on wet ash using a model aggregate hopper suggest that certain factors, including the quantity stored, the period of time in the hopper before discharge, and external vibration at the outlet, may need to be considered for the material. Changes were made to wet ash concrete mixes to match the properties of those with dry fly ash, which normally involved small reductions in w/c ratio and adjustments to superplasticizing admixture dose.

Overall, the examples demonstrate that the fresh and hardened properties of concrete containing stockpile fly ash could be controlled by adjustments to the mix in order to match those achieved by dry fly ash concretes. Clearly, the economic viability associated with these types of changes to concrete and practical issues associated with handling would require evaluation for specific materials and plants used. As noted above, the drying of fly ash could be an option for recovery of handling properties.

## 14.6 Observations and practical issues

Efforts to date leave little doubt that stockpile and ponded ash have great potential as concrete additions or supplementary cementing materials. When processed to meet current standards, these materials can perform adequately, and with some additional beneficiation, they may be capable of improved performance.

It is important to recognize that these materials have been subjected to hydration, weathering, and in some cases sedimentological processes, resulting in changes to particle-size gradation and a level of particle agglomeration for some deposits. The last of these seems more prominent for ash codisposed with scrubber material, conditioned/stockpile ash, ash with high free lime content (see Section 14.3), or stored in salt or brackish water ponds. Ash in fresh water appears less susceptible to these changes.

After examining many samples and cases of stored ash in the United Kingdom, the United States, and China, it is safe to conclude that each ash deposit is different and will require site-specific testing and evaluation to determine recoverability and processing strategies. In this sense, stored ash is more like a mineral deposit than an industrial by-product.

A number of ash ponds in the eastern United States have been studied. They show little or no agglomeration and have been amenable to high levels of beneficiation. Test data to date indicate that the restoration of gradation to levels approaching or exceeding the original ash is important to the performance of recovered ash.

There is a wide variety of processing techniques available for ash recovery and to separate unwanted components such as carbon, classify the ash particles by size and thicken the beneficiated ash, and dry the product. Following initial screening, froth flotation has been demonstrated to achieve significant reductions in carbon and magnetite has been recovered with spiral and magnetic separators. Hydraulic classification has been demonstrated to be effective for producing a range of particle sizes, including high-performance ultrafine fractions at high levels of recovery. These processes may be aided by the proper selection of dispersants or flocculating agents to improve classification efficiency and dewatering.

The existing mineral processing industry is more than adequate to meet the needs of processing and recovery of stored ash. Companies, in some cases with more than a century of experience, are capable of providing individual components as well as complete processing systems. Other options such as combustion or drying, followed by dry processing methods, may also play a role in recovery.

The direct use of conditioned/stockpile fly ash in concrete has been shown to have promise, although some losses in workability—which tended to increase with storage time—were found. Reductions were also noted for compressive strength, particularly with prolonged storage and at later test ages. In comparing concrete mixes with wet ash at equal slump/28-day strength to those with dry ash (e.g., changes in w/c ratio, superplasticizing admixture dose), various aspects of performance were generally similar. Most properties tended to become poorer if fly ash had a high free lime content, hence this type of material may not be suitable for wet storage and recovery. The economics associated with modifying concretes and requirements for handling are other issues that would need to be considered with regard to the adoption of conditioned/stockpile ash.

## References

American Coal Ash Association. (2003). *Fly ash facts for highway engineers*. Washington, DC: Federal Highway Administration [74 pp.].

American Coal Ash Association. (2016). Fly ash production and use with percent. https://www.acaa-usa.org/Portals/9/Files/PDFs/2015-Survey_Results_Charts.pdf Accessed 24.10.16.

American Society for Testing and Materials. (2015). *C618. Standard specification for coal fly ash and raw or calcined natural pozzolan for use in concrete*. West Conshohocken, PA: American Society for Testing and Materials.

American Society of Testing and Materials. (2014). *C1202. Rapid chloride penetrability test*. West Conshohocken, PA: American Society for Testing and Materials.

British Broadcasting Corporation. (2015). UK's coal plants to be phased out in 10 years. www.bbc.co.uk/news/business-34851718.

British Standards Institution. (1996). *BS 1881-208. Testing concrete. Recommendations for the determination of the initial surface absorption of concrete*. London, UK: British Standards Institution.

British Standards Institution. (1994). *BS EN 451-1. Method of testing fly ash. Determination of free calcium oxide content*. London, UK: British Standards Institution.

British Standards Institution. (2012). *BS EN 450-1. Fly ash for concrete: Definition, specifications and conformity criteria*. London, UK: British Standards Institution.

Carroll, R. A. (2015). Coal combustion products in the UK and the potential of stockpile ash. In *World of Coal Ash international conference, 2015, Nashville, TN, USA*. www.flyash.info.

Clarke, B. (1992). Structural fill. In R. K. Dhir & M. R. Jones (Eds.), *The use of PFA on construction: Proceedings of a National Seminar, Dundee, February 1992* (pp. 21–32). Dundee: University of Dundee.

Concrete Society. (2011). *Cementitious materials: The effect of GGBS, fly ash, silica fume and limestone fines on the properties of concrete*. Technical Report 74 Camberley, Surrey, UK: The Concrete Society.

Cooper, S. (2015). Recycling and reusing coal ash. *World Coal*. http://www.worldcoal.com/.

Dhir, R. K., Hewlett, P. C., & Chan, Y. N. (1989). Near surface characteristics and durability of concrete—Intrinsic permeability. *Magazine of Concrete Research*, *41*(147), 87–97.

Dhir, R. K., Jones, M. R., Munday, J. G. L., & Hubbard, F. H. (1985). Physical characterisation of UK pulverized-fuel ash for use in concrete. *Magazine of Concrete Research*, *37*(131), 75–87.

Dhir, R. K., McCarthy, M. J., & Halliday, J. E. (2004). Demonstration project using conditioned PFA as a cement component in concrete. Technical Report CTU/2504, Department of Trade and Industry (70 pp.).

Dhir, R. K., McCarthy, M. J., & Tittle, P. A. J. (1999). Developing applications for conditioned and lagoon PFA in concrete construction. *Concrete*, *33*(10), 34–38.

Dhir, R. K., McCarthy, M. J., Tittle, P. A. J., & Kii, K. H. (2000). Use of conditioned PFA in concrete: Strength development and critical durability. Concrete Technology Unit, University of Dundee, Report: CTU/1500 (Project Number 041033.003) (131 pp.).

Drzymala, J., Gorke, J. T., & Wheelock, T. D. (2005). A flotation collector for the separation of unburned carbon from fly ash. *Coal Preparation*, *25*, 67–80.

Duvallet, T. Y., Robl, T. L., Henke, K. R., Zhou, Y., & Harris, D. (2016). Coal ash by-product from Shanxi Province, China, for the production of Portland–calcium sulfoaluminate. *Coal Combustion and Gasification Products*, *8*, 1–7.

Duve, T. (2015). Seaborne trades of fly ash and global trends of cementitious products. In *Ashtrans conference 2015*. http://ashtrans.eu/presentations%202015.html Accessed 04.04.16.

Eisele, T. C., & Kawatra, S. K. (2002). Use of froth flotation to remove unburned carbon from fly ash. *Mineral Processing and Extractive Metallurgy Review*, *23*, 1–10.

European Coal Combustion Products Association. (2016). Utilisation. http://www.ecoba.com/ecobaccputil.html Accessed 24.10.16.

Groppo, J. G., & Brooks, S. M. (1995). Method of removing carbon from fly ash. U.S. Patent 5,456,363.

Groppo, J. G., & Honaker, R. (2009). Economic recovery of fly ash-derived magnetics and evaluation for coal cleaning. In *World of coal ash*. www.flyash.info.

Groppo, J. G., & Robl, T. L. (2001). Ashes to energy: The Coleman station project. In *International fly ash symposium, Lexington, Kentucky, USA* (pp. 205–215).

Harris, T., & Wheelock, T. D. (2008). Process conditions for the separation of carbon from fly ash by froth flotation. *International Journal of Coal Preparation and Utilization*, *28*, 133–152.

Heidrich, C., Feuerborne, H. -J., & Weir, A. (2013). Coal combustion products: A global perspective. In *World of Coal Ash conference, 2013, Lexington, KY* (p. 17).

Jewell, R., Robl, T. L., & Groppo, J. G. (2005). Advanced multi-product coal utilization by-product processing plant. Technical Progress Report for the Period July 31, 2003–December 31, 2004. U.S. Department of Energy Cooperative Agreement No. DE-FC26-03NT410781.

Khambeker, J., & Barnum, R. A. (2012). Fly ash handling: Challenges and solutions. *Power Engineering*, *116*(2), 10.

Kilgour, C. L. (1991). Use of agglomerated and micronized fly ash in Portland cement concrete. In *American Coal Ash Association, symposium 9, Paper 14* [pp. 1–14].

Li, G., Deng, L., Liu, J., Cao, Y., Zhang, H., & Ran, J. (2015). A new technique for removing unburned carbon from coal fly ash at an industrial scale. *International Journal of Coal Preparation and Utilization*, *35*, 273–279.

McCarthy, M. J., Dhir, R. K., Halliday, J. E., & Wibowo, A. (2006). Role of PFA quality and conditioning in minimising damaging ASR in concrete. *Magazine of Concrete Research*, *58*(1), 49–61.

McCarthy, M. J., Jones, M. R., Zheng, L., & Dhir, R. K. (2008). New approach to fly ash processing and applications to minimise wastage to landfill. Report CTU/4068 (144 pp.).

McCarthy, M. J., Jones, M. R., Zheng, L., Robl, T. L., & Groppo, J. G. (2013). Characterizing long-term wet-stored fly ash following carbon and particle size separation. *Fuel Journal*, *111*, 430.

McCarthy, M. J., Tittle, P. A. J., & Dhir, R. K. (1998). Lagoon PFA: Feasibility for use as a binder in concrete. *Materials and Structures*, *31*, 699–706.

McCarthy, M. J., Tittle, P. A. J., & Dhir, R. K. (1999). Characterisation of conditioned PFA for use as a cement component in concrete. *Magazine of Concrete Research*, *51*(3), 191–206.

McCarthy, M. J., Tittle, P. A. J., & Dhir, R. K. (2000). Influences of conditioned PFA as a cement component in concrete. *Magazine of Concrete Research*, *52*(5), 329–343.

McCarthy, M. J., Tittle, P. A. J., Dhir, R. K., & Kii, K. H. (2001). Mix proportioning and engineering properties of conditioned PFA concrete. *Cement and Concrete Research*, *31*, 321–326.

Mensa-Biney, R. K., & Marten, E. H. (2007). An integrated approach to processing coal combustion ash and organic bio-solids. In *World of coal ash 2007, Covington, OH*. www.flyash.info.

Raask, E. (1982). Pulverized fuel ash constituents and surface characteristics in concrete applications. In J. G. Cabrera & A. R. Cursens (Eds.), *The use of PFA in concrete: International symposium: Vol. 1* (pp. 5–16). Leeds: University of Leeds.

Raymond, S. (1961). Pulverized fuel ash as embankment material. *Proceedings of the Institution of Civil Engineers*, *19*, 515–536.

Robl, T. L., & Groppo, J. G. (2003). Technology and methodology for the production of high quality polymer filler and super-pozzolan from fly ash. U.S. Patent 6,533,848.

Robl, T. L., & Groppo, J. G. (2011). Method for hydraulically separating carbon and classifying coal combustion ash. U.S. Patent 7,963,398.

Robl, T. L., Groppo, J. G., Jackura, A., & Tapp, K. (2006). Field testing of an advanced multi-product coal by-product processing plant at Kentucky Utilities Ghent power plant. In *Ashtech, 2006, Birmingham* [pp. 1–7].

Robl, T. L., Groppo, J. G., Rathbone, R., Marrs, B., & Jewell, R. (2008). Pilot demonstration of technology for the production of high value materials from the ultra-fine (PM 2.5) fraction of coal combustion ash. Final Report, DOE. Contract No. DE-FC26-03NT41726.

Sear, L. K. A. (2001). *The properties and use of coal fly ash: A valuable industrial by-product*. London, UK: Thomas Telford.

Sierra Club. (2015). United States phases out 200th coal plant as momentum for renewable energy grows. Press release July 2015.

Smalley, N., Michael, P., & Watt, J. H. (2006). Implementation of a Rocktron PFA beneficiation process plant. In *Ashtech, 2006, Birmingham* [pp. 1–7].

Thomas, M. D. A. (2013). *Supplementary materials in concrete*. Boca Raton, FL: Taylor & Francis [210 pp.].

Tyra, M. A., Groppo, J. G., Robl, T. L., & Minster, T. (2003). Using digital mapping techniques to evaluate beneficiation potential in a coal ash pond. *International Journal of Coal Geology*, *54*, 261–268.

Walker, A., & Wheelock, T. D. (2006). Separation of carbon from fly ash using froth flotation. *Coal Preparation*, *26*, 235–250.

Yasuda, M., Niimura, T., Iizawa, M., & Shimada, Y. (1991). Possibility of using wet-stored ash as material for concrete. In *American Coal Ash Association, symposium 9, Paper 18* [pp. 1–15].

# Fly ash refinement and extraction of useful compounds

# 15

*H.W. Nugteren*
Delft University of Technology, Delft, The Netherlands

## 15.1 Quality improvement

This chapter summarizes the options for chemically treating and refining fly ash to improve its quality. The reader is also referred to an in-depth treatise on fly ash quality, with respect to both technical and environmental quality aspects, that was produced by Nugteren (2008, 2010). This addresses quality requirements, quality consistency, and methods and technologies for quality improvements.

The main factors controlling both the environmental and technical quality of coal fly ash are fuel composition and combustion technology. Using high-quality coal may be a solution to assure standards in ash quality, depending on the combustion technology used, as shown below. However, economic constraints are the driving forces towards the usage of low-quality coals. Further, a growing awareness for the necessity of sustainable development and reduction of $CO_2$-emissions has led to an increase in co-combustion of various types of wastes and refuse-derived biomass and cultivated biomass. Fuel additions such as “petcoke” (residue from oil refineries) and certain types of biomass may alter the physical and chemical characteristics of fly ash. However, this will not mean that the quality as produced has to be taken for granted. Coal preparation and cleaning has been used for some time to increase energy recovery and decrease sulfur content; the smart blending of coals and other fuels is applied to maintain ash quality. A good example of such precombustion practices is the KEMA Trace Model (Meij, 1997).

At present, most coal combustion takes place in powder coal-injection furnaces and the implementation of low-$NO_x$ technology has decreased operation temperatures and, therefore, influenced the fly ash quality by lowering the degree of vitrification. Lower temperatures also have effects on the amount of unburned carbon particles in the ash. Tuning combustion conditions through online LOI and $NO_x$ measurements can be seen as syn-combustion practice to maintain the consistency of ash quality. $NO_x$ emissions are also controlled by adding ammonia or ammonia-based reagents to the fuel, which then may result in ammonia contaminated fly ash. Ammonia vapors at construction sites are considered to be a serious health hazard for workers, therefore ammonia has to be removed before the ashes can be used in most applications. Pressurized fluidized bed combustion may be an important technique in the future to overcome many of the problems as stated above, especially when high rates of co-combustion of various residues and biomass are required (Nugteren, 2010).

**Coal Combustion Products (CCP's).** http://dx.doi.org/10.1016/B978-0-08-100945-1.00015-0

Ash quality requirements can only be met when the power industry operates within narrow limits. Through the development of new techniques to improve fly ash quality, the industry can operate within a wider window, both for operational conditions and fuel properties, and still produce ash of quality within required specifications for use.

The challenge is to control fly ash quality after it has been separated from the flue gas, that is by postcombustion technologies. This will (Nugteren, 2010):

- Guarantee continuation of the traditional fly ash market in the building industry
- Open routes for and facilitate higher value applications (e.g., zeolites, geopolymers, mineral fillers, soil amendments, absorbents, fire resistant materials, waste stabilization, etc.)
- Facilitate bulk unbound applications such as site preparation, dikes, railway tracks, and functional landfilling
- Give power plants the freedom to apply different combustion technologies, such as fluidized bed combustion
- Make it possible to use coals that are less expensive and are of lower quality ("battle coal")
- Possibly allow the use of higher quantities of co-combustion of an even wider variety of secondary fuels, such as biomass, petcokes, and RDF (refuse derived fuel).

### 15.1.1 Improving technical quality

The *technical quality* of ash refers to how the ash performs in a given application; it is mainly reflected by the chemical and physical properties of the ash. The technical quality is generally considered good if the ash performs equal or better than other commercially available materials used for the same application (Nugteren, 2008). Technical quality requirements for cement, concrete, and other building materials type applications are laid down in international and local standards such as BS (British), ASTM (American), and EN (European). The most important ones are listed in Nugteren (2008) and in Chapter 4.

The aim is to improve the technical quality in such a way that after the treatment, the ash can be used in certain applications for which it disqualifies without treatment. In general it deals with applications in *bound form*. Most quality improvement technologies in this category are based on physical separation technologies as used in mineral processing. Examples are the removal of unburned carbon by applying carbon burnout, electrostatic separation, classification and blending, and flotation. Magnetic separation for the removal of iron minerals and density separations for the recovery of cenospheres also belong to this category.

For the removal of ammonia from fly ash produced when ammonia reagent were added to the fuel, chemical methods can also be used. Wetting fly ash with a bit of water, while carefully dosing lime, is claimed to be suitable to recover 100% of the ash and to reuse the ammonia in the plant (Gasiorowski & Hrach, 2000; Bittner, Gasiorowski, & Hrach, 2001).

### 15.1.2 Improving environmental quality

The *environmental quality* refers to the impact ash has on the natural environment. Information on the environmental quality is obtained by standardized (leaching) tests believed to be valid for the prediction of the future behavior of a combustion residue under natural conditions. Many different test methods have been developed in different countries; for example, the TCLP (toxicity characteristic leaching procedure) in the US, EN12457 in the EU, BS tests in the UK, DIN tests in Germany, and NEN tests in the Netherlands (Nugteren, 2008).

The results of such tests are compared to environmental requirements set down in directives. The environmental quality dictates the type of application allowed for the ash. It depends largely on the form in which the ash is exposed to the natural conditions. If the ash is land filled or used as a granular material, the behavior under direct leaching becomes the key property to be considered. But if used in a bound or molded form, leaching will generally be reduced, and diffusion leaching of the bound products or monoliths becomes the main exposure route. The interaction between ash and the natural environment (i.e., the environmental quality) depends largely on the concentrations of trace elements and their chemical speciation, although particle size distribution and major element concentrations (Ca and S) also have an influence (Nugteren, 2010).

After having carried out extensive mass balance studies in various power plants in the Netherlands, Meij, van der Kooij, van der Sluys, Siepman, and van der Sloot (1983) introduced the relative enrichment factor (RE) for elements in combustion residues. The *RE* factor governs the partition of elements among different combustion by-products: bottom ash, fly ash, gypsum, wastewater, fly dust, and flue gas. The *RE* for an element *X* is defined as

$$REx = \frac{[X]_{ash}}{[X]_{coal}} \frac{\text{ash content of coal}}{100}.$$

If $RE = 1$ for an element for a particular combustion residue, it means that the enrichment of that element in that residue is equal to the coal to ash ratio. Referring to fly ash with 10% ash in coal, such an element will have a 10 times higher concentration in the fly ash than in coal. If $RE < 1$, the element is depleted; with $RE > 1$, the element is enriched. On the basis of *RE* factors for fly ash, the elements were divided into three classes:

- Class I elements with $RE \approx 1$: Mostly nonvolatile elements that compose the clean, glassy spherical particles of fly ash belong to this group: Al, Ca, K, Mg, Si, and Ti.
- Class II elements with $RE > 1$: Volatile elements that condense within the installation on the ash particles: As, Ba, Cd, Cr, Cu, Mo, Na, Ni, P, Pb, Sb, V, and Zn.
- Class III elements with $RE < 1$: Highly volatile elements that (partly) escape from the installation and report preferentially to flue gases: B, Br, Cl, Hg, N, S, and Se.

Elements of Class II are mostly found on the outer shell of fly ash particles, and the small quantity of elements of Class III present in fly ash is almost exclusively located on the surface of the particles. Meij and Krijt (1993) estimated the relative amounts present on the surface of fly ash particles for a number of elements. In accordance with this classification of the elements, they found that 50–90% of most environmentally hazardous elements, such as Se, B, Mo, As, Sb, Cd, Zn, Cu, and V, are located on the outer surface of fly ash particles. As the surface of ash particles is highly reactive, leaching of these elements will readily occur.

In 2007 the Dutch government published a new Soil Quality Decree (SQD, 2007, Besluit Bodemkwaliteit), replacing the former decree on building materials (BMD). The rules were simplified in the Soil Quality Regulation (annex to the SQD). Emission values are directly measured on the applied materials with tests NEN 7373 and NEN 7375. Three categories are distinguished and for each of them, there is a single list of emission threshold values:

- Molded building materials (or bound forms); emissions to be tested with NEN 7375
- Unmolded building materials (or unbound forms); emissions to be tested with NEN 7373
- ICM (isolation, control, and monitoring) building materials; also to be tested with NEN 7373. For ICM materials, the emission requirements are less strict than for unmolded materials that are applied freely.

The aim of technologies for ash treatments to improve the environmental quality (leaching characteristics) is to change the ash properties in such a way that the treated ash can be used in *unbound form* for bulk applications, such as base material for roads and building ground elevation works. Simply said, these methods can be characterized as ash-washing technologies with or without the usage of extracting agents and other auxiliary systems. An overview of ash washing research and technology up to 2008 can be found in Reijnders (2005) and Cox, Nugteren, and Janssen-Jurkovičová (2008).

The main drawback of the use of wet forced leaching is the transfer of polluting elements from a large, yet fairly manageable solid into a still larger, highly mobile liquid, as high L/S ratios are required for obtaining residues that comply with leaching standards. The decontamination of the liquid streams becomes the main problem. In combination with the recovery of valuables from ashes, this could, however, still be a feasible technology, as higher extractant concentrations are used; decontamination of the liquids may be achieved simultaneously with the recovery processes of the targeted elements. In this respect the research done on the forced leaching may, in combination with hydrometallurgical principles, be a starting point in research for recovery of valuables from ash.

It is possible to remove a high percentage of trace elements from fly ash by extraction with water. Free lime (CaO) quickly dissolves and makes the pH move toward the Portlandite equilibrium at 12.5. This limits the Ca removal at given L/S ratio. Dissolution of anhydrite accounts for considerable sulfate removal and also adds to the Ca removal. The only elements of environmental concern that are extracted in water along with Ca and S are Mo and Se. By using a four step countercurrent washing procedure with an effective L/S of 9, the following removal was obtained: 12% Ca; 38% $SO_4^{2-}$; 32% Mo and 19% Se (Nugteren, Janssen-Jurkovícová, & Scarlett, 2001, 2002).

In the follow-up work (Nugteren et al., 2001, 2002), the selection criteria for extraction reagents were: (1) high extraction for the elements critical for passing the leaching requirements of the Dutch Building Materials Decree (BMD) and (2) low extraction of the major elements in the fly ash. Oxalate and citrate buffers, EDTA and ammonium and sodium carbonate solutions turned out to be the most promising reagents. With these reagents, extractions for sulfate and Mo up to 100% were obtained. Se was extracted up to 70% and extraction of Cr, Sb, and V was found between 10% and 20%. The dissolution of free lime also caused pH increase in the case of extraction with the buffers and EDTA, as the fly ash itself acted as a strong alkaline buffer. During this pH change, some of the already extracted elements may reprecipitate in a rather mobile form (As, Cr, Sb, Se, V); therefore strength of solution and reaction times are important parameters for a washing process.

When washing with water as a preextraction step, similar removal percentages could be obtained with much lower reagents concentrations. However, the overall extraction did not increase.

The washing of fly ash resulted in an improvement of the leaching behavior of the residues for Cr, Mo, Se, and $SO_4^{2-}$. However, Sb and V leaching increased. Compliance with the leaching requirements of the BMD could not be reached. This was probably caused by the reprecipitation of mobilized elements during washing. For Se and Sb, for which extremely low limit leaching values apply, the small amount present in the moisture left behind after filtration play a role as well. When washing with water is used as a pretreatment before extraction with the reagents, the leaching does not improve. The matrix of the ash particles seem to have been attacked too severely.

Su and Wang (2011) compared arsenic and selenium leaching from raw ash and water-washed ash and found that leaching was either increased or remained the same after washing with deionized water. They concluded that this was due to removal of the surface layers of the ash particles, but that the adsorption strength of As and Se species onto the surface was not affected by the washing.

Kashiwakura et al. (2009) reported the removal of 60%–80% of boron in a bench scale test from coal fly ashes using extraction in a 0.1 M HCl solution with an L/S ratio of 10 and only 10 min of extraction time. This turned out to be sufficient for the treated ash to leach boron below the Japanese regulatory limit.

In follow-up studies from the same research group, Kashiwakura et al. (2010, 2011) concentrated on the removal of arsenic and selenium. For this purpose, they used a sulfuric acid extraction liquid with an L/S ratio of 1 and 10 min extraction time in bench scale testing with fly ash samples of 60 kg. The liquid-solid separation was performed in a centrifuge (200 rpm), and the solids were rinsed with water at an L/S ratio of 2 to remove residual acids and then submitted to the regulatory tests. It was found that the pH should be maintained near 0 in order to ensure removal of arsenic as $H_3AsO_4$ and selenium as $H_2SeO_3$. If pH increased as leaching proceeds under the influence of dissolution of Ca-compounds, these species may be transferred into $H_2AsO_4^-$, $HAsO_4^{2-}$, and $HSeO_3^-$, which adsorb easily onto the surface of the ash particles. In the case of arsenic, the precipitation of $FeAsO_4$ if Fe(III) is freely available in the leaching solution may also play a role. When subsequently submitted to regulatory leaching tests, these species may readily be redissolved at alkaline pH. To ensure the complete removal of arsenic and selenium, the pH of the leaching solution must be kept below 0.2, which may be achieved by controlling the $H_2SO_4$ concentration in the solvent. In an extreme case, this leads to solvents with 2 M $H_2SO_4$. To the eluted acid solution remaining after centrifugation, caustic soda was added for neutralization. The resultant sludge containing the polluting elements was dried and fired and disposed in a designated landfill. It was reported that in general less than 10 kg of solid waste remained per ton of treated ash.

#### 15.1.2.1 Supercritical fluid extraction

Metal extraction using supercritical fluids was mainly tested on MSWI ashes (Kersch, Peretó Ortiz, Woerlee, & Witkamp, 2004) but can potentially be applied to coal combustion ashes as well. Successful extraction with supercritical $CO_2$ of most cation species can be achieved when the right chelating agents are used; however, extraction of anion species seems more difficult. In a study using a synthetic solid waste matrix, nearly 100% extraction of Zr, Hf, U, and Cd was achieved using Cyanex 272 as chelating agent and methanol as modifier (Ghoreishi, Hedayati, & Ansari, 2016). This may open perspectives for the recovery of valuable compounds from fly ash (Section 15.2).

#### 15.1.2.2 Other technologies

Treatment of acid and alkaline fly ashes with ferrous sulfate in a L/S ratio of 30 reduces the mobility of oxyanions of As, B, Cr, Mo, Se, and V between 20% and 90%; however, the mobility of some cations may be increased, notably for Ni and Sr (Bhattacharyya, Donahoe, & Patel, 2009).

## 15.2 Extraction of valuable compounds

Apart from physical separation technologies for the removal of certain components from ash (for example, cenospheres), chemical and metallurgical technologies can be used to concentrate certain elements from ash. Some of the methods listed under Section 15.1.2 can be transitional in the sense that both environmental quality improvement and recovery of the removed elements is beneficial (for example, extraction with selective ligands).

As such, metal extraction from fly ash can have two combined objectives, both increasing the feasibility of such processes: (1) the production of metals and (2) leaving behind a residue that has become more appropriate for construction purposes compared to the original fly ash. In this respect, not only must the economic viability of the intended processes be taken into account, but also their environmental impact. As there is a tendency for more and more internalization of external costs, it makes sense to compare total costs (production + external costs) for the alternatives to produce certain metals or components. Such external costs, whether expressed in single-issue indicators such as the carbon footprint or more complex damage-based or prevention-based indicators (ecocosts), must then be calculated for both routes of production; that is, the production from primary ores and from fly ash. The lowest total costs will at the long term be the most feasible. For example, certain rare earth metals produced from primary ores in China seem cheaper than produced from fly ash. However, when external costs are taken into account, this may not be the case. (Re) developing primary production from deposits in the western world will result in even higher production prices, in favor for developing processes for extraction from fly ash.

The main drivers for obtaining metals from fly ash are:

- waste management
- environmental issues
- scarcity of resources from primary ores, in technical, economic, or geopolitical sense
- growing demand for exotic and critical metals

With the rapid development of computing and communication technology, the demand for base metals, precious metals, and exotic metals has increased enormously during the first decades of the 21st century. As an illustration, data from the National Research Council (USA) and Intel shows the increasing complexity of computer chips over time. In the 1980s, only 12 out of the 92 naturally occurring elements were used for the production of computer chips, whereas this increased to 16 in the 1990s and 61 in the 2000s. This increase was mainly due to the use of transition metals and rare earth metals. Add to this the growing demand for special elements in displays (In, Sc), turbine engines (Re), wind turbines (Nd, Dy), high-performance alloys (Sc), photovoltaic cells (Ga, Ge), batteries (Li, Rare Earth Elements), and catalysis (platinum group elements), it becomes clear why the extraction of such elements has increased by factors between 2 and 10 over the last decades.

Most of those elements occur in nature only in low-grade ore deposits or as minor by-products from deposits mined for base metals. Due to the increase in demand, the production has shifted in recent times to even lower grades. Further, for REE the production is almost limited to a single country (China), although resources are fairly well distributed all over the globe. For other elements, such as Nb and Ta, the production depends significantly on illegal mining operations (Africa). Apart from generating geopolitical issues, such circumstances promote neither efficient recovery nor decent environmental protection measurements. As a result, this may lead to fast exhaustion of resources for some of the elements that are essential to the development of renewable energy systems; therefore governments and international institutions have determined lists of so-called critical materials or elements. There exist many definitions for critical materials, but all of them contain elements of supply security, essential function in products, difficulty of substituting, and difficulty of recycling (Peck, 2016). Materials are often plotted in a two-factor diagram, with the economic importance on one axis and the risk of supply shortages on the other axis. Materials scoring high in both factors are classified as critical materials.

The EU definition of critical materials (Pellegrini, 2014) followed this classification and resulted in a list of critical elements (i.e., Li, Be, Mg, Sc, Cr, Co, Ga, Ge, Y, Nb, In, Sb, W, Platinum Group Metals, and Rare Earth Elements) and nonelements (i.e., borates, magnesite, silicon metal, coking coal, fluorspar, natural graphite, and phosphate rock). More advanced and complicated schemes for the determination of the criticality of materials are available from the work of Graedel (Graedel et al., 2012; Graedel, Harper, Nasser, & Reck, 2013). Although there is no agreed global list of critical materials, the US Department of Energy published lists of critical materials for different countries (Bauer et al., 2010).

Many of the elements appearing in critical material lists are present in variable quantities in combustion residues and have been recorded to be extractable from them.

As such, coal fly ashes may serve as alternatives, so far not yet considered recourses for these elements. In view of enrichment in some particular ashes and the quantities available worldwide, production of critical materials from fly ash may even alleviate the global situation by transferring some of these materials away from those lists. Global markets, market prices, and actual security of supply makes it beneficial to invest in recovery technologies of specifically those critical materials from fly ashes. Moreover, some of the largest deposits in the world of a few critical elements, such as Sc, Ge, Ga, and others, are found associated with coal deposits (Gomes, Mayes, Rogerson, Stewart, & Burke, 2016; Dai et al., 2012; Seredin, 2012; Seredin & Dai, 2012; Seredin, Dai, Sun, & Chekryzhov, 2013) and may be of crucial importance for the development of renewable energy technologies, wind and photovoltaics, and electronics. Therefore coal technology for high-metal coals will still be needed in the future, eventually with combustion as an easy preconcentration technology, from which metals become the primary product and energy a by-product.

One of the most recent and most comprehensive literature studies on the recovery of metal values from coal fly ash was performed by Lucinda Tolhurst and is available from Lucid Insight (Tolhurst, 2014). This review report is based on more than 300 scientific papers, patents, and business releases and was complemented by interviews with 28 fly ash experts. The interest in the recovery of metal values from coal ash was supported by an analysis of ashes from different coal power stations, showing metal values worth over $40,000 per ton of ash at current metal prices in some cases, as shown in Fig. 15.1 (Tolhurst, 2015). The highest values are contributed by scandium and germanium, but dysprosium, aluminum, yttrium, neodymium, gallium, and titanium also show values of interest. It should be noted that except for scandium, the minimum concentration in the ashes is almost zero, and the commercial interest is restricted to exceptionally high concentrations in ashes from particular coal sources. In a recent study on the REE content of US fly ashes, Taggart, Hower, Dwyer, and Hsu-Kim (2016) also recognized the importance of evaluating the content of critical REEs compared to total REEs. The highest concentrations of almost 600 mg kg$^{-1}$ total REEs were found in ashes derived from Appalachian coals. Notably, around 35% of the REEs were critical REEs as recognized by the authors (Nd, Eu, Tb, Dy, Y, and Er), much higher than the 15% reported for primary ores from which these elements are currently extracted.

As is known from earlier work, shown previously and summarized in Cox et al. (2008), the most volatile trace elements will condense on the surface of fly ash particles during their formation. Therefore these elements become enriched in the finer fractions of the ash due to an enhanced surface-to-volume ratio for such fractions. A similar observation was found for REE in a fly ash from China (Joshi, 2013a, 2013b), in which the total content of REE was twice as high in the finest fraction ($<30$ μm) compared to the coarsest fraction ($>125$ μm). However, enrichment of REE in the finer fractions seems not to be a general phenomenon, as some authors do not find such enrichment (Scott, Deonarine, Kolker, Adams, & Holland, 2015). Similar fractionation was found between lighter and denser particles in fly ashes from Poland (Blissett, Smalley, & Rowson, 2013). Preferred concentrations of the elements of interest among different fly ash fractions offers the opportunity of applying simple pretreatment methods to reduce the amounts of materials for metallurgical processing and restrict the environmental impacts of such processing.

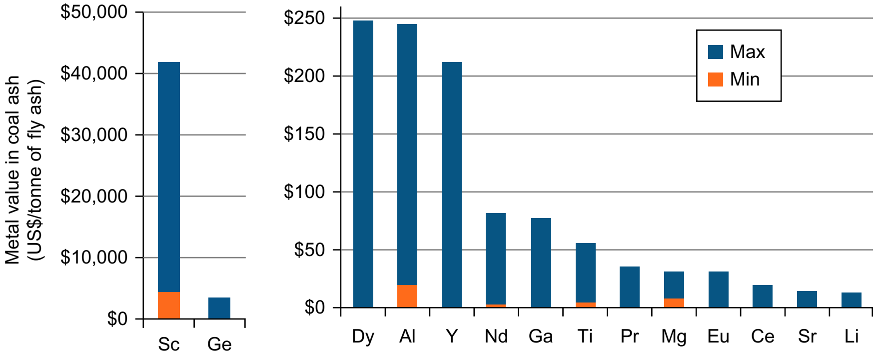

**Fig. 15.1** Valuation for selected metals based on concentrations in various fly ash samples (US$/ton fly ash). Metal prices date from Sep. 2014.
From Tolhurst, L. (2015). Commercial recovery of metals from coal ash. 2015 World of coal ash (WOCA) conference in Nasvhille, TN, 5–7 May 2015 (pdf available on http://www.flyash.info/); with data from Seredin, V. V., & Dai, S. (2012). Coal deposits as potential sources for lanthanides and yttrium. *International Journal of Coal Geology, 94*, 67–93; Medina, A., Gamero, P., Querol, X., Moreno, N., De Leon, B., Almanza, M., et al. (2010). Fly ash from a Mexican mineral coal 1: Mineralogical and chemical characterization. *Journal of Hazardous Materials, 181*, 82–90; Arroyo, F., Font, O., Fernández-Pereira, C., Querol, X., Juan, R., Ruiz, C., et al. (2009). Germanium recovery from gasification fly ash: Evaluation of end-products obtained by precipitation methods. *Journal of Hazardous Materials, 167*, 582–588, Arroyo, F., Font, O., Fernández-Pereira, C., Querol, X., Chimenos, J. P., & Zeegers, H. (2009). Germanium and gallium extraction from gasification fly ash: Optimisation for up-scaling a recovery process. World of coal ash conference, 2009 (pdf available on http://www.flyash.info/); Mardon, S. M., & Hower, J. C. (2004). Impact of coal properties on coal combustion by-product quality: Examples from a Kentucky power plant. *International Journal of Coal Geology, 59*, 153–169; Zhang, Y., Talbott, J. L., Wiedenmann, L., DeBarr, J., & Demir, I. (1997). Determination of germanium content in coal ash by wavelength-dispersive X-ray fluorescence spectrometry and inductively coupled plasma—mass spectrometry. In: Proceedings of the Denver X-ray conference, *Advances in X-ray Analysis, 41*, 879–891; Mayfield, D. B., & Lewis, A. S. (2013). Environmental review of coal ash as a resource for rare earth and strategic metals. World of coal ash conference 2013.

Determining the value of the elements present in coal ashes is one thing, but extracting them from the ashes is quite another. However, as we will soon show, the last decade has seen an increase in research in this area.

### 15.2.1 Production of aluminum from coal ash

The first activities regarding the production of aluminum from coal fly ash date from the 1950s, when the Eastern European countries suffered from a bauxite embargo during the Cold War. In 1953, small-scale industrial production started in Poland using a sinter process to produce alumina and Portland cement simultaneously (Grzymek, 1976).

In the 1970s and 1980s, recovery of aluminum from coal fly ash to compensate for a shortage of available bauxite ores was reconsidered. Direct acid leaching was proposed, as well as alkaline leaching flow sheets, sometimes combined with pretreatment by sintering. The drawback of these leaching processes is that only aluminum present in the amorphous phases is extractable. Fly ashes with a significant amount of mullite or other crystalline alumina-silicates (e.g., pyroxenes or feldspars) will have a low level of extractable alumina compared to the bulk alumina composition. Mullite may also form networks of tiny crystals on the surface of glassy fly ash spheres and even prevent the leaching liquids to come into contact with the amorphous core of such particles. Processes are described in various papers (Burnet, Murtha, & Dunker, 1984), and Cox (2008) gives an overview of the early literature.

After some decades without little further development because of no economic needs arising, in recent years there is an increasing interest from China. Yao, Xia, Sarker, and Chen (2014) gives an overview of available process options ranging from sinter processes (with lime, salt, soda and other agents), direct acid leaching (DAL) to chlorination processes (HiChlor process). High-aluminum fly ashes from Inner Mongolia that contain 40%–45% $Al_2O_3$ and in some cases up to 50% have been listed by the state as encouraged and preferential policy for alumina recovery. Alumina reserves from these coal deposits have been estimated to contain the equivalent of 3.2 times the proven bauxite resources of China. Since 2010, several industrial operations have started using different recovery technologies, together accounting for the production capacity of more than 5 million tonnes of alumina per year, as well as large amounts of by-products, such as calcium and sodium silicate, silica, and zeolites (Yao et al., 2014).

Alumina can be enriched in fly ashes by bioleaching with *Bacillus barbaricus* to remove part of the silica, a process that is enhanced by a water-wash pretreatment (Sen, Das, Bandyopadhyay, Dash, & Raut, 2016). The authors report an alumina increase from 25.45% to 34.72% with a fly ash from Odisha (India). The silica content decreases from over 60% to 40%, and the extracted $SiO_2$ may be used for the manufacturing of silica products. This approach seems a way to render more fly ashes suitable for alumina recovery.

When aluminum is extracted from high-aluminum coal fly ash (between 40% and 50% $Al_2O_3$) using an hydrothermal alkaline process, a fly ash residue results with a high sodium content (up to 20 wt%). Such residues cannot be used directly in most of the common fly ash applications due to occurring alkali-aggregate reactions. Li, Hui, Wang, Bao, and Sun (2015) developed a hydrothermal washing procedure ($T = 185°C$; NaOH 50 g/L; $t = 2$ h; $L/S = 40$) to remove sodium from these residues. This brought the $Na_2O$ content in the residues down to 0.6 wt% with the possibility of reusing the washed $Na_2O$ in alumina extraction.

A chloride-based extraction technology for the recovery of aluminum was recently patented by the Canadian Orbite Technologies Inc. (Boudreault, Fournier, & Primeau, 2015). Extractions based on hydrochloric acid are developed primarily for aluminum, but they cover all valuable materials from fly ash, including Fe, MgO, $TiO_2$, Sc, Ga, Ge, and REEs.

### 15.2.2 Extraction and recovery of V and Ni

*Aspergillus* and *Penicillium* are heterotrophic fungi that are often used for the recovery of valuable metals from solid materials. An example of this technology is the simultaneous extraction of vanadium and nickel from an Iranian coal fly ash containing 30 g $kg^{-1}$ of V and almost 20 g $kg^{-1}$ of Ni using *Aspergillus niger* and *Penicillium simplicissimum* (Rasoulnia & Mousavi, 2016). Slurry leaching with a pulp density in the order of 30 g $L^{-1}$ for 7 days at a temperature of 60°C leached 90%–97% of the vanadium and approximately 50% of the nickel. Moreover, the residue turned out to be detoxified, according to the TCLP test.

### 15.2.3 Extraction and recovery of Ga, Ge, and associated elements

An analysis of alkaline industrial residues by Gomes et al. (2016) revealed that when recovering 5% of the metal content from coal fly ash, assuming a Ga content in coal fly ash of 40–60 mg $kg^{-1}$, this would for Ga mean a production of three to four times the actual world production, which is significantly higher than for the other elements analyzed (Co, La, Li, Se, V). Much work in this respect is done by the research group of Dai in cooperation with the group of Seredin on Chinese and Russian coal deposits (Dai et al., 2012; Seredin, 2012; Seredin & Dai, 2012; Seredin et al., 2013). Unfortunately, the main focus is on the metal content of coal and not on the metals content of the fly ash, but with a reported enrichment factor between 6 and 10, a fair idea of the possibilities for metal values in ash is suggested. They report an average Ga content for Chinese coals of 6.55 mg $kg^{-1}$, as compared to the world average of 5.8 mg $kg^{-1}$. More importantly, a few coal deposits have Ga contents >30 mg $kg^{-1}$; notably the Heidaigou Surface Mine's coal has an average of 45 mg $kg^{-1}$ and an estimated reserve of 45,000 t of Ga, making it a huge gallium ore deposit (Dai et al., 2012). This coal is burnt in the Jungar power plant, from which the fly ash also has a very high $Al_2O_3$ content (>50%) and may serve as a resource for aluminum, gallium, and several other elements.

Another review of Ga in coal and combustion residues is given by Qin, Sun, et al. (2015). In coal, Ga shows inorganic affinity, therefore the dominant form in ash is $Ga_2O_3$. Only at high combustion temperatures can gaseous species form (GaCl, Ga, GaO, $Ga_2O$ and $Ga_2S$), which may disappear with the flue gases; therefore Ga is normally enriched with a factor of 6–10 compared to the coal. The authors suggest that in addition to the Ga removal methods mentioned in the previous paragraphs, Ga can also be removed by precipitation after leaching, which is integrated in the process they developed for the simultaneous recovery of lithium and aluminum from predesilication coal ash. This technology, described in a different paper, is also of broad interest, since Li is recognized as a critical element as well (Qin, Zhao, Li, & Zhang, 2015).

According to Dai et al. (2012), the largest Ge deposit in the world is the Yimin Coal in Inner Mongolia, with approximately 4000 t Ge and a concentration of up to 470 mg $kg^{-1}$; also the third largest deposit of Ge is incorporated into a coal layer in the Spetzugli coal in Eastern Russia. Other deposits, such as in Shengli and Lincang coals in China, even have higher concentrations of Ge, up to 850 mg $kg^{-1}$ in some ore bodies, but have lower total reserves. Associated with Ge occurrences in these coal seams, also enrichment of other elements occur such as W, Be, U, Cs and Nb, to the extent that part of the Lincang coal is even mined for its uranium. There exist other coal- and lignite-hosted uranium deposits that are mined in China, with uranium concentrations up to 7000 mg $kg^{-1}$ (Yili Basin Lignite), which are also high in Mo and Re (Dai et al., 2012).

Spanish research groups concentrated their work on the recovery of germanium, gallium, and vanadium from gasification fly ash (Font et al., 2007; Arroyo, Font, Fernández-Pereira, Querol, Juan, et al., 2009; Arroyo, Font, Fernández-Pereira, Querol, Chimenos, 2009), but they also applied their metallurgical processes to leachates from coal fly ashes in general (Arroyo & Fernández-Pereira, 2011). The gasification fly ash had a germanium concentration in the range of 200–400 mg $kg^{-1}$, a gallium concentration in the range of 150–300 mg $kg^{-1}$, and a vanadium concentration between 0.4 and 0.6 wt% (Font et al., 2007).

Gallium extraction yields of 60%–68% were achieved in a 0.7–1 M NaOH solution in a L/S ratio of 5 at 25°C for 6 h (Font et al., 2007). In a recirculation system the Ga concentration in the liquid could be increased to around 200 mg $L^{-1}$. With carbonation from bubbling the solution with $CO_2$, 99% of the gallium could be precipitated, and after a few purification steps, the final product had a Ga purity of 30%. This was considered an economically feasible end product at the time. For vanadium a maximum extraction of 64% was achieved at the expense of much higher NaOH concentrations, which, to the contrary, was not considered a feasible operation (Font et al., 2007).

In a follow-up study, Arroyo et al. (2014) tested different extractants for Ga leaching on IGCC fly ash and found the highest yield (71%) for 24 h leaching with $H_2SO_4$. NaOH leaching with the same ash under the same conditions resulted in 64% yield.

Germanium was leached from the fly ash by hot water (90°C) to give a solution with 35 mg $L^{-1}$ that could be enriched by germanium sorption onto activated carbon or by solvent extraction (Arroyo, Font, Fernández-Pereira, Querol, Juan, et al., 2009). Germanium was then precipitated as $GeS_2$ by addition of $H_2S$, or as an organic Ge-complex by the addition of 1,2-dihydroxy benzene pyrocatechol (CAT) and cetyltrimethylammonium bromide (CTAB). More than 99% of the germanium was recovered from the solutions to yield a product with more than 90% hexagonal-$Ge_2O$ purity.

Zhang and Xu (2016) achieved 94% germanium recovery from an exceptionally high germanium-rich coal fly ash from Inner Mongolia, China (>0.6% Ge). In a pilot plant operation with 500 g of ash, they used vacuum reduction assisted by 10% of coke addition at 1473 K and 1–10 Pa for 40 min.

### *15.2.4 Extraction of REE and associated elements*

Many of the reported Nb-Ta-Zr-Hf-REE-Ga deposits associated with coal deposits are in fact of volcanogenic origin and are either intimately intergrown with coal seams or else some of the metals have migrated into the coal (Dai et al., 2012). Nevertheless, in the Songzao coalfield, Nb concentration may be as high as 275 mg $kg^{-1}$ in the burnt coal, and the resulting fly ash may be considered as a niobium ore.

The ease of recovering REE from fly ash depends largely on the solubility of these elements in acids. Therefore Taggart et al. (2016) determined both total content and nitric acid extractable REE; they found that up to 70% of the REEs could be digested with heated nitric acid. It was noted that the extractable part was highest in high Ca fly ashes. However, it has been found before that REE in fly ash are evenly distributed over the glass phase of fly ash particles (Hower et al., 2013), probably because the high Ca content enhances a larger portion of the ash particles to dissolve in nitric acid.

Seredin and Dai (2012) reviewed the contents of yttrium and Lanthanides in coal deposits worldwide and concluded that coal deposits should be carefully analyzed during exploitation to recognize the potential values they may contain for their content in those elements. Whether from terrigenous, volcanogenous, from infiltration of meteoric waters or hydrothermal origin, the combustion by-products from such coals may present promising materials for the recovery of yttrium and Lanthanides.

## 15.3 Integral treatment technologies

These are conversion technologies by which the fly ash is to be converted into a new product by chemical engineering processes. The most important among those products are zeolites. Chemically similar to zeolites, but amorphous in nature and different in properties are geopolymers, which were covered in Chapter 8. Other examples of products include polyalkenoate cements and sialon ceramic materials.

### *15.3.1 Conversion into zeolites*

Reviews and state-of-the-art technologies on the conversion of coal fly ash into zeolites are given by Querol, Moreno, Umaña, et al. (2002), Querol and Moreno (2008), Nugteren (2008), and Ahmaruzzaman (2010). These papers provide extensive literature reviews of the development of the research and processes since the first recognition by Höller and Wirsching (1985) that coal fly ash could be utilized as a precursor for zeolites. In this first study, Höller and Wirsching synthesized an already remarkable variety of zeolites from fly ash: analcime, chabazite, faujasite, hydroxysodalite, phillipsite, zeolites F, HS, J, M, P, and X.

In general, zeolites synthesized from coal fly ash via direct conversion in a hydrothermal alkaline environment yield products that are a mixture of zeolites and residual fly ash. Such products contain a maximum of 70% zeolites, often 50% or even less. An interesting innovation was the two-step approach first reported by Hollman, Steenbruggen, and Janssen-Jurkovicova (1999) and further developed by Querol, Moreno, Andres, et al. (2002). The precursor elements Si and Al were in the first step extracted from fly ash into an alkaline solution that was later used for the synthesis of pure zeolites. In this way, there was more steering in synthesis conditions possible, and therefore the desired zeolite species could be produced in pure form. An extra parameter was the $SiO_2$ to $Al_2O_3$ ratio, which could be varied by adding aluminum through the addition of spent anodizing etch solutions from the aluminum industry. In this way, pure zeolite A and zeolite X could be synthesized. Depending on the characteristics of the fly ash the suitability of fly ash for silica extraction varies widely and was studied to select the most appropriate fly ashes for zeolite synthesis (Moreno et al., 2004).

In recent years, most of the studies are simply confirmations of what has been shown before. This probably has to do with the fact that the production of zeolites from fly ash can hardly compete with zeolites produced from primary materials. On the one hand, this is because of the impure nature of fly ash zeolites produced through direct conversion, and on the other hand, because of high production costs when produced through the two-step approach. However, some interesting work is reported from South Africa, where the work of Du Plessis, Ojumu, Fatoba, Akinyeye, and Petrik (2014) attracted attention because it focused on the fate of (trace) elements during synthesis. It was found that when the two-step approach was followed, the majority of the elements reported to the solid zeolite product. However, when a fusion-assisted process was used as a pretreatment step, most of the elements ended up in the solid waste. In both cases the liquid wastes were equally contaminated with toxic elements (As, Pb, Hg, Al, and Nb). It was further reported that by using the fusion-assisted approach, the yield of Si and Al was only in the order of 20%, far too low for being an economical process.

### 15.3.2 Other products

*Glass polyalkenoate cements* were produced from coal gasifier slag with an Si/Al ratio close to unity and a Ca/Al ratio greater than or equal to 0.5. The slag is reacted with polyacrylic acid (PAA) to form a cement that may find application in the building industry (Sullivan & Hill, 2008).

Another interesting topic is the conversion into *nonoxide Sialon ceramic materials* (composed of Si, Al, O, and N), which was first shown by Kudyba-Jansen, Hintzen, and Metselaar (2001). They successfully treated fly ashes of different compositions by carbothermal reduction and nitridation to synthesize these ceramic powders. Not only was β-Sialon powder obtained, but due to free available Ca in the fly ashes, also Ca-α-Sialon ceramic powders could be made. The synthesized Sialon powders were densified to produce ceramics, and by the combination of β- and α-Sialon, composite ceramics were made that combine the excellent properties of both Sialon modifications. For β-Sialon ceramics, similar properties were obtained compared to β-Sialon ceramics made of clays.

In a series of articles, Qiu, Hlavacek, and Prochazka (2005) and Qiu and Hlavacek (2005a, 2005b, 2005c) studied the carbonitridation of coal fly ash for the production of Sialon whiskers at a low cost. The addition of decomposable and indecomposable salts turned out to promote whisker formation and had a positive effect on the nitridation extent of the fly ash. Using 4% of different inorganic salts as indecomposable additives was found to have a strong effect on the nitridation reaction. $BaCl_2$ turned out to be the most effective additive studied; however, results were also dependent on the fly ash properties and sources.

Another example is given by Zhao, Wang, Yu, and Zhang (2015), who produced Sialon whiskers at 1420°C from coal fly ash. They showed that the whisker morphology was dependent on the reaction time through the formation mechanism. When fly ash liquid droplets form and be transformed into whiskers by chemical vapor deposition on the substrate surface, this will first result in bead-like whiskers. With prolonged time the liquid phases will become exhausted, and rod-like whiskers will be formed instead.

## 15.4 Concluding remarks

Forced leaching as a chemical refinement method for achieving environmentally sound combustion residues seems to force the problematic elements from the ash into a solution. However, in combination with the recovery of valuables from ashes, efficient and economically feasible processes for the decontamination of solid and liquid residues with the simultaneous recovery of targeted elements become options.

Even when targeting for a renewable energy future, there is still a need for coal technology, as the largest and easiest accessible deposits of metals crucial for new energy technologies and electronics are found associated with coal deposits. Combustion will then be the first and easiest concentration method of the metals with energy as a by-product. The quantities available in ash may be high, but the concentrations of the targeted metals are low in the order of 0.1%–0.01%, and the extractable quantities may be much lower than 100%. This is probably the reason that no commercial extraction has begun as yet. Therefore research should now concentrate on finding the reasons for low and variable extractability, which is determining the speciation of the metals in the ash and how that depends on ash properties and combustion conditions. Further, there is a need for inexpensive classification or other pretreatment methods to enhance metal concentrations in selected fractions, thereby reducing the amount of materials to be handled and subjected to the final extraction processes. Finally, demonstration and pilot operations are needed to show that the findings from laboratory research can be scaled up to commercial operations.

Integral conversion processes for coal fly ash (e.g., the conversion into zeolites) seem attractive, but their major drawback is that the products partly consist of unconverted fly ash, rendering such products less valuable compared to products from primary resources.

## References

Ahmaruzzaman, M. (2010). A review on the utilization of fly ash. *Progress in Energy and Combustion Science*, *36*, 327–363.

Arroyo, F., & Fernández-Pereira, C. (2011). Recovery of germanium from real fly ash leachates by ion-exchange extraction. *Minerals Engineering*, *24*, 35–41.

Arroyo, F., Font, O., Chimenos, J. M., Fernández-Pereira, C., Querol, X., & Coca, P. (2014). IGCC fly ash valorisation. Optimisation of Ge and Ga recovery for an industrial application. *Fuel Processing Technology*, *124*, 222–227.

Arroyo, F., Font, O., Fernández-Pereira, C., Querol, X., Chimenos, J. P., & Zeegers, H. (2009a). Germanium and gallium extraction from gasification fly ash: Optimisation for up-scaling a recovery process. In: *World of coal ash conference, 2009* [pdf available on http://www.flyash.info/].

Arroyo, F., Font, O., Fernández-Pereira, C., Querol, X., Juan, R., Ruiz, C., et al. (2009b). Germanium recovery from gasification fly ash: Evaluation of end-products obtained by precipitation methods. *Journal of Hazardous Materials*, *167*, 582–588.

Bauer, D., et al. (2010). *US Department of Energy. Critical materials strategy*. Published by the US DoF Office of Policy and International Affairs (PI).

Bhattacharyya, S., Donahoe, R. J., & Patel, D. (2009). Experimental study of chemical treatment of coal fly ash to reduce the mobility of priority trace elements. *Fuel*, *88*, 1173–1184.

Bittner, J., Gasiorowski, S., & Hrach, F. (2001). Removing ammonia from fly ash. In: *In Proc. Int. Ash Uti. Symp. (on CD), 22–24 October, Kentucky, USA*.

Blissett, R. S., Smalley, N., & Rowson, N. A. (2013). An investigation into six coal fly ashes from the United Kingdom and Poland to evaluate rare earth element content. *Fuel*, *119*, 236–239.

Boudreault, R., Fournier, J., & Primeau, D. (2015). Processes for treating fly ashes. Patent CA 2,862,307.

Burnet, G., Murtha, M. J., & Dunker, J. W. (1984). *Recovery of metals from coal ash*. Ames, IA: Ames Laboratory, US DOE Iowa State University.

Cox, M. (2008). Recovery of values from combustion ashes. In M. Cox, H. W. Nugteren, & M. Janssen (Eds.), *Combustion residues, current, novel and renewable applications* (pp. 369–378). Chichester: John Wiley and Sons Ltd.

Cox, M., Nugteren, H. W., & Janssen-Jurkovičová, M. (Eds.), (2008). *Combustion residues, current, novel and renewable applications*. Chichester: John Wiley and Sons Ltd.

Dai, S., Ren, D., Chou, C.-L., Finkelman, R. B., Seredin, V. V., & Zhou, Y. (2012). Geochemistry of trace elements in Chinese coals: A review of abundances, genetic types, impacts on human health, and industrial utilization. *International Journal of Coal Geology*, *94*, 3–21.

Du Plessis, P. W., Ojumu, T. V., Fatoba, O. O., Akinyeye, R. O., & Petrik, L. F. (2014). Distributional fate of elements during the synthesis of Zeolites from South African coal fly ash. *Materials*, *7*, 3305–3318.

Font, O., Querol, X., Juan, R., Casado, R., Ruiz, C. R., López-Soler, A., et al. (2007). Recovery of gallium and vanadium from gasification fly ash. *Journal of Hazardous Materials*, *A139*, 413–423.

Gasiorowski, S. A., & Hrach, F. J. (2000). Method for removing ammonia from ammonia contaminated fly ash. US Patent 6,077,494.

Ghoreishi, S. M., Hedayati, A., & Ansari, K. (2016). Experimental investigation and optimization of supercritical carbon dioxide extraction of toxic heavy metals from solid waste using different modifiers and chelating agents. *Journal of Supercritical Fluids*, *117*, 131–137.

Gomes, H. I., Mayes, W. M., Rogerson, M., Stewart, D. I., & Burke, I. T. (2016). Alkaline residues and the environment: A review of impacts, management practices and opportunities. *Journal of Cleaner Production*, *112*, 3571–3582.

Graedel, T. E., Barr, R., Chandler, C., Chase, T., Choi, J., Christoffersen, L., et al. (2012). Methodology of metal criticality determination. *Environmental Science and Technology*, *46*, 1063–1070.

Graedel, T. E., Harper, E. M., Nasser, N. T., & Reck, B. K. (2013). On the materials basis of modern society. *PNAS*, *112*, 6295–6300.

Grzymek, J. (1976). Prof. Grzymek's self-disintegration method for the complex manufacture of aluminium oxide and Portland cement. In: *Proceedings of sessions 105th AIME annual meeting, Las Vegas, NV* (pp. 29–39).

Höller, H., & Wirsching, U. (1985). Zeolites formation from fly ash. *Fortschritte der Mineralogie*, *63*, 21–43.

Hollman, G. G., Steenbruggen, G., & Janssen-Jurkovicova, M. (1999). A two-step process for the synthesis of zeolites from coal fly ash. *Fuel*, *78*, 1225–1230.

Hower, J. C., Groppo, J. G., Joshi, P., Dai, S., Moecher, D. P., & Johnston, M. N. (2013). Location of Cerium in coal-combusion fly ashes: Implications for recovery of Lanthanides. *Coal Combustion and Gasification Products*, *5*, 73–78.

Joshi, P. (2013a). A low cost rare earth elements recovery technology. In: *Paper presented at the world of coal ash conference, Lexington, KY*.

Joshi, P. (2013b). Final report phase I: A low-cost rare earth elements recovery technology. EPA Extramural Research.

Kashiwakura, S., Kubo, H., Kumagai, Y., Kubo, H., Matsubae-Yokoyama, K., Nakajima, K., et al. (2009). Removal of boron from coal fly ash by washing with HCl solution. *Fuel*, *88*, 1245–1250.

Kashiwakura, S., Ohno, H., Kumagai, Y., Kubo, H., Matsubae, K., & Nagasaka, T. (2011). Dissolution behavior of selenium from coal fly ash particles for the development of an acid-washing process. *Chemosphere*, *85*, 598–602.

Kashiwakura, S., Ohno, H., Matsubae-Yokoyamaa, K., Kumagai, Y., Kubo, H., & Nagasaka, T. (2010). Removal of arsenic in coal fly ash by acid washing process using dilute $H_2SO_4$ solvent. *Journal of Hazardous Materials*, *181*, 419–425.

Kersch, C., Peretó Ortiz, S., Woerlee, G. F., & Witkamp, G. J. (2004). Leachability of metals from fly ash: Leaching tests before and after extraction with supercritical $CO_2$ and extractants. *Hydrometallurgy*, *72*, 119–127.

Kudyba-Jansen, A. A., Hintzen, H. T., & Metselaar, R. (2001). Ca-α/β-sialon ceramics synthesised from fly ash—Preparation, characterization and properties. *Materials Research Bulletin*, *36*, 1215–1230.

Li, H., Hui, J., Wang, C., Bao, W., & Sun, Z. (2015). Removal of sodium ($Na_2O$) from alumina extracted coal fly ash by a mild hydrothermal process. *Hydrometallurgy*, *153*, 1–5.

Meij, R. (1997). Prediction of environmental quality of by-products of coal-fired plants; elemental composition and leaching. In: *WASCON'97, Houthem St. Gerlach, The Netherlands*. Amsterdam: Elsevier.

Meij, R., & Krijt, G. D. (1993). Databank spoorelementen deel 3 poederkoolvliegas. KEMA report no.63597-KES/WBR 93-3113.

Meij, R., van der Kooij, J., van der Sluys, J. L. G., Siepman, F. G. C., & van der Sloot, H. A. (1983). The emission of fly ash and trace species from pulverised coal fired utility boilers. In: *VIth world congress on air on air quality, Paris*.

Moreno, N., Querol, X., Andrés, J. M., López-Soler, A., Janssen-Jurkovicová, M., Nugteren, H., et al. (2004). Determining suitability of a fly ash for silica extraction and zeolitisation. *Journal of Chemical Technology and Biotechnology*, *79*, 1009–1018.

Nugteren, H. W. (2008). Limitations of combustion ashes: 'From Threat to Profit'. In: M. Cox, H. Nugteren, & M. Janssen (Eds.), *Combustion residues, current, novel and renewable applications* (pp. 137–198). Chichester: John Wiley and Sons Ltd.

Nugteren, H. W. (2010). *Secondary industrial minerals from coal fly ash and aluminium anodising waste solutions* [PhD thesis]. Delft University of Technology [pdf available from Delft Library Repository].

Nugteren, H. W., Janssen-Jurkovícová, M., & Scarlett, B. (2001). Improvement of environmental quality of coal fly ash by applying forced leaching. *Fuel*, *80*, 873–877.

Nugteren, H. W., Janssen-Jurkovícová, M., & Scarlett, B. (2002). Removal of heavy metals from fly ash and the impact on its quality. *Journal of Chemical Technology and Biotechnology*, *77*, 389–395.

Peck, D. (2016). *Prometheus missing: Critical materials and product design* [PhD thesis]. Delft University of Technology [pdf available from Delft Library Repository].

Pellegrini, M. (2014). *Report on critical raw materials for the EU*. Report of the Ad hoc Working Group on defining critical raw materials European Commission, DG Enterprise and Industry.

Qin, S. J., Sun, Y., Li, Y., Wang, J., Zhao, C., & Gao, K. (2015a). Coal deposits as promising alternative sources for gallium. *Earth-Science Reviews*, *150*, 95–101.

Qin, S. J., Zhao, C., Li, Y. H., & Zhang, Y. (2015b). Review of coal as a promising source of lithium. *International Journal of Oil, Gas and Coal Technology*, *9*, 215–229.

Qiu, Q., & Hlavacek, V. (2005a). Carbonitridation of fly ash. II. Effect of decomposable additives and whisker formation. *Industrial and Engineering Chemistry Research*, *44*, 2477–2483.

Qiu, Q., & Hlavacek, V. (2005b). Carbonitridation of fly ash. 3. Effect of indecomposable additives. *Industrial and Engineering Chemistry Research*, *44*, 7352–7358.

Qiu, Q., & Hlavacek, V. (2005c). Carbonitridation of fly ash. 4. Hydrolysis of nitrided fly ash. *Industrial and Engineering Chemistry Research*, *44*, 7359–7365.

Qiu, Q., Hlavacek, V., & Prochazka, S. (2005). Carbonitridation of fly ash. I. Synthesis of Sialon-based materials. *Industrial and Engineering Chemistry Research*, *44*, 2469–2476.

Querol, X., & Moreno, N. (2008). Zeolites. In M. Cox, H. Nugteren, & M. Janssen (Eds.), *Combustion residues, current, novel and renewable applications* (pp. 240–260). Chichester: John Wiley and Sons Ltd.

Querol, X., Moreno, N., Andres, J. M., Janssen, M., Towler, M., Stanton, K., et al. (2002a). *SILEX, Recovery of major elements from coal fly ashes*. Final report, BRITE–EURAM Program BRPR-CT98-0801 Commission of the European Communities.

Querol, X., Moreno, N., Umaña, J. C., Alastuey, A., Hernandez, E., & Lopez-Soler, A. (2002b). Synthesis of zeolites from coal fly ash: An overview. *International Journal of Coal Geology*, *50*, 413–423.

Rasoulnia, P., & Mousavi, S. M. (2016). V and Ni recovery from a vanadium-rich power plant residual ash using acid producing fungi: *Aspergillus niger* and *Penicillium simplicissimum*. *RSC Advances*, *6*, 9139–9151.

Reijnders, L. (2005). Disposal, uses and treatments of combustion ashes: A review. *Resources, Conservation and Recycling*, *43*, 313–336.

Scott, C., Deonarine, A., Kolker, A., Adams, M., & Holland, J. (2015). Size distribution of rare earth elements in coal ash. In: *WOCA 2015*.

Sen, S. K., Das, M. M., Bandyopadhyay, P., Dash, R. R., & Raut, S. (2016). Green process using hot spring bacterium to concentrate alumina in coal fly ash. *Ecological Engineering*, *88*, 10–19.

Seredin, V. V. (2012). From coal science to metal production and environmental protection. *International Journal of Coal Geology*, *90–91*, 1–3.

Seredin, V. V., & Dai, S. (2012). Coal deposits as potential sources for lanthanides and yttrium. *International Journal of Coal Geology*, *94*, 67–93.

Seredin, V. V., Dai, S., Sun, Y., & Chekryzhov, I. Y. (2013). Coal deposits as promising sources of rare metals for alternative power and energy-efficient technologies. *Applied Geochemistry*, *31*, 1–11.

SQD. (2007). Dutch soil quality decree (Besluit Bodemkwaliteit). *Staatscourant*, *469*. 3 December.

Su, T., & Wang, J. (2011). Modelling batch leaching behaviour of arsenic and selenium from bituminous coal fly ashes. *Chemosphere*, *85*, 1368–1374.

Sullivan, A., & Hill, R. (2008). Glass polyalkenoate cements. In M. Cox, H. Nugteren, & M. Janssen (Eds.), *Combustion residues, current, novel and renewable applications* (pp. 276–289). Chichester: John Wiley and Sons Ltd.

Taggart, R. K., Hower, J. C., Dwyer, G. S., & Hsu-Kim, H. (2016). Trends in the rare earth element content of U.S.-based coal combustion fly ashes. *Environmental Science and Technology*, *50*, 5919–5926.

Tolhurst, L. (2014). Commercial recovery of metals from coal ash—Global review. Commercial report from lucid insight (available from lucinda@lucid-insight.com), 112 pages.

Tolhurst, L. (2015). Commercial recovery of metals from coal ash. In: *2015 World of coal ash (WOCA) conference in Nasvhille, TN, 5–7 May 2015* [pdf available on http://www.flyash.info/].

Yao, Z. T., Xia, M. S., Sarker, P. K., & Chen, T. (2014). A review of the alumina recovery from coal fly ash, with a focus in China. *Fuel*, *120*, 74–85.

Zhang, L., & Xu, Z. (2016). An environmentally-friendly vacuum reduction metallurgical process to recover germanium from coal fly ash. *Journal of Hazardous Materials*, *312*, 28–36.

Zhao, H., Wang, P. Y., Yu, J. L., & Zhang, J. (2015). A mechanistic study on the synthesis of β-Sialon whiskers from coal fly ash. *Materials Research Bulletin*, *65*, 47–52.

This page intentionally left blank

# Part Four

# Coal products and the environment

This page intentionally left blank

# Coal products and the environment

# 16

*T. Adams*[*], *T. Robl*[†]
[*]American Coal Ash Association, Lexington, KY, United States, [†]University of Kentucky, Lexington, KY, United States

## 16.1 Environmental benefits of coal product recycling

This book is focused on beneficially recycling coal combustion materials. There are many uses for these products but the role that coal ash products in construction is probably the most critical. Portland cement concrete is the most important material of construction that we have. It is strong, durable, and formed from common ingredients found throughout the world, primarily limestone and shale with small amounts of gypsum. However, it is energy intensive and releases a large amount of $CO_2$ from the calcination of limestone. Its role as the third largest anthropologic source of carbon emissions is well documented and represents over 3.5 billion tons of $CO_2$ annually.

The most effective way to minimize these emissions is to use supplementary cementitious materials (SCMs). Coal fly ash is the most abundant and economic SCM. It both replaces Portland cement and improves a wide range of its key engineering characteristics of concrete and its environmental durability, extending the life of structures and reducing future emissions. Its use can easily reduce the global warming potential (GWP) of concrete by 20%–30%. Coal ash is also in the process of replacing shale in the fabrication of Portland cement itself, reducing the impact of the mining of this commodity.

Synthetic gypsum from flue-gas desulfurization is also a coal combustion product with a major environmental impact. Its widespread availability has transformed the manufacturing of wall board (i.e., plasterboard) in North America, where on a weight basis, it has become the most important material in single- and multiple-occupancy homes. Globally, it has become an important source of plaster cements and boards and has largely supplanted natural gypsum in Portland cement manufacture.

There are many organizations dedicated to the recycling of these materials including: the American Coal Ash Association (ACAA), which is approaching its 50th anniversary; the UK Quality Ash Association (UKQAA); European Coal Combustion Productions Association (ECOBA); Association of Canadian Industries Recycling Coal Ash (CIRCA); Ash Development Association of Australia (ADAA); the South African Coal Ash Association; and the Asian Coal Ash Association, as well as

**Coal Combustion Products (CCP's).** http://dx.doi.org/10.1016/B978-0-08-100945-1.00016-2

organizations in India and Russia.[1] Many other organizations, such as the American Concrete Institute[2] and the Electric Power Research Institute (EPRI), also support the beneficial reuse of coal products.

The first chapter in this section, written by Lionel Lemay, the vice president for sustainable development of the US National Ready Mix Association, addresses coal products in green construction and the history of the sustainable construction movement. The contribution of coal products in improving life cycle and reducing the carbon footprint of construction is discussed, as well as other benefits, such as asphalt additives and soil stabilization. The future challenges of increasing coal products in construction are also discussed.

## 16.2 Risk assessment in the management of coal products

Our purpose in the next chapters is not to engage in the larger debate of climate change and carbon emissions; rather, it is to focus on the direct risks associated with managing and handling the materials themselves. Coal products are a major mineral resource and must be managed optimally. We believe this is best done through beneficial reuse and recycling, and many environmentalists concur. The US Environmental Protection Agency (EPA), after its finding that coal ash was not hazardous in the year 2000, actively promoted ash recycling, giving out awards annually to the best recycling projects.

This changed on Dec. 22, 2008, when the large ash pond at the Tennessee Valley Authority's Kingston power plant partially collapsed and spilled some 4 million $m^3$ of ash slurry into the Emory River. Another spill took place on Feb. 2, 2014 at a Duke Power plant in North Carolina, which affected the Dan River. Compared to Kingston, this ash spill was tiny, but politically and legislatively, its impact was just as great.

The Kingston spill was very large and shocking. It occurred after a substantial rainy period late at night without any witnesses to the actual event. The media attention and national outcry over the spill was intense. The focus of many environmental organizations shifted from air emissions to combustion byproducts. The US EPA quickly acted to reclassify ash as a hazardous material and regulated it under Subtitle C of the Resource Conservation and Recovery Act (RCRA) as a reversal of two previous findings. This change in policy was due to public outcry, pressure from environmental

---

[1] American Coal Ash Association, 28800 Country Club Drive, Farmington Hills, MI; Asian Coal Ash Association, No. 1 Guangzhuang East Chaoyang District, Beijing; European Coal Combustion Productions Association (ECOBA), Klinkestr. 27-31, D-45136 Essen; Association of Canadian Industries Recycling Coal Ash (CIRCA), Post Office 60, Shubenacadie, NS, Canada; South African Coal Ash Association, P.O. Box 50172, 0097 Moreleta Village, 452 Danehill, Furrow Street, Equestria, Pretoria, South Africa; UK Quality Ash Association, Willow House, Kingswood Business Park, Holyhead Road, Albrighton, Wolverhampton; Ash Development Association of Australia, Level 1, Suite 2, 336 Keira Street, PO Box 1194, Wollongong NSW 2500, Australia; Coal Ash Institute of India, (A Society Incorporated), Conmat Technologies Private Limited, CF-318, Salt Lake, Kolkata.

[2] American Concrete Institute (ACI), 38800 Country Club Drive, Farmington Hills, MI; Electric Power Research Institute (EPRI), 3420 Hillview Ave, Palo Alto, CA.

organizations, and the way in which environmental laws are administered in the United States. With a hazardous classification, ash would be directly regulated by the US EPA, while nonhazardous waste is regulated by the individual states.

Although the US EPA proposed a workaround for beneficial reuse, a hazardous classification would have hampered these efforts and prevented its utilization in many applications. When the US EPA conducted a series of town hall meetings to review the proposed reclassification, the negative impact on ash utilization proved to be a major consideration. After more than 8 years of hearings and other deliberations, the US EPA's final rule, published on Jul. 27, 2016, regulated coal ash as nonhazardous under subtitle D of RCRA. Although some issues are still being ironed out, a uniform national standard for monitoring and insuring the safety of ponded and landfilled ash is now in place in the United States, which will ultimately replace a patchwork of local and state regulations. In addition, there are ongoing attempts to pass bipartisan legislation in the US Congress to simplify and clarify the regulation of coal ash.

Probably the best lesson learned from the Kingston ash spill was that the cooperation between local, state, and federal authorities, along with the utilities, could quickly mobilize a major successful cleanup effort. Most of the ash was removed from the river in the first 10 months after the spill. The Emory River was reopened in late spring 2010 for full use. It continues to supply safe drinking water that complies with all federal standards.

These two major events and the studies and findings they triggered are covered in the next chapter by Prof. John Daniels. The events themselves are chronicled along with the environmental and human health investigations and the impacts on regulatory framework. Discussions of sustainable closure and postclosure care are also presented.

Another lesson learned is that fly ash is not hazardous or toxic, at least in the usual sense. The Kingston and subsequent Dan River spills triggered some of the most extensive and intensive environmental studies of all time. Hundreds of thousands of tests and measurements were made on the environment as well as on flora and fauna affected. It was determined that there was little or no environmental impact after the cleanup.

The environmental effects associated with coal ash are addressed in the chapter written by Dr. Lisa Bradley, a toxicologist. Dr. Bradley presents a discussion of what it means for something to be toxic, constituents present in coal ash and human and ecological risk assessment, how exposure is evaluated and risk level targeted, and how all this may be related to the Kingston and Dan River spills. An interesting discussion of the differences between how the European testing of the toxicity of ash compares to that of the United States is also included.

Since Kingston the use of slurry ponds to manage coal ash has fallen into disfavor in the United States. They might not be illegal or impossible to build, but new ponds must be much more heavily engineered, and they must be lined and monitored. The signals from the US EPA have not been subtle on this issue, and many utilities are rapidly converting their ash systems to dry handling and closing their ponds. The North Carolina State legislature mandated a review of all the ponded ash in the state following the Dan River spill. Ponds were given three classifications, and the ponds representing the most imminent threat were ordered closed with the ash transported to approved lined landfills.

Another major trend affecting ash utilization and its environmental impact is the closing of many coal-fired power plants. A recent study found more than 170 coal-fired power plants in the United States are either closed or slated to be closed in the near term or are being converted to other fuels, primarily natural gas.[3] This is reflective of trends in many other countries. There are many causes for this; environmental regulations are clearly a factor for some, but probably more important is the greater availability and lower cost of natural gas. Natural gas-fired plants are also much simpler and cleaner to operate.

Many or most of the affected coal-fired power plants have ash ponds associated with them, and most are unlined. At best, these sites can be capped and remain in place, but they will still require decades of monitoring. Many will require some level of remediation to protect groundwater. At worst, some will have to be relocated at great cost and risk.

The closure of an ash pond must take many factors and variables into consideration. Some, like groundwater aquifers, are site specific. Choices must be made to minimize risk to the environment and human health, as well as the long-term liability for the utilities and their rate payers. This will require some careful and thorough risk assessment. The assessment of these risks is addressed in the next chapter written by Mrs. Ari Lewis, a risk assessment specialist with the Gradient Corporation. Issues such as balancing short-term and long-term risk associated with pond closures are considered, along with best management practices and corrective actions to manage these risks.

## 16.3 Ash as an internationally traded commodity and the future of the industry

The last chapter in this book brings us full circle. It is not about risk, but reward. David Harris, the executive director of the Asian Coal Ash Association, presents a summary of the rapidly changing market dynamics of coal ash, projected to reach $98 billion in sales by 2020. The loss of point sources of coal ash products from plant closures in some parts of the world, combined with an oversupply in other parts, is already developing the dynamics of ash being traded as an international commodity. The demand for a lower-carbon built environment will continue, increasing both the demand and value of high-performing fly ash produced through beneficiation. Consideration of the cost and risks associated with what amounts to the perpetual care of retired ash storage facilities will undoubtedly lead to the recovery and beneficiation of ash from these sites as well. In short, the future for ash is bright, and it belongs to the international recycling trade.

---

[3] Institute for Energy Research, Power plant Closures, 2016, http://instituteforenergyresearch.org/topics/policy/power-plant-closures/.

# Coal combustion products in green building

# 17

*L. Lemay*
National Ready Mixed Concrete Association, Silver Spring, MD, United States

## 17.1 Introduction

The keys to high performance in cementitious construction materials are dependent on coal combustion products. High strength, durability, and low environmental impacts are all attributes that coal combustion products, such as fly ash, bottom ash and flue gas desulfurization (FGD) Gypsum, can impart to building products. With the advent of the green building movement over the last two decades, owners, designers, contractors, and product manufacturers are challenged to meet new goals for lowering the environmental footprint of the buildings they design, build, and operate while maintaining and or improving product performance. Coal combustion products can help meet these challenges.

Modern society relies on buildings, roadways, public transportation, water, and infrastructure to function effectively. But these modern amenities place a heavy burden on the environment. It takes raw materials, energy, and other resources to make building products, as well as to build a structure and operate it throughout its lifetime. At the end of their useful lives, structures are demolished. Some of the materials can be recycled, but many are placed in landfills, adding further to environmental burden. Although buildings and infrastructure provide a nearly incalculable societal benefit, anything that can be done to reduce the environmental footprint of structures can also help to reduce the environmental burden.

## 17.2 What is green building?

There are many definitions of green building. One definition provided in an article by the US Green Building Council (USGBC) is as follows:

> *Green building is a holistic concept that starts with the understanding that the built environment can have profound effects, both positive and negative, on the natural environment, as well as the people who inhabit buildings every day. Green building is an effort to amplify the positive and mitigate the negative of these effects throughout the entire life cycle of a building.*
>
> (Kriss, 2016)

**Coal Combustion Products (CCP's).** **http://dx.doi.org/10.1016/B978-0-08-100945-1.00017-4**

USGBC developed the Leadership in Energy and Environmental Design (LEED) green building rating system with this definition in mind. The LEED system, for example, described in detail in Section 17.4, provides strategies for designing a green building from cradle to grave, taking into account the entire life cycle, including site location, public transportation, building orientation, water use, energy use, indoor air quality, and product and material impacts.

Most of the strategies revolve around reducing life cycle impacts for the entire building. For example, for the energy and atmosphere credit, the strategy is to minimize energy consumption, encourage renewable energy, and reduce emissions, including greenhouse gasses and ozone depleting chemicals, among others. Approximately one-third of the credits for LEED certification are focused on energy reduction. For the location and transportation credit, the primary objective is to reduce emissions from vehicles by promoting public transportation and alternative fuel vehicles as a way to lower greenhouse gas emissions. For products and materials, the concept is to minimize the energy of production, including associated emissions such as greenhouse gasses, and to minimize impacts on land, society, and human health from the extraction of raw materials and manufacturing.

Strategies for reducing the environmental burden of the manufacturing process include

- reducing the need for raw materials by using more efficient methods, innovative materials, or recycled materials
- reducing the transportation distances to manufacturing and construction sites
- reducing the energy needed to manufacture a product
- improving the durability of a product, thus reducing the need for maintenance and replacement
- making a product more recyclable at end of life

Fly ash contributes to these strategies in many ways that will be described in greater detail later in this chapter.

### *17.2.1 Climate change*

The increase in the average temperature of the Earth's atmosphere and oceans as a result of the buildup of greenhouse gasses in the atmosphere is called climate change or global warming. Climate scientists are now positive that greenhouse gasses emitted into the atmosphere through human activity are the primary cause of climate change. Sources of greenhouse gas emission include burning fossil fuels for everything from fueling our cars and trucks, heating and cooling our buildings, and manufacturing the products we use every day, including building products and materials. Climate change is also caused by deforestation, as trees serve a primary role as carbon sink. Other sources of greenhouse gas emissions include natural occurrences such as volcanic eruption and other human activities such as raising livestock, agriculture, landfill emissions, and use of chlorofluorocarbons in refrigeration systems.

Scientists predict that global warming will result in several things, including a rise in sea levels, an increase in the intensity of extreme weather, and a change in the amount and pattern of precipitation. All of this leads to changes in agricultural yields, as well as glacier retreat, species extinctions, and widespread disease. Ultimately, these effects could severely impact the Earth's ability to support life, therefore any opportunity to reduce greenhouse gas emissions or the concentration of greenhouse gasses in the atmosphere is considered to be a positive effort.

As mentioned above, LEED and other green building standards and rating systems do not necessarily focus entirely on greenhouse gas emissions, but many of the strategies are related to reducing those effects of climate change that are attributed to greenhouse gas emissions. Greenhouse gas emissions, either during the manufacture of building products, or during the operation of a structure, such as a building, roadway or other infrastructure system, is one way of measuring environmental impact. Generally, though not always, the more greenhouse gasses that are emitted into the atmosphere, the more harm is done to the environment, such as acidification, smog formation, and ozone depletion, along with other effects, such as ecosystem degradation and disease.

Over the last several years, there has been a greater focus on climate change and its effects on the planet. Carbon dioxide ($CO_2$) emissions have become a surrogate for green building metrics, with an effort made to reduce $CO_2$ and other greenhouse gas emissions.

## 17.3 How do CCPs contribute to green products?

### 17.3.1 Fly ash concrete

*Increased strength*: Fly ash, when used in concrete, makes structures like highways, bridges, tunnels, and buildings stronger and more durable (Vanita, Gupta, & Sachdeva, 2010). The ultimate compressive strength of fly ash concrete, due to the pozzolanic reaction, continues with time and is generally higher than similar Portland cement-only concretes. As climate change will continue to produce stronger hurricanes and tornadoes, wildfires, and floods, increasing the strength of a structure to resist natural disasters will reduce the environmental impact of a structure. If a structure has a longer service life and reduces the need for maintenance or repair, it in turn reduces the amount of greenhouse gasses emitted during the entire life of the structure.

*Reduced permeability*: Fly ash concretes are less permeable and thus protect against corrosion of reinforcing steel more effectively by making it less likely for water to flow through the concrete to the reinforcing steel. The pozzolanic reaction improves the microstructure of concrete compared to Portland cement concrete. Fly ash concretes can be 5–20 times less permeable than Portland cement concretes. Corrosion of the reinforcement is a major cause of structures that are exposed to weather, thus fly ash concrete can help extend the service life of a structure, which in turn reduces the amount of greenhouse gasses emitted.

*Sulfate resistance*: Class F fly ash can improve the sulfate resistance of concrete. The primary reason for this is that the continued pozzolanic reaction blocks the capillary pores in the cementitious paste, which reduces the flow of water and sulfate ions into concrete. Reduced availability of lime also has been attributed to improving sulfate resistance.

*Alkali-silica reactivity* (*ASR*) *resistance*: ASR results in the expansion of reactive forms of silica (aggregates) when sufficient water and alkalis are present, which can lead to the cracking and deterioration of concrete. Fly ash reduces the propensity of ASR expansion by reducing permeability of concrete, thus limiting the ability for water to reach a reactive aggregate and when Class F fly ash chemically binds the alkalis in concrete. Most Class C fly ashes are less effective in reducing ASR. Again, improving the durability of concrete exposed to weather (concrete on the interior of a building is not subject to ASR because no moisture is present) increases the service life of a structure and thus reduces greenhouse gas emissions.

*Freezing and thawing resistance*: One precaution, however, is that fly ash concretes may be susceptible to freezing and thawing damage (surface scaling), thus the building code for concrete recommends the maximum fly ash in concrete be limited to 25% when the concrete will be exposed to deicing chemicals (ACI 318-14, 2014). Keep in mind, though, that this is only a factor when concrete is exposed to deicing chemicals. When concrete is exposed to weather in moderate climates and when it is protected from the weather, most concrete will not be affected by freezing and thawing; therefore there is no limit to fly ash content.

*Embodied global warming potential* (*GWP*): One of the greatest benefits of concrete is to reduce the embodied GWP of concrete. GWP is usually stated in kg of carbon dioxide equivalents ($CO_2e$) per unit of product. For concrete, that number is stated in kg $CO_2e/m^3$ or kg $CO_2e/yd^3$. Since Portland cement has a relatively high GWP, it is a priority to find a strategy to optimize the amount of cement in concrete in order to reduce the embodied impacts of concrete.

As with all manufacturing processes, cement manufacturing requires energy to produce. $CO_2$ is generated from the use of fossil fuels in the heating process and from calcination, which is when calcium carbonate is heated and broken down to calcium oxide with the release of $CO_2$. On average, 1040 kg of $CO_2$ are emitted for every 1000 kg (2205 lb) of Portland cement produced in the United States (Portland Cement Association, 2016). The resultant GWP of average concrete (30 MPa or 4000 psi) made with Portland cement in the United States is ~416 kg $CO_2$ per $m^3$ (318 kg $CO_2e/yd^3$). By reformulating the concrete with a 30% replacement of Portland cement with fly ash, the same concrete in the United States would have a GWP of 325 kg $CO_2e/m^3$ (249 kg $CO_2e/yd^3$), which is a 22% decrease from the Portland cement concrete (NRMCA IW EPD, 2014).

The primary reason is that fly ash, a by-product of coal-fired electric power generation, is considered to have a very small environmental footprint. There is no energy associated with "manufacturing" fly ash, unless there is some processing involved to beneficiate the fly ash for use in concrete. Most fly ash used in concrete does not require beneficiation. Only the GWP from transportation impacts are attributed to the fly ash, which is considerably smaller than the GWP of Portland cement.

Furthermore, any replacement of Portland cement with fly ash reduces the impacts associated with mining raw materials. Also, fly ash used in concrete also reduces the amount of materials sent to landfills, a fate the fly ash would have if it were not used for a beneficial purpose.

In addition to the benefits on hardened concrete, fly ash can enhance the properties of fresh concrete, resulting in further environmental impact reduction.

*Water demand reduction*: Fly ash particles are spherical in shape, which reduces the demand for water for a given slump target for concrete. A fly ash concrete with 25% fly ash can reduce water demand by 6%–10%. Since fresh water is a limited resource, anything to reduce the water needed for concrete is an environmental benefit.

*Enhanced workability*: Fly ash improves the flow of concrete, which helps improve workability. Fly ash tends to result in longer set times, making the finishing process more efficient. Fly ash concrete also has better pumping characteristics than Portland cement concrete. All of these characteristics result in a concrete that is easier to place, which means that less energy is used, resulting in reduced environmental impacts.

*Reduced heat of hydration*: Since the pozzolanic reaction occurs at a later stage, the heat of hydration of fly ash concrete is lower than Portland cement concrete. This is critically important for mass concrete applications, be it for a mass building foundation, bridge abutment, or large concrete dam. High heat of hydration can cause cracking and other deterioration of concrete, so anything that can improve the durability of concrete can benefit the life cycle impacts of a structure.

*Economic benefit*: Fly ash is typically less costly than Portland cement, which can result in economic savings for concrete applications. In addition, using fly ash can result in reduced cost for power utilities, as the byproduct can be used for beneficial use instead of long-term land fill and protection.

> *Economic benefits can include job creation in the beneficial use industry, reduced costs associated with CCR [Coal Combustion Residues, including fly ash] disposal, increased revenue from the sale of CCRs and savings from using CCRs in place of other more costly materials.*
>
> *EPA's Beneficial Use Risk Evaluation (Environmental Protection Agency, 2014)*

*Health concerns*: Coal combustion products, including fly ash, are not hazardous and are therefore safe for human health when managed properly. Coal ash has been studied extensively for decades by universities and government regulatory agencies; the US Environmental Protection Agency and other government bodies have determined that coal ash is nonhazardous (Environmental Protection Agency, 2014). The chemical constituents of coal ash are commonly found in many everyday products and natural materials, including soil (AECOM, 2012). Chemical constituents in fly ash are bound in concrete (MIT Concrete Sustainability Hub, 2010).

According to a 2012 survey conducted by the National Ready Mixed Concrete Association (NRMCA), about 98% of ready mixed concrete companies used fly ash in some of their concrete over that time period (NRMCA, 2012). According to the American Coal Ash Association (ACAA), more than half of the concrete produced in the United States uses fly ash as a substitute for traditional Portland cement. Concrete routinely contains 40% fly ash, but that amount can reach 70% or more in massive elements such as walls, girders, dams, and foundations (American Coal Ash Association, 2016).

### 17.3.2 Controlled low-strength materials

Controlled low-strength materials (CLSM), sometimes called flowable fill, is generally used as an economical alternative backfill material to compacted granular and is mostly made with fly ash instead of Portland cement. One of the main uses of CLSM is as backfill for utility trenches, but it can also be used for structural fill for foundation subbase or pavement base. It is sometimes used to fill abandoned mines, tunnels, and underground storage tanks. The key benefit of CLSM is that it is flowable. That means it eliminates the need for workers to get into pits and trenches to compact traditional granular fill. CLSM can reach areas typically difficult to reach by machinery since it can be delivered by a ready mixed concrete truck and pumped into place.

In general, CLSM is a low-strength concrete often made with significant amounts of fly ash and small amounts of Portland cement and filler, such as sand. The key to CLSM, in most applications, is that it remains at a low enough strength that it can be excavated at a later date. Strengths should be 50 psi for hand excavation and up to 200 psi for machine excavation. Strengths can go higher for fill where excavation is not anticipated. It also helps improve the speed of construction and worker safety.

### 17.3.3 Geopolymers

Geopolymer concrete combines an alkaline liquid with a geological source material containing silicon and aluminum to form a binder that does not use any Portland cement. Because the chemical reaction that takes place is a polymerization process, the material is called a geopolymer. The geological source material can come from naturally occurring materials such as kaolites and clays or by-product materials such as fly ash, silica fume, slag, rice-husk ash, etc. Fly ash, being one of the most abundant source materials with the necessary properties, is the most commonly used source material for geopolymer concrete. The alkaline liquids come from soluble alkaline metals such as sodium or potassium such as combinations or sodium hydroxide and potassium hydroxide and sodium silicate or potassium silicate.

The mechanical properties of geopolymer concrete is similar to that of Portland cement concrete, and therefore can be used as a substitute for Portland cement. Geopolymer concrete gains strength similar to Portland cement concrete, is resistant to sulfate attack, has good acid resistance, and undergoes very little creep and drying shrinkage. It is ideal where durable concrete is a must. Structural tests on reinforced concrete elements such as beams and columns demonstrate similar behavior to ordinary Portland cement concrete.

One drawback is that the alkaline liquid is expensive to manufacture, and thus geopolymer concrete has not been commercialized to replace ordinary Portland cement concrete. However, some companies have commercialized it for specialty applications where high fire or chemical resistance is required. Obviously, if the process could be made more economical, it would provide an excellent opportunity to lower the environmental footprint of concrete construction.

### 17.3.4 Asphalt

Fly ash can be used as an economical mineral filler in hot mix asphalt. Although fly ash does not react with chemical constituents of asphalt like it does with Portland cement concrete, it does enhance some of the properties of asphalt. For example, it can help increase the stiffness of the asphalt mortar matrix, resulting in reduced rutting of the pavement. It also helps reduce asphalt drain down during construction, and ultimately results in improved durability because the amount of asphalt binder is held more consistent throughout the mixture. By improving the durability of asphalt and increasing the recycled content, fly ash can help reduce the environmental impact of pavements.

### 17.3.5 Soil stabilization

Fly ash can be mixed with soil to improve the density, water content, plasticity, strength, and other engineering properties of soil that would otherwise be unsuitable for construction applications, such as road base or structural fills. Class C-Fly ash alone or Class-F fly ash blended with lime or other cementing material are mixed with soil and water with grading equipment. This methodology is used to stabilize road base, stabilize embankments, control expansive soils, and reduce moisture content to permit compaction of soil. The use of fly ash in soil stabilization and modification may be subject to local environmental requirements. One of the primary uses of fly ash in soil stabilization is to improve the compressive and shear strength of soils. Using fly ash for soil stabilization reduces environmental impacts by reducing the need to remove unsuitable soil and replacing it with engineered fill, thus eliminating the expense and environmental burden of transportation.

### 17.3.6 Wallboard

Calcium sulfate is a naturally occurring mineral commonly known as gypsum. Gypsum is mined all over the world to make gypsum wallboard, as a cement additive and as plaster. Synthetic gypsum, or calcium sulfate, is a by-product of the flue-gas desulfurization or scrubbing process at coal-fired electric power plants. Just like naturally occurring gypsum, synthetic gypsum can also be used to make gypsum wallboard, which reduces the need to use virgin materials and thus reduces the impact of construction.

## 17.4 How coal combustion products are treated in the green building standards

### 17.4.1 Leadership in energy and environmental LEED

Since its inception in the mid-1990s, the LEED green building rating system has been used to reduce environmental impacts of the built environment. LEED has been a market transformation device affecting all sectors of the construction industry, including concrete production and construction. The system is credit-based, allowing projects to earn points for environmentally friendly strategies employed during the design and construction process. With each new version, the USGBC, developers of LEED, has increased the targets and scope for reducing environmental impacts related to building design, construction, and maintenance.

LEED v4, released in Nov. 2013 and was made mandatory for LEED projects in Oct. 2016, continues the momentum with a number of advancements that will likely change the way design professionals, contractors, and product manufacturers do business. Many credits, such as Stormwater Management, Heat Island Reduction, and Optimized Energy Performance, are refined, but maintain the same intent. Others, such as material and resource (MR) credits, challenge product manufacturers to disclose their environmental, social, and health impacts in third-party validated reports.

LEED v4 has six main credit categories:

- Location and transportation
- Sustainable sites
- Water efficiency
- Energy and atmosphere
- Materials and resources
- Indoor environmental quality

Each credit category is divided into credits that outline the intent, requirements, technologies, and strategies for meeting each credit. Credits are broken down into individual points. Additional points can be earned for integrative process, innovation, and regional priority credits.

Because of concrete's versatility, there are many applications where concrete can be used in a building project, from foundation and superstructure to sidewalks and parking lots. That means concrete can contribute to every credit category. More detail about how concrete can be used for LEED v4 credit can be found in Concrete's Contribution to LEED (CSR011, 2014). But suffice it to say that fly ash concrete can be used for nearly every application within a building and thus also contribute to every credit category in LEED v4.

Where fly ash can directly support LEED v4 certification is in the MRs credit category. In the past versions of LEED, the focus of material impacts has been on single attributes such as recycled content, rapid renewability, or regional materials. While these attributes are important, they only tell part of the story. A product could perform well in one attribute but poorly in another. The new LEED v4 MR credits attempt to take a holistic look at materials by adopting life-cycle assessment (LCA) and product disclosure and optimization.

LCA is the investigation and evaluation of the environmental impacts of a product, process or service. LCA evaluates all stages of a product's life to determine its environmental life cycle impacts. LCA is the most comprehensive approach to determining environmental impacts of a building. A detailed explanation of LCA can be found in Section 17.5. There is one credit in LEED v4 called Building Life-Cycle Impact Reduction that rewards three points if the building has lower life-cycle impacts than a reference building.

Product disclosure means reporting environmental, social, and health impacts through third-party verified reports, including environmental product declarations (EPDs), corporate sustainability reports (CSRs), and health product declarations (HPDs), among others. There are three Building Product Disclosure and Optimization credits, and each offers two points. The first point (Option 1), Disclosure, requires the project use 20 permanently installed products that disclose impacts using EPDs, CSRs, and/or HPDs. In LEED v4, a "product" is defined by the distinct function it serves. That means concrete has the advantage of contributing significantly because of its wide range of applications or functions. For example, footings, foundations walls, shear walls, bearing walls, columns, beams, slabs, sidewalks, and parking areas, each of which has a unique mix design, would all be considered different products in LEED v4 and therefore contribute significantly to the 20 required products.

The second point (Option 2), Optimization, requires a certain minimum value of building products to demonstrate they are performing better than industry baselines for environmental, social, and health impacts. The second option limits the contribution of structure and enclosure to 30% of the qualifying products on a cost basis. However, the value of products manufactured and extracted within 100 miles (160 km) of the project site is doubled, meaning concrete can contribute significantly to this option, as concrete is almost always manufactured and extracted locally.

### *17.4.2 Building life-cycle impact reduction*

This credit offers several options for reducing the impact of buildings, mostly centered on existing building adaptation and reuse. However, for new buildings, Option 4 of the credit encourages the use of LCA to demonstrate lower environmental impacts of the proposed building over a baseline building. The project is awarded three points for conducting a whole building LCA of the project's structure and enclosure that demonstrates a minimum of 10% reduction, compared with a reference building, in at least three of following six impact categories:

- Global warming potential (required)
- Reduce ozone depletion
- Land/water acidification
- Eutrophication
- Tropospheric ozone
- Nonrenewable energy

No impact category assessed as part of the LCA may increase by more than 5% when compared with the reference building. Concrete structures have always been known for durability and long service life. Therefore, they decrease the environmental impacts associated with reconstruction, repair, and maintenance and can often demonstrate the lowest life-cycle impacts. As described in Section 17.5, concrete is made with fly ash and along with other supplementary cementitious material (SCMs) can contribute significantly to lowering environmental impacts of concrete. That means a design team can use "average" concrete to conduct an LCA for the reference building, then use high fly ash content concrete for the proposed building to demonstrate a significant reduction in environmental impacts.

### 17.4.3 Building product disclosure and optimization—EPDs

EPDs are reports published by product manufacturers that provide third-party-verified information regarding the environmental performance of their product (see Section 17.5). Option 1 (Disclosure) awards one point for using 20 permanently installed products in the building that have published EPDs. Under this credit, a plant specific EPD is more desirable (worth the full product), but industry average EPDs (worth half a product) can be used if site specific EPDs are not available. There are no requirements for reducing environmental impacts; simply disclosing the product's environmental impacts will support this credit. Concrete producers with EPDs will be able to contribute significantly to this credit because of the wide range of concrete products on most projects.

Option 2 (Optimization) awards one point if 50%, by cost, of all products in the building can demonstrate that their products perform better than the industry average or baseline environmental impacts. The concrete industry has developed an industry-wide EPD for concrete and an industry benchmark report for concrete that provides average impacts for a variety of mix designs, which means concrete producers can compare their impacts to these baselines and formulate products that have lower environmental impacts than average. As shown in Section 17.5, fly ash concrete can have significantly lower impacts than average concrete.

### 17.4.4 Building product disclosure and optimization—Sourcing of raw materials

Option 1 (Disclosure) awards one point for selecting 20 products verified to have been extracted or sourced in a responsible manner. Responsible sourcing strategies include commitments to long-term ecologically responsible land use, reducing environmental harms from extraction and/or manufacturing processes, and meeting applicable standards or programs voluntarily that address responsible sourcing criteria. The credit requires CSRs from 20 different products, which means concrete producers with a CSR can contribute a significant number of products to this option.

Option 2 (Optimization) awards one point if 25%, by cost, of all products in the building have demonstrated leadership in the sourcing of raw materials. Several pathways are provided for meeting this option, including responsible forestry and material reuse and recycling, among others. Concrete products can contribute to the recycled content pathway because most concrete contains recycled materials, such as fly ash and slag, and in some cases, recycled aggregate.

### 17.4.5 Building product disclosure and optimization—Material ingredients

Option 1 (Disclosure) of this credit provides one point if 20 products in the building disclose chemical ingredients in their products using an accepted methodology. Option 1 requires reporting of chemical ingredients of products to at least 1%

(or 1000 ppm) in a HPD or under another approved program, such as GreenScreen or Cradle to Cradle. HPDs are reports that allow manufacturers to present building product ingredients in a format that is consistent and includes information on product ingredients, product testing, regulatory compliance, health hazards, and risks. Concrete producers with HPDs can contribute many products to this option.

Option 2 (Optimization) provides one point if 25%, by cost, of all products in the building are verified to have improved life-cycle impacts by optimizing their material ingredient chemistry. Concrete is typically an inert material and has one of the lowest levels of volatile organic compounds and off-gassing when compared to other commonly used building materials and can likely meet the credit requirement.

As described in Section 17.3, fly ash has minimal human health impact if handled properly. In addition, fly ash providers can help concrete producers meet this credit by submitting and verifying HPDs themselves (NRMCA, 2016).

## 17.5 Measuring impacts of construction materials using LCA

### 17.5.1 Life-cycle assessment

LCA is one of the tools used to measure the environmental impacts of a project, product, or process. LCA is a standard methodology by which all of the inputs (materials, energy, etc.) and outputs (emissions to air, water, land, etc.) are accounted for. The outputs are characterized into a set of environmental impacts such as GWP, ozone depletion potential, acidification potential, eutrophication potential, and photochemical ozone creation/smog potential, among others. The LCA methodology allows a design professional to model a project or product and investigate several options during the design process to minimize environmental impacts.

Fig. 17.1 provides a schematic of a typical LCA process. LCA was originally developed as a way to measure the environmental impact of a manufacturing process, but more recently, the concept has been extended to structures. The analysis can be performed for a building product or building project. Inputs include raw materials and energy. Life-cycle stages include raw material acquisition, manufacturing, product use, and finally, recycling or waste management. The outputs, many of which impact the environment negatively, include atmospheric emissions, waterborne wastes, solid wastes, co-products, and other releases.

An example where LCA might be used is on a major bridge project to estimate the difference between the environmental impacts of a project made with more durable materials versus a project built with less durable material. By conducting an LCA over the life of the structure, one could evaluate the overall impacts of the project including the impacts of operating the bridge, repair, and replacement. One could possibly justify using products with higher embodied impacts if it could be shown that the impacts over the life of the structure are lower.

Another example where LCA could be used is to evaluate the life-cycle impacts of a building. For a building (and for most structures), the operational stage is typically

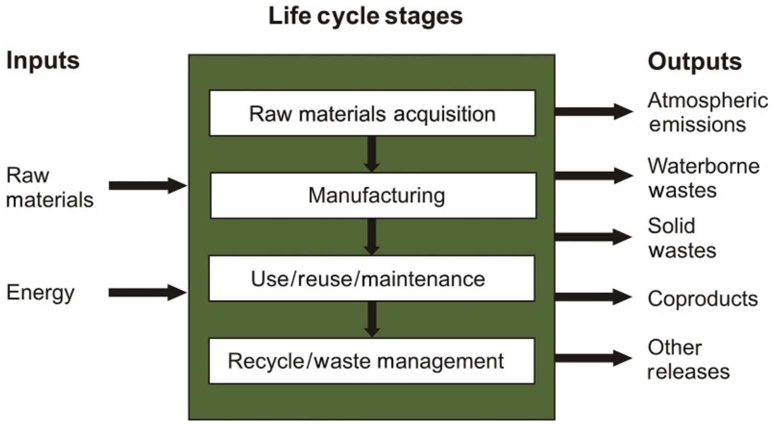

**Fig. 17.1** Life-cycle stages, inputs and outputs for life-cycle assessment. From Environmental Protection Agency.

the longest and most impactful. Impacts from heating and cooling buildings far outweigh the impacts during the other life-cycle stages. That being said, calculating the environmental impacts of a building is very complex. In addition to the operational energy and associated environmental impacts, a design professional also must have information about the products and materials used in the building. The environmental information about products is usually communicated in a document called EPD. Armed with environmental impacts of building products along with the environmental impacts of operating the building, they could calculate the life-cycle impacts over a period of 60 years (or longer).

EPDs are third-party-verified (certified) reports published by product manufacturers that provide information regarding the environmental impacts of their product. The EPD basically reports the LCA results in a uniform fashion. One can think of an EPD as a nutrition label for a product, but instead of providing information such as calories, fat content and carbohydrates, an EPD provides information about environmental impacts.

Industry trade groups typically help develop a Product Category Rule that provides instructions on how to conduct the LCA for a specific product category, such as concrete, carpeting, wood, ceiling tile, etc. It is most desirable to have plant- or site-specific data for conducting an LCA for the product. In cases where plant specific data does not exist, industry average data are sometimes used. Ideally, LCAs for products are conducted for the entire life cycle or from "cradle to cradle." However, in some cases, it may be preferable to conduct partial LCAs such as "cradle-to-gate" type analyses where only the first two life-cycle stages, raw material acquisition and manufacturing, are included because this data is needed to conduct the more comprehensive LCA for a building or other structure.

Green building standards, such as LEED v4, Architecture 2030 Challenge, International Green Construction Code, Green Globes, Envision, Greenroads, and Invest have all adopted LCA and EPDs as a way to evaluate environmental impacts of projects. As a result of the green building movement, there are several LCA software tools available in the marketplace. Each has unique features with regards to ease of use, focus (building or infrastructure), datasets, etc. Some examples include

- Athena Impact Estimator for Buildings[1]
- Athena Pavements LCA[2]
- Gabi[3]
- SimaPro[4]
- Tally[5]

### 17.5.2 Example of how fly ash can reduce full life-cycle impacts

Research at the Massachusetts Institute of Technology (MIT) conducted a full LCA for 12-story, 46,321 $m^2$ (498,590 $ft^2$) commercial building (see Fig. 17.2; Ochsendorf et al., 2011). The building was analyzed for two climates, Phoenix and Chicago, and for two different structural materials, concrete and steel. The annual operating energy, determined using the EnergyPlus[6] building energy analysis software, was conducted for a 60-year life cycle. The GWP was quantified using $CO_2e$ for several purposes,

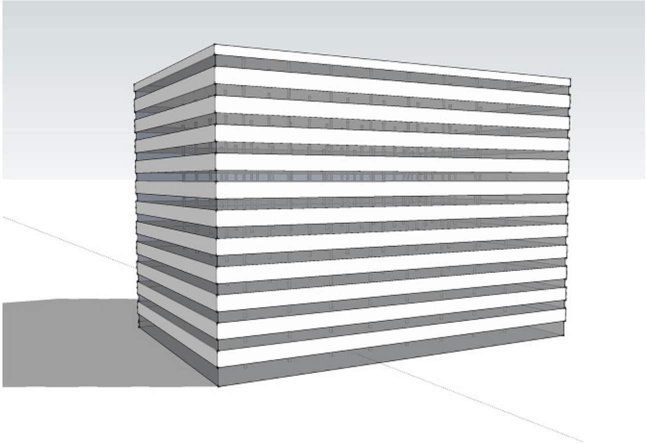

**Fig. 17.2** Twelve story commercial building used for full LCA by MIT.

---

[1] Athena Impact Estimator for Buildings. Athena Sustainable Materials Institute. http://www.athenasmi.org/our-software-data/impact-estimator/.

[2] Athena Pavement LCA. Athena Sustainable Materials Institute. http://www.athenasmi.org/our-software-data/pavement-lca/.

[3] GaBi LCA Software. Thinkstep. http://www.gabi-software.com/international/index/.

[4] SimaPro. Pré Consultants. https://www.pre-sustainability.com/simapro.

[5] Tally. A joint development project from KT Innovations, thinkstep, and Autodesk. http://choosetally.com/.

[6] EnergyPlus. US Department of Energy. http://apps1.eere.energy.gov/buildings/energyplus/.

including benchmarking emissions for current construction practices, comparing impacts of concrete versus steel and understanding the relative magnitude of impacts for different life-cycle stages.

The analysis demonstrated that the greenhouse gas emissions due to operational energy of the benchmark buildings are responsible for 95%–96% of life-cycle emissions. Compared to the steel structure, the concrete building has approximately the same embodied emissions (preuse, maintenance, and end-of-life stages), but have lower operating emissions (operational stage), which can lead to similar life-cycle emissions over time. For all cases considered, the concrete buildings had similar emissions over 60 years as the steel alternatives. The LCA research drew several conclusions, including

- Concrete and steel commercial buildings have a similar embodied GWP of 42 lbs $CO_2e/ft^2$ (205 kg $CO_2e/m^2$).
- Thermal mass of an exposed concrete frame can provide heating, ventilation and air conditioning (HVAC) savings of 7%–9% compared to a steel frame. This accounts for 2% savings in annual operating emissions.
- Over a lifetime of 60 years, the $CO_2e$ emissions of the concrete building were slightly lower than the steel alternative (see Fig. 17.3).
- The steel and concrete buildings have very similar emissions over the full life cycle and the choice of structural material does not dramatically influence the total emissions.

Finally, several recommendations for reducing life-cycle emissions of concrete buildings were presented. In particular, the GWP reduction effects of SCMs in concrete, such as fly ash, were quantified. Additional options for reducing operating emissions were introduced and quantified within the full life cycle. There are a number of potential emissions reduction strategies for concrete buildings, and LCA provides guidance for future environmental improvements, including

- Increasing SCM substitution (such as fly ash) in the concrete building from 10% to 25% can decrease preuse GWP by 4.3%.
- Lighting control and low-lift cooling can decrease the operating energy requirements for concrete buildings. Low-lift cooling takes advantage of the high heat capacity of concrete and is effective when building cooling loads are reduced through control of internal and solar heat loads.

In this example, considering the full life LCA or cradle-to-grave LCA, the use of fly ash does help reduce the environmental impact of the building over the life cycle of the building, but only by a relatively small amount because the majority of the impacts occur during the use stage, where fly ash has no effect on lowering the impacts.

### 17.5.3 Example of how fly ash can reduce embodied impacts

In this example the authors conducted a cradle-to-gate LCA to determine the embodied impacts of concrete on a building to compare the GWP of a reference building using average mixes with moderate amounts of SCMs (both fly ash and slag cement) and a proposed building using mix designs that have relatively high volumes of fly ash and slag cement. The building is an 18-story residential tower located in the northeast

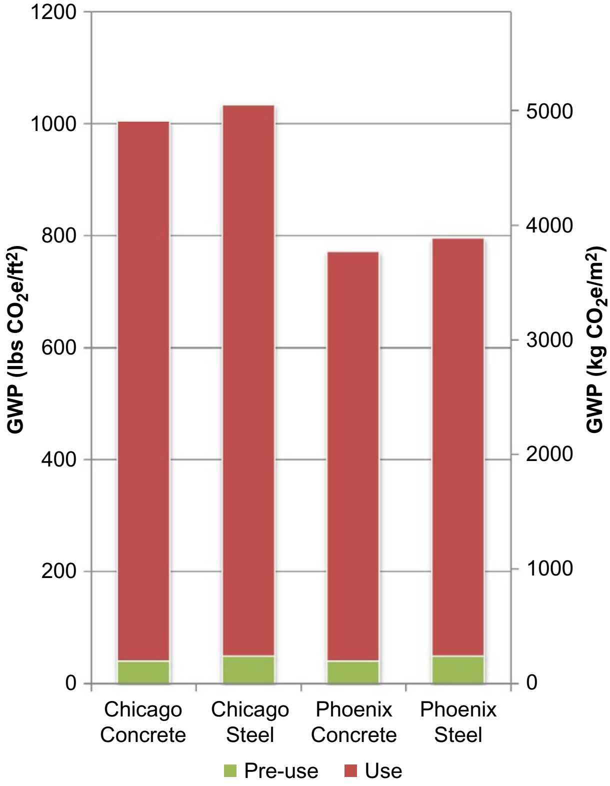

**Fig. 17.3** Total global warming potential (GWP) over 60-year lifespan for a 12-story concrete and steel commercial building in two different climate zones.

United States. For illustration purposes, only six different mix designs are selected for the project. In reality, a project of this size might have more than six mix designs. Compressive strengths for each structural element are identified in Fig. 17.4.

The first step in the analysis is to identify average concrete mixes for the reference building. In 2014, the NRMCA published benchmark mix designs and their environmental impacts for eight different regions in the United States (NRMCA, 2014). For this example, we will use the benchmark mix designs for the reference building for the Northeast region.

The next step is to estimate mix designs that have a significantly lower GWP than the benchmark mixes that still meet the performance criteria (strength, durability, etc.). Keep in mind that concrete requiring high early strength should be limited to around 30% replacement of fly ash or slag. Concrete that does not require early-age strength such as footings, basement walls, and even some vertical elements such as columns and shear walls, could have as much as 70% fly ash and/or slag and could be tested at 56 or 90 days instead of 28 days to account for slower strength gain. Start with mix designs from the NRMCA IW EPD (2014). A summary of the concretes selected for the reference and proposed building are provided in Tables 17.1–17.3.

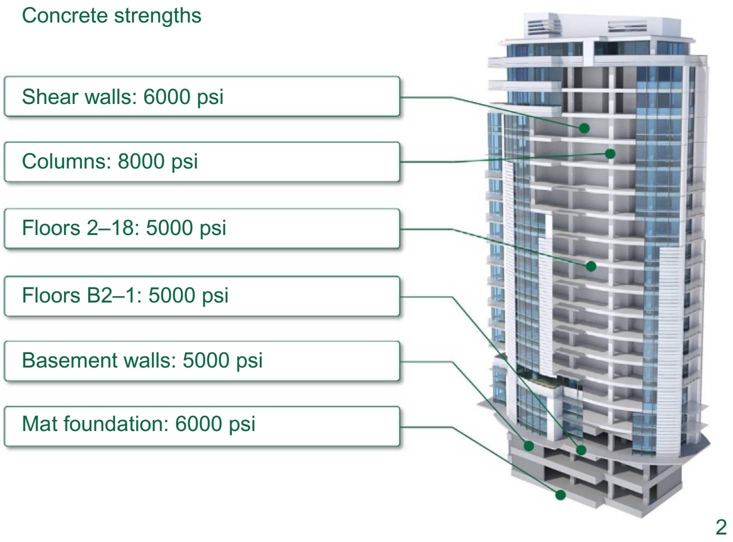

**Fig. 17.4** Specified compressive strength of concrete for an 18-story residential tower.

**Table 17.1** **Summary of concrete selected for an 18-story residential tower**

| Concrete element | Element dimensions | Concrete volume ($\text{yd}^3$) | Reference (benchmark) mixes (psi) | Proposed design mixes (fly ash slag) |
|---|---|---|---|---|
| Mat foundation | $9600\ \text{ft}^2 \times 8'$ | 2844 | 6000 | 6000 psi<br>40% slag<br>30% fly ash |
| Basement walls | $400' \times 24' \times 15''$ | 444 | 5000 | 5000 psi<br>40% slag<br>30% fly ash |
| Floors B2–1 | $9600\ \text{ft}^2 \times 3 \times 12''$ | 1067 | 5000 | 5000 psi<br>40% fly ash |
| Floors 2–18 | $9600\ \text{ft}^2\ 17 \times 9''$ | 4533 | 5000 | 5000 psi<br>30% fly ash |
| Shear walls | $25' \times 40' \times 206' \times 12''$ | 7630 | 6000 | 6000 psi<br>30% slag<br>20% fly ash |
| Columns | $24'' \times 24'' \times 206' \times 12$ | 366 | 8000 | 8000 psi<br>30% slag<br>20% fly ash |

Table 17.2 **Mix designs selected for the reference building**

| Concrete element | Reference (benchmark) mixes (psi) | Portland cement ($lbs/yd^3$) | Slag ($lbs/yd^3$) | Fly ash ($lbs/yd^3$) |
|---|---|---|---|---|
| Mat foundation | 6000 | 782 | 119 | 82 |
| Basement walls | 5000 | 741 | 112 | 78 |
| Floors B2–1 | 5000 | 741 | 112 | 78 |
| Floors 2–18 | 5000 | 741 | 112 | 78 |
| Shear walls | 6000 | 782 | 119 | 82 |
| Columns | 8000 | 967 | 147 | 102 |

Table 17.3 **Mix designs selected for the proposed building**

| Concrete element | Reference (benchmark) mixes (psi) | Portland cement ($lbs/yd^3$) | Slag ($lbs/yd^3$) | Fly ash ($lbs/yd^3$) |
|---|---|---|---|---|
| Mat foundation | 6000 | 256 | 342 | 256 |
| Basement walls | 5000 | 242 | 323 | 242 |
| Floors B2–1 | 5000 | 512 | 0 | 341 |
| Floors 2–18 | 5000 | 581 | 0 | 249 |
| Shear walls | 6000 | 427 | 256 | 171 |
| Columns | 8000 | 503 | 302 | 201 |

Using the Athena Impact Estimator for Buildings (Athena IE) software, define a reference building and proposed building. Athena IE software has the NRMCA benchmark mixes and the NRMCA IW EPD mixes preloaded into the software. It also allows the user to define new mixes based on the existing mixes in the library or completely new mixes, if that information is available, as it was for several mixes in this example.

Once all the concrete information is defined for each project, the user can then run a report that will provide the estimated GWP, along with other impacts, for each building. The reference building will represent the largest GWP and the proposed designs will represent lower GWP. The results for this example showed that the reference building has a GWP for concrete of 6.14 million kg $CO_2$ while the proposed building has a GWP for concrete of 3.92 million kg $CO_2$, meaning that the high volumes of fly ash and slag mixes resulted in 36% reduction in GWP (Fig. 17.5).

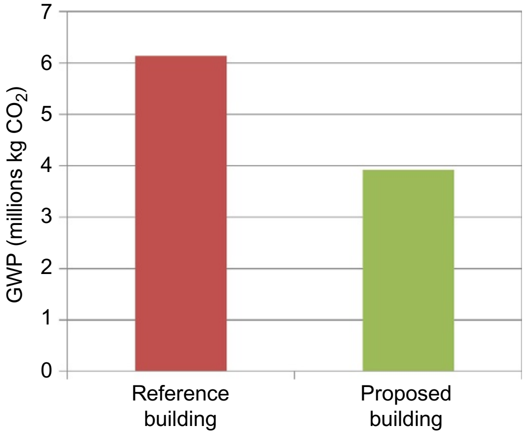

**Fig. 17.5** Global warming potential of reference building (average use of fly ash) versus proposed building (significant use of fly ash).

## 17.6 Standard specifications and project specifications

Modern standard specifications rarely have limitations for the use of fly ash in concrete. Building Code Requirements for Structural Concrete (ACI 318-14, 2014) and accompanying Specifications for Structural Concrete (ACI 301-16, 2016) does not have limitations for the use of fly ash in concrete except for concrete exposed to freezing and thawing. When concrete is exposed to deicing chemicals, then the maximum amount of fly ash is 25% of total cementitious materials. For concrete building construction, there are few limitations to using fly ash in concrete.

Unfortunately, project specifications often incorrectly provide additional limitations on fly ash use for all concrete, sometimes as low as 15%, regardless of the concrete's exposure to weather and deicing chemicals. And in some cases, on projects that are identified as green projects, specifiers require minimum fly ash contents as a way to reduce the environmental impacts of concrete. The problem with these minimum and maximum requirements is that they may lead to unintentional consequences. Artificially limiting fly ash may increase project cost or reduce the durability of a project. By artificially requiring a minimum amount of fly ash, it may cause slowed strength gain and therefore not meet the contractor's needs.

The authors recommend avoiding limitations on fly ash in concrete other than what is required in the standard specifications. Many of the limitations that do end up in project specifications are from a time (40 years ago) when the mechanisms and benefits of fly ash were not completely understood, and those limitations have remained in the specifications through generations without justification.

## 17.7 Challenges and opportunities for greater use of CCPs

Not all coal combustion products (CCPs) produced at coal-fired power plants are used in a beneficial way. A significant portion of product is landfilled each year, which increases environmental burdens. One challenge for the construction industry is to make more significant effort to specify CCPs for construction. All too often, there are unnecessary limitations on the amount of fly ash in project specifications that can be used in concrete or other applications, which hinders the use of fly ash. In addition, in many parts of the world, cold weather in the winter months combined with the slower set times of fly ash concrete result in a reduced use of fly ash in concrete. On top of that, winter months have the lowest construction volumes, hence reducing demand for fly ash. This presents a challenge to the utility companies because power generation doesn't decrease to the same degree. This poses a challenge to fly ash marketers because most do not have the storage capacity to inventory large amounts of fly ash throughout the winter months, and so some of the CCPs are simply landfilled.

Another challenge is negative perceptions of fly ash. As a result of fly ash spills in Tennessee and North Carolina, fly ash was investigated by the US EPA as a potentially hazardous material. In the end the agency ruled that beneficial use of CCPs are not hazardous and would not be regulated as such. However, the perception of the US EPA even suggesting that CCPs might be hazardous was enough to make many designers and specifiers rethink its use in construction. It appears that based on the continued growth of fly ash use in construction that this setback may have been temporary, but it likely decelerated growth at least for several years.

Increased regulation on emissions from power plants have also affected the properties of CCPs. Therefore sources of construction grade fly ash and other by-products have been reduced. In addition, a move towards renewable energy has reduced demand for coal-fired power plants. All this results in fewer sources of construction grade CCPs. Some fly ash marketers are compensating by treating fly ash that is out of specification to bring it within specification. Others are mining previously landfilled fly ash and processing it into proper specification. These are positive steps, but any additional processing required for CCPs, especially fly ash, increases cost and environmental impact.

Thankfully, the green building movement is still strong and is expected to grow. This means that demand for lower impact concrete and other building products will continue to expand. High-volume fly ash concrete mixes, fly ash-modified asphalt binders, and synthetic gypsum wallboard will continue to have a demand in green buildings and infrastructure. The advent of geopolymers and the potential to upscale the manufacturing process show promise. CCPs will continue to be a key strategy to help reduce the impact of construction materials for decades.

## References

American Coal Ash Association. (2016). https://www.acaa-usa.org/About-Coal-Ash/What-are-CCPs/Fly-Ash. (Accessed June 28, 2016).

*Building code requirements for structural concrete (ACI 318-14).* (2014). Farmington Hills, MI: American Concrete Institute.

*Coal ash material safety.* (2012). Chelmsford, MA: AECOM.

*Coal combustion residual beneficial use evaluation: Fly ash concrete and FGD gypsum wallboard.* (2014). Environmental Protection Agency.

*CSR011—Concrete's contribution to LEED v4.* (2014). Silver Spring, MD: National Ready Mixed Concrete Association.

*Environmental product declaration for Portland cement.* (2016). Skokie, IL: Portland Cement Association.

Kriss, J. (2016). *What is green building?* Washington, DC: US Green Building Council. (2016). http://www.usgbc.org/articles/what-green-building. (Accessed July 2016).

*Locking mercury into concrete.* (2010). Cambridge, MA: MIT Concrete Sustainability Hub.

*NRMCA material ingredient reporting guidance methodology and guide to LEED v4 material ingredient reporting.* (2016). Silver Spring, MD: RMC Research & Education Foundation.

*NRMCA member industry-wide EPD for ready mixed concrete.* (2014). Silver Spring, MD: National Ready Mixed Concrete Association.

*NRMCA member national and regional life cycle assessment benchmarks (industry average) report.* (2014). Silver Spring, MD: National Ready Mixed Concrete Association.

Ochsendorf, J., et al. (2011). *Methods, impacts, and opportunities in the concrete building life cycle.* Cambridge, MA: Massachusetts Institute of Technology Concrete Sustainability Hub.

*Specifications for structural concrete (ACI 301-16).* (2016). Farmington Hills, MI: American Concrete Institute.

*The 2012 NRMCA supplementary cementitious materials use survey.* (2016). Silver Spring: National Ready Mixed Concrete Association. http://www.nrmca.org/aboutconcrete/NRMCA%20SCM%20SurveyinfocusJune%202012final.pdf. (Accessed July 2016).

Vanita, A., Gupta, S. M., & Sachdeva, S. N. (2010). Concrete durability through high volume fly ash concrete (HVFC) a literature review. *International Journal of Engineering, Science and Technology*, *2*(9), 4473–4477.

# Coal ash in context

## 18

*L.J.N. Bradley*
Haley & Aldrich, Inc., Burlington, MA, United States

## 18.1 Introduction

Coal ash has been in the news since late 2008 due to unintentional releases, federal rulemaking on disposal, and state regulatory activities. Invariably, coal ash is labeled "toxic coal ash," as though it was one word. This is not correct, and it represents a misunderstanding on the part of many members of the press.

An informed discussion of coal ash, especially in the public arena, is in dire need of context. The purpose of this chapter is to provide such context in a technically sound and scientifically defensible manner.

## 18.2 Overview

Information provided here includes what coal ash is and its composition. The potential for materials or the constituents in those materials to pose a risk to human health is evaluated using methods the US Environmental Protection Agency (USEPA) developed and are referred to as human health risk assessment. This methodology evaluates the potential for a material to be toxic, and the potential for human exposure to the material to evaluate risk. These are important concepts, because as already noted, coal ash is frequently referred to as "toxic coal ash" in the popular press, without an actual discussion of either its relative toxicity or exposure.

In this section the basics of risk assessment are introduced, and the two most important concepts, evaluation of toxicity and evaluation of exposure, are discussed. USEPA has used the tools of risk assessment to develop health risk-based screening levels (RSLs) for constituents in soils and water that are used to evaluate environmental data. Governmental data for coal ash are discussed in relation to these screening levels. In addition to evaluating its trace element components, studies conducted under European regulatory programs to test the potential toxicity of coal ash as a whole material are discussed.

An important component of a risk evaluation is the development of a conceptual site model (CSM) that identifies the source, how constituents may move in the environment, and if there are any complete exposure pathways from a source to a "receptor" (such as humans or animals). This type of exposure pathway analysis is a key part of any site-specific environmental evaluation, and its application to coal ash management areas is discussed.

The potential release to groundwater is an important pathway for coal ash management facilities, and this pathway is discussed in detail. The use of a tiered risk-based

**Coal Combustion Products (CCP's).** http://dx.doi.org/10.1016/B978-0-08-100945-1.00018-6

approach for addressing this pathway is presented. Such tiered approaches are common in federal and state risk assessment applications. To put this pathway into context, a discussion of USEPA’s national risk assessment for coal ash disposal for the drinking water pathway is presented.

## 18.3 What is coal ash?

Coal ash is the unburned/unburnable material remaining after the combustion of coal. Coal is a type of sedimentary rock that is a natural component of the earth’s crust, and the inorganic minerals and elements it contains are also naturally occurring. Coal was formed over millions of years from the compaction of decayed plant matter with soils and sediments. The soils and sediments contained minerals, and these minerals were taken up into the plants as they grew. It is the organic component of coal that is burned to produce energy, and the inorganic minerals and elements that remain after combustion make up what we know as coal ash. These same minerals are present in the soils in the United States today and throughout the world.

The two major types of coal ash are fly ash and bottom ash. Fly ash is coal ash that exits from a combustion chamber in the flue gas and is captured by air pollution control equipment; it generally consists of very small particles with high surface area and a higher proportion of metals on the surface (see Chapter 2 for details). Bottom ash consists of agglomerated ash particles that are too large to be carried in the flue gases and instead adhere to the boiler walls or fall through open grates to an ash hopper at the bottom of the boiler; they generally consist of larger chunks of relatively inert material. Both of these materials have chemical and physical properties that make them useful products in a variety of applications, including the use of fly ash to replace Portland cement in concrete and the use of bottom ash as a replacement for aggregate material in lightweight concrete applications. Although not technically an “ash,” synthetic gypsum or flue-gas desulfurization (FGD) products are considered to be a coal combustion residual (CCR) by USEPA and are created as part of sulfur emission control processes. Synthetic gypsum is commonly used for making wallboard and is also used as an agricultural soil amendment. Coal ash that is not beneficially used is generally disposed of in impoundments or landfills.

## 18.4 What constituents are present in coal ash?

Fig. 18.1 compares the relative amounts of major and minor components in coal ash and other naturally occurring materials (after EPRI, 2010). It is important to understand that the constituents that are the focus of news stories about coal ash are the so-called trace elements because they are present in such low concentrations (in the milligrams per kilogram [mg/kg] or part per million [ppm] range). Together, the trace elements generally make up less than 1% of the total mass of these materials, either rocks and soil or coal ash. To put these concentrations into context, a mg/kg or ppm is equivalent to:

- 1 penny in a large container holding $10,000 worth of pennies
- ¼ cup of water in a backyard swimming pool
- 1 second in 11.5 days
- 1 in. in 15.8 miles

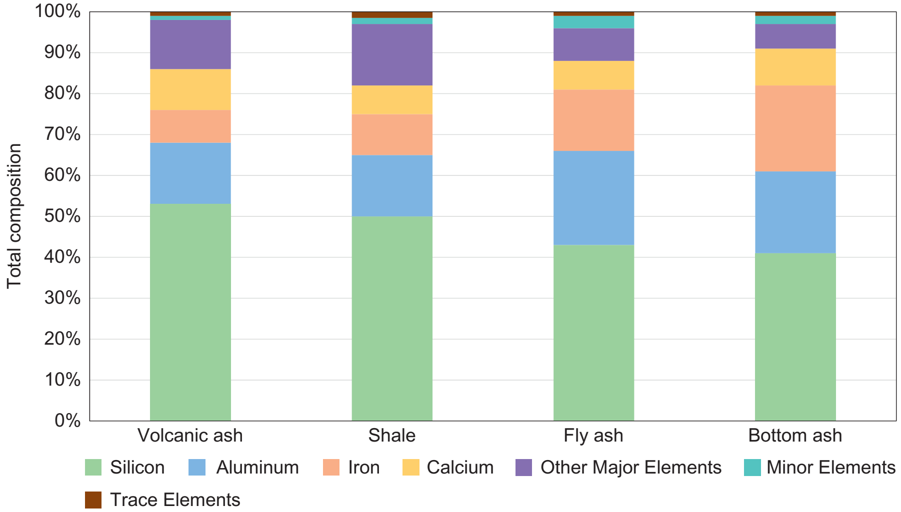

Figure developed based on EPRI data.
Source: EPRI, 2010. Comparison of Coal Combustion Products to Other Common Materials – Chemical Characteristics. Report No. 1020556. Available for download at www.epri.com.

**Fig. 18.1** Composition of coal combustion products compared to rock and volcanic ash.

Note that when considering concentrations in water, a part per million (ppm) is the same as a water concentration of a milligram per liter (mg/L). The comparisons above apply to water concentrations as well.

Tables 18.1 and 18.2 present constituent concentration data for fly ash and bottom ash, respectively, from US Geological Survey (USGS) sources (USGS, 2011); there is more discussion of these data later in the chapter.

These trace elements have been referred to by the press, by members of the community, and in legal proceedings as “toxic.” The implication is that any level of these trace elements is toxic and that there is no safe level of exposure to any of these elements. It is also inferred that these trace elements are only present in the environment due to releases from coal ash. These assumptions are not consistent with scientific facts.

## 18.5 Coal ash constituents in US soils

All of these substances occur naturally in our environment. USGS data demonstrate the presence of these constituents in the soils across the United States. A USGS report (USGS, 2014) provides concentration data and maps for 45 elements in three depths of soil for the continental United States. For example, Fig. 18.2 shows maps for arsenic, mercury, and selenium in the uppermost surface soil, and Fig. 18.3 shows the same for beryllium, cadmium, and nickel.

These soils are found in our backyards, schools, and parks, and because of their presence in soil, these constituents are also present in the foods we eat. Some of these constituents are present in our vitamins, as shown in Fig. 18.4. Thus we are exposed to these trace elements in our natural environment every day.

**Table 18.1** Summary statistics—fly ash

| Constituent | FOD | Minimum detect | Maximum detect | Mean detect | Median | 10%ile | 50%ile (Q2) | 90%ile |
|---|---|---|---|---|---|---|---|---|
| *Five state summary statistics for fly ash (a) (b) (c)* | | | | | | | | |
| Antimony | 76:76 | 0.982 | 22.4 | 3.947 | 2.88 | 1.695 | 2.88 | 8.595 |
| Arsenic | 76:76 | 7.3 | 93.8 | 27.21 | 20.95 | 14.55 | 20.95 | 57.95 |
| Barium | 76:76 | 336 | 5730 | 2372 | 1745 | 389 | 1745 | 5050 |
| Beryllium | 76:76 | 1.69 | 32.7 | 5.166 | 2.875 | 2.215 | 2.875 | 11.35 |
| Cadmium | 76:76 | 0.312 | 3.29 | 0.831 | 0.791 | 0.462 | 0.791 | 1.24 |
| Chromium | 76:76 | 33.7 | 984 | 180.5 | 100.6 | 36.1 | 100.6 | 360 |
| Cobalt | 76:76 | 14.5 | 264 | 32.1 | 28.65 | 15.35 | 28.65 | 41.25 |
| Copper | 76:76 | 55.1 | 692 | 134.2 | 139.5 | 64.6 | 139.5 | 186.5 |
| Lead | 76:76 | 14.4 | 293 | 43.66 | 33.8 | 23.65 | 33.8 | 64.85 |
| Lithium | 76:76 | 13.2 | 560 | 63.47 | 30.15 | 21.75 | 30.15 | 110.5 |
| Manganese | 76:76 | 105 | 966 | 379.8 | 217.5 | 158.5 | 217.5 | 908 |
| Mercury | 76:76 | 0.0127 | 1.15 | 0.276 | 0.128 | 0.0243 | 0.128 | 0.844 |
| Molybdenum | 76:76 | 4.95 | 90.5 | 15.67 | 8.705 | 5.755 | 8.705 | 35.25 |
| Nickel | 76:76 | 17.3 | 572 | 127.2 | 107 | 20 | 107 | 234.5 |
| Selenium | 76:76 | 1.03 | 22.5 | 7.208 | 6.09 | 2.175 | 6.09 | 12.55 |
| Strontium | 76:76 | 319 | 2400 | 1093 | 700.5 | 375 | 700.5 | 2290 |
| Thallium | 76:76 | 0.312 | 21 | 1.576 | 0.77 | 0.418 | 0.77 | 3.295 |
| Uranium | 76:76 | 0.682 | 34.1 | 7.422 | 7.37 | 0.848 | 7.37 | 12.7 |
| Vanadium | 76:76 | 106 | 1660 | 266.2 | 251 | 111.5 | 251 | 363.5 |
| Zinc | 76:76 | 33.1 | 848 | 121.8 | 106 | 51.55 | 106 | 184.5 |

Notes:
FOD: Frequency of detection—Number of detected results: Total number of samples.
(a) Statistics calculated using ProUCL version 4.1 (USEPA, 2011).
(b) Data from USGS. (2011). *Geochemical database of feed coal and coal combustion products (CCPs) from Five Power Plants in the United States*. Data Series 635. Available at: http://pubs.usgs.gov/ds/635/.
(c) Units are mg/kg.
*Source*: ACAA. (2012). *Coal ash material safety: A health risk-based evaluation of usgs coal ash data from Five US Power Plants*. American Coal Ash Association. Available at: https://www.acaa-usa.org/Portals/9/Files/PDFs/ACAA_CoalAshMaterialSafety_June2012.pdf.

**Table 18.2** Summary statistics—bottom ash

| Constituent | FOD | Minimum detect | Maximum detect | Mean detect | Median | 10%ile | 50%ile (Q2) | 90% ile |
|---|---|---|---|---|---|---|---|---|
| *New Mexico, Ohio, and Wyoming Power Plants summary statistics for bottom ash (a) (b) (c)* | | | | | | | | |
| Antimony | 48:48 | 0.401 | 3.2 | 0.869 | 0.797 | 0.488 | 0.797 | 1.15 |
| Arsenic | 48:48 | 1.24 | 18.1 | 5.036 | 4.775 | 1.744 | 4.775 | 7.344 |
| Barium | 48:48 | 474 | 2990 | 1545 | 1435 | 486.8 | 1435 | 2840 |
| Beryllium | 48:48 | 2.99 | 10.3 | 5.429 | 4.085 | 3.206 | 4.085 | 9.316 |
| Cadmium | 27:48 | 0.104 | 0.425 | 0.165 | 0.148 | 0.1132 | 0.148 | 0.2056 |
| Chromium | 48:48 | 17.5 | 461 | 150 | 72 | 19.47 | 72 | 397.5 |
| Cobalt | 48:48 | 7.29 | 55 | 28.92 | 36.05 | 7.818 | 36.05 | 49.46 |
| Copper | 48:48 | 40.4 | 148 | 76.03 | 59.8 | 41.81 | 59.8 | 135.6 |
| Lead | 48:48 | 7.59 | 40 | 15.56 | 15.8 | 8.79 | 15.8 | 20.01 |
| Lithium | 48:48 | 29.5 | 120 | 76.78 | 90.15 | 33.64 | 90.15 | 106 |
| Manganese | 47:48 | 145 | 347 | 266.9 | 266 | 214.8 | 266 | 324 |
| Mercury | 15:48 | 0.0123 | 0.155 | 0.047 | 0.0229 | 0.01474 | 0.0229 | 0.1122 |
| Molybdenum | 48:48 | 2.15 | 10.2 | 4.55 | 3.215 | 2.493 | 3.215 | 8.465 |
| Nickel | 48:48 | 28.8 | 255 | 106 | 74.45 | 31.29 | 74.45 | 214.6 |
| Selenium | 37:48 | 0.121 | 1.28 | 0.382 | 0.253 | 0.136 | 0.253 | 0.8814 |
| Strontium | 48:48 | 270 | 2680 | 1105 | 588.5 | 291.7 | 588.5 | 2563 |
| Thallium | 41:48 | 0.102 | 1.96 | 0.459 | 0.446 | 0.128 | 0.446 | 0.747 |
| Uranium | 48:48 | 5.27 | 11 | 8.229 | 9.045 | 5.597 | 9.045 | 9.96 |
| Vanadium | 48:48 | 69.4 | 591 | 223 | 206.5 | 72.65 | 206.5 | 512.1 |
| Zinc | 48:48 | 26.5 | 152 | 57.8 | 57.85 | 28.19 | 57.85 | 91.44 |

Notes:

FOD: Frequency of detection—Number of detected results: Total number of samples.

(a) Statistics calculated using ProUCL version 4.1 (USEPA, 2011). ProUCL does not calculate summary percentiles for datasets with nondetect values. Therefore, cadmium, mercury, manganese, selenium, and thallium percentiles calculated using Microsoft Excel for detected values only.

(b) Data from USGS. (2011). *Geochemical database of feed coal and coal combustion products (CCPs) from Five Power Plants in the United States*. Data Series 635. Available at: http://pubs.usgs.gov/ds/635/.

(c) Units are mg/kg.

*Source*: ACAA (2012). *Coal ash material safety: A health risk-based evaluation of USGS coal ash data from Five US Power Plants*. American Coal Ash Association. Available at: http://www.acaa-usa.org/associations/8003/files/ACAA_CoalAshMaterialSafety_June2012.pdf.

**Fig. 18.2** Arsenic, mercury and selenium distribution in surface soils collected from a depth of 0–5 cm, conterminous United States.

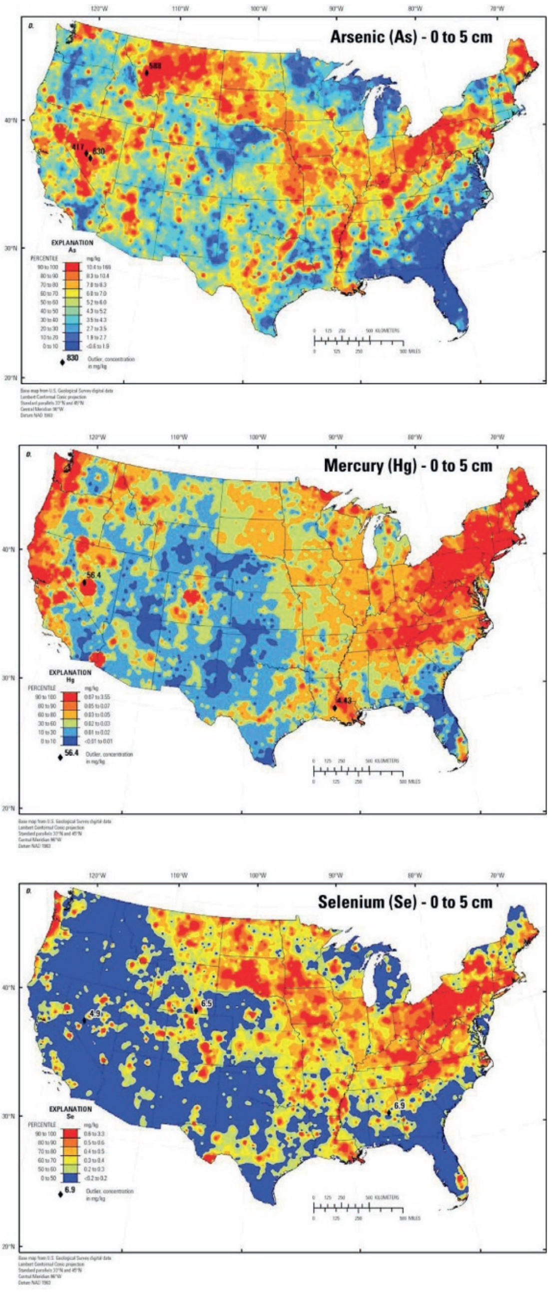

**Source:**
**USGS, 2014. Geochemical and Mineralogical Maps for Soils of the Conterminous United States.**
**http://pubs.usgs.gov/of/2014/1082/**

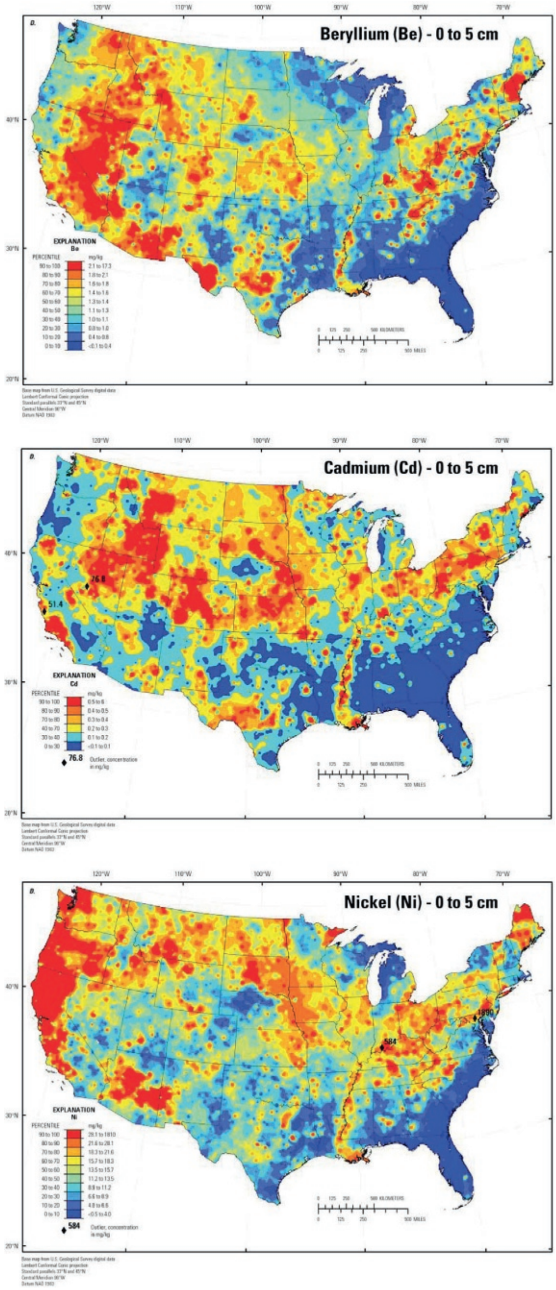

**Fig. 18.3** Beryllium, cadmium and nickel distribution in surface soils collected from a depth of 0–5 cm, conterminous United States.

**Source:**
**USGS, 2014. Geochemical and Mineralogical Maps for Soils of the Conterminous United States.**
**http://pubs.usgs.gov/of/2014/1082/**

**Fig. 18.4** Constituents present in vitamins that are also present in coal combustion products.

| Multivitamin/Multimineral for women supplement facts | | |
|---|---|---|
| Vitamin/Mineral | Amount per serving | Percent daily value |
| Vitamin A | 3,500 IU | 70% |
| Vitamin C | 100 mg | 167% |
| Vitamin D | 1,000 IU | 250% |
| Vitamin E | 35 IU | 117% |
| Vitamin K | 50 mcg | 63% |
| Thiamin | 1.1 mg | 73% |
| Riboflavin | 1.1 mg | 65% |
| Niacin | 14 mg | 70% |
| Vitamin B6 | 5 mg | 250% |
| Folic acid | 400 mcg | 100% |
| Vitamin B12 | 50 mcg | 833% |
| Biotin | 30 mcg | 10% |
| Pantothenic acid | 5 mg | 50% |
| Calcium | 300 mg | 30% |
| Iron | 8 mg | 44% |
| Phosphorus | 20 mg | 2% |
| Iodine | 150 mcg | 100% |
| Magnesium | 100 mg | 25% |
| Zinc | 15 mg | 100% |
| Selenium | 22 mcg | 31% |
| Copper | 0.5 mg | 25% |
| Manganese | 2.3 mg | 115% |
| Chromium | 52 mcg | 43% |
| Molybdenum | 50 mcg | 67% |
| Chloride | 72 mg | 2% |
| Potassium | 80 mg | 2% |
| Nickel | 5 mcg | * |
| Silicon | 2 mg | * |
| Vanadium | 10 mcg | * |
| Lutein | 300 mcg | * |

Notes:
*Daily Value not established.

🟨 Constituents present in coal ash (EPRI,2010).

## 18.6 Human health risk assessment

Human health risk assessment is a process used to estimate the chance that contact with constituents in the environment may harm people now or in the future (USEPA, 1989). There are four components to the process: (1) hazard identification, (2) exposure assessment, (3) toxicity assessment, and (4) risk characterization.

In this type of risk assessment, exposure to mixtures or complex materials is evaluated on a per constituent basis. This is the main approach used in the United States for environmental risk assessment, and Sections 18.6–18.12 discuss this approach in detail. Section 18.13 provides an evaluation of the toxicity of coal ash as a mixture, using information from the European Union (EU).

The USEPA applies these components to evaluate environmental conditions in two separate but complementary ways. First, when conducting a site-specific risk assessment, the USEPA applies these components in a four-step process: (1) the constituents and their concentrations in environmental media (such as soil or water) are identified for evaluation, (2) the ways that people may be exposed to the constituents in the environment are identified and estimates of how much of a constituent someone may be exposed to are made using information from USEPA sources, (3) the information on potential constituent toxicity is obtained from USEPA sources, and (4) this information on exposure and toxicity is combined to develop estimates of potential risk. This methodology is described in the USEPA's Risk Assessment Guidance for Superfund, Part A (USEPA, 1989).

Essentially, risk is a function of exposure and toxicity:

$$\text{Risk} = \text{Exposure} \times \text{Toxicity}$$

Thus if something is essentially nontoxic, then there is no risk. If something can be toxic, the risk to human health depends on the level of exposure. More importantly, if there is no exposure, there is no risk. The concepts of toxicity and exposure are discussed below.

## 18.7 Ecological risk assessment

Like humans, animals (or ecological "receptors") can be exposed to constituents in the environment that may be potentially harmful. Because ecological receptors are in more intimate contact with their habitat, they have a greater chance of being exposed to environmental constituents than humans. The concepts in the risk assessment process for ecological receptors is very similar to those for human health risk assessment, but differ in that (a) there can be hundreds of types of receptors (e.g., birds, mammals, fish, reptiles, amphibians, and invertebrates) and (b) laboratory testing can be directly performed to assess the degree of hazard either by exposing laboratory animals to site media in a controlled setting or by collecting and evaluating ecological receptors from a site (e.g., benthic macroinvertebrates and fish) for laboratory evaluation.

However, unlike with humans, there is limited data on each of the various species that may be exposed at a site. Therefore several common, well-studied species are selected as "surrogate" receptors, and different exposure scenarios are built around those more familiar animals. Food chain models can also be used to evaluate how constituents can move through an ecosystem. These models evaluate the movement of constituents from lower "trophic level" species, such as single-celled algae, to fish, and then all the way up to higher trophic level species, or animals at the top of the food chain (e.g., herons, eagles, and even humans).

Most importantly, the toxicological principles are also the same in that risk (or hazard) is directly proportional to the degree of exposure and the potency of the constituents to which ecological receptors are exposed. In other words, to understand whether an effect is occurring, there needs to be an understanding of the dose/response relationship; that is, the extent to which an increasing exposure ("dose") can result in an increase (large or small) in the probability of an adverse effect ("response").

Ecological risk assessment is segregated into two general categories: aquatic and terrestrial. Aquatic risk assessments address wetland and water body habitats (e.g., rivers, streams, lakes, and ponds). Terrestrial risk assessments are generally applied to sites where soils may be impacted. Both address the concept of risk, but the concept of a "threshold" effect is more commonly employed. For example, a "safe" water quality or sediment quality criterion may be promulgated at the state or federal level and as long as a site-related concentration is below that benchmark, there will be no relative hazard to aquatic organisms. Likewise, very conservative soil screening values are developed for terrestrial organisms.

An exceedance of a laboratory-identified toxic threshold or regulatory benchmark for a particular environmental medium, however, does not automatically mean a receptor is at risk. Thresholds and benchmarks are derived to be conservative, in that they are considered protective of all species; however, they may not directly apply to a specific site, and the species and exposure assumptions may be different. One important site-specific difference is the foraging patterns of animals, many of which forage over a wide area (known as a home range) and are thus exposed to an "average" concentration, not just a single constituent concentration measured at a single location. Some also seasonally migrate in and out of areas, which reduces their potential for exposure.

Another aspect of ecological risk assessment is the concept of bioconcentration and/or bioaccumulation. Many constituents are metabolized and generally eliminated from the body. The inorganics associated with coal ash are generally taken up and eliminated from the body efficiently. However, some constituents, such as mercury, can accumulate in receptor tissues such that their body burden can be higher than for other constituents. Thus small amounts of constituents in the environment can be taken up by an organism and move up the food chain from lower to higher trophic level species.

The ecological risk assessment process is also conducted in a step-wise manner following the traditional ecological risk assessment paradigm. These steps are similar to those used in a human health risk assessment: problem formulation, exposure and toxicity assessment, and risk characterization. The difference lies in the types of receptors, the characterization of the habitat that supports the animals, and the food chain evaluation. USEPA has developed a detailed guidance for conducting ecological risk assessments used in federal and state programs (USEPA, 1997, 1998).

The USEPA has a very comprehensive eight-step process for the evaluation of risk to ecological receptors in the context of the ecological risk assessment paradigm (USEPA, 1997, 2015b). Step 1 consists of collection of available data. Step 2 is comprised of the development of a CSM and includes an initial screening process that utilizes hazard quotients (HQs). A HQ is simply the ratio of the environmental concentration (e.g., soil, water, sediment, and biota) to the ecological effect benchmark (typically a toxicity reference value). Decision rules are then applied to determine whether there is a potential for adverse effects. If the resulting HQ is equal to or less than unity (1), the potential for adverse effects due to that constituent is considered negligible and, therefore, can be dropped from further consideration of risk for the applicable exposure pathway. For values above unity, the potential for adverse effects to the receptor cannot be ruled out. At this decision point, additional investigation and/or a refinement of the risk assessment (e.g., using more realistic benchmarks, conducting field surveys, addressing bioavailability, and conducting laboratory bioassays) is conducted (USEPA, 1997, 1998). It is always important to keep in mind that the screening process depends upon the application of conservative assumptions, consistently biasing the results towards overestimating potential risks.

As discussed in the USEPA ecological risk assessment guidance (USEPA, 1999), information should be of sufficient quantity and quality to allow the risk assessor to make an informed decision about causality between levels of constituents and effects; that is, if the observed or predicted effect on the population or community is of sufficient magnitude, severity, extent, and duration to constitute harm and whether these effects appear to exceed the natural changes in the components typical of similar nonsite-impacted habitats (i.e., reference areas).

## 18.8 What does it mean for something to be toxic?

It is also important to understand that all constituents and materials that we encounter in our natural environment can be toxic. What determines whether a toxic effect actually occurs is how a person is exposed to the constituent, the amount of constituent to which someone may be exposed, and the timing and duration of that exposure. Without sufficient exposure the science tells us that there are no toxic effects. Put another way, when a toxic effect is demonstrated by a particular constituent, it is generally caused by high levels of exposure over a long-term duration. The fundamental principles here are:

- All constituents can exert toxic effects (from aspirin to table salt to water to minerals).
- For such toxic effects to occur, exposure must occur at a sufficiently high level for a sufficiently long period of time.
- If there is no exposure, there is no risk.

Aspirin can provide a simple real-world example of this concept. Aspirin is a safe and effective medication. It is present in many homes and used by many Americans. “Low-dose” aspirin is used by many adults on a daily basis to serve as a blood thinner to prevent strokes and heart attacks. Two aspirin every four hours can be taken to address headaches or muscle aches. However, it would be fatal if someone were to ingest an entire bottle of full-strength aspirin. Thus while there are many benefits to aspirin use, as noted in many toxicology texts, “it is the dose that makes the poison.”

This concept extends to all exposures to our environment. The type of effect and the nature of the effect that can be exerted by a constituent depend on the magnitude of the exposure or dose. At low exposures or doses, there may be no effects or minimal effects. As the exposure or dose increases, effects can occur, and those effects can be toxic at higher exposures and doses. Virtually everything can be toxic if the exposure or dose is high enough. Conversely, a constituent can only exert an effect if there is an exposure to the constituent. If there is no exposure, there is no effect, toxic or otherwise.

## 18.9 How is exposure evaluated?

In addition to understanding toxicity, to determine if there is a risk posed by a constituent, we also have to understand the potential for exposure. A CSM is used to evaluate the potential for human exposure to constituents that may have been released to the environment. Some of the questions posed during the CSM evaluation include:

> *What is the source? How can constituents be released from the source? What environmental media may be affected by constituent release? How and where do constituents travel within a medium? Is there a point where a receptor (human or ecological) could contact the constituents in the medium? Are the constituent concentrations high enough to potentially exert a toxic effect?*

The first step in developing the CSM is the characterization of the setting of the area of interest and the surrounding area. Current and potential future uses of the area and people who may potentially contact the environmental media of interest are then identified. Potential exposure scenarios and pathways are developed that describe how people may contact constituents released to the environment. Barriers to access, including engineering and institutional controls, are considered when evaluating whether a specific exposure pathway is complete.

For an exposure pathway to be complete, the following conditions must exist (as defined by USEPA, 1989):

1. A source and mechanism of chemical release to the environment.
2. An environmental transport medium (e.g., air, water, soil).
3. A point of potential contact with the medium by a receptor.
4. A receptor exposure route at the contact point (e.g., inhalation, ingestion).

A receptor in this context is a human that could hypothetically contact constituents that have been released to the environment. Unless all of the four above conditions are met, the potential exposure pathway will be deemed incomplete. Only complete exposure pathways can result in exposure to humans.

The concept of the complete exposure pathway is fundamental to risk assessment. If there is no complete exposure pathway, then there is no exposure by humans to the constituents, and there is no risk to human or ecological health. Thus unless all of the four listed conditions are met for a given environmental scenario, there is no complete exposure pathway, and there will be no human health or ecological risk posed by that scenario.

## 18.10 Target risk levels

Two types of risk are evaluated in a human health risk assessment: noncancer and cancer (USEPA, 2016a).

### 18.10.1 Target risk levels for noncancer effects

For noncancer effects, the USEPA toxicity values identify a level of exposure that is expected to not produce adverse effects. This safe level is the toxicity value, and is very conservative.

Under USEPA guidance, a predicted level of exposure to a constituent in the environment is compared to the noncancer toxicity value by using a ratio of the exposure to the toxicity value. If the predicted exposure is lower than the toxicity value, the ratio (also called a hazard quotient or HQ) is below 1, and no adverse effects are expected. [Exposure/Toxicity Value = Hazard Quotient]. If the exposure is higher than the toxicity value, the ratio is above 1. However, a result greater than 1 does not mean that adverse effects will necessarily occur. It means only that there is the potential for such effects based on this USEPA screening method, and further risk analysis is needed to decide if an actual, significant risk would exist. Thus, USEPA's target risk level for noncarcinogens is 1 (USEPA, 1991). When HQs are added, the sum is termed a hazard index (HI). If the initial HI is greater than one, then the HQs are summed for constituents that affect the same target organ or target endpoint (i.e., all HQs for constituents whose toxicity values are based on liver effects are added to derive a target endpoint-specific HI). It is the target endpoint-specific HI that is compared to the risk target of 1. Where the initial HI is below one, a target endpoint analysis is not needed.

### 18.10.2 Target risk levels for potential cancer effects

For constituents classified as potential carcinogens, the predicted level of exposure to a constituent is multiplied by a toxicity value developed by the USEPA that is used to predict the chance of cancer occurring as a result of the exposure, and the result is referred to as the cancer risk (USEPA, 2016b). USEPA defines a target risk range for potential carcinogens of one in one million (1 in 1,000,000 or $1 \times 10^{-6}$) to one in ten thousand (1 in 10,000 or $1 \times 10^{-4}$). Thus the USEPA target risk range is between one in one million and one in ten thousand chance of developing cancer as the result of a specific exposure. A risk that falls within that range (1 in 10,000 to 1 in 1,000,000) or below that range is considered acceptable.

The target risk range is based on USEPA guidance. Specifically, USEPA provides the following guidance (USEPA, 1991):

> *"Where the cumulative carcinogenic site risk to an individual based on reasonable maximum exposure for both current and future land use is less than $10^{-4}$, and the non-carcinogenic hazard quotient is less than 1, action generally is not warranted unless there are adverse environmental [i.e., non human-health] impacts."*
>
> *"The upper boundary of the risk range is not a discrete line at $1 \times 10^{-4}$, although EPA generally uses $1 \times 10^{-4}$ in making risk management decisions. A specific risk estimate around $10^{-4}$ may be considered acceptable if justified based on site-specific conditions."*

To understand the USEPA target risk range in context, it is important to recognize that the background cancer risk in the United States is generally one in two for men

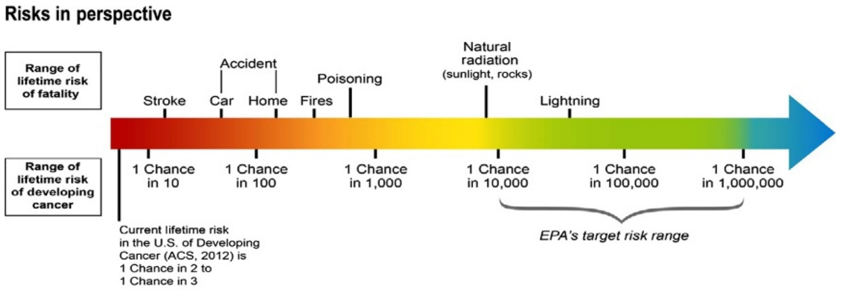

*- Adapted from U.S. EPA 450/3-90-022, Mar. 1991, http://www.epa.gov/air/oaqps/air_risc/3_90_022.html (1996)*
*- American Cancer Society. 2012. Cancer Facts and Figures 2012.*
*http://www.cancer.org/acs/groups/content/@nho/documents/document/acspc-024113.pdf*

**Fig. 18.5** Risks in perspective.

(0.5 or $5 \times 10^{-1}$) and one in three for women (0.33 or $3.3 \times 10^{-1}$), based on statistics published annually by the American Cancer Society (ACS, 2016). Thus the USEPA regulatory target risk range is 4–6 orders of magnitude lower than the background cancer rates in the U.S. This is illustrated graphically in Fig. 18.5. The background cancer rate in the United States is shown on the left-hand side of the arrow, with risk levels decreasing towards the right. The USEPA target risk range is shown on the right-hand side of the risk arrow. The other risks illustrated on the arrow are the risk of fatalities based on measurements for the US population. Risks of occurrence of these outcomes would be higher (i.e., those risks would move to left-hand side on the risk arrow); for example, the risk over a lifetime of being hit by lightning is 10 times higher than the risk of dying from a lightning strike, according to the National Weather Service (NWS, 2015). Thus the target risk range USEPA uses for regulatory decision making is lower than a person's chances of being struck by lightning.

## 18.11 USEPA uses toxicity and exposure information for environmental assessment

USEPA uses the steps of risk assessment and information on the potential toxicity of constituents and assumptions about exposure to identify concentrations of trace elements in soil in a residential setting that are considered by USEPA to be protective for humans (including sensitive groups) over a lifetime. Specifically, residential soil screening levels are levels that are protective of a child and adult's daily exposure to constituents present in soil or a solid matrix over a residential lifetime. In the context of regulatory decision making, at sites where constituent concentrations fall below these screening levels, no further action or study is warranted under the federal Superfund program. The USEPA provides screening levels for constituents in residential soil (and other media, including tap water) for over 750 constituents (USEPA, 2016a).

Fig. 18.6 shows these residential soil screening levels for the trace elements that are present in coal ash (USEPA, 2016a). The USEPA considers it safe for children to be exposed to these concentrations of each of these trace elements in soils on a daily basis throughout their lifetime. What this tells us is that by developing these residential

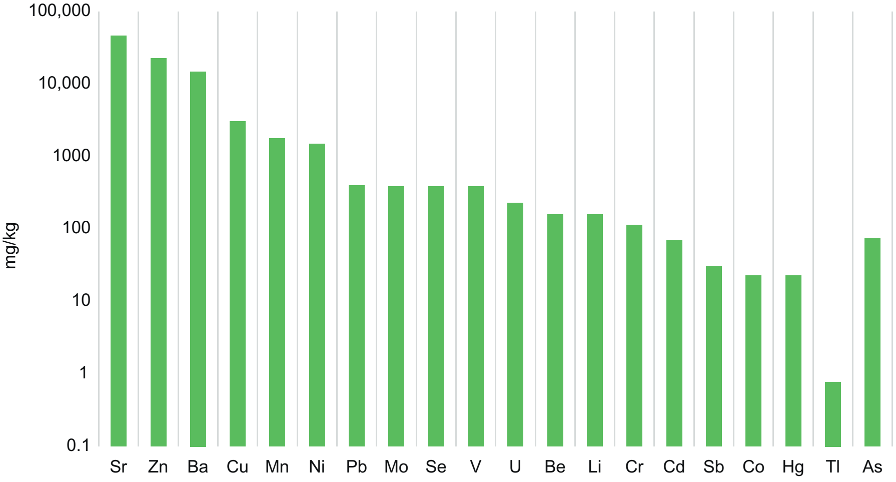

Source: USEPA, 2016. Residential soil screening levels. May. https://www.epa.gov/risk/regional-screening-levels-rsls

**Fig. 18.6** USEPA regional screening levels for residential soils.

soil-screening levels, the USEPA considers the presence of these levels of these constituents in soils to be safe for humans, even for exposure on a daily basis. It is, therefore, simply not true that there are no safe levels of exposure to these constituents.

This concept is also true for ecological receptors. Ecological screening levels are designed to provide a conservative estimate of the concentration to which an ecological receptor can be exposed without experiencing adverse health effects. Due to the conservative methods used to derive screening levels, it can be assumed with reasonable certainty that concentrations below screening levels will not result in any adverse effects to survival, growth, and/or reproduction, and, therefore, no further evaluation is necessary. Concentrations above conservative RSLs, however, do not necessarily indicate that a potential ecological risk exists, but rather that further evaluation may be warranted.

## 18.12 Using USEPA screening levels to evaluate coal ash

With only a few exceptions, constituent concentrations in coal ash are below human health screening levels developed by the USEPA for residential soils and are similar in concentration to background US soils. The American Coal Ash Association (ACAA) released a study, titled "Coal ash material safety: A health risk-based evaluation of USGS coal ash data from five US power plants," that evaluated data on constituent concentrations in a variety of coal ashes from across the United States (ACAA, 2012). The report addressed the potential risk to human health from direct contact with coal ash.

Fig. 18.7 shows the range of concentrations of trace elements in fly ash (top panel) compared to the USEPA residential soil screening levels for these trace

**Comparison of 10th and 90th percentile USGS database constituent concentrations in fly ash and background levels in US soils to the USEPA regional screening levels for residential soils**

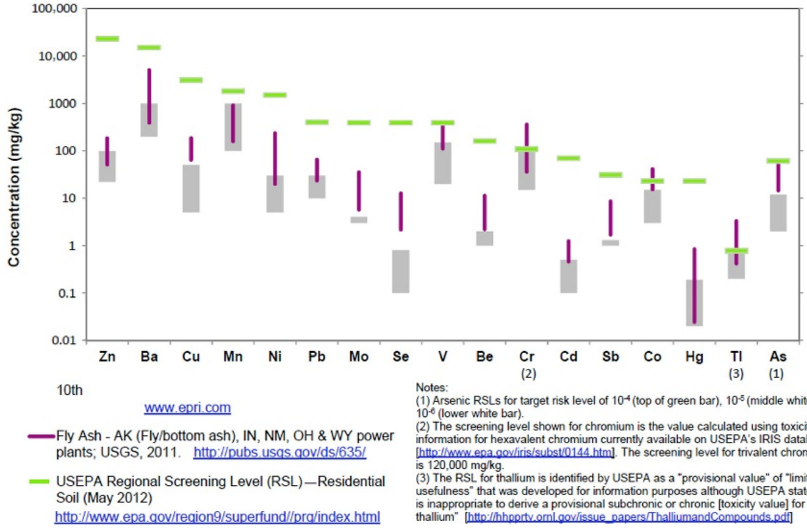

Notes:
(1) Arsenic RSLs for target risk level of $10^{-4}$ (top of green bar), $10^{-5}$ (middle white bar), $10^{-6}$ (lower white bar).
(2) The screening level shown for chromium is the value calculated using toxicity information for hexavalent chromium currently available on USEPA's IRIS database [http://www.epa.gov/iris/subst/0144.htm]. The screening level for trivalent chromium is 120,000 mg/kg.
(3) The RSL for thallium is identified by USEPA as a "provisional value" of "limited usefulness" that was developed for information purposes although USEPA states "it is inappropriate to derive a provisional subchronic or chronic [toxicity value] for thallium" [http://hhpprtv.ornl.gov/issue_papers/ThalliumandCompounds.pdf]

**Comparison of 10th and 90th percentile USGS database constituent concentrations in bottom ash and background levels in US soils to the USEPA regional screening levels for residential soils**

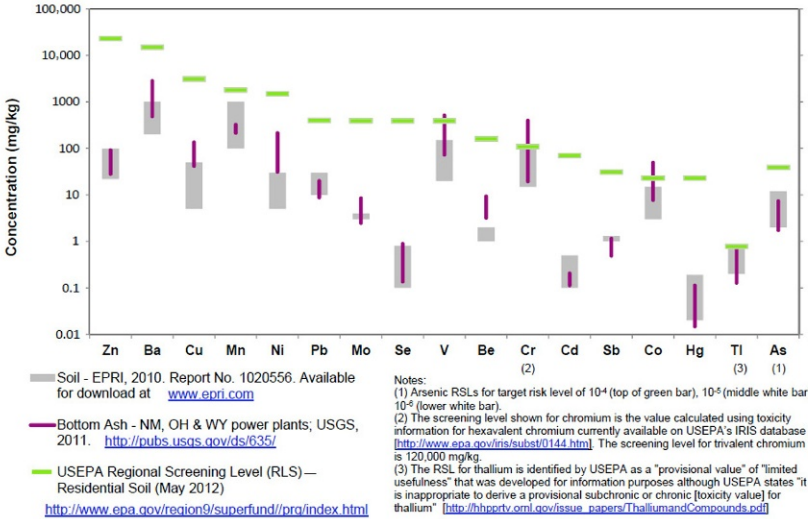

Notes:
(1) Arsenic RSLs for target risk level of $10^{-4}$ (top of green bar), $10^{-5}$ (middle white bar), $10^{-6}$ (lower white bar).
(2) The screening level shown for chromium is the value calculated using toxicity information for hexavalent chromium currently available on USEPA's IRIS database [http://www.epa.gov/iris/subst/0144.htm]. The screening level for trivalent chromium is 120,000 mg/kg.
(3) The RSL for thallium is identified by USEPA as a "provisional value" of "limited usefulness" that was developed for information purposes although USEPA states "it is inappropriate to derive a provisional subchronic or chronic [toxicity value] for thallium" [http://hhpprtv.ornl.gov/issue_papers/ThalliumandCompounds.pdf]

**Fig. 18.7** Fly ash and bottom ash comparisons.

elements and background concentrations from USGS data. The vertical purple bars represent the 10th to 90th percentile ranges for each constituent in fly ash. The vertical gray bars represent the 10th to 90th percentile ranges for each constituent in background soils in the United States. The horizontal green bars identify the USEPA RSL for residential soils. The bottom panel shows the same comparison for bottom ash. Of the 20 trace elements evaluated in the full report, 15 are present in *all* ashes included in the evaluation at concentrations *less* than the USEPA screening levels for residential soils. These are: antimony, barium, beryllium, cadmium, copper, lead, lithium, manganese, mercury, molybdenum, nickel, selenium, strontium, uranium, and zinc. Concentrations of five constituents range to above the residential soil screening level in some but not all of the coal ashes: arsenic, chromium, cobalt, thallium, and vanadium. Moreover, these concentrations are only slightly above the screening levels.

## 18.13 Studies testing the toxicity of coal ash

The previous seven sections have discussed the per-constituent approach to risk assessment that is most commonly used in the United States. The ACAA report showed that constituent concentrations in coal ashes are generally similar to those in US soils, and the results indicate that with few exceptions, constituent concentrations in coal ash are below screening levels for residential soils. To evaluate coal ash as a material rather than as its components parts, studies of coal ash with respect to various types of potential toxic effects have been conducted under the EU Registration, Evaluation, Authorization, and Restriction of Chemicals program (REACH, 2007). REACH enforces strict guidelines on companies that manufacture, import, or use 1 ton of chemicals per year or more in the EU. These companies must collect information on the properties of the substances and communicate it to the European Chemical Agency (ECHA) through a registration dossier. REACH uses a weight of evidence approach to categorize scientifically valid information from animal and human toxicity data that are available. REACH requires the submission of information on substance identity, physicochemical properties, mammalian toxicity, ecotoxicity, environmental fate, including abiotic and biotic degradation, and information on manufacture and uses, as well as risk management measures.

The mammalian (i.e., applicable to human health) testing results are classified based on degrees of the severity of toxicity in terms of dose response. Chemicals that have low or no toxicity at high levels of dose are "not classified," meaning that exposure is not likely to cause a hazard. While some of the information on the registrations is proprietary, the results of the toxicity testing are available. Available mammalian data were compiled for materials classified as "Ashes, Residues" with an EC# 931-322-8, where the EC# is a unique seven-digit identifier that is assigned to chemical substances for regulatory purposes within the EU by the regulatory authorities. The results are shown in Table 18.3. A wide range of mammalian toxicity tests (7 publications and 25 study reports for a total of 34 studies) has been conducted on coal ash

**Table 18.3 REACH CCP human health toxicity data for "Ashes, Residues" EC# 931-322-8**

| Endpoint | Publications | Study reports | Conclusion |
|---|---|---|---|
| *REACH CCP human health toxicity data (a)* | | | |
| Acute oral toxicity | 0 | 3 | Not classified as hazardous |
| Acute inhalation toxicity | 1 | 0 | Not classified as hazardous |
| Acute dermal toxicity | 0 | 2 | Not classified as hazardous |
| Skin irritation | 0 | 8 | Not classified as hazardous (7)<br>Inconclusive (1) |
| Eye irritation | 0 | 4 | Not classified as hazardous (3)<br>Inconclusive (1) |
| Skin sensitization | 0 | 2 | Not classified as hazardous |
| Repeated dose inhalation toxicity | 3 | 0 | Not classified as hazardous |
| Repeated dose oral toxicity | 1 | 1 | Not classified as hazardous |
| Genetic toxicity | 1 | 4 | Not classified as hazardous |
| Reproductive toxicity | 1 | 1 | Not classified as hazardous |
| Carcinogenicity | NA | NA | Not classified as hazardous |
| Total | 7 | 25 | 34 |

Notes:
CCP: Coal combustion product.
EC#: European Commission Number.
NA: Not available.
REACH: Registration, Evaluation, Authorization and Restriction of Chemical substances.
(a) Information on REACH obtained from the European Chemicals Agency, Chemical Substances Search (http://echa.europa.eu) and the search term: Ashes, Residues EC# 931-322-8.

under the REACH program, and all of the results indicate "Not Classified as Hazardous." This means that the results of the toxicity tests on coal ashes either showed no toxic responses or very mild responses at high levels of exposure; such results do not warrant classification as a hazard under the REACH system, and thus a conclusion of "Not Classified as Hazardous" was made.

Environmental data (i.e., aquatic toxicity) may be required as part of the dossier submitted in support of registration under REACH. Included in the REACH dossier for CCP "Ashes, Residues" EC# 931-322-8 is both acute and chronic aquatic toxicity data. In accordance with the classification labeling and packaging (CLP) requirements, the hazard classification for the acute and chronic aquatic toxicity endpoints requires evaluation of data at three trophic levels (fish, invertebrates (crustacea), and algae). In addition, the data is looked at as a whole, giving higher weight to those studies conducted in accordance with standard methods and good laboratory practice

(GLP). Once the entire dataset has been reviewed for the endpoint the overall classification for the substance for both acute and chronic aquatic toxicity is proposed within the dossier. A summary of the key studies for each tropic level and endpoint are summarized in Table 18.4. As part of the overall REACH dossier for CCP "Ashes, Residues" (EC# 931-322-8), no classification was proposed for the aquatic toxicity endpoints based on an extensive set of studies; that is, the determination was made that the ashes are "Not Classified as Hazardous."

Thus the results of the extensive study on the mammalian and aquatic toxicity of coal ash as a whole material, not just its component parts, under the REACH program indicate that coal ash is "Not Classified as Hazardous."

**Table 18.4** **REACH CCP summary of key aquatic toxicity studies for "Ashes, Residues" EC# 931-322-8**

| Endpoint (b) | Test guideline | Study duration | Effect level | Classification (c) (d) |
|---|---|---|---|---|
| *REACH CCP aquatic toxicity studies (a)* | | | | |
| Acute toxicity fish | OECD Guideline 203 | 96 hours | LL50 > 100 mg/L | Not classified as hazardous |
| Acute toxicity invertebrates | OECD Guideline 202 | 48 hours | EL50 > 100 mg/L | Not classified as hazardous |
| Acute toxicity algae | OECD Guideline 201 | 72 hours | EL50 = 30 mg/L | Not classified as hazardous |
| Chronic toxicity invertebrates | OECD Guideline 211 | 21 days | NOEL = 2.2 mg/L | Not classified as hazardous |
| Chronic toxicity algae | OECD Guideline 201 | 72 hours | NOEL = 4.6 mg/L | Not classified as hazardous |

Notes:
CCP: Coal combustion product.
EC#: European Commission Number.
EL50: Effective loading 50%.
LL50: Lethal loading 50%.
NOEL: No observable effect level
OECD: Organization for economic cooperation and development.
REACH: Registration, Evaluation, Authorization, and Restriction of Chemical Substances
(a) Information on REACH obtained from the European Chemicals Agency, Chemical Substances Search (http://echa.europa.eu) and the search term: Ashes, Residues EC# 931-322-8.
(b) A chronic toxicity study for fish was also presented in the REACH dossier; however, a NOEC could not be derived based on the data and therefore was not included in the table above.
(c) As part of the overall REACH dossier for CCP "Ashes, Residues" (EC# 931-322-8), no classification was proposed for the aquatic toxicity endpoints.
(d) In addition to the key studies presented in the table above a number of supporting studies were also summarized in the REACH dossier. The results from these studies support the conclusions based on the key studies that no classification is warranted for the acute or chronic aquatic toxicity endpoints.

## 18.14 Site-specific conceptual site models

As noted above, CSMs are used on a site-specific basis to evaluate the potential for exposure and risk posed by constituents at a given facility or coal ash management area. The CSM is used to identify potentially complete exposure pathways by evaluating the source → transport → environmental medium → exposure linkage. The CSM can then be used to identify where data gaps may exist by asking the question: What data are needed to determine if the exposure pathway is complete, and if so, is there is a risk associated with that pathway?

It is also important to remember in the context of a CSM that not all complete exposure pathways result in a risk to human health. For a human health risk to exist, the exposure must be of a sufficient magnitude and frequency. If the exposure pathway is complete, but the magnitude or concentration of a constituent in the environmental medium is below health risk-based levels, then the exposure would not pose an adverse risk. Thus an exposure pathway could be complete, but it will be insignificant on a health risk basis.

The following is a general discussion of a CSM for a coal ash management facility. The purpose of this discussion is to identify the potential components of the source → transport → environmental medium → exposure linkage. Because workers are addressed by facility health and safety plans and OSHA requirements, the receptors of interest for this discussion are members of the public and ecological receptors.

Generally, coal ash is managed in a landfill/stacking operation or in an impoundment. While newer landfills and impoundments may be lined, historically liners were not commonly used. The operations of a coal-fired power plant require large amounts of cooling water, thus these power plants are commonly located along large bodies of water, generally rivers, and consequently the coal ash management facilities are also located on or near a river or large body of water. These coal ash management facilities constitute the source term for the CSM.

Potential exposure pathways include:

- Direct contact with the coal ash at the management facility.
- Inhalation of air-borne dust generated at the management facility.
- Leaching of constituents from the coal ash into water, migration of that water into groundwater and subsequent transport with groundwater flow to downgradient areas, and ultimately discharge to a surface water body.

Each of these potential exposure pathways is discussed in turn below.

As power plants are generally secure facilities, direct contact with coal ash at a disposal facility by a member of the public is not a complete exposure pathway. Even if direct contact exposure was to occur, the majority of constituent concentrations in coal ashes are below health RSLs for a daily residential exposure scenario, as previously discussed.

The residential scenario upon which the USEPA RSLs are formed (USEPA, 2016a) also includes a component that addresses the inhalation of an airborne dust pathway, and thus the USEPA's RSLs are protective of that potential inhalation exposure. Based on this comparison, dust that could be generated from a landfill operation or an inactive dewatered area of an impoundment is unlikely to be transported offsite at a concentration that could pose a risk to human health. This conclusion is supported by the CCR risk assessment conducted by the USEPA in support of the CCR rule-making (USEPA, 2014b). From Section 3.5.1 of the risk assessment:

> *"EPA calculated ambient air concentrations that result from windblown dust from landfills under uncontrolled and controlled management scenarios. Risks were estimated for based on short-term (i.e., acute) and long-term (i.e., chronic) exposures. Under the uncontrolled management scenario, concentrations of arsenic were found to pose acute risks and PM2.5 was found to exceed the 24-hour NAAQS [National Ambient Air Quality Standards]. However, all risks fell below selected criteria under the controlled management scenario. Based on these results, EPA did not retain exposures to ambient air for further analysis. Even with the conservative assumptions used here, risks fell below selected criteria when dust controls were considered. Thus, these screening results are sufficient to characterize high-end risks for this pathway, and the controls required by the rule are considered protective."*

This leaves the groundwater pathway as the primary pathway for potential exposure. Both the physical and chemical characteristics of the coal ash are affected by the origin (chemistry) of the original coal as well as the processes within the power plant that create the coal ash. These factors in turn affect the behavior of these materials in the environment, specifically the potential for constituents to migrate from the coal ash into groundwater systems. The release of constituents from coal ash in a disposal area via leaching and subsequent transport in the environment is the most complicated potential exposure pathway, consisting of:

1. *Partitioning of constituents in coal ash to water via a process called leaching*. The resultant water is referred to as leachate or ash porewater. This partitioning is a function of the type of coal ash, its physical characteristics, the concentration of the constituent in the coal ash, the solubility of the constituent, and the chemical properties of the infiltrating or ambient water including pH, among other factors.
2. *Movement of constituents in the leachate from the disposal area through the underlying soil column to the underlying groundwater*. Attenuation of constituent concentrations in the leachate can occur in the soil column due to adsorption and chemical reaction with the soils. In some cases, these attenuating mechanisms in the unsaturated zone may not apply if the ash is in direct contact with groundwater.
3. *Movement of constituents with groundwater flow in the uppermost groundwater zone*. Constituent concentrations will initially dilute when mixed with the groundwater flow, and further attenuation in concentration can take place via dispersion with groundwater flow and via reactions with the soil matrix through either adsorption and/or a chemical reaction.
4. *Upon a groundwater discharge to surface water, constituent concentrations will mix with the surface water*. Where surface water bodies are large, there is more surface water in which this mixing can occur.

Receptors that could contact constituents released via these potential exposure pathways include:

1. Groundwater:
   a. Users of groundwater. For this receptor pathway to be complete, the drinking water well (or spring) would have to be located hydraulically downgradient of the coal ash management area and located where constituents released from coal ash leachate are present in the groundwater.
2. Surface water:
   a. Users of surface water, if the surface water intake is located downstream of the coal ash management area.
   b. Recreational users of the surface water body, including swimmers, boaters, and anglers.
   c. Ecological/wetland-dependent receptors in the surface water body.

Site-specific evaluation of each of these potential exposure pathways is needed to determine if they are complete.

For use of groundwater as drinking water, a determination first needs to be made as to whether the potential receptor point is located downgradient from a coal ash management area. If a receptor point is in a downgradient location, then groundwater sampling and analysis can be used to identify whether coal ash-derived constituents are present at the receptor point at concentrations that are above background levels and then at concentrations that are above drinking water standards and/or RSLs.

For the evaluation of surface water, it can be measured directly, or groundwater data can be used as an input to models, either simple or complex, to predict current and/or future surface water concentrations. These modeled and/or measured data can also be used in a site-specific risk evaluation.

## 18.15 How is risk assessment used on a site-specific basis?

Once a CSM has been developed, generally a tiered risk-based approach is used to evaluate the data based on the potentially complete exposure pathways identified in the CSM. This is the logical approach used by the USEPA for it various regulatory programs, including the Superfund program, and the process is described in the User's Guide for their RSLs (USEPA, 2016a). The approach is common to many state programs.

A tiered risk-based approach is a process that moves from simple to more complex evaluations using increasingly more site-specific data and refinements. For example:

- Tier 1—Simple screening by comparison to RSLs
- Tier 2—Use of site-specific data to refine the RSLs
  - Consider whether exposure pathway is complete or not
  - Consider simple refinements to regulatory default exposure assumptions
  - Consider the applicability of toxicity information used in the screening levels (ecological component)
- Tier 3—Detailed site-specific risk assessment or development of site-specific screening levels or cleanup levels (can include probabilistic evaluation)

For example, whether or not a drinking water pathway is identified as complete at a given site, comparison of groundwater data to drinking water standards [such as federal maximum contaminant levels, or MCLs (USEPA, 2012)] and to USEPA RSLs (USEPA, 2016a), is a conservative first step in the risk assessment process.

RSLs are designed to provide a conservative estimate of the concentration to which a person (receptor) can be exposed without experiencing adverse health effects. Due to the conservative methods used to derive RSLs, it can be assumed with reasonable certainty that concentrations below screening levels will not result in adverse health effects and that no further evaluation is necessary. Concentrations above conservative RSLs do not necessarily indicate that a potential risk exists, but they do indicate that further evaluation may be warranted.

Human health RSLs for groundwater are generally derived to be protective of the use of groundwater as a drinking water source. Human health RSLs for surface water are generally derived to be protective of the use of surface water as a drinking water source and the consumption of fish from a surface water body. The drinking water screening levels are also protective of recreational uses of a surface water body (such as swimming or boating) because drinking water exposure is of a higher magnitude and frequency.

Constituent concentrations below drinking water standards are unlikely to pose risk via other groundwater or surface water exposure pathways, and these constituents can be eliminated from further evaluation at this step. Similarly, there are no complete groundwater exposure pathways for ecological receptors, but comparison of groundwater data to ecological RSLs is a conservative first step that can be used to focus further evaluation on those constituents whose concentrations may be above the RSLs.

In the second tier of evaluation, modeling can be used to predict environmental media concentrations (for which data are not available) or to predict future concentrations, and/or more realistic screening levels can be used that reflect the potentially complete exposure pathways. For example, if groundwater is not used as a source of drinking water, but it discharges to a surface water body where a public drinking water intake exists some distance away, then the modeling that accounts for constituent fate and transport between the point of discharge and the drinking water intake can be used to predict surface water concentrations at the intake point, which can then be compared to drinking water standards. Alternatively, surface water concentrations, either predicted or measured, can be compared to RSLs calculated for recreational exposures (e.g., incidental ingestion and dermal contact while swimming).

The third tier of evaluation is generally a full risk assessment of those constituents that did not “screen out” in previous steps. Even in a second-tier evaluation, RSLs generally employ conservative assumptions and target risk levels. Tier three can utilize site-specific exposure pathways, site-specific exposure assumptions, and more detailed fate and transport modeling, and the results can be compared to a full-target risk range, rather than a specific target risk level. Risk drivers, if any, are identified at the end of this evaluation and can be the focus of remedial action.

Another important concept in a risk assessment is the weight of evidence approach. This considers that single results above a screening value, whether generic or site specific, do not indicate harm, and that results need to be considered spatially and temporally. USEPA recognized this in its CCR Final Rule (USEPA, 2015a). Groundwater monitoring requirements include sample collection over time, definition of background conditions, and statistical comparison of downgradient results to upgradient results before a determination can be made if there is a release or a condition where a constituent is present in groundwater above a standard that would require regulatory action.

## 18.16 How common is a complete groundwater drinking water pathway?

As previously noted, for a drinking water pathway to be complete, the drinking water well would have to be located hydraulically downgradient of the coal ash management area, and the well would have to be screened in the aquifer where constituents may have been released. A well that is located downgradient of a coal ash management area but screened (i.e., draws water from) at a depth that is 100 or more feet below ground surface is unlikely to be impacted by a release, especially if there is a geological layer that serves to separate the shallow groundwater from the deeper groundwater (called an aquitard). Similarly a drinking water pathway would not be complete for a well that is located hydraulically downgradient of the coal ash management area and screened at a shallow depth, but is not within the area of groundwater affected by coal ash leachate.

The USEPA’s CCR Rule (USEPA, 2015a) is based on a risk assessment that evaluated potential risk to users of groundwater as drinking water. Although the USEPA made improvements to how the risk assessment groundwater modeling was conducted, no context is provided for how common a complete groundwater drinking water pathway in areas downgradient of a coal ash management area may be in the United States.

The USEPA states in the CCR Rule “Under sections 1008(a) and 4004(a), EPA must establish national criteria that will operate effectively in the absence of any guaranteed regulatory oversight (i.e., a permitting program), to achieve the statutory standard of “no reasonable probability of adverse effects on health or the environment” at all sites subject to the standards.” USEPA has used the results of the CCR risk assessment to support the conclusion that there is a reasonable probability of adverse effects on health or the environment, therefore, national standards are needed for CCR disposal.

Specifically, the 90th percentile risk result for arsenic (III) for surface impoundments ($2 \times 10^{-4}$) is the only result that is above the $1 \times 10^{-5}$ risk level, which is the initial “level of concern” used by the USEPA for candidates for regulation. All other risks are at or below the $1 \times 10^{-5}$ level. Arsenic (III), lithium, and molybdenum for the surface impoundment scenario are above the target HQ of 1. The USEPA also notes “No 90th percentile risks above ecological criteria were identified for either surface impoundment or landfills. No 50th percentile risks above human health or ecological criteria were identified for either surface impoundment or landfills.” However, the surface impoundment risks are provided without reference to what populations in the United States may be affected.

As part of the evaluations conducted to help inform USEPA's rulemaking process after releasing the proposed CCR Rule in 2010, the Electric Power Research Institute (EPRI) conducted an aerial evaluation of over 500 coal-fired power plants in the United States. They identified less than 3,000 structures that could be dwellings located downgradient of a coal ash management area, in areas not likely served by municipal water. Based on US Census data that identifies 2.6 persons per household in the United States (USCB, 2016), potentially 7770 people out of 318,857,056 people in the United States in 2014 (USCB, 2016) may have been living downgradient of a coal ash management area and may have been using drinking water from a well. It is not possible from this analysis to determine if such wells exist, and if they would be screened in the area of an aquifer impacted by coal ash leachate. Thus, the USEPA's national risk assessment for coal ash disposal and the resulting risk estimates could at most apply to less than 0.002% of the US population.

The Preamble to the Rule identifies the highest "90th percentile nationwide probabilistic risk results" as an excess lifetime cancer risk of $2 \times 10^{-4}$ for arsenic (III) for an unlined surface impoundment. This hypothetical cancer risk is equivalent to a 2 in 10,000 chance of developing cancer over a lifetime. Assuming that all of the 7770 people identified above could potentially be using shallow groundwater downgradient from an unlined surface impoundment as drinking water, hypothetically one or two cancer cases could occur in this population.

To put these results in perspective, it is important to compare these estimated results to the rate of cancer incidence in the United States. The American Cancer Society (ACS, 2016) provides annual reports on the rate of cancer incidence in the US population. The statistics published in 2016 indicate that one in two males and one in three females will develop cancer over their lifetime (these statistics do not include cases of skin cancer). For this estimated downgradient population of 7770 and a US population that is 50% male/female (USCB, 2016), this equates to 3237 background cancer cases, which is well above the hypothetical one or two cancer cases that could occur, as estimated by USEPA as a result of releases from a coal ash surface impoundment.

## 18.17 Risk evaluations of the TVA Kingston release

The most salient information about the potential impact of coal ash-derived constituents on an aquatic environment is provided by the extensive studies conducted by the Tennessee Valley Authority (TVA) under the USEPA-led Superfund program under a baseline ecological risk assessment (TVA, 2012a). These studies are summarized in a series of technical papers recently published in the peer-reviewed journal *Integrated Environmental Assessment and Management* (IEAM, 2015).

The papers in this series address the potential ecological effects of the residual ash in the Watts Bar Reservoir. The investigation was conducted under USEPA regulatory authority, using a consensus-based approach that involved the regulatory agencies, stakeholders, and the public to ensure that the study was designed and executed to meet the wide range of objectives representing the diverse group of participants.

The papers include the following: problem formulation for the river system to set the stage for the quantitative ecological evaluation; sediment toxicity test procedures and results; benthic community analysis techniques and results; methods and results of evaluation of risk to fish and riparian and aquatic wildlife; an extensive analysis characterizing risk to the insectivorous tree swallow; and finally how the Baseline Ecological Risk Assessment (BERA) results were used in the postdredging management decisions made in the context of USEPA regulatory programs.

The evaluations were constructed to be conservative; that is, they were likely to overestimate rather than underestimate risk. Even under this conservative scenario, results show that:

- Collectively the data and analyses indicate that ash and ash-related constituents pose negligible risks to the fish communities.
- It appears that where ash comprises less than approximately 40% of the sediment, there are no discernible impacts to the benthic community; toxicity that occurred in areas with >40% ash in the sediment was primarily correlated with exposure to arsenic, where arsenic levels were significantly greater than the probable effects concentration for benthic systems for arsenic of 33 mg/kg. The results also suggest that native sediments, where residual ash is <40% have some capacity to bind arsenic, thereby reducing its bioavailability.
- The severity of the initial effects appeared to be limited to the physical smothering of benthic organisms, and the benthic community recolonized the ecosystem quickly.
- Conditions at the site appear to have resulted in short-term impacts to the benthic community, with a quick response occurring after the bulk of the ash was removed from the system. The analysis of benthic community structure showed, at most, a weak correlation with the percent of ash in the sediment, further illustrating the lack of benthic invertebrate population and community-level effects.
- For wildlife, TVA evaluated risks using a weight of evidence approach, using multiple lines of evidence to evaluate the potential toxicity of 17 different receptors representing a broad range of species, feeding habits and behaviors, trophic levels, assessment metrics, and sampling seasons. The results indicate minimal ecological risk to most organisms and only low risks to insectivorous birds.

These results indicate the resiliency of ecosystems in being able to respond and recover from a catastrophic release of coal ash, and the importance that the immediate dredging activities had in shaping that outcome.

While this series of papers addresses the ecological evaluation of the release, the evaluation of human health was also an important component of the larger project. These evaluations include the following:

- A Human Health Risk Assessment was conducted under USEPA oversight and guidance, and the results indicated no ash-related risks to humans that exceeded USEPA guidelines for acceptable risk (TVA, 2012b).
- The Agency for Toxic Substances and Disease Registry (ATSDR) and the Tennessee Department of Health (TDOH) Public Health Assessment to address potential effects of exposure to the ash after the release concluded, "no harm to the community's health is expected from touching the coal ash. This includes children who might touch the ash while playing" (ATSDR, 2010).
- Oak Ridge Associated Universities (ORAU) and Vanderbilt University Medical Center conducted a health study of participating area residents and concluded, "No adverse health

> effects were found among those Roane County residents who elected to participate in medical evaluations following the Dec. 2008 fly ash spill at TVA's Kingston Fossil Plant" (ORAU, 2010a, 2010b).

These technically sound and scientifically defensible results are in stark contrast to the dire predictions of harm that were reported soon after the release.

The results presented here show overall that risks were demonstrated to be low or negligible across the ecosystem, with risks to a few ecological receptors identified as either moderate (benthic) or low (tree swallows). However, ecological community-based evaluations showed few to no measureable impacts. As discussed in more detail in the papers (IEAM, 2015), USEPA regulation addresses leaching to groundwater as the pathway of concern, with subsequent groundwater flow into surface water bodies. The evaluation of the Kingston release can be seen as a worst-case scenario for ecological exposures to ash and ash-related constituents of interest in a primarily flowing/river aquatic environment, and here for the direct release of coal ash to the river, conservatively estimated ecological risks were determined to be limited in magnitude and likelihood.

## 18.18 Evaluations of the Dan River spill in North Carolina

On Feb. 2, 2014, there was a coal ash release from the Duke Energy Dan River Steam Station in Eden, NC, to the Dan River. Approximately 38,000 tons of coal ash were released due to a failed pipe below an ash pond. It is important to provide context for this event; the release was much smaller than the Kingston release, and the river exhibited recovery from the release much as at Kingston. Several studies have been conducted of the Dan River, as discussed below.

### *18.18.1 Agricultural study*

A North Carolina State University report was published in Apr. 2014, titled "Assessment of trace-element impacts on agricultural use of water from the Dan River following the Eden Coal Ash Spill" (NC State, 2014). The report concludes:

- Total concentrations of trace elements ("total metals") in the Dan River water declined sharply from maximum levels that were typically measured 1 day after the ash release.
- Concentrations measured 2.2 miles downriver of the spill site were equivalent to upstream concentrations within 3 days after the coal ash release.
- River water is suitable for use as irrigation water on crops and as drinking water for livestock.
- Trace-element influx during flooding of agricultural areas will have only a marginal impact on soils and crops.

### *18.18.2 Health evaluation of the Dan River*

The North Carolina Department of Health and Human Services (DHHS) conducted an evaluation of the potential health threats as a result of the release. In Jul. 2014, they concluded (NC DHHS, 2014):

- DHHS is recommending lifting the recreational water advisory after evaluating the most recent available surface water and sediment data from the Dan River downstream from the coal ash spill.
- DHHS has evaluated sediment and surface water data collected after the work was completed that confirms that no incidental ingestion or skin contact risk exists for the sediment or the river water.
- Contaminants associated with the coal ash spill are at levels that should not pose a health risk during recreational use of the river.
- A potential fish and shellfish consumption hazard still exists immediately downstream of the release. DHHS recommends that people not consume any fish or shellfish collected from the Dan River in North Carolina downstream of the Duke Power-Eden spill site. As of Jul. 2016, this advisory has not been lifted (NC DHHS, 2016).

### *18.18.3 Health evaluation of the Kerr Reservoir*

In May 2014, the USEPA issued a fact sheet addressing community concerns over use of the Kerr Reservoir, which is 80 miles downstream of the Dan River facility (USEPA, 2014a). USEPA concluded, "There have been no exceedances in human health screening in the surface water samples collected from Kerr Reservoir for contaminants of concern from the coal ash." The agency also notes that the Dan River and Kerr Reservoir were already under fish advisories prior to the release due to constituents not related to coal ash.

### *18.18.4 Benthic evaluation of the Dan River*

In Nov. 2014 the NC Department of Environmental Quality (DEQ) released a statement about their evaluation of aquatic insect communities upstream and downstream of the Dan River spill (NC DEQ, 2014).

In Oct. 2014 the DEQ sampled upriver and downriver of the Dan River spill for "benthic macroinvertebrates, or small insects and other invertebrate animals that live on or near the bottom of the Dan River. Benthic macroinvertebrate species diversity and population estimates provide an excellent indicator of the overall health of a body of water." The State notes, "The populations from the upstream and downstream sites were similar and were considered 'Excellent,' which is the highest biological rating available."

Much like at Kingston, the Dan River ecosystem has thus rebounded from the release.

## 18.19 Evaluations of private well water in the vicinity of North Carolina ash ponds

North Carolina passed the Coal Ash Management Act (CAMA) of 2014 (CAMA, 2014), which is primarily administered by the North Carolina Department of Environment and Natural Resources (DENR), now the NC DEQ.

Among other things, CAMA requires a survey of drinking water supply wells within a half-mile radius downgradient of a coal ash impoundment. Implementation of this requirement has resulted in private well testing within any direction of an ash impoundment. Included in the sampling program were wells identified by NC DEQ as background wells. The data collected from this effort are publicly available:

- DEQ Private Well Data (NC DEQ, 2015a)
- DEQ Reference or Background Private Well Data (NC DEQ, 2015b)

According to DEQ records, over 300 private wells and 24 background wells were sampled (NC DEQ, 2015c).

The vast majority of the results meet federal primary drinking water standards. However, the NC DHHS conducted health risk evaluations for 327 wells, and 288 of the wells received “Do Not Drink” recommendations. Vanadium and hexavalent chromium are the most common reasons for a “Do Not Drink” recommendation, based on DHHS-specific screening levels (NC DHHS, 2015). NC DEQ uses a screening level for vanadium that is unique, and at least two orders of magnitude lower than the USEPA tap water RSL (USEPA, 2016a). DHHS uses a screening level for hexavalent chromium of 0.07 micrograms per liter (μg/L); slightly higher than the USEPA tapwater RSL of 0.035 μg/L (USEPA, 2016a), but still a very low level.

The state has not made a determination as to whether the wells are impacted by coal ash. Review of the publicly available data indicates that the indicators of coal ash release to groundwater, boron and sulfate, are either not present or not elevated in the private wells.

Groundwater reports for each coal-fired utility owned by Duke Energy in North Carolina have been posted on the NC DEQ website (NC DEQ, 2015d). A review of the maps indicates that with the exception of one location, groundwater from ash management areas at each of these facilities is flowing towards major bodies of water and away from areas where private wells are located. Thus it is unlikely that the private wells are impacted by coal ash management in these areas. This then indicates that the concentrations of vanadium and hexavalent chromium in the private wells are not related to coal ash releases, but may instead be due to natural background conditions. Hexavalent chromium is discussed in more detail in the next section.

### *18.19.1 Hexavalent chromium*

As previously noted, the presence of very low levels of hexavalent chromium in groundwater both in the vicinity of Duke Energy ash basins and at reference/background locations has resulted in a public focus on this constituent. Many metals can exist in different oxidation states; for some metals, the oxidation state can have different toxicities. This is the case for chromium, which exists in two common oxidation states: trivalent chromium (chromium-3, Cr[III], Cr3 or Cr+3), and hexavalent chromium (chromium-6, Cr[VI], Cr6 or Cr+6).

USEPA’s Integrated Risk Information System (IRIS) (USEPA, 2016b) is the source of final USEPA-approved toxicity values. Currently on IRIS (USEPA, 2016b), an oral noncancer toxicity value or reference dose (RfD) is available for trivalent chromium. Trivalent chromium is essentially nontoxic, as evidenced by its RSL for residential soil of 120,000 mg/kg, and the tapwater RSL of 22,000 μg/L (USEPA, 2016a). It can be bought as an over-the-counter supplement and is included in most vitamins.

Hexavalent chromium has been concluded to be a human carcinogen by the inhalation route of exposure, as identified on IRIS (USEPA, 2016b). For hexavalent chromium, IRIS provides an inhalation cancer toxicity value for potential inhalation carcinogenic effects, and an oral RfD and inhalation noncancer toxicity value or reference concentration (RfC). Note that the oral noncancer dose response value (RfD) for hexavalent chromium is based on a study where no adverse effects were reported. The tapwater RSL for hexavalent chromium is 0.035 μg/L (USEPA, 2016a); however, this value is much lower than the current toxicity values on IRIS would provide and much lower than the current federal MCL for chromium of 100 μg/L. The reason for this will be described shortly.

Recent studies by the National Toxicology Program (NTP) have shown that when present in high concentrations in drinking water, hexavalent chromium can cause gastrointestinal tract tumors in mice (NTP, 2008). Note that the drinking water concentrations in the NTP study were very high. The lowest exposure level in the test was 5000 μg/L—this is 50 times higher than the MCL of 100 μg/L for total chromium and 143,000 times higher than the RSL developed from the study of 0.035 μg/L.

Note that if the tap water RSL for hexavalent chromium was calculated using the final USEPA toxicity values available on IRIS, a value 44 μg/L would result. The tap water screening level that appears on the RSL table (0.035 μg/L; USEPA, 2016a) is derived from other sources, as will be described shortly.

IRIS does not present an oral cancer toxicity value for hexavalent chromium; a value developed by the New Jersey Department of Environmental Protection (NJDEP, 2009), which was similarly developed by the California Environmental Protection Agency (CalEPA), was used in the development of the RSLs. The USEPA developed a draft oral cancer dose-response value for hexavalent chromium, based on the same study, and it was the same as the NJDEP value. However, it should be noted that USEPA's Science Advisory Board (SAB) provided comments in Jul. 2011 on the draft USEPA derivation of the oral cancer slope factor (CSF) for hexavalent chromium and indicated many reservations regarding the assumptions of the mode of action and in the derivation itself (SAB, 2011). Thus the value used to develop the RSLs for hexavalent chromium has been called into question by USEPA's peer review panel.

Currently, there is much scientific debate about whether the mode of action of hexavalent chromium in very high concentrations in drinking water (as used in the NTP study) is relevant to the low concentrations most likely to be encountered in environmental situations (Proctor et al., 2012). Based on detailed studies of mechanism of action, an RfD has been developed in the literature that is protective of both the noncancer and cancer effects of hexavalent chromium in drinking water and corresponds to a safe drinking water equivalent level of 210 μg/L (Thompson et al., 2014), which is above the current MCL for total chromium. Thus the current MCL is protective. This is in contrast to the proposed CalEPA drinking water level of 10 μg/L (CalEPA, 2014) and the USEPA RSL of 0.035 μg/L, which are orders of magnitude below this risk-based level.

Two regulatory agencies have reviewed the MOA literature and have developed noncancer toxicity values for the oral exposure to hexavalent chromium that are protective of potential carcinogenic effects at high doses.

- Health Canada (2015) has developed a drinking water level for hexavalent chromium of 100 μg/L.
- The Texas Commission on Environmental Quality (TCEQ, 2016) has released a draft noncancer oral toxicity value for hexavalent chromium that equates to a drinking water screening level of 100 μg/L. A TCEQ toxicologist published a paper reviewing the basis of the MOA that supports this derivation (Haney, 2015).

Data from the American Water Works Association (AWWA, 2004) indicates that the average background level of hexavalent chromium in water supplies in the United States served by groundwater is 1.1 μg/L, though many of the results were below the limit of detection in the study of 0.2 μg/L. The majority of the detected results in groundwater in the AWWA study ranged from 1 to 10 μg/L, with a maximum of 52.6 μg/L.

To understand the occurrence of hexavalent chromium and other constituents in US drinking water that are currently not regulated under the Safe Drinking Water Act, the USEPA is conducting a nationwide survey of public water systems (PWS) under the Third Unregulated Contaminant Monitoring Rule (UCMR3; USEPA, 2015c, 2015d). In the United States as a whole, the average hexavalent chromium concentration in public water systems is 0.58 μg/L and ranges from 0.015 to 97.38 μg/L. The average concentration of hexavalent chromium in public water systems in North Carolina is 0.13 μg/L and ranges from 0.015 to 9.1 μg/L (Cr6 Study, 2016; USEPA, 2015c, 2015d).

A study has been conducted on the occurrence of hexavalent chromium in groundwater in the Piedmont region of North Carolina (Vengosh et al., 2016). The authors conclude:

> *"We show that Cr(VI) is the predominant species of dissolved Cr in groundwater and elevated levels of Cr and Cr(VI) are found in wells located both near and far (>30 km) from coal ash ponds. The geochemical characteristics, including the overall chemistry, boron to chromium ratios, and strontium isotope (87Sr/86Sr) variations in groundwater with elevated Cr(IV) levels, are different from those of coal ash leachates. Alternatively, the groundwater chemistry and Sr isotope variations are consistent with water-rock interactions as the major source for Cr(VI) in groundwater. Our results indicate that Cr(VI) is most likely naturally occurring and ubiquitous in groundwater from the Piedmont region in the eastern United States."*

Thus the average background concentrations of hexavalent chromium in US public water supplies and in groundwater in North Carolina are well above the USEPA RSL for tap water of 0.035 μg/L, a value based on an uncertain draft toxicity value and is not consistent with recent regulatory developments.

Prior to 2009, there were no regulatory reasons to use analytical methods to detect hexavalent chromium in groundwater below 100 μg/L. Now that analytical methods have been developed to measure at least down to 0.1 μg/L, it is clear that hexavalent chromium is present in groundwater at very low levels; however, the recent information on its toxicity demonstrates that these low levels are not of health concern.

## 18.20 Summary

In summary, while coal ash has been portrayed in the press as "toxic," careful evaluation demonstrates that constituent concentrations are similar to those in background soils across the United States, and the majority of constituents are present in coal ash at concentrations below conservative RSLs for a residential soil scenario. Moreover, toxicity studies on coal ash conducted under the EU REACH program consistently show a result of "No Hazard."

Leaching to groundwater and the subsequent discharge to surface water is a potentially complete exposure pathway for most coal ash management facilities. But the detailed work on the Kingston release indicates that even a large release of material to a river has not resulted in long-lasting effects; this has also been borne out at Dan River. The Kingston and Dan River studies demonstrate that following a release of coal ash directly into a river, the aquatic system rebounds in a short period of time; aquatic ecosystems are very resilient.

We live in a complex world, one that increasingly requires at least a basic understanding of science and scientific principles of research: hypothesis generation, hypothesis testing, and deriving conclusions based on the strength of the data. Preconceived notions of what the answer should be and/or distrust of funding sources do not have a place in our pursuit of knowledge. We need to use that knowledge to ensure that we are making rational and health-based decisions in our personal and public lives. As a community, we need to focus our concern and activism on issues that generally warrant them, and spend our time and money on efforts that can result in demonstrable improvements to our health and environment.

## References

ACAA. (2012). *Coal ash material safety: A health risk-based evaluation of USGS coal ash data from five US power plants*. American Coal Ash Association. Available at: https://www.acaa-usa.org/Portals/9/Files/PDFs/ACAA_CoalAshMaterialSafety_June2012.pdf.

ACS. (2016). *Cancer facts & figures 2016*. Atlanta: American Cancer Society. Available at: http://www.cancer.org/research/cancerfactsstatistics/cancerfactsfigures2016/.

ATSDR. (2010). Public Health Assessment—Tennessee Valley Authority (TVA) Kingston fossil plant coal ash release. *Prepared by the Tennessee Department of Health under a cooperative agreement with the Agency for Toxic Substances and Disease Registry, September 7,* Available at http://www.atsdr.cdc.gov/HAC/pha/TVAKingstonFossilPlant/TVAKingstonFossilPlantFinalPHA09072010.pdf.

AWWA. (2004). *Occurrence survey of boron and hexavalent chromium*. American Water Works Association. Available at: http://www.waterrf.org/publicreportlibrary/91044f.PDF.

CalEPA. (2014). *Chromium-6 drinking water MCL*. California Environmental Protection Agency. State Water Resources Control Board. Available at: http://www.waterboards.ca.gov/drinking_water/certlic/drinkingwater/Chromium6.shtml.

CAMA. (2014). *North Carolina Coal Ash Management Act. Senate Bill S729v7*. Available at: http://www.ncleg.net/Sessions/2013/Bills/Senate/PDF/S729v7.PDF.

Cr6 Study. (2016). *The Cr(VI) MOA research study. Hexavalent chromium in U.S. Drinking Water*. Available at: http://cr6study.info/crvi-moa-study-resources/hexavalent-chromium-in-u-s-drinking-water/.

EPRI. (2010). *Comparison of coal combustion products to other common materials*. Electric Power Research Institute. September 2010. Report No. 1020556. Available at: http://www.epri.com/.

Haney, J. (2015). Consideration of non-linear, non-threshold and threshold approaches for assessing the carcinogenicity of oral exposure to hexavalent chromium. *Regulatory Toxicology and Pharmacology*, *73*, 834–852.

Health Canada. (2015). *Chromium in drinking water*. Document for Public Consultation. Available at: http://www.healthycanadians.gc.ca/health-system-systeme-sante/consultations/chromium-chrome/document-eng.php.

IEAM. (2015). *Special series: Ecological risk assessment for residual coal fly ash at Watts Bar Reservoir, Tennessee*. Integrated Environmental Assessment and Management. Available at: http://onlinelibrary.wiley.com/doi/10.1002/ieam.v11.1/issuetoc.

NC DEQ. (2014). *Insects in Dan River downstream of Feb. 2 coal ash spill appear to be thriving, state tests show*. North Carolina Department of Environmental Quality. Available at: http://portal.ncdenr.org/c/journal/view_article_content?groupId=4711509&articleId=23477514.

NC DEQ. (2015a). *Updated well water testing results and information posted*. North Carolina Department of Environmental Quality. Available at: http://deq.nc.gov/blog/2016-01-12/updated-well-water-testing-results-and-information-posted-1.

NC DEQ. (2015b). *Groundwater reconnaissance well water sampling study results posted*. North Carolina Department of Environmental Quality. Available at: http://deq.nc.gov/blog/2016-01-12/groundwater-reconnaissance-well-water-sampling-study-results-posted.

NC DEQ. (2015c). *Summary of well testing near coal ash ponds*. North Carolina Department of Environmental Quality. Available at: https://ncdenr.s3.amazonaws.com/s3fs-public/document-library/Summary%20of%20well%20testing%20near%20coal%20ash%20ponds%207_8_Final.pdf.

NC DEQ. (2015d). *DENR posts groundwater assessment reports for duke energy coal ash facilities*. North Carolina Department of Environmental Quality. Available at: http://deq.nc.gov/blog/2016-01-12/denr-posts-groundwater-assessment-reports-duke-energy-coal-ash-facilities.

NC DHHS. (2014). *DHHS revises health advisories for the Dan River*. North Carolina Department of Health and Human Services. Available at: http://www.ncdhhs.gov/news/press-releases/dhhs-revises-health-advisories-dan-river-area.

NC DHHS. (2015). *DHHS screening levels*. Department of Health and Human Services, Division of Public Health, Epidemiology Section, Occupational and Environmental Epidemiology Branch. Available at: http://portal.ncdenr.org/c/document_library/get_file?p_l_id=1169848&folderId=24814087&name=DLFE-112704.PDF.

NC DHHS. (2016). *Current fish consumption advisories for North Carolina—Dan River*. Available at: http://epi.publichealth.nc.gov/oee/fish/advisories.html.

NC State. (2014). *Assessment of trace-element impacts on agricultural use of water from the Dan River following the Eden Coal Ash Spill*. Department of Soil Science, College of Agriculture and Life Sciences, North Carolina State University. Available at: http://www.soil.ncsu.edu/documents/Assessment%20of%20Trace%20Elements-Dan%20River%20Water-Agriculturev2.pdf.

NJDEP. (2009). *Derivation of ingestion-based soil remediation criterion for Cr+6 based on the NTP chronic bioassay data for sodium dichromate dihydrate*. Division of Science, Research and Technology New Jersey, Department of Environmental Protection. Risk Assessment Subgroup of the NJDEP Chromium Workgroup. Available at: http://www.state.nj.us/dep/dsr/chromium/ingestion-cr.PDF.

NTP. (2008). *NTP Technical Report on the toxicology and carcinogenesis studies of sodium dichromate dihydrate (CAS No. 7789-12-0) in F344/N rats and B6C3F1 mice (drinking water studies), NTP TR 546. NIH Publication No. 08-5887*. National Toxicology Program. Available at: http://ntp.niehs.nih.gov/ntp/htdocs/lt_rpts/tr546.PDF.

NWS. (2015). *How dangerous is lightning?* National Weather Service, National Oceanographic and Atmospheric Administration. Available at: http://origin-www.nws.noaa.gov/om/lightning/odds.shtml.

ORAU. (2010a). *Kingston Project Surveillance Program—Baseline medical screening results*. Oak Ridge Associated Universities. Available at: http://www.orau.org/documents/kingstonproject/Kingston-Fly-Ash-Results-Report.pdf.

ORAU. (2010b). *ORAU Kingston Project medical screening results—At a glance*. Oak Ridge Associated Universities. Available at: http://www.orau.org/documents/kingstonproject/At-a-Glance-Brochure.pdf.

Proctor, D. M., Suh, M., Aylward, L. L., Kirman, C. R., Harris, M. A., Thompson, C. M., et al. (2012). Hexavalent chromium reduction kinetics in rodent stomach contents. *Chemosphere*. On-line pre-print of article in press. Available at: http://www.sciencedirect.com/science/article/pii/S0045653512005978.

REACH. (2007). *Registration, evaluation, authorization and restriction of chemicals*. Regulation (EC) No 1907/2006 of the European Parliament. Available at: https://echa.europa.eu/regulations/reach.

SAB. (2011). Consolidated comments from the external peer review (final). In *Peer review workshop for EPA's draft toxicological review of hexavalent chromium*. Available at: https://cfpub.epa.gov/ncea/iris_drafts/recordisplay.cfm?deid=221433.

TCEQ. (2016). Proposed Development Support Document (DSD) hexavalent chromium oral reference dose. Texas Commission on Environmental Quality. June. Available at: http://www.tceq.com/assets/public/implementation/tox/dsd/proposed/june2016/hexchromoral.pdf.

Thompson, C. M., Kirman, C. R., Proctor, D. M., Haws, L. C., Suh, M., Hays, S. M., et al. (2014). A chronic oral reference dose for hexavalent chromium-induced intestinal cancer. *Journal of Applied Toxicology*, *34*, 525–536. Available at: http://onlinelibrary.wiley.com/doi/10.1002/jat.2907/ePDF.

TVA. (2012a). *Baseline Ecological Risk Assessment (BERA). Kingston ash recovery project non-time critical removal action, river system*. Document No. EPA-AO-050. Tennessee Valley Authority. Available at: http://www.epakingstontva.com/Phase%203%20Documents/BERA/Appendix%20I%20BERA/App%20I%20BERA.pdf.

TVA. (2012b). *Baseline Human Health Risk Assessment. Kingston Ash recovery project non-time critical removal action, river system*. Document No. EPA-AO-052. Tennessee Valley Authority. Available at: http://www.epakingstontva.com/Phase%203%20Documents/BERA/App%20H%20BHHRA%202012-07-11.pdf.

USCB. (2016). *QuickFacts*. U.S. Census Bureau. Available at: http://quickfacts.census.gov/qfd/states/00000.html.

USEPA. (1989). *Risk Assessment Guidance for Superfund: Volume I. Human health evaluation manual (Part A). Interim final. Office of emergency and remedial response*. Washington, D.C.: U.S. Environmental Protection Agency. EPA 540/1-89/002. Available at: http://www.epa.gov/risk/risk-assessment-guidance-superfund-rags-part.

USEPA. (1991). *Role of the Baseline Risk Assessment in Superfund remedy selection decisions*. OSWER Directive #9355.0-30. April. U.S. Environmental Protection Agency. Available at: http://www.epa.gov/oswer/riskassessment/baseline.htm [Note—USEPA is in the process of updating its website, so old links no longer work, but pages are not redirected. This reference can currently be found here: http://www.lm.doe.gov/cercla/documents/rockyflats_docs/SW/SW-A-005200.pdf].

USEPA. (1997). *Ecological Risk Assessment Guidance for Superfund: Process for designing and conducting ecological risk assessments*. US Environmental Protection Agency, Solid Waste and Emergency Response, OSWER 9285.7-25. PB97-963211. EPA 540-R-97-006. Available at: http://www.epa.gov/risk/ecological-risk-assessment-guidance-superfund-process-designing-and-conducting-ecological-risk.

USEPA. (1998). *Guidelines for ecological risk assessment. Risk Assessment Forum*. Washington, D.C.: U.S. Environmental Protection Agency. EPA/630/R-95/002F. Available at: http://www.epa.gov/sites/production/files/2014-11/documents/eco_risk_assessment1998.pdf.

USEPA. (1999). *Issuance of final guidance: Ecological Risk Assessment and Risk Management Principles for Superfund sites. Memorandum from S. Luftig to Superfund National Policy Managers, Region 1–10*. OSWER Directive 9285.7–28 P. Available at: http://www.epa.gov/sites/production/files/2015-10/documents/implementation-metals-memo.pdf.

USEPA. (2011). Statistical Software ProUCL 4.1 for Environmental Applications for Data Sets with and without Nondetect Observations. Software: http://www2.epa.gov/landresearch/proucl-software, and User's Guide: http://www2.epa.gov/sites/production/files/2015-03/documents/proucl_v5.0_user.PDF.

USEPA. (2012). *USEPA 2012 edition of the drinking water standards and health advisories*. U.S. Environmental Protection Agency. Available at: http://rais.ornl.gov/documents/2012_drinking_water.pdf.

USEPA. (2014a). *Information update—Kerr Reservoir*. Eden North Carolina Ash Spill. Available at: http://www.epa.gov/sites/production/files/2014-06/documents/eden-nc-coal-ash-spill-info-update.pdf.

USEPA. (2014b). *Human and Ecological Risk Assessment of coal combustion residuals*. EPA-HQ-RCRA-2009-0640-11993. Available at: http://www.regulations.gov.

USEPA. (2015a). Hazardous and solid waste management system; disposal of coal combustion residuals from electric utilities; final rule. 40 CFR Parts 257 and 261. *Federal Register*, *80* (74), 21302–21501. Available at: https://www.gpo.gov/fdsys/pkg/FR-2015-04-17/pdf/2015-00257.pdf.

USEPA. (2015b). *USEPA Region 4 Ecological Risk Assessment supplemental guidance interim draft*. Available at: http://www.epa.gov/sites/production/files/2015-09/documents/r4_era_guidance:document_draft_final_8-25-2015.pdf.

USEPA. (2015c). *The Third Unregulated Contaminant Monitoring Rule (UCMR3): Data summary*. Last updated January 2015. http://www.epa.gov/dwucmr/third-unregulated-contaminant-monitoring-rule.

USEPA. (2015d). *The Third Unregulated Contaminant Monitoring Rule (UCMR3): Occurrence data*. Last updated January 2015. http://www.epa.gov/dwucmr/third-unregulated-contaminant-monitoring-rule.

USEPA. (2016a). *USEPA regional screening levels*. U.S. Environmental Protection Agency. Available at: http://www.epa.gov/risk/regional-screening-table.

USEPA. (2016b). *Integrated Risk Information System (IRIS). Environmental criteria and assessment office*. Cincinnati, OH: U.S. Environmental Protection Agency. Available at: http://cfpub.epa.gov/ncea/iris/index.cfm.

USGS. (2011). *Geochemical database of feed coal and Coal Combustion Products (CCPs) from five power plants in the United States. Data series 635*. U.S. Geological Survey. Available at: http://pubs.usgs.gov/ds/635/.

USGS. (2014). *Geochemical and mineralogical maps for soils of the conterminous United States*. U.S. Geological Survey. Available at: http://pubs.usgs.gov/of/2014/1082/.

Vengosh, A., Coyte, R., Karr, J., Harkness, J. S., Kondash, A. J., Ruhl, L. S., et al. (2016). Origin of hexavalent chromium in drinking water wells from the piedmont aquifers of North Carolina. *Environmental Science & Technology Letters*. http://dx.doi.org/10.1021/acs.estlett.6b00342.

# Environmental impact and corrective action

# 19

*J.L. Daniels*[*], N.E. Carriker[†]
[*]UNC Charlotte, Charlotte, NC, United States, [†]Tennessee Valley Authority, Knoxville, TN, United States

## 19.1 Introduction and context

The spills that occurred at the Kingston Fossil Plant in Tennessee and the Dan River Steam Station in North Carolina provide well-documented case studies from which generalizable insights can be gleaned. While radically different in terms of their root cause analysis, site characteristics, spill size, and nature, these two sites were the impetus to regulation, legislation, and massive data collection efforts. The intent of this paper is to provide an integrated discussion of these developments with an aim toward informing evolving policy and practice at all coal combustion residuals (CCR) facilities, especially ash impoundments that are closing. Specifically the objectives are to summarize and discuss (1) the background and chronology of both spills; (2) review site assessments, as well as impacts to surface and groundwater quality; (3) review approaches to corrective action; (4) discuss sustainable closure and postclosure care; and (5) provide an overall framework for managing CCR that is universally relevant throughout the developed and developing world.

### *19.1.1 Context of the TVA and Duke Energy ash spills*

"Costs of cleaning toxic coal ash pits grows clearer." This is the headline of a story by Associated Press (AP) reporter Emery P. Dalesio that appeared in the Chattanooga Times Free Press (Dalesio, 2016) and other newspapers around the country on Feb. 8, 2016, 7 years after the unprecedented Tennessee Valley Authority (TVA) Kingston ash spill into the Emory River and 2 years after a smaller spill from Duke Energy's Dan River Steam Plant near Eden, NC. Nominally about the cleanup costs of the TVA and Duke Energy spills, most of this AP story describes leaching of "toxic heavy metals" in these "toxic, liquefied wastes" into groundwater, and a presumed associated public health threat. It says the TVA spill destroyed 40 homes (the actual number was 3) and is reminiscent of predictions by some that the TVA Kingston spill would

Synopsis: Reviews the environmental impact of the coal ashspills, including site assessment data (e.g., soil/river sediment, surface water, groundwater, biota, etc.) and corrective action. In situ sampling, monitoring, testing, and modeling; sustainable closure, net environmental effects, in context of state and federal regulation. Implications to corrective action and closure at other sites.

**Coal Combustion Products (CCP's).** **http://dx.doi.org/10.1016/B978-0-08-100945-1.00019-8**

cause the collapse of fisheries in Watts Bar Lake, the 39,000-acre TVA reservoir into which the Emory River flows (e.g., Chattanooga Times Free Press, 2009).

So what actually happened in these two spills? What were the ecological and human health impacts and risks? What effects did these spills have on coal ash regulations?

### *19.1.2 The TVA Kingston and Duke Dan River spills—What happened?*

The TVA Kingston spill occurred shortly after 1 a.m. on Dec. 22, 2008, when a dike around an ash disposal cell failed, releasing 5.4 million $yd^3$ of ash into the Emory River in an event that lasted less than an hour. The ash slide physically destroyed one home and damaged two others to the point that they were no longer habitable. Fig. 19.1 is an oblique aerial photo taken shortly after the slide that shows the extent of ash spilled. The embayment in the middle of the photo (the area to the left of the "Emory River" caption and above the "Fly ash spill area" caption, all the way to the left edge of the photo) was completely filled in with ash from which all the water was displaced. The tidal wave caused by the displaced water knocked over part of a concrete skimmer wall spanning the power plant's cooling water intake channel and damaged about 20 boathouses. Ash also completely filled the channel of the Emory River and initially spread as much as 3.5 miles upstream and at least two miles downstream. Rainfall in the weeks shortly after the spill increased the volumetric flowrate of the river that carried ash as far as 21 miles downstream to Watts Bar Dam. Cenospheres, that fraction of the ash that is especially small and hollow, floated on the river surface and provided a visual impact of the spill for miles. As such, the remediation effort involved excavation and dredging as well as surficial collection.

The Dan River spill was first detected on Feb. 2, 2014. It resulted from the collapse of an ostensibly corroded 48 in. (1.2 m) corrugated metal pipe (CMP) that was used to

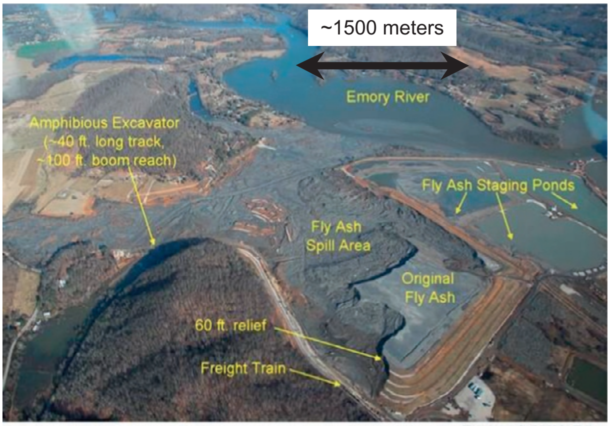

Photo taken 01/08/09 by TVA.

**Fig. 19.1** Aerial photo taken Jan. 8, 2009 showing the extent of the Kingston ash spill into the Emory River and the two embayments adjacent to the power plant.

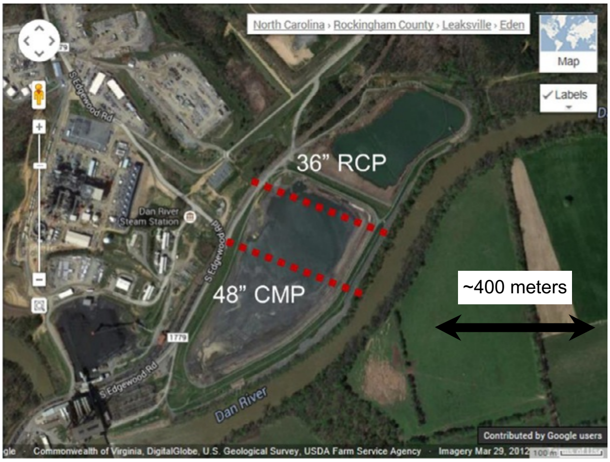

**Fig. 19.2** Aerial view of the Dan River Steam Station, along with the approximate locations of pipes used to convey stormwater: (48″/1.2 m CMP) and secondary leaking pipe (36″ RCP).

convey site stormwater under the ash pond. The breach in the CMP allowed for water and ash to flow into the pipe and discharge into the Dan River. The majority of the discharge occurred within 24 h, during which about 39,000 yd$^3$ of material spilled into the river. In addition, a separate 36 in. (0.91 m) reinforced concrete pipe (RCP) was found to be leaking as well. Both of these pipes were grouted in place and taken out of service. Because flow in the Dan River upstream of the plant is unrestricted, flows from subsequent rain events washed trace amounts of ash as far as 70 miles downstream to South Boston, VA. A plan view of the site is provided in Fig. 19.2.

Within a year, TVA removed most of the spilled ash from the Emory River by hydraulic and mechanical dredging, shipping about 3 million yd$^3$ (2.2 million m$^3$) to a landfill in Alabama. Over the next 3 years, TVA removed about 2.5 million yd$^3$ (1.9 million m$^3$) from two embayments adjacent to the plant and returned it to a reengineered landfill on site. Approximately 400,000 yd$^3$ (304,000 m$^3$) of material was left in the lower 1.7 miles (2.7 km) of the Emory River and the 4-mile (6.4 km) reach of the Clinch River downstream of the mouth of the Emory River. That area has legacy contamination of mercury and Cesium-137 from activities conducted in the 1950s and 1960s at the US Department of Energy (US DOE) Oak Ridge facilities. A Comprehensive Environmental Response, Compensation and Liability Act (CERCLA) Remedial Investigation/Feasibility Study conducted in the early 1990s (US DOE, 1996) resulted in Records of Decision (US DOE, 1995, 1997) selecting Monitored Natural Attenuation as the Remedial Action for those contaminants. Dredging ash from those parts of these two rivers was determined to be likely to disturb those sediments, causing more risk to human health and the environment than leaving it in place and allowing it to mix with native sediments and be covered by fresh sediments to remediate the ash-contaminated sediments.

Most of the ash from the Dan River spill was in layers too thin to remove by dredging. Over the course of several months, Duke Energy removed a total of about

4000 $yd^3$ from three areas of the river. The remainder of the ash was spread over a large area by river flows and is gradually being covered by fresh river sediments.

### 19.1.3 Public, legislative, and regulatory scrutiny

Both the TVA and Duke Energy spills received immediate and intense public scrutiny. At Kingston, an environmental advocacy organization was on the river within days collecting samples for analysis. Several outside experts offered their opinions to the press on possible environmental consequences of the spill, and the Tennessee Department of Environment and Conservation (TDEC) was characterized as having too close a relationship with TVA. Several Congressional committees scheduled hearings at which the outside experts testified, along with TVA and TDEC officials. A similar scenario unfolded for the Dan River spill: Many of the same environmental organizations and outside experts weighed in with the press, the North Carolina Department of Environmental Quality (NCDEQ) was described as having too close a relationship with Duke Energy, and state legislative committees quickly intervened.

Ultimately, both spills stimulated broader regulation of coal ash disposal. By Mar. 2009, Environmental Protection Agency (EPA) had ordered all utilities to assess the stability of dikes around all their coal ash impoundments. EPA then moved forward on proposed rules regulating coal ash disposal that had been stalled for several years, eventually issuing the CCR rules on Apr. 17, 2015. These rules follow Subtitle D of Resource Conservation and Recovery Act (RCRA) (2012), which manages fly ash as a solid, rather than hazardous waste, and prescribes schedules for assessments to be conducted for closure of ash ponds and landfills.

In North Carolina, public and political pressures led to the quick passage of the North Carolina Coal Ash Management Act (CAMA) into law without the governor's signature on Sep. 20, 2014. This legislation addressed virtually all aspects of coal ash disposal and reuse and set up a process by which all coal ash impoundments were to be classified and closed according to specific methods and timelines. The legislation also created the Coal Ash Management Commission (CAMC) to review the classifications by the NCDEQ and closure plans as submitted by Duke Energy. The CAMC was also created to recommend appropriate changes in the law itself, and in that respect, the law includes a built-in mechanism to reconcile policy goals with evolving science and engineering data. The CAMC was subsequently challenged in state court and dissolved by the governor in Mar. 2016. New legislation was developed to modify the CAMA was passed by the General Assembly and signed by the governor on Jul. 15, 2016.

### 19.1.4 Environmental and human health investigations

During the time EPA was developing the CCR rules, TVA was aggressively conducting a broad range of investigations to assess the extent of the Kingston ash spill, its effects on the environment and public health, and alternatives for disposal of the recovered ash. Among other things, those investigations

1. Measured depths of ash deposited in the Emory, Clinch, and Tennessee Rivers.
2. Evaluated whether the spill had adverse effects on fish, aquatic invertebrate, or amphibian populations.
3. Determined body burdens of CCR-related contaminants in 17 different types of ecological receptors, ranging from algal "slime" (periphyton) to birds of prey.
4. Examined the chemical content and leachability of Kingston ash, including developing new methods for analyzing ash.
5. Measured concentrations of CCR-related contaminants in surface waters and groundwater.
6. Modeled groundwater flow through the coal ash cell for several different configurations of containment structures and landfill caps.
7. Modeled sediment resuspension, mixing with native sediments, and downstream transport under several flow scenarios.

Several of the investigations were performed by independent university and National Laboratory researchers, all of whom were encouraged to publish their findings in peer-reviewed journals. As a result, more than 50 technical articles have been published on the results of the TVA Kingston investigations (e.g., IEAM, 2015, a series of eight papers published as a special issue; Greeley, Elmore, McCracken, & Sherrard, 2013; Otter, Bailey, Fortner, & Adams, 2012).

Similarly, the Dan River ash spill prompted several environmental investigations. Most of those focused on identifying where the spilled ash was deposited downstream, the feasibility of recovering it, and its effects on river water quality. Key findings from both sets of investigations are briefly discussed in this chapter.

## 19.2 Regulatory framework (as relevant for corrective action of surface impoundments)

Much of the regulatory framework for evaluating and managing legacy impoundments derives from the RCRA of 1976. The impetus for RCRA legislation was focused on solid and hazardous waste management while coal fly ash was explicitly exempted through the Bevill Amendment, so named after a member of the US House of Representatives, Thomas Bevill (D) of Alabama.

Most of the ~735 impoundments in the United States were built between 1950 and 1980. During this time, science and engineering was beginning to recognize the need to design systems for isolating solid, hazardous, and nuclear wastes from the natural environment. Previously, all of these waste types were disposed of in any low-lying depression, with virtually no protection from the hydrologic cycle. Coal fly ash as a material was understood principally in terms of its soil-like properties, with applications to road construction and concrete production. As such, the industry was unaware that ash also should be treated as waste and isolated from groundwater and surface water features. Therefore the majority of these ponds were unlined and constructed adjacent to rivers and streams.

The leachability characteristics for ash are typically much lower than for RCRA-defined wastes, as can be assessed by comparing the maximum reported solid phase concentrations of trace elements shown in Fig. 19.3. Coal ash is derived from

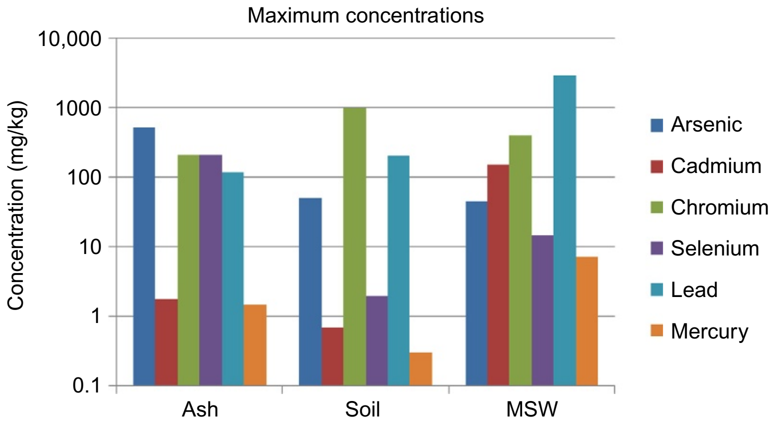

**Fig. 19.3** Comparison of maximum reported concentrations for coal fly ash, soil, and municipal solid waste.

Data from Lindsay, W. L. (1979). *Chemical equilibria in soils*. John Wiley, as cited in *Ground Water Issue, Behavior of Metals in Soils*. EPA/540/S-92/018; National Institute of Standards and Technology. (1998). *A study of the metal content of municipal solid waste*. Chemical Science and Technology Laboratory, NIST (prepared for US DOE); US EPA. (2009). *Characterization of coal combustion residues from electric utilities—Leaching and characterization data*. EPA-600/R-09/151. US Environmental Protection Agency. December.

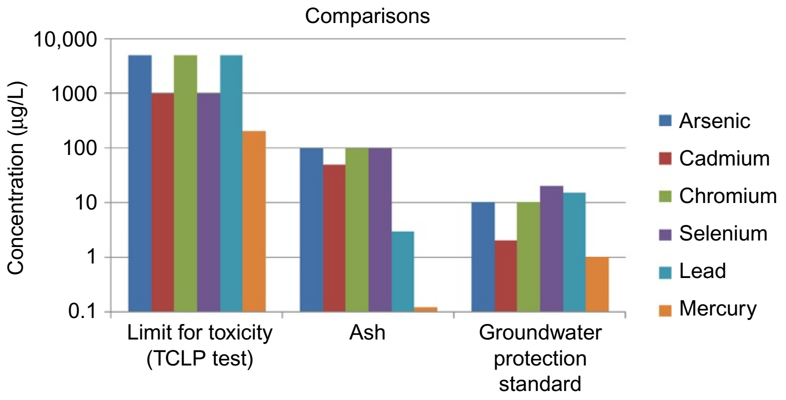

**Fig. 19.4** Comparison of a typical coal fly ash relative to the toxicity threshold set by US EPA Method 1311 and groundwater protection standards in North Carolina.

coal that is mined from the subsurface in contact with soil and rock. So it follows that soil also contains trace elements. Municipal solid waste, while also not considered hazardous, contains a broader array of contaminants, given the biological component in that waste stream.

Although the leachate from coal fly ash is often significantly less than the limits specified as toxic by the Toxicity Characteristic and Leaching Procedure (US EPA Method 1311), it can often exceed the lower threshold set for the protection of groundwater, as shown in Fig. 19.4.

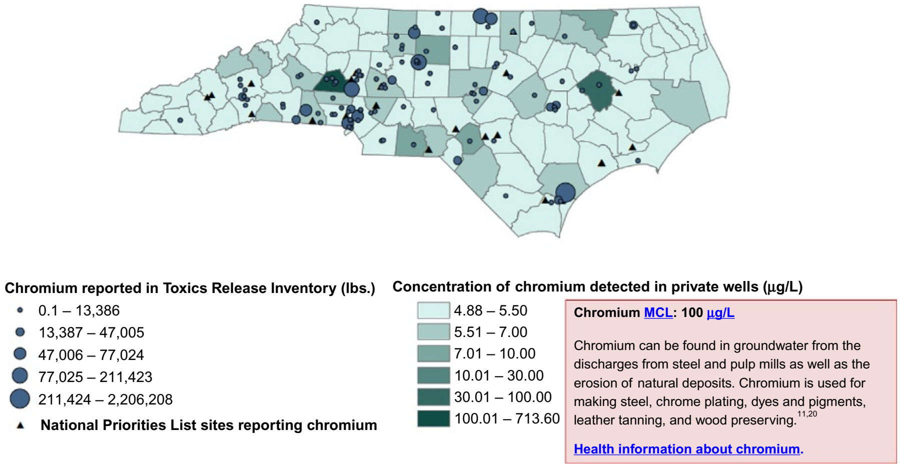

Chromium can be found in groundwater from the discharges from steel and pulp mills as well as the erosion of natural deposits. Chromium is used for making steel, chrome plating, dyes and pigments, leather tanning, and wood preserving.[11,20]

**Fig. 19.5** Concentrations of chromium detected in North Carolina private well water (µg/L), average 1988–2010.
Courtesy of UNC Superfund Research Program—Research Translation Core, Funded by an ARRA supplement from NIEHS (P42-ES005948) 2009–11.

As suggested by Fig. 19.4, while coal fly ash is not hazardous, some ashes can leach constituents at concentrations that exceed groundwater protection standards. These standards can vary according to whether there is a state-specific limit versus federal primary drinking water standards. For example, the federal drinking water standard for chromium is 100 µg/L, while the groundwater protection standard in North Carolina is 10 µg/L. This difference gives rise to confusion among members of the public, especially given that, like all other constituents in coal ash, chromium is occurs in nature and thus would be present in groundwater at concentrations between 10 and 100 µg/L, as shown in Fig. 19.5.

Since chromium occurs naturally in groundwater, federal and state regulatory structures explicitly call for the delineation of a site-specific background concentration. The governing principle is that serving as a source of drinking water is the highest and best use of groundwater. Consequently, any industrial activity (e.g., a leaking surface impoundment) should not result in a deterioration of quality, typically defined as contaminant concentrations that either exceed groundwater protection standards or the applicable background concentration.

In the case of either the federal EPA CCR rule or the NC CAMA legislation, data are required to demonstrate the extent to which unlined ash basins may adversely impact groundwater. This involves performing a site assessment, inclusive of soil, groundwater, and surface water sampling. Site assessments are generally iterative in nature, with initial data collection informing subsequent data collection plans. If an impoundment is unlined and is found to be contaminating groundwater beyond the applicable protection standard, then the impoundment must cease receiving ash and be either retrofitted or closed. Given that most ash ponds are both unlined and are impacting groundwater, nearly all are in some phase of the closure process. Moreover, the impact to groundwater must be addressed through a corrective action process that ends when groundwater has been restored to the protection standards at the site boundary. This entire process, from site assessment, corrective action, and ultimate closure is described in more detail in the following chapters.

## 19.3 Site assessments

### *Coal ash characteristics*

Over the last quarter-century, coal ash probably has been studied and analyzed at least as much as, and probably more than, any other industrial waste product. These investigations include a wide range of scientific and engineering disciplines, with many examining the chemical composition of both fly ash and bottom ash, the potential for the leaching of ash constituents under varying environmental conditions and the potential ecological effects of the leached constituents. So what have we learned about the composition of coal ash and its effects on the environment?

Chemical composition: Coal ash is comprised mainly of aluminosilicate mineral glasses formed from elements naturally present in coal. There is some variation in the composition of ash depending on coal types and sources, combustion temperatures, and burner designs. Most elements in coal ash occur at concentrations within or slightly higher than the ranges for each element as found in the earth's crust, as shown in Table 19.1.

Fly ash is composed of spherical particles varying from about 0.1 μm to 1 mm, with a median diameter of about 15–25 μm. These glasses also contain iron, manganese, calcium, and trace elements such as arsenic, selenium, copper, chromium, strontium, and others. See Chapter 2 for more details.

As fly ash is composed of spherical particles of varying sizes, it exhibits some unusual physical properties. Fly ash easily forms slurries when mixed with water, but when a slurry is allowed to stand without physical agitation, the material settles to the bottom and the particles tend to be tightly compact, driving out interstitial water and resulting in a cement-like solid that is inhospitable for burrowing organisms.

**Table 19.1** **Typical composition of coal fly ash**

| **Component/mineral** | **Typical range (%)** |
|---|---|
| Silicon dioxide ($SiO_2$) | 34–58 |
| Aluminum oxide ($Al_2O_3$) | 20–40 |
| Iron oxide ($Fe_2O_3$) | 4–24 |
| Calcium oxide (CaO) | 2–30 |
| Magnesium oxide (MgO) | 1–6 |
| Sulfur trioxide ($SO_3$) | 0.5–4 |
| Trace elements (e.g., antimony, arsenic, cadmium, chromium, cobalt, copper, lead, molybdenum, nickel, selenium, uranium, and vanadium) | <1%<br>Typically part per million to part per billion levels |

Data from Oweis, I. S., & Khera, R. P. (1998). *Geotechnology of waste management*. PWS Publishing Company, 472 p.; US Geological Survey. (2015). Trace elements in coal ash. Fact Sheet, 2015-3037.

Fly ash has nearly the same density as sand and it mixes readily with sandy sediments. That has proven to be fortuitous at Kingston. Since the bedload in the Emory River is mostly sand, the ash remaining after the completion of dredging is rapidly being diluted by native sediments.

Bottom ash also is composed of mostly aluminosilicate glasses, but is irregular in shape and contains higher concentrations of iron, manganese, and other major elements (Oweis & Khera, 1998).

Although the elemental composition of coal ash is similar to that of the earth's crust, because of its relatively recent origin as a combustion by-product, several constituents typically are enriched in coal ash leachate as compared to soil leachates. Among others, these include barium, boron, arsenic, selenium, strontium, calcium, magnesium, and thallium. As a result of the highly oxidizing combustion environment, many are present in their highest valence states in freshly generated ash. When water is added, depending on factors such as pH and the oxidation-reduction potential, some constituents may be reduced to lower valence states and react with other constituents to form precipitates. Others remain dissolved in the water, but may adsorb onto soil particles as the water moves through the soil and enters streams.

Boron, arsenic, and selenium exist in aqueous solution as oxyanion complexes, thus they are less likely to adsorb onto negatively charged soil particles and are among the more mobile components of coal ash. The US EPA recommends that boron, calcium, chloride, fluoride, pH, sulfate, and total dissolved solids be used as indicators for the detection monitoring of impacts of coal ash impoundments on groundwater quality. If a statistically significant increase beyond background concentrations is observed, then assessment monitoring is required, inclusive of antimony, arsenic, barium, beryllium, cadmium, chromium, cobalt, fluoride, lead, lithium, mercury, molybdenum, selenium, thallium, radium 226, and radium 228 (combined).

Arsenic is often a focus of environmental investigations because of its toxicity to humans at high concentrations. Selenium also is often a focus because it is both a toxicant and teratogen at levels only slightly higher than those at which it is an essential nutrient. In addition, selenium is of concern because it, along with mercury, bioaccumulates in the food chain.

Toxicity is a function of dose. The toxicity of a chemical to organisms is a product of dose and exposure. Some chemicals, such as oxygen or aspirin, require high levels before they become toxic. Dioxins, in contrast, have characteristics that result in toxicity at exceedingly small doses or exposures. Some factors that can reduce the potential toxic effects of CCR-derived chemicals to aquatic life include chemical reactions with other constituents that may reduce bioavailability (e.g., precipitation, oxidation, or reduction), adsorption onto solid phases, and dilution within the receiving water.

## *TVA Kingston environmental investigations*

Much of the scientific literature on environmental consequences of coal ash or coal ash constituents, such as selenium, published prior to the TVA Kingston spill were for lacustrine (lake-like) aquatic environments, rather than for flowing streams (e.g., Lemly, 1997, 2002; Ohlendorf, Hothem, & Welsh, 1989). As a consequence, early predictions of effects of the TVA Kingston and Duke Energy Dan River spills were based on the previously published studies. However, these two spills, as well as an Aug. 2005 spill into the Delaware River from PPL's Martin Creek plant, were in more riverine environments that provide continuing sources of fresh water, reducing both dose and exposure to most ecological receptors.

TVA's investigation of possible environmental effects of the Kingston ash spill were extensive. The numbers of samples collected, the variety of scientific and engineering disciplines represented, the range of environmental media sampled, and the quality of data collected certainly places the Kingston spill among the most comprehensively investigated environmental events recorded. The cost of the investigations approached $60 million over a 5-year period and resulted in over 15,000 samples and over 400,000 chemical analyses. Nearly every imaginable type of analysis was performed at some point. This included analyses of water, porewater, and sediment chemistry; radiological characteristics; physical characteristics of ash and sediments; ash and sediment leaching; biological population and community structure assessments; bioaccumulation of CCR-derived chemicals in insects, spiders, fish, birds, reptiles, and mammals; studies of sediment resuspension, mixing with native sediments, and downstream transport and redeposition; flood risk; water and sediment toxicity; human health risks; and an ecological risk assessment that included 17 different receptor organisms. At one point an investigator observed, "Anything that eats, breathes, flies, swims, walks, crawls, or just photosynthesizes is at risk of becoming part of a statistic in a table of results, sacrificing its life (or at least part of its anatomy) for the benefit of science."

These wide-ranging investigations resulted in numerous technical reports and peer-reviewed publications (e.g.,;Beck, Hopkins, & Jackson, 2013 Mathews et al., 2014; Rivera et al., 2015; Van Dyke, Steen, Jackson, & Hopkins, 2013). The following will briefly summarize key findings:

An immediate concern after the spill was that the ash would dry and become mobilized by the wind, then be transported offsite, exposing residents to airborne ash particulates. In addition, on-site recovery operations had the potential to stir up dry ash on roadways that would be transported from the site in dust clouds. TVA addressed those issues by implementing an on-site dust management plan and by establishing both on-site and off-site air monitoring programs. Moreover, the majority of the ash has been capped in place onsite. As a result, the on-site monitoring never detected contaminants exceeding Occupational Health and Safety Administration (OSHA) standards for worker safety. Similarly, the off-site monitoring, which included seven stations surrounding the plant, never recorded exceedances of US EPA ambient air quality standards during the period of ash recovery operations.

Groundwater monitoring was performed at several wells around the perimeter of the site, as well as within the ash cell. Because of the relatively simple groundwater flow pattern, one upgradient and two downgradient wells eventually were approved to evaluate compliance with groundwater protection standards. Results from those (and other) wells indicated that while concentrations of several constituents increased as water passed through the ash in the cell, only concentrations of arsenic exceeded groundwater protection standards, and only for the first part of 2009 (Fig. 19.6)

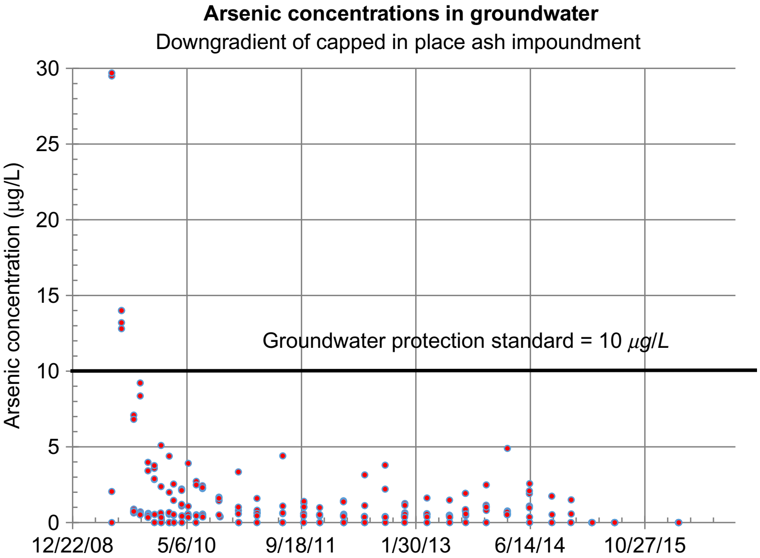

**Fig. 19.6** Groundwater monitoring results at capped-in-place impoundment at TVA Kingston.

(TVA, 2014). Fig. 19.6 also demonstrates the efficacy of the cap-in-place solution, in conjunction with slurry walls, which resulted in a reduction in concentration of arsenic.

Groundwater transport modeling conducted in support of the selected remediation showed that after containment of the recovered ash within a cell surrounded by a perimeter subsurface containment wall with a clay cap, the maximum fluxes of arsenic and selenium to the Emory River via groundwater would be <23 and 17 mg/day, respectively (TVA, 2011, 2012, 2013).

Some impacts of the spill were obvious. Spilling 5.4 million yd$^3$ of solid material into the Emory and Clinch Rivers buried aquatic insect larvae, freshwater mussels, and some turtles under up to 8 m of ash. It effectively dammed the Emory River, temporarily creating an impounded pool in what had been a mostly unregulated stream, changing the nature of the aquatic habitat.

There were immediate impacts to water quality. High levels of turbidity and both dissolved and suspended materials were present in the water column for a few days following the spill, and for a few days after subsequent high streamflow events. Daily monitoring at stations from upstream of the spill to 20 miles downstream found that the suspended solids quickly settled to the bottom of the river, with downstream and upstream water quality very similar within a week following the spill. Until dredging to remove ash from the river was completed in the summer of 2010, high flows from rainfall events resuspended spilled ash for brief periods. Toxicity testing of dredge plume water performed throughout the period of dredging found no significant toxic effects to laboratory test organisms (Sherrard, Carriker, & Greeley, 2015).

Nearly all the native sediments in the lower six miles of the Emory River and in a shorter reach of the Clinch River were completely covered by varying depths of ash immediately following the Kingston spill. TVA began removing ash from the Emory River within 3 months and evaluated the potential for dredging ash from the Clinch River. The much shallower ash deposits in the Clinch River and the presence of legacy radioactivity from Department of Energy activities at Oak Ridge led to the decision to not dredge ash from the Clinch River or from the lower 1.8 miles of the Emory River. Ash depths and percent ash composition of sediments throughout the affected reaches were characterized by 269 sediment core samples collected in a grid pattern. Results of the grid sampling identified locations for which whole-sediment toxicity testing was performed.

Over 1600 sediment samples were collected from 2009 to 2013. Chemical analysis of the sediments and porewaters and with leaching tests identified several contaminants of potential ecological concern, with attention ultimately focusing on arsenic as the constituent most likely responsible for observed toxicity in laboratory bioassays. Arsenic in ash-contaminated sediments varied linearly with percent ash.

However, as shown in Fig. 19.7, plotting porewater arsenic concentration versus percent ash in sediments suggested the native Emory River sediments have some capacity to bind arsenic, apparently attenuating porewater arsenic concentrations and reducing

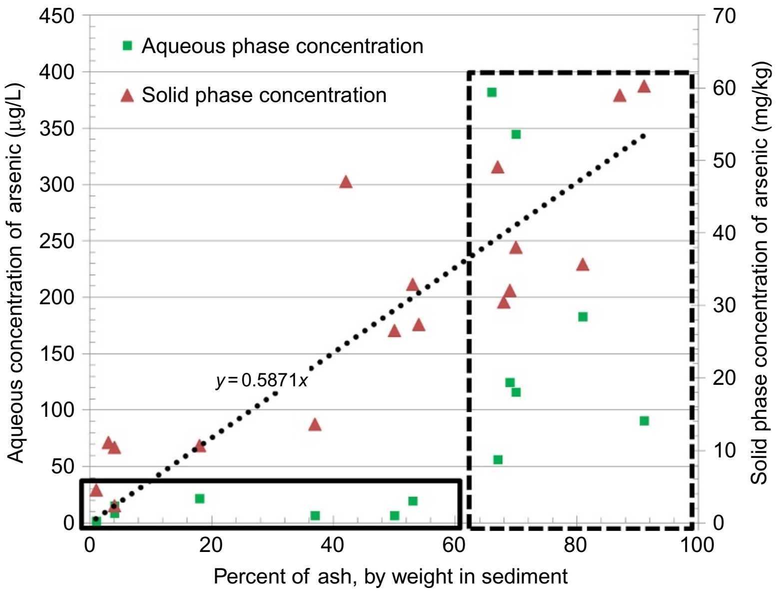

**Fig. 19.7** Aqueous and solid phase concentrations of arsenic; as a function of percent of ash mixed with Emory River sediment. The *dashed line* represents a linear fit of solid phase arsenic concentration with percent of ash in sediment. The *solid and dashed boxes* capture aqueous phase arsenic concentration. Arsenic becomes available in the aqueous phase only when the percent of ash mixed with sediment exceeds 50%.

its bioavailability at <40% ash in sediments. Above ~50% sediment ash, porewater arsenic increased approximately linearly with increasing ash in sediments.

Whole sediment toxicity testing found little evidence of toxicity when ash comprised <40% of the sediment. At higher ash concentrations, any observed toxicity was partly the result of tight packing, making the material an unsuitable habitat for burrowing insect larvae, and partly associated with arsenic in the sediments and porewaters (Sherrard et al., 2015).

The fish population and community structure information (including larval fish surveys), and benthic population and community information showed that the impact on those two ecosystem components was short-lived. Benthic invertebrates had begun recolonizing the ash-impacted areas within a few months, and fish communities were similar to other nearby streams and to previously documented conditions within about 2 years, after dredging was completed (Bevelhimer, Adams, Fortner, Greeley, & Brandt, 2014; Rigg et al., 2015). Turtle populations also recovered quickly, with no significant differences in estimated turtle biomass per hectare for ash-impacted and control areas (Van Dyke, Steen, Jackson, & Hopkins, 2014).

A broad range of organisms (e.g., periphyton, littoral zone macrophytes, aquatic insect larvae, snails, fish, turtles, spiders, birds, and raccoons) were collected and analyzed for tissue concentrations of a suite of up to 26 different elements. The organisms collected ranged from primary producers to top-level predators and included a variety of feeding guilds. In addition to whole-body analyses, individual tissues (e.g., blood, egg, ovary, muscle, claw, feather, skeleton, and viscera) were analyzed for several types of organisms. Aquatic insect larvae and snails were analyzed before and after purging intestinal tracts.

These bioaccumulation results showed that for nearly all organisms, the levels of some CCR-derived contaminants (mainly arsenic, selenium, and strontium) were higher for samples collected near the spill site than at reference sites. However, tissue concentrations didn't exceed threshold levels reported in the literature for causing adverse population effects, and they began to decrease over time after ash was removed from the river (Beck et al., 2013; Mathews et al., 2014; Van Dyke et al., 2013).

For all organisms collected, investigators recorded the incidence of structural deformities (e.g., fish scoliosis, bird leg, or bill deformities); physical characteristics (e.g., length, weight, external parasites); and measures of fecundity (turtle and bird egg weight and volume, clutch size, hatching success, and fledgling survival). In addition to metals and metalloids, fish blood was analyzed for enzymes indicative of overall health or particular types of stresses, and fish ovary tissues were examined histologically for egg condition. The physical condition of fish (length/weight ratios, incidence of deformities and parasite infestations, presence of skin lesions, etc.) also was recorded as an overall assessment of fish health.

Except for evidence of stress to resident fish during the spring of 2009, when both habitat and food sources near the spill site were severely impacted, and there were some small, but statistically insignificant differences in some field observations for tree swallow clutch size, there was no evidence of increased teratogenic or reproductive effects on fish, turtles, or birds in ash-impacted areas. Laboratory exposures of fathead minnow eggs and larval fish to Kingston ash also found no indication of adverse effects, nor did histopathological examination of ovary tissues of field-collected bluegill, bass, or catfish (Greeley, Elmore, McCracken, & Sherrard, 2014).

Potential human health risks of the spilled ash were evaluated both for ash recovery workers and for a wide range of residents, recreationists, fishermen, and others who might be exposed to the spilled or recovered ash. Individual workers performing different recovery tasks were randomly selected to wear personal industrial hygiene air monitors, since inhalation of ash particles was judged to be the most likely route of exposure for onsite workers. Results of thousands of samples collected in this manner found no exceedances of OSHA standards for inhalation of silica, As, or Se.

A Baseline Human Health Risk Assessment (Jacobs Engineering, 2012) considered multiple potential routes of exposure for adult and child residents with potential domiciles on the recovered ash, as well as swimmers, boaters, fisherpersons, and beachcombers. The risk assessment used conservative assumptions for exposure via consumption of untreated Emory Rover water, inhalation of dust, incidental ingestion of ash by children playing on areas underlain by recovered ash, and consumption of CCR-contaminated fish. Of all the various possible combinations of receptor and exposure route, the only combination that resulted in a risk exceeding EPA's guideline of $10^{-6}$ for increased cancer risk (i.e., one additional case of cancer per million inhabitants) was a child living and playing on an area underlain by recovered ash. Since the recovered ash is in a cell that will never be classified for residential or recreational use that is a purely theoretical situation.

Similarly, the Baseline Ecological Risk Assessment (BERA; Arcadis, 2012) considered 17 different ecological receptors ranging from primary producers (periphyton, or algal "slime") to top predators (osprey and raccoons), with site-specific data available for all but a couple of receptors. The results showed that the only receptors for which there were potential ecological risks were aquatic insect larvae and insectivorous birds, and those were, at most, moderate risks. Consequently, the approved remedial action for ~500,000 yd$^3$ of residual ash left in the river system after conclusion of dredging was Monitored Natural Recovery (MNR), and the long-term monitoring plan focuses on concentrations of arsenic and selenium in mayflies (larvae and adults) and tree swallows (an obligate insectivorous bird). The monitoring results show continuing declines in those elements in birds and mayflies sufficient that EPA and TDEC approved eliminating tree swallow monitoring after 2015. Although the BERA did not indicate a need to monitor fish, because the area supports a popular sport fishery, TVA has chosen to continue monitoring fish populations, fish health, and fish body burdens of arsenic and selenium in the Clinch and Emory Rivers near Kingston to confirm the continuing lack of ecological effects of the residual ash.

## *Dan River environmental investigations*

The NCDEQ monitored the impact of the Duke Energy spill to the Dan River by measuring upstream and downstream concentrations of over 40 different elements. The impact was found to be evident in terms four constituents: aluminum, arsenic, copper, and iron. Aluminum and iron concentrations in the Dan River typically exceed North

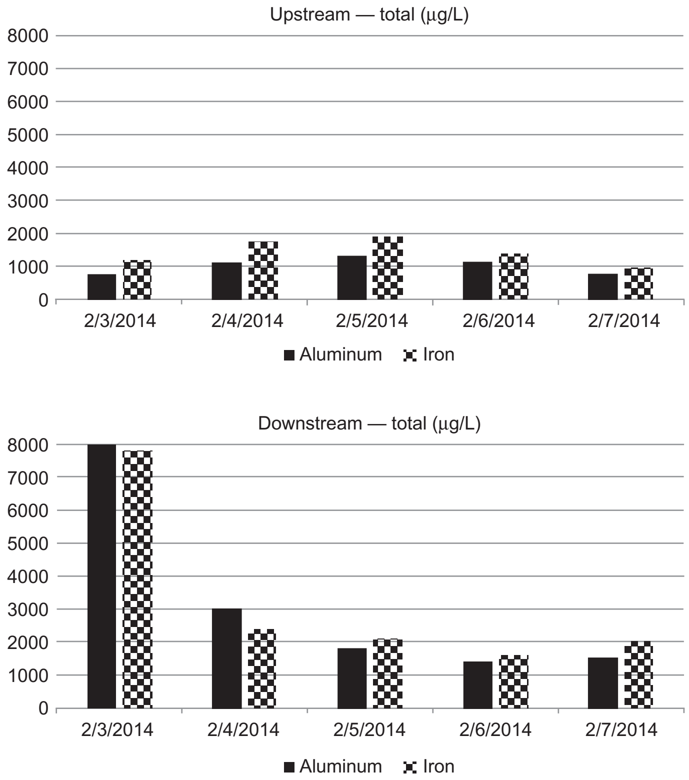

**Fig. 19.8** Upstream and downstream concentrations of unfiltered samples after the Dan River spill (arsenic and copper visible in Fig. 19.9).

Carolina Water Quality Standards for Aquatic Health, given as 87 µg/L (Al) and 1000 µg/L (Fe) for total concentration. Upstream and downstream measurements are shown in Fig. 19.8.

A similar effect can be observed for arsenic and copper, with applicable standards of 10 µg/L (As) and 7 µg/L (Cu), as shown in Fig. 19.9 with a smaller scale for clarity. The estimated spill volume of 102,000 m$^3$ (27 million gallons) represented a fraction of the volume of water flowing in the Dan River at the time.

As noted in Fig. 19.9, the principal effect of the spill was found to be arsenic and copper for ~2 days after the spill. Overall, these results mesh quite well with what would be predicted on the basis of typical leaching characteristics and flow volume.

For example, measured arsenic values were approached 40 µg/L for 1 day after the spill, which is consistent with the dilution provided by the Dan River. Fig. 19.10 provides a comparison of the actual flow rate of the Dan River at a location 14 miles upstream from the plant in comparison to estimates of the flow duration of the spill, estimated to have occurred between 3 and 24 h. As noted in the figure, the actual flow rate of the Dan River was ~27 m$^3$/s as compared to a maximum of 10 m$^3$/s for 3 h or 1 m$^3$/s for 24 h.

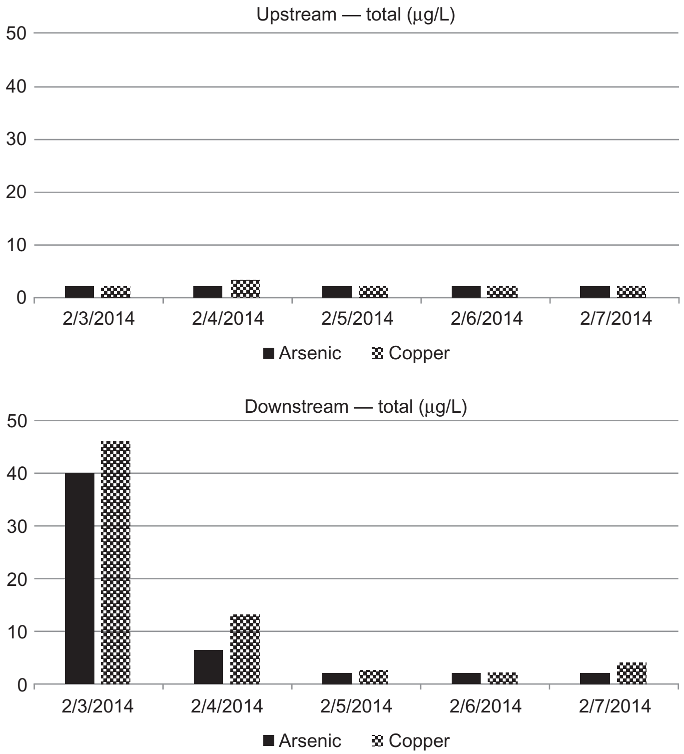

**Fig. 19.9** Upstream and downstream concentrations of arsenic and copper in unfiltered samples after the Dan River spill.

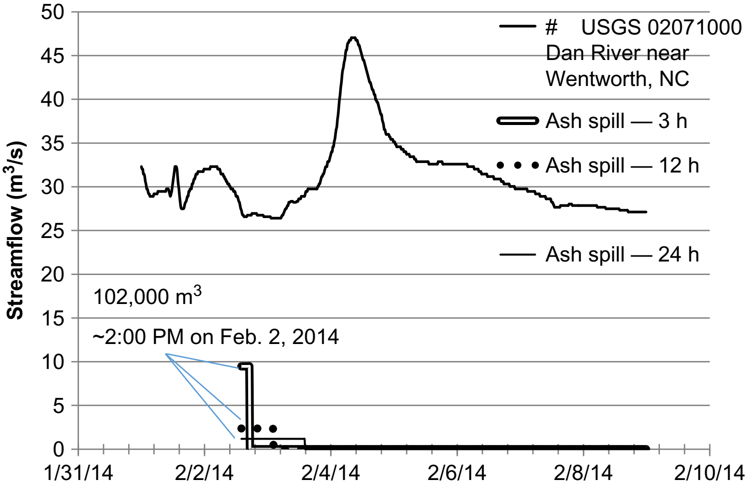

**Fig. 19.10** Flowrate of Dan River just upstream of spill, as compared to estimated spill volume and time.

As the foregoing graphs indicate, effects on the Dan River water quality have been minimal, with no indication of long-term consequences.

## 19.4 Corrective action

Corrective action is required when groundwater has been contaminated beyond the applicable groundwater protection standard. If background concentrations are greater than the protection standard, those levels become the standard. When defining groundwater impact, the EPA CCR rule requires at least one monitoring well that is located upgradient of the impoundment and another three downgradient. However, the complexity and size of most impoundments requires far more. For example, in North Carolina, $\sim$25 wells were installed for each impoundment.

Prior to the EPA CCR, most ash basins were enveloped by a compliance boundary beyond which they had to meet groundwater protection standards. In North Carolina the compliance boundary is 152 m (500 ft) from an impoundment permitted before 1983, or the property boundary, whichever is less. The maximum distance for the boundary was reduced to 76 m (250 ft) for impoundments permitted after 1983. The significance of distance between an impoundment and a compliance boundary is the provision for natural attenuation (e.g., dilution, dispersion, and physical/chemical reactions) to reduce contaminant concentrations below groundwater protection standards. In the EPA CCR rule, the compliance boundary is the waste boundary itself; that is, there is no buffer or allowance for natural attenuation to occur. Groundwater protection standards must be met in the uppermost aquifer. The waste boundary is defined as the vertical plane downgradient of the impoundment, which extends into the uppermost aquifer. The uppermost aquifer is defined by the point nearest to the natural ground surface to which the aquifer rises during the wet season. A conceptual image of these boundaries are provided in Fig. 19.11.

In evaluating whether coal ash has impacted groundwater at the waste boundary, the EPA CCR rule requires a minimum of eight independent samples from each background and downgradient monitoring well. The results from these samples are first subjected to detection monitoring, which is performed to evaluate whether an impoundment has resulted in a statistically significant increase in boron, calcium, chloride, fluoride, pH, sulfate, or total dissolved solids. These constituents were selected because of their mobility and general association with coal ash leachate. For example, the EPA CCR rule notes that calcium was added, "because it is an indicator of the extent of leaching from fly ash and FGD gypsum and because of the strong demonstrated link between the leaching of calcium and arsenic, which is one of the primary risk drivers identified in the risk assessment." If detection monitoring is positive, then assessment monitoring is required, which includes antimony, arsenic, barium, beryllium, cadmium, chromium, cobalt, fluoride, lead, lithium, mercury, molybdenum, selenium, thallium, and radium 226 and 228 (combined). If one or more of these constituents is found at statistically significant levels above groundwater protection standards or background, then corrective action is required. Corrective action requires additional wells and sampling to further delineate the contaminant plume. In

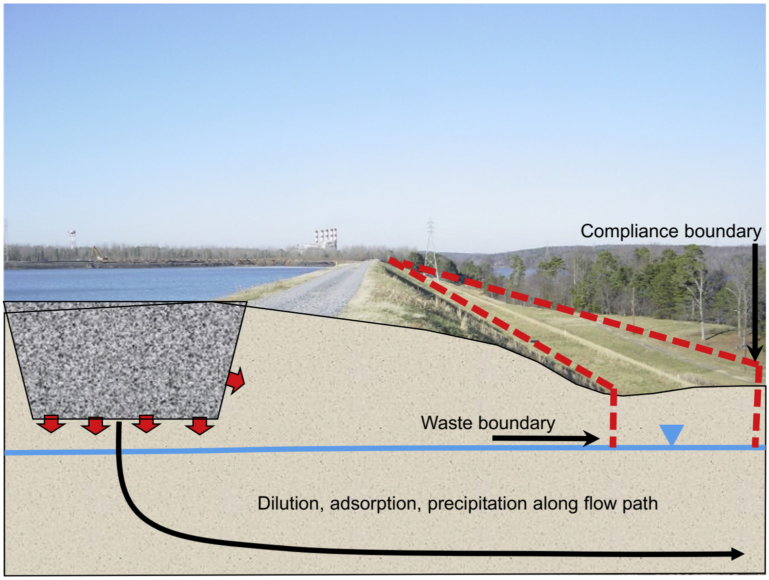

**Fig. 19.11** Distinction between the waste boundary and a compliance boundary.

the case of NC CAMA, this requirement is to determine the horizontal and vertical extent of contamination. Corrective action involves both source control and groundwater remediation. Source control measures include excavation of the ash, capping (e.g., with geomembranes, compacted clay or water repellent additives), vertical barriers, or some method of in situ stabilization (e.g., with lime, cement, or grout mixtures). Groundwater remediation involves processes to reduce contaminant concentrations, including pump and treat, injection of reactive additives (e.g., zero-valent iron or activated carbon) and monitored natural attenuation.

An approach to corrective action is described using the Dan River Steam Station as a case study. The results from Dan River are very much representative of ash basins throughout the United States. Fig. 19.12 provides an aerial view of the Dan River Steam Station, superimposed with groundwater equipotential lines.

As would be predicted in a typical slope aquifer system, groundwater follows the general topography. Fortunately, the requirement that power plants be constructed near a major river or lake means that the prevailing groundwater is in that direction and away from private residences, which may rely on drinking water. Contaminated groundwater that reaches surface water is attenuated and typically unmeasurable when mixed with a reasonably large and fast moving surface water body. The source of contamination is a nonpoint source in terms of the Clean Water Act, analogous to an agricultural runoff. This is principally because the distribution of contaminants is discontinuous and intermittent as they enter a surface water body. The distribution is a function of the prevailing reactivity and tortuosity of the subsurface, which varies dramatically according to the heterogeneous nature of soils and sediment. This is in stark contrast to contaminants that emerge distinctly from a point source (e.g., an

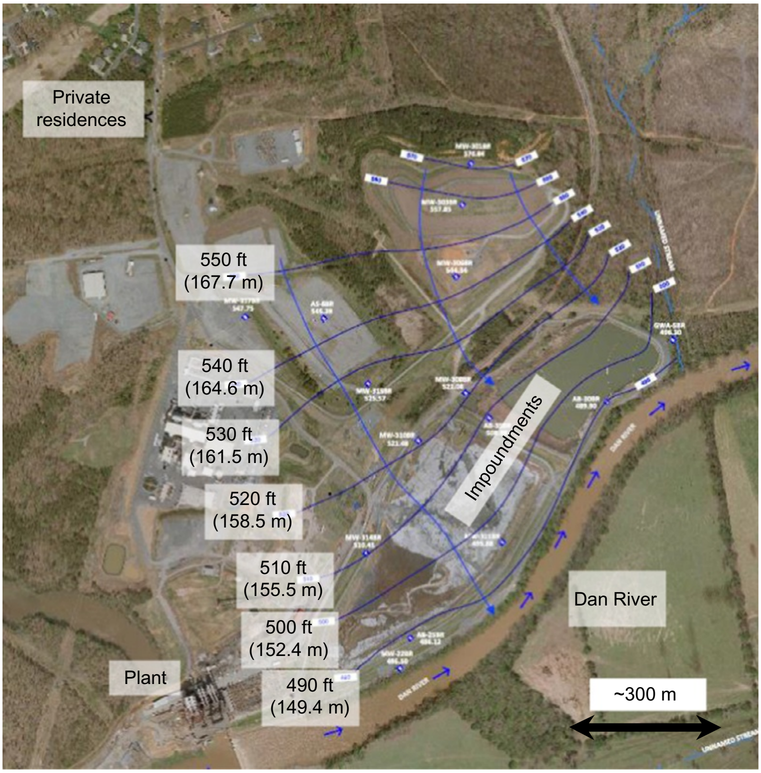

**Fig. 19.12** Groundwater equipotential lines superimposed on Dan River Steam Station Site. From Comprehensive Site Assessment, HDR, Inc., Available from North Carolina Department of Environmental Quality.

outfall pipe). This is true in the case of the Dan River, where the flowrate of the river is several orders of magnitude greater than the flowrate of adjoining aquifer. For example, groundwater velocity in aquifers is often measured in meters per day, as opposed to meters per second or minute in a river.

Groundwater flow to the Dan River downgradient of the ash impoundments was calculated to be 0.007 $m^3/s$ (0.25 cfs), whereas the mean annual flow in the Dan River is 51 $m^3/s$ (1817 cfs). To consider low-flow conditions, the smallest flowrate observed for 1 or 7 days over a 10-year period (1Q10/7Q10) in the Dan River is 7.5 $m^3/s$ (264 cfs) and 10.8 $m^3/s$ (382 cfs). As such, the dilution factor (groundwater flowrate plus river flowrate divided by the groundwater flowrate) is at least 1057, while on average it is 7268. These calculations can be readily computed for other sites. Given the limiting composition and leachability of CCR (e.g. see Fig. 19.4 or Thorneloe, Kosson, Sanchez, Garrabrants, & Helms, 2010) it is generally not possible for groundwater contaminated by ash impoundments to subsequently have a meaningful influence on surface water quality.

Sampling of the monitoring wells at the Dan River Steam Station revealed that the majority of horizontal and vertical impacts to groundwater can be represented by boron, total dissolved solids, or sulfate. Data from monitoring wells installed near the surface, at an intermediate depth and in bedrock, are all collapsed together to provide the combined area, where exceedances of groundwater protection standards occurred, as shown in Fig. 19.13.

The comprehensive site assessments provide data on the groundwater elevation, direction of flow, and contaminant concentrations. Data are also required to determine the extent to which contaminants react (e.g., sorption or precipitation) with site soils as they travel through the vadose zone or in groundwater. In the case of the Dan River site, soil samples were collected during monitoring well installation and subjected to batch and column sorption evaluation, as described by Daniels and Das (2014). Briefly, in the case of batch testing, soil samples are subjected to simulated groundwater with varying contaminant concentrations. The concentrations are measured before and after. If the aqueous contaminant concentration after exposure

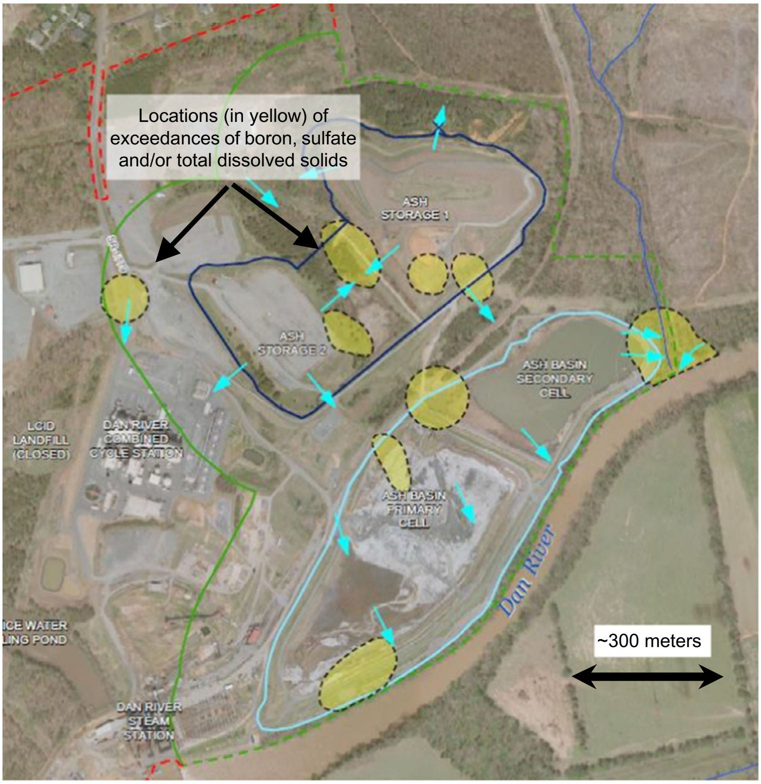
Locations (in yellow) of exceedances of boron, sulfate and/or total dissolved solids

**Fig. 19.13** Plan view of groundwater exceedances due to ash impoundments.
From Comprehensive Site Assessment, HDR, Inc., Available from North Carolina Department of Environmental Quality.

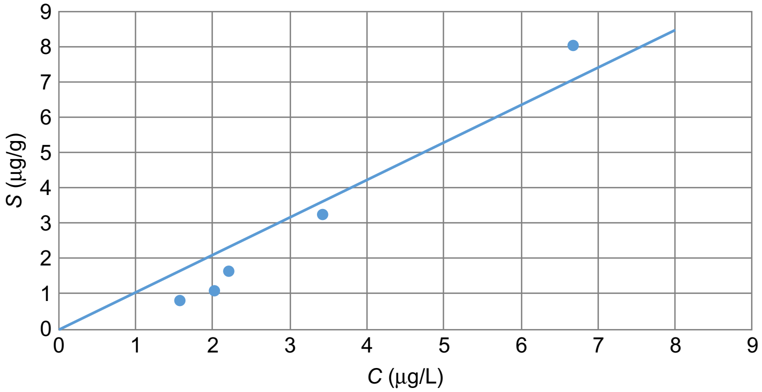

**Fig. 19.14** Batch equilibrium (at 24 h) relationship between aqueous phase ($C$) and solid phase concentrations ($S$) of arsenic for Dan River site soils ($K_d = 1000$ mL/g).
From Corrective Action Plan, HDR, Inc., Available from North Carolina Department of Environmental Quality.

(e.g., shaking in a test tube) has reduced, that reduction is attributed to sorption to the soil. Similarly, column tests are conducted by subjecting columns of soil to a continuous injection of simulated contaminated groundwater. Effluent measurements are made, and the time required for the injected contaminant concentration to appear can be used as an indicator of soil/contaminant reactions. Example results from soil samples taken from the Dan River site for batch (Fig. 19.14) and column (Fig. 19.15) arsenic conditions are presented below. The data are used to generate partition coefficients ($K_d$), which quantify the extent of partitioning from the aqueous to the solid phase, subject to various assumptions and limitations, including local equilibria and reaction reversibility.

In addition to knowledge of the contaminant concentrations and their affinity for site soils and groundwater interaction, speciation is also required. For example, when evaluating the environmental or human health risks associated with exposure, different chemical forms of the same constituent can have significantly different impacts. Fig. 19.16 provides a plot of the measured oxidation reduction potential (displayed in Eh) and pH from the Dan River site, superimposed on a standard Pourbaix diagram for both arsenic and chromium. The Pourbaix diagram provides an estimate of the dominant species of arsenic. Monitoring well measurements typically report total arsenic concentrations, whereas these data provide information on the oxidation state. Inspection of Fig. 19.16 reveals that virtually all of the arsenic is in the pentavalent ($H_3AsO_4$), hexavalent ($H_2AsO_4^-$), or septavalent forms ($HAsO_4^-$). For arsenic, it is typically the trivalent state that is more toxic than the other forms. The significance of the state varies by contaminant. For chromium, it is the hexavalent state ($CrO_4^{2-}$) that is more toxic than the trivalent ($Cr^{3+}$) form. The Eh and pH conditions at the Dan River site favor the naturally occurring and less toxic trivalent form of chromium.

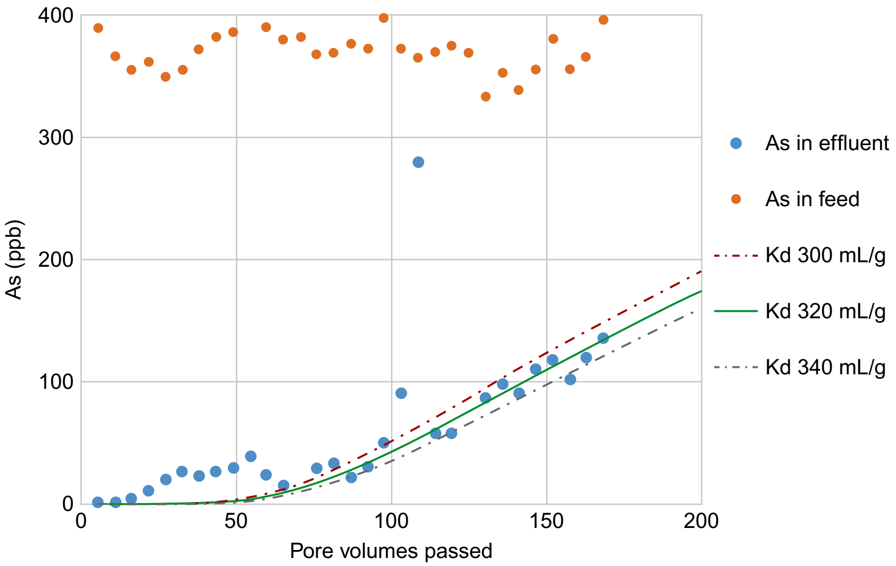

**Fig. 19.15** Column sorption of arsenic passed through columns Dan River site soils. From Corrective Action Plan, HDR, Inc., Available from North Carolina Department of Environmental Quality.

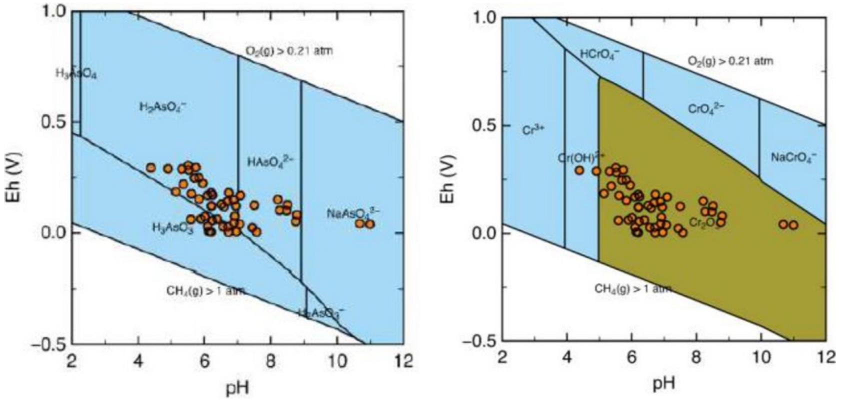

**Fig. 19.16** Speciation data for arsenic (left) and chromium (right) from the Dan River site. From Corrective Action Plan, HDR, Inc., Available from North Carolina Department of Environmental Quality.

In general the purpose of this data is to establish the extent of groundwater contamination and how that will change in the future under various corrective action scenarios. Future predictions require a three-dimensional model. The model is constrained by the hydrologic and chemical data. The basis for hydrologic data includes well logs, rivers, streams, and ditches, whereas chemical data include measured contaminant concentrations and leachability/sorption data. The process of groundwater modeling follows the typical approach (e.g., ASTM D5447), whereby the model is calibrated by adjusting the hydraulic conductivity and recharge until the head predicted by the model in any given monitoring well is close to the field-measured value. The extent to which this is successful is often judged by the root-mean-square error, which should be $<10\%$ for a comparison between model and field measured values of head. Similarly, in terms of contaminant transport, the model predicted concentrations are compared against field-measured values of concentration. In the case of Dan River, the model was used to compare the effect of excavation versus leaving the ash in place on groundwater concentrations, as shown in Figs. 19.17 and 19.18.

The foregoing figures confirm that excavation may be used as a method of source control. However, other methods can be equally or more effective without the need to excavate and transport ash. The selection of excavation for Dan River was not based on concerns for groundwater impact or any other technical (e.g., seismic stability) driver. Rather, the removal was required by NC CAMA because of the visibility associated with the original spill. Other methods of source control include: dewatering the impoundment and placement of an impermeable cap over the remaining CCR;

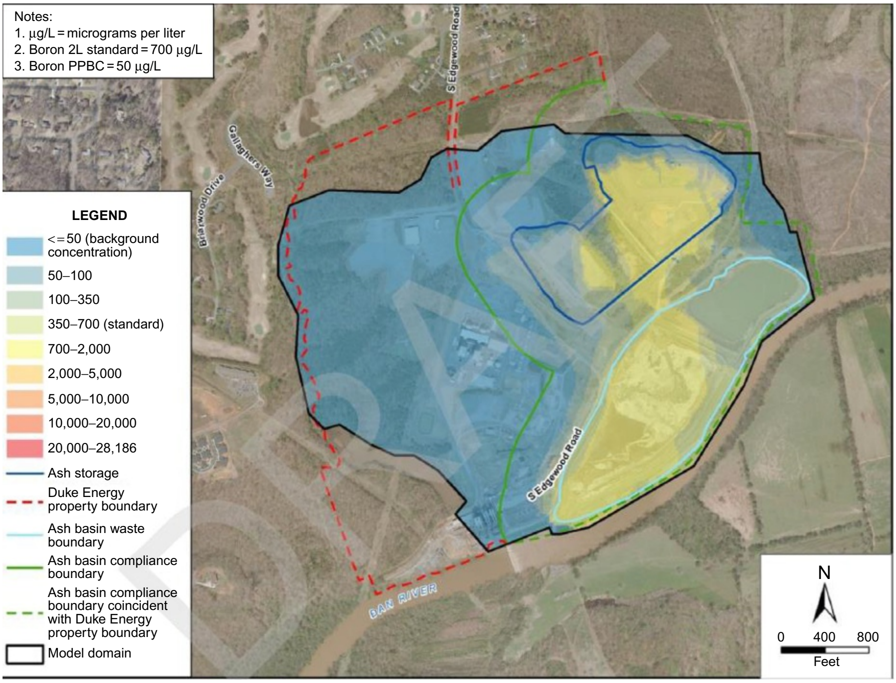

**Fig. 19.17** Model predictions for shallow groundwater at the Dan River Site in the year 2115 with the ash left in place (i.e., do nothing).
From Corrective Action Plan Part 2, HDR, Inc., Available from North Carolina Department of Environmental Quality.

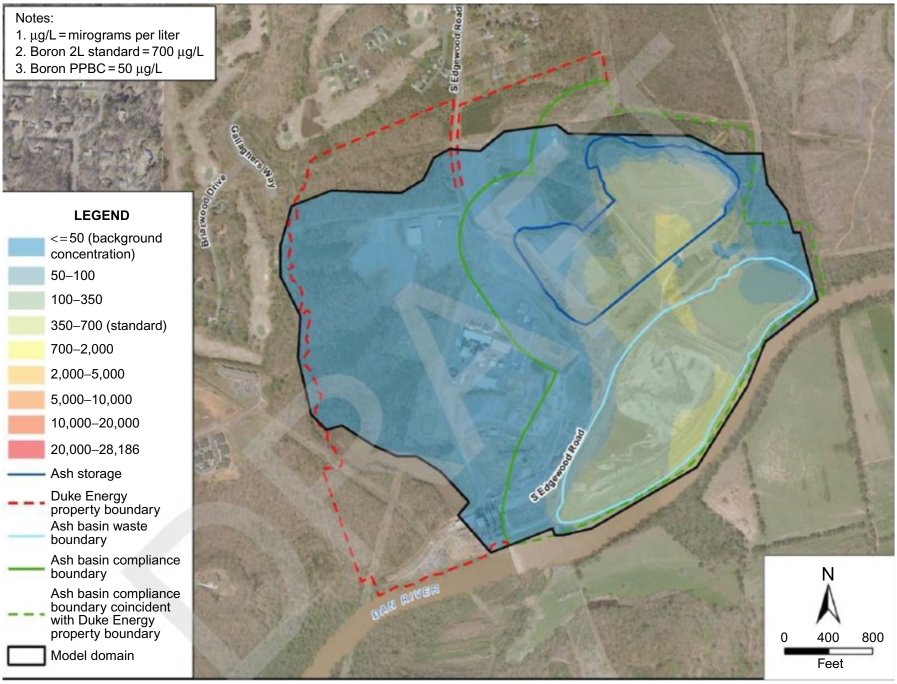

**Fig. 19.18** Model predictions for shallow groundwater at the Dan River Site in the year 2115 for ash excavation.
From Corrective Action Plan Part 2, HDR, Inc., Available from North Carolina Department of Environmental Quality.

installation of upgradient or downgradient vertical slurry walls; stabilization of the ash with lime, cement or grout material; and extraction/treatment of the groundwater. Beyond source control, a remedy must be selected to restore groundwater quality. Methods to improve groundwater quality include in situ injection of additives to encourage contaminant precipitation or sequestration, vertically placed permeable reaction walls, and monitored natural attenuation, as well as extraction/treatment. Extraction/treatment, also known as "pump and treat," is both an approach to source control and a method of groundwater remediation. Groundwater remediation techniques have evolved considerably, and there are numerous case studies and textbooks that summarize the efficacy of different approaches (e.g., Lagrega, Buckingham, & Evans, 2001; Sharma & Reddy, 2004).

According to the EPA CCR rule, remedies must (1) be protective of human health and the environment, (2) attain groundwater protection standards, (3) control the source of contamination, (4) remove contaminated material released from the impoundment, and (5) comply with other waste management standards (e.g., per general RCRA requirements). The EPA also specifies myriad criteria and related factors by which a remedy can be selected, including such considerations as the time required to complete corrective action, its efficacy, and the magnitude of risk reduction. Risk, as discussed in previous chapters, requires a threat (e.g., ash impoundment with high concentrations of contaminants), a continuous exposure pathway (e.g., aquifer is connected to source of drinking water), and a receptor (e.g., human, aquatic species, etc.). Historically, risk has been used as the basis on which to decide the extent of remediation required. For example, if there are no human or ecological receptors, then the standard of practice for hazardous waste sites has been to tolerate greater concentrations of contaminants. With respect to coal ash regulated as a solid waste, the US EPA does not relax the applicable standard because the CCR rule is self-implementing (i.e., enforced by citizen lawsuits). The rule states that since there is no permitting process, a risk-based approach to groundwater correction is "too susceptible to potential abuse." However, in the case of soil, the EPA CCR rule does not require contamination to be completely removed, noting that such requirements are not imposed "even for hazardous waste units." In sum, groundwater must be cleaned to groundwater protection standards; however, soil may remain contaminated. Notwithstanding the numerous methods for source control, the most efficient is expected to involve capping in place (with geomembranes, compacted clay, or possibly water repellent additives, such as organosilanes) or the use of slurry wall barriers. Likewise, the most efficient method for groundwater remediation is likely to include monitored natural attenuation, whereby existing soils are used to retard and/or sequester contaminants of concern, in conjunction with dispersion and dilution. Ultimate decisions are site-specific and may involve a hybrid of options, inclusive of limited excavation, isolated stabilization, and other treatment methods. Ideally, any and all options will also encourage and allow for subsequent beneficial use.

## 19.5 Sustainable closure and postclosure care

In the context of ash basin closure, corrective action is a component of the closure and postclosure plans that define the final disposition of ash and overall site development. These plans should be considered living documents in the sense that evolving data may require changes to the plan. For example, if a beneficial use opportunity (e.g., highway construction project, concrete production, etc.) emerges, then provisions can be made to the plan to accommodate that reality. Moreover, as with all engineering activities, the plans should be sustainable. In what is perhaps the best definition of sustainability, the United Nations World Commission on the Environment and Development states that sustainability is "development that meets the needs of the present without compromising the ability of future generations to meet their own needs" (United Nations, 1987). It is the needs that must be clarified, as well as the associated impacts of meeting these needs. In some sense, needs can be described in terms of benefits, and we can compare the benefit associated with any given alternate corrective action. The US DOE has published a framework with which to perform an analysis of net environmental benefits. The US DOE defines net environmental benefits as the gains in environmental/ecological services achieved by a given corrective action, minus the negative impacts to the environment required to implement the corrective action. The US DOE notes that for contaminated sites, a typical analysis typically includes (US DOE, 2003):

- leaving contamination in place
- physically, chemically, or biologically remediating the site through traditional means
- improving ecological value through onsite and offsite restoration alternatives that do not directly focus on removal of chemical contamination
- a combination of those alternatives

For example, some ash impoundments have long since been dewatered and are covered by forest. There is an ecological cost associated with tree removal, habitat disturbance, excavation, transportation, and placement of ash at some other distant location. When evaluating options, such impacts must be compared to the impact posed by allowing the ash to remain in place.

For sites in which groundwater/surface water impacts are the primary risk drivers, employing excavation as a remedy creates additional risk. The additional risk from excavation and transporting ash from one location to another can exceed the risk posed by leaving the ash in place. Additional risk drivers include fatalities and injuries from excavation and transportation, as well as ecological disturbance.

The foregoing discussion makes it clear that there are positive and negative consequences associated with any corrective action plan. Full excavation and redisposal of ash elsewhere, as well as the full and complete remediation of groundwater, may address source control and corrective action objectives while engendering other risks to human health and the environment. As such, a full analysis must be conducted on any given option, taking into consideration factors beyond groundwater contamination. The US EPA acknowledges these broader concerns in the CCR rule, noting that any selected remedy must consider risks posed to the community by excavation, transportation, and redisposal.

As such, closure planning must include a broader life-cycle analysis, with impacts not just to the immediate aquifer, but the surrounding community and environment at large. Methods and guidance to accomplish this have been developed by the Gradient Corporation (e.g., EPRI, 2015), US EPA (e.g., ITRC, 2011; US EPA, 2015), the US DOE (e.g., US DOE, 2003), ASTM (e.g., ASTM E2893-13, 2013), and others (e.g., Reddy & Adams, 2015).

The US EPA describes this type of analysis as "green remediation," noting (US EPA, 2010):

> *Green remediation is intended to reduce the demand placed on the environment during cleanup actions and to conserve natural resources. Like all activities, each stage of the remedial process (discovery, assessment, characterization, design and construction, operation of treatment and containment remedies, monitoring and maintenance of remedies, etc.) produces an environmental footprint. Environmental and community effects from cleanup activities, including fossil fuel consumption, emission of GHG and air pollutants, disruption to water cycle balances, and soil erosion, need to be considered.*

The US EPA notes that there are five core elements of green remediation: (1) energy, (2), air and atmosphere, (3) water, (4) land and ecosystems, and (5) materials and waste. For any given proposed corrective action or ultimate closure plan, the impact in each of these areas should be quantified using best available practices. Moreover and notwithstanding the EPA's commentary on risk-based corrective action in the CCR rule, the standard of care requires that each of the impacts to each of these core areas be evaluated and compared in the context of environmental risk assessment.

There are exceptions, however. As with hazardous waste sites and landfills and municipal solid waste landfills, postclosure care is generally required for ash impoundments that have been closed. Postclosure care typically refers to the activities that will ensure the integrity of source control measures (e.g., the performance of a final cover or other components of an engineered system). It also addresses systems that evaluate system efficacy (e.g., groundwater monitoring systems). The postclosure period is typically defined as 30 years, although extensions are applied as needed to address ongoing or emerging concerns. As with site assessment, corrective action and closure planning, the process is iterative and actions are informed by data.

## 19.6 Conclusion

The environmental impacts of the spills that occurred at the Kingston Fossil Plant in Tennessee and the Dan River Steam Station in North Carolina were principally short-term effects on surface water quality, with longer-term impacts to groundwater quality. In particular, at these and most other sites in which CCR impoundments have been constructed, there is a main stem river downgradient of the facility. These and most other rivers have an assimilative capacity that well exceeds the plausible potential for significant contamination by CCR, as defined by the leaching characteristics of ash and river flow rate. In the case of the TVA, the primary impact was a complete filling of the river's bathymetry with coal ash. In the case of Dan River, the primary impact was discoloration with suspended ash particles, as well as short-term (<3 days) exceedances of aluminum, arsenic, copper, and iron. Environmental impacts, however, are not relegated to accidents and spills. Virtually all CCR impoundments were constructed without liners, and while ash does not leach trace elements at levels that would qualify it as toxic or hazardous, it does leach contaminants at levels that exceed groundwater standards. These concentrations will move downgradient from any given impoundment toward the nearest surface water body (i.e., river or lake). Processes of natural attenuation, including dilution, precipitation and sorption, will reduce these concentrations with time. The extent to which these reductions are sufficient without other intervention (e.g., excavation, capping, slurry walls, groundwater treatment, etc.) will depend largely on the extent to which risk-based corrective action is allowed. The CCR Rule published in 2015 did not allow for risk-based corrective action; however, it does allow for a comparison of methods as part of "remedy selection." Moreover, the EPA and engineers in general have long recognized the importance of net environmental benefits and life-cycle assessment as part of efforts to make environmental remediation less resource intensive and community intrusive. To that end, as with the preservation, renewal, or remediation of all civil infrastructure, the principles of sustainability apply.

# References

Arcadis. (2012). Kingston ash recovery project non-time critical removal action river system baseline ecological risk assessment. Document no. EPA-EO-050. August 3.

ASTM E2893-13. (2013). *Standard guide for greener cleanups*. Developed by committee E50.04. West Conshohocken, PA: ASTM International.

Beck, M. L., Hopkins, W. A., & Jackson, B. P. (2013). Spatial and temporal variation in the diet of tree swallows: Implications for trace element exposure following habitat remediation. *Archives of Environmental Contamination and Toxicology*, *17*, 133–141.

Bevelhimer, M. S., Adams, S. M., Fortner, A. M., Greeley, M. S., & Brandt, C. C. (2014). Using ordination and clustering techniques to assess multi-metric fish health response following a coal ash spill. *Environmental Toxicology and Chemistry*, *33*, 1903–1913.

Chattanooga Times Free Press. (2009). Emory River at 'tipping point'. May 19.

Dalesio, E. P. (2016). Costs of cleaning toxic coal ash pits grows clearer. *Chattanooga Times Free Press*. Associated Press news story appearing in the February 8, 2016 issue.

Daniels, J. L., & Das, G. (2014). Practical leachability and sorption considerations for ash management. In *Geo-congress 2014* (pp. 362–376). Reston, VA: ASCE.

Electric Power Research Institute (EPRI). (2015). Relative impact framework for evaluating coal combustion residual surface impoundment closure options. 3002006286.

Greeley, M. S., Elmore, L. R., McCracken, M. K., & Sherrard, R. M. (2013). Effects of sediment containing coal ash from the Kingston ash release on embryo-larval development in the fathead minnow, *Pimephales promelas* (Rafinesque, 1820). *Bulletin of Environmental Contamination and Toxicology*, *92*, 154–159.

Greeley, M. S., Elmore, L. R., McCracken, M. K., & Sherrard, R. M. (2014). Effects of sediment containing coal ash from the Kingston ash release on embryo–larval development in the fathead minnow, *Pimephales promelas* (Rafinesque, 1820). *Bulletin of Environmental Contamination and Toxicology*, *92*, 154–159.

Integrated Environmental Assessment and Management. (2015). Special series: Ecological risk assessment for residual coal fly ash at watts bar reservoir, Tennessee. *Integrated Environmental Assessment and Management*. Available at http://onlinelibrary.wiley.com/doi/10.1002/ieam.v11.1/issuetoc.

ITRC. (2011). *Green and sustainable remediation: A practical framework*. November, prepared by The Interstate Technology & Regulatory Council Green and Sustainable Remediation Team. http://www.itrcweb.org/GuidanceDocuments/GSR-2.pdf.

Jacobs Engineering. (2012). *Kingston ash recovery project non-time-critical removal action river system baseline human health risk assessment*. Document no. EPA-EO-052. July 11.

Lagrega, M. D., Buckingham, P. L., & Evans, J. C. (2001). *Hazardous waste management* (2nd ed.). New York: McGraw-Hill. 1202 p.

Lemly, A. D. (1997). Ecosystem recovery following selenium contamination in a freshwater reservoir. *Ecotoxicology and Environmental Safety*, *36*, 275–281.

Lemly, A. D. (2002). Symptoms and implications of selenium toxicity in fish: The Belews Lake case example. *Aquatic Toxicology*, *57*, 39–49.

Mathews, T., Fortner, A. M., Jett, R. T., Morris, J., Gable, J., Peterson, M. J., et al. (2014). Selenium bioaccumulation in fish exposed to coal ash at the Tennessee Valley Authority Kingston spill site. *Environmental Toxicology*, *33*, 2273–2279.

Ohlendorf, H. M., Hothem, R. L., & Welsh, D. (1989). Nest success, cause-specific nest failure, and hatchability of aquatic birds at selenium-contaminated Kesterson Reservoir and a reference site. *The Condor*, *91*, 787–796.

Otter, R. R., Bailey, F. C., Fortner, A. M., & Adams, S. M. (2012). Trophic status and metal bioaccumulation differences in multiple fish species exposed to coal ash-associated metals. *Ecotoxicology and Environmental Safety*, *85*, 30–36.

Oweis, I. S., & Khera, R. P. (1998). *Geotechnology of waste management*. Boston, MA: PWS Publishing Company. 472 p.

Reddy, K. R., & Adams, J. A. (2015). *Sustainable remediation of contaminated sites*. New York, NY: Momentum Press. 160 p.

Resource Conservation and Recovery Act (2012). 42 U.S.C. §§6901-6992k. Subchapter I—General provisions. *Environmental law deskbook*.

Rigg, D., Wacksman, M., Iannuzzi, J., Baker, T. F., Adams, S. M., & Greeley, M., Jr. (2015). Assessing ecological risks to the fish community from residual coal fly ash in Watts Bar Reservoir, Tennessee. *Integrated Environmental Assessment and Management*, *11*, 88–101.

Rivera, N., Kaur, N., Hesterberg, D., Ward, C. R., Austin, R. E., & Duckworth, O. W. (2015). Chemical composition, speciation, and elemental associations in coal fly ash samples related to the Kingston ash spill. *Energy & Fuels*, *29*, 954–967.

Sharma, H. D., & Reddy, K. R. (2004). *Geoenvironmental engineering. Site remediation, waste containment, and emerging waste management technologies*. New York, NY: John Wiley and Sons. 968 p.

Sherrard, R. M., Carriker, N. E., & Greeley, M. S. (2015). How toxic is coal ash? A laboratory toxicity case study. *Integrated Environmental Assessment and Management*, *11*, 88–101.

Thorneloe, S. A., Kosson, D. S., Sanchez, F., Garrabrants, A. C., & Helms, G. (2010). Evaluating the fate of metals in air pollution control residues from coal-fired power plants. *Environmental Science and Technology*, *44*(19), 7351–7356.

TVA. (2011). *Kingston Ash recovery project, groundwater flow and transport model report*. Document no. EPA-RPT-1002, prepared for the Tennessee Valley Authority, Revision 01, July 25.

TVA. (2012). *Addendum to the Kingston ash recovery project, groundwater flow and transport model report*, Document no. EPA-RPT-1002A, prepared for the Tennessee Valley Authority, Revision 00, July 3.

TVA. (2013). *Addendum 2 to the Kingston ash recovery project, groundwater flow and transport model report*. Document no. EPA-RPT-1002B, prepared for the Tennessee Valley Authority, Revision 00, April 29.

TVA. (2014). Groundwater monitoring report. In *June 2014 Quarterly monitoring event, September 8*, Knoxville, TN: Tennessee Valley Authority.

United Nations. (1987). *Report of the World Commission on Environment and Development*. New York, NY: United Nations.

US Department of Energy. (2003). *A framework for net environmental benefit analysis for remediation or restoration of petroleum contaminated sites*. ORNL/TM-2003-17.

US DOE. (1995). *Record of decision for the lower Watts Bar Reservoir*, Document no. DOE/OR/02-1373&D3. US Department of Energy. September.

US DOE. (1996). *Remedial investigation/feasibility study of the Clinch River/Poplar Creek Operable Unit, Oak Ridge, Tennessee*. DOE/OR/01-1393&D3. US Department of Energy.

US DOE. (1997). *Record of decision for the Clinch River/Poplar Creek Operable Unit, Oak Ridge, Tennessee*. DOE/OR/02-1547&D3. US Department of Energy.

US EPA. (2010). *Superfund green remediation strategy*. Office of Solid Waste and Emergency Response, US Environmental Protection Agency.

US EPA. (2015). 40 CFR Parts 257 and 261. Hazardous and solid waste management system; disposal of coal, combustion residuals from electric utilities. Final rule. *Federal Register*, *80*(74).

Van Dyke, J. U., Steen, D. A., Jackson, B. P., & Hopkins, W. A. (2013). Interspecific differences affect egg trace element concentrations after a coal fly ash spill. *Environmental Science and Technology*, *47*, 13763–13771.

Van Dyke, J. U., Steen, D. A., Jackson, B. P., & Hopkins, W. A. (2014). Maternal transfer and embryonic assimilation of trace elements in freshwater turtles after remediation of a coal fly ash spill. *Environmental Pollution 194*, 38–49.

# Storage of coal combustion products in the United States: Perspectives on potential human health and environmental risks

# 20

*A. Lewis**, *A. Bittner**, *K. Radloff**, *B. Hensel*†
*Gradient, Cambridge, MA, United States, †Electric Power Research Institute, Palo Alto, CA, United States

## 20.1 Background

Although coal began to be used as an energy source in North America in the late 1800s, it was not until the 1960s that coal-fired electricity generation became the major means of energy production in the United States (ACF, 2005). A similar trend was true in Europe as well. In the United Kingdom, coal-fired electricity generation was nearly equal to coal-fired steel production through the 1960s before becoming the dominant use in the 1970s (UK DBEIS, 2016). The rise in coal-fired electricity generation necessitated the development of waste management practices for coal combustion products (CCPs), which were now being generated in larger volumes via this process. In the United States, the American Coal Ash Association (ACAA), which has published information on CCP generation since the mid-1960s, reports that ~25 million short tons of CCP were generated in 1966, an amount that steadily increased until about 2000, when CCP production volumes leveled off at ~120 million short tons [108 metric tonnes (MTs)] (ACAA, 2015). Although a significant portion of CCPs are recycled and reused beneficially, according to the latest ACAA products and use report, about half of CCPs are disposed of as waste in the United States. In contrast, within the EU (specifically the EU-15), 90.5% of CCP was beneficially reused, 2.4% was stockpiled for future use, and only 7.1% was disposed in 2008 (Feuerborn, 2011). Similar percentages were reported thorough the 2000s (EEA, 2007). The current estimate of how much CCP is produced worldwide is about 780 MTs (Heidrich, Feuerborn, & Weir, 2013). The largest producers of CCPs outside the United States are China (395 MTs) and India (105 MTs), with significant increases in CCP production expected as these countries continue to develop (Heidrich et al., 2013). Currently, ~30% of the CCPs produced in China and 75% of the CCPs produced in India are disposed of as waste (Heidrich et al., 2013).

CCPs generated in high volumes include fly ash, bottom ash, boiler slag, and flue-gas desulfurization products. These CCPs are routinely comanaged with other

**Coal Combustion Products (CCP's).** http://dx.doi.org/10.1016/B978-0-08-100945-1.00020-4

lower-volume utility wastes, most commonly coal mill rejects, floor/yard drain wastewater, demineralizer reagent, air heater/precipitator wash, and coal pile run-off. When these wastes are managed together with CCPs, they can significantly change the combined waste's pH (EPRI and USWAG, 1997; US EPA, 2009a). Therefore, comanaged waste can modify the leaching potential of CCP constituents, which is of greater concern in surface impoundments than in landfills.

As described in more detail in the following sections, two main types of CCP management methods have developed over time: wet storage of CCP in surface impoundments or ponds and dry storage in landfills. In 2013, as part of a request for information from utilities to support CCP management regulations, the US EPA published information on existing surface impoundments and landfills (active and inactive) in the United States. Although the survey covered surface impoundments for utility wastewater as well as CCPs, its results indicated there were well over 700 active surface impoundments and 300 landfills that managed CCPs in the United States at that time; many more inactive impoundments also exist (US EPA, 2016). These results, which were made available to the public, indicated that the earliest existing CCP surface impoundment was opened in 1914, with hundreds beginning to operate in the period of 1950–80. This information is consistent with a survey of CCP management facilities conducted by the Electric Power Research Institute (EPRI), which reported that the number of these facilities started to grow in 1960; that growth continued through 1985, at which time the number of facilities began to decline.

## 20.2 History of evaluation of potential human health and ecological risk associated with CCP management

The generation of high volumes of CCPs, in conjunction with federal initiatives to regulate waste management practices, had led to in-depth examinations of the potential risks associated with CCP management in the United States. Shortly after the passage of the Resource Conservation and Recovery Act (RCRA), the US Congress passed the Solid Waste Disposal Act Amendment of 1980 (commonly referred to as the Bevill Amendment). This regulation specifically exempted "fly ash waste, bottom ash waste, slag waste, and flue gas emission control waste generated primarily from the combustion of coal or other fossil fuels" (US Congress, 1980). However, at the same time, the Act called for the US EPA to evaluate adverse effects on human health and the environment caused by the disposal and beneficial reuse of CCP (US Congress, 1980). The first report in which the US EPA addresses these issues was published in 1988 (US EPA, 1988). While acknowledging potential groundwater contamination from CCP leachate as a possible environmental issue, the agency's analysis offered the "tentative" conclusion that the actual potential for exposure of human and ecological populations is likely to be minimal and that CCP waste management practices at the time appeared to be adequate for protecting human health and the environment (US EPA, 1988). This conclusion was largely based on the examination of case reports, groundwater monitoring data collected around active facilities, and general information about the environmental conditions that affect the leaching of CCP constituents from waste management facilities.[1] Also, the report concluded that these constituents did not meet hazardous waste criteria because they are unlikely to be corrosive, reactive, or ignitable; in general, metals in CCP leachate were not present above the toxicity characteristic leaching procedure (TCLP) threshold. However, this report only addressed large-volume CCP wastes and did not consider that these wastes were often comanaged with other utility wastes.

To further examine the potential risks to human health and the environment from CCPs, the US EPA released a subsequent analysis of CCP risk potential in 1999. This analysis involved a more thorough risk assessment that not only considered human health risks from exposure to CCPs via groundwater, but also examined "above ground" pathways, including risks from the inhalation and ingestion of CCPs via air and soil, as well as direct contact. The US EPA concluded in its report to Congress that "co-managed wastes generated at coal-fired utilities, including petroleum coke combustion wastes as well as wastes from other fuels co-fired with coal, generally present a low inherent toxicity, are seldom characteristically hazardous, and generally do not present a risk to human health and the environment" (US EPA, 1999). This conclusion was modified in the associated regulatory determination, in which the US EPA acknowledged that, "The composition of these wastes could present danger to human health and the environment under certain conditions" (US EPA, 2000). Additionally, because more damage cases (see sections below for the specific definition and description of damage cases) had been identified and because there were few comprehensive regulatory programs at the state level, the US EPA decided that national regulations for the management of CCPs in landfills and surface impoundments should be developed (US EPA, 2000). Also at this time, the US EPA determined that the use of CCP as minefill should be evaluated separately (US EPA, 2000).

The mandate to establish federal criteria for the management of CCPs reopened an examination of the potential human health and ecological impacts of CCP waste management. This latest analysis resulted in a draft risk assessment report in 2007, which was reissued in 2010 in response to public comments and finalized in 2014 (US EPA, 2007a, 2010, 2014a). The overarching conclusion of the most recent risk assessment was that managing CCP waste in unlined surface impoundments has the potential to result in significant human health risks (from exposure to CCPs via drinking water ingestion), as well as adverse impacts on the environment. The report also concluded that the human health risks posed by surface impoundments with synthetic liners and landfills (again, from exposure to CCPs via drinking water ingestion) were negligible. The results of this risk assessment, in large part, form the basis for the requirements put forth in the 2015 CCR Rule, "Hazardous and Solid Waste Management System; Disposal of Coal Combustion Residuals From Electric Utilities" (US EPA, 2015a).

---

[1] The regulatory determination associated with this analysis was not published until 1993 but ultimately stated, "that regulation under Subtitle C of RCRA is inappropriate for the four waste streams that were studied because of the limited risks posed by them and the existence of generally adequate State and Federal regulatory program" (US EPA, 1993).

More details on the results of US EPA's evaluations of the human health and environmental risks posed by CCP waste management practices are presented in subsequent sections of this chapter.

The approach to CCP waste regulation in the EU reflects the substantial reuse of CCP there. Fly ash and furnace bottom ash are regulated in the EU as waste under the Waste Framework Directive [Directive 2008/98/EC] (European Parliament, 2008). However, once the material is prepared for reuse, it is no longer considered a waste and is instead considered a product regulated under Registration, Evaluation and Authorisation of Chemicals, or REACH [Regulation (EC) No 1907/2006] (EC, 2006). Construction products made from CCPs must further meet the standards outlined in the Construction Products Regulation (CPR) [Regulation (EU) No 305/2011] (EC, 2016).

## 20.3 Damage cases

There have been several instances in which CCP management practices at specific US facilities have been associated with groundwater or surface water contamination. When the EPA identifies proven cases of contamination, these cases are referred to as "damage cases" (see definition of damage case below). These cases have played a part in the regulatory determinations regarding the US federal requirements for CCP management facilities. Most notably, in 2008, one of the containment dikes at the Kingston facility in Tennessee failed, releasing ~5.5 million cubic yards of CCP, covering about 300 acres of land and flowing into the Emory River (Industrial Economics, Inc., 2015). Although some properties in the vicinity of the CCP spill experienced physical property damage, a recent authoritative report concluded, "There is little evidence of substantial toxicity-derived service loss in the vicinity of the Kingston facility" (Industrial Economics, Inc., 2015). This highly visible incident highlighted the potential risks associated with the failure of surface impoundment containment systems. While the structural stability of impoundments is a key issue with respect to potential human health and ecological impacts from the storage of CCPs in impoundments, it will not be addressed further in this chapter.

Historically, other incidents have raised awareness of the potential adverse impacts of CCP surface impoundment effluent discharging into lakes, nearby wetlands, or other aquatic habitats. One example includes an incident that occurred at Belews Lake, North Carolina, which involved "extensive impacts on fish populations due to direct discharge to a surface water body" (US EPA, 2007b).

In 2007, the US EPA released a comprehensive report documenting 67 CCP sites that it categorized as proven or potential damage cases. The US EPA defined proven damage cases as those:

1. With documented exceedances of primary federal maximum contaminant levels (MCLs) or other health-based standards measured in groundwater at sufficient distance from the CCP management unit, indicating that CCP constituents have migrated to the extent that they could pose human health risks.

2. In which a scientific study demonstrates there is documented evidence of another type of damage to human health or the environment (e.g., ecological damage) caused by the CCP management facility.
3. In which there has been an administrative ruling or court decision with an explicit finding of specific damage to human health or the environment caused by the CCP management facility.

Potential damage cases were defined as those with

1. Documented exceedances of primary MCLs or other health-based standards measured only directly beneath or in very close proximity to the CCP management facility.
2. Documented on-site or off-site exceedances of secondary MCLs or other nonhealth-based standards.

In damage cases in which a facility comanages CCPs with other types of industrial waste, it was necessary for the CCPs to be clearly implicated in the reported damage. EPRI collected data and information from the power companies responsible for the 67 facilities covered in the US EPA damage case report and performed an independent review (EPRI, 2010). Four of the facilities turned out to be oil ash management facilities, rather than CCP management facilities. Roughly half of the remaining 63 facilities were surface impoundments.

### 20.3.1 Surface impoundment damage case summary

All of the 31 surface impoundments categorized by the US EPA as damage cases were constructed prior to 1990, with most constructed prior to 1980 (Fig. 20.1). Only two of these surface impoundments were built with liners, although some of them were either retrofitted with liners or contained newer cells constructed with liners (EPRI, 2010). The prevalence of older, unlined surface impoundments being classified as damage cases by the US EPA can be contrasted with information provided later in this chapter that shows most CCP management facilities constructed since about 1990 have been lined.

Groundwater and surface water were reportedly the affected media for 22 and 9 of the surface impoundment damage cases, respectively (EPRI, 2010). EPRI (2010) compiled information on 22 documented exceedances of groundwater quality standards at the surface impoundments where groundwater impacts were reported. Such exceedances were documented for 18 of these 22 damage cases; in 9 of these 18 cases, the exceedances included concentrations of CCP constituents that were higher than an MCL. In most of these cases, the exceedances were measured in on-site monitoring wells. However, in two cases, the off-site exceedances of groundwater quality standards were reported, with one of these being an exceedance of the MCL for cadmium.

According to the EPRI (2010) data, concentrations of sulfate and boron in groundwater most frequently exceeded state or federal groundwater quality standards (exceedances of these two constituents were measured at more than 75% of the surface impoundments, at which concentrations of these constituents were monitored [eight sites minimum; see Fig. 20.2]). Arsenic was the only other constituent with exceedances measured at more than half of the surface impoundments at which

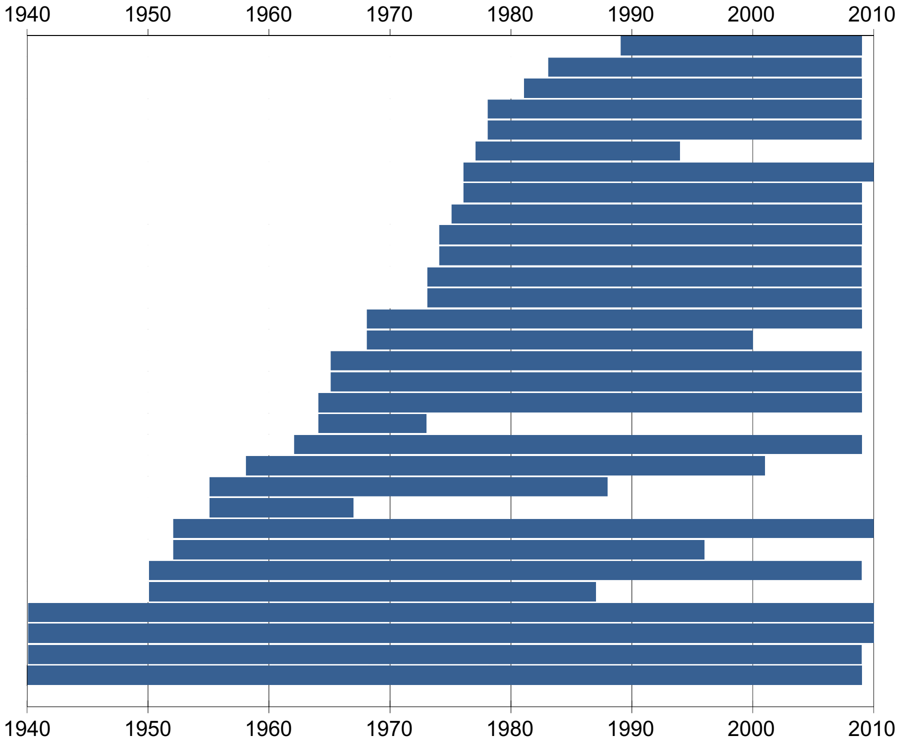

**Fig. 20.1** Periods of operation for surface impoundment damage cases. Starting dates are unknown for surface impoundments for which bars extend back to 1940.

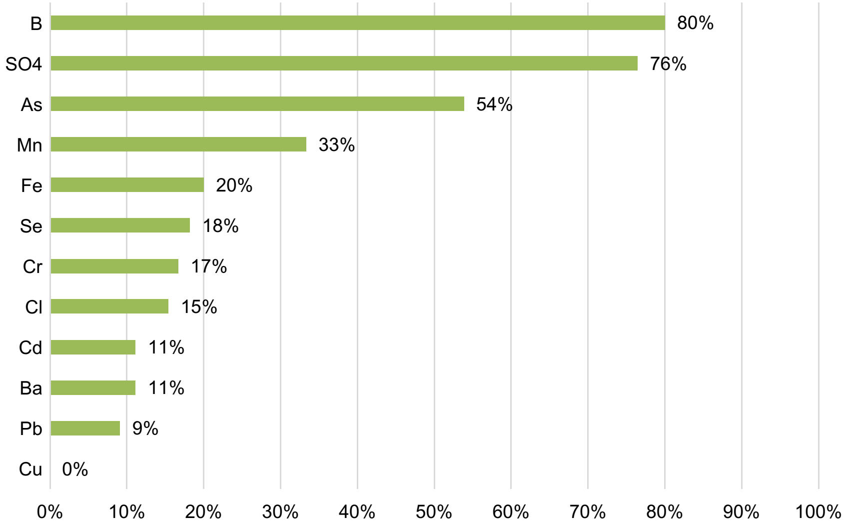

**Fig. 20.2** Percentage of damage case surface impoundments at which monitored constituents exceeded applicable groundwater quality standards.
From Electric Power Research Institute (EPRI). (2010).

concentrations of this constituent were monitored (Fig. 20.2). Conversely, barium, cadmium, chloride, chromium, copper, iron, lead, and selenium exceedances were reported at fewer than 25% of the surface impoundments at which concentrations of these constituents were monitored (see Fig. 20.2).

### 20.3.2 Landfill damage case summary

All of the 32 CCP landfills classified as damage cases by the US EPA were constructed prior to 1990, with most constructed prior to 1980. Most of the landfills (25 out of 32) were either entirely unlined or contained older cells that were unlined (Fig. 20.3). Only four of the damage case landfills were fully lined, and only one of these had a leachate collection system (EPRI, 2010). The likelihood of older, unlined landfills being classified as damage cases by the US EPA can be contrasted with information provided later in this chapter, showing that most CCP management facilities constructed since 1990 have been lined. This observation led EPRI (2010) to conclude that the CCP landfills classified as damage cases by the US EPA are not representative of current landfill construction practices.

Groundwater impacts were listed as the affected media for all 32 of the damage case landfills (EPRI, 2010). EPRI (2010) compiled information on the documented exceedances of groundwater quality standards at these landfills. Exceedances were documented in 27 of the 32 cases, and in 12 cases, measured concentrations of certain constituents were higher than their corresponding MCL. In most cases, the exceedances were measured in on-site monitoring wells; however, in six cases, off-site exceedances were reported, with two of these being exceedances of an MCL (arsenic at one site and selenium at another).

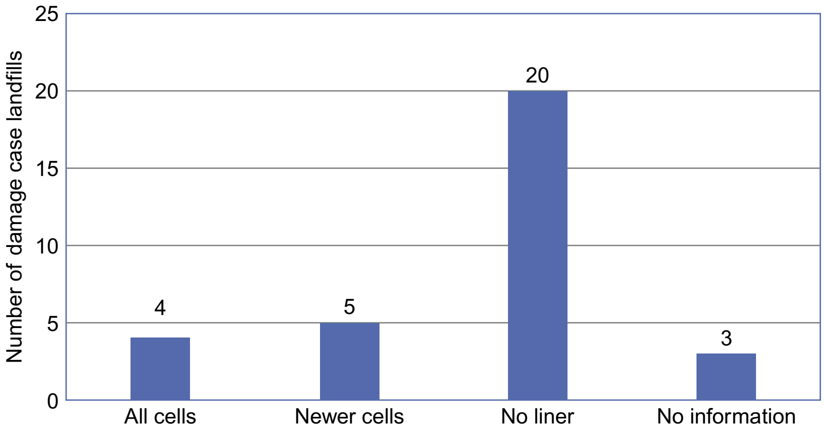

**Fig. 20.3** Liner status for landfills identified by US EPA (2007b) as proven or potential damage cases.
From Electric Power Research Institute (EPRI). (2010).

According to the EPRI (2010) data, the constituents that most frequently exceeded state or federal groundwater quality standards at the 32 damage case landfills were sulfate and boron. More than 75% of the landfills at which these constituents were monitored reported such exceedances (eight sites minimum; see Fig. 20.4). Iron and manganese were the only other constituents that exceeded groundwater quality standards at more than half of the landfills at which these constituents were monitored (Fig. 20.4). Conversely, no exceedances were reported for mercury, silver, copper, and zinc at any of the damage case landfills at which concentrations of these constituents were monitored (eight sites minimum; see Fig. 20.4).

### 20.3.3 Damage case follow-up

Since the release of the 2007 damage case report by the US EPA, it has identified several more damage case candidates, while other groups have suggested an additional 90 damage cases. The US EPA considered both the EPRI (2010) report and the additional suggested damage cases and revised its damage case assessment in the preamble to the CCR Rule. This reevaluation resulted in some of the 2007 damage cases being reclassified and some of the newly suggested damage cases being rejected, but it ultimately added to the total number of designated damage cases. The revised number of damage cases, as determined by the US EPA, is 40 proven and 113 potential (80 FR 21453; US EPA, 2014b). Based on these assessments, the US EPA concluded that

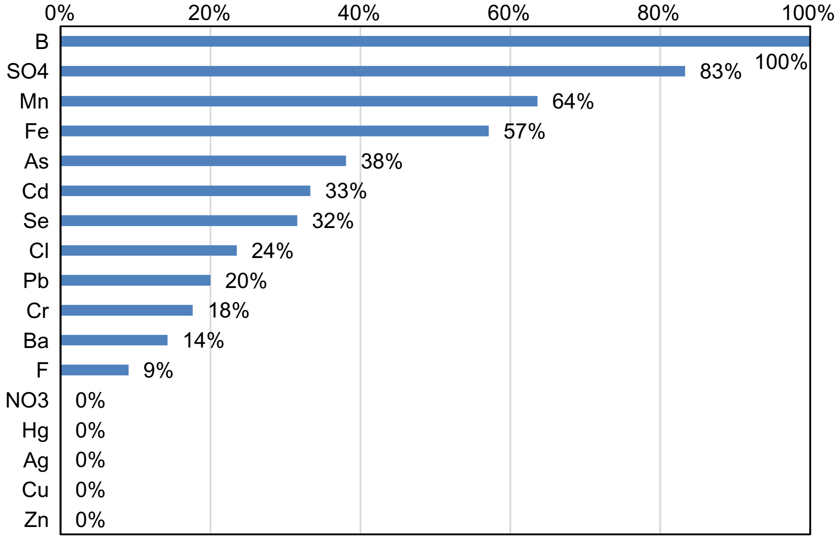

**Fig. 20.4** Percentage of damage case landfills at which monitored constituents exceeded applicable groundwater quality standards.
From Electric Power Research Institute (EPRI). (2010).

the "CCR damage case record corroborates the findings of the risk analysis by demonstrating the greater vulnerability of groundwater (and surface water) to wet disposal (i.e., surface impoundments)" (80 FR 21453; US EPA, 2014b). The US EPA also concluded:

> *the damage cases show a direct correlation between the absence of liners and groundwater impacts, and illustrate that whereas in general the design of waste units—particularly surface impoundments—has improved over time, a notable portion of CCR impoundments constructed in the last two decades still lack a protective liner, thus presenting a potential threat to groundwater.*
>
> *(40 FR 21458; US EPA, 2014b)*

The conclusions the US EPA presents with the 2015 CCR Rule have not yet been evaluated by an independent third party.

## 20.4 Exposure pathways

Throughout the CCP risk assessment and damage case evaluation process conducted by the US EPA, several human and ecological exposure pathways have been identified and evaluated. The complete set of plausible exposure pathways associated with CCP exposure were articulated by the US EPA in its final risk assessment (US EPA, 2014a) and are depicted in Fig. 20.5. Note that the figure provided below is for exposure pathways associated with surface impoundment CCP storage, but landfill pathways are qualitatively similar. As noted above, in the most recent US EPA risk assessment, the impacts of the release of CCP constituents to groundwater and the subsequent discharge of contaminated groundwater to surface water were identified as key risk pathways for both human health and ecological endpoints. Prior risk assessments of CCPs had focused on "nonwater" exposure pathways and determined that the potential human health or ecological risk from exposure to CCPs via these pathways were minimal (US EPA, 1998). Most recently, the US EPA evaluated potential inhalation risks from fugitive dust generation at landfills and concluded that best practices for landfill management are unlikely to pose a risk to human health; more specifics on best practices for landfill management and potential fugitive dust risks are provided in Section 20.8.

## 20.5 Facility design

As noted in the damage cases and CCP risk assessment results, the design of a CCP management facility is an important consideration for minimizing the potential for the system to cause adverse environmental impacts. The design of a CCP management unit takes many site-specific factors into account, including, but not limited to: the configuration of available land, geologic and hydrogeologic considerations, the engineering properties of the CCP and of soils available for liner and cover, and material

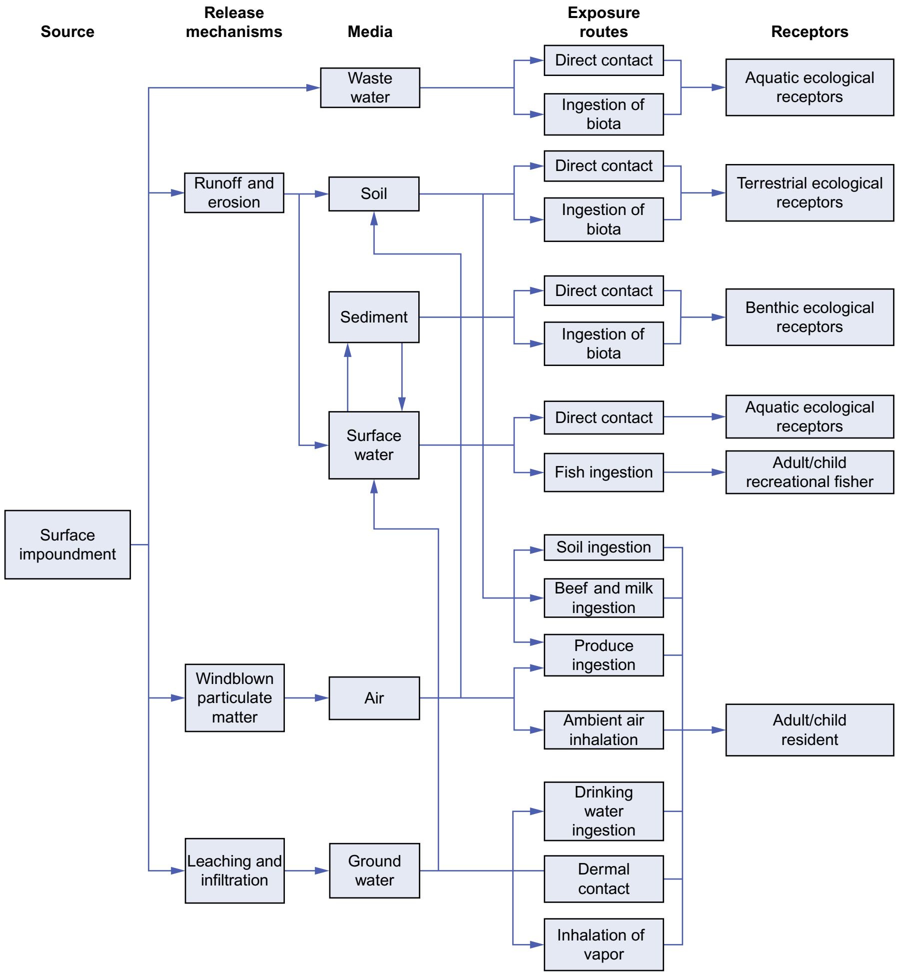

**Fig. 20.5** Key exposure pathways associated with CCP storage in surface impoundments. From US EPA. (2014a). *Human and ecological risk assessment of coal combustion residuals (final)* (1237 p.). Office of Solid Waste and Emergency Response (OSWER), Office of Resource Conservation and Recovery, December. Available from http://www.regulations.gov/#!documentDetail;D=EPA-HQ-RCRA-2009-0640-11993.

availability and cost. This section focuses on the past, present, and future high-level aspects of CCP management facility design that can affect the facility's impact on the environment.

## 20.5.1 Surface impoundments versus landfills

As mentioned in the Background section, two primary management methods for CCPs that are not beneficially re-used or placed in former mines are

- Wet placement of CCPs in surface impoundments, usually by piping a slurry of CCP and water to the impoundment.
- Dry placement, often via truck transport, of CCPs in landfills.

Prior to the 1980s, surface impoundments were the predominant type of CCP management facility. Over time, the percentage of surface impoundments has decreased and the percentage of landfills has increased. Landfills accounted for 35% of storage facilities pre-1980; this increased to 66% by 1995 and to 68% by 2004, based on surveys by the Electric Power Research Institute and the Utility Solid Waste Activities Group, EPRI and USWAG (1997) and the US DOE and US EPA (2006). This trend toward utilizing landfills as the primary type of CCP management facility is expected to continue in the future, due to the requirements put forth in the CCR Rule (US EPA, 2015a, Subpart D) and effluent limitation guidelines (US EPA, 2015b).

## 20.5.2 Liners and leachate collection systems

Just as the type of facility has evolved over time, the use of liners has also evolved over time (Fig. 20.6). CCP management units constructed prior to the 1980s often did not have engineered liners. By the 1990s the majority of new CCP management units had an engineered liner, and by the 2000s, almost all newly constructed units had an engineered liner. The predominant types of liner systems for both surface impoundments and landfills are listed as follows.

- *Compacted clay*: Clay is compacted to achieve a very low hydraulic conductivity (often, but not always, $1 \times 10^{-7}$ cm/s).
- *Synthetic*: Man-made material, such as high-density polyethylene (HDPE) or polyvinyl chloride, is used as a barrier to contain leachate within the facility.
- *Composite*: A synthetic barrier is placed over compacted clay.
- *Geocomposite liners* (*GCLs*): A product with a lower layer of material containing a high-swelling clay (e.g., bentonite) attached to an upper layer consisting of a synthetic material.

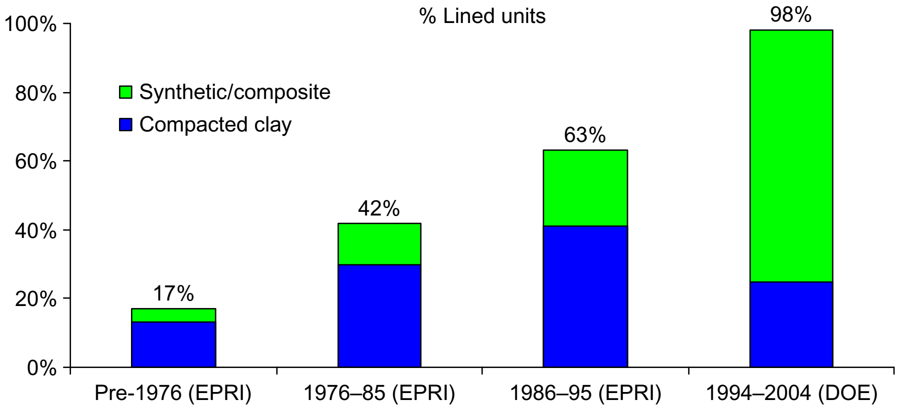

**Fig. 20.6** Results from surveys by the Electric Power Research Institute and the Utility Solid Waste Activities Group (EPRI and USWAG, 1997) and the US DOE and US EPA (2006) showing the types of liners used in CCP management units constructed during selected periods.

A leachate collection system is used to collect and remove leachate as it accumulates on top of the liner. Leachate collection systems are principally used in landfills and are not typically included in liner designs for surface impoundments. There are no statistics available on how frequently leachate collection systems have been used in CCP management systems over time.

The CCR Rule (40 CFR 257 Subpart D; US EPA, 2015a) requires that a new CCP landfill or surface impoundment cell constructed after 2015 have a composite liner and that new landfill cells constructed after 2015 have a leachate collection system. There is a provision in the CCR Rule allowing for alternative liners (e.g., GCL) to be used if it is at least as effective as the composite liner. The liner and leachate collection system requirements in the CCR Rule do not retroactively apply to existing landfills and surface impoundment cells.

## 20.6 Hydrogeological environment

This section presents a summary of several key hydrogeological factors that may affect the human health and environmental risks associated with CCP management facilities.

*Waste type*: The total elemental content and leaching potential of each element varies between different material types (e.g., coal ash, fly ash, and comanaged wastes) and depends on site-specific conditions (US EPA, 2009a). Comanagement of CCPs with other lower volume utility wastes drives the pH to more acidic or basic extremes, with measured pHs of landfilled CCPs ranging from 3 to 13 (US EPA, 2009a). Typical coal ash has a pH between 10 and 11. Coal refuse tends to be very acidic due to the high sulfate content and will reduce the pH of comanaged waste below a pH of 7. In contrast, flue-gas desulfurization wastes are basic and increase the waste pH above 11. EPA has promoted the Leaching Environmental Assessment Framework (LEAF) to provide a robust dataset for evaluating the leaching potential of CCPs under different disposal scenarios, as well as for beneficial reuse (US EPA, 2014c). Compared to the toxicity characteristic leaching procedure (TCLP) and synthetic precipitation leaching procedure, LEAF and its analogous European counterparts provide a more refined characterization leaching potential over a larger range of possible environmental scenarios.

*Soil type/hydraulic conductivity*: The soil type and hydraulic conductivity of an aquifer underlying a CCP management facility can affect risks for human and ecological receptors by impacting the migration rate of CCP constituents in groundwater. Constituent migration will be slower in low-conductivity deposits (e.g., silts and clays) than in high-conductivity deposits (e.g., sands and gravels). CCP constituent plumes migrating through low-conductivity soils will take longer to reach downgradient receptors (e.g., potential drinking water wells and surface waters) than plumes migrating through high-conductivity soils. In some cases, low-conductivity soil deposits may prevent CCP constituents from reaching downgradient receptor locations.

*Hydraulic gradient*: The hydraulic gradient of the aquifer underlying a CCP management facility is another parameter that impacts the rate of CCP constituent migration in groundwater. High hydraulic gradients will result in faster migration of CCP constituents in groundwater and earlier detection of observed impacts at downgradient receptor locations. High infiltration rates from CCP surface impoundments containing pooled water and saturated ash may induce the formation of a groundwater mound underneath the surface impoundment. A groundwater mound will increase the hydraulic gradient and consequently will increase the migration rate of CCP constituents in groundwater.

Groundwater velocity, which is a function of hydraulic conductivity and hydraulic gradient, also affects CCP constituent plume dispersion. Mechanical dispersion is caused by individual particles of groundwater migrating on different flow paths through a porous medium. Fast-moving plumes will have higher dispersion rates than slow-moving plumes (Eq. 20.1).

$$D = \alpha \cdot v \tag{20.1}$$

where $D$ is the mechanical dispersion coefficient; $\alpha$ is the aquifer dispersivity; and $v$ is the groundwater seepage velocity.

Mechanical dispersion will affect the observed concentrations of CCP constituents at downgradient receptor locations. For example, high dispersion rates may cause observed CCP constituent concentrations to be lower at groundwater receptor locations along the plume centerline compared to plumes with low dispersion rates (Fig. 20.7). Conversely, when compared to low dispersion rates, high dispersion rates may cause observed CCP constituent concentrations to be higher at groundwater receptor locations off the plume centerline (Fig. 20.7).

*Aquifer geochemistry*: Constituents in CCP leachate may undergo sorption reactions with naturally occurring compounds in soil and groundwater underlying CCP management facilities. Common naturally occurring adsorbents include ferric oxides and organic matter (HydroGeoLogic, Inc., & Resource Management Concepts, Inc., 2003). The ratio of the sorbed constituent concentration to the dissolved constituent concentration is referred to as the partition coefficient ($K_d$). Partition coefficients are used to calculate a retardation factor, which relates the

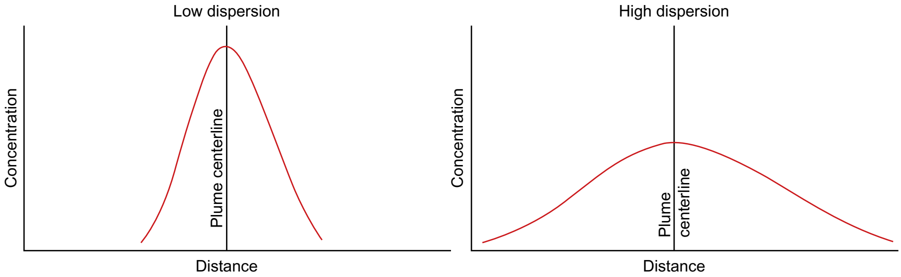

**Fig. 20.7** Example plume cross-sections for low and high dispersion rates.

transport rate of the constituent to the surrounding groundwater velocity. Although partition coefficients may vary nonlinearly depending on the constituent concentration, groundwater pH, and adsorbent concentration, high partition coefficients are indicative of a high degree of sorption and, will result in slower CCP constituent migration rates and lower groundwater concentrations of CCP constituents at downgradient receptor locations.

*Redox conditions*: Reduction-oxidation (redox) conditions in a groundwater aquifer can impact potential risks resulting from CCP constituents released into the groundwater. Many constituents common to CCP leachate, such as arsenic and selenium, may be found in multiple valence states. The predominant valence state for each constituent is partly determined by the groundwater redox conditions. For example, in an aerobic aquifer, arsenic may be more commonly found in its +5 valence state; however, if groundwater conditions are suboxic and favor chemical reduction, arsenic may be present in its +3 valence state. The migration rates of metals with multiple valence states can be quite different. Table 20.1, based on data obtained from the US EPA’s 2014 CCR risk assessment (US EPA, 2014a), presents the median saturated zone partition coefficient for surface impoundments containing comanaged CCP for different arsenic and selenium species. Because partition coefficients are an indication of a constituent’s propensity to sorb to adsorbents in an aquifer, they can be used to estimate relative constituent transport velocities; constituents with a low partition coefficient will migrate faster in groundwater than constituents with high partition coefficients.

Based on the data, arsenic (III) can be expected to migrate in groundwater about 100 times faster than arsenic(V), and selenium(VI) can be expected to migrate in groundwater about 5,000,000 times faster than selenium(IV).

*Precipitation/infiltration rates*: Precipitation can cause CCP leachate to migrate vertically downward into soils and groundwater underlying the CCP management facility. High rates of precipitation will increase the infiltration rate; consequently, the mass flux of CCP constituents migrating out of the management facility will increase.

*Intersecting/nonintersecting water table*: At some CCP management facilities, the water table intersects the CCP in the bottom of the landfill or surface impoundment. These scenarios may impact the human health and ecological risks posed by the CCP management facility by affecting the mass flux of CCP constituents that migrate from

**Table 20.1** **Median partition coefficients for arsenic and selenium species**

| CCP constituent | Median saturated zone partition coefficient ($cm^3/g$) |
|---|---|
| Arsenic(III) | 0.87 |
| Arsenic(V) | 110 |
| Selenium(IV) | 650 |
| Selenium(VI) | 0.00012 |

From US EPA. (2014a). *Human and ecological risk assessment of coal combustion residuals* (*final*) (1237 p.). Office of Solid Waste and Emergency Response (OSWER), Office of Resource Conservation and Recovery, December. Available from http://www.regulations.gov/#!documentDetail;D=EPA-HQ-RCRA-2009-0640-11993.

the facility to the surrounding environment. For CCP management facilities at which the water table does not intersect the bottom of the landfill or surface impoundment (a nonintersecting groundwater scenario), the primary mass flux mechanism of CCP constituents from the facility to the surrounding environment is the vertical downward infiltration of soluble CCP constituents into soils underlying the surface impoundment (Fig. 20.8). CCP leachate may continue to migrate downward until it reaches groundwater. For CCP management facilities at which the water table intersects the bottom of the landfill or surface impoundment (an intersecting groundwater scenario), there are several mechanisms that may cause a mass flux of CCP constituents from the facility to the surrounding environment (Fig. 20.9). Similar to the nonintersecting groundwater scenario, CCP leachate may infiltrate vertically downward into the groundwater underlying the facility. In addition, the lateral flow of groundwater through the CCP in the bottom of the landfill or surface impoundment constitutes another mass flux mechanism.

*Surface water characteristics*: The characteristics of surface waters near CCP management facilities can impact the human health and ecological risks posed by such facilities. When CCP constituents discharge from a facility to surface water, either directly or via groundwater, the discharge stream will mix with the surface water, causing an attenuation in aqueous concentrations. There will be a lower rate of attenuation for surface waters with a low flowrate or low volume and a higher rate of attenuation for surface waters with a high flowrate (e.g., major rivers) or high volume (e.g., large lakes). Furthermore, the water column's turbidity can affect aqueous surface water concentrations of CCP constituents. CCP constituents will partition between sorbed (sediment and suspended solids) and dissolved phases (sediment porewater and water column).

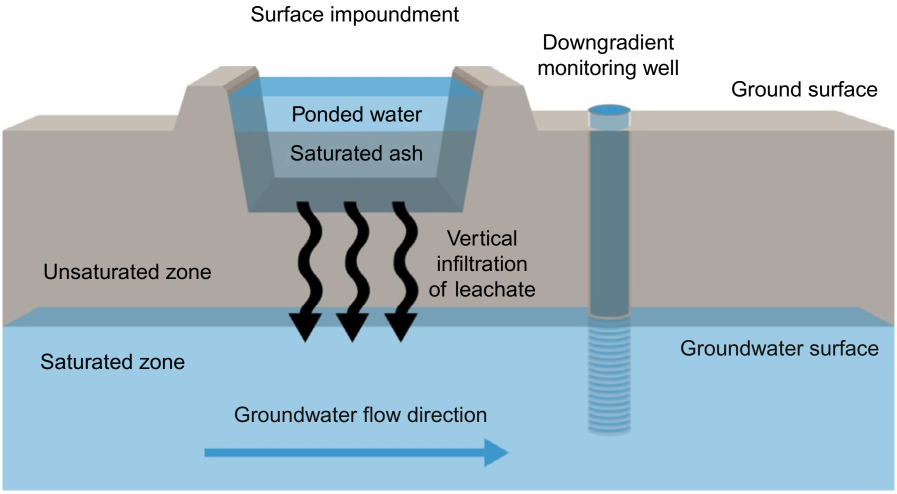

**Fig. 20.8** Simplified CCP surface impoundment schematic: nonintersecting groundwater scenario.

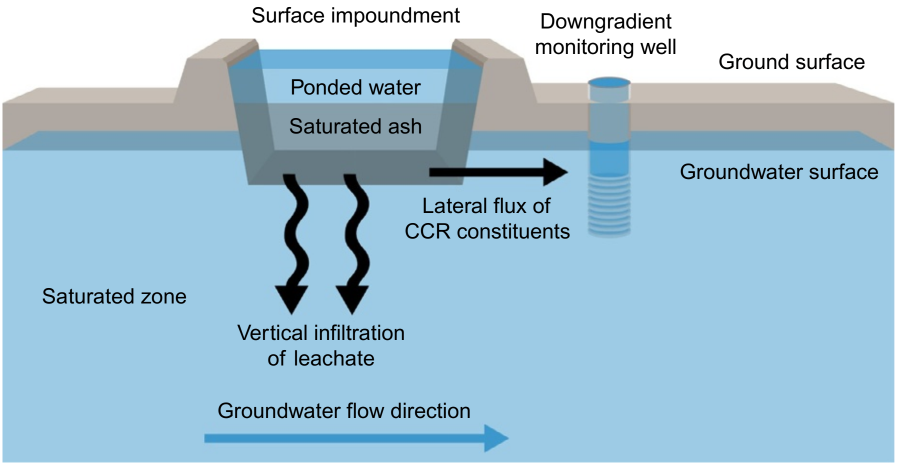

**Fig. 20.9** Simplified CCP surface impoundment schematic: intersecting groundwater scenario.

## 20.7 Human health and environmental impacts associated with storing CCP in surface impoundments

As summarized in Section 20.4, CCP constituents may be released from surface impoundments to the surrounding environment in a couple of different ways. The primary mechanisms by which releases occur are the infiltration of leachate to groundwater underlying the surface impoundment and direct discharge of wastewater or embankment seeps into nearby surface water bodies. This section provides a discussion of the potential human health and environmental impacts and risks associated with these release mechanisms.

### *20.7.1 Leachate infiltration and groundwater migration*

During the operation of the CCP management system, CCPs may be sluiced as a slurry into a surface impoundment for storage and treatment. The CCP settles to the bottom of the surface impoundment, building up over time until the impoundment is either dredged or closed. A layer of pooled water may accumulate on top of the CCP in the surface impoundment. This water may decant into an adjacent retaining structure, discharge to a surface water body, evaporate, or infiltrate into soils underlying the surface impoundment. In unlined surface impoundments, the hydraulic head caused by the column of pooled water and saturated CCP in the impoundment may cause soluble CCP constituents to migrate downward into the soils underlying the impoundment. Subsequently, this CCP leachate may migrate vertically downward through those underlying soils until it reaches groundwater.

CCP constituents can be transported through groundwater, which could potentially impact downgradient human and ecological receptors, which may be exposed via the ingestion of impacted groundwater or by dermal contact with impacted groundwater or surface water. Impacted groundwater may also discharge to nearby surface water bodies, potentially impacting human and ecological receptors. Human receptors may also be exposed to CCP constituents via direct contact with impacted surface water during recreational activities or through the ingestion of fish. Benthic and aquatic ecological receptors may also be exposed to CCP constituents via direct contact with impacted sediment and groundwater/surface water or via the ingestion of impacted sediment biota.

In its 2014 CCR risk assessment, the US EPA performed probabilistic modeling to characterize the risks to human and ecological receptors exposed to groundwater and surface water impacted by leachate from CCP surface impoundments (US EPA, 2014a). The US EPA used site-specific, regional, and national data in its risk assessment. Additionally, multiple models were used to simulate the infiltration of CCP leachate from surface impoundments, the migration of CCP constituents in groundwater, and the mixing of groundwater that discharges to surface water. The US EPA calculated the median (50th percentile) and high-end (90th percentile) risks to human health due to the ingestion of groundwater and fish impacted by CCP constituents, as well as environmental risks from impacted surface water and sediments.

The US EPA's CCR risk assessment concluded that ingestion of impacted groundwater at the 90th percentile was the only exposure pathway that resulted in human health risks above acceptable risk thresholds (e.g., a cancer risk of $10^{-5}$ and a noncancer hazard quotient of 1). No unacceptable human health risks were identified at the 50th percentile. A summary of the US EPA's calculated human health risks from CCP constituents released from surface impoundments is provided in Table 20.2. No environmental risks were identified at either the 50th or 90th percentiles in excess of relevant ecological criteria for surface water and sediment.

### 20.7.2 Direct discharge of wastewater and seeps

Pooled water in a CCP surface impoundment may be discharged into a nearby surface water body. Potential exposure pathways for human receptors exposed to surface water impacted with CCP constituents include ingestion of impacted fish, direct contact with surface water (e.g., via recreation), and incidental ingestion of surface water. Additionally, aquatic and benthic organisms may be impacted by CCP constituents in surface water and sediment. However, discharges of wastewater from CCP surface impoundments into a surface water body are typically regulated under National Permit Discharge Elimination System (NPDES) permits. Individual permits may impose restrictions on flowrates and the quality of the wastewater discharged to surface water, thus ensuring that conditions protective of human health and the environment are maintained in the surface water body.

Occasionally, unregulated seeps may flow from CCP surface impoundments into nearby surface waters. These seeps form due to the daylighting of the phreatic surface adjacent to the surface impoundment. Often, seeps may be a result of an insufficient surface impoundment embankment design and/or construction. Human health and ecological exposure pathways for human and ecological receptors exposed to CCP constituents via seeps are similar to those for direct discharges of CCP constituents to surface water.

**Table 20.2** **Summary of US EPA's 90th percentile cancer and noncancer risks from ingestion of groundwater and fish impacted by CCP constituents released from surface impoundments**

| CCP constituent and risk type | 90th percentile calculated risk | |
|---|---|---|
| | **Groundwater ingestion** | **Fish ingestion** |
| ***Cancer risk*** | | |
| Arsenic(III) | *$2 \times 10^{-4}$* | $2 \times 10^{-7}$ |
| Arsenic(V) | $1 \times 10^{-5}$ | $5 \times 10^{-9}$ |
| Chromium(VI) | $6 \times 10^{-7}$ | – |
| ***Noncancer risk*** | | |
| Arsenic(III) | *5* | – |
| Arsenic(V) | 0.4 | – |
| Boron | 0.6 | – |
| Cadmium | 0.04 | <0.01 |
| Cobalt | 0.01 | – |
| Fluoride | 0.2 | – |
| Lead | <0.01 | – |
| Lithium | *2* | – |
| Mercury | – | 0.02 |
| Molybdenum | *2* | – |
| Selenium(IV) | – | <0.01 |
| Selenium(VI) | – | 0.05 |
| Thallium | 0.9 | 0.04 |

– Represents the risks were not calculated for constituent and pathway.

*Notes*: Italicized values indicate exceedances of acceptable risk thresholds—cancer risk of $10^{-5}$ and a noncancer hazard quotient of 1.

From US EPA. (2014a). *Human and ecological risk assessment of coal combustion residuals* (*final*) (1237 p.). Office of Solid Waste and Emergency Response (OSWER), Office of Resource Conservation and Recovery, December. Available from http://www.regulations.gov/#!documentDetail;D=EPA-HQ-RCRA-2009-0640-11993.

## 20.8 Human health and environmental impacts associated with storing CCP in landfills

Generally, similar exposure pathways can be evaluated for human and ecological receptors exposed to CCP constituents released from landfills as for CCP constituents released from surface impoundments. However, risks to human health and the environment from groundwater and surface water pathways impacted by CCP constituents are generally greater for surface impoundments than for landfills. This is due to the lower infiltration rates of CCP constituents from landfills relative to surface impoundments. The lower risk to groundwater and surface water (from water infiltrating into landfills and leaching metals from the disposed material) posed by CCP landfills was highlighted in the 2014 CCR risk assessment, which found that no CCP constituents released to groundwater from landfills posed a human health risk. Interestingly, when the US EPA conducted its landfill evaluation, it only calculated risks for those CCP constituents that showed risk exceedances in the surface impoundment assessment. The reason was that if CCP constituents leaching from surface impoundments were not associated with unacceptable groundwater impacts, it could be reasonably confident that landfills would also not be associated with unacceptable impacts as well (US EPA, 2014a). A summary of the US EPA's calculated human health risks from CCP constituents released from landfills is provided in Table 20.3.

Human and ecological receptors also have the potential to be exposed to CCP constituents released from landfills via runoff and erosion. In its 2014 CCR risk assessment, the US EPA included both controlled and uncontrolled landfill management scenarios (i.e., scenarios in which current, more realistic landfill management practices are employed and those scenarios in which they are not). The US EPA determined that all risks for human and ecological receptors were below criteria under a

**Table 20.3 Summary of US EPA's 90th percentile cancer and noncancer risks from ingestion of groundwater and fish impacted by CCP constituents released from landfills**

| | 90th percentile calculated risk | |
|---|---|---|
| **CCP constituent and risk type** | **Groundwater ingestion** | **Fish ingestion** |
| ***Cancer risk*** | | |
| Arsenic(III) | $5 \times 10^{-6}$ | – |
| Arsenic(V) | $7 \times 10^{-8}$ | – |
| Chromium(VI) | $7 \times 10^{-8}$ | – |
| ***Noncancer risk*** | | |
| Arsenic(III) | 0.1 | – |
| Arsenic(V) | <0.01 | – |
| Boron | <0.01 | – |
| Cadmium | – | – |
| Cobalt | <0.01 | – |
| Fluoride | –[a] | – |
| Lead | – | – |
| Lithium | –[a] | – |
| Mercury | – | 0.01 |
| Molybdenum | <0.01 | – |
| Selenium(IV) | – | – |
| Selenium(VI) | – | – |
| Thallium | 0.08 | – |

– Represents the risks were not calculated for constituent and pathway because surface impoundment risks were considered to be de minimis.

*Notes*: There are no exceedances of acceptable risk thresholds—cancer risk of $10^{-5}$ and a noncancer hazard quotient of 1.

[a] Data were not available to model this constituent for landfills.

From US EPA. (2014a). *Human and ecological risk assessment of coal combustion residuals (final)* (1237 p.). Office of Solid Waste and Emergency Response (OSWER), Office of Resource Conservation and Recovery, December. Available from http://www.regulations.gov/#!documentDetail;D=EPA-HQ-RCRA-2009-0640-11993.

controlled management scenario in a screening assessment; therefore they did not conduct a further probabilistic assessment of risks from exposure to the CCPs constituents released from landfills via runoff and erosion (US EPA, 2014a). The US EPA concluded that the management controls required by the CCR Rule were sufficiently protective of human and ecological receptors, and it deemed further characterization of high-end risks from these exposure routes unnecessary.

Fugitive (i.e., wind-blown) dust has the potential to be a more significant route of exposure for human receptors exposed to CCP constituents for landfills. The US EPA has evaluated the potential impacts of fugitive dust emissions from landfills twice via different approaches. An initial screening evaluation was conducted as part of the ruling in 2009 (US EPA, 2009b). In this evaluation, the US EPA assumed a worst-case, yet highly improbable scenario in which an entire landfill would be exposed to wind constantly until the end of its useful life. In practice, CCP landfills are typically divided into smaller operating cells within the overall landfill footprint, and they typically employ several different dust control practices (see section on landfill management and dust control). To assess the potential risks from fugitive particulate matter (PM), the US EPA compared the results of their screening modeling (using the SCREEN3 model) to the 24-h National Ambient Air Quality Standards (NAAQS) for PM ($PM_{10}$ and $PM_{2.5}$). This is an inappropriate action for two reasons: SCREEN3 predicts total suspended PM (TSP), while the NAAQS is for $PM_{10}$ and $PM_{2.5}$; and SCREEN3 estimates 1-h maximum concentrations, while the NAAQS are for 24-h and annual average concentrations. Despite these modeling and analysis limitations, the US EPA reached the preliminary conclusion that there was a "strong likelihood that dry-handling would lead to the NAAQS being exceeded absent fugitive dust controls" (US EPA, 2009b, p. 11).

The US EPA updated the screening analysis of fugitive dust to address concerns about risks from inhaling wind-blown dust from CCP landfills in its 2014 CCR risk assessment. The US EPA conducted screening-level modeling with AERSCREEN and AERMOD to estimate dust dispersion and deposition rates associated with landfills during their operational period. Unlike the approach the US EPA used in its 2010 assessment, this more refined modeling evaluated specific concentrations of CCP constituents using the estimated 90th percentile concentrations of those constituents present in whole CCP waste. In doing so, it allowed for the evaluation of acute and chronic human health risks from specific metals using a variety of human health benchmarks, as well as for an assessment of the potential for those CCP constituent concentrations to exceed the NAAQS standards. As noted above, the US EPA included both controlled and uncontrolled landfill management scenarios in this assessment. The US EPA did not identify any human health risks above their selected criteria under the controlled management scenario. The only potential risks identified under the uncontrolled management scenario were due to $PM_{2.5}$ exceedances of the 24-h NAAQS and arsenic concentrations above the acute (not the chronic) benchmark criterion; the US EPA employed the California Environmental Protection Agency (CalEPA) Acute Reference Exposure Level (REL) for the acute arsenic benchmark criterion). Based on these findings, the US EPA did not further evaluate human health and environmental risks associated with fugitive dust emissions from CCP landfills using a probabilistic approach. The US EPA did determine that the results of the more refined screening assessment sufficiently demonstrated that the CCP landfill management controls required by the 2015 CCR Rule would be protective of human health.

### 20.8.1 Landfill management and dust control

Over the years, management practices that limit potential impacts to groundwater and air (i.e., fugitive dust) have developed. These best practices are reflected in the 2015 CCR Rule (40 CFR part 257.80; US EPA, 2015a), which establishes minimum criteria for new and existing CCP landfills, including lateral expansions of CCP landfills. These criteria are

- *Location*: For new landfills, CCP cannot be placed in the following regions: above the uppermost aquifer, in a wetland, within a fault area, within seismic impact zones, or in unstable areas. For existing landfills, CCP cannot be placed in unstable areas of the landfill.
- *Liner design*: New CCP landfills must have composite liners that include two adjacent layers—a geomembrane and two feet of compacted soil—or an alternative liner that has the same effectiveness as a composite liner. New landfills must also operate a leachate collection and removal system. Existing landfills are not subject to these requirements, but they must meet the other groundwater monitoring guidelines in the CCR Rule.
- *Structural integrity*: Periodic assessments must be made of hazard potential classification (i.e., potential for economic loss, environmental damage, or damage to infrastructure from impoundment failure), structural stability, and safety factors.
- *Operating criteria*: Landfills must comply with several specific requirements, including fugitive dust management (to be discussed), surface water run-on and run-off controls, and completion of periodic inspections.
- *Groundwater monitoring and corrective action*: Wells must be installed for groundwater monitoring, and procedures must be set for analyzing collected samples for CCP constituents of concern.
- *Closure and postclosure*: When CCP landfills are closed, all applicable standards must be followed, including postclosure groundwater monitoring and corrective action programs.
- *Recordkeeping*, *notification*, *and public posting*: CCP landfill operating records must be stored and shared with appropriate state and Native American tribal representatives, as well as the public.

To ensure fugitive dust control, the CCR Rule (40 CFR part 257.80; US EPA, 2015a) also requires that owners and operators of CCP landfills place only "conditioned" CCP in landfills, which is CCP that has sufficient moisture content to prevent wind-blown fugitive dust emissions, but not so much moisture that free liquids can separate from solid-phase CCP (US EPA, 2015a). The CCR Rule requires that landfill CCP conditioning be maintained through regular application of water or chemical dust suppressants, but does not specify the type or amount of suppressant that should be used. Rather, the CCR Rule requires landfill owners and operators to develop a fugitive dust control plan that details the fugitive dust control methods used, as well as yearly fugitive dust control reports that document all fugitive dust control measures applied to the CCP, all citizen complaints received, and any corrective measures taken.

CCP tends to repel water (i.e., it is hydrophobic), and therefore fugitive dust control measures rely on strategies to enhance CCP surface wetting (Peterson, 2011). Blazek (2003) presents four categories of control measures

- *Water sprays with surfactants*: Chemical surfactants reduce the surface tension of the water, thereby increasing the adsorption of the liquid on the surface of the CCP.
- *Foam*: A foam forms a barrier between the CCP and the air, thereby inhibiting fugitive dust emissions.
- *Emulsion*: An emulsion forms a seal over the CCP, thereby inhibiting fugitive dust emissions.
- *Water sprays with binders*, *humectants*, *and/or surfactants*: These water sprays combine surfactants (which increase the adsorption of liquid onto the CCP surface), binders (which increase the period of suppression by preventing the loss of moisture), and humectants (e.g., salts, which slow the evaporation of moisture).

Water sprays can be applied to airborne dust, CCP transfer points (i.e., points at which CCP is dumped or dropped), and other areas with the potential for fugitive dust emissions (e.g., CCP placed in landfill cells that are not vegetated or haul roads), and can be automatically controlled using electronic systems (Blazek, 2003; Peterson, 2011). Emulsions are commonly used to seal the top of CCP piles or to coat the CCP prior to transport (Blazek, 2003).

## 20.9 Corrective actions

As discussed in the sections above, certain environmental conditions and facility designs may facilitate the leaching of CCP constituents to underlying groundwater. In instances in which groundwater contamination does occur, there are several corrective action technologies that are routinely implemented at CCP management facilities. In general, the technologies can be grouped into source control (capping, excavation, installing a retrofit liner, and in situ soil stabilization and solidification, or ISS) and groundwater plume control (barrier walls, pump and treat, in situ injection, permeable reactive barriers, or PRBs). In some instances, multiple corrective action technologies may be implemented at the same site, depending on the potential risks to human health and the environment posed by the groundwater contamination. A summary of the corrective action technologies that may be implemented at CCP management facilities is presented below.

### *20.9.1 Source control*

- *Capping* consists of installing an impermeable cap (e.g., geomembrane, compacted clay, or similar structure) over the top of a CCP management facility to prevent infiltration of CCP constituents to groundwater. Capping is a proven technology that can be effective under a variety of hydrologic environments. It is relatively easy to implement and will likely be more cost effective than other control source measures.
- *Excavation and removal* consists of dewatering CCP in the surface impoundment and excavating the dried material so that it can be redisposed of in a different facility, often a lined landfill. Excavation and removal will relocate all CCP source material, thereby preventing any future

contaminant mass flux to groundwater and eliminating the need for long-term maintenance of the former disposal facility. Depending on the location of the landfill used for redisposal, this approach may have a significant impact on the surrounding community due to truck traffic while the CCP is being relocated from the surface impoundment to the landfill. The cost of excavation and removal is generally high in relation to other corrective action measures.

- A *retrofit liner* is an impermeable (e.g., HDPE) liner that is meant to be installed underneath the CCP in the management system, which is achieved by temporarily moving the CCP while the liner is constructed. Such a liner can provide an effective source control barrier between the CCP and the environment. Retrofitting CCP surface impoundments is difficult and requires double handling of the ash (i.e., remove ash out of the impoundment, then replace after the liner is installed) as the liner is installed.
- *ISS* involves injecting a cement-like slurry and mixing it with the CCP at the bottom of a surface impoundment to create a concrete-like layer of stabilized or solidified material. ISS can be implemented without the need for excavating CCP in order to improve the structural properties of the surface impoundment and stabilize CCP located below the water table.

### 20.9.2 Plume control

- Installing a *barrier wall* requires excavating trenches to the depth of a confining geological unit and pouring in concrete to create a subterranean wall around a surface impoundment. The CCP management facility can remain in operation during the installation of a barrier wall. Barrier walls are proven technologies that can effectively contain plumes of groundwater impacted by CCP constituents. However, barrier walls require long-term operation and maintenance of hydraulic control systems (i.e., pumping inside the barrier wall) to be effective.
- *Pump and treat* systems consist of pumping wells that extract contaminated groundwater in order to contain and limit the migration of impacted groundwater plumes. The extracted groundwater must be treated prior to discharging it to another location. Pump and treat is a proven technology; however, it may involve lengthy durations of remediation if not paired with a source control measure.
- *In situ injection* involves installing chemical injection wells to treat or immobilize the groundwater contamination. Minimal site disruption is required, and the injection can readily be targeted to focus on specific treatment zones, although the implementation of such systems is not yet proven at CCP management facilities. Changing groundwater geochemical conditions may render the system less effective over time.
- Installing a *PRB* requires excavating a trench and filling it with a slurry that includes chemicals or materials that can treat or immobilize groundwater contamination. Groundwater will continue to flow through the barrier. PRBs have not yet been proven in the field for all CCP-related constituents. Replenishing the PRB media may be required, depending on the source loading and groundwater flow characteristics.

## 20.10 Impacts associated with surface impoundment closure alternatives

The new requirements of the CCR Rule may pose several challenges for surface impoundment operators, which has prompted many utilities to reexamine their waste management practices, with many utilities opting for dry (i.e., landfill) over wet (i.e., surface impoundment) CCP storage. Also, the CCR Rule mandates that all inactive surface impoundments be closed. The options for closing a surface impoundment fall into two main categories

- Closure-in-Place (CIP), which involves leaving the CCP in the surface impoundment and dewatering, backfilling, and capping the surface impoundment.
- Closure-by-Removal (CBR), which involves dewatering the surface impoundment, excavating the CCP from the surface impoundment, transporting the material by truck or rail to a newly constructed landfill, and redisposing of the CCP in that landfill.

When deciding how to close a surface impoundment in a way that will maximize the human health and environmental benefits of its closure, several factors need to be considered. In addition to evaluating the potential impacts of the closure activities on groundwater and surface water, the short-term risks associated with each closure option must be weighed.

Groundwater protection will be an important consideration when selecting the most appropriate way to close a surface impoundment, but air impacts from fugitive dust and diesel equipment should also be examined, as well as potential accidents associated with CCP transport under the different closure options. Energy expenditures and resource consumption under the different closure options may also be important factors to consider. Although there will be site-specific conditions associated with each surface impoundment that will dictate the most appropriate closure options to use for the surface impoundment, in general, closing a surface impoundment using CBR will be associated with more short-term emissions from diesel and fugitive dust, truck accidents, and resource consumption than CIP (EPRI, 2016). The relative groundwater and surface water impacts of these two closures options are very specific to the site and cannot be generalized. In particular, intersecting versus nonintersecting groundwater at a facility may be a particularly important consideration when evaluating the human health and ecological risks posed by potential surface impoundment closure scenarios. Ultimately, because of the large number of site features and closure activities that may be present, a site-specific evaluation will need to be conducted in order to determine which closure option is most beneficial.

## 20.11 Summary

The disposal of CCPs has occurred over many decades. In that time, through continued study and monitoring, scientists, engineers, and regulators have gained a better understanding of the types of human health and environmental risk that may be associated with disposal. The lower intrinsic risk of dry versus wet storage has emerged as a key issue, both with respect to the possible impacts of structural dam failure, as well as the potential of contaminants to leach to groundwater. However, over time there has been an increased awareness of the potential for adverse impacts resulting from CCP disposal facilities; this awareness has triggered greater implementation of methods to limit adverse environmental impacts, such as liners and the development of other corrective actions. Additionally the development of best practices to control fugitive dust has limited potential risk via air exposures. Further considerations for environmentally friendly disposal include optimizing the beneficial impacts associated with closing surface impoundments, making use of existing CPPs for beneficial use applications, and planning for sustainable disposal of newly generated CCPs.

# References

American Coal Ash Association (ACAA). (2015). *2014 coal combustion product (CCP) production & use survey report.* 1 p., December. Available from https://www.acaa-usa.org/Portals/9/Files/PDFs/2014ReportFinal.pdf.

American Coal Foundation (ACF). (2005). *Timeline of coal in the United States.* 2 p. Available from: http://www.paesta.psu.edu/sites/default/files/timeline_of_coal_in_the_united_states.pdf.

Blazek, C. F. (2003). The role of chemicals in controlling coal dust emissions. In: *Paper presented at the American Coal Council PRB coal use: Risk management strategies & tactics course, Dearborn, MI, June 25-26.* 16 p. Available from http://www.powerpastcoal.org/download/coal-dust-the-role-of-chemicals-in-controlling-coal-dust-emissions.

European Environment Agency (EEA) (2007). EN10: Residues from combustion of coal for energy production. 11 p. http://www.eea.europa.eu/data-and-maps/indicators/en10-residues-from-combustion-of/residues-from-combustion-of-coal Accessed 28.12.16.

Electric Power Research Institute (EPRI). (2010). *Evaluation of coal combustion product damage cases. Volume 1: Data summary and conclusions (final).* 1020553 (68 p.), July.

Electric Power Research Institute (EPRI). (2016). *Relative impact framework for evaluating coal combustion residual (CCR) surface impoundment closure options.* 3002007543, May.

Electric Power Research Institute (EPRI), & Utility Solid Waste Activities Group (USWAG). (1997). Coal combustion by-products and low-volume wastes comanagement survey (final). TR-108369 (67 p.), December.

European Commission (EC). (2006). Regulation (EC) No 1907/2006 of the European Parliament and of the Council of 18 December 2006 concerning the Registration, Evaluation, Authorisation and Restriction of Chemicals (REACH), establishing a European Chemicals Agency, amending Directive 1999/45/EC and repealing Council Regulation (EEC) No 793/93 and Commission Regulation (EC) No 1488/94 as well as Council Directive 76/769/EEC and Commission Directives 91/155/EEC, 93/67/EEC, 93/105/EC and 2000/21/EC. *Official Journal of the European Union* L(396), 1–849.

European Commission (EC). (2016). *Construction products [CPD/CPR regulations].* https://ec.europa.eu/growth/single-market/european-standards/harmonised-standards/construction-products_en (Accessed November 29, 2016).

European Parliament. (2008). Directive 2008/98/EC of the European Parliament and of the Council of 19 November 2008 on waste and repealing certain directives. Council of the European Union. *Official Journal of the European Union* L 312, 3–30. November 22. http://eur-lex.europa.eu/legal-content/EN/TXT/PDF/?uri=CELEX:32008L0098&from=EN. (Accessed November 30, 2016).

Feuerborn, H. (2011). Coal combustion products in Europe—An update on production and utilisation, standardisation and regulation. In: *Presented at the World of Coal Ash (WOCA) conference, Denver, CO, May 9-12.* 18 p. http://www.flyash.info/2011/007-feuerborn-2011.pdf (Accessed November 28, 2016).

Heidrich, C., Feuerborn, H. J., & Weir, A. (2013). Coal combustion products: A global perspective. In: *Paper presented at the 2013 World of Coal Ash conference, Lexington, KY, April 22-25*. 17 p.

HydroGeoLogic, Inc., & Resource Management Concepts, Inc. (2003). *EPA's Composite Model for Leachate Migration with Transformation Products* (*EPACMTP*) *technical background document*. Report to US EPA, Office of Solid Waste. EPA-HQ-RCRA-2006-0984-0027 (490 p.), April.

Industrial Economics, Inc. (2015). *Tennessee Valley Authority Kingston Fossil Fuel Plant Coal ash release natural resource damage assessment restoration and compensation determination plan* (*Final*). Report to Tennessee Dept. of Environment and Conservation (TDEC); Tennessee Valley Authority (TVA); US Fish and Wildlife Service (68 p.), May 26.

Peterson, E. (2011). *An aid to fugitive material control in coal ash applications. In: Paper presented at the World of Coal Ash (WOCA) conference, Denver, CO, May 9-12*. 7 p. Available from http://www.flyash.info/2011/001-felde2011.pdf.

United Kingdom, Department for Business, Energy & Industrial Strategy (UK DBEIS) (). *Historical coal data: Coal production, availability and consumption 1853 to 2015. August 25.* https://www.gov.uk/government/statistical-data-sets/historical-coal-data-coal-production-availability-and-consumption-1853-to-2011 (Accessed November 28, 2016).

US Congress. (1980). *Public law 96-482: An act to amend and reauthorize the Solid Waste Disposal Act [Solid Waste Disposal Act Amendments of 1980]*. PL 96-482; 94 Stat 2334, October 21. Available from https://www.gpo.gov/fdsys/pkg/STATUTE-94/pdf/STATUTE-94-Pg2334.pdf.

US Dept. of Energy (US DOE) & US EPA. (2006). *Coal combustion waste management at landfills and surface impoundments, 1994-2004—A decade of improvement* (*draft for external peer review*). EPA-HQ-RCRA-2006-0796-0003 (240 p.), February 13.

US EPA. (1988). *Report to Congress: Wastes from the combustion of coal by electric utility power plants. Final report*. Report by ICF, Inc. to US EPA. National Technical Information Service (NTIS) EPA/530/SW-88/002a; NTIS PB88-177977 (386 p.), February.

US EPA. (1993). Final regulatory determination on four large-volume wastes from the combustion of coal by electric utility power plants. *Federal Register*, *58*(August 9), 42466–42482.

US EPA. (1998). *Draft final report: Non-groundwater pathways, human health and ecological risk analysis for fossil fuel combustion phase 2* (*FFC2*). Report by Research Triangle Institute, Center for Environmental Analysis to US EPA, Office of Solid Waste (139 p.), June 5.

US EPA. (1999). *Report to congress: Wastes from the combustion of fossil fuels. Volume I—Executive summary*. Office of Solid Waste and Emergency Response (OSWER). EPA 530-S-99-010, March. Available from http://www.epa.gov/epaoswer/other/fossil/volume_1.pdf.

US EPA. (2000). Notice of regulatory determination on wastes from the combustion of fossil fuels; final rule. *Federal Register*, *65*(99), 32214–32237.

US EPA. (2007a). *Human and ecological risk assessment of coal combustion wastes* (*draft*). Report by RTI to US EPA, EPA-HQ-RCRA-2006-0796-0009 (333 p.), August 6. Office of Solid Waste.

US EPA. (2007b). *Coal combustion waste damage case assessments*. EPA-HQ-RCRA-2006-0796-0015 (70 p.), July 9. Office of Solid Waste.

US EPA. (2009a). *Characterization of coal combustion residues from electric utilities—Leaching and characterization data*. Report by Kosson, D., Sanchez, F., Kariher, P., Turner, L. H., Delapp, R., & Seignette, P. to US EPA. EPA-600/R-09/151 (215 p.), December.

US EPA. (2009b). *Inhalation of fugitive dust: A screening assessment of the risks posed by coal combustion waste landfills* (*draft*) (43 p.), September. Office of Solid Waste and Emergency Response (OSWER).

US EPA. (2010). *Hazardous and solid waste management system; identification and listing of special wastes; disposal of coal combustion residuals from electric utilities (proposed rule)*. 283 p. Available from http://www.epa.gov/epawaste/nonhaz/industrial/special/fossil/ccr-rule/index.htm#propose.

US EPA. (2014a). *Human and ecological risk assessment of coal combustion residuals (final)*. Office of Solid Waste and Emergency Response (OSWER), Office of Resource Conservation and Recovery. (1237 p.), December. Available from http://www.regulations.gov/#!documentDetail;D=EPA-HQ-RCRA-2009-0640-11993.

US EPA. (2014b) *CCR damage case database*. Office of Solid Waste and Emergency Response (OSWER), Office of Resource Conservation and Recovery (ORCR). Submitted to US EPA Docket. EPA-HQ-RCRA-2009-0640-12123, December 18. Available from https://www.regulations.gov/document?D=EPA-HQ-RCRA-2009-0640-12123.

US EPA. (2014c). *Leaching test relationships, laboratory-to-field comparisons and recommendations for leaching evaluation using the Leaching Environmental Assessment Framework*. EPA 600/R-14-061 (357 p.), September. Office of Research and Development. http://www.vanderbilt.edu/leaching/wordpress/wp-content/uploads/600r14061-Lab-to-Field-LEAF1.pdf. (Accessed November 28, 2016).

US EPA. (2015a). Hazardous and solid waste management system; disposal of coal combustion residuals from electric utilities (final rule). *Federal Register*, *80*(74), 21302–21501. 40 CFR Parts 257 and 261. April 17.

US EPA. (2015b). Effluent limitations guidelines and standards for the steam electric power generating point source category (final rule). *Federal Register*, *80*(212), 67838–67903. 40 CFR 423, November 3. Available from https://www.gpo.gov/fdsys/pkg/FR-2015-11-03/pdf/2015-25663.pdf.

US EPA. (2016). *Frequent questions about the coal ash disposal rule*. June 7. Available from https://www.epa.gov/coalash/frequent-questions-about-coal-ash-disposal-rule.

# Ash as an internationally traded commodity

# 21

*D. Harris*
Asian Coal Ash Association, Beijing, China

## 21.1 Introduction

Dramatic shifts in global patterns of supply and demand have increased interest in fly ash as an internationally traded commodity. Large volume production markets, led by China and India, are expected to have surplus supplies in the hundreds of millions of tons through 2030 and beyond. At the same time, the quantity and quality of supplies are diminishing in developed markets. Relative demand is high in geographies such as California, Western Europe, and the Middle East, where ash utilization techniques are advanced and construction material standards allow for high levels of substitution in cement, concrete and other applications. This chapter will focus on fly ash as the highest volume and most important coal combustion product, with the greatest potential for increased international trade. There may be opportunities for global trade in FGD gypsum, though markets are limited and supply/demand volumes are expected to be significantly less than fly ash. Bottom ash, due to its relatively low value, will likely see only small volumes in international trade, possibly across nearby borders or within consolidated bulk shipments.

Global fly ash sales are expected to reach $98 billion by 2020 with a five-year CAGR of 5.5%.[1] Performance, cost, and, increasingly the environmental benefits of fly ash are expected to continue driving demand in all markets, with Asia Pacific leading the growth in demand. Some of this demand may be offset by the increased use of alternative supplementary cementitious materials (SCM), such as ground granulated blast furnace slag (GGBFS). Ash and slag can work optimally as complimentary SCMs, but some substitution is possible in markets where certain SCM faces supply/quality limitations or prohibitive pricing.

Logistics costs and infrastructure are always critical cost considerations in bulk material trade. The Baltic Dry Index (BDI), an indication of global bulk commodity freight prices, currently sits at historic lows. This is expected to continue for the next three years at least, and it could keep total delivered costs in check if bulk commodity buyers can negotiate longer-term agreements or purchase their own ships during the down market.

Environmental concerns around loading and unloading will delay a full realization of international trade potential, as will limited infrastructure capacity. However, the

---

[1] http://www.bccresearch.com/pressroom/avm/uptick-in-global-construction-to-spur-growth-in-scm-market; BCC Research LLC, 49 Walnut Park, Building 2, Wellesley, MA 02481, Telephone: 866-285-7215; Email: editor@bccresearch.com.

**Coal Combustion Products (CCP's).** **http://dx.doi.org/10.1016/B978-0-08-100945-1.00021-6**

economics based on the price differential between SCMs and cement production prices, appear to justify an investment in port and transport capacity to meet the growing demand.

Other barriers to international trade include construction material standards that lag behind technology developments, as well as continued designation of CCPs as hazardous materials in some markets. Efforts are being made in developed and developing markets to adapt standards and regulatory frameworks to facilitate greater beneficial utilization and trade. Coordination around fly ash standards in different jurisdictions would also help to expand the global marketplace.

Additional sources of demand may come online should standards develop in a way that higher volumes are permitted for use in cement, concrete, and other mature applications. Emerging technologies present a wild card, which is that a number of technologies currently under development have the potential to significantly impact global fly ash demand. Should advances in aluminium extraction, geopolymers, industrial ceramics, or other applications prove commercially viable, they could represent hundreds of millions of tons per year in additional consumption. On the supply side, improvements in ash beneficiation techniques could produce marketable materials from the billions of tons of ash currently stockpiled in global landfills.

## 21.2 High-volume surplus markets

Growth in global fly ash supplies will be driven by coal-fired energy production China, India, and Southeast Asia. The economic advantages of coal power in these markets include lower financial costs per unit of power, a large and relatively young fleet of installed capacity, and a domestic industry highly geared to coal-power related equipment supply, fuel supply, and operations. Additionally, China and India rank third and fifth in the world by coal reserves, respectively, while the United States, Russia, and Australia rank first, second, and fourth, respectively. For both China and India, domestic coal reserves and installed capacity have strategic value in that they support national energy independence.

### 21.2.1 China

#### 21.2.1.1 Production

Chinese fly ash production rates, as reported by officially recognized bodies, indicate 500 to 600 million tons of ash produced in 2015. China's growth in energy consumption has slowed since 2014, in line with the slowing of the overall domestic economy. Coal consumption has slowed from around six percent annual growth during the last decade and is now expected to grow at less than 0.5 percent each year through to 2025.[2] In absolute terms, however, growth in coal consumption and ash production volumes are substantial. With an average ash content of around 28 (Li, 2003), Chinese domestic coals rank amongst the highest in the world, trailing only India amongst the

---

[2] http://www.eia.gov/forecasts/ieo/world.cfm, http://www.bp.com/content/dam/bp/pdf/energy-economics/energy-outlook-2016/bp-energy-outlook-2016-country-insights-china.pdf.

major coal producing countries. With 3.7 billion tons of coal consumed in 2015, an average of only 0.3% growth in coal consumption would mean 2.5–3 million tons of additional fly ash added to Chinese supplies each year.[3] This would add another 20–25 million tons to annual production figures by 2025.

Official Chinese fly ash production and utilization rates, as reported by institutes and departments recognised by the government, indicate 500–600 million tons of ash produced in 2016 (Cui, 2016) with a utilization rate of around 70%. Some observers question the accuracy of these official figures, and in particular question claims about utilization rates. Even with the best of intentions, calculating accurate total fly ash productions figures in China is complicated by a lack of both monitoring and transparency. While the guidelines and policies governing ash collection and ash disposal are reasonably clear in their content and comprehensive in their scope, monitoring and enforcement of regulations are lacking in some important production regions.

The financial cost of installing and using ash collection systems is relatively high, with electrostatic precipitation systems estimated at 30–80 USD/kWe capital cost and 5 USD per kW per year for operation and maintenance. Ash transportation and disposal costs can add another 3–15 USD per ton, depending on regulations and the distance to be travelled. Given such high operating costs, power station operators in areas with weak regulation or enforcement may avoid proper collection and disposal. For example, by switching off collection systems (typically overnight), ash can be disposed of into the atmosphere with substantial a cost savings. The China Academy of Sciences has estimated that coal combustion is responsible for between 19% and 34% of PM2.5 in Beijing and the surrounding areas in Hebei province.[4] Researchers have found evidence of fly ash being a significant contributor to PM2.5 levels in the eastern metropolitan areas of Shanghai and Chengdu, the capital of the southwestern province of Sichuan (Tao et al., 2014). Modern ash collection systems are designed to collect more than 99.7% of the ash produced. With systems installed and deployed properly, these volumes of fly ash should not be present in the atmosphere. In a scenario where only 15% of power stations turn off their collection systems for 8 h a day, that would represent an additional 25–30 million tons of undocumented fly ash production each year.

Other irresponsible methods of disposal include dumping ash onto land or bodies of water without proper liners or containment systems. These disposal practices are not officially reported, but again as a scenario, if only 10% of power stations were collecting and dumping 20% of their ash ‘off the record’, it would represent millions of tons of production for which it is currently unaccounted.

China’s recent history of recognizing and creating policy to address environmental challenges suggests that the scope for this type of negligence will decrease. Laws and policies related to air, water, and soil pollution are improving in their scope, though monitoring and enforcement naturally lag behind central and provincial government level edicts. Policies place clear responsibility for ash collection on producers and

---

[3] 3.7 Billion × 0.3% growth = 11.1 million tons × 25% ash content = 2.78 million tons of fly ash.

[4] Institute of Atmospheric Physics, Chinese Academy of Sciences.

clearly indicate that commercial benefits should go to the consumers. Implementation is not without its challenges, but overall it is expected that China will continue to strengthen regulations, increase the monitoring of emissions at power stations, and enforce responsible disposal. These measures should serve to increase the amount of ash collected by power stations, adding to total supplies. The added costs incurred by power stations may stimulate investments in ash reduction techniques, such as coal washing, or the pursuit of alternative utilization methods.

Penalties for noncompliance should be both deterrent (i.e., designed to dissuade others from non-compliance) and punitive. Punitive penalties should reflect the degree to which society may be harmed by the negligent or purposeful release of pollutants into the atmosphere or contamination of soil, groundwater, or marine environments. Policy makers and regulators should also encourage the development of beneficial utilization so that the costs of adopting beneficial-use methods and technologies are preferable to the risks and costs of noncompliance.

#### *21.2.1.2 Utilization*

The officially recognized fly ash utilization rate is 70% (Cui, 2016), implying that an unutilized portion of 150–180 million tons from the 500 to 6000 million tons of total production. Utilization is concentrated in cement (44%), concrete walling products (28%), and ready-mix concrete (16%), with other low-value applications making up the road base and mine shaft fill making up the balance (12%).

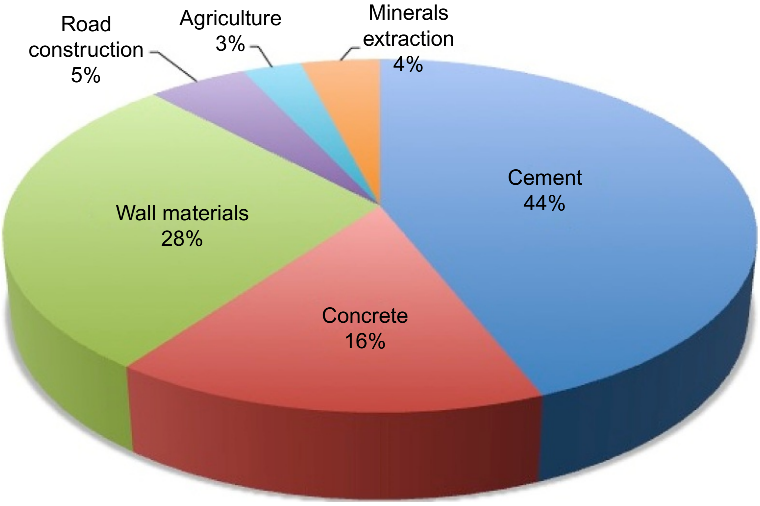

Incentives for the utilization of ash, such as VAT exemption for achieving recycled content thresholds in some construction products, are designed to further support utilization. Carbon trading markets, implemented on an experimental scale in 2015, have yet to create clear demand-side stimulation for lower-carbon material technologies. The central government has recently announced environmental sustainability guidelines focused on soil, following earlier proclamations focused on air and water sustainability. When these are implemented at local levels, they should improve the monitoring of landfill management by increasing the costs of landfilling, which should increase incentives for the beneficial usage of more material.

As with policies governing collection and disposal, practical implementation of policies intended to stimulate demand is often slow. Navigating the required pathways to gain formal approvals and then actually receiving the defined benefits is often a significant challenge for private entrepreneurs and state-owned enterprises alike. Some of the policies face conflicting government goals. For example, adjusting building material standards to allow for higher amounts of fly ash in cement and concrete production would reduce demand for Portland cement at a time when the Chinese government is working to eliminate serious overcapacity in the sector.

Despite the difficulties in enforcement, the intention and direction of government policies strengthening fly ash collection, disposal and utilization regulations is clear. Efficacy of policies and regulations in China tend to improve over time, perhaps even improving to the extent that they will have a measurable impact on fly ash demand. However, unless these policies drive substantial breakthroughs in higher ash substitution in cement and concrete or support commercialization of new high-volume applications, the increases in demand will not significantly alter expected surpluses.

### 21.2.1.3 Declines in domestic cement and concrete consumption

Chinese domestic demand for cement and concrete are expected to remain flat through 2020, trailing the global average. Demand will likely see declines thereafter as the country's development shifts away from investment-led growth, despite recent efforts to support distressed property and construction material industries.

In mid-2016, in response to the slowest growth in 25 years the central government began acting to support the property and construction sectors. Infrastructure investments remains key in cushioning the hard-hit steel and cement industries, though recent stimulus measures to support infrastructure and housing construction are believed to be unsustainable. In early October 2016, the International Monetary Fund (IMF) indicated that Chinese total debt levels were becoming dangerously high, noting that the Chinese "economy's dependence on credit is increasing at a dangerous pace, intermediated through an increasingly opaque and complex financial sector." The IMF further suggested that China should rein in the credit growth and cut off support to "unviable" state-owned enterprises, "accepting the associated slower GDP growth… By maintaining high near-term growth momentum in this manner, the economy faces a growing misallocation of resources and risks an eventual disruptive adjustment" (World Economic Outlook, 2016).

While there is support for downstream industries that may sustain fly ash demand in China in the short term (i.e., cement and concrete producers vis-a-vis property and infrastructure spending), demand is expected to remain flat in the mid term (2–5 years) and decline over the long term (>5 years).

#### 21.2.1.4 Surplus ash

The effects of sustained total coal power production levels, the likely increase in total ash collection volumes (through greater monitoring and enforcement of collection), and the fall in traditional demand suggests that existing annual surpluses will continue and likely grow. Based on two scenarios published by the Asian Coal Ash Association in December 2016, surplus fly ash volumes in China are expected to remain between 144 million and 243 million tons per year through 2025. At this range of projected accumulation, the current stockpile of two billion tons of fly ash in landfills may double to four billion during this period.

The below table illustrates two simplified scenarios that provide an estimated range for Chinese fly ash surplus through 2030. In the first scenario, production is kept at the same level through 2030. Coal will remain an important part of China's energy mix for the next 30–40 years, and while some models estimate moderate growth in absolute coal power production in China, others predict that the total coal production volumes have plateaued. Utilization predicts total fly ash consumption to remain in line with total cement production, using this figure as a proxy based on cement volumes being indicative of the demand for total construction materials.

The second scenario maintains the utilization growth figures while adjusting the production figures moderately upward (from 0.07% to 2% annual growth). The factors that may result in this larger growth in fly ash production include: (a) improvements in regulations and enforcement, such that a greater percentage of fly ash produced is captured and accounted for, as opposed to being, rather than released into the atmosphere or dumped in unregistered landfills; (b) coal power maintains its share of the energy mix, due to higher oil prices or the failure of renewables to meet expectations.

The models are highly simplified and could be sensitized to many variables not considered here. Total fly ash consumption and production during this period may be affected, for example, by emerging technologies, a surge in regional infrastructure development, a change in standards that allow for greater fly ash additions to cement or concrete, or unpredictable shifts in global energy markets. Overall, however, the projected ranges should provide a reasonable framework for estimating surplus volumes based on current knowledge.

#### 21.2.1.5 International trade: Opportunities

Considering geographic location, supply-and-demand patterns, and total delivered logistics costs, Chinese ash producers have a number of potential export markets, including:

1. Australia
2. United States (West Coast)
3. Western Europe
4. South Korea
5. Southeast Asia

While there have been Chinese ash exports to these and other markets over the last 10 years, the trade has been largely limited to containerized bulk bags. Total exports are estimated to be less than three million tons per year.

| China fly ash production and utilization projections | | | | | | | Millions of tons | | | | |
|---|---|---|---|---|---|---|---|---|---|---|---|
| **Scenario 1** | **Growth** | **2016** | **2017** | **2018** | **2019** | **2020** | **2021** | **2022** | **2023** | **2024** | **2025** |
| Production | 1.00 | 565.00 | 565.00 | 565.00 | 565.00 | 565.00 | 565.00 | 565.00 | 565.00 | 565.00 | 565.00 |
| Utilization | 1.01 | 395.50 | 398.27 | 401.06 | 403.86 | 406.69 | 409.54 | 412.40 | 415.29 | 418.20 | 421.13 |
| Surplus | | 169.50 | 166.73 | 163.94 | 161.14 | 158.31 | 155.46 | 152.60 | 149.71 | 146.80 | 143.87 |
| Notes: | • Production assumes coal consumption has plateaued and will remain at current consumption rates through 2040; based on WEO2015<br>• Utilization assumes ash consumption will grow at same rate as cement consumption, based on CW Group forecast of 0.07% growth | | | | | | | | | | |
| **Scenario 2** | **Growth** | **2016** | **2017** | **2018** | **2019** | **2020** | **2021** | **2022** | **2023** | **2024** | **2025** |
| Production | 1.02 | 565.00 | 576.30 | 587.83 | 599.58 | 611.57 | 623.81 | 636.28 | 649.01 | 661.99 | 675.23 |
| Utilization | 1.01 | 395.50 | 399.46 | 403.45 | 407.48 | 411.56 | 415.67 | 419.83 | 424.03 | 428.27 | 432.55 |
| Surplus | | 169.50 | 176.85 | 184.38 | 192.10 | 200.02 | 208.13 | 216.45 | 224.98 | 233.72 | 242.67 |
| Notes: | • Growth in production assumes uniform energy demand growth (two percent) and that coal will remain as the same percentage of energy mix<br>• Utilization assumes ash consumption will grow at same rate as cement consumption, based on CW Group forecast of 0.07% growth | | | | | | | | | | |

Producers and prospective export customers are currently investigating infrastructure, as wella as the regulatory and financial requirements for bulk powder exports and imports. Some details regarding the demand in these markets, as well as considerations and challenges around bulk fly ash powder exports/imports, are discussed below.

## 21.2.2 India

### 21.2.2.1 Production

Coal is expected to remain central to Indian power generation for the next 40–50 years.[5] At 152 watts per person (2014), per capita annual domestic electricity consumption in India is less than half the worldwide average (385 watts) and less than 1/3rd of China's per person consumption (474 watts per person).[6] Strong growth in manufacturing and an additional 580 million consumers are boosting electricity demand by 4.9% per year in India. Total energy consumption is expected to reach nearly 3300 TW h in 2040, with the installed capacity growing from 290 GW in 2015 to nearly 1100 GW in 2040. Half of the net increase in coal-fired power generation capacity worldwide will occur in India.

There is an overwhelming dependence on domestic high-ash coal for power generation in India.[7] According to the latest report of the Central Electricity Authority, between April and September 2015, 132 thermal power plants (TPPs) of 58 utility companies having an installed capacity of 130,428 MW consumed 251.69 million tonnes of coal with an average ash content of 33.23%. This led to the generation of 83.64 million tonnes of coal ash during a sixth-month period, out of which only 46.87 million tonnes (or 56.04%) was beneficially utilized. The total installed capacity of coal based TPSs in India is 186,492.88 MW as of October 31, 2016. Annual figures are roughly double the sixth-month figures, and the increased capacity suggests total ash production of approximately 240 million tonnes at present.[8]

### 21.2.2.2 Utilization

Current utilization in India is concentrated in cement 42%; bricks and tiles 13%; mine filling 11%; kand reclamation 11%; roads and fly-overs 5%; agriculture 2%; ash dyke raising 7.5%; concrete 1%; and miscellaneous 7.5%. This pattern of use has been in practice for the last several years, and the overall utilization of fly ash has been in the range of 55%–62%.

India is expected to post the fastest growth in cement demand of any major national market, advancing 8.0% per year through 2019. The growth drivers, in addition to

---

[5] http://www.worldenergyoutlook.org/media/weowebsite/2015/FactsheetIndia.pdf.

[6] http://www.askci.com/finance/2015/01/20/1013378nyi.shtml (China); Ministry of Statistics and Programme Implementation, India "Energy statistics 2015"—page 48, 57 (India).

[7] https://www.pwc.in/assets/pdfs/industries/power-mining/icc-coal-report.pdf.

[8] Notes from Dr. Anjan Chatterjee, Nov. 12th, 2016.

growing incomes, include: reduction in the average size of the household (due to increased nuclearization of families), reduction in the average age of homeowners, increased availability of housing finance, and a favorable tax regime.[9] Growth in other ash consumption areas is expected to maintain a similar growth pattern to cement.

While these applications will certainly add some demand for fly ash, it is not likely to offset the increased supplies described above. Increased demand for exports may improve utilization rates, but it will be difficult to gain any meaningful volumes outside of their traditional markets.

### *21.2.2.3 Surplus ash*

Growth in total ash supplies in India will be offset to some degree by an anticipated growth in cement and other construction materials consumption. The Asian Coal Ash Association produced two scenarios that estimate the surplus fly ash volumes in India will remain between 81 million and 114 million tons per year through 2025.

The two simplified scenarios provide an estimated range for Indian fly ash surplus through 2025. The first model assumes steady growth in coal power production at 4.9% per year through 2025 production, based on the World Energy Outlook 2015 paper.[10] The first scenario further models fly ash consumption growth at 9% through 2025, tracking projected cement demand growth as a proxy for total fly ash demand. Coal will remain an important part of China's energy mix for the next 30–40 years. While some models estimate moderate growth in absolute coal power production in China, others predict that the total coal production volumes have plateaued. Utilization predicts total fly ash consumption to remain in line with total cement production, using this figure as a proxy based on cement volumes being indicative of total construction materials demand.

The second scenario maintains the utilization growth figures while adjusting the production figures moderately upward (from 0.07% annual growth to 2% annual growth). The factors that may result in this larger growth in fly ash production include: (a) improvements in regulations and enforcement, such that a greater percentage of fly ash produced is captured and accounted for, as opposed to being released into the atmosphere or dumped in unregistered landfills; (b) coal power maintaining its share of the energy mix due to higher oil prices or failure of renewables to meet expectations.

The models are by definition simplifications that could be sensitized to many variables not considered herein. Total fly ash consumption and production during this period may be affected, for example, by emerging technologies, a surge in regional infrastructure development, a change in standards that allow for greater fly ash

---

[9] http://www.ijemr.net/April2014Issue/AStudyOnFutureMarketingTrendsIndianCementIndustry(154-156).pdf.

[10] http://www.worldenergyoutlook.org/media/weowebsite/2015/FactsheetIndia.pdf.

| | **Growth** | **2016** | **2017** | **2018** | **2019** | **2020** | **2021** | **2022** | **2023** | **2024** | **2025** |
|---|---|---|---|---|---|---|---|---|---|---|---|
| Production | 1.05 | 240.00 | 251.76 | 264.35 | 277.57 | 291.44 | 306.02 | 321.32 | 337.38 | 354.25 | 371.96 |
| Utilization | 1.08 | 134.00 | 144.72 | 156.30 | 168.80 | 182.31 | 196.89 | 212.64 | 229.65 | 248.02 | 267.87 |
| Surplus | | 106.00 | 107.04 | 108.05 | 108.76 | 109.14 | 109.13 | 108.68 | 107.73 | 106.23 | 104.10 |
| Notes: | Growth in production assumes uniform energy demand growth (4.9%) and that coal will remain the same percentage of energy mix<br>Utilization assumes ash consumption will grow at same rate as growth in cement consumption | | | | | | | | | | |

| | **Growth** | **2016** | **2017** | **2018** | **2019** | **2020** | **2021** | **2022** | **2023** | **2024** | **2025** |
|---|---|---|---|---|---|---|---|---|---|---|---|
| Production | 1.05 | 240.00 | 251.76 | 264.35 | 277.57 | 291.44 | 306.02 | 321.32 | 337.38 | 354.25 | 371.96 |
| Utilization | 1.08* | 134.00 | 144.72 | 156.30 | 168.80 | 182.31 | 196.89 | 210.67 | 225.42 | 238.94 | 253.28 |
| Surplus | | 106.00 | 107.04 | 108.05 | 108.76 | 109.14 | 109.13 | 110.64 | 111.96 | 115.31 | 118.68 |
| Notes: | Growth in production assumes that uniform energy demand growth (4.9%) and that coal will remain the same percentage of the energy mix. | | | | | | | | | | |

---

*Utilization assumes a gradual decline in cement/construction materials consumption from 8% to 5% per year, starting in 2022 through 2030.

additions to cement or concrete, or unpredictable shifts in global energy markets. Overall, however, the projected ranges should provide a reasonable framework for estimating surplus volumes based on current knowledge.

### *21.2.2.4 Policies*

Policy regarding the use and disposal of fly ash are handled by the Ministry of Environment, Power and Climate Change (MOEFCC). The current regulation is dated January 2016 and stipulates that cost of transportation of fly ash up to 100 km from the power station needs to be borne by the concerned generator. Transportation cost from 100 to 300 km is to be shared between the generator and the consumer. The regulation requires mandatory use of fly ash products in all government schemes and monthly reporting of fly ash stocks.

Again, the problem with the policies has been implementation. Although there are state-level monitoring committees, the speed of implementation has been slow.[11]

### *21.2.2.5 International trade: Opportunities*

Although Indian traders have exported fly ash in small consignments, ash as an international commodity has not received much attention in the domestic industry. The sales cycle can be lengthy, starting with laboratory sample approvals and often requiring additional field trials, making the market less desirable for ash traders. Consignment sizes range from a few hundred to a few thousand tonnes each. While export-import data services provide some insight into international trade, reliable export statistics are difficult to determine, as several ash-based products are often shipped under the 26219000 HS code number. A reasonable estimate based on the trade data is that exports may not exceed a couple of million tonnes per year. Main ports for export include Mundra in Gujrat, Tuticorin in Tamil Nadu, Sabarmati, Nhava Shiva, Kolkata, and some others. The importing countries are Qatar, Kenya, UAE, Japan, and Sri Lanka. Cenospheres are also exported from India in consignment sizes of kilogram quantities, typically by air cargo from various parts of the country. Export to Bangladesh from Kolkata port in small barges is a regular trade from the coastal TPSs in West Bengal. It is reported that Tata Power has done some ground work to export up to 90,000 tonnes of fly ash per year to Middle East from the western ports.

Potential export markets for Indian ash include:

1. Middle East
2. Australia
3. Africa
4. Western Europe
5. United States (West Coast)

---

[11] Notes from Dr. Anjan Chatterjee, Nov. 12th, 2016.

### 21.2.3 Southeast Asia

Coal-fired generating capacity has grown in the region over the past decade, with significant additional capacity already in the pipeline in Vietnam, Malaysia, Indonesia, and Taiwan. In the IEO2016 reference case, the coal-fired generating capacity in non-OECD Asia (excluding China and India) nearly doubles from 2012 to 2040.[12]

Many countries in the Asia/Pacific region will post strong growth in cement consumption, including Vietnam, Indonesia, and Pakistan.

In Vietnam, where electricity demand has been increasing at a rapid pace in recent years, there are ambitious plans to increase the coal-fired generating capacity. As of January 2016, more than 12 GW of coal-fired capacity was under construction, and there are plans to add an additional 60 GW of new coal-fired generating capacity by 2030. The majority of the coal will by imported from Australia and Indonesia.[13]

## 21.3 International trade: Challenges

Major barriers for export include the cost of inland transport, port expenses, and shipping costs for relatively small consignments and lengthy approval procedures for export, import, and transport permits. For ash traders, all of these barriers result in export being less attractive than the domestic sales. As supply constraints hit key markets, upward price pressure on SCMs will push buyers and suppliers to tackle these and other challenges to developing new international supply chains.

### 21.3.1 High-quality coastal supplies already contracted

Coastal power stations, due to their proximity to major urban areas, tend to be better managed in terms of production consistency and environmental standards. In China and India in particular, coastal power stations tend to mill coal more finely, use superior emissions to control technologies, and have a tendency to use higher-quality coal blends. The result is higher quality and greater consistency in fly ash chemical and physical properties, to the extent that the material is more desirable to local cement manufacturers and those in other domestic markets along the coast. This material is typically allocated in multiyear contracts.

Adding to this, coastal urban areas usually have high volume demand for construction materials. Coastal power stations are often fully contracted to supply cement-grade fly ash, as well as the run of station ash and bottom ash to serve this demand. This is particularly clear in China, where coastal cities such as Shanghai and Shenzhen have seen dramatic urban development over the last 20 years. During this period, both cities have been net importers of fly ash, drawing from both inland and domestic coastal sources.

[12] http://www.eia.gov/forecasts/ieo/coal.cfm.

[13] http://www.eia.gov/forecasts/ieo/coal.cfm.

The cost of loading material onto vessels, whether in containers or bulk, is much lower at coastal power stations due to lower local land transport costs. As a result, coastal power stations have been logical first choices for exporters/importers, and many have already developed either domestic coastal markets for their ash or export markets.

### 21.3.2 Production moving away from the coast

In earlier stages of economic development, coal power stations are often located along the coasts to take advantage of access to coal resources (through coastal trade and imports) and proximity to energy consumers. As economies develop, coal power production typically moves away from coastal areas. This trend is notable in China, where over the last decade the central government has specifically focused on relocating coal power production away from the coast. China's coal power production base has shifted towards the central, west, and northern regions of the country, where domestic coal resources are most abundant. In the United States the majority of coal power stations are located more than 100 km from the coast. In California, coal-fired generation is projected to serve about three percent of California's electricity consumption by 2024; this generation is expected to decline to zero by 2026.[14] The Californian market already suffers from severe ash shortages, with expensive synthetic alternatives currently under development. In the United Kingdom, there is no coal power in Scotland, and all ash is currently being imported from Germany. In England and Wales, all remaining coal power stations are mandated to close by 2025, though they are likely to close earlier.

The relocation of ash production away from seaports brings increased transportation costs when moving the material from source to port, raising the FOB cost and limiting the number of addressable export markets. It also raises delivered costs to the high-demand domestic coastal markets.

### 21.3.3 Road and rail infrastructure

China's rail and road infrastructure is well developed, though transport costs from main fly ash production regions (Shanxi, Inner Mongolia) to the coast still add 10–20 USD per ton.

In India, inadequate rail infrastructure and a lack of dedicated freight infrastructure limit the ability for exports to bring supplies to the coast from the interior. "Decades-long projects including dedicated freight lines have yet to be completed, and several rail projects have stalled, including the 93-km Tori-Shivpur-Kathautia line to provide access to coal mines in Jharkhand, which was begun in 1999 and scheduled to be completed in 2005, but was only half complete as of 2015."[15]

---

[14] http://www.energy.ca.gov/renewables/tracking_progress/documents/current_expected_energy_from_coal.pdf.

[15] http://www.eia.gov/forecasts/ieo/footnotes.cfm#138.

### 21.3.4 Export infrastructure

China has spent nearly three decades investing in infrastructure to support raw material imports and exports. Infrastructure has also been developed to support a vibrant domestic coastal trade in raw construction materials. As a result, the country has a large bulk powder export capacity with storage facilities and ports that can accommodate large bulk vessels. Much of this capacity is currently underutilized due to a decline in domestic demand, resulting in competitive port charges that should reduce overall export costs. In addition, there is abundant capacity to export powders in bulk bags. This is a higher cost option, but may be viable in markets where cement prices justify the added cost.

In India, export facilities for bulk powder are more limited. Most of the ash being exported currently is done so in bulk bags, with volumes typically a few hundred to a few thousand tons per shipment. It is reported that Tata Power has done some groundwork to export up to 90,000 tons of ash per year to the Middle East. Such volumes are not likely to yet justify major infrastructure investment, but may be an indicator of things to come. Indian export volumes could grow substantially and justify investments in bulk shipment capabilities if exporters are able to secure purchase agreements to fulfill some of the growing demand described in this chapter.

### 21.3.5 Import infrastructure

#### 21.3.5.1 Bulk powder

Bulk powder unloading of fly ash can be done at import terminals that currently handle bulk cement and GGBS. Capacity issues at import facilities create a bottleneck for importers, and the approvals process to allow nonpneumatic vessels can be lengthy, costly, and uncertain. Many ports within reasonable distance to the main markets have a preference for container ships or at best pneumatic vessels due to the risk of dust emissions during unloading and unwanted discharge during cleaning. Naturally, importers want to get their material as close as possible by sea freight to the end-use location in order to reduce more expensive land transport costs.

Building an additional import capacity requires substantial investment in shore-based offloading equipment and warehousing. To justify these expenditures, importers need to develop confidence that they have access to long-term, reliable, quality supplies from at least one resource, with additional options preferable so as to reduce risk.

#### 21.3.5.2 Bulk bags

Bulk bags can be used to pack and transport fly ash, eliminating the need for specialized shore- or vessel-based offloading equipment. Environmental concerns with dust emissions are also less of a concern. The 1 or 1.5 ton bulk bags can be packed in the cargo hold of the vessel and removed with a standard gantry crane. While avoiding the capital costs or capacity restrictions of bulk powder imports, shipping by bulk bag incurs additional costs due to the cost of the bag, the cost of filling the bag, and the cost of emptying the bag by the customer. The debagging process can also be messy, with expensive equipment often necessary to contain fugitive dust. While this method of delivery works in markets where local cement or SCM supplies are relatively expensive, the added cost and additional processing required in debagging make this a less desirable or unviable option for large-volume trading in established markets.

#### *21.3.5.3 Pneumatic vessels*

Pneumatic vessels avoid many of the environmental concerns that port authorities have during both export and import. Pneumatic vessels also eliminate the need for offloading equipment at the port of destination, reducing capital expenditure requirements for importers. However, the global fleet of pneumatic vessels is limited, with a relatively small cargo capacity on an average vessel. As of 2013, there were only 11 self-discharging vessels globally with a capacity greater than 19,000dwt.[16] Current ocean freight costs for chartering pneumatic vessels are considerably higher, with current rates two to three times higher than standard bulk ships.

Importers will need to compare total costs of chartering or acquiring and operating bulk vessels with the total costs of chartering or acquiring and operating pneumatic vessels. Bulk vessels require additional investment in import infrastructure for offloading and have greater regulatory restrictions. Pneumatic vessels are more expensive to purchase or operate, but require less import infrastructure and are typically less of an environmental concern to port authorities.

### *21.3.6 Environmental and regulatory challenges*

Bulk powder vessels face restrictions at many ports due to environmental regulations. Primary concern is fugitive dust emissions during loading and unloading. Pneumatic vessels face fewer restrictions at ports, as they tend to provide better containment of dust.

Other regulatory challenges include restrictions on transporting or importing material designated as hazardous waste in some countries. After a long regulatory process, the US EPA in 2014 determined that fly ash would be classified under a subcategory of hazardous waste. This designation allows for relative ease of transport and beneficial use in cement, concrete, and other applications. Other countries, such as Indonesia, classify fly ash as hazardous waste. While responsible material handling should be practiced with any bulk powder material, the hazardous waste designation adds substantial cost and complexity to transporting and utilizing ash.

### *21.3.7 Quality and standards*

Only a small percentage of power stations or ash managers in China, India, and other surplus markets are presently equipped with sufficient facilities or expertise to provide fly ash that meet specifications for cement in the United States, Australia, and Europe. The main challenges are the ability to supply ash over sustained periods with

[16] http://ashtrans.eu/2013%2008%2026%20KGJ%20Cement%20Presentationx.pdf.

consistent chemical and physical properties. Consumers of fly ash need to adjust their supply chains and mix designs around specific ash profiles; fluctuations outside of tolerable limits can cause unacceptable disruption to their supply chains. Maintaining consistently low levels of LOI and consistent fineness are the main challenges. Proven methods to control for these parameters are well understood in the industry, but justifying the investments in equipment, training, and quality control and monitoring require credible long-term sales prospects.

Part of the difficulty in building consistent quality ash supplies is a lack of coordination in international standards. There is evidence that increased coordination around fly ash standards in different jurisdictions would help to create a broader global marketplace. Prior to standardization, some EU members utilized 100% of the coal combustion products produced in their country, while others only utilized 10% due to differing regulations. The EU laws that have harmonized differing standards take precedent over national laws and have benefitted the fly ash industry by requiring fly ash to be utilized more widely throughout the EU (Hans-Joachim, 2005).

## 21.4 International trade: Opportunities

Decreasing local demand and increasing costs of disposal in high-volume surplus markets may combine to justify the costs of investing in the quality production and logistics required to export fly ash to high value markets. A “first-mover” opportunity exists for those producers willing to make the investments in infrastructure and put in place quality control programs that satisfy sophisticated and demanding international customers.

At the time of writing, ocean freight rates are at historical lows and are expected to remain depressed for the next 2–3 years due to vessel oversupply and a slowdown in global commodity markets. Early movers are in a position to lock in competitive pricing for near to mid-term contracts while ship owners are desperate for business. The price of bulk vessels is also at historical lows, with many shipbuilders struggling for new orders. This may motivate some large-volume customers to invest in their own fleets and secure long-term purchase agreements as part of a strategic raw material procurement program.

### *21.4.1 Diminishing supplies in key markets*

A number of key markets have seen steady declines in fly ash supplies over the last decade, including the United States, Western Europe, and Australia. Fly ash production in these markets has declined primarily as a result of the retiring of coal power capacity and an infrastructure investment shift towards nuclear, gas, and renewable energy.

The American Coal Ash Association publishes fly ash production and utilization figures from 2000. According to the published figures, production has seen a steady decline from around 72 million tons in 2006 to 45 million tons in 2015.[17] Utilization

---

[17] https://www.acaa-usa.org/Portals/9/Files/PDFs/2015-Survey_Results_Charts.pdf.

has remained between 20 and 30 million tons during the same period. Coal power stations in the United States are being retired at a rapid rate, with nearly 5% of installed capacity retired in 2015 alone.[18] Policy changes in the new Trump administration aimed at reviving the coal industry may result in increased fly ash production volumes in the near term, but price competition from natural gas and the improving economics of renewables suggest that the long-term trend for American coal and fly ash production will be a steady decline.

In Europe (EU15[19]), there has been a steady overall decline in coal consumption since 1995,[20] with corresponding decreases in fly ash production tracked by the European Coal Combustion Products Association. Some of this decline can be attributed to the slowdown in industrial demand due to the 2008 financial crisis, but more meaningful longer-term impact is likely caused by political decisions relative to CO2 reduction and an increased focus on energy production through renewables. Air-quality regulations are likely to continue forcing plant closures, and renewable energy will continue to surge, while European energy demand will be weak in general. Currently, production (2015) is 32 million tons, of which approximately 92% is used. As supplies continue to diminish in these markets, demand will quickly outstrip supplies.

In contrast to the EU15, the total amount of CCPs in EU-28 did not decrease substantially, as EU12[21] countries generate a larger share of their energy from coal-fired power plants. ECOBA estimates total CCPs for the EU28 countries at $>$ 105 million tons (2015), implying EU12 countries were producing $>$73 million tons in 2015. ECOBA has not published figures on utilization rates, but due to less development in these markets, it is expected to be considerably lower. Ash trading within the EU is already established and will likely increase, given the asymmetrical supply and demand. The high costs of land transport, however, will restrict much of this trade, and exporters from the East Coast of America or Asia may emerge to meet Western European fly ash demand.

The supply problems in the United Kingdom have emerged quickly. At the end of 2015, the UK had adequate amounts of fly ash to meet domestic demand. It is now expected that there will be a 200,000–300,000 ton shortfall to supply current demand. The UK withdrawal from the EU may further complicate imports and increase the price of European ash. The price of fly ash increased from 10 euros per ton (delivered) to 20–30 Euros per ton in a six-month period in 2016. Fly ash stockpiles that existed in Germany and the Netherlands just last year have already been consumed. The impact on global trade has been rapid for other countries too. Trade flows of fly ash from northern Europe to the United States, accounting for sizeable volumes in 2015, have all but stopped.

---

[18] http://www.ibtimes.com/coal-power-waning-nearly-5-us-capacity-retired-2015-aging-plants-lose-ground-2333207.

[19] Belgium, Denmark, France, Germany, Greece, Ireland, Italy, Luxembourg, the Netherlands, Portugal, Spain, United Kingdom, Austria, Finland, Sweden.

[20] http://www.eiu.com/industry/article/741997658/coals-last-gasp-in-europe/2014-07-09.

[21] Belgium, Denmark, France, Germany, Greece, Ireland, Italy, Luxembourg, the Netherlands, Portugal, Spain, United Kingdom.

### 21.4.2 Quality declines

Average ash quality in many markets has also seen a decline in the last decade. Low NOx burners, widely adopted in new power station designs following the 1970 Clean Air Act Amendment in the United States, are designed to reduce the amount of nitrogen oxides emitted during coal combustion. The process typically involves lower combustion temperatures and results in higher levels of unburned carbon (LOI) in fly ash. In most cement standards, LOI is a critical specification that requires a certain percentage, typically below 5% in most standards and below 2% in more stringent specifications. While a number of postcombustion processes have been developed to address this higher LOI from low-NOx burners, the added capital and operating costs have often been unviable for ash producers. Rising cement costs and an increasing scarcity of local fly ash supplies in some markets may cause wider-spread adoption of carbon removal technologies, but the overall costs and quality will need to compete with total delivered cost of imports from more distant markets.

The changing role of renewables in the overall energy mix also impacts fly ash quality. Daytime demand in markets such as Australia is being met by solar power. Coal power, previously the base load power supplier, now shut down in the morning and need to be reignited in the evening. The re-ignition process involves using kerosene as the initial fuel to fire up the boiler. Coal is then slowly added until coal is the sole fuel source. The ash during the period where kerosene is being employed is much higher LOI than the pure coal burn. Quality ash supply volumes from these power stations are therefore reduced substantially, and the process of separating the lower LOI ash from the higher LOI ash introduces additional management and operating costs.

### 21.4.3 Increased demand for supplementary cementitious materials (SCMs) globally

Demand for supplementary cementitious materials (SCM) depends heavily on the global construction industry. Global infrastructure development, particularly in Asia Pacific, Latin America, Africa, and the Middle East, should drive demand for SCMs through 2020.

Global fly ash sales totalled an estimated $75 billion in 2015, account for over 70% of the volume and almost 95% of the revenue in the global SCM market.[22] Fly ash revenue is expected to reach $98 billion by 2020 with a five-year CAGR of 5.5%.[23] Comparatively accommodative regulations governing the use of fly ash in

---

[22] http://www.bccresearch.com/pressroom/avm/uptick-in-global-construction-to-spur-growth-in-scm-market; BCC Research LLC, 49 Walnut Park, Building 2, Wellesley, MA 02481, Telephone: 866-285-7215; Email: editor@bccresearch.com.

[23] http://www.bccresearch.com/pressroom/avm/uptick-in-global-construction-to-spur-growth-in-scm-market; BCC Research LLC, 49 Walnut Park, Building 2, Wellesley, MA 02481, Telephone: 866-285-7215; Email: editor@bccresearch.com.

Asia Pacific supported high consumption, with the region accounting for the majority of global trade, followed by North America.

Demand for supplementary cementitious materials globally is driven by a number of key benefits. Economically, substituting a portion of Portland cement with SCMs reduces operational manufacturing costs, as current prices are typically less than ordinary Portland. SCMs such as fly ash and GGBS are more capital efficient; as industrial by-products, they do not require significant capital investments in manufacturing capacity. To the degree that SCMs can replace Portland cement, they reduce the need for capital investment in new cement manufacturing assets required to meet market demand.

SCMs add performance improvements to blended cements. When added correctly, fly ash improves the workability of fresh concrete and enhances strength, durability, and resistance to sulfate attack in hardened concrete.

The primary benefits of increased SCM content are performance and cost. However, heightened environmental awareness, accompanied by policies and legislation that support products with lower embodied energy are playing an increasing role in buyer and supplier decisions. The environmental benefits first emerged as drivers in Japanese and European markets, but other markets are now following the lead. The Middle East is a major contributor to this trend, with the government of the UAE implementing regulations in 2015 that require all major infrastructure projects and substructures to use at least 60% slag or ash-containing cements.

In Europe, the new Fehmarn Belt bridge/tunnel has specified only fly ash cement. This project, connecting Denmark and Germany and led by the respective governments, will be a reference case for construction and engineering companies and may lead to greater adoption of fly ash cements in the region and globally.[24]

There is an upward trend in increasing the volumes of fly ash additive permitted in cement and concrete. Australian standards currently permit a 7.5% addition of fly ash in the cement kiln, and the industry is trialling 12.5% additions. The European standard allows for 22.5% fly ash to be milled with clinker. The Chinese standard for ordinary Portland cement (GB 175-2007) allows for up to 40% fly ash additive. Chinese concrete standards allow for between 15% and 70% fly ash, with high w/c prestressed concrete at the lower end of the scale and roller compacted concrete at the upper end.

## 21.5 Summary

The long-term trend will see continual declines in fly ash supplies in the United States, Western Europe, and Australia with little to no domestic supplies in most of Africa and the Middle East. Short-term shifts in attitudes and policy towards coal power generation, most notably in America, may cause increased supplies, but the low cost of natural gas and declining cost of renewables will likely limit the impact of any coal revival policies.

---

[24] http://www.globalcement.com/magazine/articles/994-lower-scm-supplies-demand-a-change-in-approach.

Sustained or increasing surpluses of fly ash in China, India, Southeast Asia, and Eastern Europe will create a growing imbalance in geographic supply and demand, stimulating growth in international trade. Delivered prices for cement-grade fly ash will approach and possibly even surpass the delivered price of cement in developed markets, where environmental considerations increase the costs of building cement manufacturing capacity and reward the use of materials with lower embedded energy.

A number of other variables may impact supply and demand. Environmental, health, and safety regulations in exporting and importing countries may impact supply and demand. Supply may be thus impacted through restrictions on use in some applications, restricting or adding cost and complexity to the import/export process or prohibitive regulations regarding local transportation. Demand may be stimulated through carbon credits, tax incentives, or feature projects that validate and give profile to use of high-volume fly ash cements (such as the aforementioned German-Danish Fehmarn Belt bridge/tunnel).

One factor that may have the largest impact on fly ash demand is also the least predictable. Investments in emerging technologies for fly ash utilization have focused on a broad number of product applications and markets. A number of these may achieve technical and commercial breakthroughs that could increase fly ash demand.

Geopolymers, which are alkali-activated cements that use fly ash and GGBS as their main component, have received a substantial amount of investment and interest, particularly in China, India, and Australia. With low-embedded energy and high proportions of recycled content, geopolymer cement systems offer promising benefits. However, technology developers have yet to overcome the disadvantages inherent in the use of alkaline activators, which include higher costs and health and safety issues due to their caustic nature. Workability is another key barrier to widespread adoption, as set times for geopolymers are typically very rapid, and retarders only add additional cost. Nonetheless, with the amount of investment and interest, there is a chance that these barriers will be at least partly overcome. Due to the large addressable market size for geopolymer cement and concrete products, even moderate success would have significant impact on fly ash demand in respective markets; upside demand increase could be in the hundreds of millions of tons globally.

Metal extraction, particularly the extraction of aluminium, has seen investments in the hundreds of millions of dollars in China, where some ashes have more than 50% aluminium oxide content. If the technologies prove to be commercially viable, fly ash could replace bauxite as feedstock for aluminium smelting in some markets. The potential volumes for this application would see demand for higher aluminium ashes increase by tens of millions of tons per year. Thus far, efforts such as the Datang processing facility in Inner Mongolia have demonstrated technical capability, but operating costs, particularly those associated with neutralizing the strong alkali solutions used in the process, have prevented commercial viability.

A number of companies have invested in developing methods for using fly ash as a substitute for clays in the manufacturing of industrial ceramics. Fly ash is essentially the unburned clay and trace minerals and metals present in the coal during combustion. While chemically similar, fly ash has unique physical properties that are derived from having been fired at high temperature and converted into fine particulate.

Technology developers demonstrated the ability to produce a range of industrial ceramics with beneficial properties and a promising cost base. An example is in the manufacture of ceramic tiles, wear-resistant ceramics, and refractories using 40–80% fly ash substitute for industrial clays. Moderate market share for fly ash-derived refractories and ceramic tiles alone would represent tens of millions of tons of ash demand each. Whether such technologies can be deployed at full scale with commercial viability remains to be seen.

On the supply side, advancements in ponded ash beneficiation could unlock billions of tons of fly ash currently stockpiled in landfills. The prospect of diminishing supplies, and the acknowledged costs and risks of maintaining ash ponds in the United States, have propelled research and development in ponded ash beneficiation over the last decade. As quality ash supplies become scarcer and more expensive, the ability to upgrade lower quality stocks will become increasingly valuable.

## References

Cui, Y. (2016). Current situation and development trend of fly ash utilization in china. In *Institute of Technical Information for Building Materials Industry of China (ITIBMI), Coal Ash Asia Conference September 24*.

Hans-Joachim, F. (2005). Coal ash utilization over the world and in Europe. In: *Workshop on Environmental and Health Aspects of Coal Ash Utilization, November 23–24*. www.flyash.info/2011/007-feuerborn-2011.pdf.

Li, W. (2003). *Coal and Clean Coal Technologies: Similarities and Differences between China and USA*. Presentation at Harvard University, December 10.

Tao, J., Gao, J., Zhang, L., Zhang, R., Che, H., Zhang, Z., et al. (2014). PM2.5 pollution in a megacity of southwest China: Source apportionment and implication. *Atmospheric Chemistry and Physics*, *14*, 8679–8699.

World Economic Outlook. (October 2016). *Subdued Demand: Symptoms and Remedies*. Research Dept. p. 33.

# Index

Note: Page numbers followed by *f* indicate figures and *t* indicate tables.

WOODHEAD PUBLISHING SERIES IN ENERGY

*Maximize the potential of coal ash and other coal combustion wastes with this detailed guide to their geochemistry, preparation for use, applications, and toxicology.*

**Coal Combustion Products** provides a detailed overview of the different waste materials produced during power generation from coal, exploring their nature, beneficiation techniques, applications, and environmental impacts. Strong focus is placed on coal fly ash, bottom ash, and flue gas desulfurization materials and their employment in cement, concrete, gypsum products, aggregates, road construction, geotechnics, and agriculture, among other products and industries.

Part One of this book focuses on the nature of coal ashes, with chapters on their origin, generation, and storage, both in ponds and landfill. The coal combustion by-products produced as a result of clean coal technologies are the focus of the final chapter in the section. The next group of chapters in Part Two considers the utilization of different waste materials, including the key products coal fly ash, bottom ash, and flue gas desulfurization materials. This is followed by a contribution reviewing the latest research into innovative and advanced uses for coal ash.

After an introduction to ash quality problems and quality monitoring, Part Three concentrates on the essential area of by-product beneficiation techniques, and how to maximize the quality of materials for the end user. Topics covered include separation methods, thermal processing, and chemical passivation. The final part of the book addresses environmental issues, including the use of coal combustion by-products in green construction materials and the essential health and safety considerations associated with their use.

Key features:

- An essential reference on the nature, reactivity, beneficiation, potential, and environmental risks of coal-combustion by-products
- Contains an in-depth review of the origin and geochemistry of coal ash
- Explores the utilization of coal combustion by-products as supplementary cementitious materials to reduce the anthropomorphic greenhouse gas emissions associated with the use of Portland cement concrete
- Describes the essential area of the toxicology of coal combustion by-products

**Dr Thomas L. Robl**, Senior Advisor for the Materials Technologies Group at the University of Kentucky Center for Applied Energy Research, USA

**Anne Oberlink**, Senior Research Scientist, Materials Technologies Group at the University of Kentucky Center for Applied Energy Research, USA

**Rod Jones**, Professor of Civil Engineering, School of Science and Engineering, University of Dundee, Scotland

ENERGY AND ENVIRONMENTAL
ENGINEERING

ISBN 978-0-08-100945-1

9 780081 009451

ELSEVIER

WP
WOODHEAD
PUBLISHING
An imprint of Elsevier
elsevier.com/books-and-journals